University of Strathclyde

Department of Pure and Applied Chemistry

A Chemical Probe for TIGAR

A thesis submitted to the University of Strathclyde in part fulfilment of regulations for the degree of Doctor of Philosophy in Chemistry.

Steven Kay

Supervised by Professor Nicholas C. O. Tomkinson

2019

FLY LEAF

This thesis is the results of the author's original research. It has been composed by the author and has not been previously submitted for examination, which has led to the award of a degree.

Signed: Steven Kay

Date: 15/08/19

Abstract

The University of Strathclyde has established a partnership with the Beatson Institute to initiate this multidisciplinary project, bringing together three academic researchers; Prof. Nick Tomkinson (Chemistry), Dr Blair Johnston (Modelling) and Prof. Karen Vousden (Biology). The project primarily applied a standard SAR approach following the design, target synthesis, biological evaluation and data analysis cycle, to develop a chemical probe for the emerging tumour suppression target, TP53 Induced Glycolysis and Apoptosis Regulator (TIGAR). Upon optimisation, these tool compounds were then used to dissect the fundamental biology associated with this target, specifically in cancer models developed within the Vousden laboratory.

The phosphatase TIGAR plays a key role in the flow of metabolites within two key biological pathways; glycolysis and the pentose phosphate pathway (PPP). The regulation of these pathways is crucial for the stability and growth of cancer cells, which highlighted TIGAR as a potential therapeutic target. Currently, there are no chemical tools for the interrogation of TIGAR, and its downstream functional effects. Here, a novel series of 2-amino thiophene-3-cabomate benzoic acid derivatives were designed, synthesised, and biologically evaluated, as potential TIGAR inhibitors. A summary of the optimisation achieved during the SAR studies is highlighted in **Figure 1**, from initial hit compound **58** to lead compound **338**. Ligand **338** exhibited a half-maximal inhibitory concentration in the nanomolar range. Pharmacokinetic studies demonstrated that **338** possessed a sufficiently robust PK profile for potential use within *in vivo* studies. The selectivity and cellular activity of lead compound **338** has yet to be tested, however, compound **184** exhibited a promising selectivity profile and phenocopied the effects of siRNA in cell based studies.

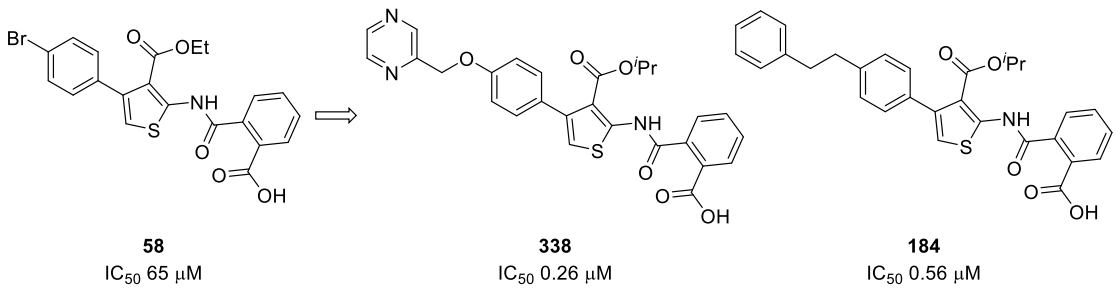

Figure 1: Summary of SAR from initial hit 58 to lead compound 338. Structure of ligand 184.

Acknowledgements

I would like to thank my supervisor, Professor Nicholas Tomkinson, for his continuous support and guidance throughout the year as well as the wealth of knowledge that he enlightens me with. I would like to extend my gratitude to the Tomkinson group for their constant support throughout the year and for making my time in the lab both enjoyable and fortuitous.

I would also like to thank my second supervisors, Dr Blair Johnston and Professor Karen Vousden for both their knowledge input and for allowing me to work in their respective laboratories.

Thank you to Simon Mackay for providing his medicinal chemistry expertise and aiding in the progression of the project.

Thanks to Louise Young for allowing me to perform my biological assay within her laboratory and for constant help and advice.

I would like to thank Tony Vassileou and Dr Murray Robertson for demonstrating the AI software used to perform the allosteric site prediction and the pharmacophore generation software respectively, and also for their help and friendship throughout this time.

I would like to extend my gratitude to Dr Ming Yang for showing me how to carry out the biological assessment of the compounds made on this project.

I would also like to acknowledge the sponsors of this project, Cancer Research UK (CRUK), for allowing me to carry out my research in state of the art laboratories.

Finally, I would like to thank my fiancée, Jayde McLellan and my family and friends, for all their help and support throughout my time at the University of Strathclyde.

Table of Contents

Abbreviations - Biological terms

ADP -	Adenosine diphosphate
AP -	Alkaline phosphatase
APC -	Adenomatous polyposis coli
ATP -	Adenosine triphosphate
BAX -	bcl-2-like protein 4
2,3-BPG -	2,3-bisphosphoglycerate
CC1 -	Cys-based class I
CC2 -	Cys-based class II
CC3 -	Cys-based class III
CDC -	Cell division cycle
CDK -	Cyclin-dependent kinase
CD45 -	Protein tyrosine phosphatase receptor type C
DDT -	1,4-Dithiothreitol
DNA -	Deoxyribonucleic acid
DSP -	Dual-specificity phosphatase
ERK1 -	Extracellular signal-regulated kinase 1
ERK2 -	Extracellular signal-regulated kinase 2
F-1,6-BP -	Fructose-1,6-bisphosphate
F-2,6-BP -	Fructose-2,6-bisphosphate
F-6-P -	Fructose-6-phosphate
FBP-1 -	Fructose-1,6-bisphosphatase
FBPase-2 -	Fructose-2,6-bisphosphatase
G-6-P -	Glucose-6-phosphate
GSH -	Glutathione
HAD -	Haloacid dehalogenase
HP -	Histidine phosphatase
KD -	Knockdown
Ki -	Inhibitory constant
KO -	Knockout
MptpA -	*M. tuberculosis* protein tyrosine phosphatase A
MptpB -	*M. tuberculosis* protein tyrosine phosphatase B
$NADP^+$ -	Nicotinamide adenine dinucleotide phosphate
NADPH -	Nicotinamide adenine dinucleotide phosphate-H

PD -	Proton donor
PFK-1 -	Phosphofructokinase-1
PFK-2 -	Phosphofructokinase-2
3PG -	3-Phosphoglycerate
PHP -	Protein histidine phosphatase
Pi -	Phosphate
PPM -	Metal-dependant phosphatase
PPP -	Pentose Phosphate Pathway
PPPL -	Phosphoprotein phosphatase like
PTP1B -	Protein tyrosine phosphatase 1B
p21 -	Cyclin-dependent kinase inhibitor 1
R-5-P -	Ribose-5-phosphate
ROS -	Reactive oxygen species
RTR1 -	RNA polymerase II subunit B1 CTD phosphatase
SHP-1 -	Src homology-2 domain containing protein tyrosine phosphatase-1
SHP-2 -	Src homology-2 domain containing protein tyrosine phosphatase-2
STAT -	Signal transducer and activator of transcription
TIGAR -	TP53-induced glycolysis and apoptosis regulator
TP53 -	Tumour protein 53
UBASH3B -	Ubiquitin-associated and SH3 domain-containing protein B

Amino acid abbreviations are provided in Section 9.1. page 343

Abbreviations - Chemical & miscellaneous terms

Ac -	Acetate
Bn -	Benzyl
Bu -	Butyl
d -	Distilled
DABAL-Me_3 -	*bis*(Trimethylaluminium-1,4-diazobicyclo[2.2.2]octane adduct
DAST -	Diethylaminosulfur trifluoride
DiFMUP -	6,8-Difluoro-4-methylumbelliferyl phosphate
DMF -	*N*,*N*-Dimethylformamide
DMSO -	Dimethylsulfoxide
DS -	Discovery Studio
EC_{50} -	Concentration when 50% effective
Et -	Ethyl
HBA -	Hydrogen bond acceptor
HBD -	Hydrogen bond donor
H-Bond -	Hydrogen bond
Hepes -	4-(2-Hydroxyethyl)-1-piperazineethanesulfonic acid
HRMS -	High Resolution Mass Spectrometry
^{i}Bu -	Isobutyl
IC_{50} -	Concentration at 50% inhibition
^{i}Pr -	Isopropyl
LC-MS -	Liquid chromatography - mass spectrometry
LRMS -	Low Resolution Mass Spectrometry
MD -	Molecular dynamics
Me -	Methyl
Ms -	Mesylate
M.wt -	Molecular weight
NMR -	Nuclear magnetic resonance
PCC -	Pyridinium chlorochromate
PDB -	Protein data bank
Ph -	Phenyl
SAR -	Structure activity relationship
SID -	Shared information data model
^{t}Bu -	*tert*-Butyl

TCA -	Trichloroacetic acid
THF -	Tetrahydrofuran
TLC -	Thin layer chromatography
TMS -	Trimethylsilyl

1. Introduction

1.1. Post translational modifications

Post translational modifications (PTMs) are covalent chemical modifications which occur at all steps of a protein's life cycle, increasing their functional diversity, by adding or removing functional groups. The identification and understanding of PTMs, along with the proteins that perform these transformations, is imperative to our study of cell biology, and disease treatment/prevention. The most abundant PTMs are phosphorylation and dephosphorylation which are performed by kinase and phosphatase enzymes, respectively.[1]

1.2. General phosphatase overview

The human genome contains approximately 200 protein phosphatases, which were recently categorised in 2017 by Chen *et al*. into 10 protein folds, 21 families and 178 subfamilies, based on their genomic and evolutionary relationships.[2] **Figure 2** represents the 10 protein folds for the classification of human phosphatases.[2]

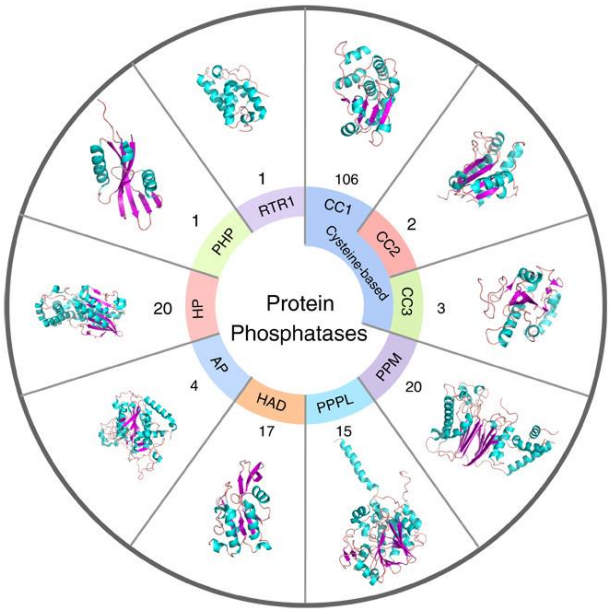

- CC1: Cys-based class I
- CC2: Cys-based class II
- CC3: Cys-based class III
- PPM: metal-dependant phosphatase
- PPPL: phosphoprotein phosphatase like
- HAD: haloacid dehalogenase
- AP: alkaline phosphatase
- HP: histidine phosphatase
- PHP: protein histidine phosphatase
- RTR1: RNA polymerase II subunit B1 CTD phosphatase

Figure 2: Protein phosphatases categorised into 10 structural folds. Numbers indicate the number of phosphatases within each classification.[2]

Classification of the protein phosphatases into 10 different structural folds implies that a variation in the evolutionary origin of these proteins exists. However, three of the folds (CC1, CC2 and CC3) are comprised of a shared catalytic motif (CX_5R), as

they all contain a nucleophilic cysteine residue, which indicates that these 3 folds may share similar evolutionary pathways.

The human phosphatases and their evolutionary relationships with each other are represented by the human phosphatase phylogenetic trees (Figure 3).[2] Each tree represents one of the 10 folds described in **Figure 2** with subsequent branching detailing the individual phosphatases within families and subfamilies. These phosphatase phylogenetic trees were designed and segregated, based on the sequence of a respective phosphatases catalytic domain and the biological function(s).

The majority of human phosphatases (more than half) are grouped into the CC1 fold, as it contains the two largest families of protein phosphatases; the protein tyrosine phosphatase (PTP) and the dual-specificity phosphatase (DSP) families. The first of these is a family which plays a key role in intracellular signalling pathways and has been linked to multiple disease states.[3] For these reasons, the PTP family has received a significant amount of attention from the scientific community, in order to further understand their biological functions and to establish whether these phosphatases can be targeted with tool compounds in disease models. The PPM and PPPL folds are made up of phosphatases with phosphorylated serine/threonine specificity and illicit a variety of functional effects. The histidine phosphatases all contain a nucleophilic histidine residue which directly performs the dephosphorylation process. The remaining trees include phosphatases which have more specific functions.[4-6]

Figure 3 also details the evolutionary relationships and origins of each individual phosphatase through colour coding of every single branch within the phylogenetic trees. Each branching event indicates where a new family or subfamily was created and the organism within which this evolutionary change occurred, is highlighted through the colour scheme, allowing for the tracking of evolutionary pathways.

Due to the significant physiological and pathological role that phosphatases adopt in our biological systems, they are considered to be important targets for drug discovery, particularly within oncology.[7]

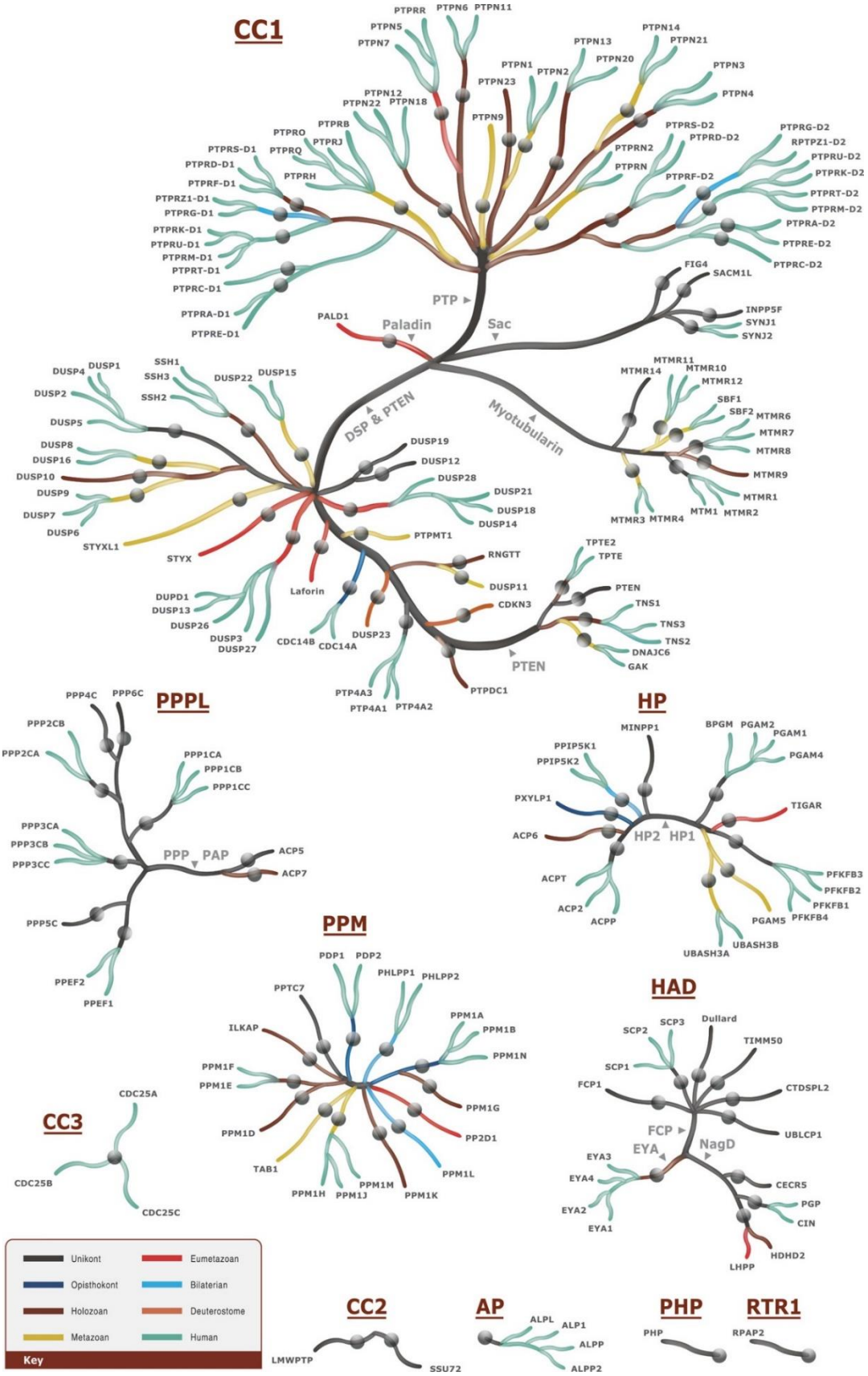

Figure 3: Human protein phosphatase phylogenetic trees. Families depicted by triangles and subfamilies by circles. Branches coloured based on evolutionary origin.[2]

1.2.1. Protein phosphatase structure

The general structure for phosphatases is more complex than their kinase counterparts, as kinases effectively act as ‘shuttlers’ transferring a phosphate group from one component, adenosine triphosphate (ATP), to another (substrate). As they are always interacting with ATP, their adopted structure is relatively similar. In the case of phosphatases however, they directly perform the removal of the phosphate group and so, the structure of the protein has adapted depending on the structural nature of the specific substrate, resulting in no typical overall structure. However, since all phosphatases extract the same functional group (phosphate) from their substrates, the catalytic site within each family of phosphatases remains highly conserved (Figure 4).[8]

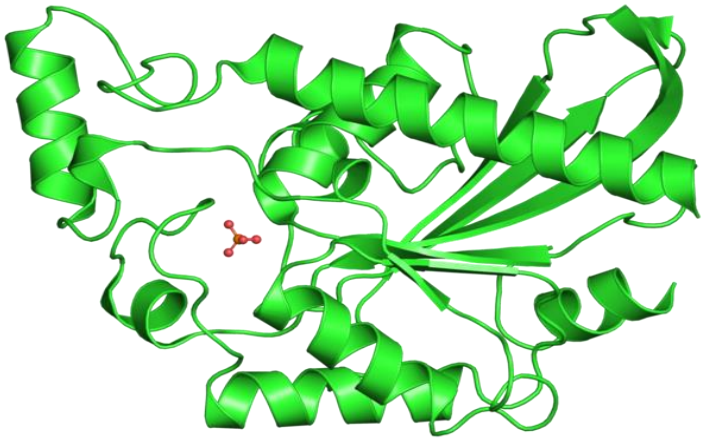

Figure 4: Example of protein phosphatase structure (PDB = 3DCY).

In general, the catalytic sites of protein phosphatases are moderate to large in size. They are open and positively charged in nature, as they need to incorporate substrates, which vary in size, from small molecules to a protein. The substrates always have a high charge density as they contain at least one, in some cases two, negatively charged phosphate groups, resulting in the fact that even small molecules require a large relative space due to increased repulsion from the charged functionalities. The catalytic sites generally contain positively charged residues (arginine, lysine, histidine) which aid in the stabilisation of the negatively charged phosphate group, to enable dephosphorylation to occur readily.[9] A table of amino acids is attached in Section 9.1. page 347.

1.2.2. Mode of action

The function of protein phosphatases is to act as a catalyst in the removal of the phosphate group, from a small molecule substrate or phosphorylated protein, onto a nucleophilic residue (serine, threonine, tyrosine, or histidine) of the phosphatase, in a cellular process known as dephosphorylation. The phosphate group is then released from the phosphatase by a water molecule to regenerate the active enzyme and a free phosphate ion (Pi). Dephosphorylation is a reversible process and addition of a phosphate group to a specific substrate is catalysed by another enzyme known as a kinase, which uses ATP as a phosphate source, resulting in the phosphorylated protein and a molecule of adenosine diphosphate (ADP) (Figure 5).[10-11]

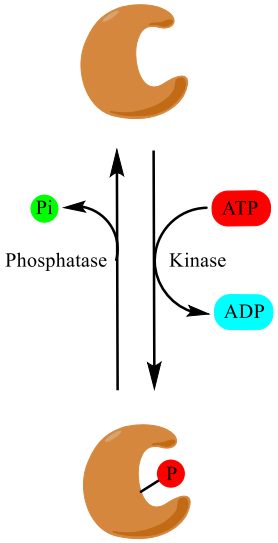

Figure 5: Phosphatase mode of action.[12]

Phosphorylation and dephosphorylation are two of the most ubiquitous post translational modifications (PTMs) used in cellular signal transduction pathways, both of which are reversible (Figure 5).

1.2.3. Therapeutic potential

Phosphorylation and dephosphorylation may result in a conformational change of the substrate, which can in turn result in the extensive modulation of the substrates biological function. As a result, these PTMs act to regulate fundamental cellular processes such as apoptosis, cell cycle progression and cell growth. This is a result of the intricate part protein kinases and phosphatases play in facilitating transduction within cell signalling pathways (Figure 6).[13]

Signal transduction occurs when a signalling event (e.g. cellular stress) activates a particular receptor, which can then trigger a cascade of biochemical events, often *via* kinases and/or phosphatases inside the cell, creating a net response. Kinases and phosphatases themselves are known to be activated by other kinases or phosphatases, and can organise into phosphorylation cascades (Figure 6).[13] The overall control of these pathways is known as phosphoregulation.[14]

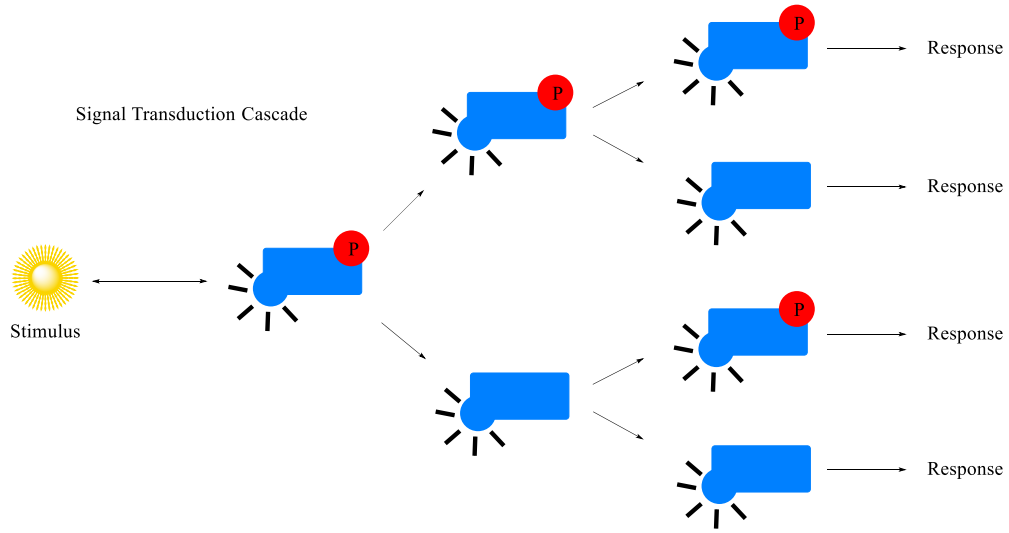

Figure 6: Theoretical example of a signal transduction cascade.[12]

The balance between activation/deactivation of these cascades is extremely delicate and so unsurprisingly, the modification of signal transduction pathways (e.g. *via* oncogenic mutation) can lead to the aberrant functioning of a cell, and in turn cancer. The potential to establish a degree of control over cell division and death has resulted in both kinases and phosphatases becoming attractive therapeutic targets.[15]

Interest in the last few decades has fundamentally resided with protein kinases, which have been deemed more targetable, and to have more specific applications than their phosphatase counterparts.[14] The main reason for this is the nature of the kinase orthosteric site, which tends to be deeper compared to the shallow sites normally observed with phosphatases. Kinase active sites are also generally more flexible and lipophilic, which has enabled a general binding mode to be established for small molecules within this protein family. Designing chemical tools which fit this binding mode and identifying areas of the active site that drove potency, could also be effectively rationalised. In contrast, phosphatase active sites act directly upon their phosphorylated substrate(s), and therefore establishing a generic binding mode

has been exceptionally difficult. Additionally, to out-compete natural substrates, phosphatase inhibitors generally need to possess a minimum of one anionic functionality that can mimic the negatively charged phosphate group, present on the substrate (Figure 7).[16-18] Achieving cell permeability and target specificity is made somewhat more challenging due to this factor, which has reduced the attraction in phosphatases as drug targets in comparison to their kinase counterparts.

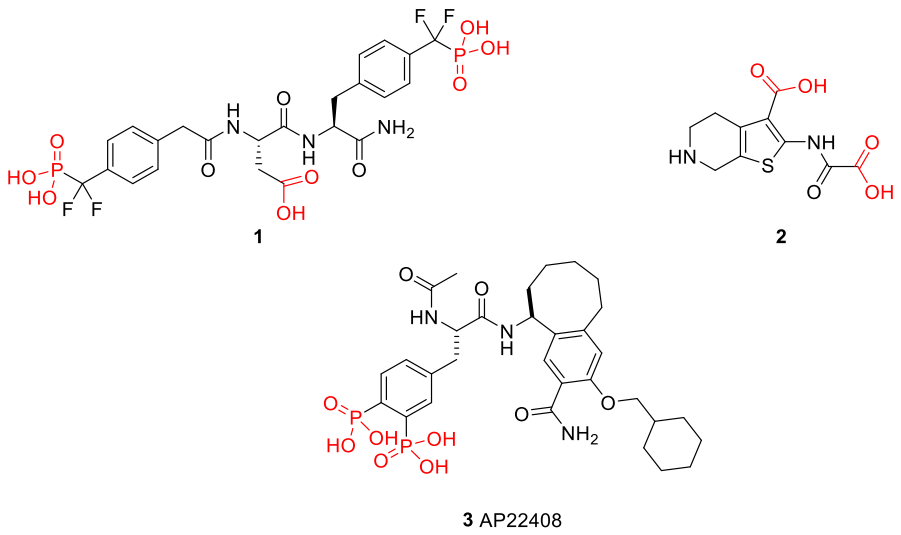

Figure 7: Examples of phosphatase inhibitors: anionic functional group(s) highlighted in red.[16-18]

Recent research, however, has generated an ever-growing recognition that protein phosphatases have imperative roles in the maintenance of phosphorylation levels within cells, which is crucial for the normal function of cellular processes.[7,19] Due to the part these proteins play in physiological regulation, phosphatase enzymes effectively govern severe pathological diseases, including cancer, diabetes, inflammatory diseases, cystic fibrosis and cardiovascular diseases.[20-21]

Multiple reviews have been published describing recent advances in the available methods for studying protein phosphatases.[22-23] Recent advances in available structural data, computational modelling, compound library make-up and assay types have also led to new chemical tools for this challenging target class.[24-25] Further development of small molecule probes, comprised of differing scaffolds, may provide the structural foundations from which future therapeutics can be developed, in order to target the phosphatase family and ameliorate their role in disease. However, at this time, the discovery of small molecules that function under *in vivo* conditions for phosphatases remains difficult.[26] As a consequence, our understanding

of phosphatases, their interaction with substrates and their individual, specific biological functions is severely underdeveloped. The need for efficient chemical probes that can provide an insight to these fundamental areas is at an all-time high. Primarily, this project aims to add to the ever-growing library of tool compounds by targeting a phosphatase from a sub-family that has received very limited attention, in order to further our understanding within the phosphatase interactome.

1.3. Protein Tyrosine Phosphatases

Protein tyrosine phosphatases are the largest sub family within the entire phosphatase interactome, consisting of 108 members that are further classified based on catalytic domain sequence homology, substrate specificity and cellular localisation. Numerous PTPs have been strongly linked to multiple disease states including diabetes, obesity and cancer (Table 1).[3] Aberrant PTP signalling within cells has now been related to multiple human cancers, with the individual PTPs being classed as either oncogenic or tumor suppressing phosphatases. Overexpression of oncogenic phosphatases and a depletion of tumor suppressing phosphatases have been observed in malignant cells.[3] These significant findings have ensured that the majority of research studies surrounding phosphatases over the past two decades have been focused upon this particular group.[3]

Table 1: Example tyrosine phosphatases and associated disease states.[26]

Tyrosine phosphatase	Disease
PTP1B	Diabetes, obesity
MptpA/B	Tuberculosis
CD45	Alzheimer's disease, autoimmune disease, inflammation
SHP1	Obesity, Noonan syndrome
SHP2	Leukaemia

Intensive targeting towards PTPs has fuelled an increase in the number of small molecule inhibitors that interact with the orthosteric site of this key protein class. The vast majority of PTP inhibitors are designed with the aim of binding within the active site of the respective PTP, and normally contain a phosphate mimetic group which is

immune to the dephosphorylation process, i.e. non-hydrolytic. Ligands designed in this manner are then able to exploit the cationic nature of the catalytic residues, however as previously stated, selectivity against other PTPs can become a hindrance. A selection of PTP inhibitor compounds, with associated IC_{50} values and specific targets, are detailed in Figure 8.[26]

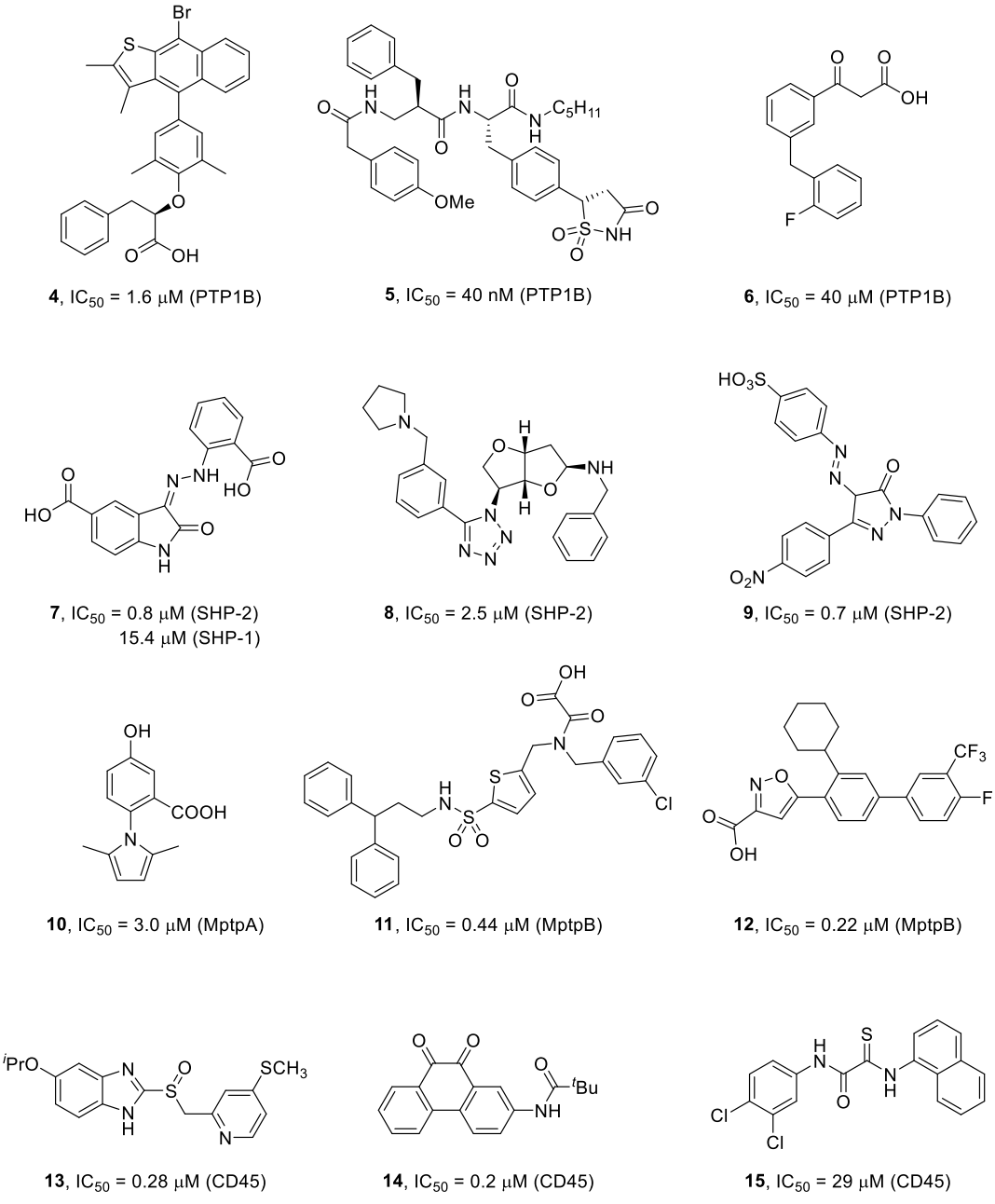

Figure 8: Selected PTP inhibitors.[26]

Key examples include protein tyrosine phosphatase 1B (PTP1B) ligand **4**, which reached phase II clinical trials for treatment of Type II diabetes, before being

discarded due to multiple undesired side-effects and limited *in vivo* potency.[27] Src homology-2 domain containing protein tyrosine phosphatase-2 (SHP-2) inhibitor **7** exhibited only moderate potency but was crucially selective against Src homology-2 domain containing protein tyrosine phosphatase-1 (SHP-1) and PTP1B, as well as possessing sufficient cell permeability. Inhibitor **9** restricts tumor growth in various human tumor cell lines by preventing the activation of extracellular signal-regulated kinase 1/2 (Erk1/2), by inhibiting an oncogenic mutant of SHP-2.[28] *M. tuberculosis* protein tyrosine phosphatase B (MptpB) ligand **12** is recognised as the most potent inhibitor for this PTP to date, according to the literature and was also found to be selective (≥ 35 fold) against a screening panel of various PTPs.[29] Protein tyrosine phosphatase receptor type C (CD45) inhibitor **14** was reported as a potent compound (0.2 μM), with anti-proliferative activity against T-cells in the range of 0.1 μM. **14** was found to be a reversible inhibitor even though it is hypothesised to temporarily modify the nucleophilic cysteine residue through the formation of a hemi-thioketal.[30]

Recognition of the therapeutic potential phosphatases possess has been generated from observing the key physiological role that these enzymes perform. PTPs were the first family to receive significant appreciation for their biological roles, which resulted in the stable development of a wide range of potent inhibitors with diverse applications and proven functional effects.[16, 26] Limited selectivity and a lack of pharmacological astuteness are appreciated factors that medicinal chemistry efforts will have to improve upon, in order to progress more compounds towards clinical trials. Nevertheless, the extensive efforts on the PTP front, provides a platform to build upon for future endeavours. Also, with only a limited number of phosphatases currently being examined from a chemistry perspective, there could perhaps be new targets which prove to be more promising, and may lead to the development of more efficient inhibitors.

1.4. TIGAR

1.4.1. Origin

The protein phosphatase chosen for this project is the **T**P53-**i**nduced **g**lycolysis and **a**poptosis **r**egulator (TIGAR). The TIGAR protein was discovered in the Vousden laboratories by a co-supervisor on this project, Prof. Karen Vousden, as recently as 2006.[31] Tumour protein 53 (TP53) is regarded with crucial importance as it is the

main protein that conserves genomic stability and inhibits malignant development, when a cell is placed under stress.[32] TP53 functions as a tumour suppressor, and it has been established that the TP53 gene is the most mutated gene in human cancer, again demonstrating its crucial role in cancer prevention. Both of these functions have resulted in TP53 being termed the 'guardian of the genome' as the TP53 pathway determines cell survival or death upon its activation.[33]

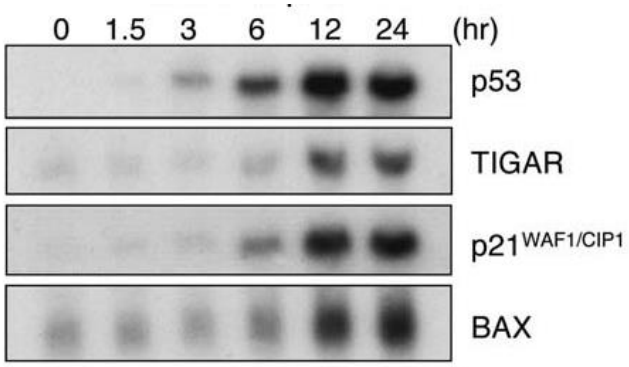

Figure 9: Northern blot showing expression of p53, TIGAR, p21WAF1/CIP1, and BAX to occur on approximately the same time scale.[31]

TP53 mainly acts indirectly by inducing a number of different target genes to carry out a specific role. One of these inducible genes is TIGAR, which functions by inhibiting glycolysis and protecting cells from oxidative stress.[31] The TIGAR gene contains two possible TP53 binding sites and microarray analysis of gene expression demonstrated that the induction of TIGAR expression by TP53, occurred within the same time frame as the expression of other directly induced TP53 target genes (p21, BAX) (Figure 9).[31] This information demonstrates the importance of TIGAR's biological function in relation to the functions of other TP53 induced proteins.

1.4.2. Histidine phosphatase

The TIGAR protein is a histidine phosphatase and is therefore part of the histidine phosphatase superfamily of proteins (Figure 10). Histidine phosphatases are a functionally diverse group of twenty proteins that share a highly conserved catalytic core, containing a nucleophilic histidine residue, which directly performs the dephosphorylation process. The superfamily is composed of two branches; the larger branch 1 where TIGAR is placed, which contains mainly sugar-based phosphatases, and the smaller branch 2 which contains mainly acid based phosphatases.[34] Sequence similarity of the phosphatases between and within the two principal branches of the

family has been identified as being very different, with the highest sequence similarity across the family being 53% and a low of 9%.[34] This is thought to be due to the differing evolutionary origins of the family members, which for example include eumetazoan (TIGAR), metazoan, holozoan and human origins.[2] **Figure 10** depicts TIGAR on a single evolutionary chain within branch 1 and shows that TIGAR has no isomeric forms, potentially increasing the chances of selectivity for a developed chemical probe, against other members of the family.

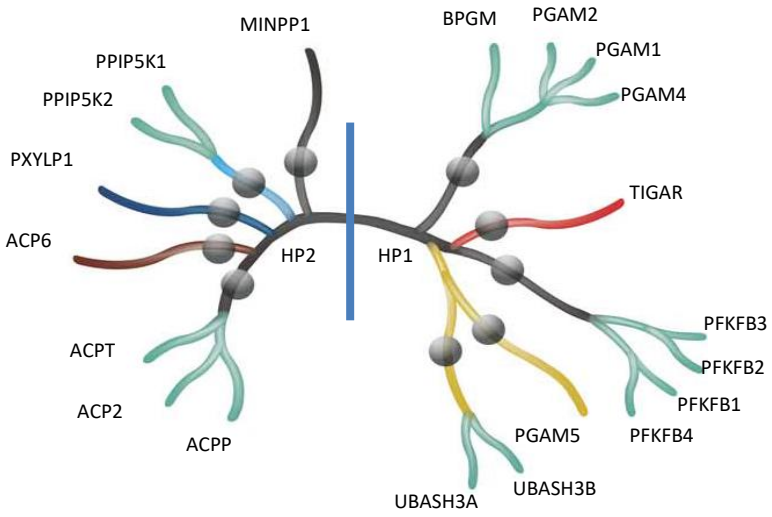

Figure 10: Histidine phosphatase phylogenetic tree.[2]

The TIGAR structure is approximately 30 kDa in weight and exists as a monomeric structure in solution.[35] The crystal structure of TIGAR has been studied in reasonable detail since its discovery in 2006, with full characterisation of the protein being obtained for multiple homologs. Attempts have also been made to crystallise the structure with the natural substrate present; however, this has been unsuccessful to date.[35] This may be due to the kinetics of the dephosphorylation reaction as one or two phosphate (Pi) molecules are observed in these crystal structures (Figure 11), indicating that the dephosphorylation event has already occurred.

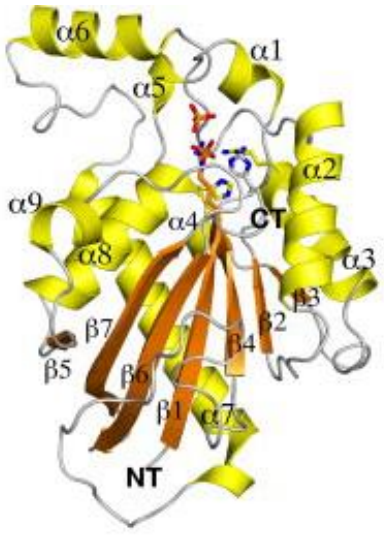

Figure 11: TIGAR structure. Two bound phosphate molecules and key residues in the active site are shown as sticks (NT = N-terminus, CT = C-terminus) PDB = 3E9C.[35]

As predicted, the overall TIGAR structure contains a common histidine phosphatase fold (Figure 11). The core of the protein is created from an α-β-α sandwich with a central mixed stranded β-sheet (β1–β7), which is in turn verged by two α helices (α3 and α8) on either side. The catalytic site area of the protein is then sealed off by three helices (α1, α5 and α6), which are formed by two insertions between β1/α2 and β3/α7. The central β-sheet is partially covered in TIGAR by a novel loop formed from an extra insertion between β4 and α7, which is not observed in other histidine phosphatases.[35]

The catalytic core of histidine phosphatases is highly conserved and unsurprisingly, is comprised of the same four cationic residues. The four residues consist of the key nucleophilic histidine residue (His11), two flanking arginine residues (Arg10 and Arg61) and a second histidine residue (His198) (Figure 12). A generic proton shuffler, which varies between aspartate and glutamate, aids in the dephosphorylation process and completes the catalytic quintet of residues. Another common motif that is highly conserved across histidine phosphatases is the RHG (arginine, histidine, glycine) motif. The glycine residue (or alanine in some cases) packs tightly against the core, and the backbone carbonyl group of this residue forms an essential hydrogen bond with the nucleophilic histidine residue, which ensures that the histidine is present in the optimum orientation for catalysis (Figure 12).[34] The high conservation level of this glycine motif across the family illustrates how important the histidine conformation is for catalysis.

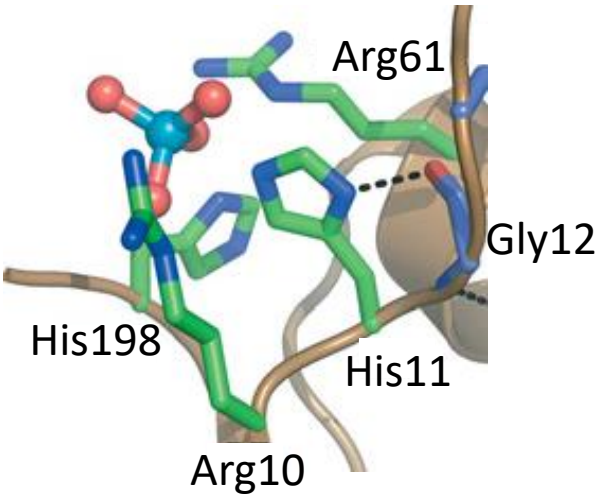

Figure 12: Catalytic core of TIGAR displaying the key hydrogen bond of glycine to histidine.[34]

During dephosphorylation, the two arginine residues and the second histidine residue form stabilising interactions, such as hydrogen bonds and electrostatic interactions, with the phosphate group of the substrate before, during and after the reaction has occurred. This intricate hydrogen bond network enables the phosphate group to adopt the appropriate orientation inside the phosphate binding pocket, by negating the repulsive forces of the negatively charged functional group. Additional neutral residues can aid in the phosphate groups stabilisation, through the formation of additional hydrogen bonds. A proposed mechanism for dephosphorylation by histidine phosphatases is shown in **Figure 13**.

In Step 1, the optimally aligned histidine residue nucleophilically attacks the phosphorus atom of the phosphate through one of its nitrogen atoms, with subsequent protonation of the leaving group by a nearby proton donor residue (aspartate or glutamate). The dephosphorylated product is then released so that it can leave the active site while the remaining phosphate is directly bound to the histidine residue. Step 2 consists of catalyst regeneration and the release of the free phosphate ion. The negatively charged proton donor residue formed in the first step regains a proton by deprotonating, and in turn, activating a water molecule present in the active site. This water molecule then undergoes nucleophilic attack on the phosphorous atom of the histidine bound phosphate. The imidazole functionality of the histidine group acts as an excellent leaving group (pKa ~6.9) and so is released to produce a free phosphate ion, regenerating the nucleophilic residue for the next dephosphorylation cycle. The negative charge of the free phosphate ion is once again stabilised by the catalytic

amino acids before eventually being cleared from the protein in order for the catalytic site to be re-established (Step 3).

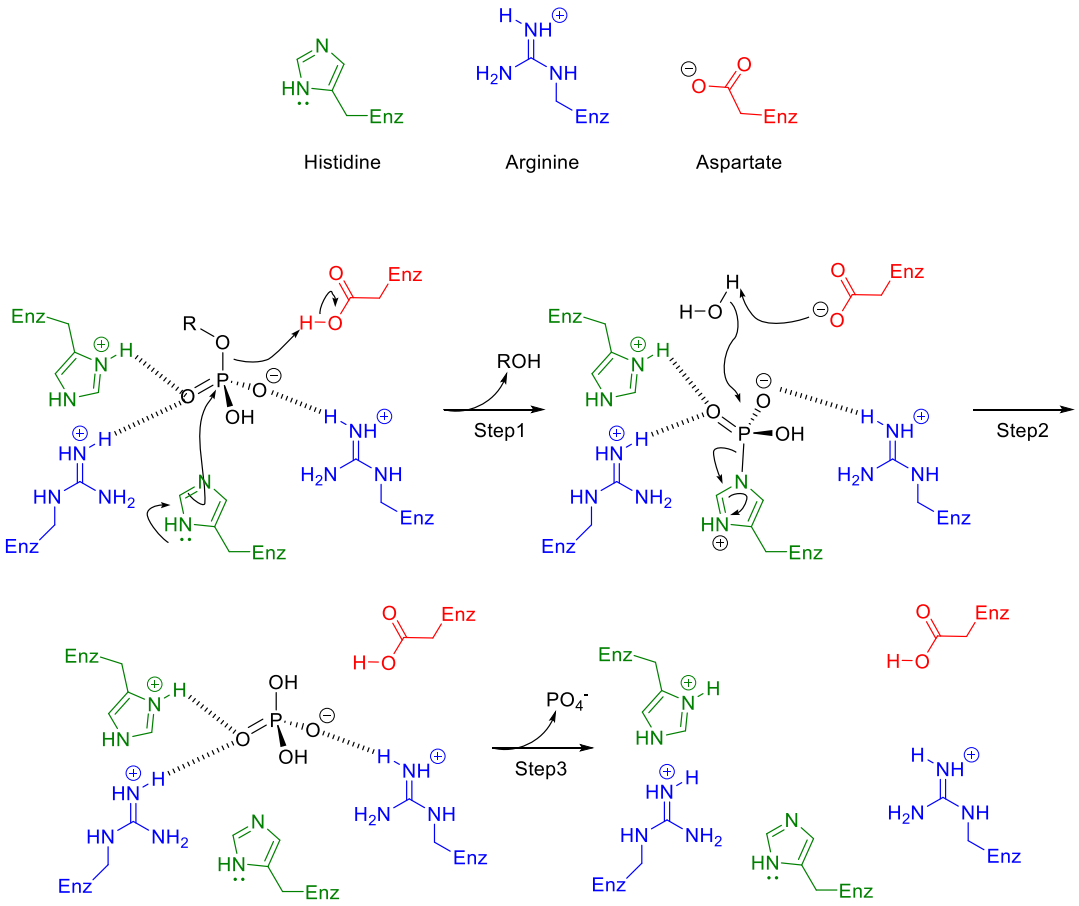

Figure 13: Proposed mechanism for histidine phosphatase dephosphorylation.[34]

1.4.3. Therapeutic relevance

As previously stated in Section 1.4.1, TIGAR functions by inhibiting glycolysis and protecting cells from oxidative stress when it is activated by TP53. The processes by which TIGAR accomplishes this are complex and indirect, however, conclusions about its therapeutic relevance can still be easily drawn in relation to its function. A schematic of TIGAR's established signalling pathway, coupled with the cellular responses which underpin its biological function, are detailed in **Figure 14**.

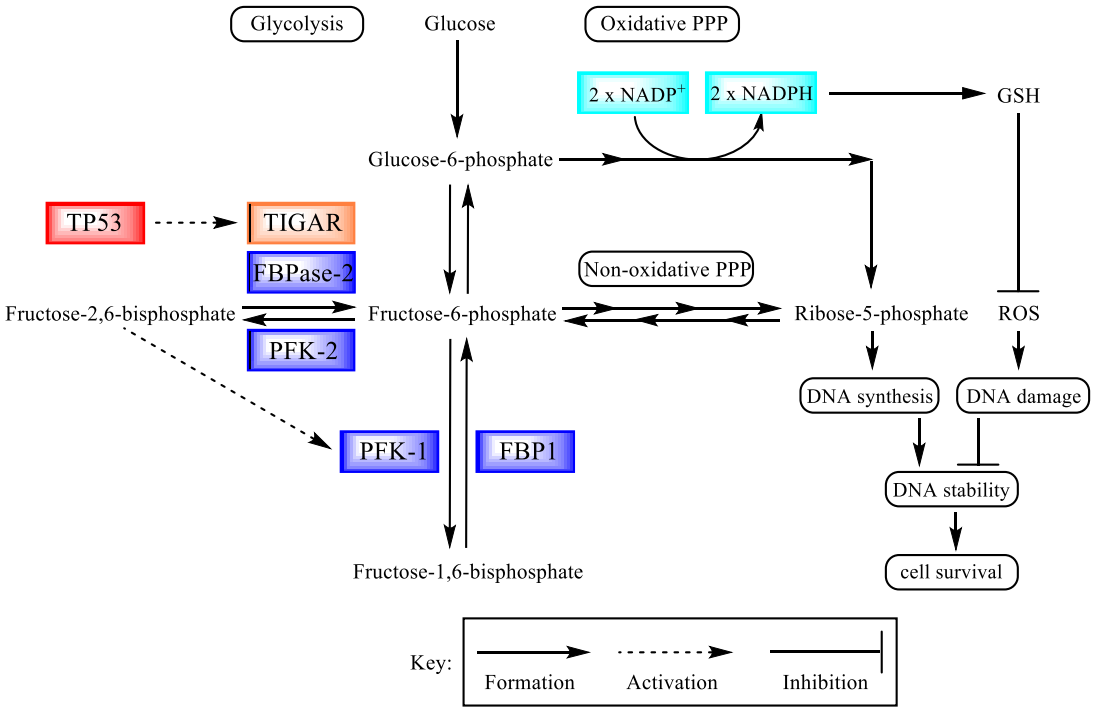

Figure 14: TIGAR signalling pathway and related cellular processes.

TIGAR operates as a bisphosphatase and shares similarities with the domains of other bisphosphatases such as the bifunctional phosphofructokinase-2/fructose-2,6-bisphosphatase (PFK-2/FBPase-2), despite a lack of amino acid conservation. As such, under cellular stress, once TP53 initiates TIGAR expression, TIGAR functions in an analogous manner to FBPase-2 by reducing intracellular levels of fructose-2,6-bisphosphate (F-2,6-BP), which is a robust allosteric activator of phosphofructokinase-1 (PFK-1). PFK-1 acts by catalysing the conversion of fructose-6-phosphate (F-6-P) to fructose-1,6-bisphosphate (F-1,6-BP) which drives the cellular degradation of glucose, also known as glycolysis. F-2,6-BP also has a secondary function as it inhibits fructose-1,6-bisphosphatase (FBP-1) which counteracts PFK-1 activity (Figure 14).[36]

Under normal cellular conditions, with no form of stress and where TIGAR activity has not been induced by TP53, F-2,6-BP increases the rate of glycolysis through the above two processes, resulting in a normal amount of F-6-P and glucose-6-phosphate (G-6-P) being present in the cell. Both of these substrates can then move into two different branches, non-oxidative and oxidative respectively, of another critical process within cells, known as the Pentose Phosphate Pathway (PPP). The PPP is

vital as it produces ribose-5-phosphate (R-5-P), which is the key building block in nucleotide synthesis and also produces nicotinamide adenine dinucleotide phosphate-H (NADPH) from nicotinamide adenine dinucleotide phosphate ($NADP^+$) through its oxidative pathway, which assists antioxidant function. Once F-6-P and G-6-P are processed through the PPP, the R-5-P produced is used for DNA synthesis/repair, which results in increased DNA stability and cell survival. It is this property that enables TIGAR to act as a tumor suppressor under low levels of cellular stress. The NADPH lead to the synthesis of glutathione (GSH), an antioxidant, which can in turn dampen the number of reactive oxygen species (ROS). However, some ROS species will still remain which can cause DNA damage, resulting in decreased DNA stability and potentially cell death through oxidative stress (Figure 14).[37] Low levels of oxidatively induced apoptosis allows TIGAR to display tumor suppressor characteristics under these circumstances by keeping cell survival rates in check.

When a cell is placed under high levels of oxidative stress (e.g. malignant cells), TIGAR no longer functions as a tumor suppressor, as it becomes heavily overexpressed. Under increased levels of oxidative stress TP53 will bind to the TIGAR gene resulting in a substantial increase in TIGAR expression and activation. TIGAR then acts by significantly degrading F-2,6-BP, which results in an overall inhibition of glycolysis. Upon this degradation, F-2,6-BP will no longer allosterically activate PFK-1, preventing the conversion of F-6-P to F-1,6-BP. Additionally, F-2,6-BP now fails to inhibit the FBP-1 which increases the production of F-6-P. Therefore, not only is less F-6-P being broken down by PFK-1 but more is also being produced by FBP-1, which consequently inhibits glycolytic flux downstream of this point. At this stage, the increased concentrations of glycolytic metabolites, G-6-P and F-6-P, can enter the PPP. The increased concentrations force a flux into the oxidative portion of the PPP, which amplifies the levels of R-5-P and NADPH that are produced, resulting in an amplification of DNA synthesis and the production of GSH respectively. In turn, this ends with highly improved DNA stability and a reduction in ROS levels. Decreased ROS levels provide reduced DNA damage and a restriction in oxidatively induced apoptosis. The overall outcome is an increase in the rate of malignant cell survival and increased protection from ROS-induced cell death.[36]

Under normal cellular stress, the above activities would be viewed as a standard response, however, if TP53 underwent a mutation or if another oncogenic mutation was to occur, which resulted in the over-expression of TIGAR, then it can easily be seen how the jump from protection to malignant cell development can be made, resulting in the possible contribution of TIGAR to cancer development.

1.4.4. TIGAR in cancer

Evidence already exists which suggests that TIGAR levels must be carefully regulated during a TP53 response.[36] Overexpression of TIGAR has been observed in a number of cancers, such as primary colon cancer, glioblastoma and invasive breast cancer.[38,39,40] Expression of TIGAR, and other p53 promoted proteins, supports an antioxidant response which can aid cell survival under low levels of stress, and has been proposed to preclude cell malignancies.[37]

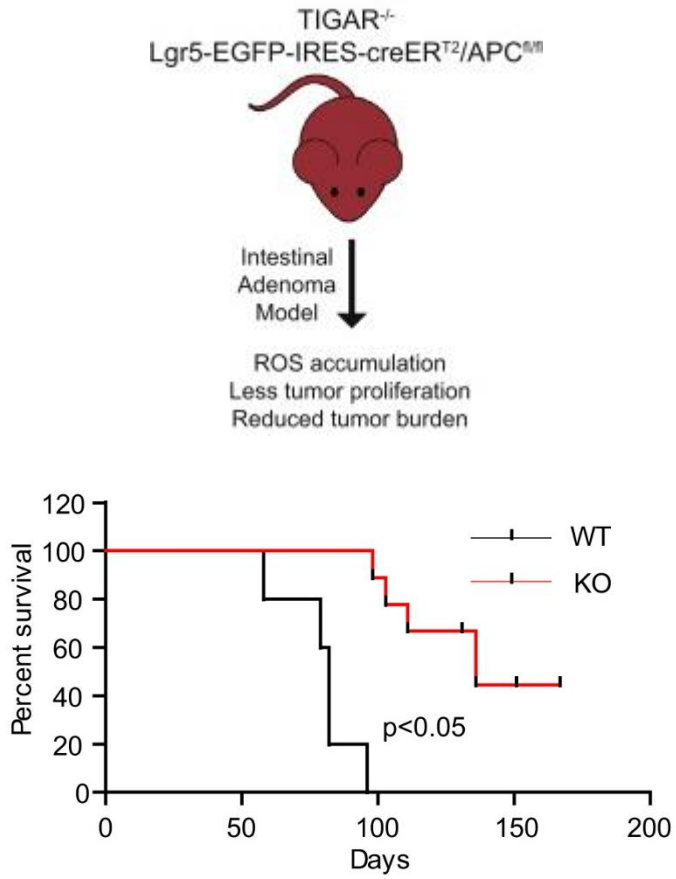

Figure 15: TIGAR deficiency reduced tumor burden and increased survival rates (percentage of mice not reaching pre-defined tumor growth limit) in a mouse model of intestinal adenoma.[39]

However, studies have also reported that TIGAR expression is amplified in mouse/human tumors and tumor cell lines, demonstrating that TIGAR contributes to both tissue regeneration and tumor development.[39] **Figure 15** describes the effects of TIGAR on tumor burden, with respect to a mouse model of intestinal adenoma. This particular cancer model was generated by using a gene trap (Lgr5-EGFP-IRES-creER^{T2}/APC$^{l/fl}$) to delete the tumor suppressor gene adenomatous polyposis coli (APC). In order to observe the effects due to TIGAR absence, genetic knock out (KO) techniques were implemented. The study depicted in **Figure 15**, performed by Cheung *et al*, identified three key changes in the absence of TIGAR; (1) an accumulation was observed in the levels of cellular ROS species which we know can induce apoptosis; (2) less tumor proliferation was observed; and (3) overall there was a reduced tumor burden. Percentage survival was defined as the percentage of test subjects that had not reached a defined tumor growth limit due to cell proliferation. The percentage survival graph further supports the above observations, as in the TIGAR wildtype (WT) experiment, percentage survival had reached zero just under 100 days. However, the experiments in which TIGAR KO was implemented depicted a 100% survival rate after 100 days and a > 40% survival rate after 150 days.

Together, the data demonstrates that the metabolic regulation displayed by TIGAR is crucial for tumor cell survival and proliferation within the intestinal adenoma mouse model. This aberrant need for TIGAR function by tumors is glaringly depicted at the 100 days mark, where WT TIGAR models have a 0% survival rate and the KO TIGAR models have a 100% survival rate. In the KO studies, ROS species cannot be depleted, meaning that oxidatively induced apoptosis is not inhibited and the cancer cells are therefore unable to proliferate. This assessment was strongly supported by the fact that the tumor cells could be rescued through the addition of ROS scavengers. Re-introduction of WT TIGAR to KO species was also able to rescue tumor cells, proving that the observed effects were due to an absence of TIGAR function. These findings suggest that unregulated TIGAR expression may promote the progression of cancer/tumorigenesis, and that the inhibition of TIGAR expression could provide a therapeutic advantage.

1.4.5. TIGAR Unknowns

Evidence has shown that TIGAR expression is preserved in tumour cells containing a TP53 mutation and that TP53 may still exert some control over TIGAR expression which may influence tumorigenesis.[39] However, additional studies have demonstrated that p53-independent TIGAR expression has been observed in a wide range of cancer cell lines where no wild-type p53 is present.[41] Expression of TIGAR in various human tumor types can therefore be completely unrelated to the levels of WT p53, suggesting that there is an alternative pathway for TIGAR regulation.

Downstream effects from the dephosphorylation of F-2,6-BP to F-6-P by TIGAR have been investigated by multiple research groups and our understanding of this relationship is constantly growing. However, new information has also established that TIGAR can convert 2,3-bisphosphoglycerate (2,3-BPG) to 3-phosphoglycerate (3PG) with a higher catalytic efficiency than that of converting F-2,6-BP to F-6-P (Figure ***16***). The absence of TIGAR was also found to consistently increase the concentration of 2,3-BPG by approximately 5-fold, although the physiological relevance of this metabolism has yet to be discovered.[42]

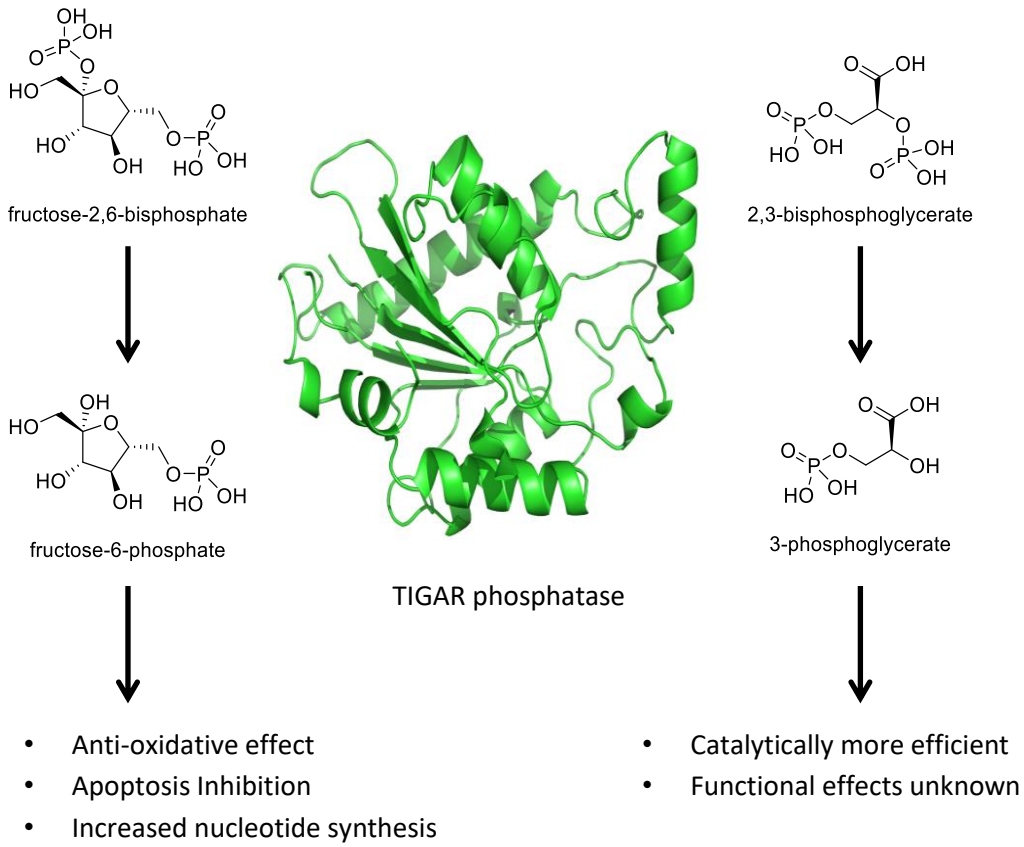

Figure 16: TIGAR substrates and known information of downstream effects.

These findings clearly demonstrate that there are still significant amounts of information to be uncovered with regards to the regulation of TIGAR expression during cellular stress. The precise downstream effects of TIGAR function on multiple phosphorylated substrates and how cells determine which substrate TIGAR should act upon, at any given time, are fundamental questions which still need to be answered. The expansion of the TIGAR substrate pool, and the associated increase in the complexity of this phosphatases downstream functional effects, should be considered when performing any further investigations. Any supplementary tools that can contribute to the unravelling of this complicated and intricate histidine phosphatase would be invaluable in the pursuit of further knowledge regarding this target.

1.5. Small molecule probes

Since the discovery of TIGAR only occurred recently (2006), the majority of its biological functions, and the particular interactions the protein has with cellular substrates remain unknown. The need for a biological tool to allow further investigation into these aspects of the TIGAR profile is high. There are currently no small molecule probes for TIGAR, therefore any initial starting probe, and in time, a more selective chemical tool, would allow a more in-depth understanding of this important bisphosphatase to be achieved.

1.5.1. What is a chemical probe?

A chemical probe/tool is generally described as a small organic molecule, which binds to a macromolecule, such as a protein and initiates a particular response. This response can be the activation or deactivation of another cellular substrate, downstream of the initial target. In the current climate chemical probes are, alongside aspects such as molecular biology and genetic techniques, proving to be essential in furthering our understanding of the genome and expanding the number of druggable targets.

Probes typically facilitate the investigation of chemical and biological space by creating a starting point for analogues to be developed, with the potential of generating a drug. They also allow the exploration of cellular processes and can aid in the understanding of the functions of specific genes and proteins, within signal

transduction cascades. These in turn, have driven our understanding of the physiology and pathology of a wide range of diseases.[43]

Small molecule probes allow for the potential validation of new therapeutic targets and provide a proof of concept for addressing a specific molecular target, pathway or process using a small molecule. They are also designed to inhibit/activate a specific function of the protein instead of affecting all roles of the protein, as these may be intricate processes, of which the modulation is undesirable.

Two examples of established chemical probes are SNS-032 and IC87114, which target the CDK2 and PI3K kinases respectively, and have allowed the elucidation of their biological functions (Figure 17).[44-45]

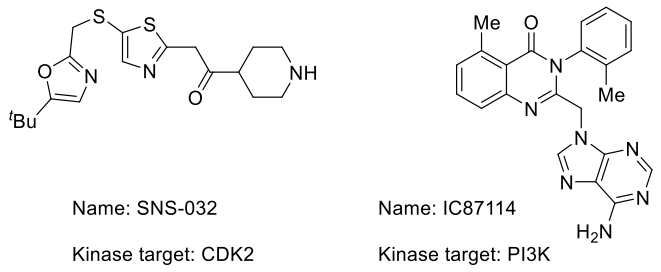

Figure 17: **Examples of established probes and their kinase targets.**

The key point in defining a chemical probe is that they allow researchers to validate a molecular target by demonstrating that a specific effect occurs, through the modulation of the target's function, when a particular synthetic molecule is bound. This allows a biomarker to be established for a particular disease state (e.g. cancer), which substantially boosts the chances of developing a successful drug candidate. As a result, the confidence in progressing through clinical trials will be greatly increased when embarking on a costly drug-discovery programme. Modern day drug-discovery programmes are increasingly more likely to not be undertaken, unless proper validation of a molecular target has been obtained, highlighting the requirement for high-quality chemical probes.[43]

1.5.2. Requirements for an efficient probe

Evidence suggests that the scientific community has taken a strong interest in chemical probes, and their impact on chemistry/biology is constantly growing with advancing technologies. More specifically however, the time and effort being spent

on the discovery of inhibitors/probes has resulted in only a small fraction of the human phosphatase interactome being characterised. Groups of chemists at the forefront of medicinal chemistry have recently expressed the need to focus on developing probes, instead of drug molecules, to further our understanding of uncharacterised proteins.[46] This in turn, could have an immediate impact on drug discovery efforts through better understanding and more focused targeting. The constraints that apply to the discovery of a 'drug like' compound can be relaxed to an extent, allowing more room to manoeuvre.

The central issues associated with chemical probes have been poor aqueous solubility and a lack of specificity regarding the target. Growing interest in this area has led to a number of researchers attempting to establish general guidelines to follow when synthesising small molecule chemical probes for assessing the broader biological effects of target modulation (Figure 18).[47-48]

Figure 18 outlines the main sections into which the parameters for successful chemical probes can be organised including chemical properties, biological potency, selectivity and context of use. All of these factors are brought together to provide an assessment of how relevant a small molecule probe is for exploring biological function.

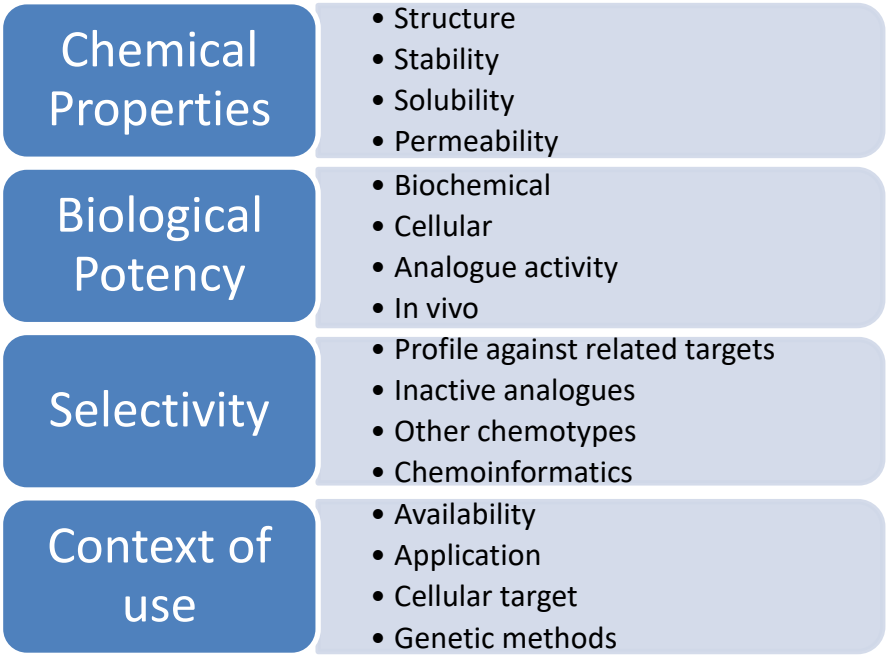

Figure 18: Four main areas and related criteria for successful chemical probes.[43]

Frye[47] summarised the main criteria displayed in **Figure 18** to produce a more concise set of principles to follow when designing a new chemical probe. This defined a correlation between a molecular target and the resulting biological effect from modulating that target.

1. **Molecular profiling**: Must be able to relate the *in vitro* profile to the cellular or *in vivo* profile by acquiring sufficient *in vitro* potency and selectivity data.
2. **Mechanism of action**: Should have enough mechanistic data against the desired molecular target to allow elucidation of the qualitative and quantitative effect (dose dependency) on a target-dependent action, in either a cell-based assay or a cell-free assay that recapitulates a physiologic function of the target.
3. **Identity of the active species**: Physical and chemical property data should be proficient in allowing the probe to be used in *in vitro* and cell-based assays where any conclusions drawn from the results are associated with the probe's original structure or a well-defined analogue.
4. **Proven utility as a probe**: Acceptable cellular activity should be attained so as to prove/disprove at least one hypothesis on the part played by a molecular target in a cell's response to alterations in the environment.
5. **Availability**: Free access to the chemical probe by the academic community with no limitations. An accompanying structurally related negative control should also be available for comparison.

The main point to highlight from the above set of principles is that other than point 5, the remaining principles are all assessed using gathered data, and so the strictness of the values will depend on the environment that the probe is used in, and the degree of knowledge already established in that area. If little is known for the desired area then the parameters may be relaxed, as with new biological targets such as TIGAR, valuable information can still be attained with a probe that is less than ideal. Probe credentials are therefore based on numbers and not assumed based on the structure of the small molecule. This is so that the biologists can use the most effective chemical probes available for biological studies.

Since there is currently no chemical probe reported to target TIGAR, a small molecule, which can be used to investigate the intricacies of this protein, is highly sought after by our biological collaborators at CRUK. In the past, obtaining selective

chemical probes has been hindered by multiple aspects, most notably the fact that the active sites of the proteins (e.g. phosphatases and kinases) are highly conserved, resulting in many cases with limited selectivity. In this project we aim to develop a chemical probe with a promising selectivity profile and an optimised potency.

1.6. Orthosteric site Targeting

The orthosteric site of TIGAR is comprised of a large and open pocket with an abundance of polar residues surrounding the phosphatase binding section in particular. The site consists of a significantly cationic nexus buried at the base, which attracts the anionic phosphate group of the substrate and anchors the molecule in the correct position for dephosphorylation. There are five key highly conserved catalytic residues, four of which (Arg10, His11, Arg61 and His198) are all positively charged at physiological pH. The cationic nature of these residues provides the necessary stabilisation of the incoming anionic phosphate group, which is held in an optimal orientation to enable the catalytic dephosphorylation process. The final catalytic residue present in TIGAR's orthosteric site is a glutamate (Glu89), which hangs just above the cationic quartet. These residues, along with the strategically placed glycine residue (Gly12), which holds His11 in the optimum trajectory for the process, are highlighted in **Figure 19.**

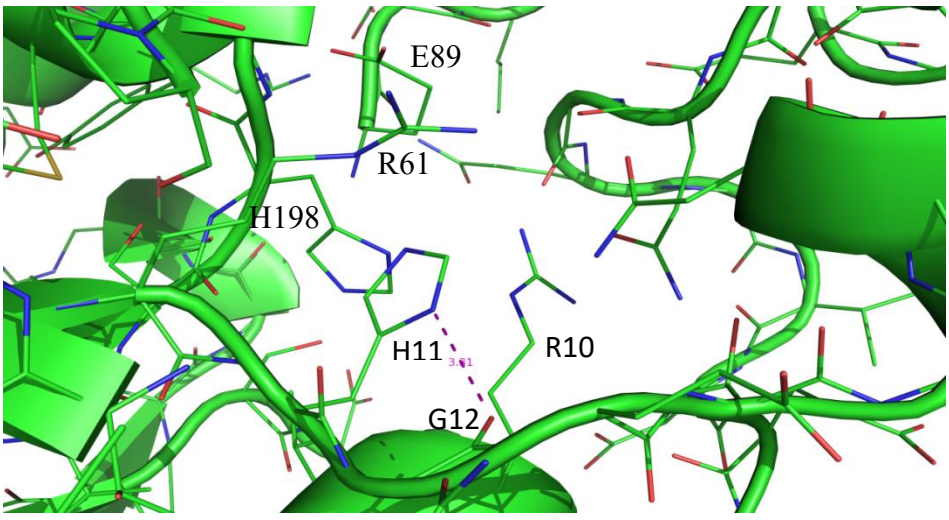

Figure 19: TIGAR orthosteric site; Key catalytic residues Arg10, His11, Arg61 and His198 along with the additional highly conserved Gly12 residue are labelled.

Based on this information, in order to effectively target the orthosteric site and out-compete the natural substrate, the designed small molecule will most likely

require, at least in the first instance, a functional group which is negatively charged at physiological pH. Securing an electrostatic interaction within the phosphate binding pocket should favourably position the small molecule, to permit further growth towards additional pockets within the binding site of TIGAR. The binding site is also open and relatively large in size, so the probe may require a relatively large amount of steric bulk, in order to spatially fill the pocket and maximise desirable interactions.

1.6.1. Current landscape of histidine phosphatase modulators

Histidine phosphatases are essentially unknown territory with respect to designing and developing small molecule probes. Literature searches have identified that examples of synthetic modulators which interact with this sub family of phosphatases are limited. Of the reported cases that do exist, the tool compounds are not even specific to histidine phosphatases, as researchers have so far only used established protein tyrosine phosphatase inhibitors. These compounds are used without the incorporation of any subsequent selectivity generating modifications, which results in the inhibitors binding promiscuously, to the selected histidine phosphatase.[49-50] As a result, these compounds are highly inefficient chemical probes, and are therefore not robust enough to generate reliable and accurate data.

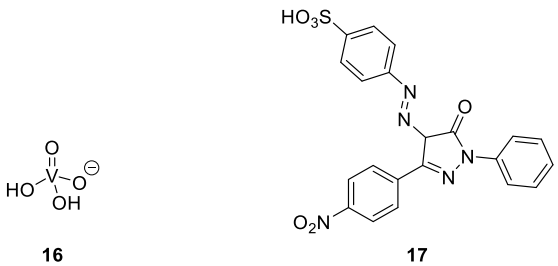

16 **17**

Figure 20: Literature reported inhibitors currently used for targeting histidine phosphatases.[49]

One example is where the metal ion based inhibitor, pervanadate (Figure 20, **16**) which essentially mimics a free phosphate ion, was used to study the histidine acid phosphatase ACPT (testicular acid phosphatase). Pervanadate provides no starting point for a structural activity relationship (SAR) study as it is only a simple fragment ion. Ubiquitin-associated and SH3 domain-containing protein B (UBASH3B or STS-1) inhibition with the known tyrosine phosphatase SHP-2 inhibitor, PHPS1 (Figure 20, **17**), provides a second reported example of a small molecule inhibitor.

However, again no structural changes were made to PHPS1 to drive selectivity towards UBASH3B, making this tool compound a very inefficient probe for interrogating a histidine phosphatase.

As a result, there are effectively no established small molecules that have been specifically designed for any histidine phosphatase, exposing a significant gap in our chemical arsenal. This shortage of information outlines the complete lack of attention that the histidine phosphatase family has received from the chemistry community, epitomised by the lack of published chemical probes. Clearly, this heavily limited number of histidine phosphatase inhibitor species highlights a striking need for more effort and focus to be directed towards expanding this chemical library.

1.7. Proposal

Phosphorylation is the most common reversible protein PTM with up to 30% of all proteins being phosphorylated at any given time.[51] Whilst substantial clinical success in cancer has been achieved with kinases as drug targets,[52] addressing phosphatases with small molecules has received significantly less attention, despite their accordant potential as drug targets. The primary challenge in understanding the basic biology of phosphatases, and thus validating them as targets, is the achievement of selectivity across members of the family. Therefore, the ability to drive potency towards a specific target, whilst engineering selectivity, is highly desirable, particularly for phosphatase inhibitors as this quality has proven challenging to achieve so far.

This project brings together multiple disciplines in the form of a collaborative triad, which includes experts within synthetic chemistry, computational chemistry and biology, with the overall purpose of delivering a validated chemical probe for the target phosphatase. The well-established and robust cycle of molecular modelling/ligand design, target synthesis, biological evaluation and data analysis will be used to drive SAR studies around a hit compound scaffold (Figure 21). Upon chemical probe potency and selectivity optimisation, drug metabolism and pharmacokinetics (DMPK) profiles will be generated for selected inhibitors, to assess their suitability for cellular and/or *in vivo* studies. Lead compounds will then be employed, by our biology based collaborators, to dissect the fundamental biology associated with this target, specifically in cancer models developed within the Vousden laboratory.

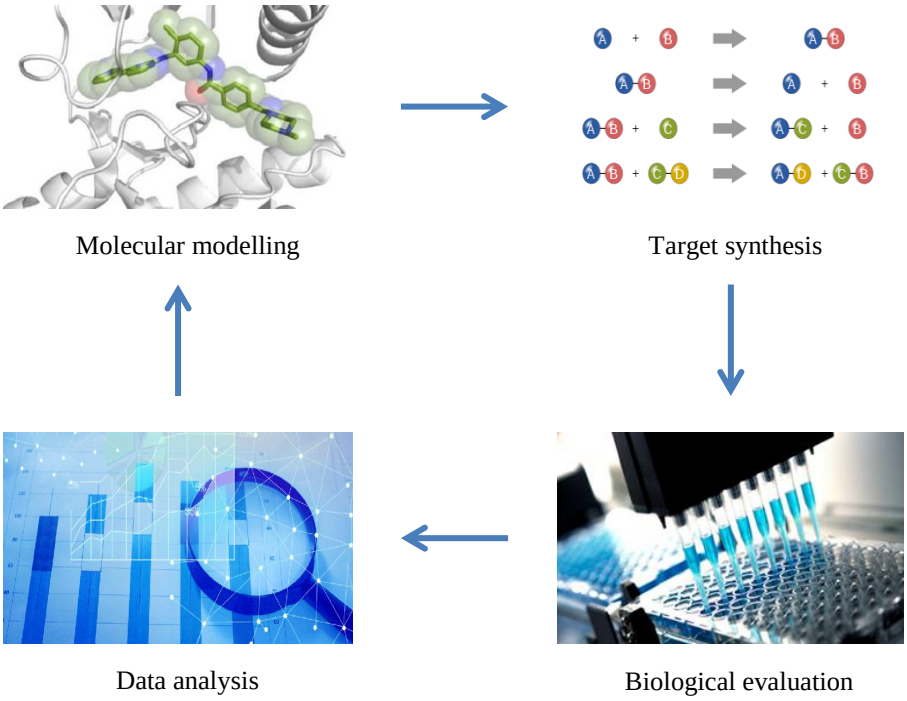

Figure 21: SAR cycle diagram for project.

At this point in time, TIGAR currently has no associated chemical probes, resulting in the fact that even a probe with low efficiency may allow for the determination of some intricacies of its biological function. For this reason, the stringency by which we judge the efficaciousness of our tool compounds will be relaxed to an extent, in order to ensure that there are no missed opportunities for informative results.

This work has the potential to produce the first small molecule probe for the human phosphatase TIGAR. A tool compound would also be an invaluable addition to the exceptionally limited/non-existent chemical library, for the interrogation of the histidine phosphatase family in general.

2. Aims

The first aim of the project was to attempt to identify a primary scaffold, from which to build upon and expand our investigations. No chemical starting point was pre-determined before the project, as no probes currently exist for TIGAR, and probe data is very limited with regards to histidine phosphatases in general. However, the natural substrates (fructose-1,6-bisphosphate **18** and fructose-2,6-bisphosphate **19**) shown in **Figure 22**, were identified and so we decided to begin by synthesising non-hydrolytic mimics of these compounds.

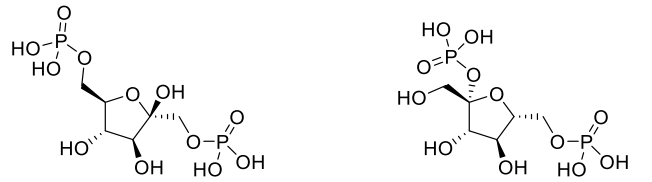

Figure 22: Natural substrates of TIGAR.

The overall primary aim of this project was to design and synthesise a potent chemical tool compound for TIGAR with sufficient selectivity and DMPK profile, for efficient target engagement.

A secondary aim was to generate cellular potency within a cancer cell line and for the inhibitor to exhibit a functional effect upon target engagement.

The final aim of the investigation would be to develop a compound capable of undergoing *in vivo* studies, through an immunocompromised mouse model, within the Vousden research laboratory.

3. Biological assay

3.1. *In vitro* colorimetric phosphatase assay

Abcam's phosphate assay provides an easy, quick and sensitive means of assessing phosphate levels over a wide range of concentrations. The kit contains 500 µL of 10 mM phosphate standard and 15 mL of phosphate reagent. The assay utilises a proprietary formulation of malachite green and ammonium molybdate, which forms a chromogenic complex with phosphate ions, giving an intense absorption band around 650 nm. Phosphate concentrations between 1 µM and 1 mM can be directly determined. The assay is carried out using a 96 well plate and all runs were performed in duplicate.

Phosphate standard preparation:

Dilute 10 µL of the 10 mM phosphate standard to 990 µL with distilled water (dH_2O) and mix well to generate a 100 µM working phosphate standard. Add 0, 10, 20, 30, 40, 50 µL of the 100µM phosphate standard to individual wells. Adjust the volume to 100 µL with dH_2O to generate 0, 20, 40, 60, 80, 100 µM of phosphate standard.

Sample preparation:

Initially, a 50 mM DMSO solution of each sample is prepared, before the samples undergo further dilution to the desired concentration for the particular assay.

Controls:

1 µL DMSO, 25 µL of substrate (80 µM), 25 µL of enzyme (1 µg/mL); negative control.

1 µL of DMSO, 25 µL of substrate (80 µM), but no enzyme; positive control.

1 µL of DMSO, 25 µL of enzyme (1 µg/mL), 25 µL of an inactive substrate (80 µM), for TIGAR (glucose-6-phosphate); positive control.

All reported concentrations are final assay concentrations.

TIGAR assay buffer:

25 mM KCl, 1 mM $MgCl_2$, 1 mM DTT **(**1,4-dithiolthreitol) 20 mM Hepes (4-(2-hydroxyethyl)-1-piperazineethanesulfonic acid) (pH 7.1)[42]

Protocol:

1. 1 µL of each sample (at the desired concentration) is added to individual wells on the plate.
2. Controls are prepared.
3. 25 µL of a 160 µM buffer solution of enzyme is added to the appropriate wells with subsequent incubation at room temperature for 5 minutes.
4. The phosphate standards were made up during this time.
5. 25 µL of a 160 µM buffer solution of substrate (fructose-1,6-bisphosphate) is added to the appropriate wells before the plate is incubated at 37 °C for 30 minutes.
6. Reactions are quenched with 50 µL of 10% trichloroacetic acid (TCA), including controls and phosphate standards.
7. 100 µL of dH_2O is added to all wells to bring the volume to 200 µL.
8. 30 µL of phosphate reagent is added to each well. Further incubation at room temperature for 15 minutes is allowed before absorbance is read at 650 nm.

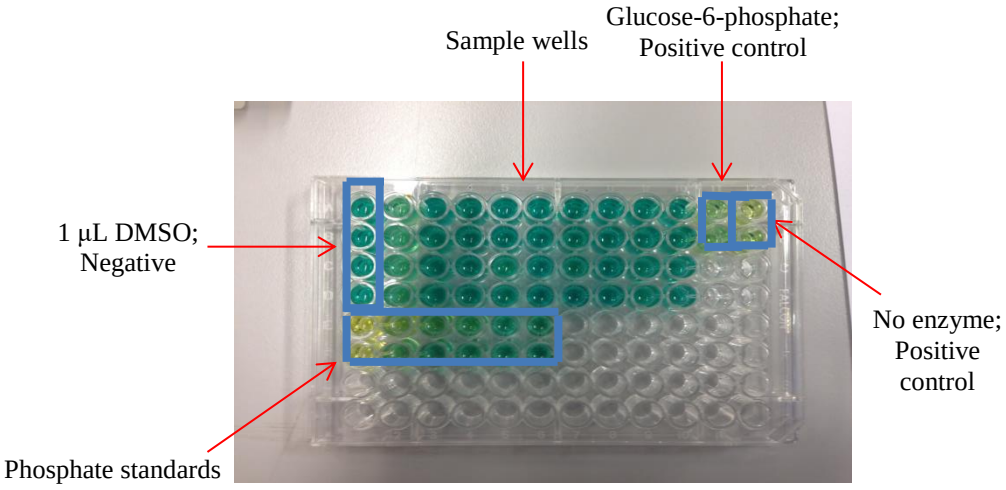

Figure 23: Detailed typical plate after assay protocol has been performed.

The phosphate concentration at each absorption value could easily be identified by referring to a graph of the phosphate standard concentrations vs absorption values. By taking the absorption value of the negative DMSO control as 100% dephosphorylation/phosphate ion concentration, the percentage inhibition of each sample was determined by using this value as a baseline. Dose response curves were

generated by performing the assay across a concentration gradient for each ligand. IC_{50} values were subsequently calculated as an n=3 using GraphPad Prism software.

4. Results and discussion

4.1. Orthosteric site - natural substrate mimetics

As stated in the proposal section, we elected to pursue the synthesis of a chemical probe for the orthosteric site, as there are currently no tool compounds available for interaction with TIGAR. A natural starting point for the targeting of the active site was the structure of two closely related natural substrates (fructose-1,6-bisphosphate **18** and fructose-2,6-bisphosphate **19**) (Figure 24), upon which an attempt was made to directly mimic the core structure.

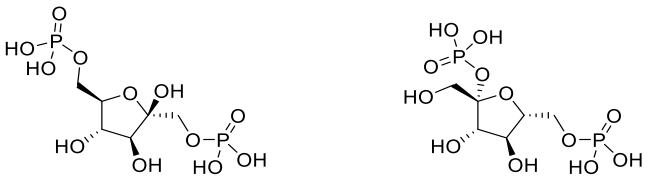

Figure 24: Natural substrates of TIGAR.

The two endogenous TIGAR ligands are both bisphosphates with only one of the phosphates on each ligand being removed during dephosphorylation. In order to effectively mimic these compounds, it was proposed that they should be modelled in the active site. Obtaining a crystal structure of the active site bound ligands is very difficult as the dephosphorylation process occurs rapidly, leaving only a free phosphate ion within the binding site. To gain an idea of how they bound to the target, both ligands were docked using the Gold 5.2.2. modelling software (Figure 25, PDB: 3DCY).

Figure 25 demonstrated multiple key features regarding the binding pose of F-2,6-BP **2** (Purple) which may have proven useful in the design of our chemical probe. First, it was observed that one of the respective phosphate groups (**a**) adopts several interactions (magenta) with the catalytic residues of the phosphate binding pocket. The other segments of the endogenous ligand (including the second phosphate group (**b**)) occupy the remainder of the site, forming secondary interactions with multiple residues located around the pocket. The tetrahydrofuran (THF) core acts as an anchoring scaffold by holding the phosphate groups in the appropriate spatial arrangement. The first series of compounds was therefore based

around this scaffold, with the idea that they would adopt a similar binding pose, and form key interactions within the active site.

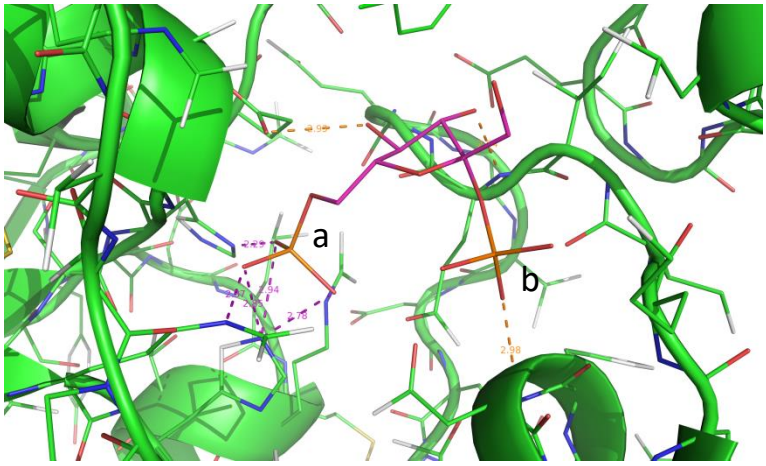

Figure 25: Fructose-2,6-bisphosphate 2 Purple docked in the orthosteric site of TIGAR; hydrogen bonds to catalytic residues shown in magenta, secondary stabilising hydrogen bonds shown in orange; Substrate phosphate groups labelled as a) and b).

4.1.1. Phosphonate/phosphonic acid series

4.1.1.1. Hypothesis

This first series of ligands prepared was based around the formation of a direct mimic of the natural substrates that could adopt similar interactions without undergoing dephosphorylation. Mimics of the phosphate group have been well documented in the literature[26, 53-54] and are based around two main criteria; the spatial size of the group and the net charge, since phosphates are negatively charged (pKa ~3) at physiological pH. The most common method for imitating a phosphate group, but still negating its ability to be dephosphorylated, is to replace the oxygen atom alpha to the phosphate group with a carbon atom, shutting down the enzymatic process.[53] The application of this concept, coupled with the removal of the furan scaffold and replacement with a phenyl ring to provide a more tractable synthetic route, led to the mono/*bis* phosphonate/phosphonic acid series of ligands (**20** and **21**) (Figure 26). A variety of both acids and esters were synthesised with varying substitution patterns and chain length at the carbon alpha to the phosphate group.

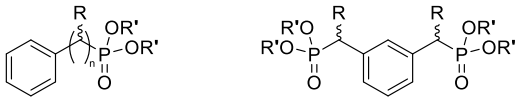

20 **21**

Figure 26: General structure of mono/bis phosphonates/phosphonic acids.

4.1.1.2. Synthetic routes

As these particular phosphate bio-mimetics were well established, there was substantial literature precedent for their synthesis.[16, 26] Below is the synthetic route and additional synthetic steps that were implemented for the synthesis of the mono phosphonate compounds (Scheme 1).

Scheme 1: Synthetic route for mono-phosphonate compounds.

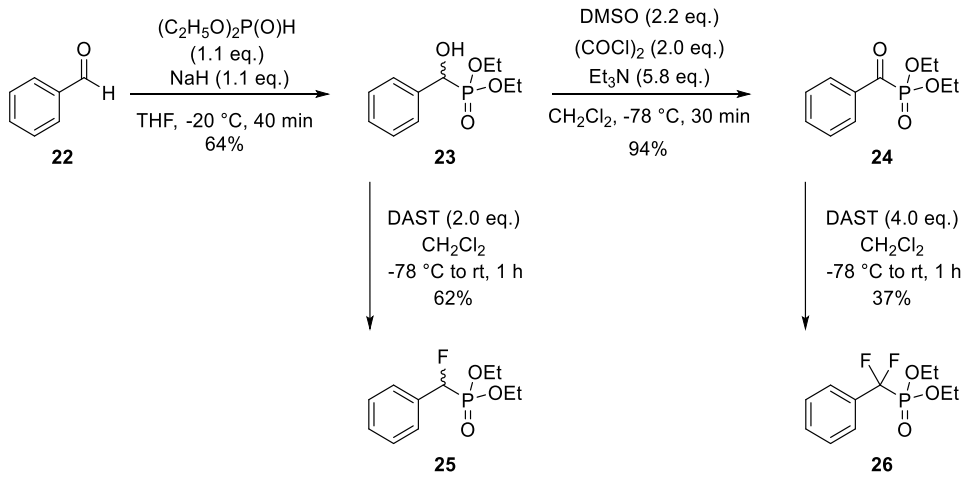

22 **23** **24** **25** **26**

Treatment of commercially available benzaldehyde **22** with diethyl phosphite ($(C_2H_5O)_2P(O)H$) and sodium hydride (NaH) in THF, afforded compound **23** (64%) after aqueous work-up and purification *via* column chromatography.[16] Compounds **24** and **25** were then both synthesised from compound **23**. Multiple oxidations were attempted for the synthesis of **24** from **23** before arriving at the Swern oxidation.[55] Both a pyridinium chlorochromate (PCC) and a manganese dioxide (MnO_2) oxidation were examined,[16] as these were successful for the oxidation of similar substrates in the literature, however, each reaction proved unsuccessful. There seemed no straightforward reasoning as to why the MnO_2 reaction did not work, however, the ^{1}H NMR spectra of the PCC reaction showed partial hydrolysis of the phosphonate ester, suggesting that the acidic nature of the reaction was a problem.

As a result, the Swern oxidation was performed, which resulted in the successful preparation of **24** (94%) without the need for further purification, after acidic work-up. Both compounds **23** and **24** were reacted with diethylaminosulfur trifluoride (DAST) (2.0 eq. and 4.0 eq., respectively) under similar conditions to afford, after aqueous work-up and purification *via* flash column chromatography, mono-fluoro **25** (62%) and gem di-fluoro **26** (37%), respectively.[16]

A selection of the corresponding bisphosphonates were then synthesised *via* the same synthetic route but with double the amount of equivalents for each reagent in the sequence (Scheme 2). Compound **28** was synthesised from **27** in 67% yield, **29** was prepared in 2 steps (67 and 53% yields, respectively) and the mono-fluorinated *bis*-ester **30** was also isolated after 2 steps (67 and 78% yields, respectively).

Scheme 2: Synthetic route for bisphosphonate compounds.

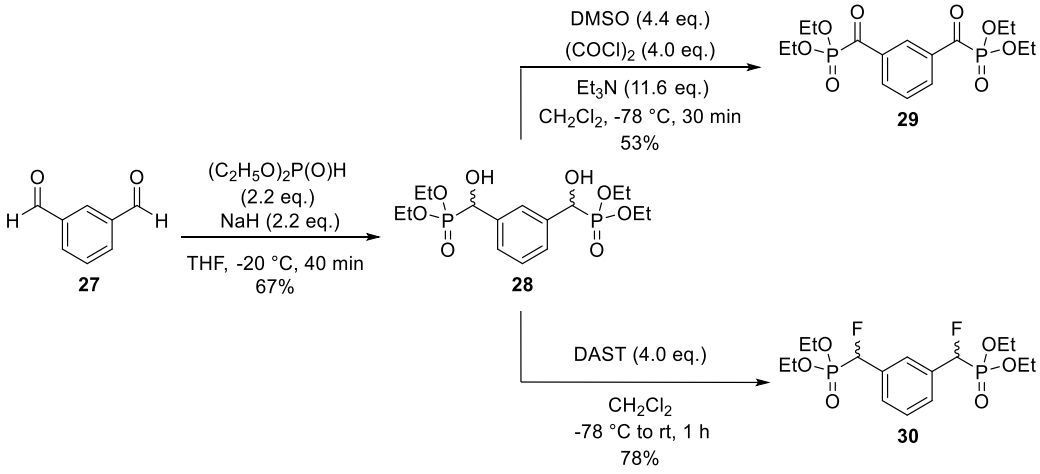

Two additional mono-phosphonate compounds were also synthesised to explore the effects of having a non-functionalised carbon alpha to the phosphonate ester (compound **32**) and the effects of varying the carbon chain length (compound **34**) (Scheme 3).

The palladium-catalysed coupling of benzyl bromide **31** with $((C_2H_5O)_2P(O)H)$ provided **32** (35%) after purification.[56] Treatment of 2-phenylethylbromide **33** and $((C_2H_5O)_2P(O)H)$ with caesium carbonate (Cs_2CO_3) and tetrabutylammonium iodide (TBAI) afforded **34** (56%) after purification.[57]

Scheme 3: Synthetic steps for phosphonates 32 and 34.

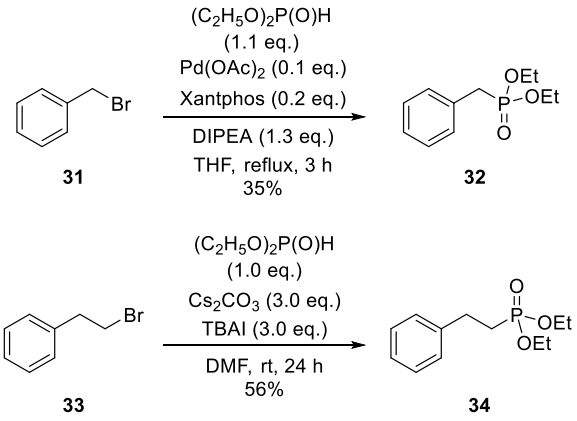

The final *bis*phosphonate ester of this series was prepared using the same procedure detailed in **Scheme 3**, for the synthesis of compound **32**, but with an increased number of equivalents for each reagent (Scheme 4). The palladium catalysed coupling of the dibromide **35** with ($(C_2H_5O)_2P(O)H$) successfully yielded **36** (37%) following purification.[56]

Scheme 4: Synthesis of bisphosphonate 36.

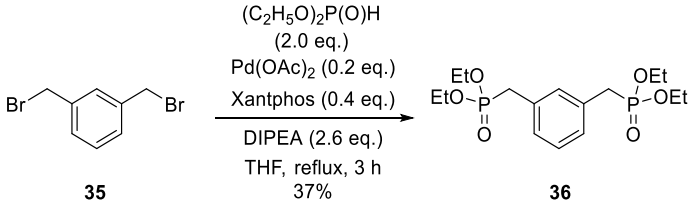

The corresponding phosphonic acids for selected phosphonate esters, were prepared in a single step, as shown in **Scheme 5**. Each phosphonate ester (compounds **23**, **34**, **28**, and **30**) was reacted with an excess of bromotrimethylsilane (TMSBr) in dry acetonitrile (MeCN) for 3 hours. Excess TMSBr was removed *in vacuo* through multiple co-evaporations with toluene (PhMe) and methanol (MeOH) to afford the corresponding phosphonic acid derivatives (compounds **37–40**).[58]

Scheme 5: Synthesis of phosphonic acid derivatives.

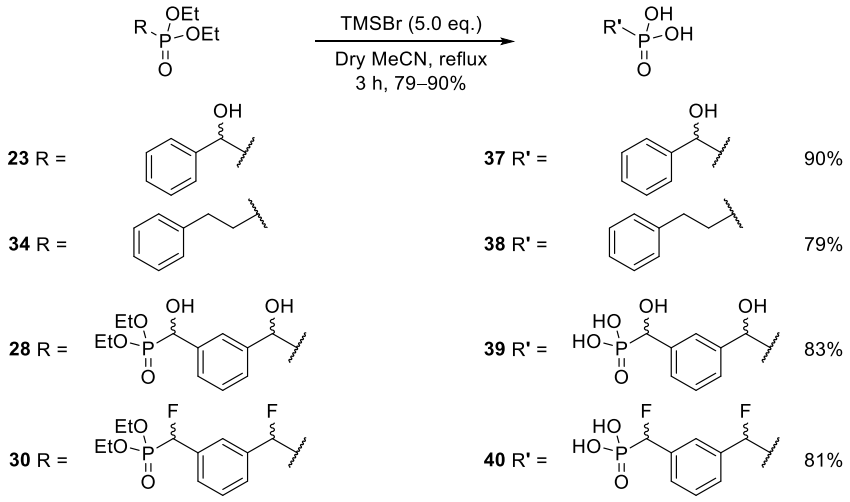

4.1.1.3. Biological evaluation

Each of the compounds synthesised throughout this project were screened in the *in vitro* assay described in Section 3.1. As the initial objective was to find a molecule with some form of activity, a single point assay at a single concentration was performed on each individual compound. If affinity for the protein was observed then IC_{50} (concentration at 50% inhibition) values were to be obtained by carrying out a titration curve across a range of concentrations.

The compounds in this series were screened at a concentration of 200 μM which was deemed a reasonable concentration for a hit compound, in relation to the compound's molecular weight (~150–300). Screening results for the mono- and bis-phosphonate esters of this series are displayed in **Figure 27**.

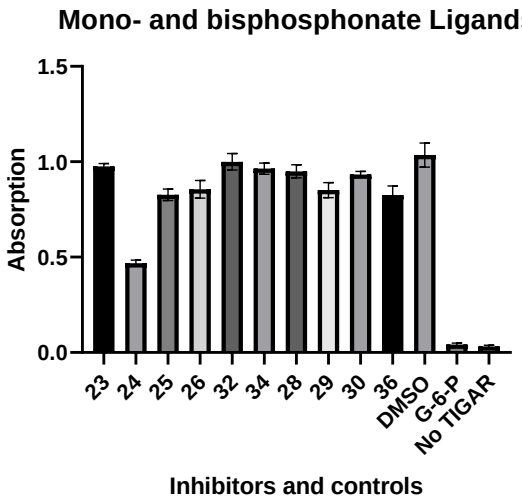

Figure 27: Graph of single point assay results for mono- and bisphosphonate compounds.

In the above graph, the DMSO, G-6-P and no TIGAR peaks are the negative and two positive controls described in Section 3.1., respectively. The value observed for the negative control peak (~1) is the baseline value for the assay, meaning that percentage inhibition of each compound was calculated using this number. For this particular series, we identified that the only ligand displaying noticeable inhibition at 200 μM was compound **24** (55% inhibition). Originally, this seemed like a promising result however, upon further analysis of the structure of **24** (Figure 28), it was proposed that inhibition was being observed due to non-specific covalent binding to one of a number of potential nucleophilic residues, in the TIGAR active site. Non-specific Covalent binding was undesirable for this chemical probe due to toxicity reasons, so the result was not followed up with any further analysis.

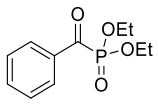

24

Figure 28: Structure of 24.

The phosphonic acids (**37**–**40**) were also screened at 200 μM and the results for these compounds are detailed in **Figure 29**. The phosphonic acids all proved to be inactive towards the target, which was interesting, as they very closely resembled the endogenous ligands and had an overall net negative charge, due to the acidic nature of the protons. The potential sub-optimal orientation of the phosphonic acid groups, in relation to the phenyl core, could be a possible reason for the observed inactivity.

These results reinforced the proposal that **24** was binding covalently, as the phosphonic acids, in theory, should have been the more effective binders due to their potential for forming electrostatic interactions. The phosphonic acids should also fit into the pocket more efficiently, as they are spatially smaller than their ester counterparts.

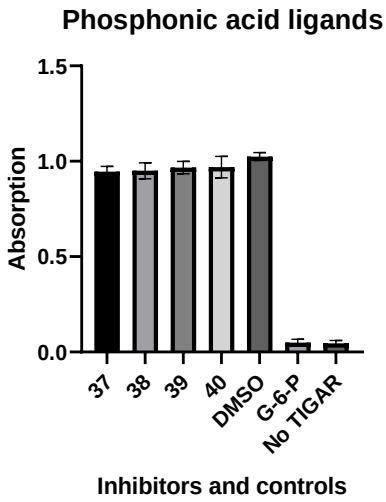

Figure 29: Graph of single point assay results for phosphonic acid compounds.

In summary, a series of phosphonate esters (**23**–**26**, **28**–**30**, **32**, **34** and **36**) and phosphonic acid (**37**–**40**) ligands were screened against TIGAR (200 µM), for initial hit identification. The majority of the ligands proved to be inactive towards the target, with only ligand **24** exhibiting activity (55% inhibition), however, the binding mode for this analogue was proposed to be undesirably covalent in nature.

4.1.2. Amido acid series

4.1.1.1. Design hypothesis

Literature searches on phosphatase inhibitors indicated that carboxylic acids could also act as effective phosphate mimetics,[59-60] presumably because they also have an acidic proton (pKa ~5) that would afford compounds with a net negative charge. Based on this knowledge, and combined with our understanding of the natural substrates, a new scaffold **41** was proposed (Figure 30).

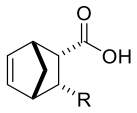

41

Figure 30: General structure of carboxylic acid-based compounds.

The compounds based around this core structure would contain a negative charge generated from the carboxylic acid and an anchor in the form of a bicyclic ring to hold the functional groups in place. These two features are analogous to the role of the functional groups in the endogenous ligands. It was proposed that the R group could be an amide, as it is a functional group with the potential to act as both a hydrogen bond donor (HBD) and a hydrogen bond acceptor (HBA). Placing an amide in this position would also make the scaffold amenable to structure activity relationship (SAR) studies as a variety of amines could be used in the synthesis.

4.1.1.2. Synthetic route

It was determined that these compounds could be prepared through Diels-Alder cycloaddition followed by nucleophilic ring-opening reactions on the appropriate cyclic anhydride.[61-62] The synthetic route for these compounds can be viewed in **Scheme 6**. Initially, cyclopentadiene **43** was formed by cracking di-cyclopentadiene **42**.[63] This was reacted with maleic anhydride in a Diels-Alder cycloaddition, to afford **44** (93%) in a high yield without the need for further purification.[64] At this stage, **44** was treated with an equimolar amount of a variety of amines, in a nucleophilic addition reaction, to afford amido acid derivatives **45**–**50** (65–95%) upon simple filtration and washing.[61-62] Endo anhydride **44** was also reacted with water (H_2O) to produce di-acid **51** (95%).[65]

Scheme 6: Synthetic route for amido acid series and dicarboxylic acid 51.

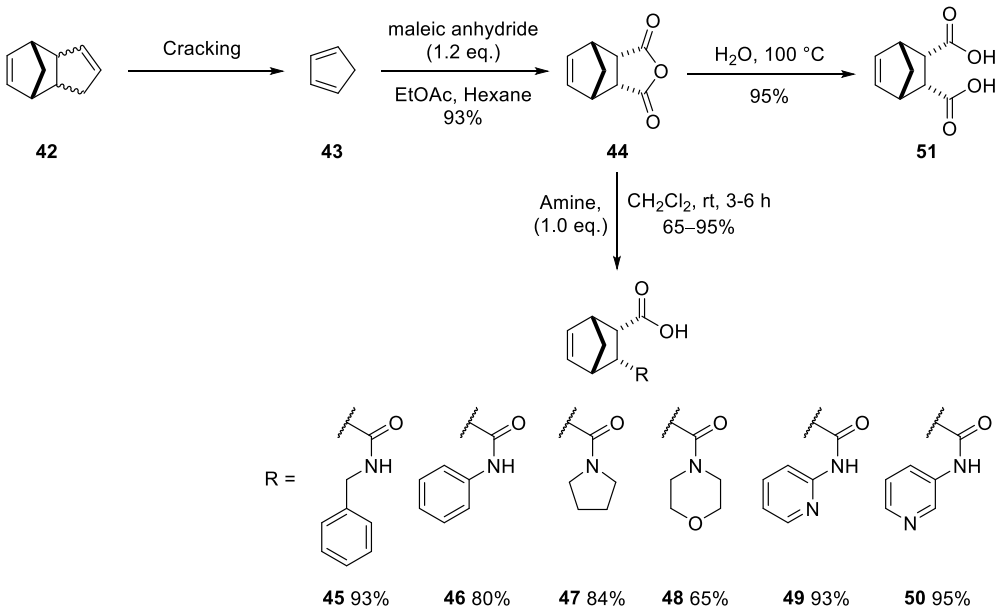

4.1.1.3. Biological evaluation

The compounds in this series were also screened at a single point concentration of 200 μM to maintain consistency within the *in vitro* assay. Screening results for the amido acids (**45**–**50**), endo anhydride **44** and di-acid **51** of this series are presented in **Figure 31**.

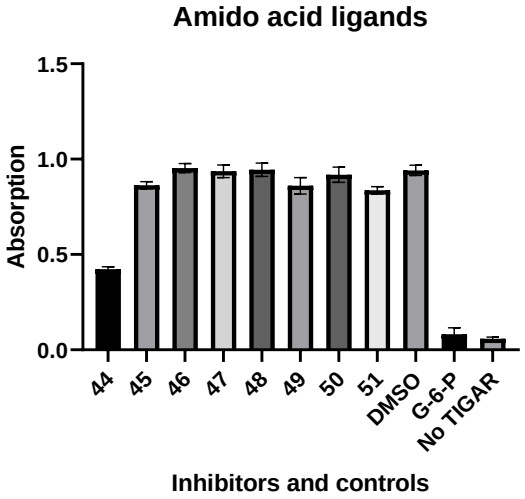

Figure 31: Graph of single point assay results for amido acid compounds.

Once again, the majority of the ligands, including all of the amido acids (**45**–**50**) and the di-acid **51**, displayed no activity against the TIGAR enzyme. The reason for this inactivity was again proposed to be potentially due, to the sub-optimal orientation of

the amide/carboxylic acid substituents, in relation to the bicyclic core. Endo anhydride **44** displayed approximately 59% inhibition. However, upon further assessment of the structure of **44** (Figure 32), a similar scenario to that observed for compound **24** from the phosphonate ester series, appeared to be occurring. Again, the amido acid type ligands should theoretically be more efficient binders, due to their exposed negative charge, which compound **44** does not possess. Therefore, it was proposed that **44** was binding irreversibly and non-specifically to the active site of the enzyme, which was unfavourable as a reversible non-covalent binder was sought.

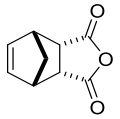

44

Figure 32: Structure of ligand 44.

In summary, the ligands synthesised on this series (**45**–**51**) proved to be inactive towards TIGAR when tested at a concentration of 200 μM. Only intermediate **44** demonstrated noticeable inhibition levels (59%), however, this was again proposed to be occurring, through a covalent modification of a nucleophilic residue within the active site of TIGAR.

4.1.2. Squaric acid series

4.1.2.1. Design hypothesis

While the first two series of compounds were being synthesised, a third series was also examined as a potential orthosteric ligand. Further literature studies had suggested that squaric acid was a bioisostere of the phosphate group due to its similar spatial boundaries and electronic properties.[53, 66] It also had a pKa of approximately 1.5, ensuring a net negative charge would be present on any derivatives. In 2004 Xie *et al*. had shown that squaric acid amide derivatives acted as inhibitors towards some tyrosine phosphatases, known as PTPases.[67] Based on all the above information, some squaric acid amide derivatives were synthesised, which were established around the structure **52** shown in **Figure 33**.

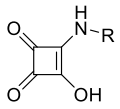

52

Figure 33: General structure for squaric acid based derivatives.

4.1.2.2. Synthetic route

It was possible to synthesise the squaric acid derivatives in a simple one-step procedure (Scheme 7). Squaric acid **53** and the appropriate amines were heated at reflux in H_2O. Upon cooling of the reaction mixtures, the corresponding amides (**54**–**57**) (70–95%) precipitated from solution and were isolated by filtration, followed by flash column chromatography.[67]

Scheme 7: Synthetic route for squaric acid series.

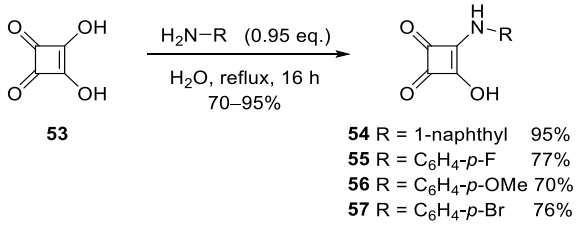

4.1.2.3. Biological evaluation

The compounds in this series were once again screened at a single point concentration of 200 μM for consistency within the *in vitro* assay. Screening results for the squaric acid derivatives (**54**–**57**) of this series are presented in **Figure 34**.

Three of the four synthesised derivatives (**55**–**57**) displayed no activity against the target, at the chosen concentration. The 1-naphthyl derivative (**54**) displayed minimal activity of approximately 25% inhibition, which indicated that the part of the binding site where the naphthyl group positioned itself, was hydrophobic in nature. This was a positive result but ultimately deemed insufficient to launch an SAR study on. Consequently, no further investigations have been made to this series, however, there still may be potential to use squaric acid as a head group on alternative building blocks.

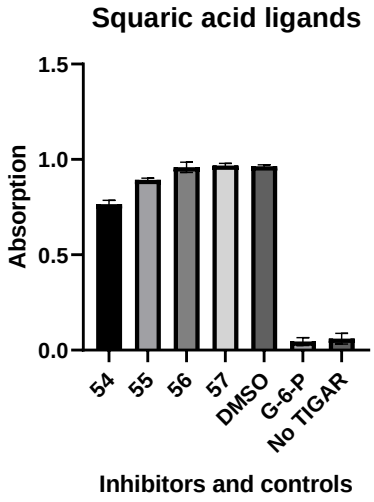

Figure 34: Graph of single point assay results for squaric acid compounds.

4.2. Orthosteric site - 2-amino thiophene scaffold

Designing non-hydrolytic mimics of the natural bisphosphate substrate structures had proven to be unsuccessful in identifying a hit compound for TIGAR, from which to perform SAR studies. Hit identification using high-throughput screening methods was unavailable on this project and current mimetic designs were only exploring a tiny fragment of the vast chemical pool. After three different series of compounds failed to provide a starting point, a decision was made to adopt a new strategy of selecting a chemical scaffold, which already demonstrated weak potency towards a phosphatase enzyme, so that investigations could permit an increase in potency and selectivity towards TIGAR. Once identified, this ligand could then be screened against TIGAR and if reasonable binding affinity was achieved, this hit compound would serve as the chemical starting point for SAR studies and the development of a chemical probe for TIGAR.

Extensive literature searches identified ligand **58** (Figure 35), a weakly potent inhibitor of the phosphatase PTP1B (100% inhibition 100 μM, 3.4% inhibition 10 μM), as an ideal fit for the previously set parameters.[68] Compound **58** was prepared and screened against TIGAR and was found to exhibit an IC_{50} value of 65 μM, which was deemed a reasonable potency for a hit compound.

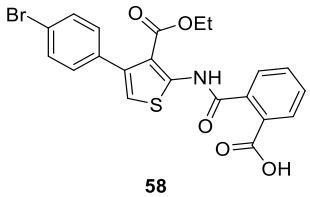

58

TIGAR IC_{50} 65 μM

Figure 35: Hit compound 58.

Development of a chemical probe for TIGAR, based upon the structure of **58**, would have to involve modification of the structure in order to increase affinity for TIGAR whilst limiting the affinity for the previous target, PTP1B. It was hypothesised that progressing in this direction would drive selectivity against the entire tyrosine phosphatase superfamily, resulting in the generation of a more efficient tool compound. Furthermore, as there is a significant volume of biological data associated with PTP1B inhibition,[69-73] selectivity over this phosphatase was deemed crucial for future cellular studies within this project.

To hypothesise whether the ability to forge selectivity for TIGAR over PTP1B was feasible, a comparison of the apo protein X-ray structures was performed. Multiple contrasts in the make-up of the orthosteric binding sites between each phosphatase were identified (Figure 36). Despite the fact that both phosphatases are comprised of a nucleophilic residue for the dephosphorylation process (PTP1B = Cys215, TIGAR = His11 green, Figure 36), the phosphate binding pocket in which they are positioned is significantly narrower within PTP1B compared to the more open equivalent pocket within the TIGAR site. This was due to the fact that the PTP1B site contains a phenylalanine 'cap' (Phe182, magenta, Figure 36) that appears orientated over the phosphate binding pocket of the active site, causing this limited space. In contrast, the active site of TIGAR has no obvious amino acid restricting access to the phosphate binding site. Another key difference between the two proteins was the electronics of the stabilising residues. PTP1B possesses a higher number of polar units (Ser216 & Tyr46, red, Figure 36) compared to basic ones (Arg221, blue Figure 36), whereas the equivalent residues for TIGAR are all basic in nature (Arg10, Arg61 & His186, blue, Figure 36). Therefore, the electronics of the phosphate binding pockets are significantly different across the two enzymes, a property that was highly likely to impact the binding affinity of any prospective ligand. Finally, from contrasting the protein surface of both proteins (Figure 36, C & D), there was a

strikingly obvious variation in the shape of the active site, between the two proteins. PTP1B appears to contain a shallow binding pocket compared to the deeper hydrophobic pocket of TIGAR. Collectively, this information suggested a realistic chance of naturally driving selectivity away from PTP1B and in favour of TIGAR, by simply growing the hit compound along the appropriate vectors for shape complementarity with the orthosteric site of TIGAR.

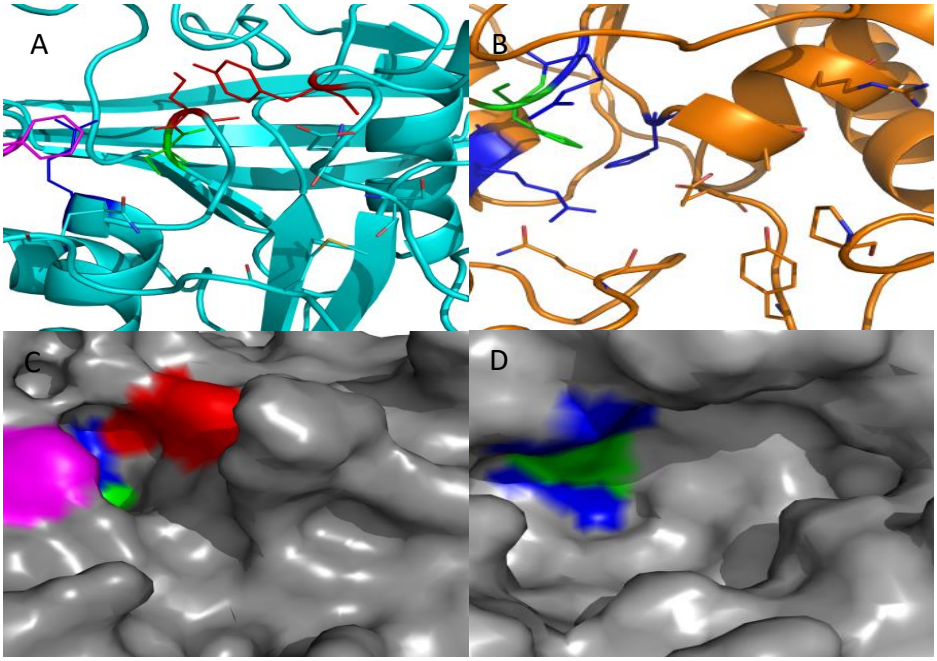

Figure 36: X-ray crystal structures of (A) PTP1B orthosteric site (cyan) (PDB: 1BZJ); (B) TIGAR orthosteric site (orange) (PDB: 3DCY); (C) PTP1B surface and (D) TIGAR surface. In both, the nucleophilic residue is coloured green (PTP1B = Cys215 / TIGAR = His11) and the basic/polar stabilising residues are coloured blue and red, respectively. (PTP1B = Ser216 & Arg221 / TIGAR = Arg10, Arg61 & His186). PTP1B lipophilic 'cap' group (Phe182) is coloured magenta.

Using the previously published TIGAR crystal structure (PDB: 3DCY), **58** was docked into the orthosteric binding site of TIGAR (Figure 37, A & B) *via* Gold molecular modelling software. A hypothetical binding mode from which to base SAR studies was then proposed through rationalisation of the mode of molecular recognition. Activity of **58** towards TIGAR can be rationalised from the computational model (Figure 37).

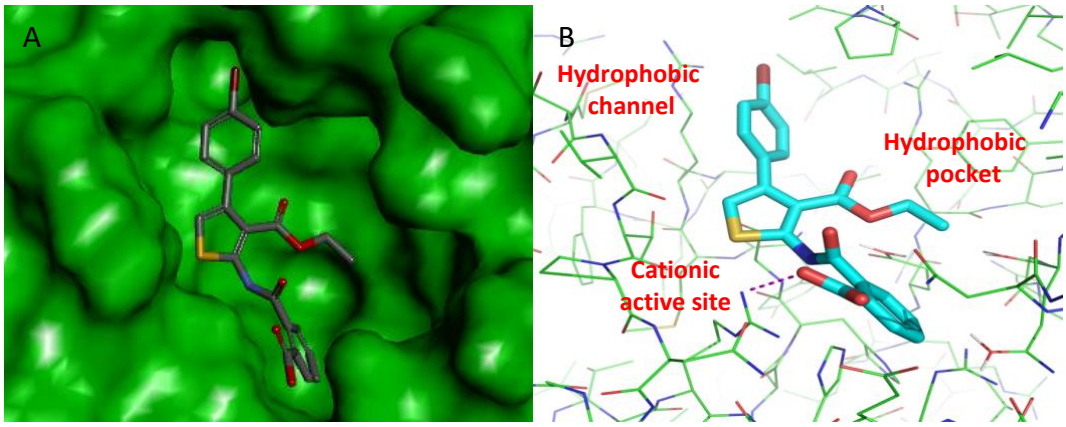

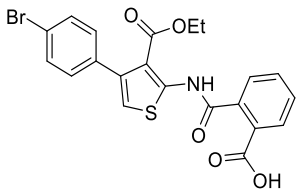

58

IC_{50} = 65 μM

Figure 37: Binding mode of 58 docked in TIGAR. (A) Surface representation of ligand 58 (grey) binding mode in TIGAR (green). (B) Amino acid level model of 58 (cyan) binding mode with key parts of the TIGAR active site labelled in red. Key electrostatic interaction is highlighted by magenta dashed line.

The anionic carboxylic acid moiety of **58** formed a key electrostatic interaction with Arg10 (Figure 37, B dashed magenta line), one of the conserved catalytic arginine residues. The carboxylate group appears to be acting as a direct isostere for the substrate phosphate functionality; providing stability and anchoring the ligand within the cationic binding site of TIGAR. The phenyl linker between the amide and carboxylate functionalities orientated itself deeper in the cavity, within a pocket generated by Gln23, Asn17 and Thr14. The 2-amino thiophene core adopted a position at the centre of the active site, establishing shape complementarity with the curve of the binding pocket, and principally increasing binding affinity through hydrophobic interactions. This core scaffold provided a platform for the remaining substituents to grow along desirable vectors for enhanced potency and selectivity. The lipophilic phenyl bromide segment extended into an open hydrophobic channel produced by Ala189, Val116 and Pro115. The Valine and Proline residues presented themselves in the form of a lipophilic 'shelf', against which the aromatic ring system packed for a favourable interaction. The 3-ethyl ester substituent situated itself in a small hydrophobic pocket formed by Leu100, and Ile22 on one side and Tyr92 on the other.

With compound **58** as a promising hit for the series, fundamental learnings from the initial docking studies were used to influence our design strategy moving forward. With the hypothesis that the optimisation of interactions in the hydrophobic pocket and further extension into the lipophilic tunnel would lead to increased potency and selectivity, modifications to hit **58** were explored.

4.2.1. SAR outline

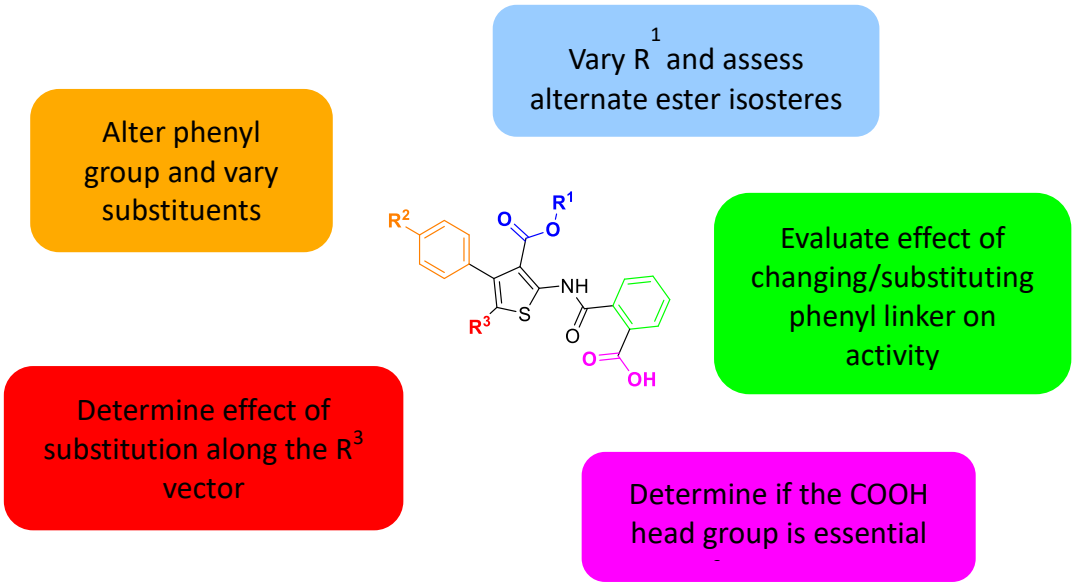

Figure 38: SAR outline for 2-amino thiophene scaffold.

The highly substituted 2-amino thiophene scaffold of **58** was an ideal platform for performing an in-depth SAR study, as this core is extremely amenable to array chemistry. Opportunities for variability within a chemical route are a greatly desired characteristic within tool compound development, and this particular framework has already produced desirable outcomes within the medicinal chemistry arena to date.[74-77] **Figure 38** details a generic chemical scaffold incorporating the 2-amino thiophene core, which outlines the key structural areas that we chose to interrogate during the SAR investigations. The 2-amino thiophene core was left unchanged throughout the SAR procedure as, according to the model, the substituents of the thiophene unit were optimally positioned for growth along the appropriate vectors of the TIGAR active site.

Key structural changes that were highlighted within the initial SAR outline, included variation in the R^1 appendage of the 3-carboxylate group (Figure 38, blue), to explore

interactions within the hydrophobic pocket where this group is positioned. From a medicinal chemistry perspective, it was proposed that the ester moiety may provide metabolic issues out with the *in vitro* assay,[78-80] so it was proposed to exchange this group for the more chemically stable amide isostere. Evaluation of the effect that substituting or altering the phenyl linker (Figure 38, green) would have on potency, was also proposed. Determining how significant the anionic nature of the carboxylic acid head group (Figure 38, magenta) was for binding affinity, by altering the head group, was hypothesised to be a potentially crucial point on the SAR study. The model portrayed a shallow pocket of space surrounding the R^3 position (Figure 38, red) and so, substitution along this vector was thought to be important in defining the spatial capacity of the binding site. Finally, growth into the hydrophobic channel *via* substitution at the R^2 position (Figure 38, orange) was proposed to be the area with the best chance for driving potency and selectivity towards TIGAR.

4.2.1.1. Multicomponent Gewald reaction

Several synthetic routes were developed to enable the synthesis of the diverse range of compounds, required for the SAR studies on this project. However, one commonality between all of the routes was that they incorporated a multicomponent coupling process, known as the Gewald reaction, for the generation of the 2-amino thiophene core. Multicomponent Gewald reactions are a well-established method for preparing this heavily substituted heterocyclic core (Scheme 8).[81-84]

Scheme 8: Multicomponent Gewald Reaction.

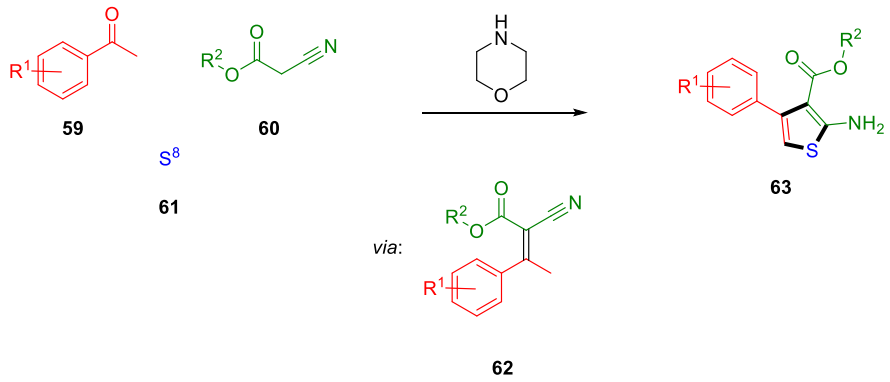

The multicomponent process involves a basic heterocyclic condensation protocol as it incorporates a ketone derivative **59** (an aldehyde may also be used to give an alternative substitution pattern) and a cyanoacetate derivative **60**, which interact in

the first step of the transformation *via* a Knoevenagel condensation. Elemental sulfur **61** then reacts with the condensation intermediate **62** to produce the 2-amino thiophene product **63** in a process that is driven by the formation of aromaticity.

Gewald reactions, and multicomponent reactions in general, offer a number of beneficial features, particularly when they are being used within an SAR programme[85-91]:

- 3 new bonds formed within a single step - difficult to do in a sequential manner.
- Generates high levels of structural diversity and molecular complexity.
- Amenable to array chemistry.
- Pendant groups produced from the reaction can undergo further functionalisation.
- Enables growth along multiple vectors.
- Efficient means of bulking out/streamlining an SAR study.

From a medicinal chemistry viewpoint, these benefits made the Gewald reaction the perfect transformation around which to base our synthetic route design, as it provided an efficient overall process to perform investigations around. The hope was that data generation would be accelerated, allowing the SAR investigations to be as extensive as possible within the time constraints of the project.

4.2.2. Ester derivative series

4.2.2.1. Design hypothesis

Initial investigations within the SAR study revolved around a variation in the R^1 appendage of the 3-carboxylate group, with the generic scaffold **64** for the series depicted in **Figure 39**.[68] Minimal alterations to the R^2 group were made at this stage, to assess how differing substitution at this position affected the binding of the R^1 group within the hydrophobic pocket.

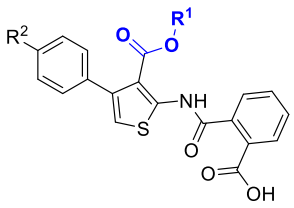

64

Figure 39: General structure of ester derivatives.

This series of compounds retained the net negative charge due to the presence of the carboxylic acid head group, allowing electrostatic interactions within the highly positively charged active site to be adopted. It was hypothesised that variation of the R^1 appendage would enable the extent of lipophilic interactions and the pocket depth to be effectively measured.

4.2.2.2. Synthetic route

The established synthetic route for the synthesis of the ester derivatives with general structure **64**, was a 2–3 step procedure, outlined in **Scheme 9**. The first reaction used the previously described multicomponent Gewald chemistry to react ketones **65** and **66** with the appropriate cyano acetate **67**, and elemental sulfur.[68]

The literature originally suggested that the Gewald reactions could be performed under microwave irradiation (100 °C, 10 min), in the presence of basic alumina (Al_2O_3) and in the absence of solvent.[68, 92] However, these conditions provided very poor conversion and resulted in the formation of numerous side-products (e.g. Knoevenagel aldol intermediates) according to ^{1}H NMR spectroscopy, even when reaction times were lengthened and the temperature was varied. A new procedure was implemented which involved using morpholine as a base and performing the reaction thermally, in the absence of solvent. Under these conditions, products **68**–**79** were easily isolated in 30–50% yields, after purification by flash column chromatography. Amino thiophenes **68**–**79** were then reacted with an equimolar amount of phthalic anhydride, to afford the corresponding thiophene amido acids (**58**, **80**–**90**, 60–86%) upon purification by flash column chromatography.[68] The synthesis of all biphenyl derivatives was originally carried out in 3-steps with the final step being a palladium-catalysed cross-coupling with phenyl boronic acid. However, this reaction proved very low yielding (average < 10%) and so an alternative strategy was sought, which resulted in the direct use of 4-acetylbiphenyl

66 in the Gewald reaction, followed by subsequent reaction with phthalic anhydride. Not only was this optimisation higher yielding, it also reduced the number of steps from 3 to 2. Hydrolysis of thiophene amido acids **58** and **81** was performed with 2.0 M sodium hydroxide (NaOH), to yield di-acid compounds **91** (71%) and **92** (76%) in good yields, after purification *via* flash column chromatography.[93]

Scheme 9: Synthetic route for 2-amino thiophene ester derivative series.

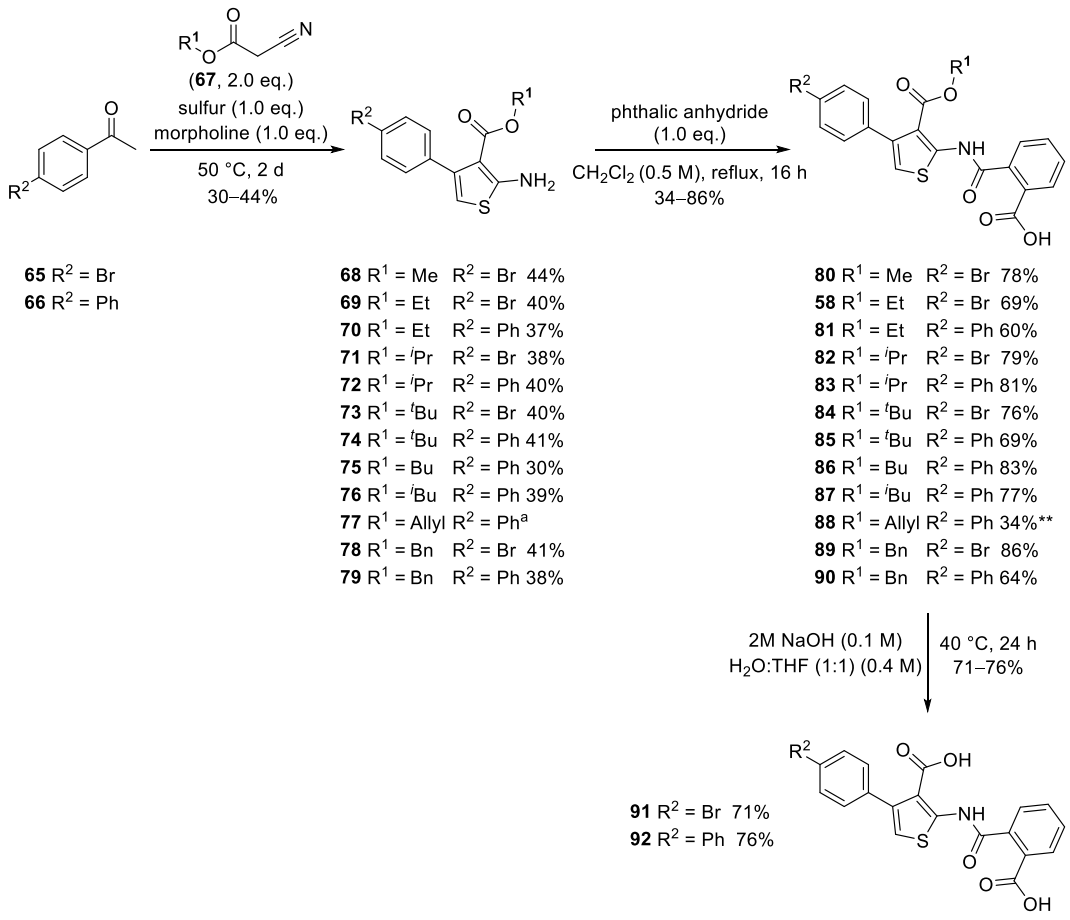

65 R^2 = Br
66 R^2 = Ph

68 R^1 = Me R^2 = Br 44%
69 R^1 = Et R^2 = Br 40%
70 R^1 = Et R^2 = Ph 37%
71 R^1 = ^{i}Pr R^2 = Br 38%
72 R^1 = ^{i}Pr R^2 = Ph 40%
73 R^1 = ^{t}Bu R^2 = Br 40%
74 R^1 = ^{t}Bu R^2 = Ph 41%
75 R^1 = Bu R^2 = Ph 30%
76 R^1 = ^{i}Bu R^2 = Ph 39%
77 R^1 = Allyl R^2 = Ph[a]
78 R^1 = Bn R^2 = Br 41%
79 R^1 = Bn R^2 = Ph 38%

80 R^1 = Me R^2 = Br 78%
58 R^1 = Et R^2 = Br 69%
81 R^1 = Et R^2 = Ph 60%
82 R^1 = ^{i}Pr R^2 = Br 79%
83 R^1 = ^{i}Pr R^2 = Ph 81%
84 R^1 = ^{t}Bu R^2 = Br 76%
85 R^1 = ^{t}Bu R^2 = Ph 69%
86 R^1 = Bu R^2 = Ph 83%
87 R^1 = ^{i}Bu R^2 = Ph 77%
88 R^1 = Allyl R^2 = Ph 34%**
89 R^1 = Bn R^2 = Br 86%
90 R^1 = Bn R^2 = Ph 64%

91 R^2 = Br 71%
92 R^2 = Ph 76%

[a] compound partially purified.

4.2.2.3. Biological evaluation

At the beginning of this series, in order to identify a hit compound for TIGAR, two compounds (**69** and **58**) were initially screened in a single point assay at 200 μM, to assess whether they demonstrated sufficient activity against the TIGAR enzyme. The results of this initial screen are shown in **Figure 40**. To our great pleasure, compound **58** (already discussed in Section 4.2. as our hit compound) displayed strong activity against the enzyme at this concentration (~85% inhibition). Compound **69** proved to be inactive against the target, which reinforced the original hypothesis that a net

negative charge would be required by the compound to achieve activity in the positively charged active site of TIGAR. When comparing the two structures of **69** and **58** (Figure 41), this observation can be rationalised due to the presence of the anionic carboxylic acid moiety in **58**, which has a high probability of forming additional electrostatic interactions within the active site of the target, compared to the neutral amine functionality of **69**.

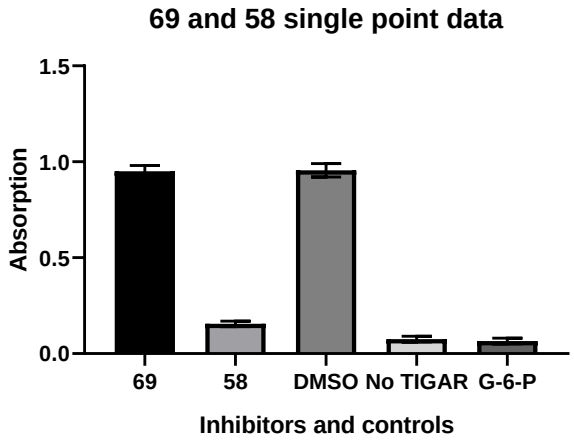

Figure 40: Graph of single point assay results for initial thiophene amido acid compounds.

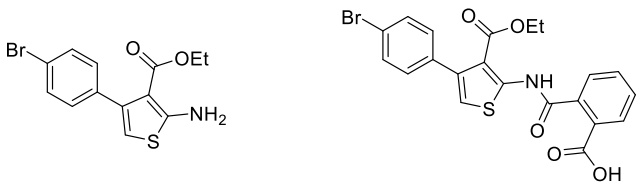

69 **58**

Figure 41: Structures of ligands 69 and 58.

A compound (**58**) had now been synthesised and screened, which displayed reasonable activity towards the target and notably, by consideration of the structure, was thought to be binding in a reversible manner. There was now a need to quantify the level of this inhibition, and confirm hit compound identification, by performing a titration curve across a concentration range and obtaining an IC_{50} value (Figure 42). All generated IC_{50} values on this project are based on 3 experiments (n=3). The hillslope value (2.3) for the curve was higher than the standard desired value of ~1, possibly due to the IC_{50} value for **58** (65 μM) being high. However, it was still decided that an SAR study would be carried out, based around hit compound **58**. IC_{50}

values for all future inhibitors on the series were calculated from the same style of graph, as the one shown in **Figure 42**, using GraphPad Prism software.

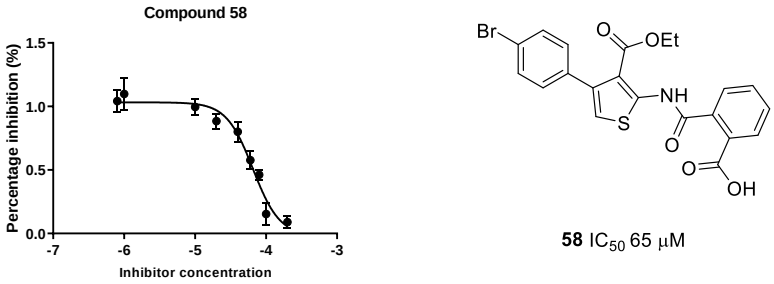

Figure 42: Dose response curve for compound 58.

Upon the discovery of hit compound **58**, SAR investigations were subsequently initiated through the generation of dose response curves, for a series of ester derivatives, so that an interrogation of the TIGAR active site could begin. Ester series assay results for compound **58** and derivatives **80**–**92** are detailed in **Table 2**.

Table 2: IC_{50} values for compounds 58 and 80–92. Compound 83 IC_{50} curve.

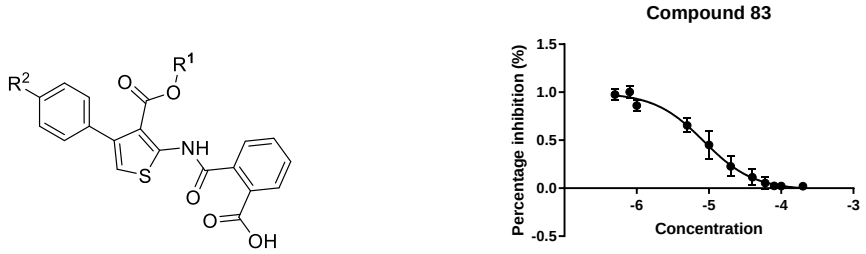

Compound	R^1	R^2	IC_{50} (µM)[a]	Compound	R^1	R^2	IC_{50} (µM)[a]
80	Me	Br	90 ± 28	**86**	Bu	Ph	2.8 ± 1.9
58	Et	Br	65 ± 5.4	**87**	^{i}Bu	Ph	1.5 ± 0.4
81	Et	Ph	48 ± 4.0	**88**	Allyl	Ph	7.0 ± 0.3
82	^{i}Pr	Br	27 ± 1.1	**89**	Bn	Br	8.0 ± 0.3
83	^{i}Pr	Ph	8.5 ± 0.5	**90**	Bn	Ph	0.92 ± 0.08
84	^{t}Bu	Br	20 ± 0.8	**91**	H	Br	> 100
85	^{t}Bu	Ph	6.8 ± 0.4	**92**	H	Ph	> 100

[a] IC_{50} calculated as n=3

The first key piece of information to be drawn from **Table 2** was that exchanging the R^2 substituent from a bromide to a phenyl ring, consistently produced a favourable increase in potency towards TIGAR (e.g. **58** 65 µM vs **81** 48 µM or **82** 27 µM vs

83 8.5 μM). With respect to the R^1 substituents, shortening the aliphatic chain from the ethyl of hit compound **58** (65 μM) to a methyl **80 (**90 μM), resulted in a loss of potency. Branching of the aliphatic chain to an isopropyl (**82** 27 μM & **83** 8.5 μM) or a *tert*-butyl functionality (**84** 20 μM & **85** 6.8 μM), delivered a consistent increase in potency compared to the parent ethyl ligands (**58** 65 μM & **81** 48 μM). A further extension of chain length *via* straight-chain butyl **86** (2.8 μM), or the branched isobutyl **87 (**1.5 μM), led to a further small improvement in potency. These numbers suggested that a ceiling exists for the binding affinity generated by aliphatic substituents and that branched groups are generally better than their equivalent straight-chain isomers. Allyl substituent **88** (7.0 μM) portrayed a negligible variance in binding affinity compared to isopropyl **83** (8.5 μM) and *tert*-butyl **85** (6.8 μM), suggesting that no additional benefits were gained from the alkene moiety within the hydrophobic pocket. A marked increase in potency was observed when incorporating a benzyl group (**89** 8.0 μM & **90** 0.92 μM) into the R^1 position. This highlighted that the hydrophobic pocket had the spatial capacity to accept a 6-membered aromatic ring substituent and that the increased lipophilicity of this group had a favourable effect on binding affinity. When R^1 = H (**91** > 100 μM & **92** > 100 μM), the dramatic change in the electronics of the carboxylic acid functionality, compared to that of the ester species, resulted in a complete loss of potency towards TIGAR (IC_{50} > 100 μM). The computational model indicated that the R^1 group was positioned within a hydrophobic pocket and so, this result reinforced the model, as the carboxylic acid moiety would be expected to exhibit a multitude of unfavourable interactions within this type of environment.

The docking studies described in **Figure 43** outlined the potential alternative binding modes that the aliphatic substituents (**83**) and the benzyl esters (**90**) may adopt, within the small hydrophobic pocket. Isopropyl **83** (Figure 43, A and C) was shown to reside in the centre of the pocket and form lipophilic interactions with multiple residues. In contrast, the benzyl ester of **90** (Figure 43, B and D) was highlighted as being too large to bind in the centre of the pocket. Instead, the benzyl motif was proposed to pack directly beneath the nearby Leu100 residue. This difference in binding mode could account for the enhanced potency of ligands containing the benzyl substituent.

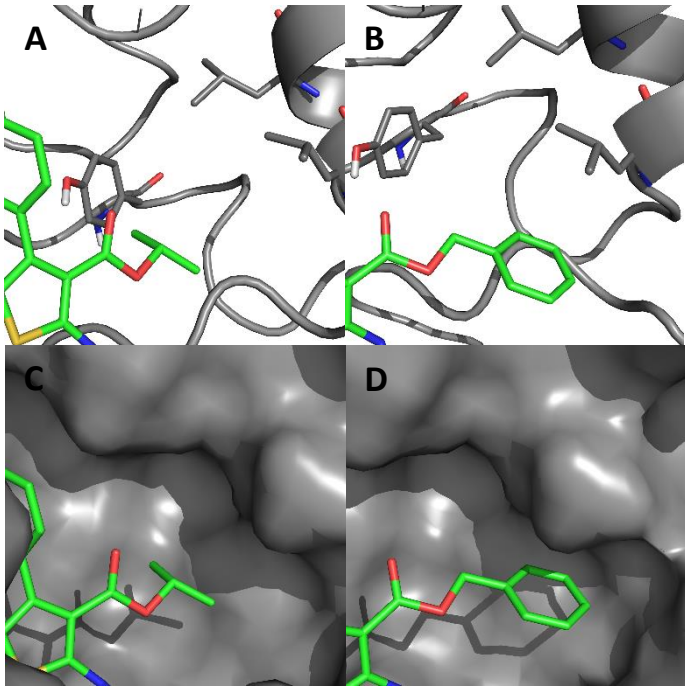

Figure 43: **Ligands 83 and 90 docked in the active site of TIGAR with ester group hydrophobic pocket highlighted. A –amino acid representation for isopropyl ester of 83; B –amino acid representation benzyl ester of 90; C – surface representation for isopropyl ester of 83; D – surface representation for benzyl ester of 90.**

In summary, this data demonstrates that a parallel exists between the lipophilicity of the R^1 groups and potency. As the Van der Waals radius of the R^1 group increases (**80** IC_{50} 90 μM to **90** IC_{50} 0.92 μM), a simultaneous growth in potency of two full log units is also observed. This conclusion was reinforced by the fact that both carboxylic acid compounds (**91** IC_{50} > 100 μM & **92** IC_{50} > 100 μM) were completely inactive, as they do not complement the hydrophobic nature of the pocket. Even though the benzyl group afforded the largest increase in potency, the decision was made not to further increase the aromatic ring count at this stage. Moving forward, the isopropyl group was selected for the choice of substituent at this position, as this functionality exhibited favourable potency without becoming too lipophilic.

4.2.3. Carboxylic acid head group series

4.2.3.1. Design hypothesis

As previously described within this report, the vast majority of phosphatase inhibitors tend to be comprised of at least one chemical motif that mimics the negatively charged nature of the substrate phosphate group.[26] Sustaining an

electrostatic interaction within the phosphate binding pocket is generally thought to be crucial for affinity towards phosphatase targets. The compounds on this series were designed to specifically probe the carboxylic acid head group, in order to assess how imperative it was for binding affinity. This part of the SAR was also prepared to assess whether the carboxylic acid functionality could be substituted for alternative groups, which still retained acidic properties at physiological pH (7.4). The proposed ligands were designed around scaffold **93** depicted in **Figure 44**, where the biphenyl and the isopropyl ester motifs from compound **83** have been retained.

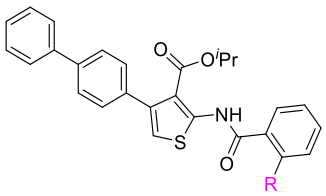

93

Figure 44: General structure of head group derivatives.

4.2.3.2. Synthetic route

Multiple synthetic routes were required for the synthesis of the different head groups on this sub-series; however, they each still incorporated the multicomponent Gewald reaction. It was determined that sulfonic acid **95** could be prepared from intermediate **72** in a single-step process (Scheme 10).

Scheme 10: Synthesis of sulfonic acid derivative 95.

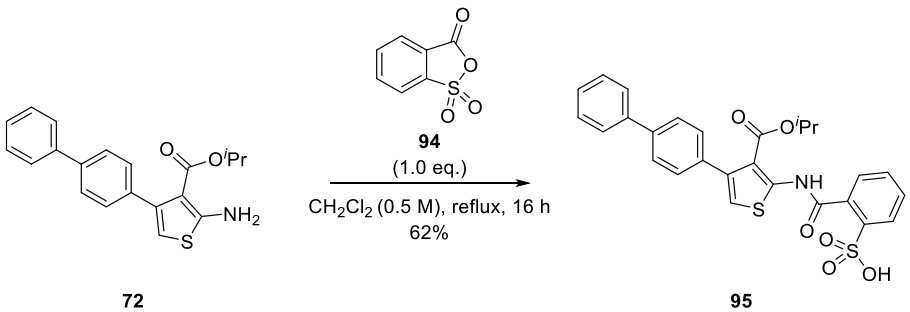

2-Amino thiophene intermediate **72** was reacted with equimolar amounts of 2-sulfobenzoic acid cyclic anhydride **94**, *via* a ring-opening transformation, to afford sulfonic acid derivative **95** in good yield (62%) upon purification by column chromatography. The chemoselectivity of the ring-opening process was proposed to

be due to the π* orbital of the carbonyl functionality being lower in energy, and therefore more available, than the corresponding σ* orbital of the S–O sigma bond.

Alternative head groups included the tetrazole analogues (**99** & **100**), which were synthesised using a convergent synthetic route, that combined products from the Gewald reaction (**71** & **72**) with the chemically tractable tetrazole intermediate **98** (Scheme 11).

Scheme 11: Synthetic route for tetrazole analogues 99 and 100.

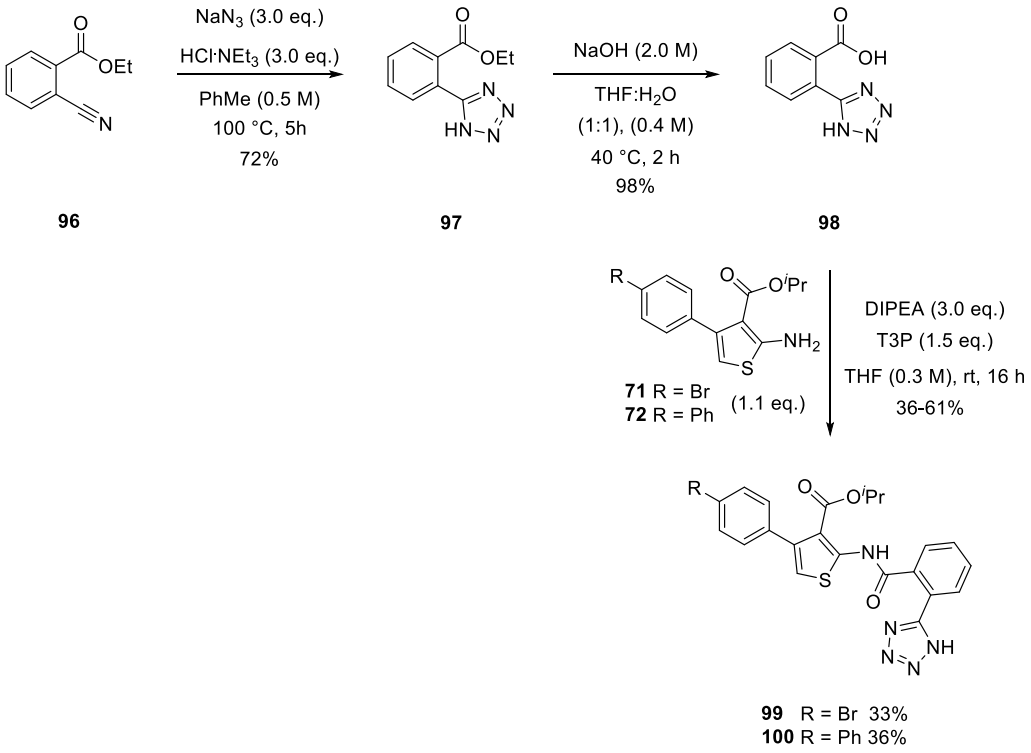

Cyano ester starting material **96** was treated with sodium azide (NaN_3) under reflux conditions to perform a [3+2] cycloaddition that afforded tetrazole ester intermediate **97** in good yield (72%), with no further purification required.[94] Tetrazole ester intermediate **97** was then hydrolysed under basic conditions (2.0 M NaOH) to produce quantitative yields (98%) of acid tetrazole intermediate **98** with no need for further purification. Acid **98** was subsequently coupled with common Gewald products **71** and **72**, using amide coupling conditions involving propyl phosphonic anhydride (T3P) as the activating reagent, to generate amides **99** and **100** in moderate yields (33% and 36%, respectively) after purification *via* column chromatography.[95]

The final compounds to be synthesised within this series were the capped ester head groups **101** and **102**. These ligands were synthesised from previously made compounds **58** and **83**, through one additional synthetic step (Scheme 12).

Scheme 12: Synthesis of capped ester compounds 101 and 102.

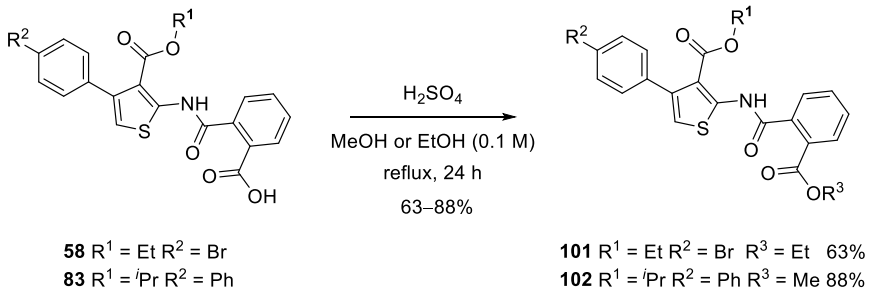

Analogues **58** and **83** were subjected to esterification conditions using EtOH (**58**) or MeOH (**83**), with catalytic amounts of H_2SO_4, to provide esterified head group compounds **101** (63%) and **102** (88%), respectively.[96]

4.2.3.3. Biological evaluation

Dose response curves were generated for all the synthesised final compounds in this series using the *in vitro* assay described in Section 3.0. **Figure 45** details the structures and IC_{50} values of the parent compounds that directly relate to the ligands prepared within this series, for comparison purposes.

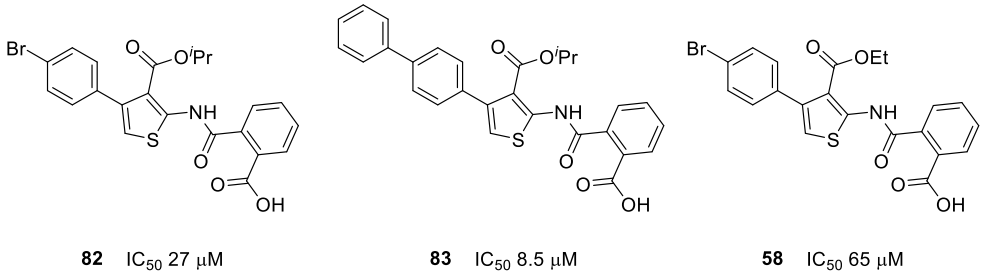

Figure 45: Parent compounds with respective IC_{50} values.

The IC_{50} values for the alternative head group are detailed in **Table 3**. Sulfonic acid analogue **95** had a comparable IC_{50} (10 μM) with that of ligand **83** (8.5 μM), demonstrating that it is possible to substitute the carboxylic acid functionality for an alternative acidic group, whilst maintaining potency. This assessment was reinforced by the IC_{50} values of tetrazole derivatives **99** (22 μM) and **100** (9.7 μM), as these were also similar to the equivalent acid head group analogues **82** (27 μM) and **83**

(8.5 μM). The predicted binding mode of tetrazole **100** is highlighted in **Figure 46**, where key electrostatic interactions with the cationic residues of the active site appear to be retained.

Table 3: IC_{50} values for compounds 95, and 99–102.

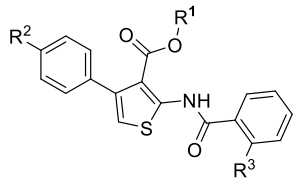

Compound	R^1	R^2	R^3	IC_{50} (μM)[a]
95	^{i}Pr	Ph	SO_2OH	10 ± 2.5
99	^{i}Pr	Br	tetrazole	22 ± 1.8
100	^{i}Pr	Ph	tetrazole	9.7 ± 1.3
101	Et	Br	COOEt	> 100
102	^{i}Pr	Ph	COOMe	> 100

[a] IC_{50} calculated as n=3

Equivalent potencies shown by tetrazoles **99** and **100** were particularly pleasing as this meant that if the carboxylic acid head group displayed metabolic issues (e.g. phase II glucuronidation)[97-98] at a more advanced point in the studies, then the metabolically stable tetrazole could be installed as a bioisosteric replacement, that should maintain equivalent potency.[99-100]

Based on the initial hypothesis for this series that the carboxylic acid head group was vital for activity at the target, it was now important to determine whether a key interaction was being formed by this functional group. When the carboxylic acids of compounds **82** and **83** were esterified (compounds **101** and **102**) to nullify the anionic properties of the head group, this resulted in a complete inactivation of the ligands (**101** > 100 μM, **102** > 100 μM). As the ligands were now neutral species, it had formerly been proposed that **101** and **102** could no longer efficiently interact with the cationic residues of the orthosteric site as no electrostatic interaction should be available. The experimental data strongly indicated that a key interaction had been perturbed, which significantly strengthened the original hypothesis. We now had an on/off switch for the activity of this scaffold through a simple one-step procedure.

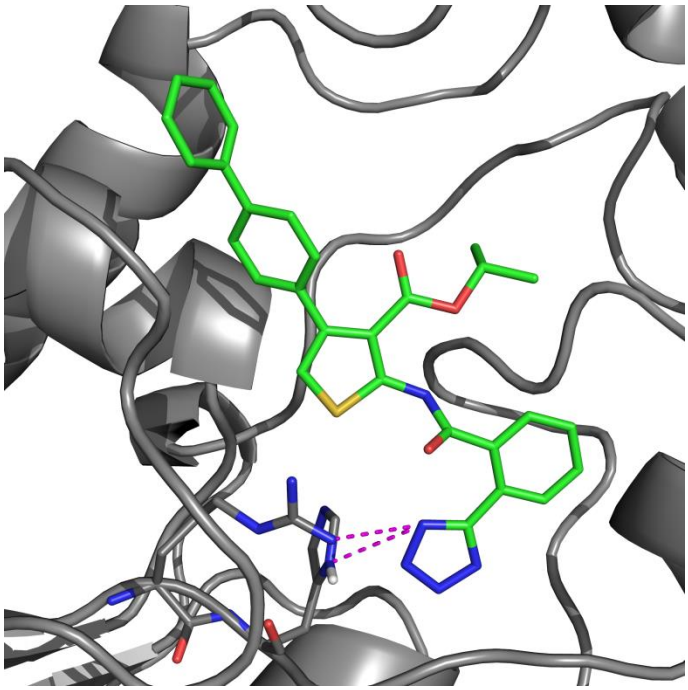

Figure 46: Tetrazole derivative 100 docked in TIGAR active site. Key electrostatic interactions are highlighted by dotted magenta lines.

In summary, the data for this series indicated that the acidic head group was required for activity of the 2-amino thiophene series towards TIGAR. Alterations in the chemical make-up of the head group were possible; however, the substituted functionalities must also exhibit anionic properties at physiological pH for maintenance of potency.

4.2.4. Phenyl linker series

4.2.4.1. Design hypothesis

SAR studies next led to performing an interrogation of the phenyl group which linked the 2-amido group of the thiophene core to the carboxylic acid head group (Figure 47). Structural linkers which differed from the phenyl group were proposed in order to see how an alteration in linker properties and/or a change in the orientation of the acidic head group would affect binding affinity. Substitution of the phenyl linker, with both non-polar and polar substituents, was also proposed, so that the nature of the pocket in which the linker orientates could be further probed.

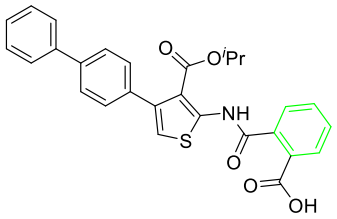

103

Figure 47: General structure of phenyl linker derivatives.

4.2.4.2. Synthetic route

Substituted derivatives of the original phenyl linker were prepared from the common intermediates **71** and **72** with a single additional ring-opening sequence (Scheme 13).

Scheme 13: Synthesis of substituted phenyl linker analogues 104–121.

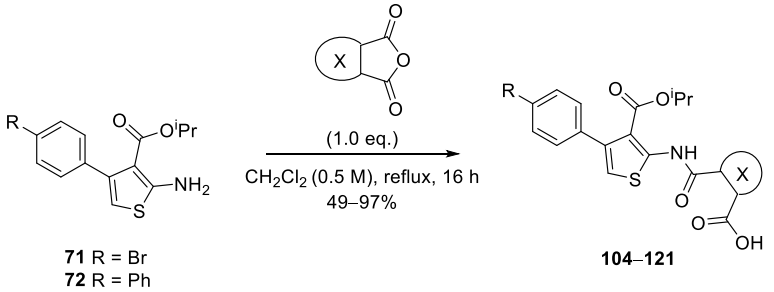

71 R = Br
72 R = Ph

104–**121**

104 R = Br X = 49%
105 R = Ph X = 82%
106 R = Br X = 73%
107 R = Ph X = 80%
108 R = Br X = 54%
109 R = Ph X = 61%
110 R = Br X = 74%
111 R = Ph X = 71%
112 R = Br X = 97%
113 R = Ph X = 88%
114 R = Br X = 89%
115 R = Ph X = 81%
116 R = Br X = 68%
117 R = Ph X = 88%
118 R = Br X = 92%
119 R = Ph X = 65%
120 R = Br X = 93%
121 R = Ph X = 88%

Intermediates **71** and **72** were reacted with a range of substituted anhydrides, under conditions developed previously (Scheme 9), to afford compounds **104**–**121** in moderate to excellent yields (49–97%). This bulked out the SAR studies with an array of phenyl linker compounds (**104**–**121**), substituted with a variety of chemical motifs that exhibited different properties. Any unsymmetrical anhydrides used for the transformation, produced an inseparable mixture of regioisomers (**104**–**117** - indicated by dashed line) after purification by column chromatography. After isolation, a decision was made to submit these mixtures for testing, with the proposal that if any of the samples proved to be particularly potent, then they would receive further scrutiny with regards to the separation of their regioisomers.

An additional sub-series of analogues (**122**–**125**) that substituted the phenyl group for alternative linker functionalities, were also prepared from common intermediate **72**, by reacting this intermediate with alternative anhydrides (Scheme 14).

Scheme 14: Synthesis of alternative linkers 122–125.

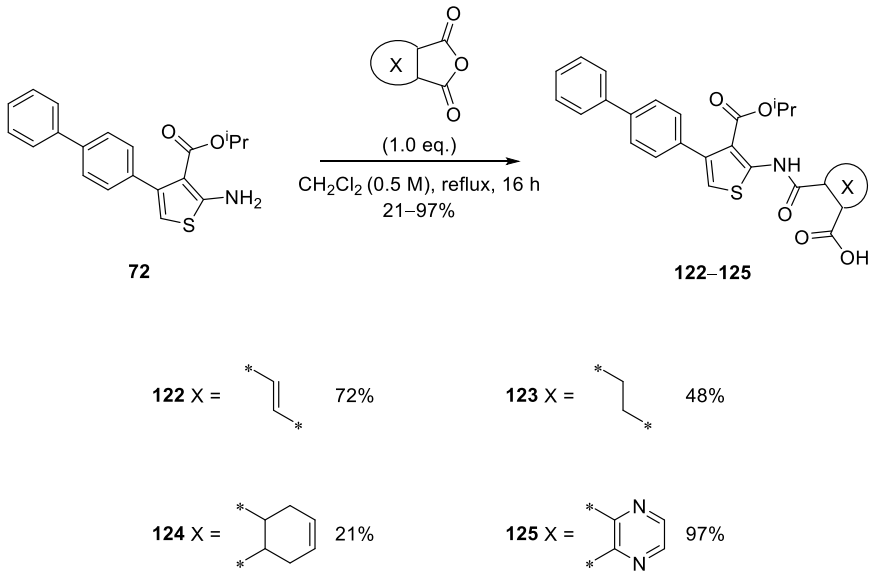

Intermediate **72** was treated with varying anhydrides to produce carboxylic acid compounds **122**–**125** in low to excellent yields (21–97%). The particularly high yield (97%) for pyrazine derivative **125** was attributed to the significantly increased electrophilicity of the carbonyl groups, due to the strong inductive effect of the fused pyrazine ring system. The lower yields associated with anhydrides **123** and **124** (48% and 21%, respectively) were thought to be due to the reduced electrophilicity of the anhydride carbonyls, and both in fact required an additional equivalent of NEt_3 and

catalytic amounts of 4-dimethylaminopyridine, for the transformation to proceed in satisfactory yields. The ^{1}H NMR spectra for compound **122** detailed a 13 Hz coupling constant for the alkene protons, which suggested that a *trans* isomer had formed. The *cis* isomer would probably be expected from the starting cyclic anhydride, however, isomerisation to the thermodynamically more stable *trans* isomer could have occurred under the reaction conditions, upon ring-opening.[101]

4.2.4.3. Biological evaluation

Figure 48 depicts the structures and IC_{50} values of the parent compounds that directly relate to the ligands prepared in this series, for comparison purposes.

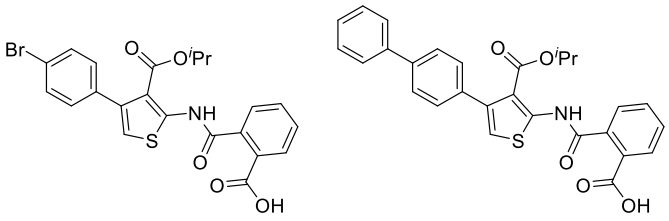

82 IC_{50} 27 μM **83** IC_{50} 8.5 μM

Figure 48: Parent compounds with respective IC_{50} values.

IC_{50} values for substituted phenyl linker ligands **104**–**121** are detailed in **Table 4**.

In comparison to the two parent compounds (**82** IC_{50} 27 μM and **83** 8.5 μM) that contain the original unsubstituted phenyl linker, the addition of a polar moiety (compounds **104** 32 μM, **105** 23 μM, **108** > 60 μM and **109** 34 μM) resulted in a universal decrease in potency. Compound **108** proved to be particularly detrimental to activity as this ligand proved to be completely inactive towards the target, highlighting the lack of available polar interactions and/or space in this area of the enzyme. Functionalisation with a charged species such as a carboxylic acid motif (compounds **106** > 60 μM and **107** > 60 μM) proved to be unfavourable, as these ligands were also both inactive, further demonstrating the non-polar nature of this section of the binding site. Mono-substituted hydrophobic substituents fared better as the 3- and 6-chloro regioisomers (compounds **110** 17 μM and **111** 7.8 μM) gave negligible increases in potency. However, 4- and 5-substituted regioisomeric mixtures of hydrophobic groups proved to be generally better as the equivalent chlorides (compounds **114** 14 μM and **115** 1.2 μM) produced more noticeable

improvements in potency. This assessment was reinforced as supplementary lipophilic 4- and 5-substituted regioisomer based ligands (**112** 21 μM, **113** 7.4 μM, **116** 16 μM and **117** 1.1 μM) also enhanced binding affinity.

Table 4: IC_{50} values for phenyl linker compounds 104–121.

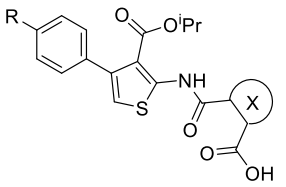

Comp.	R	X	IC_{50} (μM)[a]	Comp.	R	X	IC_{50} (μM)[a]	Comp.	R	X	IC_{50} (μM)[a]
104	Br	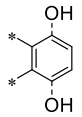	32 ± 4.2	**105**	Ph	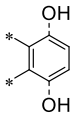	23 ± 1.6	**106**	Br	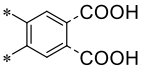	> 60
107	Ph	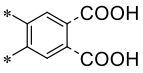	> 60	**108**	Br	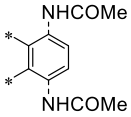	> 60	**109**	Ph	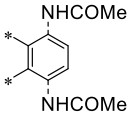	34 ± 1.5
110	Br	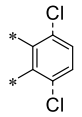	17 ± 0.9	**111**	Ph	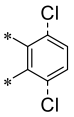	7.8 ± 1.9	**112**	Br		21 ± 0.7
113	Ph		7.4 ± 0.6	**114**	Br	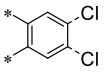	14 ± 0.4	**115**	Ph	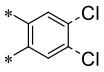	1.2 ± 0.2
116	Br	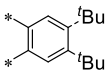	16 ± 1.0	**117**	Ph	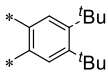	1.1 ± 0.3	**118**	Br	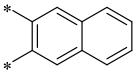	2.5 ± 0.2
119	Ph	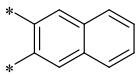	0.88 ± 0.02	**120**	Br	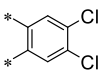	5.0 ± 1.3	**121**	Ph	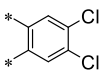	0.86 ± 0.03

[a] IC_{50} calculated as n=3

Fused naphthyl and 4,5-dichloro substituted ligands (**118** 2.5 μM, **119** 0.88 μM, **120** 5.0 μM, **121** 0.86 μM) exhibited the most significant increase in potency, with ligand **121** presenting the highest potency for this section of 0.86 μM. The compounds within this series suggested that hydrophobic growth along the vector indicated in **Figure 49** was efficient with regards to driving potency within this pocket of space.

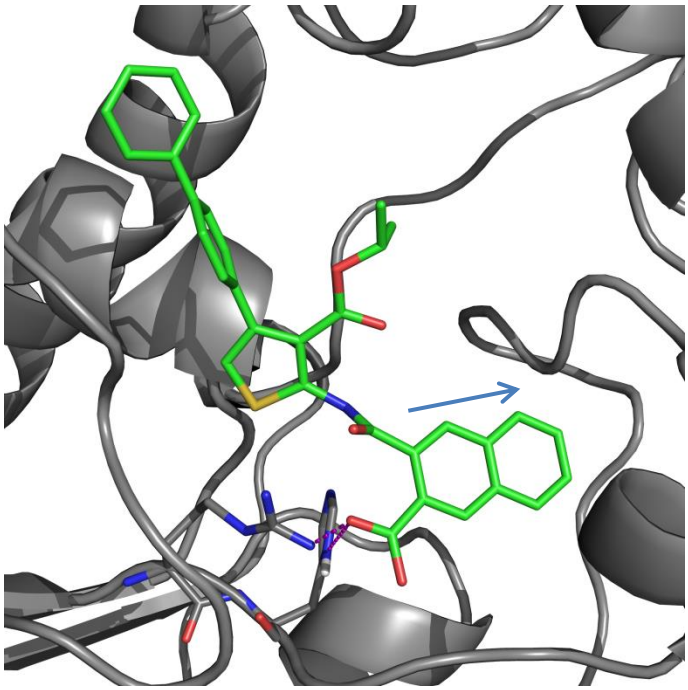

Figure 49: Naphthyl derivative 119 docked in TIGAR. Key electrostatic interactions are highlighted by dotted magenta lines with key lipophilic growth vector outlined by a blue arrow.

The IC_{50} values for the alternative linker scaffolds **122**–**125** are depicted in **Table 5**.

Table 5: IC_{50} values for alternative linker compounds 122–125.

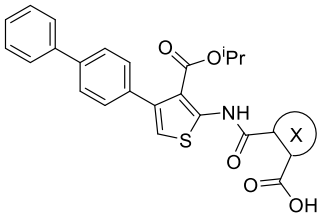

Compound	X	IC_{50} (μM)[a]
122		31 ± 24
123		> 40
124		21 ± 3.5
125		5.8 ± 3.8

[a] IC_{50} calculated as n=3

Removing the aromaticity/cyclic properties associated with the phenyl linker of the parent compound **83** (IC_{50} 8.5 μM) by changing to an alkene linker (compound **122** 31 μM), resulted in a loss in potency. This outcome was further exemplified by ligand **123** (> 40 μM) as a change to an aliphatic linker, proved to be detrimental to binding affinity towards the target. Reduced rigidity and disturbance of the optimal alignment of the carboxylate head group were proposed as the reason for this outcome. Retaining the cyclic structure of the phenyl linker **83** but removing the associated aromaticity (compound **124** 21 μM), again imparted a negative effect on potency. However, the loss of potency was not as severe as with the acyclic linkers (**122**–**123**), suggesting that the reason for this was the reduced lipophilicity of ligand **124** and that the acidic head group remained orientated in a close to ideal setting. Modifying the electronics of the linker (compound **125** 5.8 μM), and therefore the pka of the acidic head group, appeared to induce a negligible difference in binding affinity. The pyrazine linker is electron deficient compared to the parent phenyl which should theoretically result in the pka of the head group being lowered. This result suggested that modification of the acidic head group pka, has a limited effect on the overall potency of the ligands in this series.

In summary, the data within this series has demonstrated that substitution of the phenyl linker with hydrophobic substituents (compounds **110**–**121**) has a positive impact on binding affinity, particularly along the vector highlighted in **Figure 49**. Whereas, substitution with polar or charged moieties (compounds **104**–**109**) resulted in a reduction of potency. Removal of the cyclic/aromatic groups (compounds **122**–**124**) related to the phenyl linker ligand **83**, was also detrimental to potency, suggesting that the positioning of the acidic head group, and aromatic VDW interactions of the linker, were crucial for binding to TIGAR. Alteration of the linker electronics (compound **125)** and in turn the pka of the acidic head group, had minimal effect on potency. The phenyl linker group was retained for future SAR studies as a balance between potency and lipophilicity/molecular weight (M.wt). It was hypothesised that better potency gains for a similar increase in M.wt could be obtained within the channel substituent area of the SAR.

4.2.5. Channel substituent series 1

4.2.5.1. Design hypothesis

As previously described in Section **4.2.1.** the hypothetical binding mode for the series suggested that growth into the hydrophobic channel of the TIGAR active site should be the main area of focus for driving potency and potentially selectivity. A substantial amount of space was identified for hypothesised ligand occupancy, with the potential for forming several interactions with neighbouring residues (Ala189, Pro215, Val,216), at this part of the binding pocket (Figure 50). An initial series of compounds for the interrogation of this hydrophobic channel were synthesised based around the generic scaffold **126** detailed in **Figure 51**.

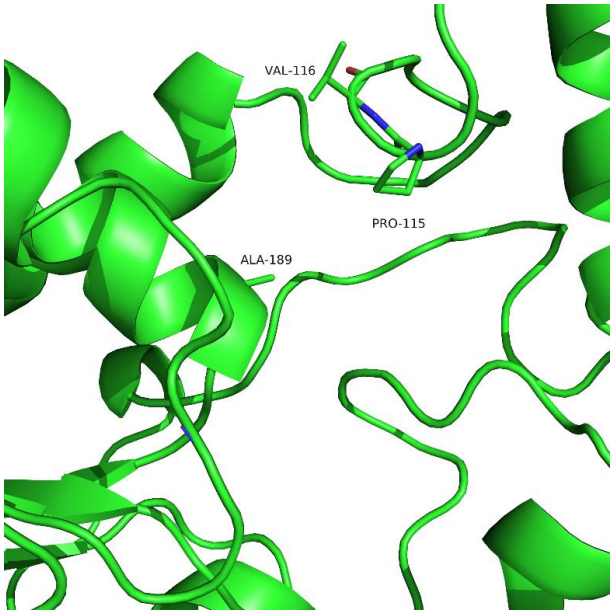

Figure 50: Identification of residues Ala189, Pro115 and Val116 that form the hydrophobic channel.

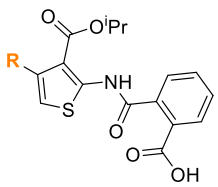

126

Figure 51: General structure of channel substituent derivatives.

4.2.5.2. Synthetic route

Most of the respective compounds within this series were synthesised using a short 2-step synthetic sequence outlined in **Scheme 15** due to the availability of the ketone starting materials. The multicomponent Gewald reaction was critical to the streamlining of this route, as it allowed very high levels of structural diversity to be achieved in a single synthetic step. This enabled efficient investigations to be made when assessing this area of the active site, through rapid expansion of the SAR library.

Scheme 15: Synthesis of compounds 167–186.

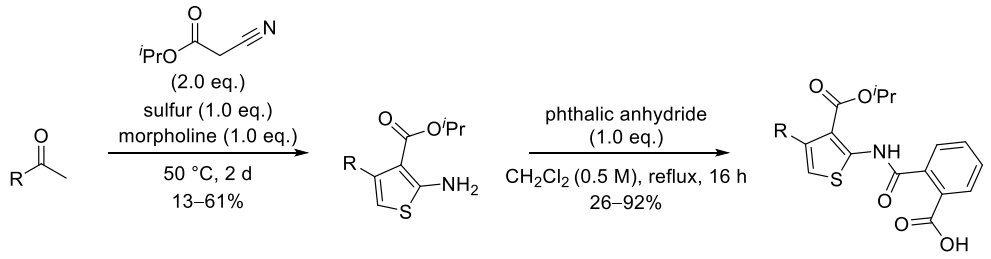

127 R = 3-pyridine	**147** R = 3-pyridine 52%	**167** R = 3-pyridine 64%
128 R = 4-pyridine	**148** R = 4-pyridine 50%	**168** R = 4-pyridine 71%
129 R = 3,5-dimethylthiazole	**149** R = 3,5-dimethylthiazole 45%	**169** R = 3,5-dimethylthiazole 48%
130 R = 1-naphthyl	**150** R = 1-naphthyl 41%	**170** R = 1-naphthyl 38%
131 R = 2-naphthyl	**151** R = 2-naphthyl 43%	**171** R = 2-naphthyl 86%
132 R = 3-quinoline	**152** R = 3-quinoline 56%	**172** R = 3-quinoline 71%
133 R = 3-isoquinoline	**153** R = 3-isoquinoline 44%	**173** R = 3-isoquinoline 92%
134 R = 2-quinoxaline	**154** R = 2-quinoxaline 61%	**174** R = 2-quinoxaline 84%
135 R = 7-methoxy-2-benzofuran	**155** R = 7-methoxy-2-benzofuran 43%	**175** R = 7-methoxy-2-benzofuran 83%
136 R = 6-benzoxazolone	**156** R = 6-benzoxazolone 13%	**176** R = 6-benzoxazolone 83%
137 R = 4-(4-morpholine)-Ph	**157** R = 4-(4-morpholine)-Ph[a]	**177** R = 4-(4-morpholine)-Ph 34%**
138 R = 4-(4-1*H*-imidazole)-Ph	**158** R = 4-(4-1*H*-imidazole)-Ph 46%	**178** R = 4-(4-1*H*-imidazole)-Ph 75%
139 R = 4-benzonitrile	**159** R = 4-benzonitrile 33%	**179** R = 4-benzonitrile 79%
140 R = 4-(4-CCH)-Ph	**160** R = 4-(4-CCH)-Ph 31%	**180** R = 4-(4-CCH)-Ph 87%
141 R = 4-(4-phenoxy)-Ph	**161** R = 4-(4-phenoxy)-Ph 30%	**181** R = 4-(4-phenoxy)-Ph 74%
142 R = 4-(4-benzyl)-Ph	**162** R = 4-(4-benzyl)-Ph 43%	**182** R = 4-(4-benzyl)-Ph 83%
143 R = 4-(4-benzyloxy)-Ph	**163** R = 4-(4-benzyloxy)-Ph[a]	**183** R = 4-(4-benzyloxy)-Ph 26%**
144 R = 4-(4-phenethyl)-Ph	**164** R = 4-(4-phenethyl)-Ph 26%	**184** R = 4-(4-phenethyl)-Ph 79%
145 R = 4-(3-benzyloxy)-Ph	**165** R = 4-(3-benzyloxy)-Ph 48%	**185** R = 4-(3-benzyloxy)-Ph 77%
146 R = 4-(2-benzyloxy)-Ph	**166** R = 4-(2-benzyloxy)-Ph 35%	**186** R = 4-(2-benzyloxy)-Ph 82%

[a] compound partially purified.

Starting ketones **127**–**146** were reacted under the standard multicomponent Gewald reaction conditions to produce intermediates **147**–**166** in low to good yields (13–61%). Ketone components with very high polarity (e.g. compound **136**) produced lower yields of the respective Gewald product (13%) due to reduced solubility within the Gewald reaction mixture. Intermediates **147**–**166** were then used to ring-open phthalic anhydride to produce final compounds **167**–**186** (26–92%) in moderate to excellent yields, exposing the key carboxylic acid head group.

Certain ketone starting materials (**190**–**193**) were not commercially available and so had to be synthesised through an additional synthetic step, before subsequently undergoing the standard multicomponent Gewald and ring-opening (Scheme 16).

Scheme 16: Synthesis of compounds 198–201.

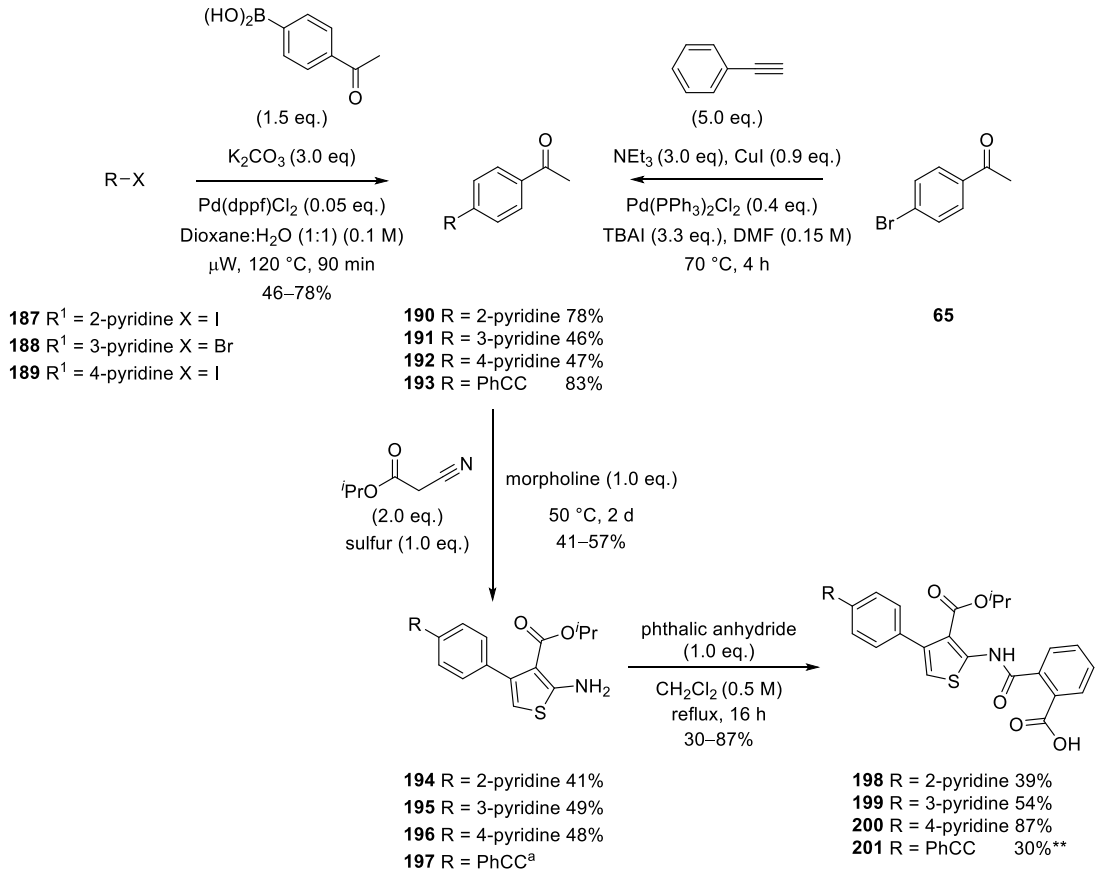

[a] compound partially purified.

Staring halides **187**–**189** were coupled with (4-acetylphenyl) boronic acid using Suzuki-Miyaura palladium-catalysed cross-coupling conditions to generate intermediate ketones **190**–**192** in moderate to good yields (46–78%).[102] 2-Pyridine substitution gave an approximate 30% increase in yield compared to the other pyridine regioisomers. This was proposed to be due to increased polarisation of the carbon halogen bond as a result of the close proximity of the nitrogen atom within the heterocycle, which would in turn aid the oxidative addition step of the catalytic cycle. 4-Bromo acetophenone **65** was coupled with phenyl acetylene through Sonagashira cross-coupling conditions to produce ketone intermediate **193** in good yield (83%).[103] Intermediates **190**–**193** were treated with the established Gewald reaction set-up to afford 2-amino thiophene intermediates **194**–**197** in moderate

yields (41–49%), before these intermediate compounds were subjected to the ring-opening of phthalic anhydride, to provide final compounds **198**–**201** in moderate to excellent yields (30–87%).

4.2.5.3. Biological evaluation

Dose response curves were generated for all the synthesised final compounds in this series using the *in vitro* assay described in Section 3.0. **Figure 52** details the structure and IC_{50} value of the parent compound that directly relates to the ligands prepared within this series, for comparison purposes.

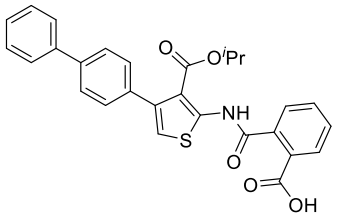

83 IC_{50} 8.5 μM

Figure 52: Parent compound with respective IC_{50} values.

The IC_{50} values for channel substituent series 1 compounds with unsubstituted and fused substituents (compounds **167**–**168** and **170**–**176**, respectively), as well as the 3,5-dimethyl thiazole ligand **169**, are described in **Table 6**.

Starting from the biphenyl appendage of the parent compound **83**, initial alterations included stripping this back to unsubstituted aromatics (compounds **167**–**168** both > 40 μM) and a 5-membered heterocycle (compound **169**, > 40 μM), to assess how limited extension into the channel, would affect potency. All of these ligands resulted in the loss of activity, demonstrating that reducing channel substituent length was undesirable and that occupying this hydrophobic channel was important for binding. Varying the R substituent for fused carbocyclic compounds gave a drop in binding affinity when compared to **83**, with a 2-naphthyl group (**171** 16 μM) being preferred to a 1-naphthyl derivative (**170** 29 μM). Further extension of the 2-naphthyl group into the channel was proposed as the reason for this potency difference. Exchanging the biphenyl of **83** for fused heterocyclic species (**172**–**176**) again produced similar negative impacts on activity for the series. 6-Membered fused heterocycles (**172** 49 μM, **173** > 60 μM and **174** 37 μM) all resulted in a reduction in potency compared to carbocycles **170** (29 μM) and **171** (16 μM). This could possibly be due

to their collective reduction in lipophilicity, as the entrance to the channel is flanked by non-polar residues. Two additional 5,6-fused heterocycles (**175** 44 μM and **176** 41 μM) were also screened against TIGAR, however, the same detrimental effects on binding affinity were once again observed. These IC_{50} values reinforced the emerging pattern, that short-length channel substituents with increased hydrophilicity, would not be tolerated within this area of the active site due to their hydrophilic nature.

Table 6: IC_{50} values for channel substituent compounds 167–176.

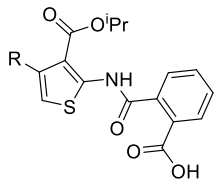

Compound	R	IC_{50} (μM)[a]
167	3-pyridine	> 40
168	4-pyridine	> 40
169	3,5-dimethylthiazole	> 40
170	1-naphthyl	29 ± 3.7
171	2-naphthyl	16 ± 2.1
172	3-quinoline	49 ± 3.9
173	3-isoquinoline	> 60
174	2-quinoxaline	37 ± 7.0
175	7-methoxy-2-benzofuran	44 ± 2.0
176	6-benzoxazolone	41 ± 2.0

[a] IC_{50} calculated as n=3

The collective data displayed for compounds **167**–**176**, strongly suggested that shortening of the biphenyl channel substituent, present in ligand **83**, consistently induced negative effects upon the binding affinity of compounds within this series. Fused aromatics performed better than unsubstituted heterocycles, with fused carbocyclic systems being preferred to the more polar fused heterocycles. Computational docking, performed at the beginning of this project, had already indicated that opportunities for desired interactions were only hypothetically possible with further growth along the channel vector.

IC_{50} values for the remaining analogues within channel substituent series 1 (**177**–**186** and **198**–**201**) are detailed in **Table 7**. The compounds in **Table 7** consist of direct mimics to parent biphenyl ligand **83**. The internal phenyl group was retained for hydrophobic interactions within the channel and the external phenyl group was varied to assess how differing electronics and substituent length would impact on potency values.

Table 7: IC_{50} values for channel compounds 177–186 and 198–201. 201 and 184 IC_{50} curves.

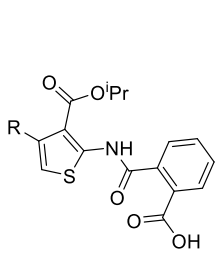

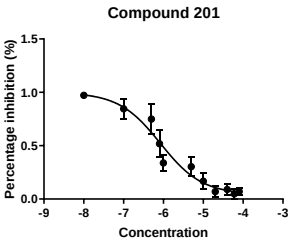

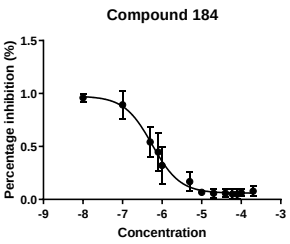

Compound	R	IC_{50} (μM)[a]
177	4-(morpholine)-C_6H_4	> 60
178	4-(1*H*-imidazole)-C_6H_4	15 ± 1.6
179	4-benzonitrile	31 ± 2.3
180	(4-CCH)-C_6H_4	9.0 ± 1.4
198	4-(2-pyridine)-C_6H_4	3.6 ± 1.8
199	4-(3-pyridine)-C_6H_4	1.4 ± 0.3
200	4-(4-pyridine)-C_6H_4	4.6 ± 0.2
201	4-phenylethynyl-C_6H_4	0.84 ± 0.03
181	4-phenoxy-C_6H_4	1.3 ± 0.2
182	4-benzyl-C_6H_4	0.72 ± 0.08
183	4-benzyloxy-C_6H_4	0.77 ± 0.05
184	4-phenylethyl-C_6H_4	0.56 ± 0.06
185	3-benzyloxy-C_6H_4	> 40
186	2-benzyloxy-C_6H_4	> 40

[a] IC_{50} calculated as n=3

Switching the external phenyl moiety for a saturated polar morpholine group (ligand **177** > 60 μM) provided an inactive ligand, highlighting that increased polarity and removal of aromaticity for substituents localised deeper within the hydrophobic channel, would not be tolerated by TIGAR. The incorporation of analogues that possessed increased polarity (compounds **178** 15 μM, **198** 3.6 μM, **199** 1.4 μM and **200** 4.6 μM), proved to be beneficial for potency. The 5-membetred imidazole

(compound **178** 15 μM) functionality afforded a subtle drop-off in activity compared to parent ligand **83** (8.5 μM), potentially due to restricted VDW interactions through decreased ring-size, however, the heterocycle was favoured compared to the saturated morpholine derivative **177** (> 60 μM). The 6-membered pyridine regioisomers (**198**–**200**) slightly improved upon the 8.5 μM IC_{50} value of compound **83** showing that biaryl species where the external ring has reduced lipophilicity, through the introduction of a heteroatom, can be tolerated within the channel to the same extent as the equivalent phenyl group. Mono-substituted triple bond derivatives (compounds **179** 31 μM and **180** 9.0 μM) displayed an interesting difference in potency. The alkyne ligand **180** exhibited activity equipotent to that of the parent phenyl, which was in keeping with the fact that alkynes are known replacements for phenyl moieties. However, the cyano analogue **179** demonstrated significantly reduced activity (31 μM), suggesting that the electronics of this group were inducing a negative interaction that the model cannot predict, as there were no obvious discrepancies.

Insertion of an alkyne linker (compound **201**) between the biphenyl functionality of ligand **83** allowed for further extension into the channel which, according to the molecular model (Figure 53), may have generated the opportunity for additional VDW interactions within the channel.

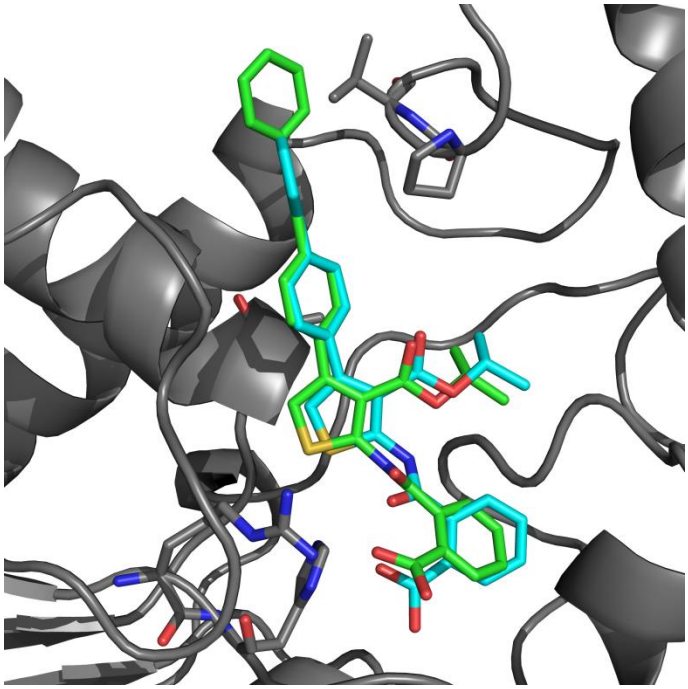

Figure 53: **4-Phenylethynyl-phenyl derivative 201 and reference compound 83 docked in TIGAR active site.**

Pleasingly, the model prediction was authenticated by an improved IC_{50} value of 0.84 μM, reinforcing the proposal that increased extension into the channel would result in potency gains.

The alkyne linker of ligand **201** was thought to be very rigid and so, this led to the development/screening of analogues **181**–**184** which introduced varying degrees of length/flexibility into the linker segment between the two aryl groups of the channel substituent R. The 4-phenoxy-phenyl derivative (compound **181** 1.3 μM) afforded a reduction in binding affinity compared to the alkyne linker analogue (compound **201** 0.84 μM), which could have been due to the reduced lipophilicity/length of the linker. However, the 4-benzyl-phenyl ligand (compound **182** 0.72 μM) produced an improved potency compared to alkyne linker **201**, indicating that maintaining a hydrophobic linker between the two aryl groups, whilst increasing flexibility, resulted in a more favoured binding mode/affinity. Extension to a 2 atom linker in the form of a 4-benzyloxy-phenyl derivative (compound **183** 0.77 μM) gave increased potency compared to the single heteroatom linker analogue **181**, signifying that linker length was fundamental to the activity of the channel substituent. 4-Phenylethyl-phenyl derivative (**184** 0.56 μM) reinforced this idea, as this 2 carbon atom linker compound displayed an approximate 200 nM increase in potency, compared to the single carbon atom linked benzyl compound (**182** 0.72 μM). The healthier potency of **184** when compared to **183** indicated that heightened hydrophobicity of the aryl linker was beneficial for binding affinity, within the lipophilic channel. The molecular docking of compound **184** (Figure 54) supported the proposal that optimum linker length and flexibility had now potentially been achieved with ligands **183** and **184**.

Docking of compound **184** highlighted that the 2-atom linker length and flexibility of the channel substituent, was potentially allowing a key interaction to be adopted by the outer phenyl functionality of compounds **183** and **184**. From the model, it was observed that the outer phenyl ring of the channel group could be extending beyond the hydrophobic channel and was instead proposed to be packing against an exposed arginine residue (Arg192), potentially forming a π-cation interaction. This positive interaction could explain the observed potency boost associated with ligands **183** (0.77 μM) and **184** (0.56 μM) compared to their single atom linker counterparts **181** (1.3 μM) and **182** (0.72 μM), respectively. Varying this external phenyl group led to

multiple new series of compounds within the SAR, which will be discussed in detail within later sections.

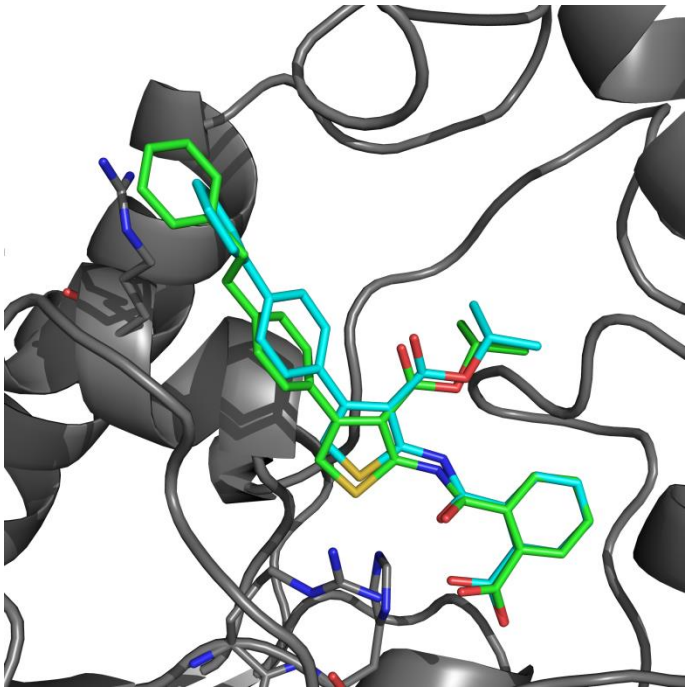

Figure 54: 4-Phenylethyl-phenyl derivative 184 and reference compound 83 docked in TIGAR active site.

Meta- (compound **185** > 40 μM) and *ortho*- (compound **186** > 40 μM) substituted benzyloxy-phenyl ligands were screened within the assay to complete the SAR investigations within this section. Molecular docking predicted that both of these analogues would be inactive towards the target due to steric clashes with the protein, as negative fit scores were calculated for both ligands when the software failed to dock them within the active site, in a feasible conformation. Assuredly, this prediction was validated by the experimental data as both compounds proved to completely lose any activity towards the target (> 40 μM).

In summary, channel substituents comprised of unsubstituted aromatic rings (compounds **167**–**168**) or fused carbocycles/heterocycles (compounds **170**–**176**) appeared to be too short in length to enable adequate occupancy of the hydrophobic channel, which resulted in weak potency values (IC_{50} > 16 μM). Phenyl groups substituted in the *para* position with a saturated polar group (compound **177** > 60 μM) were completely inactive towards TIGAR. Ligands where the phenyl of the channel appendage was *para* substituted with a polar heterocycle (compounds **178** and **198**–**200**), either gave a slight drop in potency (5-membered **178** 15 μM) or

produced a slight increase in affinity (6-membered **198** 3.6 μM, **199** 1.4 μM, **200** 4.6 μM). Conversely, benzonitrile analogue **179** (31 μM) produced a drop-off in potency from that of the parent biphenyl **83** (8.5 μM), however, phenyl alkyne derivative **180** (9.0 μM) exhibited equivalent potency compared to the parent biphenyl **83**. This demonstrated that subtle changes in electronics could sufficiently impact potency. Introduction of an alkyne linker (compound **201** 0.84 μM) generated a significant increase in potency, which indicated that activity was affected by linker length and channel occupancy. Single atom linker ligands with increased flexibility afforded both a decrease in potency (compound **181** 1.3 μM) due to reduced hydrophobicity, and also an improvement in potency (compound **182** 0.72 μM). Further extension of the linker to 2-atom units whilst maintaining flexibility, resulted in a respective increase in binding affinity for both the benzyloxy (compound **183** 0.77 μM) and the phenylethyl (compound **184** 0.56 μM) ligands, compared to their equivalent 1 atom analogues **181** and **182**, respectively. Optimal linker length of the channel substituent had now been identified and was reinforced by molecular docking, which indicated that an additional π-cation interaction was potentially occurring with ligands **183** and **184**. Finally, *meta*- and *ortho*- substituted internal phenyl ligands (compounds **185** > 40 μM and **186** > 40 μM, respectively) were observed to be completely inactive, which was supported by the molecular docking of these compounds, as a steric clash with the protein was hypothesised.

4.2.6. 5-Position series

4.2.6.1. Design hypothesis

The potential for substitution at the 5-position of the core thiophene unit, looked to be very limited according to molecular modelling studies for the series (Figure 55).

The model had hypothesised that the available physical space for growth along this vector was restricted (red region, Figure 55). However, in order to establish an extensive SAR profile for this scaffold, it was proposed that all avenues should be explored to enable complete interrogation of the target protein. Therefore, a small series of compounds were designed based around the generic scaffold depicted in **Figure 56**, with the idea of starting with minimal substitution before subsequent expansion.

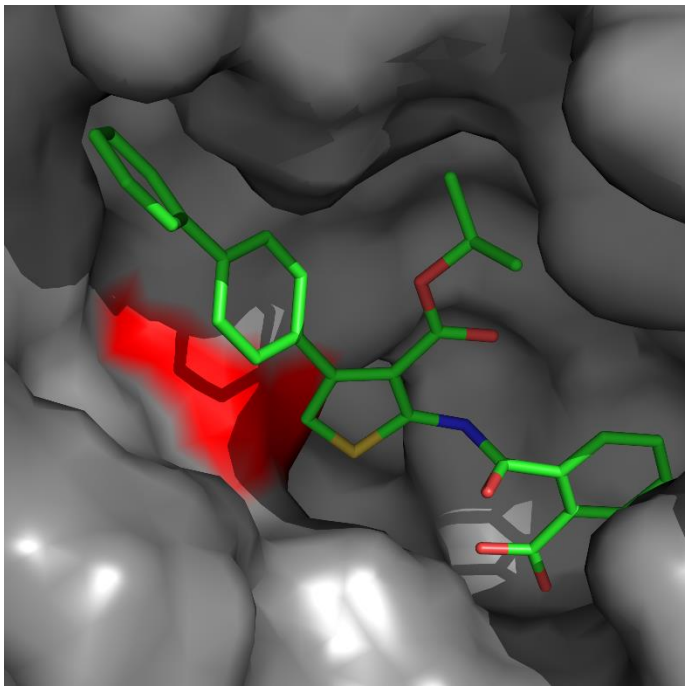

Figure 55: Compound 83 docked in TIGAR active site with surface representation. Red region highlights the hypothesised limited space available for substitution at the 5-position of the thiophene ring.

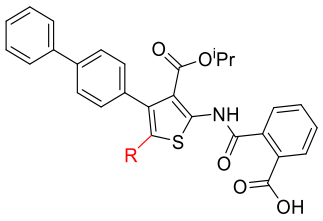

202

Figure 56: General structure of 5-substituted thiophene derivatives.

4.2.6.2. Synthetic route

The short series of compounds synthesised during this period of the SAR were generated following the 2–3 step route outlined in **Scheme 17**. Starting material **204** (R = Me) was commercially available, however, the increased alkyl chain-length derivative **205** (R = Et) was unavailable and had to be synthesised *via* an extra synthetic step, from ketone **203**.

Scheme 17: Synthesis of compounds 208 and 209.

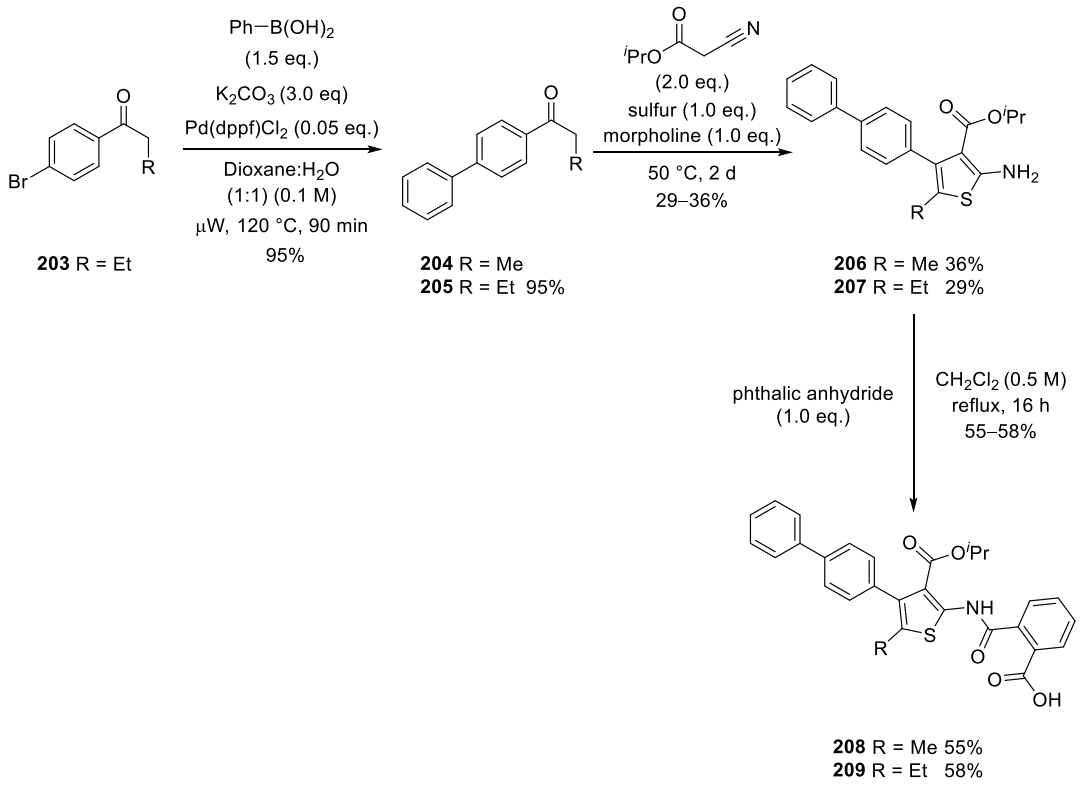

Initially, ketone **203** was reacted with phenyl boronic acid using Suzuki-Miyaura palladium-catalysed cross-coupling conditions, to produce biphenyl intermediate **205** in 95% yield.[102] Commercially available ketone **204** and synthesised intermediate **205** were then subjected to Gewald reaction conditions, to afford 2-amino thiophene derivatives **206** (36%) and **207** (29%) in moderate yields, respectively. Intermediates **206** and **207** were further functionalised *via* ring-opening of phthalic anhydride to produce final compounds **208** (R = Me, 55%) and **209** (R = Et, 58%) in good yields.

4.2.6.3. Biological evaluation

Dose response curves were generated for all the synthesised final compounds in this series using the *in vitro* assay described in Section 3.0. **Figure 57** details the structure and IC_{50} value of the parent compound that directly relates to the ligands prepared in this series, for comparison purposes.

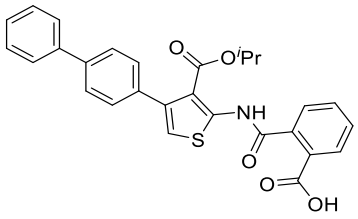

83 IC_{50} 8.5 μM

Figure 57: Parent compound 83 with respective IC_{50} values.

The IC_{50} values for 5-substituted thiophene compounds **208** and **209** are described in **Table 8**. In comparison to the 8.5 μM IC_{50} value of parent ligand **83**, 5-methyl substituted derivative **208** demonstrated an improved potency of 0.87 μM. This data highlighted that low levels of substitution were not only tolerated within this pocket of space but pleasingly, resulted in an improvement in binding affinity.

Table 8: IC_{50} values for 5-substituted compounds 208 and 209.

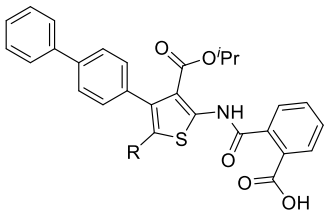

Compound	R	IC_{50} (μM)[a]
208	Me	0.87 ± 0.02
209	Et	> 40

[a] IC_{50} calculated as n=3

The experimental data for ligand **208** was reinforced by docking studies, which proposed that the 5-methyl substituent was potentially able to position favourably within the active site (Figure 58). However, further expansion along this vector to an ethyl group (compound **209** > 40 μM) proved to be detrimental to activity. Docking studies performed with ligand **209** failed as the modelling software failed to adequately fit **209** into the TIGAR active site, which also complemented the experimental results.

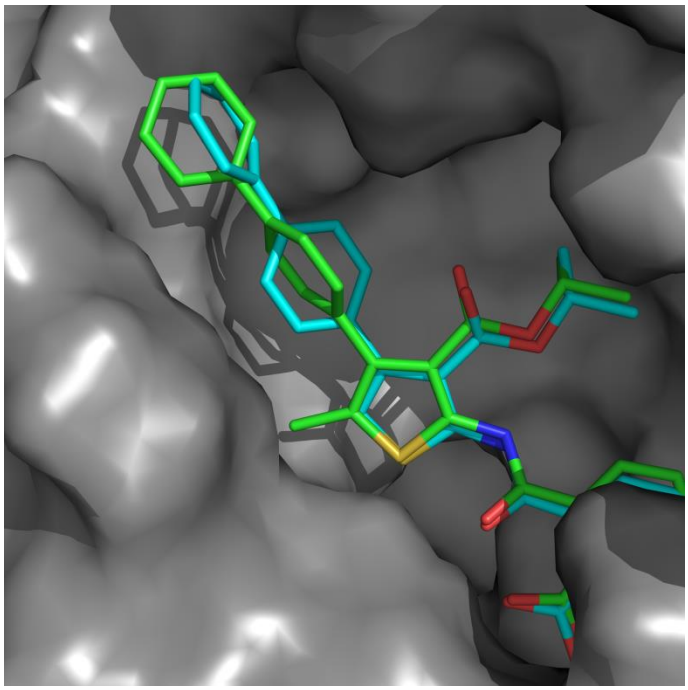

Figure 58: Compound 208 and reference compound 83 docked within the TIGAR active site. 5-Methyl substituent hypothesised to be positioned within a very shallow hydrophobic pocket.

In summary, these two ligands suggested that while a very shallow pocket of space clearly exists at this section of the TIGAR active site, there is also a very fine balance between the levels of possible substitution along this vector, for potency gain/loss. Although it was unfortunate that further expansion along this vector looked highly restricted, the experimental outcome had reinforced the established hypothetical binding mode, which was a strong positive to take from this part of the SAR study. This provided added confidence in the molecular model for the series going forward. Based on these results, further investigations into this area of the SAR were not pursued due to the observed computational and experimental evidence.

4.2.7. Hybrid series 1

4.2.7.1. Design hypothesis

The proposal to design and synthesise a few select hybrid compounds that married the optimised portions, for each section of the scaffold, was implemented at this stage of the SAR investigations. **Figure 59** displays the most potent ester derivative (compound **90** 0.92 µM), phenyl linker derivative (compound **121** 0.86 µM), channel substituent (compound **184** 0.56 µM) and 5-substituted analogue (compound **208** 0.87 µM).

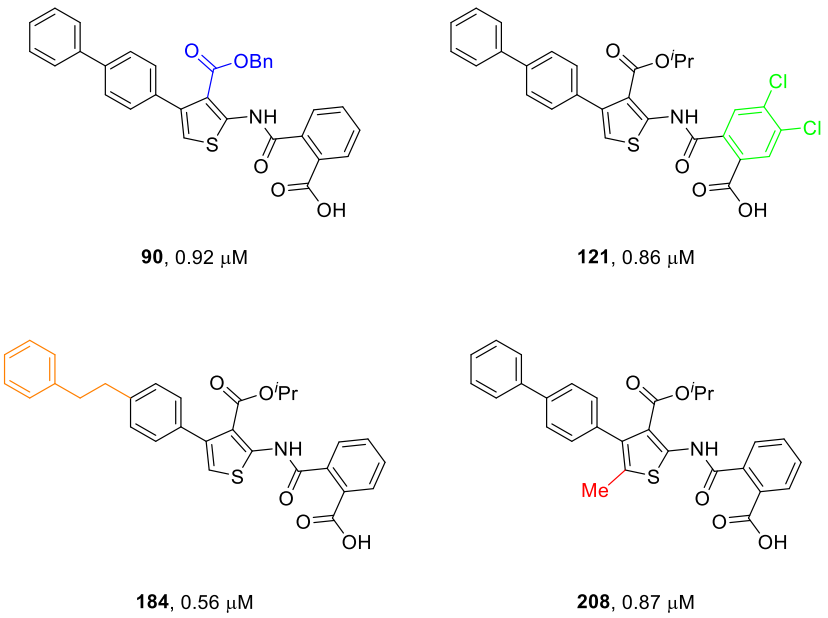

Figure 59: Optimised compounds from previous SAR series.

Hybrid compounds were then designed based around the generic scaffold **210** shown in **Figure 60**, and synthesised through different combinations of the various appendages, in order to assess the impact these changes would have upon potency. However, it was recognised that these hybrid compounds would become extremely lipophilic, as the gains in potency associated with these compounds had mainly been achieved through the optimisation of hydrophobic interactions, and therefore their overall efficiency as chemical probes would have to be questioned. Nonetheless, further expansion of the SAR data for the series, with regards to how potent the compounds could become, was deemed reason enough for initiating the synthesis of these hybrid ligands.

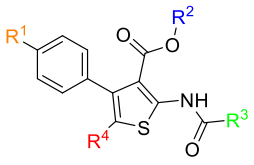

210

Figure 60: Generic scaffold for hybrid series 1 ligands.

4.2.7.2. Synthetic route

Three of the hybrid derivatives (**211**–**213**) were synthesised from common intermediates **79**, **206** and **164**, respectively, in a single-step, as these compounds had

already been formed during previous routes *via* the Gewald reaction. However, hybrid ligand **215** had to be synthesised using an additional step, from ketone starting material **144**. The synthesis for all compounds in this series is detailed in **Scheme 18**.

Scheme 18: Synthesis of compounds 211–213 and 215.

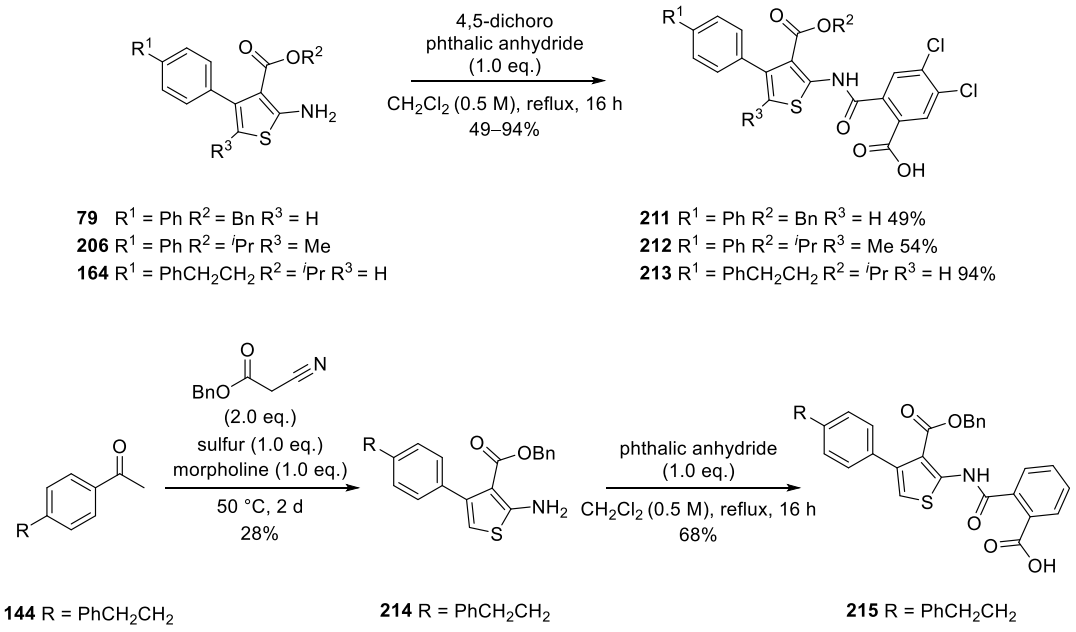

Common 2-amino thiophene intermediates **79**, **206** and **164** were subjected to ring-opening of 4,5-dichorophthalic anhydride to produced carboxylate analogues **211**, **212** and **213**, respectively, in good to excellent yields (49–94%).

Ketone **144** was reacted under standard Gewald reaction conditions to produce 2-amino thiophene intermediate **214** in moderate yield (28%). Intermediate **214** was used to perform the ring-opening of phthalic anhydride to generate final compound **215** in good yield (68%).

4.2.7.3. Biological evaluation

Dose response curves were generated for all the synthesised final compounds in this series using the *in vitro* assay described in Section 3.0. The IC_{50} values for hybrid series 1 compounds **211**–**213** and **215**, are depicted in **Table 9**.

Table 9: IC_{50} values for hybrid compounds 211–213 and 215.

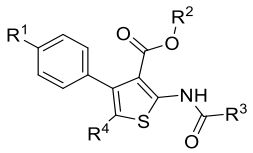

Compound	R^1	R^2	R^3	R^4	IC_{50} (μM)[a]
211	Ph	Bn	*o*-COOH-4,5-dichloro-C_6H_2-	H	0.51 ± 0.05
212	Ph	^{i}Pr	*o*-COOH-4,5-dichloro-C_6H_2-	Me	0.61 ± 0.05
213	$PhCH_2CH_2$	^{i}Pr	*o*-COOH-4,5-dichloro-C_6H_2-	H	0.31 ± 0.04
215	$PhCH_2CH_2$	Bn	*o*-COOH-C_6H_4-	H	0.19 ± 0.04

[a] IC_{50} calculated as n=3

Compound **211** combined the benzyl group of ligand **90** (0.92 μM) with the 4,5-dichloro substituted phenyl linker of compound **121** (0.86 μM), which generated a potency increase to 0.51 μM. Interestingly, this analogue demonstrated that both the R^2 and R^3 positions could simultaneously have bulky hydrophobic groups incorporated and still be able to favourably fit within the TIGAR active site. Ligand **212** brought together the 4,5-dichloro substituted phenyl linker of compound **121** (0.86 μM) and the 5-methyl of derivative **208** (0.87 μM), which again provided an increase in binding affinity (0.61 μM). The activity value for **212** (0.61 μM) was 100 nM weaker than that of ligand **211** (0.51 μM), highlighting that increased opportunities for hydrophobic substitution along the R^2 vector afforded increased potency gains, compared to the limited substitution along the R^4 vector. Analogue **213** represented a hybridisation of the 4,5-dichloro substituted phenyl linker of compound **121** (0.86 μM) and the phenyl ethyl channel substituent of derivative **184** (0.56 μM), which afforded a 200 and 300 nM increase in potency (0.31 μM) when compared to ligands **211** (0.51 μM) and **212** (0.61 μM), respectively. This was in keeping with previous results as compound **184**, which incorporated the phenyl ethyl channel substituent, was the most potent TIGAR ligand entering the hybridisation SAR studies. Therefore, the fact that the phenyl ethyl R^1 containing hybrid **213** produced an improved IC_{50} value (0.31 μM) compared to analogues **211** (0.51 μM) and **212** (0.61 μM) was consistent with all previously recorded data. The final hybrid ligand **215** combined the phenyl ethyl channel substituent of analogue **184** with the benzyl ester derivative **90**, and this produced the largest increase in potency for the

series (0.19 μM). Compound **215** was proposed to be more potent than ligands **211** (0.51 μM) and **212** (0.61 μM), for the same reasons as stated for ligand **213**. However, the improved binding affinity for **215** (0.19 μM) when compared to **213** (0.31 μM) was surprising, as the 4,5-dichloro substituted phenyl linker motif of **213** had originally exhibited a larger activity gain than the benzyl ester moiety of **215** (ligand **90** 0.92 μM vs ligand **121** 0.86 μM). This data may suggest that the extended phenyl ethyl channel functionality forces the positioning of the ligand within the active site to change, causing the benzyl ester moiety of compound **215** to adopt an alternative orientation/binding mode. Favourable VDW interactions made by the benzyl group could then be attenuated to produce an increased positive effect on potency.

In summary, all four of the hybrid compounds synthesised within this series had a desirable effect on activity. As expected, the compounds containing the phenyl ethyl channel substituent (**213** 0.31 μM & **215** 0.19 μM) afforded improved potency values compared to the hybrid ligands that incorporated the biphenyl channel substituent (**211** 0.51 μM and **212** 0.61 μM). The difference in potency between ligands **213** and **215** was proposed to be due to an alteration in the binding mode of the benzyl ester group, in the presence of the phenyl ethyl channel moiety. This may have had a positive impact on the interactions being made by this ester derivative, in the hydrophobic pocket within which it was located.

As previously stated, the gains in potency associated with these ligands were achieved through the optimisation of mainly hydrophobic interactions. As a result, these hybrid species (compounds **211**–**213** and **215**) were all extremely lipophilic with cLogP values of > 7.5. This characteristic would have a high probability of imparting a negative knock-on effect upon other physicochemical properties such as solubility, intrinsic clearance and half-life.[104] Increased lipophilicity has also been shown to increase the chances of off-target effects, which would be detrimental to the development of an efficient small molecule chemical probe.[105] As such, this part of the SAR study was used to assess potential potency gains associated with hybrid compounds, based upon the optimised substituents from the best derivatives to date, in order to widen the SAR data and increase our overall understanding of the targets active site. In terms of generating an efficient tool compound however, these ligands were considered to be unsuitable candidates for achieving this desired outcome.

4.2.8. Sp3 character series

4.2.8.1. Design hypothesis

The introduction of sp3 character into dug-like molecules has been demonstrated to exert beneficial effects upon physicochemical properties, as well as generating a reduction in promiscuity and CYP450 inhibition.[106] Therefore, in parallel to the synthesis of the hybrid series described in Section 4.2.7., the preparation of sp3 character-containing derivatives of the best ligand to date **184** (Figure 61), was undertaken. The phenyl group linked to the carboxylic acid head group was identified as the segment to be modified, due to the fact that the orientation of the head group had already been shown to be crucial and so, it was anticipated that a change in its orientation could have a pronounced effect on activity. Two compounds where the phenyl linker motif of **184** was exchanged for a bicyclic linker (compounds **216** and **217**) were proposed. These analogues were designed to gain an initial insight into the effect that the incorporation of three-dimensionality would have on ligand binding affinity.

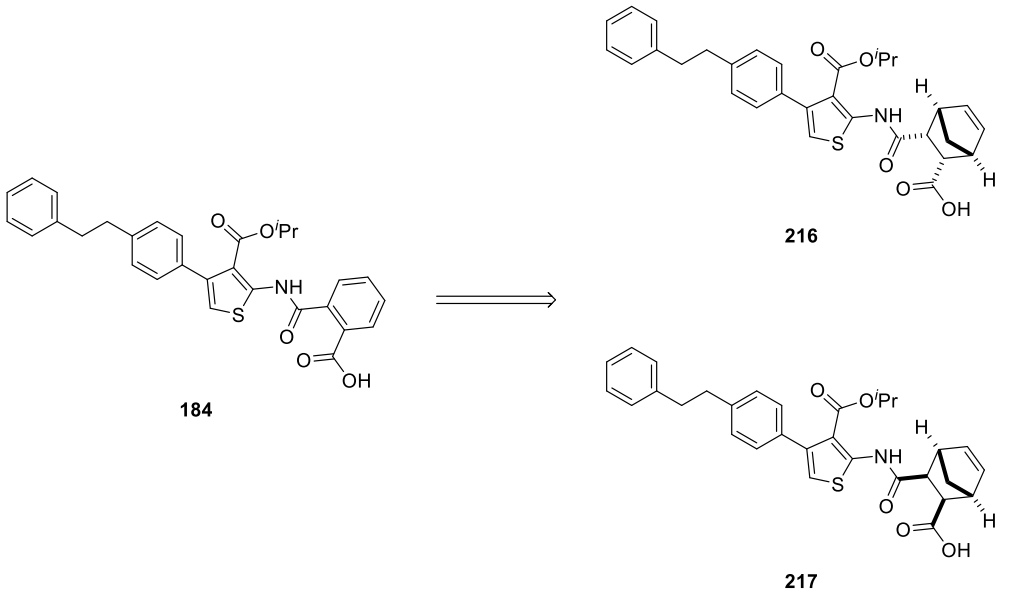

Figure 61: Proposed sp3 derivative structures based upon ligand 184.

4.2.8.2. Synthetic route

Compounds **216** and **217** were synthesised in a single synthetic step from common 2-amino thiophene intermediate **164** (Scheme 19). This permitted the streamlining of

this synthetic route in order to generate sp3 enriched analogues **216** and **217** in an efficient manner.

Scheme 19: Synthesis of compounds 216 and 217.

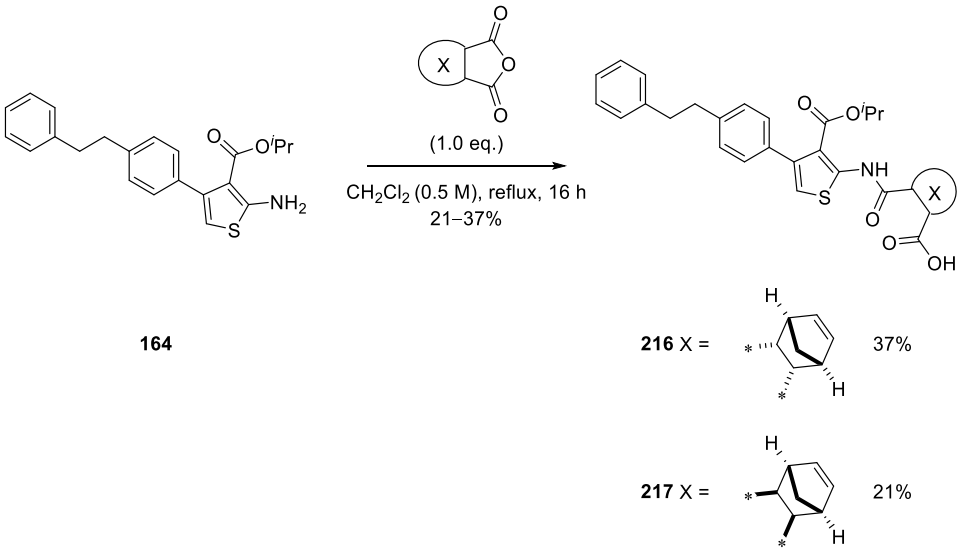

Common Gewald intermediate **164** was reacted under the general ring-opening reaction conditions for the series with the appropriate anhydride to produce final compounds **216** and **217** in low yields (21–37%). The low yields associated with this transformation were proposed to be due to the limited electrophilicity of the anhydride carbonyl groups, making nucleophilic attack from the poorly exposed lone-pair of the 2-amino thiophene derivative less favourable.

4.2.8.3. Biological evaluation

Dose response curves were generated for all the synthesised final compounds in this series using the *in vitro* assay described in Section 3.0. **Figure 62** details the structure and IC_{50} value of the parent compound **184** that directly relates to the ligands prepared in this series, for comparison purposes.

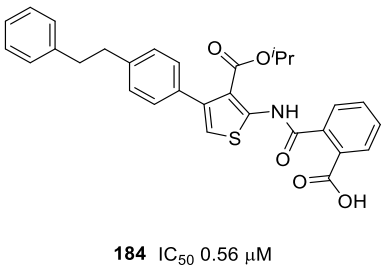

Figure 62: Parent compound 184 with respective IC_{50} values.

The IC_{50} values for sp3-hybridised ligands **216** and **217** are highlighted in **Table 10**. In comparison to the 0.56 µM IC_{50} value associated with ligand **184**, the IC_{50} data for derivatives **216** (0.82 µM) and **217** (0.95 µM) represented a loss in activity towards TIGAR. The removal of aromaticity and the depletion in lipophilicity upon moving from the phenyl of **184** to the sp3-hybridised bicyclic groups of **216** and **217**, proved to result in the dampening of activity. Pleasingly, incorporation of the three-dimensional bicycles did not result in a complete loss of target affinity, as both ligands retained sub-micromolar binding affinities. These numbers indicate that both rings adequately fit within their respective pocket of the active site and are both capable of forming favourable interactions. An approximate difference of 100 nM in potency between the two ligands highlighted that **216** (0.82 µM) adopted a subtly more optimal orientation within the orthosteric site than the diastereomeric ligand **217** (0.95 µM).

Table 10: IC_{50} values for sp3 enriched compounds 216 and 217.

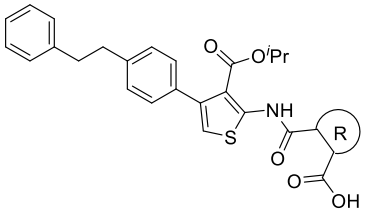

Compound	R	IC_{50} (µM)[a]
216	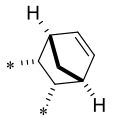	0.82 ± 0.15
217	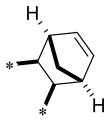	0.95 ± 0.59

[a] IC_{50} calculated as n=3

In summary, both **216** (0.82 µM) and **217** (0.95 µM) displayed reduced potency in comparison to parent ligand **184** (0.56 µM), but promisingly did not demonstrate inactivity towards the target protein, indicating that favourable binding could still be maintained. While these ligands were not as potent as the current lead compound **184**, they demonstrated sufficient potency for this type of scaffold to be considered for incorporation into lead compounds at the end of the SAR investigations. If, for

example, lead compounds at the end of the SAR have excellent potency but sub-optimal physicochemical properties and/or selectivity profiles, then these types of bicyclic motif could be introduced to improve the overall probe profile, at the expense of a slight drop in potency.

4.2.9. Amide bioisostere series

4.2.9.1. Design hypothesis

The chemical instability of the ester group was previously mentioned in the SAR outline Section 4.2.1. and it was suggested that this instability could potentially result in insufficient metabolic stability during cell and/or *in vivo* studies.[78] Substitution of the ester moiety for the more chemically stable amide isostere was suggested as a possible mitigator for the probable metabolic instability of the ester functionality. With this in mind, a new series of compounds including the amide isostere were designed, based around the generic scaffold displayed in **Figure 63**.

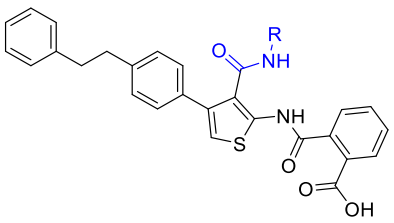

218

Figure 63: General structure of amide derivatives.

The R group appendage was heavily varied within this series, to further probe the hydrophobic pocket and identify if further potency gains could be achieved. It was possible to synthesise a wide range of substituted amides as a multitude of amines were readily available. Within the hydrophobic pocket where the amide appendage potentially positions itself, is located the Tyr92 residue, highlighted in **Figure 64**.

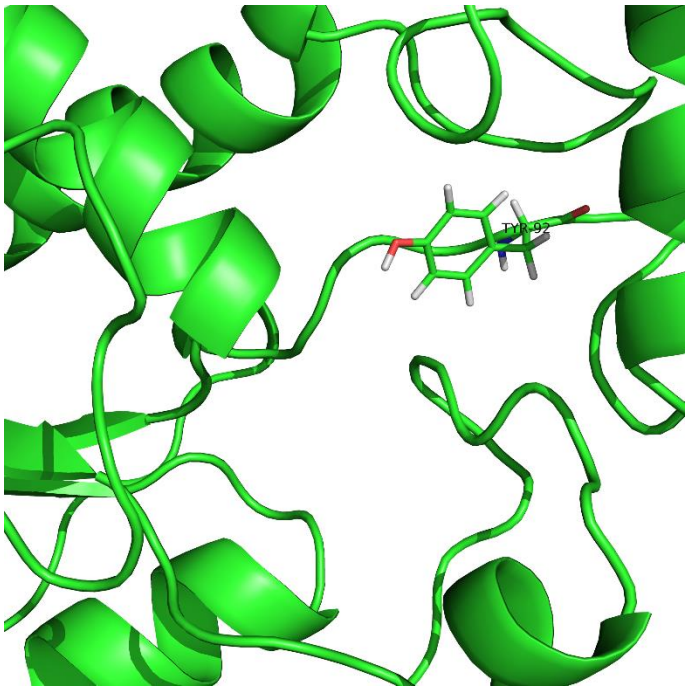

Figure 64: TIGAR active site with highlighted Tyr92 residue.

The hydroxyl unit within this head group was identified as having the potential to form hydrogen bonds with an appropriate ligand. A sub-series of compounds were designed that contained HBA atoms, to form an additional interaction with this residue, to potentially aid potency.

4.2.9.2. Synthetic route

Compounds **242**–**263** were synthesised using a 3-step synthetic route that started from common ketone starting material **144** (Scheme 20). This new synthetic sequence included the standard Gewald reaction and ring-opening steps but also introduced a single-step amidation reaction.[107] This key synthetic step permitted array chemistry to be performed with a wide range of amides being efficiently synthesised in order to greatly expand the SAR library, by invoking increased levels of structural diversity, through further functionalisation of the Gewald products.

Ketone **144** was treated with methyl cyanoacetate under general Gewald reaction conditions to afford intermediate **219** (37%) in moderate yield. Intermediate **219** was then reacted within an amidation reaction using the *bis*(trimethylaluminium-1,4-diazobicyclo[2.2.2]octane adduct (DABAL-Me_3), developed by the Woodward group,[108] and the appropriate amine to produce amide intermediates **220**–**241** (38–86%) in low to excellent yields. Intermediates **220**–**241**

were reacted in the ring-opening of phthalic anhydride to generate final compounds **242**–**263** (9–85%) in low to excellent yields.

Scheme 20: Synthesis of compounds 242–263.

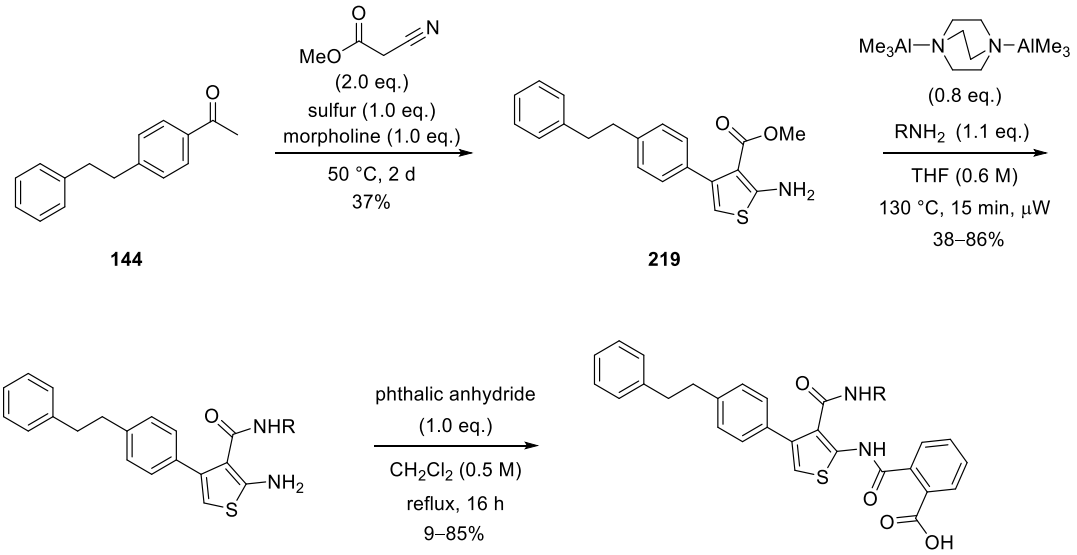

220 R = Et 38%
221 R = ^{i}Pr 74%
222 R = cyclopropyl 69%
223 R = cyclobutyl 77%
224 R = cyclopentyl 82%
225 R = cyclohexyl 72%
226 R = cycloheptyl 59%
227 R = 2-bicyclo[2.2.1]heptane 69%
228 R = methylcyclohexane 72%
229 R = CH_2CCH 40%
230 R = CH_2CF_3 80%
231 R = Ph 48%
232 R = $CH_2CH_2OCH_3$ 74%
233 R = $CH_2CH_2CH_2OCH_3$ 79%
234 R = 1-piperidine[a]
235 R = 4-THP 55%
236 R = 3-THF[a]
237 R = CH_2(3-THF) 74%
238 R = CH_2(2-THF) 60%
239 R = CH_2(2-(1,3-dioxolane)) 64%
240 R = CH_2(2-*N*-Me-pyrrolidine) 86%
241 R = CH_2CH_2(4-morpholine) 67%

242 R = Et 49%
243 R = ^{i}Pr 68%
244 R = cyclopropyl 64%
245 R = cyclobutyl 65%
246 R = cyclopentyl 64%
247 R = cyclohexyl 68%
248 R = cycloheptyl 61%
249 R = 2-bicyclo[2.2.1]heptane 71%
250 R = methylcyclohexane 70%
251 R = CH_2CCH 85%
252 R = CH_2CF_3 53%
253 R = Ph 49%
254 R = $CH_2CH_2OCH_3$ 59%
255 R = $CH_2CH_2CH_2OCH_3$ 65%
256 R = 1-piperidine 9%**
257 R = 4-THP 60%
258 R = 3-THF 39%**
259 R = CH_2(3-THF) 60%
260 R = CH_2(2-THF) 67%
261 R = CH_2(2-(1,3-dioxolane)) 57%
262 R = CH_2(2-*N*-Me-pyrrolidine) 59%
263 R = CH_2CH_2(4-morpholine) 43%

[a] compound partially purified.

The DABAL-Me_3 reagent was designed as a non-pyrophoric and more air stable variant of trimethylaluminium for safer handling and use. DABAL-Me_3 exhibits Lewis acidic properties and aided the amidation process by activating the ester carbonyl group towards nucleophilic attack by the external amine. This efficient amidation procedure offered an extra advantage over conventional amide bond forming methods, such as hydrolysis followed by amide coupling or acid chloride formation followed by nucleophilic substitution, of forming the desired amide bond

in a single step, streamlining the route. Additionally, amidation with DABAL-Me_3 mitigated the need for installing a protecting group strategy, as the increased nucleophilicity of the external amines compared to the heavily delocalised 2-amino thiophene of intermediate **219**, was enough to provide chemoselectivity. This meant that the route could be shortened by two steps and resulted in a more efficient overall synthesis.

Due to array chemistry being possible through this synthetic route, high levels of structural diversity could be generated rapidly. This enabled efficient expansion of the SAR data for the series, which aided in maximising the potential for thorough interrogation of the TIGAR active site.

4.2.9.3. Biological evaluation

Dose response curves were generated for all the synthesised final compounds in this series using the *in vitro* assay described in Section 3.0. **Figure 65** details the structure and IC_{50} value of the parent compound **184** that directly relates to the ligands prepared within this series, for comparison purposes.

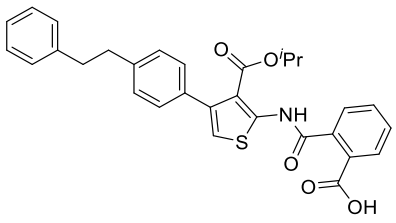

184 IC_{50} 0.56 μM

Figure 65: Parent compound with respective IC_{50} values.

The IC_{50} values for the amide bioisostere series (compound **242**–**263**) are shown in **Table 11**. The Amide derivative, where the branched isopropyl group of ester **184** (0.56 μM) was switched for the smaller ethyl (**242** 0.51 μM) chain unit, resulted in negligible changes in activity, with the ethyl unit providing a marginal increase in potency. This was interesting, as the previous ethyl (**81** 48 μM) ester species had displayed a large drop-off in activity compared to an equivalent isopropyl analogue (**83** 8.5 μM). This suggested that the amide bond was potentially adopting a different conformation compared to the ester linkage, resulting in the alteration of the substituent interactions in the process. This proposal was reinforced by the directly

comparable isopropyl ligand (**243** 0.45 μM), as this compound exhibited an approximately 100 nM improvement in potency compared to the equivalent isopropyl ester derivative (**184** 0.56 μM). This was a highly desirable result as the modification from ester to amide, had not only enhanced chemical stability but had also improved TIGAR activity. This result supported the hypothesis that the amide appendage interactions were being enhanced, due to the amide motif potentially adopting an alternative conformation, compared to its ester counterpart.

Table 11: IC_{50} values for amide bioisostere compounds 242–263. Compound 243 IC_{50} curve.

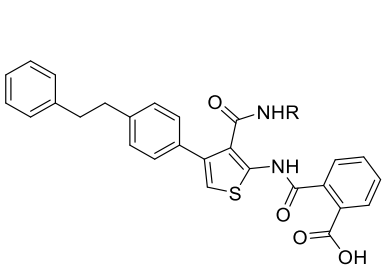

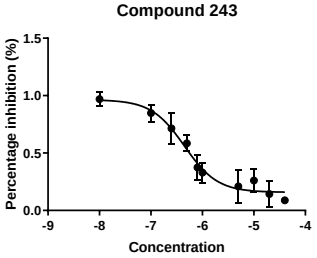

Compound	R	IC_{50} (μM)[a]	Compound	R	IC_{50} (μM)[a]
242	Et	0.51 ± 0.02	**253**	Ph	0.28 ± 0.07
243	^{i}Pr	0.45 ± 0.04	**254**	$CH_2CH_2OCH_3$	0.41 ± 0.94
244	cyclopropyl	0.51 ± 0.05	**255**	$CH_2CH_2CH_2OCH_3$	2.4 ± 0.57
245	cyclobutyl	0.48 ± 0.02	**256**	1-piperidine	0.40 ± 0.11
246	cyclopentyl	0.44 ± 0.01	**257**	4-THP	0.40 ± 0.08
247	cyclohexyl	0.38 ± 0.02	**258**	3-THF	0.48 ± 0.03
248	cycloheptyl	>20	**259**	CH_2(3-THF)	0.69 ± 0.08
249	2-bicyclo[2.2.1]heptane	>20	**260**	CH_2(2-THF)	0.36 ± 0.11
250	methylcyclohexane	0.82 ± 0.06	**261**	CH_2(2-(1,3-dioxolane))	0.31 ± 0.08
251	CH_2CCH	0.60 ± 0.01	**262**	CH_2(2-*N*-methyl-pyrrolidine)	0.48 ± 0.03
252	CH_2CF_3	0.39 ± 0.05	**263**	CH_2CH_2(4-morpholine)	> 20

[a] IC_{50} calculated as n=3

In order to determine the effect that increasing amide substituent ring size had on potency, as well as how much steric bulk could be accommodated within the pocket, a sub-series of cyclic amides with increasing ring size (**244**–**249**) were tested against TIGAR. Compared to isopropyl ligand **243** (0.45 μM), small rings such as cyclopropyl derivative **244** (0.51 μM) resulted in a loss in potency with a value comparable to that of ethyl **242** (0.51 μM). Medium ring sized cyclobutyl (**245**

0.48 µM) and cyclopentyl (**246** 0.44 µM) analogues exhibited comparable potency values, whilst the bulkier cyclohexyl group (**247** 0.38 µM) revealed a small increase in binding affinity compared to compound **243** (0.45 µM). These results demonstrated that a clear parallel existed between increasing ring size and improved potency, which reinforced the data observed within the earlier ester series of Section 4.2.2. However, upon expansion to the 7-membered cyclohexyl derivative (**248** > 20 µM) or modification to a non-planar derivative (**249** >20 µM), a complete loss of activity was observed. This data indicates that the steric capacity of the hydrophobic pocket had been discovered, and that ring sizes of > 6, as well as non-planar bicycles were not tolerated at this position of the ligand scaffold. Interestingly, incorporation of a methylcyclohexane unit (**250** 0.82 µM) delivered a drop in potency compared to parent compound **184** (0.56 µM) but did not result in complete inactivity towards the target. This result suggested that the additional rotation enabled through the methylene unit, allowed steric clashes within the pocket to be minimised to a small extent, as there was still an observed decrease in potency.

Three additional lipophilic substituent-based derivatives were evaluated in the *in vitro* assay. Alkyne analogue **251** (0.60 µM) demonstrated a marginal decrease in potency compared to that of the parent compound (**184** 0.56 µM), highlighting that linear/rigid substituents presented no immediate benefit to activity values within the series. Introduction of alternative lipophilic moieties (compounds **252** and **253**) led to more favourable potency values. Trifluoromethyl derivative **252** (0.39 µM) resulted in a small potency gain from increased lipophilic interactions as well as potential halogen hydrogen bonding. The phenyl substituent (**253** 0.28 µM) induced a more noticeable increase in potency by approximately 150 nM compared to isopropyl amide **243** (0.45 µM), presumably due to heightened VDW interactions within the pocket from the presence of the aromatic functionality.

As previously mentioned in the design hypothesis Sub-section 4.2.9.1., one of the residues involved in the formation of the hydrophobic pocket where the R groups orientate, is Tyr92, which possessed an exposed hydroxyl moiety capable of acting as a HBD. To try and exploit this potential interaction, a sub-series of substituents with the potential for acting as HBAs were screened against TIGAR to identify if a further potency increase could be achieved.

The addition of acyclic ethers (compounds **254** 0.41 µM and **255** 2.4 µM) revealed a correlation between chain length and potency; the shorter ether **254** improved potency compared to the parent ester compound **184** (0.56 µM) but the longer ether variant **255** proved detrimental to potency. This data reinforced previous patterns in this pocket that subtle variations in structure can exhibit significant changes in activity. Except for two derivatives (compounds **259** 0.69 µM and **263** > 20 µM), all tested saturated heterocyclic ligands (compounds **256–258** 0.40–0.48 µM & **260–262** 0.31–0.48 µM) afforded minor to moderate gains in potency compared to parent ester compound **184** (0.56 µM). In particular, the 1,3-dioxolane ligand (**261** 0.31 µM), which contained two HBA atoms, demonstrated the largest gain in potency. The data suggested that these compounds were potentially interacting with the hydroxyl moiety of Tyr92. Comparison of the CH_2(3-THF) ligand **259** (0.69 µM) and the CH_2(2-THF) analogue **260** (0.36) demonstrated that the positioning of the HBA atom was essential for potency, as moving the oxygen heteroatom around the ring by one atom, resulted in a 300 nM potency difference. Different heteroatoms acting as the HBA (compound **260** 0.36 µM vs **262** 0.48 µM) were also tolerated, however, oxygen-based heterocycle **260** proved to be more effective with an approximately 100 nM increase in potency. The complete loss of activity associated with ligand **263** (> 20 µM) was proposed to be related to unfavourable steric interactions. This was reinforced by molecular modelling data, as the docking programme failed to fit this ligand into the active site of TIGAR.

In summary, initial modification of the isopropyl ester **184** (0.56 µM) to the isopropyl amide **243** (0.45 µM), afforded an improvement in chemical stability as well as an approximate 100 nM increase in potency. The shorter chain-length substituent **242 (**0.51 µM), resulted in a loss of activity within the amide series (*c.f.* **243** 0.45 µM) but not as severe a loss as that experienced with the analogous compounds in the previously discussed ester Section 4.2.2., suggesting that the amide group was potentially adopting an alternative conformation compared to the ester motif. The potential extent of hydrophobic interactions and the point of steric restriction, within the small lipophilic pocket, were assessed through the formation of various cyclic amides. As R changes from the 3-membered cyclopropyl to the 6-membered cyclohexyl (compounds **244–247** 0.51–0.38 µM), a minimal but steady increase in potency occurred, which reinforced a previously described dynamic

between lipophilicity and binding affinity. However, with the 7-membered cycloheptyl group or the sp3-enriched bicycle (compounds **248** and **249** > 20 μM), the associated steric encumbrance resulted in inactivity at the target. Maintaining increased levels of steric bulk in the form of methylhexane derivative **250** (0.81 μM) resulted in a reduction in activity but not a complete loss, suggesting that the added flexibility allows a more favourable orientation to be adopted in comparison to ligands **248** and **249**. Linear alkyne ligand **251** resulted in a decrease in potency, however, introduction of alternative lipophilic moieties (compounds **252** 0.39 μM and **253** 0.28 μM) led to more favourable potency values through optimised hydrophobic and VDW interactions, with the surrounding residues of the pocket. Acyclic ether addition initially revealed a correlation between chain length and potency; the shorter ether (compound **254** 0.41 μM) improved potency but the longer variant (compound **255** 2.4 μM) proved detrimental. The majority of the saturated heterocyclic ligands (compounds **256–258** 0.40–0.48 μM & **260–262** 0.31–0.48 μM) afforded minor to moderate gains in potency. The 1,3-dioxolane ligand (**261** 0.31 μM), demonstrated the largest improvement in binding affinity. Ethyl morpholine ligand **263** (> 20 μM) was inactive towards TIGAR as the protein was unable to accommodate the steric bulk related to this derivative. The data within this series supported the design theory that a potential hydrogen bonding interaction with the exposed Tyr92 residue could be exploited for potency improvement. Positioning of the HBA atom (compound **259** 0.69 μM vs **260** 0.36 μM) and the choice of heteroatom (compound **260** 0.36 μM vs **262** 0.48 μM) within the amide substituent were also found to be influential, with regards to potency.

The amide series helped greatly to aid understanding of the properties and finer details associated with the TIGAR pocket, however, none of the tested ligands provided any significant potency advances over the original isopropyl amide. The cyclohexyl ligand **247** (0.38 μM) and the CF_3 analogue **252** (0.39 μM) both exhibited a small increase in potency compared to **243** (0.45 μM). However, these compounds had moved significantly further away from the ideal Lipinski Rule of 5 M.wt value of 500 (**247** M.wt = 552 & **252** M.wt = 552 vs **243** M.wt = 512),[109] which made the potency gain for the M.wt increase inefficient. Phenyl derivative **253** (0.28 μM) also demonstrated an improved potency compared to ligand **243** (0.45 μM) but the number of aromatic rings in compound **253** had now reached 5 in total, which was known to have a negative effect on other physicochemical properties.[110] Saturated

heterocycle derivatives **260** (0.36 µM) and **261** (0.31 µM) had also shown improvements in potency compared to isopropyl **243** (0.45 µM), however, again the potency gains were not substantial enough to justify the increase in M.wt (**260** M.wt = 554 & **261** M.wt = 556). Additionally, the dioxolane moiety of ligand **261** is a cyclic acetal functionality and therefore, may become unstable in a weakly acidic environment such as in the gut if *in vivo* studies were attempted. As a result, the isopropyl amide **243** was chosen as the optimised compound from this series to take forward into future studies.

4.2.10. Channel substituent series 2

4.2.10.1. Design hypothesis

In channel substituent 1 Section 4.2.5., it was proposed, according to the computational model for the series, that the outer phenyl ring of compound **184** (Figure 66) was possibly extending beyond the hydrophobic channel of the active site and adopting a potential π-cation interaction with an exposed arginine residue (Arg 192, Figure 66).

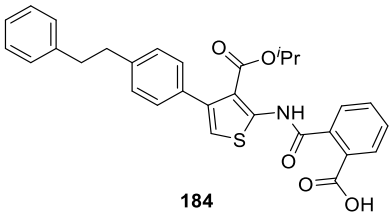

184

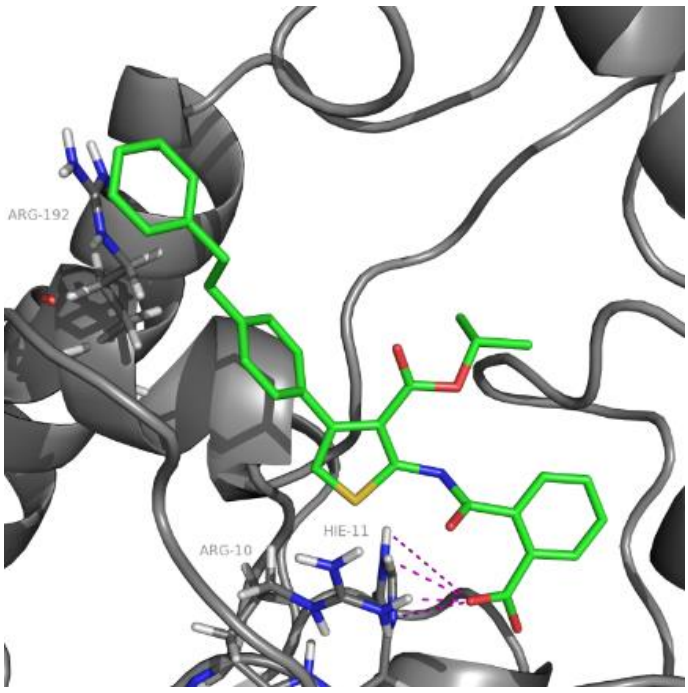

Figure 66: Compound 184 docked in TIGAR. Magenta dash = electrostatic interactions.

Using the hypothesised binding mode, it was proposed that differing the substitution pattern on the outer phenyl ring of the channel substituent with anionic functionalities, could potentially alter the interaction with the arginine residue to an electrostatic one. To test this idea, multiple compounds comprised of carboxylic acid derivatives of the outer phenyl ring were designed, based around scaffold **264** (Figure 67).

It was also hypothesised that altering the electronics of the outer phenyl group and adding in heteroatoms for potential hydrogen bonding, may also alter interactions with the exposed arginine residue. As a result, a second set of compounds, where the outer phenyl motif of **184** was varied for a range of heterocycles that differed in size and properties, were designed based around scaffold **265** (Figure 67). All compounds in this series were designed to contain the ether linkage within the channel substituent, as this made the synthetic route more tractable, allowing the efficiency of compound synthesis to be improved. The ether linkage compounds had also been hypothesised to adopt very similar binding modes to the di-methylene compound **184** within the active site, meaning that potency values should be comparable.

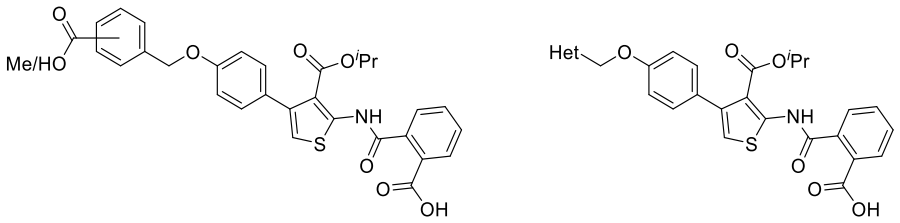

Figure 67: Channel substituent series 2 scaffolds.

4.2.10.2. Synthetic route

Carboxylic acid derivatives **277**–**280** were synthesised using the 4-step synthesis outlined in **Scheme 21**. The route included the essential multicomponent Gewald reaction and ring-opening process, as well as an initial alkylation step and an additional selective hydrolysis procedure to furnish carboxylic acid compounds **278**–**280**.

Commercially available bromide starting materials **266**–**268** were reacted with 4-hydroxy acetophenone under alkylation conditions, to produce alkylated ketones **269**–**271** (88–95%) in excellent yields.[111] Ketones **269**–**271** were then treated with the common Gewald reaction conditions using *tert*-butyl cyanoacetate, to afford 2-

amino thiophene intermediates **272**–**274** (26–33%), in low to moderate yields. 2-Amino thiophene derivatives **272**–**274** were subjected to the ring-opening of phthalic anhydride to generate carboxylic acid compounds **275**–**277** (44–74%) in moderate to good yields. The final transformation on this synthetic route involved the selective hydrolysis of intermediates **275**–**277** to furnish final di-acid compounds **278**–**280** (66–72%) in good yields.[93] The isopropyl ester had originally been used at the 3-position of the thiophene ring instead of the *tert*-butyl ester, however, this led to partial hydrolysis of the ester group which generated an undesired tri-acid species. Since the strongly basic (2.0 M NaOH) conditions for hydrolysis enforced a $B_{AC}2$ mechanism for ester hydrolysis, it was hypothesised that incorporating a *tert*-butyl ester at the 3-position of the thiophene ring, should have allowed for selective hydrolysis of the methyl ester. This theory proved to be correct as selective hydrolysis of the methyl ester was possible, however, care had to be taken when lowering the pH during work-up, as a pH value of < 5 resulted in partial *tert*-butyl group cleavage.

Scheme 21: Synthesis of compounds 277–280.

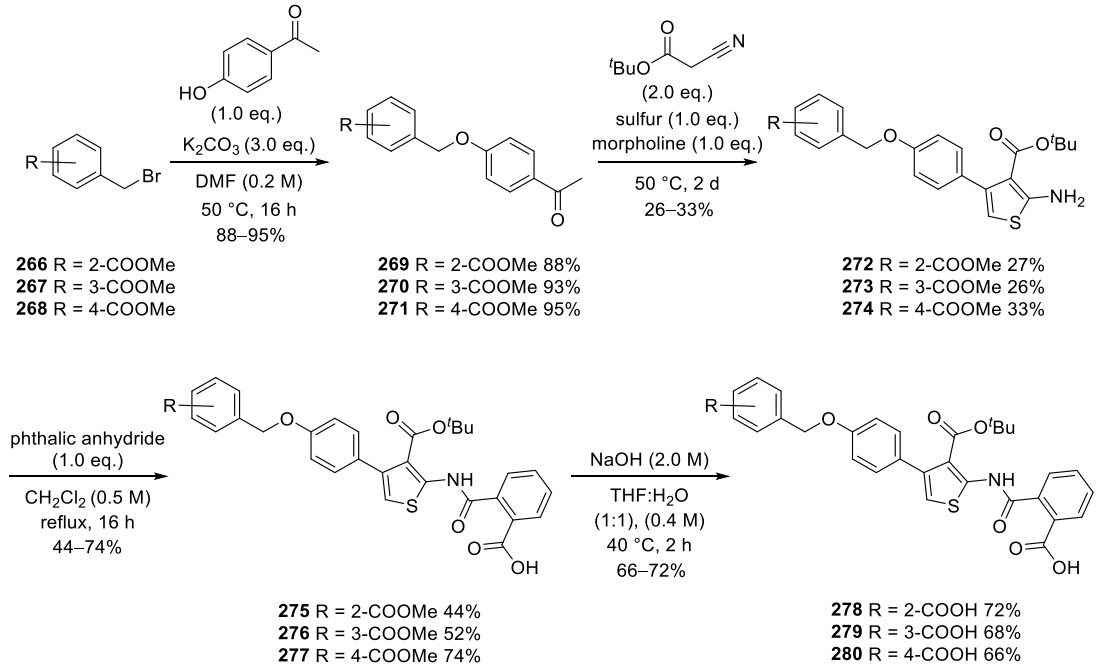

Two of the designed heterocyclic derivatives (**289** and **290**) were synthesised in their own individual 4-step synthetic routes outlined in **Scheme 22**. Both of these routes involved initial alkylation steps before 1,3-dipolar cycloaddition reactions were used to generate the respective heterocycles. Each sequence then culminated with the standard multicomponent and ring-opening steps to generate compounds **289** and **290**.

Scheme 22: Synthesis of compounds 289–290.

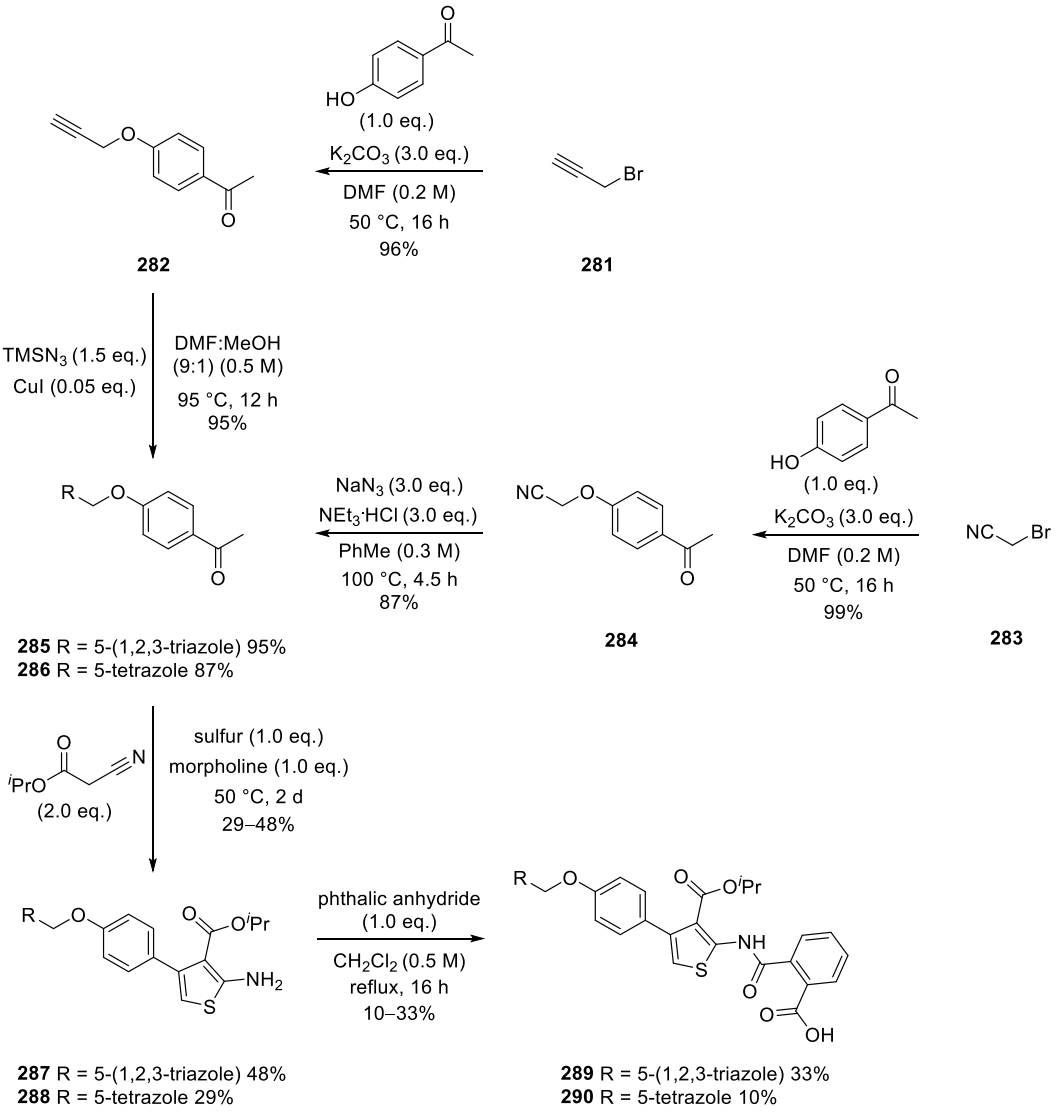

Propargyl bromide **281** was reacted with 4-hydroxy acetophenone under alkylation conditions, to afford alkyne derivative **282** (96%) in excellent yield. Compound **282** was subsequently used in a 1,3-dipolar cycloaddition reaction, more commonly known as a 'click' reaction, involving trimethylsilylazide ($TMSN_3$) and a copper(I) catalyst (CuI).[112] This produced the 5-substituted 1,2,3-triazole intermediate **285** (95%) in excellent yield. Commercially available bromo acetonitrile starting material **283** was also initially treated with 4-hydroxy acetophenone under alkylation conditions to generate cyano derivative **284** (99%) in quantitative yield. In a similar manner to intermediate **282**, compound **284** was reacted in a 1,3-dipolar cycloaddition reaction using NaN_3 to form the 5-substituted tetrazole intermediate **286** (87%) in excellent yield.[94] Both heterocyclic intermediates **285** and **286** were used as components within the Gewald reaction, along with isopropyl cyanoacetate, to produce 2-amino thiophene analogues **287** (48%) and **288** (29%) in moderate

yields, respectively. Intermediates **287** and **288** were subsequently used to ring-open phthalic anhydride in order to generate two final compounds; 1,2,3-triazole **289** (33%) and tetrazole **290** (10%) in moderate and low yields, respectively. The particularly low yields associated with the tetrazole derivative was a result of a difficult purification, as this final compound and its starting material **288** were both very polar and co-eluted from the column.

Most of the heterocycles synthesised within this series were formed through the 4-step synthetic route depicted in **Scheme 23**. This sequence involved initial activation of a starting hydroxyl motif, before subsequent alkylation to prepare the ketone component of the Gewald reaction. The last 2-steps were comprised of the standard multicomponent and ring-opening steps, which led to the formation of compounds **323**–**330**.

Scheme 23: Synthesis of compounds 323–330.

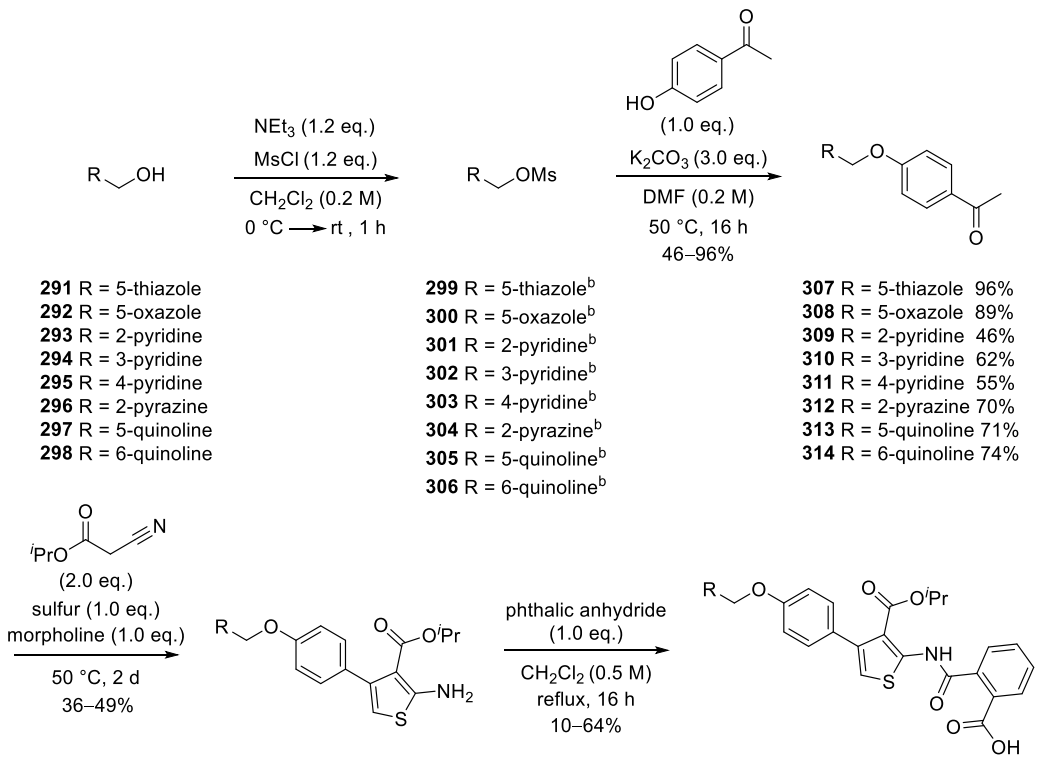

291 R = 5-thiazole
292 R = 5-oxazole
293 R = 2-pyridine
294 R = 3-pyridine
295 R = 4-pyridine
296 R = 2-pyrazine
297 R = 5-quinoline
298 R = 6-quinoline

299 R = 5-thiazole[b]
300 R = 5-oxazole[b]
301 R = 2-pyridine[b]
302 R = 3-pyridine[b]
303 R = 4-pyridine[b]
304 R = 2-pyrazine[b]
305 R = 5-quinoline[b]
306 R = 6-quinoline[b]

307 R = 5-thiazole 96%
308 R = 5-oxazole 89%
309 R = 2-pyridine 46%
310 R = 3-pyridine 62%
311 R = 4-pyridine 55%
312 R = 2-pyrazine 70%
313 R = 5-quinoline 71%
314 R = 6-quinoline 74%

315 R = 5-thiazole 47%
316 R = 5-oxazole 43%
317 R = 2-pyridine 46%
318 R = 3-pyridine 47%
319 R = 4-pyridine 41%
320 R = 2-pyrazine 36%
321 R = 5-quinoline 41%
322 R = 6-quinoline 49%

323 R = 5-thiazole 64%
324 R = 5-oxazole 53%
325 R = 2-pyridine 45%
326 R = 3-pyridine 49%
327 R = 4-pyridine 63%
328 R = 2-pyrazine 10%
329 R = 5-quinoline 51%
330 R = 6-quinoline 55%

[b] compounds unstable - used crude

The hydroxyl groups of the commercially available starting materials **291**–**298** had to initially be activated for substitution by an appropriate nucleophilic species. To this end, hydroxyl starting materials **291**–**298** were treated under mesylation conditions at 0 °C, to afford electrophilic mesylated derivatives **299**–**306**.[113] Due to the increased reactivity of the mesylate group, derivatives **299**–**306** proved to be unstable and partial decomposition was observed by ^{1}H NMR spectroscopy within half an hour of synthesis. Accurate yields could therefore not be calculated for these compounds and they were instead taken on as a crude mixture into the next step. Mesylated intermediates **299**–**306** were reacted under alkylation conditions, using 4-hydroxy acetophenone, to generate ketone derivatives **307**–**314** (46–96%) in moderate to excellent yields.[111] Isolated yields of compounds **307**–**314** varied depending on the extent of decomposition of the mesylated starting material. Ketone intermediates **307**–**314** were used as components in the Gewald reaction, along with isopropyl cyanoacetate, to deliver 2-amino thiophene derivatives **315**–**322** (36–49%) in moderate yields. Intermediates **315**–**322** were subsequently reacted in the ring-opening of phthalic anhydride to afford a multitude of highly functionalised heterocyclic analogues **323**–**330** (10–64%), in low to good yields. The lower yields such as that observed for the 2-pyrazine ligand **328** (10%), were due to difficulties involved with purification, as this final compound and its starting material **320** were both very polar and co-eluted from the column.

Derivatives **277**–**280**, **289**, **290** and **323**–**330** were prepared to further explore the hydrophobic channel and to assess the effect that changing the electronics of the outer phenyl group had on potency.

4.2.10.3. Biological evaluation

Dose response curves were generated for all the synthesised final compounds in this series using the *in vitro* assay described in Section 3.0. **Figure 68** details the structures and IC_{50} values of the parent compounds **183** and **184** that directly relate to the ligands prepared in this series, for comparison purposes.

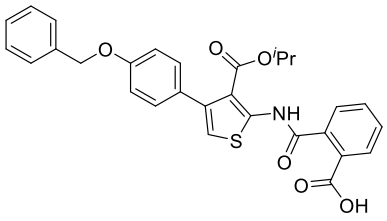

183 IC_{50} 0.77 μM

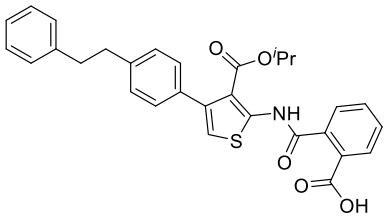

184 IC_{50} 0.56 μM

Figure 68: Parent compounds with respective IC_{50} values.

The IC_{50} values for channel substituent series 2 compounds containing a substituted phenyl group (compounds **277**–**280**) are displayed in **Table 12**.

Table 12: IC_{50} values for carboxylate compounds 277–280.

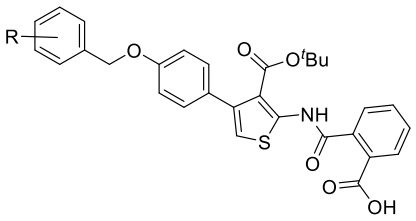

Compound	R	IC_{50} (μM)[a]
277	4-COOMe	0.82 ± 0.05
278	2-COOH	0.48 ± 0.07
279	3-COOH	0.41 ± 0.05
280	4-COOH	0.54 ± 0.08

[a] IC_{50} calculated as n=3

In comparison to parent ligand **183** (0.77 μM), the addition of a carboxylic acid to the external phenyl ring of the channel substituent (compounds **278** 0.48 μM, **279** 0.41 μM, **280** 0.54 μM) improved potency by 200–300 nM, with *meta*-substitution (**279**) proving to be superior, as this ligand also produced a 100 nM increase in potency compared to parent ligand **184** (0.56 μM). The potency associated with this sub-series was supported by docking studies, such as that of ligand **279** (Figure 69). The model hypothesised that the external phenyl ring was no longer packing against Arg192 but was instead possibly binding deeper within the pocket, which orientated the carboxylic acid appendage in a manner that allowed for potential interactions with Arg192. The *in vitro* assay data, coupled with the docking studies, suggested that the anionic carboxylic acid-based derivatives were potentially forming an electrostatic interaction with the nearby Arg192 residue. The data also

indicated that the alignment for this new interaction remained unoptimised, as a larger associated potency increase would normally be expected for this type of intermolecular binding. This hypothesis was further cemented by methylated analogue **277** (0.82 μM), as a reduction in binding affinity was observed for this compound when compared to the analogous acid derivative **280** (0.54 μM). This approximate 250 nM decrease in potency suggested that ligand **277** was still binding favourably within the TIGAR active site and that the loss in activity was not the result of a steric clash but was instead due to the theorised electrostatic interaction with the flanking Arg192 residue being potentially disrupted.

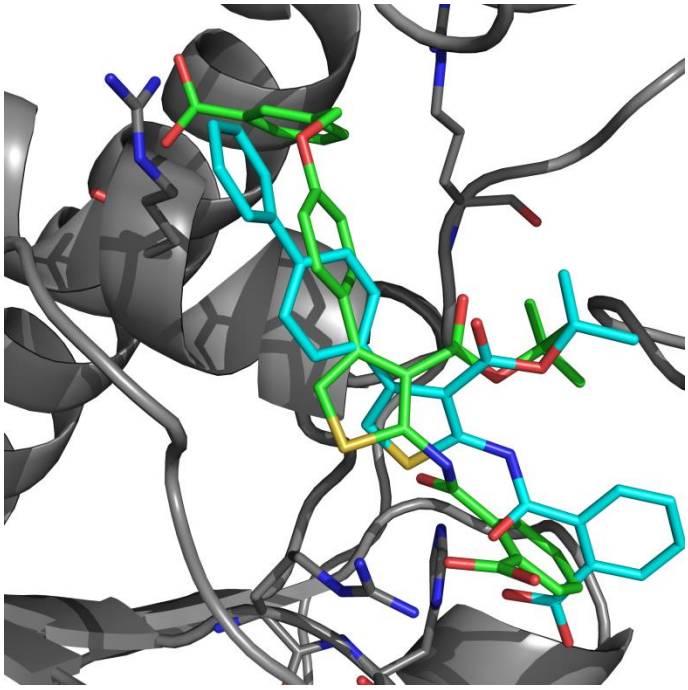

Figure 69: 3-COOH ligand 279 and reference compound 83 docked within the active site of TIGAR.

The IC_{50} data for the channel substituent series 2 ligands bearing an external heterocycle motif are described in **Table 13**. Ligands with channel substituents bearing a polar 2–3 heteroatom 5-membered heterocycle (**289** 0.67 μM, **323** 0.62 μM and **324** 0.55 μM) all generally produced a modest increase in potency compared to parent compound **183** (0.77 μM). These results suggested that the 5-membered heterocycles were potentially acting as HBA motifs and forming a favourable hydrogen bond with the neighbouring Arg192 amino acid, or that they were possibly forming a π-cation relationship, with oxazole **324** demonstrating the largest activity gain (~200 nM). However, all three ligands exhibited potencies that were either less

than or equivalent to that of the parent phenyl ethyl ligand **184** (0.56 μM), potentially highlighting that optimal alignment for intermolecular interactions between Arg192 and the heterocycles had not been achieved. A similar scenario was depicted for the anionic tetrazole analogue **190** (0.52 μM), as this ligand exhibited an increase in potency compared to benzyloxy ligand **183** (0.77 μM) but only a negligible increase in activity over ligand **184** (0.56 μM).

Table 13: IC_{50} values for channel derivatives 289, 290 and 323–330. Compound 328 IC_{50} curve.

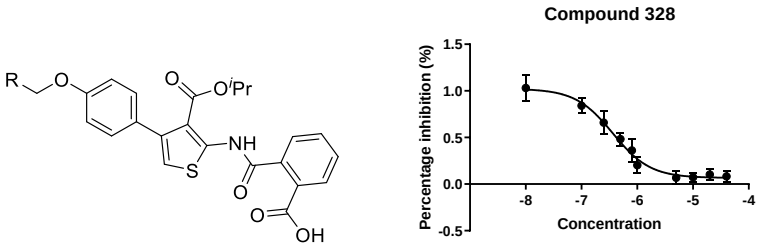

Compound	R	IC_{50} (μM)[a]
289	5-(1,2,3-triazole)	0.67 ± 0.11
290	5-tetrazole	0.52 ± 0.05
323	5-thiazole	0.62 ± 0.07
324	5-oxazole	0.55 ± 0.09
325	2-pyridine	0.43 ± 0.05
326	3-pyridine	0.48 ± 0.07
327	4-pyridine	0.59 ± 0.06
328	2-pyrazine	0.37 ± 0.03
329	5-quinoline	0.91 ± 0.10
330	6-quinoline	1.1 ± 0.06

[a] IC_{50} calculated as n=3

Incorporation of 6-membered heterocycles as the R group that contained a single heteroatom (**325** 0.43 μM, **326** 0.48 μM and **327** 0.59 μM), had varying effects on potency. The 4-pyridine channel substituent **327** (0.59 μM) displayed a similar profile to that observed with the 5-membered heterocycles, as **327** had increased potency compared to ligand **183** (0.77 μM) but was essentially equipotent with parent compound **184** (0.56 μM). This data again potentially suggested that either the nitrogen atom of the pyridine ring was acting as a HBA towards Arg192, or the pyridine ring was possibly packing against this same residue but that the interaction was sub-optimal. The 2- (**325** 0.43 μM) and 3-pyridine (**326** (0.48 μM) ligands

revealed a 100–150 nM increase in binding affinity relative to the analogous 4-pyridine derivative (**327** 0.59 μM), which indicated that hydrogen bonding or π-cation interactions had been improved. A pyrazine heterocycle, comprised of two nitrogen atoms (compound 0.37 μM), promoted a further increase in potency, to generate a new lead compound that was now 400 nM more potent than parent ligand **183** (0.77 μM) and 200 nM more potent than parent ligand **184** (0.56 μM). **Figure 70** shows a docking diagram for ligand **328**, which suggested that the pyrazine head group was no longer stacking against Arg192 but was instead proposed to be burrowing deeper into the channel and potentially forming a hydrogen bond with Arg192. The model also indicated that the second nitrogen atom of the pyrazine heterocycle was also possibly interacting with a second flanking and exposed arginine residue (Arg90), which may explain the further potency optimisation observed with compound **328** (0.37 μM).

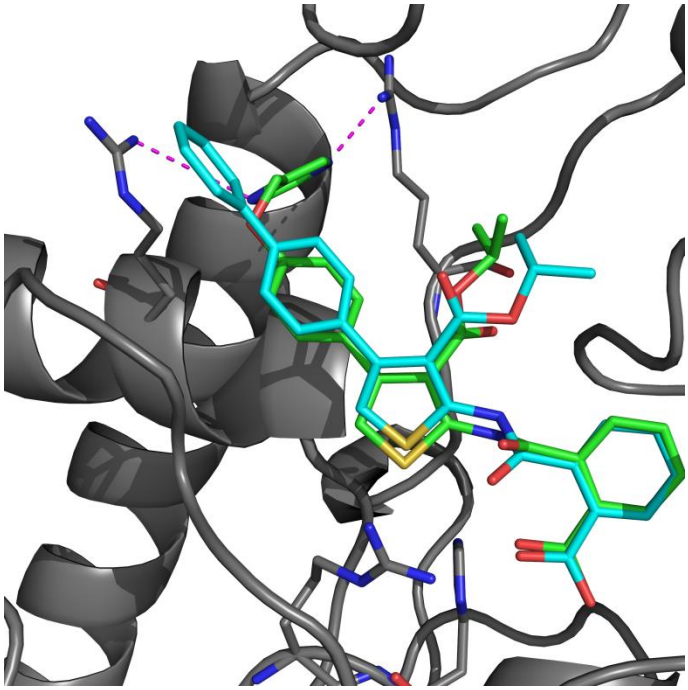

Figure 70: Pyrazine ligand 328 and reference compound 83 docked within the active site of TIGAR. Key Hydrogen bonding interactions are highlighted by magenta dashes.

The final compounds tested within this section of the SAR were fused heterocycles **329** (0.91 μM) and **330** (1.1 μM). Both of these quinoline derivatives provided a loss in activity, when compared to parent compounds **183** (0.77 μM) and **184** (1.1 μM), suggesting that any potential interactions within the channel of the active site have been disrupted. The molecular dockings of these compounds (Figure 71, A and B) highlighted potential reasons for this loss of favourable interactions. In comparison

to the docking diagram of pyrazine ligand **328** (Figure 70), both diagrams in **Figure** 71 showed that the quinoline heterocycle had possibly flipped out of the channel substituent pocket, suggesting a potential steric clash with the protein was occurring. Additionally, the quinoline segments are now both proposed to be projecting out towards solvent, which would incur a negative enthalpic penalty. Both of these proposals help to justify the observed loss in binding affinity.

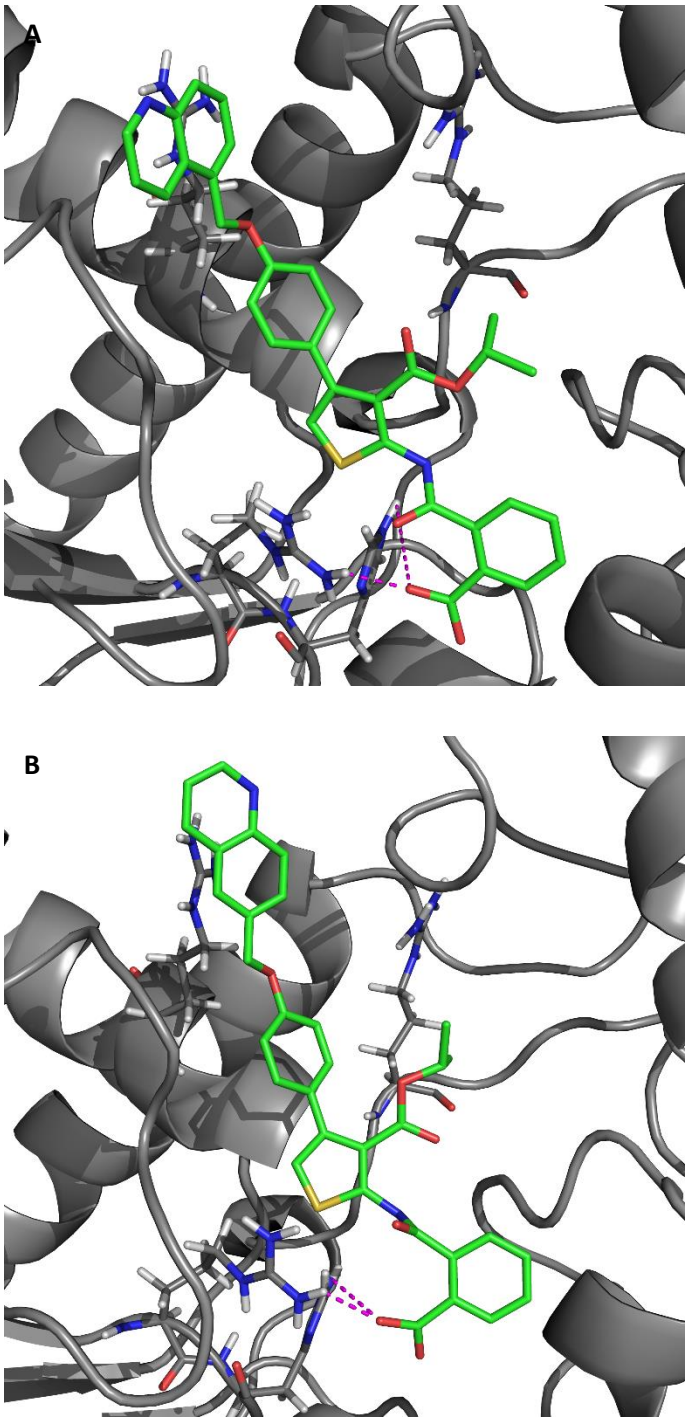

Figure 71: Quinoline ligands 329(A) and 330 (B) docked within the active site of TIGAR. Key electrostatic interactions are highlighted by magenta dashes.

In summary, accumulated data for this series of compounds indicated that substituting the terminal phenyl of ligands **183** or **184** for a heterocyclic or an anionic species, was beneficial for potency (Table 13). In comparison to parent ligand **183** (0.77 μM), the addition of a carboxylic acid to the external phenyl ring (compounds **278** 0.48 μM, **279** 0.41 μM, **280** 0.54 μM) improved potency, with *meta*-substitution (**279**) proving to be superior, as this ligand also produced a 100 nM increase in potency compared to parent ligand **184** (0.56 μM). Biochemical potency data suggested that these anionic species were potentially forming an interaction with Arg192 but that the alignment was sub-optimal. This was reinforced by methylated derivative **277** (0.82 μM) as a drop-off in potency was observed, signifying that ligand **277** was still possibly binding favourably within the pocket but that favourable electrostatic interactions with Arg192 could have been disrupted. The alternative anionic R substituent (compound **290** 0.52 μM) displayed a similar profile to the substituted acid derivatives as **290** achieved only a negligible increase in potency compared to parent ligand **184** (0.56 μM).

5-Membered heterocycles comprised of 2–3 heteroatoms (**289** 0.67 μM, **323** 0.62 μM and **324** 0.55 μM), all generally produced a modest increase in potency compared to parent compound **183** (0.77 μM). However, all of these ligands demonstrated binding affinities that were shown to be less than or equal to the activity of ligand **184** (0.56 μM). This was proposed to be due to unfavourable alignment for hydrogen bonding and/or π-cation interactions with Arg192. 6-Membered pyridine heterocycles (**325** 0.43 μM, **326** 0.48 μM and **327** 0.59 μM) generally fared better; an increase in potency was observed for all except the 4-pyridine analogue **327** (0.59 μM). The nitrogen atoms of the 2- and 3-pyridine analogues appeared to be well-positioned for interaction with Arg192. This inspired the incorporation of a pyrazine motif in ligand **328** (0.37 μM), which led to the identification of the pyrazine heterocycle as the optimised functionality for binding beyond the hydrophobic channel of TIGAR. Docking studies indicated that the pyrazine moiety was potentially acting as a HBA towards two neighbouring arginine residues instead of forming a π-cation interaction. Quinoline head groups (compounds **329** 0.91 μM and **330** 1.1 μM) proved deleterious to binding affinity. Based upon the molecular model for the series, this was proposed to be for steric reasons as both tail groups were hypothesised to be too large to position themselves in the active site, which

potentially led to them adopting an unfavourable geometry and undesirable interactions with solvent.

4.2.11. Hybrid series 2

4.2.11.1. Design hypothesis

A robust and extensive SAR study had now been performed by this stage in the project, enabling an in-depth interrogation of the TIGAR active site to be conducted. As a result, a vastly improved understanding of the characteristics, that govern the different parts of the TIGAR binding pocket, had now been established.

The final series within the SAR programme consisted of designing a second series of hybrid compounds, based around scaffold **331** (Figure 72). Hybrid ligands on this series brought together the optimised pyrazine group of **328**, for enhanced binding beyond the hydrophobic channel and the amide bioisostere **243** for improved metabolic stability. The X and Y components of the channel substituent linker portion were varied to confirm and finalise previously observed activity patterns. Metabolic hotspot analysis had identified position Z of scaffold **331** as one of multiple potential sites for oxidation when Y was an oxygen atom (Figure 73). This led to the design of a fluorinated derivative where Z = CF, as the altered electronics associated with this substitution should mitigate any metabolic problems at this position.[114-116]

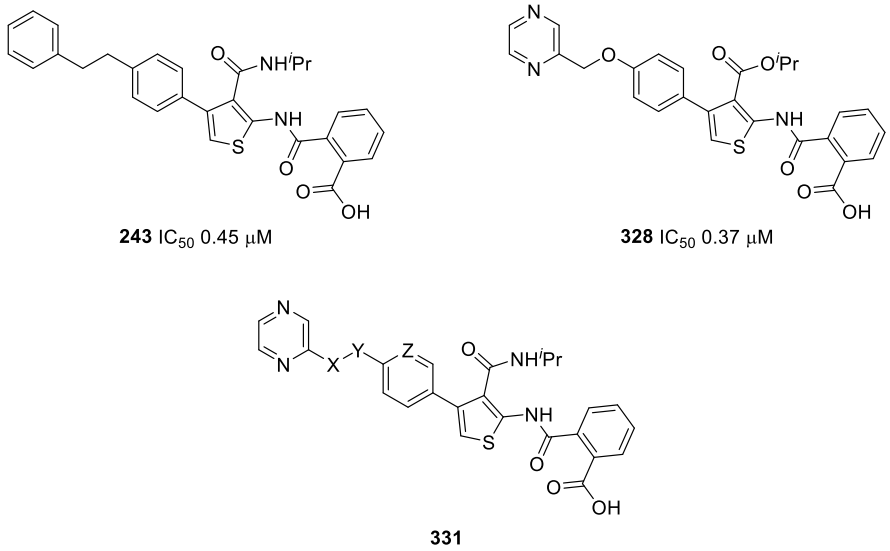

Figure 72: Optimised compounds 243, 328 and general structure of hybrid series 2 derivatives.

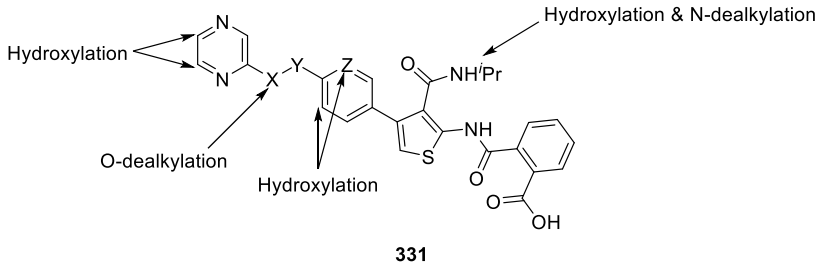

Figure 73: Potential sites of metabolism on scaffold 331 identified by metabolic hotspot analysis.

4.2.11.2. Synthetic route

Compounds **338**–**339** were synthesised in a 4-step synthetic route detailed in **Scheme 24**. Ligand **338** could be synthesised from the common ketone intermediate **312**, however, the fluorinated analogue (compound **339**) required an initial S_NAr reaction to generate fluorinated ketone component **333**, for the multicomponent Gewald reaction. The final two steps in the sequence involved standard amidation and ring-opening transformations to furnish compounds **338** and **339**.

Scheme 24: Synthesis of compounds 338 and 339.

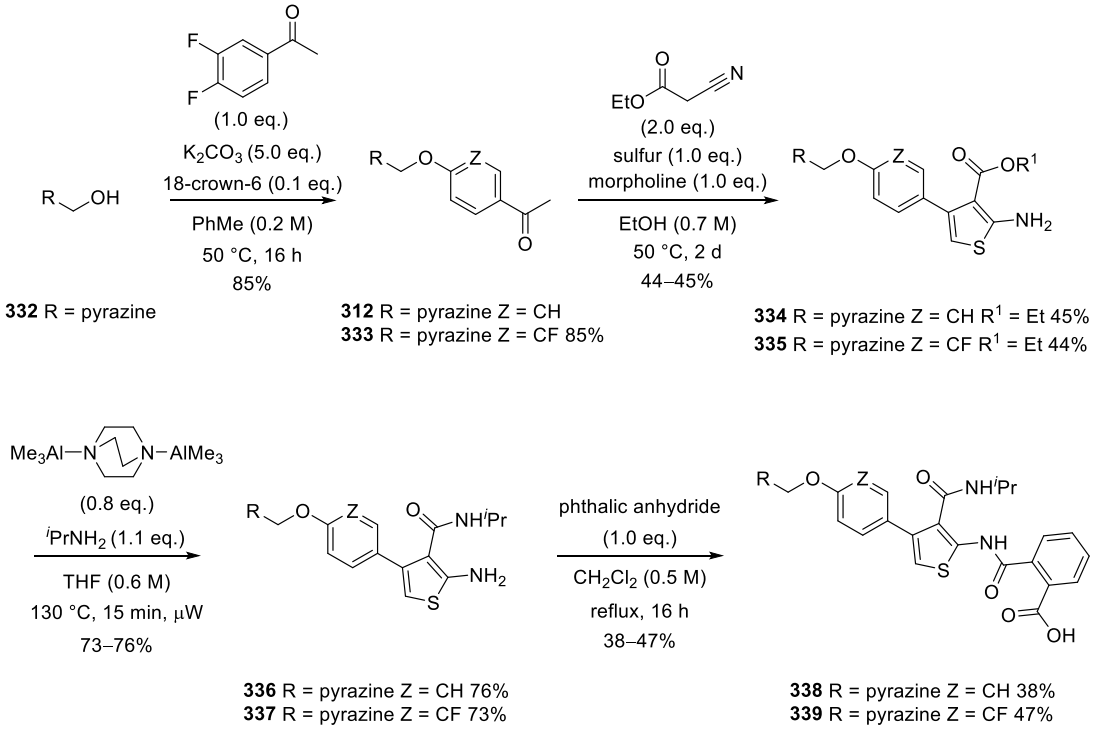

Commercially available hydroxyl starting material **332** was reacted with 3,4-difluoroacetophenone under S_NAr conditions, to produce fluorinated ketone intermediate **333** (85%), in excellent yield.[117] Sub-stochiometric amounts of

18-crown-6 were added to the reaction to expose the naked hydroxyl anion and enhance its nucleophilicity. Common ketone intermediate **312** and fluorinated ketone **333** were subsequently reacted with an appropriate cyanoacetate derivative, using Gewald reaction conditions, to afford 2-amino thiophene derivatives **334** (45%) and **335** (44%) in moderate yields. Ethyl cyanoacetate had to be used in the synthesis of intermediates **334** and **335** (R = pyrazine) for purification purposes, as the methyl ester proved inseparable from the starting ketones using column chromatography. Intermediates **334** and **335** were reacted with isopropyl amine in an amidation reaction, using the DABAL-Me_3 reagent, to generate amide analogues **336** (76%) and **337** (73%) in good yields.[107] The final synthetic step involved compounds **336** and **337** participating in the ring-opening of phthalic anhydride to afford final compounds **338** (38%) and **339** (47%) in moderate yields.

Compounds **347** and **348** were synthesised in a 4–5-step synthetic route outlined in **Scheme 25**. The synthetic sequence ended with the previously used Gewald reaction, amidation and ring-opening procedures that have governed many of the routes undertaken during the SAR studies. However, initial preparation of the ketone components for the Gewald reaction required the use of palladium catalysis to form the first ketone component **341**, followed by subsequent hydrogenation to produce the additional ketone component **342**.

Commercially available vinyl pyrazine **340** was subjected to Heck palladium-catalysed cross-coupling conditions using 4-bromoacetophenone, to selectively produce the (*E*)-alkene derivative **341** (81%) in good yield.[118] This coupling reaction was initially attempted using a ruthenium catalyst, which theoretically permitted the subsequent addition of hydrogen (H_2), for an *in situ* reduction of the resultant alkene.[119] However, this reaction proved to inefficient with regards to the initial coupling process, as no alkene coupled product was observed by a ^{1}H NMR spectrum of the crude reaction mixture. Alkene **341** was treated with hydrogenation conditions using H_2 and activated palladium on carbon (Pd/C), to afford reduced ketone intermediate **342** (87%) in excellent yield.[120] Care had to be taken during the hydrogenation step, as if the reaction was performed for a time period of more than 5 hours, then substantial secondary reduction of the pyrazine

heterocycle, to a mixture of dihydropyrazine and piperazine, was observed by ^{1}H NMR spectroscopy.

Scheme 25: **Synthesis of compounds 347 and 348.**

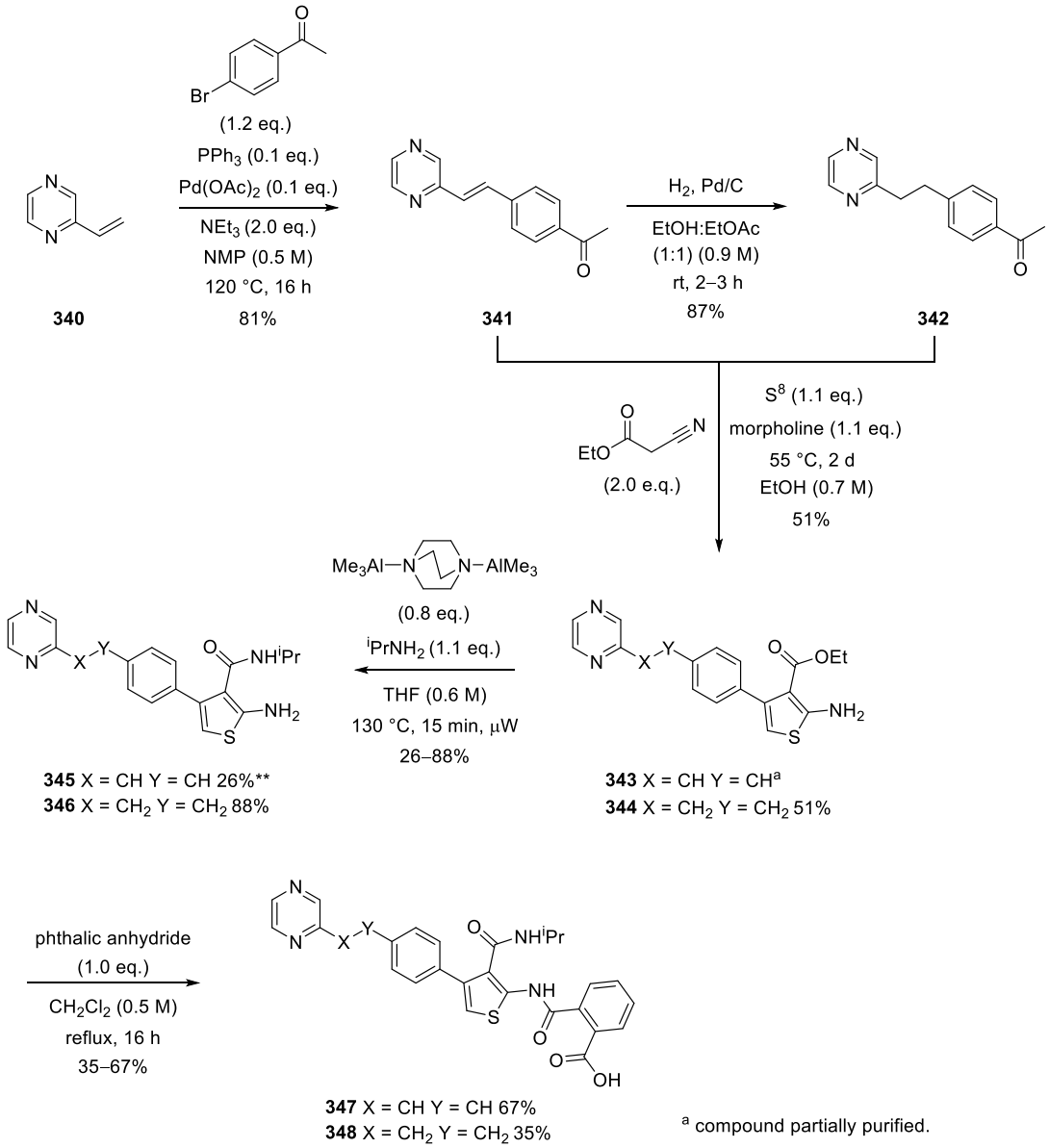

Ketone intermediates **341** and **342** were both used as components in the Gewald reaction to give 2-amino thiophene intermediates **343** (partially purified) and **344** (51%) in moderate yield. Compounds **343** and **344** were next reacted with isopropyl amine in an amidation reaction using DABAL-Me_3, to afford amide derivatives **345** (26%**) and **346** (88%) in moderate to excellent yields.[107] The final synthetic step involved using intermediates **345** and **346** as nucleophiles in the

ring-opening reaction of phthalic anhydride, to generate final compounds **347** (67%) and **348** (35%) in moderate to good yields.

4.2.11.3. Biological evaluation

Dose response curves were generated for all the synthesised final compounds in this series using the *in vitro* assay described in Section 3.0. **Figure 74** details the structures and IC_{50} values of the parent compounds **243** and **328** that directly relate to the ligands prepared within this series, for comparison purposes.

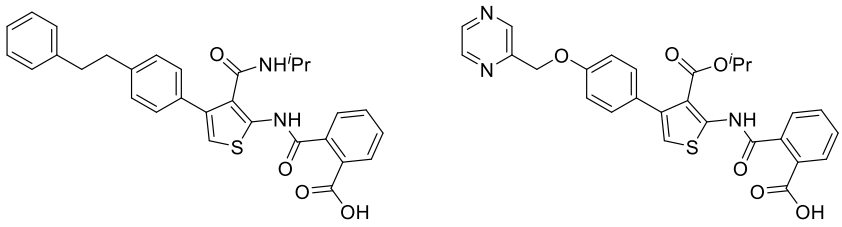

243 IC_{50} 0.45 μM **328** IC_{50} 0.37 μM

Figure 74: Parent compounds with respective IC_{50} values.

The IC_{50} values for the hybrid series 2 compounds are described in **Table 14**. In comparison to parent ligand **328** (0.37 μM), hybrid compound **338** (0.26 μM) which incorporated the amide bioisostere, generated a > 100 nM increase in potency. This result was consistent with the observed potency increase associated with the original switch from the ester motif to the amide moiety of derivative **243**. The cause of this activity increase was again reasoned to be due to a change in conformation moving from the ester to amide functionality, which may in turn influence the interactions of the hydrophobic isopropyl appendage. An expected potency improvement was also observed for ligand **338** (0.26 μM) when compared to parent ligand **243** (0.45 μM), potentially resulting from the optimised interactions provided by the pyrazine group. The internal phenyl ring, adjacent to the thiophene core, was suspected to be a potential site of metabolism. Mono-fluorination (compound **339** 0.24 μM) was performed to address this potential issue,[116] which gave a negligible change in binding affinity compared to ligand **338** (0.26 μM). This was an excellent result, as it meant that this fluorinated derivative could be used as a back-up compound within the series, in case any of the lead compounds displayed a poor metabolic profile.

Altering the ether linkage of ligand **338** (0.26 μM) for a fully aliphatic linker (compound **348** 0.14 μM) promoted a further progression in activity and produced the lead compound of the series in terms of potency. This data was again in keeping with previously observed trends within the SAR, which had also demonstrated a potency increase, when an ether linkage of the channel substituent was modified to a fully aliphatic chain. Interestingly, the (*E*)-alkene derivative **347** (0.72 μM) gave a significant drop-off in activity, suggesting that rigidifying/locking the tail group of the ligand in this conformation, has a negative effect on activity. Restricting the ability of the ligand to potentially preferentially align the nitrogen atoms of the pyrazine with the flanking arginine residues (Arg192 & Arg90), was proposed to be the cause of this loss in activity. Compound **347** explicitly demonstrated that maintaining flexibility within the linker portion of the channel substituent, was absolutely imperative for optimal binding affinity, within the orthosteric site of the TIGAR enzyme.

Table 14: IC_{50} values for hybrids 338, 339, 347 and 348. Compounds 338/348 IC_{50} curves.

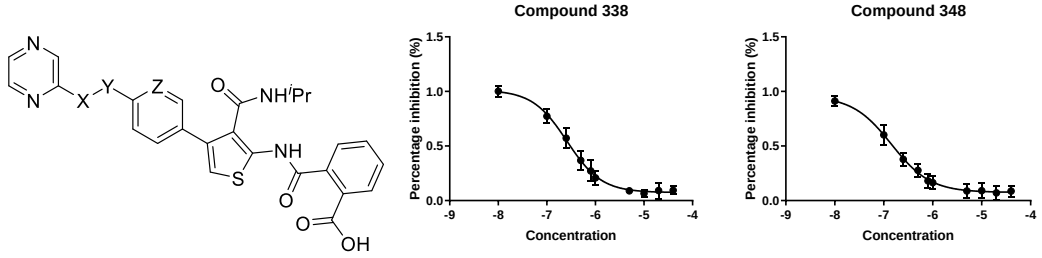

Compound	X	Y	Z	IC_{50} (μM)[a]
338	CH_2	O	CH	0.26 ± 0.05
339	CH_2	O	CF	0.24 ± 0.04
347	CH	CH	CH	0.72 ± 0.07
348	CH_2	CH_2	CH	0.14 ± 0.02

[a] IC_{50} calculated as n=3

In summary, combining parent ligands **243** (0.45 μM) and **328** (0.37 μM) to form hybrid ligand **338** (0.26 μM) resulted in an expected enhancement of target activity, based upon previously established trends within the SAR investigations. Incorporation of a fluorine atom into the internal phenyl ring (compound **339** 0.24 μM), directly linked to the thiophene core, produced a negligible potency change. Potency maintenance inferred that ligand **339** could potentially be used as an

adequate replacement within the series for any lead compounds that exhibited sub-standard metabolic profiles. Exchanging the channel substituent ether linkage (compound **338** 0.26 μM) for a completely aliphatic linker (compound **348** 0.14 μM) gave an expected potency increase, based on previously observed data within the SAR studies and generated the lead compound of the series in terms of potency. Removing the flexibility of the channel substituent linker motif (compound **347** 0.72 μM) afforded an associated depletion of potency, which demonstrated that free movement was crucial for optimal alignment of the ligand, within the active site.

The primary aim of the project was to develop a potent chemical probe for the phosphatase target TIGAR and this had now been achieved through the design, synthesis and evaluation of this final hybrid compound series.

4.2.12. Negative control compounds

In order to perform cell studies with the lead compounds of the series, our collaborators had also requested negative control compounds for use within the cellular assay. To meet this demand, derivatives **349** and **350** (Figure 75) were designed based around the proposal that removal of the channel substituent would decimate the potency of the ligand. Compound **350** additionally contained the capped methyl ester to remove any electrostatic interactions within the active site. Both ligands retained the core scaffold structure in order to be closely comparable to the test compounds, constructed around the same core unit. Compound **351** (Figure 75) was also designed, in order to develop a negative control that closely resembled the structure (including the channel substituent) of lead compounds within the series but that was methyl capped to remove target activity.

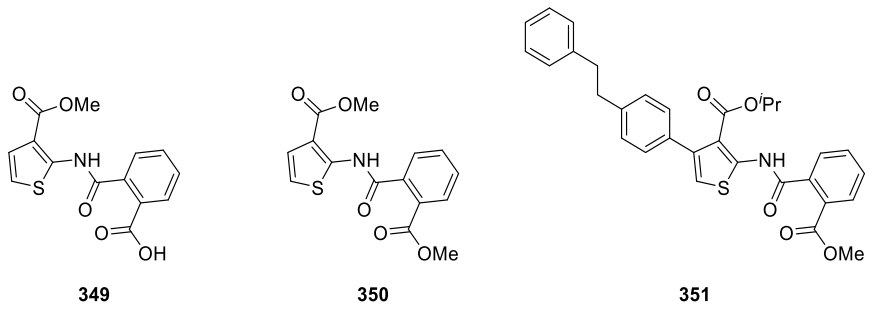

Figure 75: Structures of designed negative control species 349, 350 and 351.

Scheme 26 initially details the reaction of the commercially available 2-amino thiophene **352** with phthalic anhydride, to yield thiophene amido acid **341** (65%) in

good yield, after purification *via* flash column chromatography.[68] Compound **349** was then esterified in the presence of MeOH and H_2SO_4 to afford di-ester **350** (63%) in good yield, upon purification by flash column chromatography.[96] Common intermediate **184** was subjected to the same esterification conditions, to produce ligand **351** (93%) in excellent yield.

Scheme 26: Synthesis of compounds 349–351.

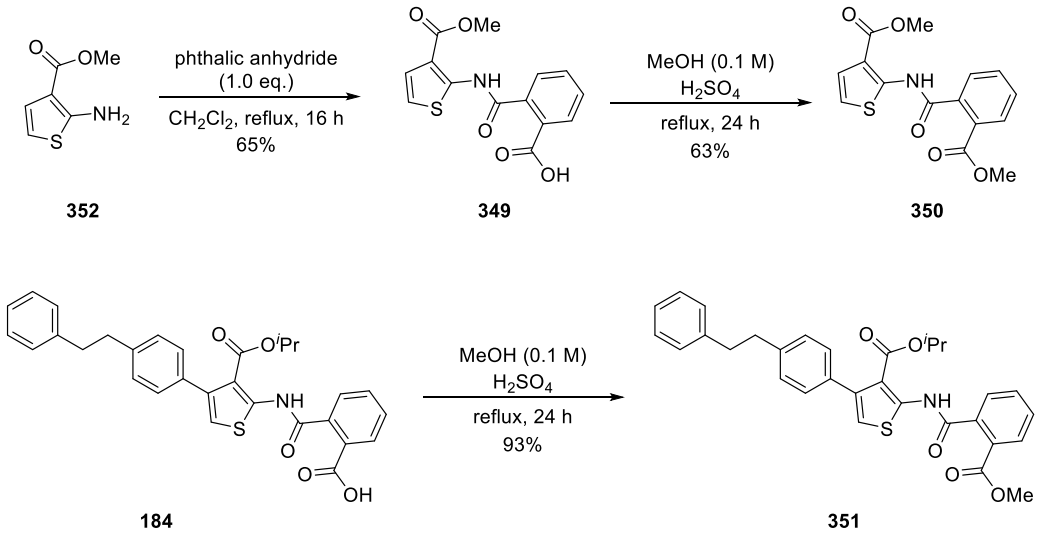

The single point assay (200 μM) results for compounds **349**, **350** and **351** are detailed in **Figure 76**. Pleasingly, analogues **349**, **350** and **351** all proved to be inactive (< 5% inhibition at 200 μM), demonstrating that the hydrophobic nature and presence of the channel substituent was crucial for activity (ligand **349**), either through the additional hydrophobic interactions or because it helped the structure adopt an optimal orientation for binding within the pocket. The electrostatic interaction between the head group and the cationic residues of the phosphate binding pocket was again demonstrated to be crucial for activity, as capped ligands **350** and **351** were both inactive.

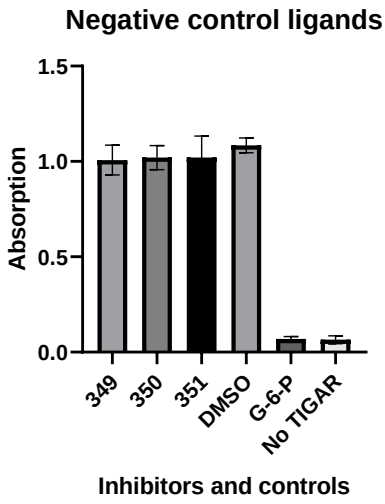

Figure 76: Graph of single point assay results for negative control compounds 349, 350 and 351.

All negative control compounds were subsequently passed on to our biological collaborators, for use in any cell studies that were performed, involving the 2-amino thiophene series.

4.2.13. SAR summary

SAR data generated during the investigation is summarised in **Figure 77**.

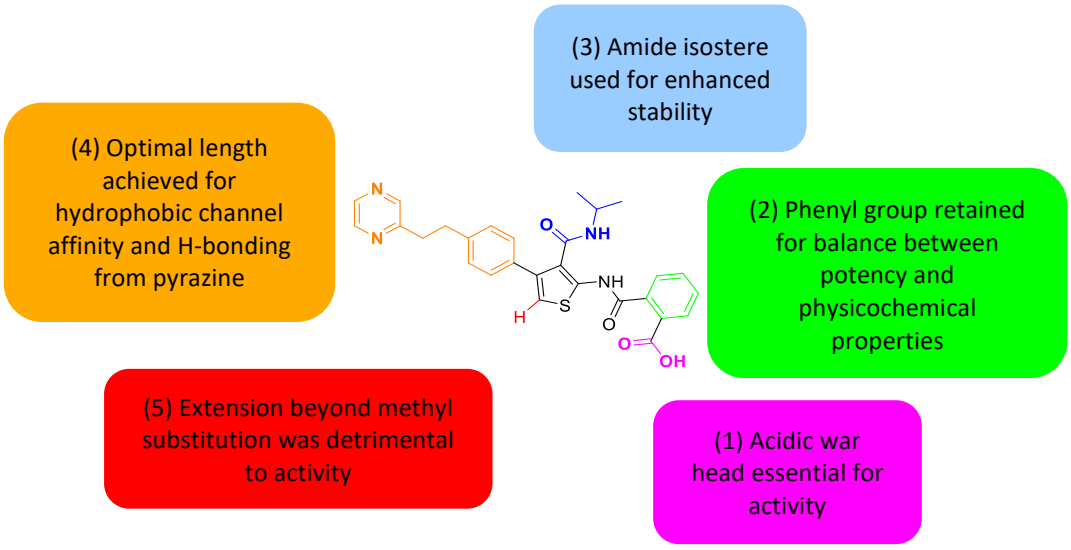

Figure 77: SAR summary for 2-amino thiophene scaffold.

In summary, (1) the anionic/acidic warhead acts by forming an electrostatic interaction with multiple cationic residues in the orthosteric site and was essential for activity; carboxylic- and sulfonic acid groups were both well-tolerated but the

carboxylic group was selected as it had a smaller impact on the total polar surface area (TPSA); a tetrazole moiety was also tolerated and has the potential to serve as a metabolically stable replacement if required;[100] (2) the phenyl linker between the amide and carboxylic acid head group was found to play a crucial role in the orientation of the head group as well as providing additional hydrophobic interactions; linkers with a smaller degree of saturation or acyclic linkers proved detrimental to activity; phenyls substituted with lipophilic moieties improved potency with a penalty in M.wt, however, the standard phenyl linker was retained as a balance between potency and desired physicochemical properties; (3) an amide isostere with a branched aliphatic chain group was selected over the corresponding ester to aid chemical stability and enhance hydrophobic interactions in the small pocket;[78] multiple amide and ester substituents positively impacted potency but many of these had questionable stability and increased M.wt values, so the isopropyl functionality was taken forward; (4) various aromatic groups, heterocycles, linker lengths/types and substituents were tested to improve binding affinity in the hydrophobic channel section of the ligand; optimal length and conformation within the channel were achieved with the aliphatic linker (CH_2CH_2), attached internally at the *para* position of a phenyl group, for favourable interactions within the lipophilic tunnel; a pyrazine group linked to the external side of the aliphatic tail unit was proposed, by virtue of molecular modelling, to be adopting hydrogen-bonding interactions with nearby amino acids (Arg192 and Arg90), and this structural change resulted in the most potent compound (0.14 μM) of the series; (5) expansion along this vector with a methyl group gave initial potency gains, however, further growth with an ethyl group exhibited a negative effect on potency; no further exploration of this SAR section was therefore performed.

4.3. Further compound data

There were several times within the project when more specific/advanced data was sought in order to complement the ongoing SAR studies. These studies enabled a deeper understanding of both the target and the synthesised tool compounds.

The overall end goal of our venture was to develop a small molecule chemical probe capable of undergoing *in vivo* studies, within a mouse model designed by our biological collaborators. In order for this to be possible, the lead compounds of the

series not only had to exhibit good *in vitro* potency towards the target, they also had to exhibit sufficient drug metabolism & pharmacokinetic (DMPK) profiles,[121] display adequate selectivity profiles and demonstrate cellular activity, by inciting a downstream functional effect upon target binding. These listed parameters for the design of an efficient tool compound, were outlined in the Aims section of the report as the major objectives for the project. The following sections shall describe the current landscape of our tool compounds, across all the required criteria that must be satisfied before *in vivo* studies can be pursued.

4.3.1. Drug metabolism & pharmacokinetic profiles

4.3.1.1. Initial DMPK profiles

In order to establish the robustness of our probe compound, it's DMPK properties had to be generated. Pharmacokinetics is defined as the impact that the systems of a living organism have on a drug molecule and involves the study of the adsorption, distribution, metabolism and elimination (ADME) of 'drug-like' compounds. A chemical probe must demonstrate satisfactory pharmacokinetic properties to ensure that the molecule will survive long enough within an organism (e.g. mouse), in order to have the opportunity to achieve its desired effect.[122] DMPK studies involve the assessment of a small molecule's pharmacokinetic profile across a range of relevant physicochemical properties. Developability metrics (e.g. Lipinski Rule of Five)[109] have been greatly refined over years of drug discovery research, to provide parameters for assessing the efficiency of chemical probe compounds. Only when a compound has displayed acceptable physicochemical properties can it be progressed towards *in vivo* studies.

SAR investigations of TIGAR led to the discovery of two lead compounds, **338** and **348**, in terms of potency. Both the structures and DMPK profiles for these ligands, plus two additional ligands (**184** and **243**) for comparison purposes, are shown in **Table 15**.

Table 15: DMPK profiles of selected compounds 184, 243, 338 and 348.

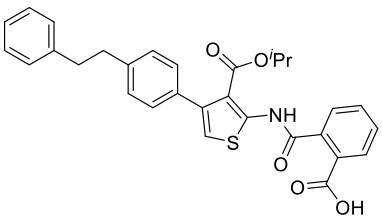

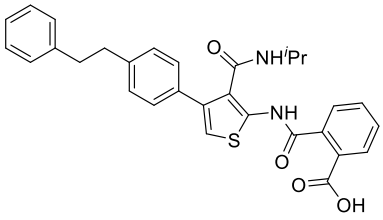

Compound	**184**	**243**
IC_{50} (μM)	0.56	0.45
cLogD	2.9	2.2
TPSA (Å^2)	92.7	95.5
M.Wt.	513	512
S9 Clearance mouse (μL/min/mg protein)	9.72	11.1
$t_{1/2}$ mouse (min)	71.3	62.2
Solubility (μM)	3.8	> 100

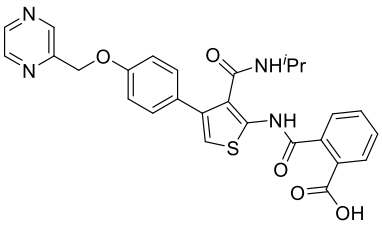

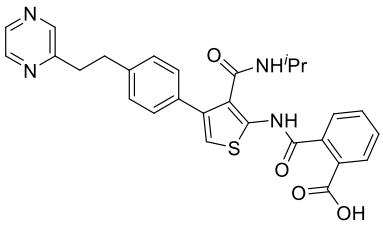

Compound	**338**	**348**
IC_{50} (μM)	0.26	0.14
cLogD	1.1	1.4
TPSA (Å^2)	129.5	120.2
M.Wt.	516	514
S9 Clearance mouse (μL/min/mg protein)	0.89	10.8
$t_{1/2}$ mouse (min)	781	64.5
Solubility (μM)	65	>100

Two initial parameters that are commonly calculated to give an idea of whether an ionisable compound (e.g. acid group) will be absorbed into the bloodstream, are cLogD and TPSA. LogD is a measurement of an ionised compounds partition coefficient between a lipophilic (octanol) and aqueous phase. Since the compound being measured undergoes ionisation, LogD calculations take into account pKa values of the ionisable functionality and therefore have to be performed at a selected pH. In most cases, the physiological pH of 7.4 is selected. If the LogD value is positive, it indicates that the drug will favour distribution into the lipophilic phase but still may not be absorbed into circulation. Compounds generally need to possess a LogD of > 2 to be well absorbed. TPSA measures the surface sum of all polar

atoms in a molecule. Well-absorbed compounds tend to have a TPSA value of < 130 Å^2. An additional parameter that was calculated was the M.wt of each ligand, which according to defined parameters, should be less than 500 in order to be considered 'drug-like'. With the pyrazine group installed, compounds **338** and **348** have significantly lower cLogD values (1.1 and 1.4, respectively) and TPSA values (129.5 Å^2, and 120.2 Å^2, respectively), compared to compounds **184** (cLogD 2.9, TPSA 92.7 Å^2) and **243** (cLogD 2.2, TPSA 95.5 Å^2) that contain a phenyl group in the equivalent position. Pleasingly, all four ligands have a positive cLogD value and reasonable TPSA values (**338** is at the upper limit), suggesting that each compound may undergo absorption in an *in vivo* experiment. All four compounds share highly similar M.wt values (**184** 513, **243** 512, **338** 516 and **348** 514) that are just above the standard 500 M.wt limit proposed by the Lipinski rules.[109]

A major cause of attrition for many chemical probes looking to undergo *in vivo* studies is metabolism by the liver.[123] The liver considers small molecules as foreign entities and works to transform these compounds into chemical forms that can be readily excreted through the kidneys. This process involves the conversion of molecules into more water-soluble species by introducing/unmasking hydrophilic groups (phase I metabolism) or by conjugating the molecule with a hydrophilic, endogenous species (phase II metabolism). Efficient chemical probes have to demonstrate stability towards the metabolic activity of the liver, in order to reach their site of action and exhibit their desired effect. A given compounds stability is measured in the form of intrinsic clearance and half-life values, which indicate the active time period that the molecule has, to induce its desired effect, before being completely metabolised and cleared from the system.[124] During the DMPK profiling, we outsourced to Cyprotex Discovery Ltd for an S9 stability experiment, which measured compound stability in a sub-cellular hepatic fraction, instead of a whole cell model. S9 assays contain the majority of phase I, and some phase II enzymes, as they are comprised of both microsomal and cytosolic enzymes, meaning that appropriate initial metabolic profiling should be achieved.[125] All values provided for this *in vitro* assay were calculated as an n=5. A lower clearance rate and a longer half-life ($t_{1/2}$) indicate that a compound has improved metabolic stability. All three compounds possessing an aliphatic linker at the channel substituent position (**184** S9 9.72 μL/min/mg protein $t_{1/2}$ 71.3 min, **243** S9 11.1 μL/min/mg protein $t_{1/2}$ 62.2 min,

348 S9 10.8 μL/min/mg protein $t_{1/2}$ 64.5 min) exhibited moderate S9 clearance and half-lives values, indicating reasonable stability in this assay. Interestingly, modification to an ether channel substituent linker (compound **338** S9 0.89 μL/min/mg protein $t_{1/2}$ 781 min) simultaneously lowered the S9 clearance value and increased the $t_{1/2}$ dramatically. This was an incredibly intriguing result when considering that only a single atom change had been made (CH_2 to O) and the data implied that ligand **338** was highly stable when exposed to phase I and phase II metabolic enzymes.

Aqueous solubility is another important physicochemical property as solubility can impact upon small molecule administration, where the compound must be soluble in the chosen medium.[126] Aqueous solubility also impacts upon a compounds ability to traverse around the systemic circulation, which is imperative for reaching the desired site of action.[126] Compound solubility is aided by ionisation as the hydration of organic ions is thermodynamically favourable, due to strong electrostatic interactions with solvent water molecules. Outsourcing to Cyprotex Discovery Ltd for turbidimetric solubility experiments was also conducted. Turbidimetric solubility measures a compounds kinetic solubility by diluting a stock DMSO solution of the respective compound into aqueous buffer.[127] All values provided for this *in vitro* assay were calculated as an n=5. Bioisostere replacement of the ester group with an amide appeared to greatly enhance solubility (compound **184** 3.8 μM vs **243** >100 μM). Upon changing from the external phenyl group (compound **184** and **243**) to a pyrazine motif (compounds **338** solubility 65 μM and **348** solubility > 100 μM), high solubility levels were pleasingly maintained, particularly for ligand **348** (solubility >100 μM).

In summary, all four ligands displayed positive cLogD values (**184** 2.9, **242** 2.2, **338** 1.1 and **348** 1.4) and satisfactory TPSA values (**184** 92.7 $Å^2$, **243** 95.5 $Å^2$, **338** 129.5 $Å^2$ and **348** 120.2 $Å^2$), indicating that each tested compound may undergo absorption during *in vivo* studies. All four compounds also possessed M.wt (**184** 513, **243** 512, **338** 516 and **348** 514) values that were just over the suggested 500 limit of the Lipinski rules. Aliphatic linker-based derivatives (**184** S9 9.72 μL/min/mg protein $t_{1/2}$ 71.3 min, **243** S9 11.1 μL/min/mg protein $t_{1/2}$ 62.2 min, **348** S9 10.8 μL/min/mg protein $t_{1/2}$ 64.5 min) possessed moderate clearance and $t_{1/2}$ values.

Pleasingly, S9 clearance values dropped dramatically when the pyrazine moiety was combined with the phenyl ether functionality (**338** S9 0.89 μL/min/mg protein $t_{1/2}$ 781 min), which also resulted in a significantly increased $t_{1/2}$ value, demonstrating that ligand **338** possessed a desirable metabolic profile. All compounds possessing the amide bioisostere exhibited enhanced solubility (**243** >100 μM **338** 65 μM and **348** > 100 μM), compared to the ester derivative (**184** 3.8 μM).

Initial DMPK profiling for ligands **338** and **348** had proven promising and so, both ligands were taken forward and subjected to testing within a hepatocyte stability assay to provide further evidence that demonstrates the robustness of these potential chemical probes.

4.3.1.2. Hepatocyte stability data

Hepatocyte stability assays are a more accurate and complete variant of the S9 assay, as hepatocytes contain the full complement of hepatic drug metabolising enzymes (phase I and phase II), which are maintained within an intact cell. For this reason, hepatocytes have become the 'gold standard' for assessing the hepatic metabolism of drug molecules and provide a valuable *in vitro* model for predicting *in vivo* hepatic clearance.[128] In order to continue progressing these chemical probes (**338** and **348**) towards further cellular, and potentially *in vivo* studies, a hepatic clearance value which produced a $t_{1/2}$ of > 20 minutes would have to be achieved.

The protocol for performing the hepatocyte stability assay is described as follows. Initially, the hepatocytes were incubated with the test compound (3 μM) at 37 °C. Samples were then removed at the appropriate time points (0, 5, 10, 20, 40, 60 minutes) into a methanol solution, containing an internal standard, in order to terminate the reaction. Following centrifugation, the supernatant was analysed by LC-MS/MS to determine the percentage of compound that remained at the given time point (Figure 78). The ln peak area ratio (compound peak area/internal standard peak area) was plotted against time and the gradient of the line was determined. Intrinsic clearance and $t_{1/2}$ values were then quantified from this data (Table 16).[128]

The percentage compound degradation data is portrayed for each ligand (**338** and **348**) in the graphs highlighted in **Figure 78**. Test compound metabolism was measured over a period of 60 minutes and the percentage of compound remaining for ligands **338** and **348** was determined at six different time intervals (**338** 0 = 100%, 5

= 86.1%, 10 = 64.9%, 20 = 51.8%, 40 = 32.8%, 60 = 26.2%, **348** 0 = 100%, 5 = 86.1%, 10 = 67.2%, 20 = 36.3%, 40 = 14.0%, 60 = 7.9%). The graph for compound **338** demonstrated a gradual depletion in the levels of test compound, and after 60 minutes 26.2% of the original compound levels were still present, suggesting reasonable stability across the 60 minute period. The equivalent graph for ligand **348** displayed an overall increased rate of degradation, as by the 60 minute increment, only 7.9% of the original compound levels remained, indicating compromised metabolic stability for **348**.

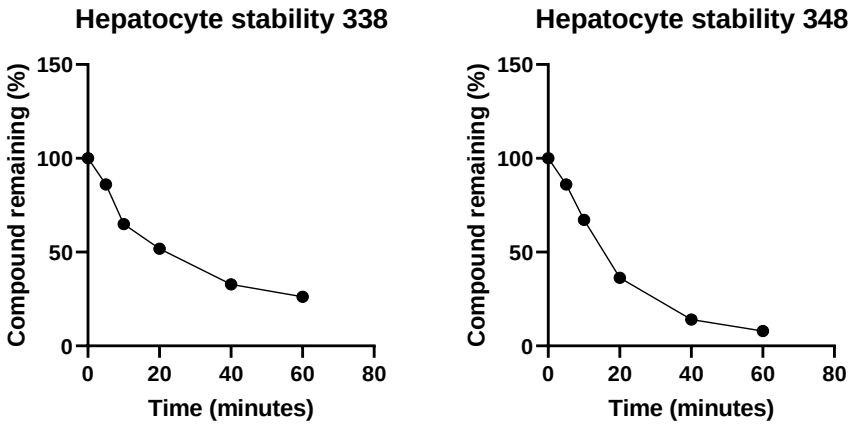

Figure 78: Hepatocyte stability graph for compounds 338 and 348.

The intrinsic clearance and $t_{1/2}$ values within hepatocyte cells for ligands **338** and **348** are displayed in **Table 16**. Consistent with the graphical data shown in **Figure 78**, both ligands demonstrated high clearance levels (**338** clearance = 54.9 μL/min/10^6 cells, **348** clearance = 88.8 μL/min/10^6 cells) and low $t_{1/2}$ (**338** $t_{1/2}$ = 25.2 min, **348** clearance = 15.6 min). Interestingly, both ligands had shown good (**348** S9 clearance = 10.8 μL/min/mg protein $t_{1/2}$ 64.5 min) and excellent (**338** S9 0.89 μL/min/mg protein $t_{1/2}$ 781 min) S9 stability profiles, so these hepatocyte stability results were surprising, particularly for ligand **338**. A potential reason for this could be that both ligands are vulnerable to phase II metabolism (e.g. glucuronidation of the carboxylic acid motif),[80] as compounds that undergo increased amounts of phase II metabolism may appear less stable in hepatocyte compared to microsomal (S9) incubations.

Ligand **348** demonstrated a particularly poor metabolic stability within the hepatocyte cells and its $t_{1/2}$ of 15.6 minutes was below the desired 20 minute mark,

that was thought to be required for an adequate *in vivo* chemical probe. As such, compound **348** was classified as possessing an inadequate metabolic profile and was therefore not progressed towards further cellular/*in vivo* studies.

Table 16: Hepatocyte stability for compound 338 and 348.

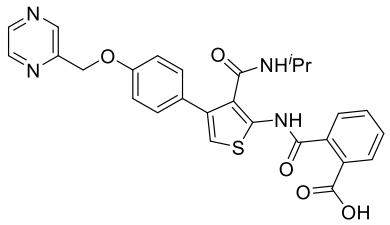

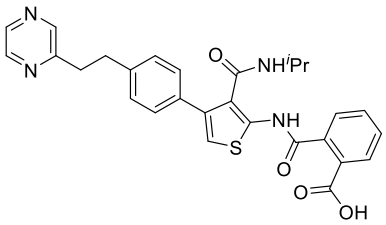

Compound	**338**	**348**
Clearance mouse (μL/min/10^6 cells)	54.9	88.8
$t_{1/2}$ mouse (min)	25.2	15.6

However, although ligand **338** did not exhibit an ideal metabolic profile, its $t_{1/2}$ value of 25.2 minutes was above the desired 20 minute mark, said to be required for a chemical probe to be robust enough to induce a desired effect within cells. Ligand **338** had therefore established a satisfactory DMPK profile and has now been passed on to our biological collaborator, Professor Karen Vousden's lab, for further cellular testing and potential *in vivo* studies.

In summary, ligands **338** and **348** were tested within a hepatocyte stability assay in order to determine their metabolic stability profiles, within intact cells. Over a 60 minute time period, compound **348** displayed a high rate of degradation, with only 7.9% of the original compound concentration remaining after 60 minutes, suggesting poor stability. In contrast, ligand **338** demonstrated a more moderate metabolic rate as 26.2% of the original compounds levels remained after 60 minutes. Analogue **348** exhibited a very high hepatocyte clearance value of 88.8 μL/min/10^6 cells and a short $t_{1/2}$ value of 15.6 minutes, which resulted in an inadequate metabolic profile. This meant that ligand **348** was not progressed towards further cellular/*in vivo* studies. Ether derivative **338** produced an improved but still high hepatocyte clearance value of 54.9 μL/min/10^6 cells and a moderate $t_{1/2}$ value of 25.2 minutes. This meant that compound **338** showed satisfactory metabolic stability, within the hepatocyte stability assay. Ligand **338** has therefore been taken forward for further testing in the form of cellular and potential *in vivo* studies.

4.3.2. Selectivity data

For a chemical probe to be deemed efficient, a second parameter that must be assessed is the selectivity shown by the tool compound against alternative targets.[129] Unfortunately, at this current stage of the project, lead compounds **338** and **348** have yet to be screened against a selectivity panel of phosphatases, as outsourcing has focussed primarily on generating DMPK profiles for these ligands. However, at an earlier point in the project when phenylethyl ligand **184** (Figure 79) was the lead compound, it was decided that a selectivity profile should be acquired for the series at this stage.

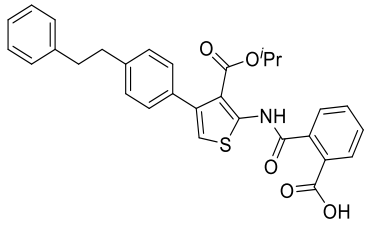

184 IC_{50} 0.56 μM

Figure 79: Ligand 184 used for selectivity studies.

Generation of phosphatase selectivity data was outsourced to Eurofins Discovery Ltd although, there was unfortunately no possibility of gathering a TIGAR selectivity profile against the Histidine phosphatase family, as this assay is currently unavailable. A tyrosine phosphatase selectivity assay, however, was available, and it was decided that ligand **184** would be tested within this *in vitro* assay, to establish an early selectivity profile for the series. Tyrosine phosphatases have received the largest amount of research attention within the phosphatase interactome and are established as physiologically relevant drug targets.[3] As such, achieving selectivity over this family would be a prerequisite for any probe compound attempting to target an alternative phosphatase family member. Additionally, it allowed us to identify if any selectivity had been generated towards TIGAR, particularly against the tyrosine phosphatase PTP1B, as the initial hit compound bearing the 2-amino thiophene scaffold (**58**) had shown weak activity towards this target.[68] Our original hypothesis regarding selectivity, had stated that growth along the vectors of the TIGAR pocket and the subsequent development of potency towards this target, should naturally result in selectivity against PTP1B.

The selectivity assay involved screening a test compound, at a single point concentration of 1 µM, against a panel of 22 different tyrosine phosphatases, listed in **Figure 81**. 6,8-Difluoro-4-methylumbelliferyl phosphate (DiFMUP) (compound **353**, Figure 80) was used as the substrate for the assay, as this compound has a low fluorescence intensity in its non-hydrolysed state, with phosphate removal producing a highly fluorescent product.[130]

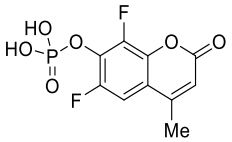

353

Figure 80: Structure of DiFMUP substrate 353 used within selectivity assay.

Control compounds were used to determine fluorescence values that relate to maximum levels of dephosphorylation (i.e. 100% phosphatase activity) for each phosphatase. The reduction in phosphatase activity, in the presence of test compound **184** could then be subsequently determined. All results depicted in the graph of **Figure 81** were performed in duplicate. The data for TIGAR from our in-house assay has been added to this graph for comparison.

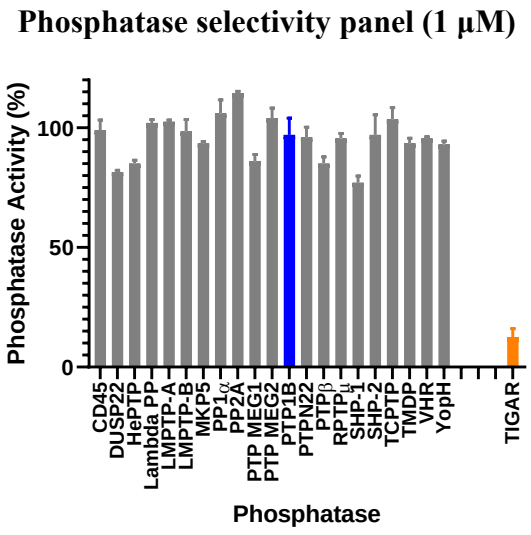

Figure 81: Tyrosine phosphatase selectivity panel with PTP1B highlighted. TIGAR data from in vitro assay added for comparison.

The phosphatase selectivity panel graph in **Figure 81** highlighted that in the presence of test compound **184**, 21/22 of the screened phosphatases demonstrated > 80% activity, with 17/22 exhibiting ≥ 93% activity. This was excellent data, as when

compared to the equivalent activity value within our own *in vitro* TIGAR assay of 12% (shown in orange in Figure 81), the numbers suggested that selectivity had been generated against a variety of physiologically relevant phosphatase enzymes. Only phosphatase SHP-1 (activity = 77%) displayed < 80% activity in the presence of ligand **184** and even this number was still high, when considering that the test compound was ran at a concentration of 1 µM. The fact that PTP1B had shown an activity of 96% when incubated with ligand **184** was extremely satisfying, particularly in comparison to the 12% activity value exhibited for TIGAR, within our own *in vitro* assay. The PTP1B and TIGAR data provided strong support for the original hypothesis, that driving potency towards TIGAR through appropriate vector growth would induce a natural selectivity paradigm against PTP1B, due to structural differences in the active site. Phosphatase panel IC_{50} values were not generated for compound **184**, so a fold selectivity value for TIGAR vs PTP1B unfortunately could not be determined, however, the single point data established a favourable selectivity profile for the 2-amino thiophene compound series in favour of TIGAR.

In summary, ligand **184** was screened against a panel of 22 physiologically relevant phosphatases at a single point concentration of 1 µM. All 22 phosphatases demonstrated ≥ 77% activity in the presence of test compound **184** and this identified that **184** showed low levels of inhibition (≤ 23%) against these phosphatases, even at a concentration of 1 µM. TIGAR activity levels (12%), determined within an in-house *in vitro* assay using ligand **171**, at an equivalent concentration of 1 µM, outlined a clear selectivity profile in favour of TIGAR. The 96% activity value associated with PTP1B, reinforced an original proposal for the project that selectivity for TIGAR against PTP1B would be generated through natural growth into the TIGAR active site. A desirable selectivity profile for the 2-amino thiophene compound series had now been established. This data showed promise for the future development of a fully selective chemical probe for TIGAR.

4.3.3. Cell studies

4.3.3.1. Glucose-fed conditions

In order to be considered an efficient tool compound, cellular activity must be established. *In vivo* studies require target engagement, therefore, a probes ability to interact with its desired target, and initiate downstream functional effects, has to be

tested within a cellular environment. Only when satisfactory cellular activity has been established, can a tool ligand be progressed to undergo *in vivo* studies.[131]

TIGAR cellular studies were performed alongside the selectivity studies described in Section 4.3.2. At this stage of the SAR investigations, ligand **184** (Figure 82) was the most potent compound and so, this probe molecule was sent to our biological collaborators (Vousden lab), for initial cell studies. These early studies were performed in order to establish multiple key properties for the chemical probe series; (1) compound permeation of the cell membrane; (2) target engagement/affinity; (3) initiation of desirable downstream functional effects.

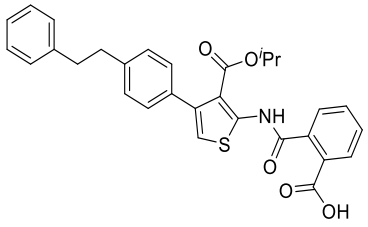

184 IC_{50} 0.56 μM

Figure 82: Ligand 184 used for cell studies.

As stated in the introductory Sections 1.4.3. and 1.4.4., TIGAR is significantly overexpressed/upregulated in multiple cancer cell types.[38-40] TIGAR overexpression results in increased DNA stability and cell survival, through an increase in R-5-P production and increased antioxidative effects, due to glycolysis inhibition and resultant flux along the oxidative PPP.[39] In order to test whether TIGAR inhibition would offer a therapeutic advantage, by reversing the observed effects of TIGAR overexpression, a cellular study had to be created, where the relationship between TIGAR inhibition and oxidative PPP produced R-5-P levels, could be measured. Measurement of oxidative PPP access was essential, as it is the TIGAR induced flux along this branch of the PPP that leads to downstream antioxidant effects/apoptosis inhibition, and increased cancer cell survival.[39, 132]

Inhibitory effects of ligand **184** on TIGAR were assessed by treating a pancreatic cancer cell line known as FA6, which had been pre-treated with menadione **354** (Figure 83) to induce oxidative stress, with inhibitor **184**. This malignant cell type was chosen, as TIGAR has been confirmed to be upregulated within these cells.[133-134] Our biological collaborators designed a very elegant method to measure R-5-P

production, from passage along the oxidative PPP, by feeding the cells with glucose molecules where two of the six carbon units were ^{13}C labelled (Yellow circles, Figure 84). As demonstrated in **Figure 84**, this allowed our collaborators to take advantage of an intrinsic property of the oxidative PPP, as when doubly labelled G-6-P was converted to R-5-P, one of the ^{13}C carbon units was removed to generate singly labelled R-5-P. This meant that any singly labelled R-5-P could be attributed to passage along the oxidative PPP and that any multiply labelled R-5-P could be associated with passage along the non-oxidative PPP (Figure 84). A study had now been developed where the functional effects of TIGAR inhibition could be accurately assessed, by providing a clear method for measuring the extent of metabolite flow through the oxidative PPP.

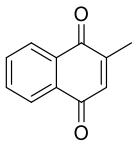

354

Figure 83: Menadione structure 354 used within cellular studies.

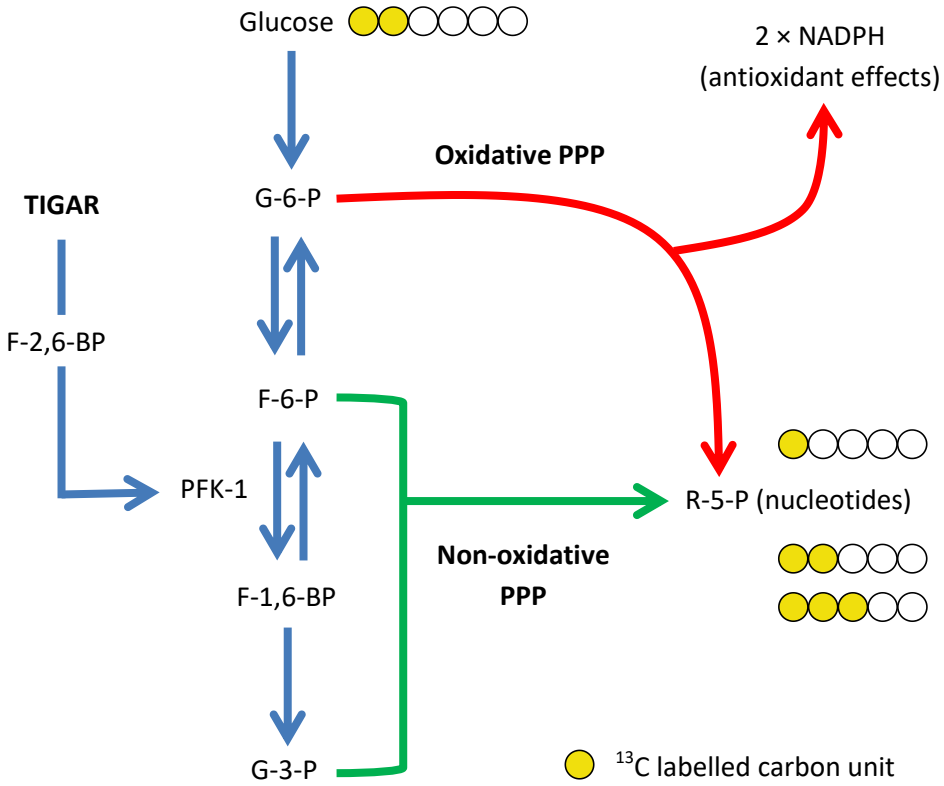

Figure 84: Pathway associated with glucose-fed cells used to determine downstream inhibitor effects on oxidative PPP production of R-5-P.

All cellular studies used a DMSO control to establish maximum concentration levels of singly labelled R-5-P (100%) produced by the oxidative PPP of malignant cells, within the FA6 cell line. This value was taken as the baseline concentration from which all other values were generated. Two negative control compounds (compounds **350** and **351** Figure 85), that had displayed inactivity towards TIGAR in the *in vitro* assay, and were comprised of the same core 2-amino thiophene scaffold as ligand **184**, were also used to reinforce the observed results from the cell studies.

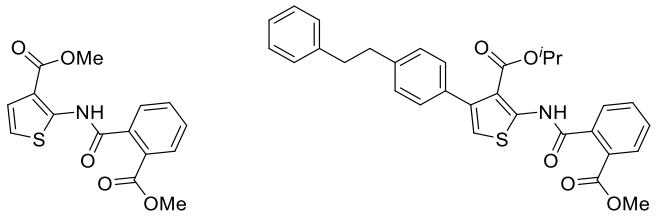

350 IC_{50} > 100 μM

351 IC_{50} > 100 μM

Figure 85: Structures of negative control compounds used for cell studies.

Before introducing probe **184**, initial knockdown (KD) studies were performed using siRNA to assess the effect of TIGAR removal on the levels of R-5-P produced through the oxidative PPP (graph A, Figure 86). The DMSO control and both negative control compounds (control 1 and control 2) all gave similar levels of maximum R-5-P production by the oxidative PPP. Graph A of **Figure 86** also demonstrated that through TIGAR KD, a depletion of singly labelled R-5-P levels to approximately half (~54%) the concentration of the DMSO control was observed. This drop in R-5-P levels revealed the expected restriction in access to the oxidative PPP upon TIGAR KD, as glycolysis should no longer be inhibited (*c.f.* controls).

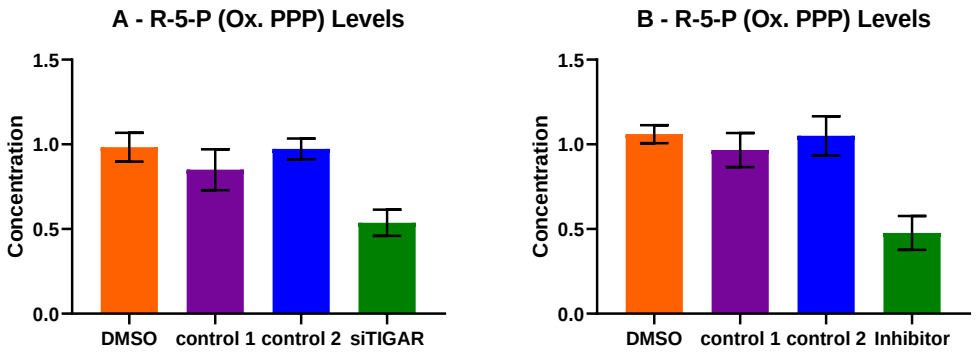

Figure 86: Singly labelled R-5-P levels produced from passage through the oxidative PPP. A - TIGAR KD studies; B - Inhibitor studies.

Equivalent studies were then conducted where instead of TIGAR KD, the FA6 cell line was treated with inhibitor **184** (graph B, Figure 86). If the inhibitor compound successfully interacted with TIGAR after crossing the cell membrane, then ligand **184** would be expected to phenocopy the results of the TIGAR KD studies. Interestingly, the chemical probe recapitulated the data observed with the KD studies, as once again the concentration of R-5-P was reduced to half (~48%) of the maximum levels displayed with the DMSO control. This was an extremely exciting result, as this data provided strong evidence that not only was ligand **184** crossing cell membranes and interacting with TIGAR, the chemical probe was also inducing downstream functional effects, by restricting access to the oxidative PPP and depleting R-5-P levels.

Additional graphs which provide further testament to the ability of inhibitor **184** to induce downstream functional effects, upon binding to TIGAR, are detailed in **Figure 87**. Upon treatment of the FA6 cell line with inhibitor **184**, the levels of F-2,6-BP increased by > 100-fold, compared to the concentration exhibited for the DMSO control. This is in keeping with TIGAR function, as if TIGAR is inhibited, then the enzyme cannot dephosphorylate and degrade F-2,6-BP levels, which generated an increased pool of this metabolite. Whereas in the DMSO control, TIGAR was at basal levels, which resulted in the degradation of this natural substrate.

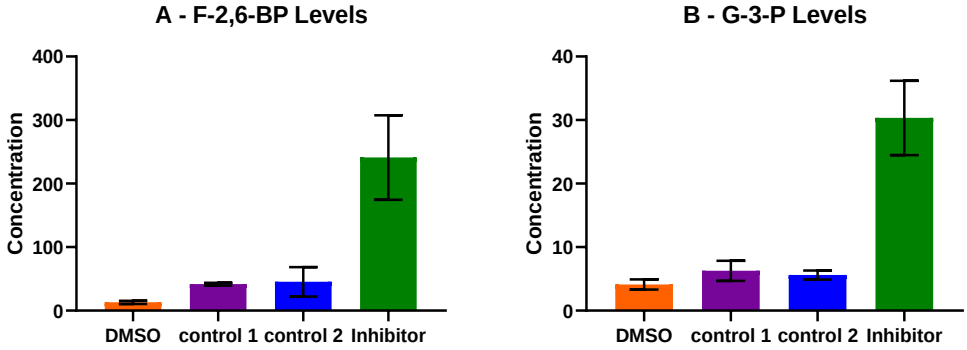

Figure 87: Concentrations of A – natural substrate F-2,6-BP levels; B – downstream glycolytic metabolite G-3-P levels.

TIGAR inhibition should theoretically result in an increased glycolytic flux, due to increased F-2,6-BP levels and a subsequent increase in PFK-1 activity.[39] To assess the effects of TIGAR inhibition on the rate of glycolysis, the concentration of a downstream glycolytic metabolite, glyceraldehyde-3-phosphate (G-3-P) was

quantified upon ligand **184** addition. In the presence of the inhibitor (graph B, Figure 87), a 7-fold increase in the concentration of G-3-P was observed in comparison to the DMSO control sample. The control samples exhibited low levels of G-3-P due to the fact that glycolysis would be inhibited when TIGAR is overexpressed and highly active. Pleasingly, this demonstrated that upon TIGAR inhibition by ligand **184**, there was a simultaneous increase in the concentration of downstream glycolytic metabolites such as G-3-P, which suggested that there was an increase in glycolytic flux and associated restricted access to the oxidative PPP.

In summary, a cellular experiment was developed that allowed the production of singly labelled R-5-P by the oxidative PPP, to be accurately measured. This was achieved by feeding pancreatic cancer cells with doubly ^{13}C labelled glucose, which took advantage of a labelled carbon unit loss, during synthesis of R-5-P through the oxidative PPP. The levels of singly labelled R-5-P were quantified in both TIGAR KD and inhibitor experiments, using an FA6 cell line treated with menadione **354**, to induce oxidative stress. Pleasingly, the inhibitor results phenocopied the KD data, as both experiments resulted in the depletion of R-5-P concentration to approximately half (KD R-5-P levels = 54%, inhibitor **184** R-5-P levels = 48%) of the maximum concentration, observed with the DMSO control. The levels of the natural substrate F-2,6-BP and the downstream glycolytic metabolite G-3-P, were additionally measured in the presence of probe **184**. Concentration levels for both species were increased (> 100-fold for F-2,6-BP, 7-fold for G-3-P), which suggested that the inhibitor was preventing the dephosphorylation of F-2,6-BP and increasing the rate of glycolysis to promote G-3-P production. Collectively, the data generated from this proof of concept model strongly suggested that inhibitor **184** was binding to TIGAR, and inducing significant downstream functional effects. This was a highly beneficial outcome, as cellular activity had now been established for the series, which greatly promoted the chances of being able to use the chemical probes on this series to perform *in vivo* studies.

4.3.3.2. Gluconeogenesis studies

Further cell studies with chemical probe **184** were performed using the pancreatic cancer cell line FA6, treated with menadione to induce oxidative stress. Section 4.3.3.1. described glucose-fed experiments that involved the use of

^{13}C labelled glucose to investigate the effects of TIGAR inhibition on glycolysis, within a malignant cell line. However, this section will discuss the experimental results concerned with glucose-starved cells, which were instead supplemented with triply labelled ^{13}C glycerol, that permitted the effects of TIGAR inhibition on gluconeogenesis to be monitored (Figure 88).

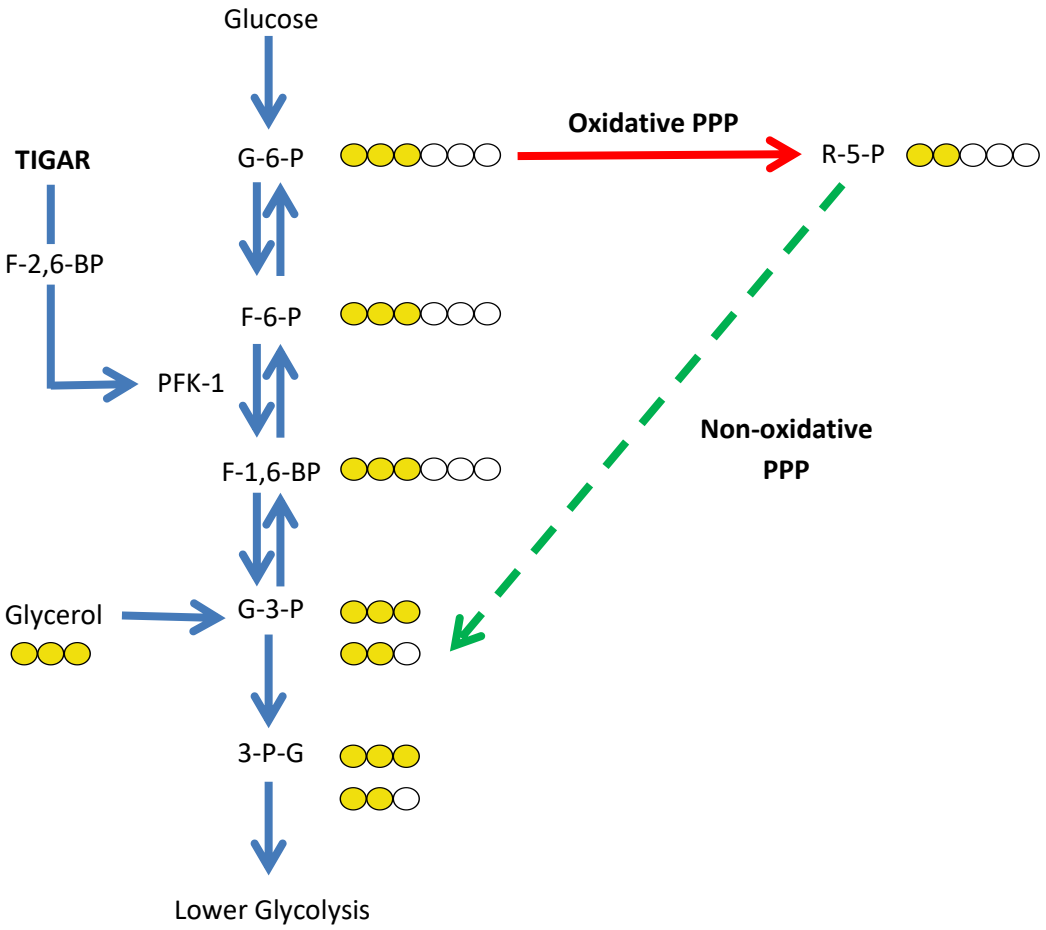

Figure 88: Pathway associated with glucose-starved cells used to determine downstream inhibitor effects on oxidative PPP production of R-5-P.

Glucose starvation meant that entry into the oxidative PPP could only be achieved, through the generation of G-6-P by gluconeogenesis from glycerol. The experiment again took advantage of the labelled carbon unit loss going from G-6-P to R-5-P, as when glycerol enters the cell it is converted to G-3-P, which can subsequently undergo gluconeogenesis to form G-6-P, that can in turn pass through the oxidative PPP to form R-5-P. At this stage, R-5-P can move through the non-oxidative branch of the PPP and re-enter glycolysis as a doubly labelled 3 carbon unit, instead of the originally fed triply labelled carbon unit (Figure 88). This means that any glycolytic

metabolites that are less than triply ^{13}C labelled have undergone gluconeogenesis and travelled through the oxidative PPP, before re-entering glycolysis through the non-oxidative PPP. This method provided a secondary means of measuring the rate of entry into the oxidative PPP and the downstream anti-apoptotic effects of TIGAR.

All cellular studies in this section used a DMSO control to establish maximum concentration levels of any measured metabolite (100%), produced by gluconeogenesis/glycolysis and/or the oxidative/non-oxidative PPP of malignant cells, within the FA6 cell line. This value was taken as the baseline concentration from which all other values were generated. Negative control compound **351** was also used to provide further support to all obtained results.

The levels of doubly labelled R-5-P obtained from the gluconeogenesis of triply labelled glycerol, followed by passage along the oxidative PPP are detailed in **Figure 89**. The negative controls (DMSO and control 1) provided the maximum concentration of doubly labelled R-5-P. Under these circumstances, TIGAR was heavily overexpressed within the malignant cells and promoted gluconeogenesis, and therefore the PPP shunt to produce doubly labelled R-5-P, by inhibiting glycolysis through F-2,6-P depletion and PFK-1 activation. Pleasingly, the introduction of ligand **184** produced a 95% decrease in the concentration of doubly labelled R-5-P. This result supported the data observed in the previous section, as the data shown here demonstrated that ligand **184** is inciting desired downstream functional effects, upon binding to TIGAR. In the presence of inhibitor **184**, F-2,6-BP degradation is greatly limited, which improved PFK-1 activation and afforded a subsequent inhibition of gluconeogenesis, due to a promotion in the rate of glycolysis.

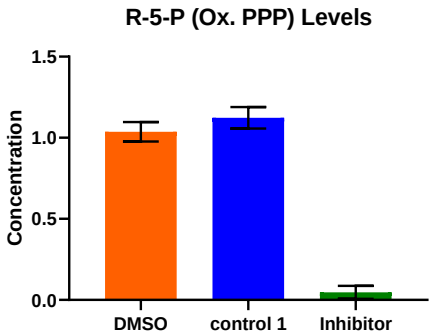

Figure 89: Doubly labelled R-5-P levels produced from gluconeogenesis and subsequent passage through the oxidative PPP.

To assess the effect of TIGAR inhibition with ligand **184** on gluconeogenesis, the concentration of triply (m+3) and doubly (m+2) labelled 3-phosphoglyceric acid (3-P-G) (Figure 90), a lower glycolysis metabolite, were measured. The data for triply labelled 3-P-G (graph A, Figure 90) represented the levels of 3-P-G when formation did not rely on passage along the oxidative PPP. Triply labelled 3-P-G levels were highlighted as being similar for both the controls (DMSO and control 1) (~100%), where TIGAR was upregulated, and the inhibitor **184** (75%), where TIGAR activity was inhibited, as the presence of triply labelled 3-P-G would be expected during both the increase/decrease of gluconeogenesis. The subtle drop-off in triply labelled 3-P-G observed for the inhibitor sample, could be due to the fact that enhanced glycolysis can result in complete removal of 3-P-G from the glycolytic pathway, through movement into the Krebs cycle.[135] Whereas increased gluconeogenesis in the absence of inhibitor **184**, resulted in the formation of products that can cycle back into glycolysis, providing an opportunity for greater maintenance of 3-P-G levels.

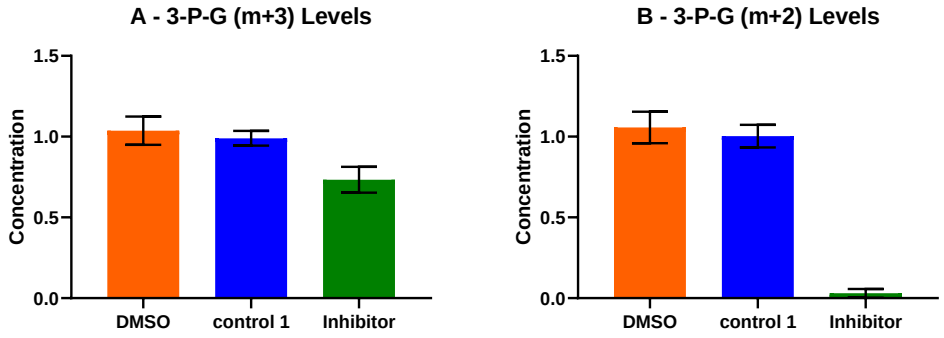

Figure 90: A - Triply labelled 3-P-G levels; B - Doubly labelled 3-P-G levels produced from gluconeogenesis and subsequent passage through the oxidative and non-oxidative PPP.

The data for doubly labelled 3-P-G (graph B, Figure 90) represents the levels of 3-P-G when formation relied upon forced gluconeogenesis from triply labelled glycerol and movement through the oxidative PPP, before re-entering glycolysis through the non-oxidative PPP. The negative controls (DMSO and control 1) provided the maximum concentration of doubly labelled 3-P-G that could be achieved through the processes just described and previously outlined in **Figure 88**. With the negative controls, TIGAR was heavily overexpressed within the malignant cells which promoted gluconeogenesis, and therefore the PPP shunt followed by subsequent re-entry into glycolysis through the non-oxidative PPP, to produce

doubly labelled 3-P-G, by inhibiting glycolysis through F-2,6-P depletion and PFK-1 activation. Pleasingly, treatment of the FA6 cell line with probe **184** generated a 98% reduction in the concentration of doubly labelled 3-P-G. This data was consistent with previously observed results, as this loss of 3-P-G levels suggested that ligand **184** was interacting with TIGAR and inducing downstream functional effects, by regulating metabolite flow within glycolysis and the PPP. TIGAR inhibition by **184** afforded increased amounts of F-2,6-BP, which promoted PFK-1 activation and an associated reduction in gluconeogenesis. This resulted in limited entry into the oxidative PPP, which meant that doubly labelled 3-P-G could not be synthesised from triply labelled glycerol.

In summary, a cellular experiment was developed that allowed the rate of gluconeogenesis to be accurately monitored. This was achieved by feeding pancreatic cancer cells with triply ^{13}C labelled glycerol. The assay took advantage of a labelled carbon unit loss during production of R-5-P, through the oxidative PPP. This then resulted in the generation of doubly labelled 3 carbon units upon re-entry into glycolysis, through the non-oxidative PPP. The levels of doubly labelled R-5-P were quantified using an FA6 cell line, treated with menadione, to induce oxidative stress. Pleasingly, inhibitor **184** resulted in the depletion of doubly labelled R-5-P concentration by 95%, when compared to the maximum concentrations observed with the DMSO control. Additionally, the levels of triply and doubly labelled 3-P-G were also measured in the presence of inhibitor **184**. A small drop (25%) in triply labelled 3-P-G concentration was observed compared to the DMSO control, suggesting that triply labelled 3-P-G levels were relatively unaffected within glycerol-fed conditions. The formation of doubly labelled 3-P-G was heavily dependent on enhanced gluconeogenesis and oxidative/non-oxidative PPP passage. Results demonstrated that doubly labelled 3-P-G concentration was significantly reduced (98%) when cells were treated with compound **184** in comparison to the DMSO control value. TIGAR inhibition by **184** produced increased F-2,6-BP levels and increased PFK-1 activation, which resulted in a substantial reduction in the rate of gluconeogenesis, in comparison to the directly opposite effects observed for the DMSO control sample. This meant the doubly labelled 3-P-G production was restricted, as the oxidative PPP could not be readily accessed by upper glycolysis metabolites. Collectively, the data generated from this alternative proof of concept

model, strongly indicated that inhibitor **184** was binding to TIGAR and inducing downstream functional effects. Cellular studies have also demonstrated that TIGAR inhibition could regulate metabolite flow, along glycolysis and the oxidative PPP. These initially observed functional effects may lay the foundations for inducing oxidative apoptosis within malignant cells.

5. Conclusions

Dephosphorylation, the removal of a phosphate group, is an extremely important post-translational modification performed by enzymes known as phosphatases. Due to the significant physiological and pathological role that phosphatases play in our biological systems, they are considered to be a key therapeutic area for drug targeting, particularly within oncology.[7] Of these phosphatases, the histidine phosphatase known as TIGAR has emerged from the Vousden laboratories as a relatively new phosphatase that has been identified as possessing considerable therapeutic potential.[39] This project aimed to design an efficient chemical probe to investigate the downstream effects of this target, and in turn, its biological function. However, as there are currently no chemical probes that target TIGAR, the development of an orthosteric regulator with good potency, selectivity, DMPK properties and cellular activity was the main aim of the project.

5.1. Orthosteric site - natural substrate mimetics

In conclusion, the initial series of compounds designed in our labs to target TIGAR, were non-hydrolytic mimics of the natural substrate F-2,6-BP, the first of which were based around the phosphonate ester/phosphonic acid scaffolds, **20** and **21** (Figure 91). The compounds in this series were designed as direct mimics of the natural substrates, as they contained functional groups of the same spatial size and charge, but with an inability to undergo dephosphorylation. Most of the compounds prepared proved to be inactive and the compound which did demonstrate activity (**24**, 55% inhibition at 200 μM) (Figure 91) was proposed to be binding non-specifically, which was an undesirable starting point for toxicity reasons.

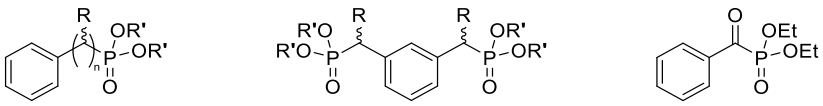

20 **21** **24**

Figure 91: Natural substrate and general structure for mono- and bis-phosphonate ester/phosphonic acid series and active compound 24.

The second and third series of synthesised natural substrate mimetics, were the amido acid **41**/**44** and squaric acid **52** derivatives (Figure 92). These compounds were planned around the hypothesis that the carboxylic acid and squaric acid

moieties could potentially mimic a phosphate group, as they would both be negatively charged at physiological pH.[26, 67] Similar biological results were obtained for these series as for the first, with the vast majority of the compounds displaying inactivity. The one compound that produced activity (**44**, 59% inhibition at 200 μM) was proposed to be binding non-specifically, which was an undesired trait.

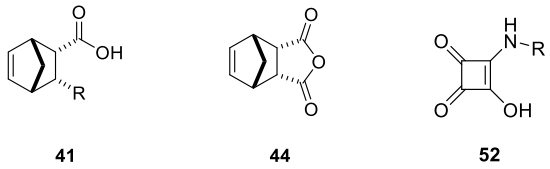

Figure 92: General structure for amido acid and squaric acid series and active compound 44.

5.2. Orthosteric site – 2-amino thiophene series

The bulk of the project and the SAR studies were based around the generic 2-amino thiophene scaffold **355** depicted in **Figure 93**. This structure type was identified in the form of hit compound **58** (Figure 93), which was found through a literature search as a weakly potent inhibitor of the tyrosine phosphatase PTP1B.[68] Hit **58** was tested against TIGAR and displayed an IC_{50} value of 65 μM. A combination of the demonstrated activity and the observation that scaffold **355** appeared highly amenable to SAR type chemistry, led to the pursuit of a chemical probe for TIGAR, through investigations into structure **355**. The core 2-amino thiophene portion was retained throughout SAR studies as this core structure allowed for appropriate vector growth within the active site of TIGAR. The coloured segments represent the portions of the scaffold that were investigated and altered during the course of the project.

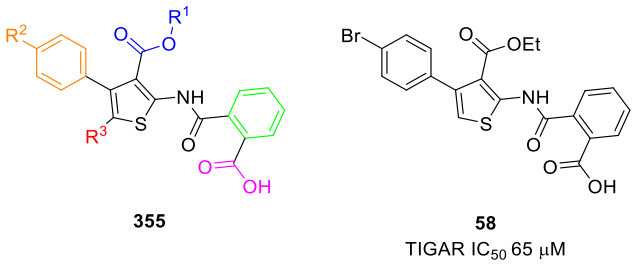

Figure 93: General structure for 2-amino thiophene series (355) and hit compound 58.

Initial investigations within the SAR study revolved around a variation in the R^1 appendage of the 3-carboxylate group, with the generic scaffold **64** for the series

depicted in **Figure 94**.[68] Minimal alterations to the R^2 group were made at this stage to assess how differing substitution at this position, affected the binding of the R^1 group within the hydrophobic pocket.

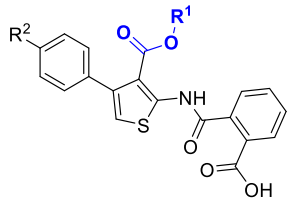

64

Figure 94: General structure for ester series.

The data for the ester series demonstrated that a parallel existed between the lipophilicity of the R^1 groups and potency, because as the VDW radius of the R^1 group increased (**81** IC_{50} 48 μM to **90** IC_{50} 0.92 μM, Figure 95), a simultaneous growth in potency of almost two full log units was observed. Moving forward, the isopropyl group of ligand **83** (Figure 95) was selected as the choice of substituent at this position, as this functionality exhibited favourable potency without becoming too lipophilic.

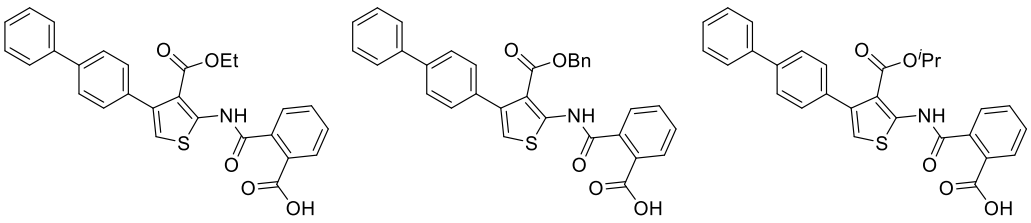

81 IC_{50} 48 μM **90** IC_{50} 0.92 μM **83** IC_{50} 8.5 μM

Figure 95: Alternative ester ligands with associated potency values.

Sustaining an electrostatic interaction within the phosphate binding pocket is generally thought to be crucial for affinity towards phosphatase targets.[26] This series of compounds were designed around scaffold **93** (Figure 96) to specifically probe the carboxylic acid head group, to assess how important it was for binding affinity and whether it could be changed for alternative acidic head groups.

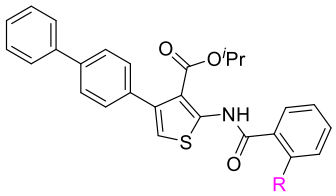

93

Figure 96 General structure of head group derivatives.

Data for this series indicated that the acidic head group was imperative for activity of the 2-amino thiophene series towards TIGAR. Alterations in the chemical make-up of the head group were possible (tetrazole **100** IC_{50} 9.7 μM, Figure 97); however, the substituted functionalities must also exhibit anionic properties at physiological pH for maintenance of potency. If the head group was capped and the anionic nature was removed (ligand **102** IC_{50} > 100 μM, Figure 97), then complete inactivity towards the target was observed.

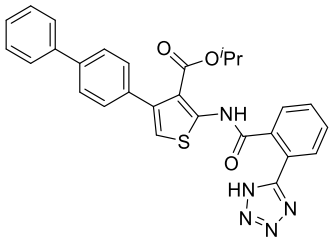

100 IC_{50} 9.7 μM

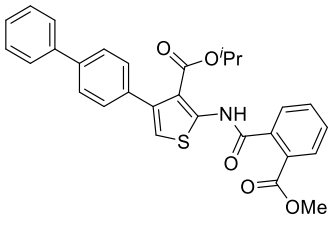

102 IC_{50} > 100 μM

Figure 97: Key head group derivatives with related potency values.

SAR studies next led to performing an interrogation of the phenyl group, which linked the 2-amido group of the thiophene core to the carboxylic acid head group (**103**, Figure 98). Alternative and substituted linkers were proposed in order to gauge how an alteration in linker properties and/or a change in the orientation of the acidic head group would affect binding affinity.

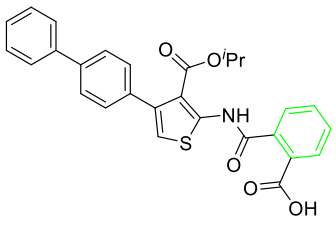

103

Figure 98: General structure of phenyl linker derivatives.

The data within this series (highlighted in Figure 99) has demonstrated that substitution of the phenyl linker with hydrophobic substituents (compound **121** IC_{50} 0.86 μM) had a positive impact on binding affinity. Whereas substitution with polar moieties (compound **107** IC_{50} > 60 μM) resulted in a loss of potency. Removal of the cyclic/aromatic properties (compounds **122** IC_{50} 31 μM) related to the phenyl linker motif, was also detrimental to potency, suggesting that the positioning of the acidic head group and aromatic VDW interactions of the linker, were crucial for binding to TIGAR. The phenyl linker group was retained for subsequent SAR studies as a balance between potency (IC_{50} 8.5 μM) and lipophilicity/M.wt.

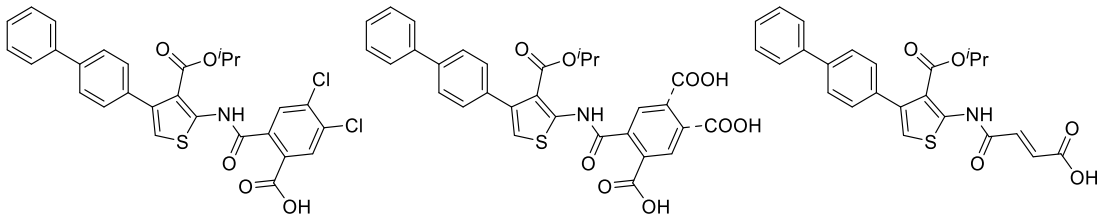

121 IC_{50} 0.86 μM **107** IC_{50} > 60 μM **122** IC_{50} 31 μM

Figure 99: Key phenyl linker derivatives with related potency values

Growth into the hydrophobic channel of the TIGAR active site was identified by initial modelling studies, as potentially being the main area of focus for driving potency and selectivity. A substantial amount of space was identified for ligand occupancy, with the potential for forming several interactions with neighbouring residues at this part of the binding pocket. An initial series of compounds for the interrogation of this hydrophobic channel were synthesised based around the generic scaffold **126** detailed in Figure 100.

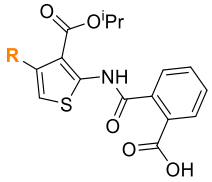

126

Figure 100: General structure of channel substituent derivatives.

Channel substituents comprised of unsubstituted aromatic rings (e.g. compound **167** IC_{50} > 40 μM) or fused carbocycles/heterocycles (e.g. compound **174** IC_{50} 37 μM) appeared to be too short in length to enable adequate occupancy of the hydrophobic channel, resulting in weak potency values. Phenyls substituted in the

para position with a saturated polar group (compound **177** IC_{50} > 60 μM) were completely inactive towards TIGAR. Ligands where the phenyl of the channel appendage was *para* substituted with an unsaturated motif, generally resulted in a slight increase in affinity (e.g. ligand **199** IC_{50} 1.4 μM). This data is highlighted in **Figure 101**.

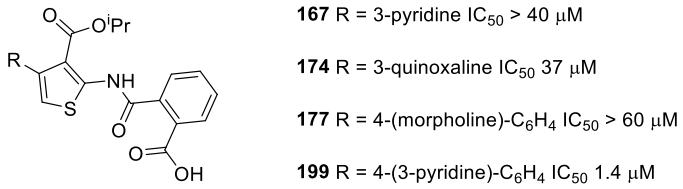

Figure 101: Key channel substituent derivatives with related potency values.

Introduction of an alkyne linker (compound **201** IC_{50} 0.84 μM) generated a significant increase in potency, showing that activity was affected by linker length and channel occupancy. Single atom linker ligands with increased flexibility afforded both a decrease in potency (compound **181** IC_{50} 1.3 μM) due to reduced hydrophobicity, and an improvement in potency (compound **182** IC_{50} 0.72 μM). Further extension of the linker to 2 atom units whilst maintaining flexibility, resulted in a respective increase in binding affinity for both the benzyloxy (compound **183** IC_{50} 0.77 μM) and the phenylethyl (compound **184** IC_{50} 0.56 μM) ligands, compared to their equivalent 1 atom analogues **181** and **182**, respectively. Optimal linker length of the channel substituent had now been identified and reinforced by molecular docking, which indicated that an additional π-cation interaction was potentially taking place with ligands **183** and **184**. Finally, substitution of alternative positions on the internal phenyl ring (e.g. **185** IC_{50} > 40 μM) resulted in complete inactivity, which was supported by the molecular docking of these compounds, as a steric clash with the protein was hypothesised. This data is outlined in **Figure 102**.

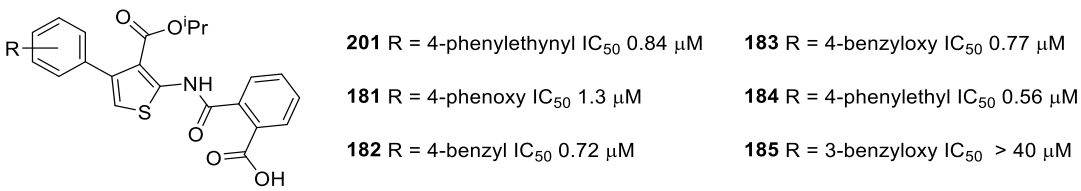

Figure 102: Key channel substituent derivatives with related potency values.

The potential for substitution at the 5-position of the core thiophene unit was proposed to be very limited, according to molecular modelling studies for the series. A small series of compounds were designed based around the generic scaffold depicted in **Figure 103**.

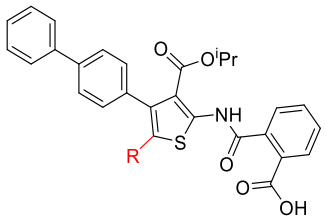

202

Figure 103: General structure of 5-substituted thiophene derivatives.

The two ligands prepared within this series (Figure 104) (**208** IC_{50} 0.87 μM, **209** IC_{50} > 40 μM) indicated that while a very shallow pocket of space clearly existed at this position of the TIGAR active site, there was also a very fine balance between the levels of possible substitution along this vector, for potency gain/loss. Based on these results, further investigations into this area of the SAR were not pursued due to the proposed computational studies and the observed experimental evidence.

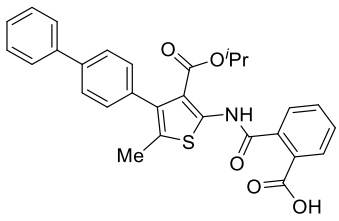

208 IC_{50} 0.87 μM

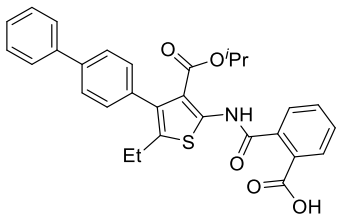

209 IC_{50} > 40 μM

Figure 104: Key 5-position substituted derivatives with related potency values.

The synthesis a few select hybrid compounds that married the optimised portions of the molecule, resulted in the formation of the ligands depicted in **Table 17**.

Table 17: **IC_{50} values for hybrid compounds 211–213 and 215.**

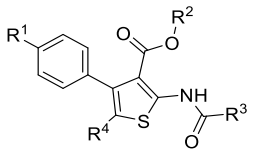

Compound	R^1	R^2	R^3	R^4	IC_{50} (μM)[a]
211	Ph	Bn	*o*-COOH-4,5-dichloro-C_6H_2-	H	0.51
212	Ph	^{i}Pr	*o*-COOH-4,5-dichloro-C_6H_2-	Me	0.61
213	$PhCH_2CH_2$	^{i}Pr	*o*-COOH-4,5-dichloro-C_6H_2-	H	0.31
215	$PhCH_2CH_2$	Bn	*o*-COOH-C_6H_4-	H	0.19

[a] IC_{50} calculated as n=3

All four of the hybrid compounds synthesised within this series had a positive effect on activity. As expected, the compounds containing the phenyl ethyl channel substituent (**213** IC_{50} 0.31 μM & **215** IC_{50} 0.19 μM) afforded improved potency values compared to the hybrid ligands that incorporated the biphenyl channel substituent (**211** IC_{50} 0.51 μM and **212** IC_{50} 0.61 μM). The difference in potency between ligands **213** and **215** was proposed to be due to an alteration in the binding mode of the benzyl ester group, due to the presence of the phenyl ethyl channel moiety. This may have had a positive impact on the interactions being made by this ester derivative with the surrounding hydrophobic residues. Unfortunately, whilst these hybrid compounds exhibited favourable potency, they also displayed concerning physicochemical properties as they were very lipophilic (> 7.5 cLogP).[104-105] As a result, the hybrid ligands developed our understanding of the TIGAR active site but were not selected for efficient chemical probe generation.

The design of sp3 character-containing derivatives of the best ligand to date **184** (Figure 105) was performed, as sp3 motifs have been shown to exert beneficial effects on physicochemical properties.[106] Two compounds (**216** and **217**, Figure 105) were tested to identify if the potency of ligand **184** could be retained. Both **216** (IC_{50} 0.82 μM) and **217** (IC_{50} 0.95 μM) displayed reduced potency in comparison to parent ligand **184** (IC_{50} 0.56 μM). However, they did not demonstrate inactivity towards the target protein, indicating that favourable binding could still be maintained when moving to sp3-enriched scaffolds. While these ligands were not as potent as the current lead compound **184**, they demonstrated sufficient potency for

this type of scaffold to be considered for incorporation into lead compounds, at the end of the SAR investigations.

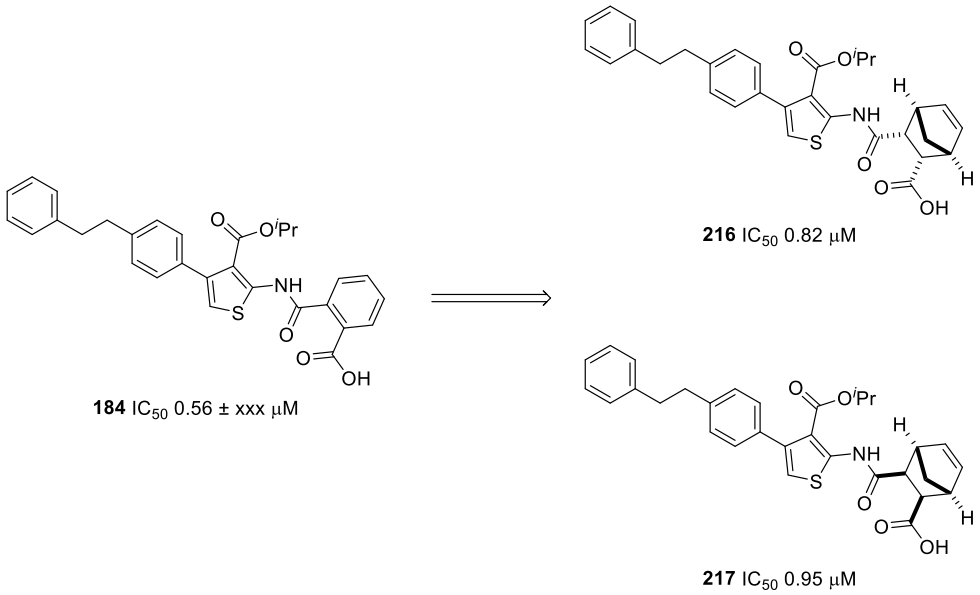

Figure 105*: *Proposed sp3 derivative structures based upon ligand 184.

The chemical instability of the ester substituent could potentially result in poor metabolic profiles during cell and/or *in vivo* studies.[78] A new series of compounds including the amide isostere, were designed to mitigate the metabolic instability of the ester functionality, based around the generic scaffold **218** displayed in **Figure 106**. The R group appendage was heavily varied within this series to further probe the hydrophobic pocket to discover if further potency gains could be achieved.

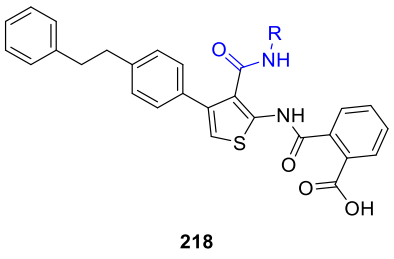

Figure 106: General structure of amide derivatives.

Initial modification of the isopropyl ester **184** (IC_{50} 0.56 μM) to the isopropyl amide **243** (IC_{50} 0.45 μM), afforded an improvement in chemical stability as well as an approximate 100 nM increase in potency. The amide series helped to aid understanding of the properties and finer details associated with the TIGAR pocket,

however, none of the ligands examined provided any significant potency advances, over the original isopropyl amide (**243**, Figure 107), that justified the associated negative impact on physicochemical properties.

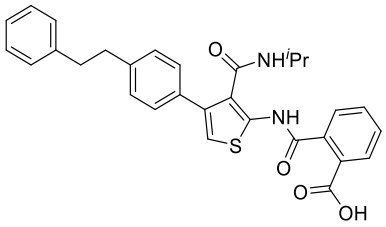

243 0.45 μM

Figure 107: Isopropyl amide 243 structure.

Using the predicted binding mode of ligand **184**, a second series of channel substituent compounds were tested, that varied substitution of the outer phenyl group (scaffold **264**, Figure 108) and incorporated a range of heterocyclic motifs to replace the outer phenyl group entirely (scaffold **265**, Figure 108).

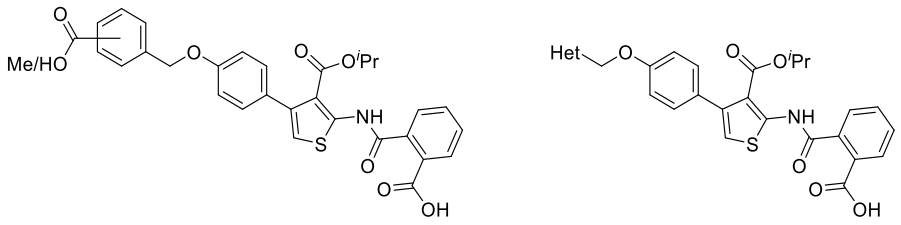

264 **265**

Figure 108: Channel substituent series 2 scaffolds.

The data for the following compounds is described in **Figure 109**. In terms of substitution of the outer phenyl group, the addition of a carboxylic acid at the *meta-* position (**279** IC_{50} 0.41 μM) provided the best binding affinity. Carboxylic acid derivatives that were capped as a methyl ester (**277** IC_{50} 0.82 μM), afforded a diminished potency but did not result in inactivation, which potentially suggested that **277** was still binding favourably within the pocket but that possible, favourable electrostatic interactions with Arg192, had been disrupted.

For the outer heterocycle-based compounds, pyrazine ligand **328** (IC_{50} 0.37 μM) generated the best potency for this series. According to modelling studies, this was potentially accomplished through the optimisation of hydrogen bonding interactions with nearby arginine residues (Arg192 & Arg90) that were exposed beyond the

hydrophobic channel. Fused heterocyclic head groups, such as 6-quinoline **330** (IC_{50} 1.1 μM), proved deleterious to binding affinity. Based upon the molecular model for the series, this was proposed to be for steric reasons, as fused heterocycles were hypothesised to be too large to effectively position themselves in the active site, which led to them potentially adopting an unfavourable geometry and undesirable interactions with solvent.

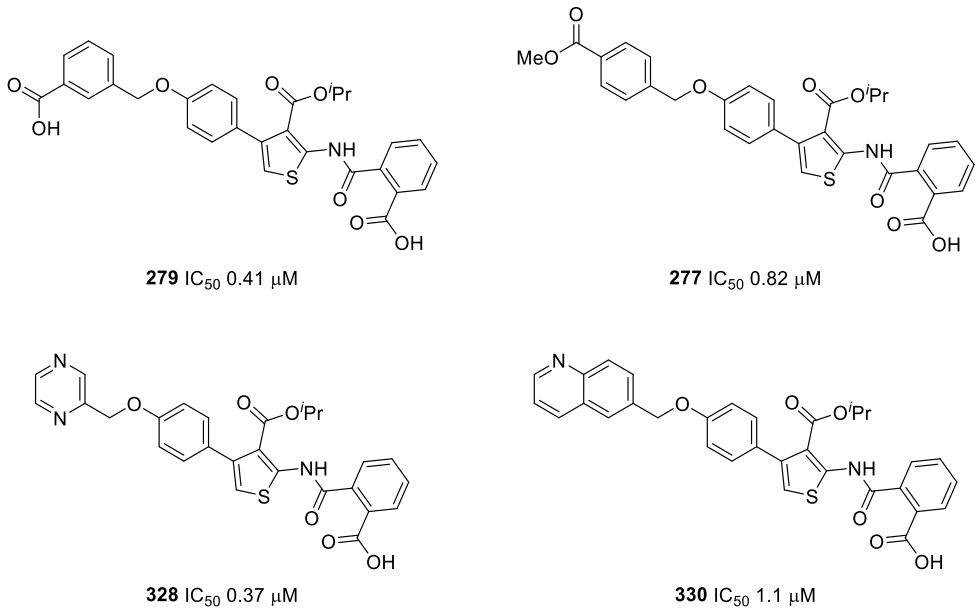

Figure 109: Key channel substituent derivatives with related potency values.

The final series within the SAR programme consisted of designing a second series of hybrid compounds, based around scaffold **331** (Figure 110). Hybrid ligands on this series brought together the optimised pyrazine group of **328**, for enhanced binding beyond the hydrophobic channel and the amide bioisostere **243**, for improved metabolic stability.

Hybrid generation within this series, using ligands **243** (IC_{50} 0.45 μM) and **328** (IC_{50} 0.37 μM), resulted in the generation of two lead compounds for the entire 2-amino thiophene compound series (**338** IC_{50} 0.26 μM and **348** IC_{50} 0.14 μM, Figure 111). A primary aim of the project was to develop a potent chemical probe for the phosphatase target TIGAR, and this had been achieved through the design, synthesis and evaluation of this final hybrid compound series. Compounds **338** and **348** were next subjected to DMPK profiling to assess whether the ligands had satisfactory physicochemical properties for further cell/*in vivo* studies.

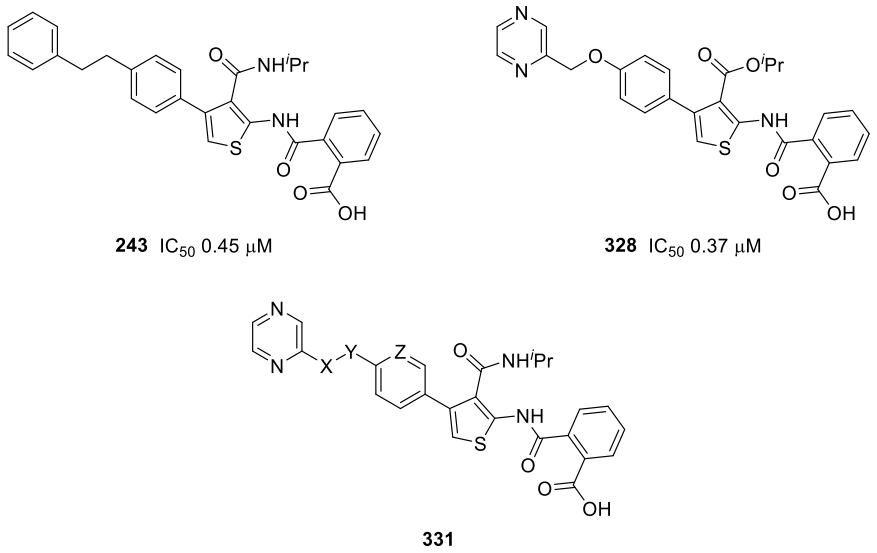

Figure 110: Optimised compounds 243, 328 and general structure of hybrid series 2 derivatives.

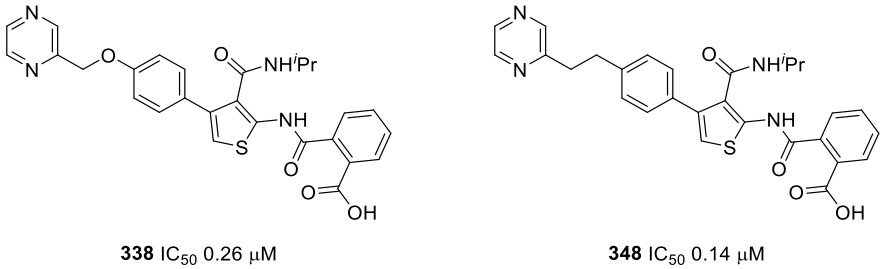

Figure 111: Key hybrid series 2 derivatives with related potency values.

SAR data generated during the investigation is summarised in **Figure 112**.

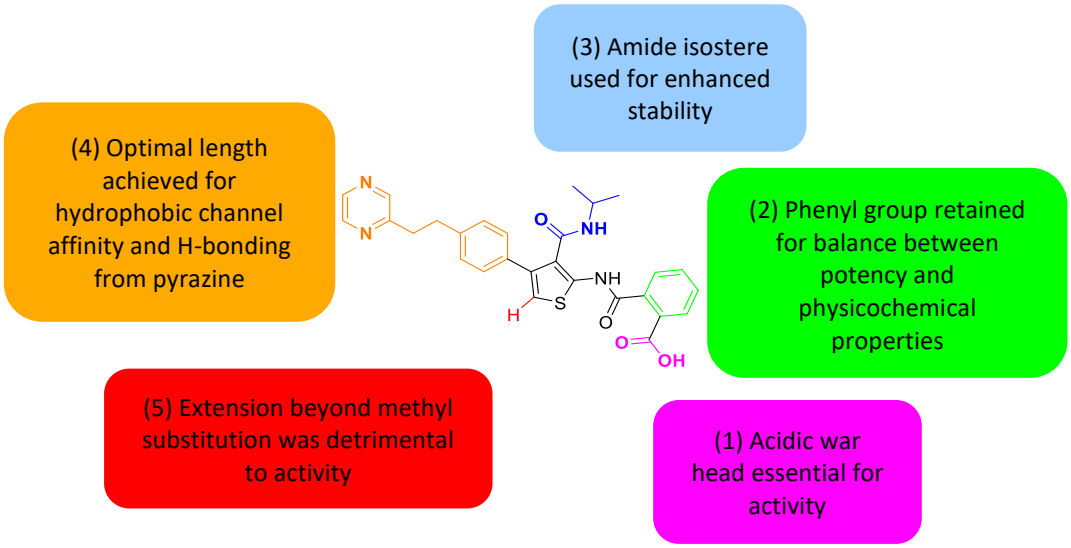

Figure 112: *SAR summary for 2-amino thiophene scaffold.*

In summary, (1) the anionic/acidic warhead acts by forming an electrostatic interaction with multiple cationic residues in the orthosteric site and was essential for activity; carboxylic- and sulfonic acid groups were both well-tolerated but the carboxylic group was selected as it had a smaller impact on the total polar surface area (TPSA); a tetrazole moiety was also tolerated and has the potential to serve as a metabolically stable replacement if required;[100] (2) the phenyl linker between the amide and carboxylic acid head group was found to play a crucial role in the orientation of the head group as well as providing additional hydrophobic interactions; linkers with a smaller degree of saturation or acyclic linkers proved detrimental to activity; phenyl groups substituted with lipophilic moieties improved potency with a penalty in M.wt. The standard phenyl linker was retained as a balance between potency and desired physicochemical properties; (3) an amide isostere with a branched aliphatic chain was selected over the corresponding ester, to aid chemical stability and enhance hydrophobic interactions in the small pocket;[78] multiple amide and ester substituents positively impacted potency but many of these had questionable stability and increased M.wt values, so the isopropyl functionality was taken forward; (4) various aromatic groups, heterocycles, linker lengths/types and substituents were tested to improve binding affinity in the hydrophobic channel section of the ligand; optimal length and conformation within the channel were achieved with the aliphatic linker (CH_2CH_2), attached internally at the para position of a phenyl group, for favourable interactions within the lipophilic tunnel; a pyrazine group linked to the external side of the aliphatic tail unit, was proposed to be adopting hydrogen-bonding interactions with nearby amino acids (Arg192 and Arg90), and this structural change resulted in the most potent compound (0.14 μM) of the series; (5) expansion along this vector with a methyl group gave potency gains, however, further growth with an ethyl group exhibited a negative effect on potency; no further exploration of this SAR position was therefore performed.

5.3. DMPK, selectivity and cell data

In conclusion, **Table 18** showed that both lead compounds displayed positive cLogD values (**338** 1.1 and **348** 1.4) and satisfactory TPSA values (**338** 129.5 $Å^2$ and **348** 120.2 $Å^2$), indicating that each tested compound may undergo absorption during *in vivo* studies. Both compounds also possessed M.wt values (**338** 516 and **348** 514) that were just over the suggested 500 limit of the Lipinski rules.[109] Aliphatic linker-based derivative **348** (S9 10.8 μL/min/mg protein $t_{1/2}$ 64.5 min) possessed

moderate clearance and $t_{1/2}$ values. Pleasingly, S9 clearance values dropped dramatically when the pyrazine moiety was combined with the phenyl ether functionality (**338** S9 0.89 μL/min/mg protein $t_{1/2}$ 781 min), which also resulted in a significantly increased $t_{1/2}$ value, demonstrating that ligand **338** possessed a desirable metabolic profile. Both compounds also exhibited enhanced solubility (**338** 65 μM and **348** > 100 μM), due to the increased polarity of the respective scaffolds. All of the above data is highlighted in Table 18. Initial DMPK profiling for ligands **338** and **348** had proven promising and so, both ligands were taken forward and subjected to testing within a hepatocyte stability assay, to provide further evidence that demonstrated the robustness of these chemical probes.

Table 18: Initial DMPK profile data for 338 and 348.

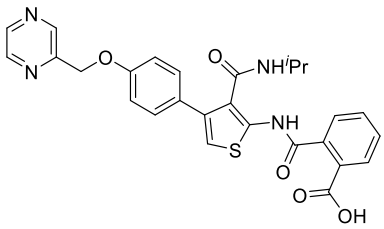

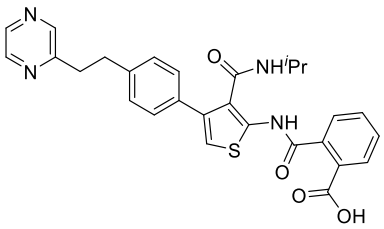

Compound	**338**	**348**
IC_{50} (μM)	0.26	0.14
cLogD	1.1	1.4
TPSA (Å^2)	129.5	120.2
M.Wt.	516	514
S9 Clearance mouse (μL/min/mg protein)	0.89	10.8
$t_{1/2}$ mouse (min)	781	64.5
Solubility (μM)	65	>100

Ligands **338** and **348** were tested within a hepatocyte stability assay, in order to further determine their metabolic stability profiles. Analogue **348** exhibited a very high hepatocyte clearance value of 88.8 μL/min/10^6 cells and a short $t_{1/2}$ value of 15.6 minutes, resulting in an inadequate metabolic profile. This meant that ligand **348** could not be progressed towards further cellular/*in vivo* studies. Ether derivative **338** showed an improved but still high hepatocyte clearance value of 54.9 μL/min/10^6 cells and a moderate $t_{1/2}$ value of 25.2 minutes, meaning that compound **338** had satisfactory metabolic stability, within the hepatocyte stability assay. Ligand **338** has therefore been taken forward for further testing in the form of cellular and potential *in vivo* studies. All of the above data is outlined in **Table 19**.

Table 19: Hepatocyte stability for compounds 338 and 348.

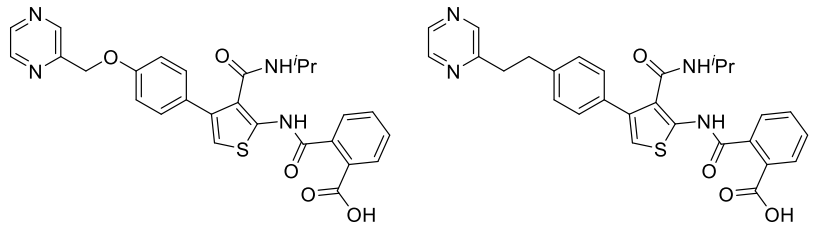

Compound	**338**	**348**
Clearance mouse (μL/min/10^6 cells)	54.9	88.8
$t_{1/2}$ mouse (min)	25.2	15.6

At this current stage of the project, lead compounds **338** and **348** have yet to be screened against a selectivity panel of phosphatases, as outsourcing has focussed primarily on generating DMPK profiles for these ligands. However, at an earlier point in the project when ligand **184** (Figure 113) was the lead compound, it was decided that a selectivity profile should be acquired for the series at this stage.

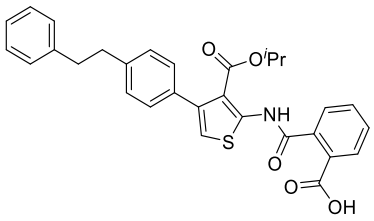

184 IC_{50} 0.56 μM

Figure 113: Ligand 184 used for selectivity studies.

Ligand **184** was screened against a panel of 22 physiologically relevant phosphatases at a single point concentration of 1 μM (Figure 114). All 22 phosphatases demonstrated ≥ 77% activity in the presence of test compound **184**. This identified that **184** showed low levels of inhibition (≤ 23%) against these phosphatases, even at a concentration of 1 μM. In comparison, TIGAR activity levels (12%), determined within an in-house *in vitro* assay using ligand **184**, at an equivalent concentration of 1 μM, outlined a clear selectivity profile in favour of TIGAR. The 96% activity value associated with PTP1B, reinforced an original proposal for the project that selectivity for TIGAR against PTP1B would be generated through natural growth into the TIGAR active site. A desirable selectivity profile for the 2-amino thiophene compound series had now been established. This data showed promise for the future development of a selective chemical probe for TIGAR.

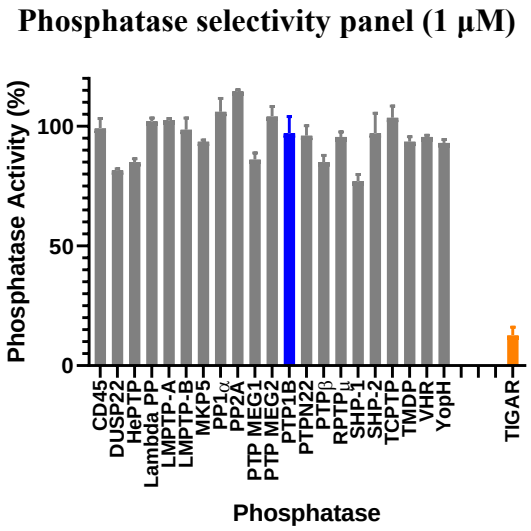

Figure 114: Tyrosine phosphatase selectivity panel with PTP1B highlighted. TIGAR data from in vitro assay added for comparison.

TIGAR cellular studies were performed at the same stage in the project as the selectivity studies. At this stage of the SAR investigations, ligand **184** (Figure 113) was the most potent compound and so, this probe molecule was sent to our biological collaborators (Vousden lab) for initial cell studies. These early studies were performed to establish multiple key properties for the chemical probe series; (1) compound permeation of the cell membrane; (2) target engagement/affinity; (3) initiation of desirable downstream functional effects. In order to test whether TIGAR inhibition would offer a therapeutic advantage by reversing the observed effects of TIGAR overexpression, a cellular study had to be created, where the relationship between TIGAR inhibition and the synthesis of R-5-P *via* the oxidative PPP, could be measured. Measurement of oxidative PPP access was essential, as it is the TIGAR induced flux along this branch of the PPP, that leads to downstream antioxidant effects/apoptosis inhibition and increased cancer cell survival.[39]

An initial cellular experiment was developed that allowed the production of singly labelled R-5-P by the oxidative PPP, to be accurately measured. This was achieved by feeding pancreatic cancer cells with doubly ^{13}C labelled glucose, that took advantage of a labelled carbon unit loss, during synthesis of R-5-P, through the oxidative PPP. The levels of singly labelled R-5-P were quantified in both TIGAR KD and inhibitor experiments, using an FA6 cell line, treated with menadione to induce oxidative stress. Pleasingly, the inhibitor results phenocopied the KD data, as both experiments resulted in the depletion of R-5-P concentration, to approximately

half (KD R-5-P levels = 54%, inhibitor **184** R-5-P levels = 48%) of the maximum concentration observed with the DMSO control. The levels of the natural substrate F-2,6-BP and the downstream glycolytic metabolite G-3-P were additionally measured in the presence of probe **184**. Concentration levels for both species were increased (> 100-fold for F-2,6-BP, 7-fold for G-3-P), suggesting that the inhibitor was preventing the dephosphorylation of F-2,6-BP and increasing the rate of glycolysis, to promote G-3-P production. Collectively, the data generated from this proof of concept model strongly suggested that inhibitor **184** was binding to TIGAR and inducing downstream functional effects. This was a highly beneficial outcome, as cellular activity had now been established for the series, which greatly promoted the chances of being able to use the chemical probes on this series, to perform *in vivo* studies.

In conclusion, a secondary cellular experiment was developed, that allowed the rate of gluconeogenesis to be accurately monitored. This was achieved by feeding pancreatic cancer cells with triply ^{13}C labelled glycerol, that took advantage of the labelled carbon unit loss, during synthesis of R-5-P through the oxidative PPP, which resulted in the generation of doubly labelled 3 carbon units, upon re-entry into glycolysis through the non-oxidative PPP. The levels of doubly labelled R-5-P were quantified using an FA6 cell line, treated with menadione, to induce oxidative stress. Pleasingly, inhibitor **184** resulted in the depletion of doubly labelled R-5-P concentration by 95%, when compared to the maximum concentrations observed with the DMSO control. Additionally, the levels of triply and doubly labelled 3-P-G were also measured in the presence of inhibitor **184**. A small drop (25%) in triply labelled 3-P-G concentration was observed compared to the DMSO control, suggesting that triply labelled 3-P-G levels were relatively unaffected within glycerol-fed conditions. The formation of doubly labelled 3-P-G was heavily dependent on enhanced gluconeogenesis and the subsequent oxidative/non-oxidative PPP. Results demonstrated that doubly labelled 3-P-G concentration was significantly reduced (98% reduction), when cells were treated with compound **184**, in comparison to the DMSO control value. TIGAR inhibition by **184** produced increased F-2,6-BP levels and increased PFK-1 activation, which resulted in a substantial reduction in the rate of gluconeogenesis, in comparison to the directly opposite effects observed for the DMSO control sample, where TIGAR was

upregulated. This meant the doubly labelled 3-P-G production was severely restricted as the oxidative PPP could not be readily accessed by upper glycolysis metabolites. Collectively, the data generated from this alternative proof of concept model, strongly indicated that inhibitor **184** was binding to TIGAR and inducing significant downstream functional effects. Cellular studies have also demonstrated that TIGAR inhibition could significantly regulate metabolite flow through glycolysis and the oxidative PPP. These initially observed functional effects using chemical probe **184** may lay the foundations for inducing oxidative apoptosis within malignant cells, which would consolidate the therapeutic value of TIGAR.[39, 132]

6. Future work

6.1. Further SAR studies and biophysical characterisation

To date on the project, an extensive SAR investigation has been performed on the 2-amino thiophene scaffold. All of the vectors available for growth with this structure have been explored in-depth to generate an expansive compound library, whose biochemical potencies have significantly developed our understanding of the properties possessed, by the TIGAR active site. This concluded with the development of two lead chemical probe compounds. The only key compound section that has yet to be examined, is the 2-amino thiophene core unit itself. Initial future work could originate around substituting this core thiophene heterocycle, for alternative core scaffolds, possessing different vectors for substituent growth (Figure 115). Alterations of this type would also demonstrate how essential the thiophene ring system and the vectors along which it directs its substituents, are for the binding affinity of this scaffold type. Modifications of the thiophene unit may result in the generation of alternative binding modes within the orthosteric site, which could potentially offer new avenues for further SAR studies.

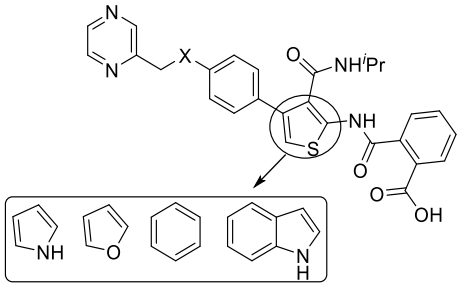

Figure 115: Summary of potential alterations of thiophene core unit.

Figure 116 highlights the molecular docking of indole derivative **356**, a possible new core scaffold. The docking studies hypothesised that **356** displayed a relatively similar binding mode to the original 2-amino thiophene core series, but that the core unit itself was orientated in a totally different manner. This could potentially generate new vectors along which to grow within the TIGAR active site, leading to a second ligand series with the opportunity for further potency development.

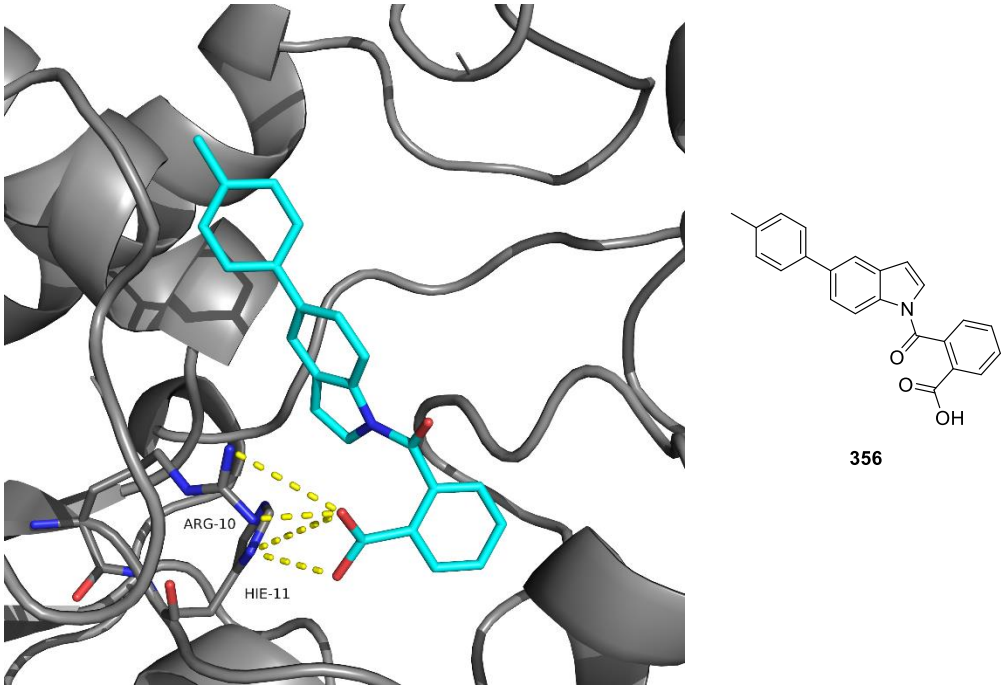

Figure 116: Indole 356 (cyan) modelled in TIGAR active site. Key electrostatic interactions highlighted by dashed yellow lines.

In terms of further alterations or substitution along the already investigated vectors, the acquisition of a crystal structure would greatly aid further potency development, with the 2-amino thiophene scaffold. Our molecular model has proven to be reasonably consistent with observed experimental data, however, we believe that the model has reached its limitations in terms of driving potency. It has been proposed that an X-ray structure of a ligand bound TIGAR sample, could be the only efficient method for identifying subtle interactions/opportunities within the binding pocket, for a further significant enhancement in potency. Selected compounds from the series have been submitted for crystallography studies with native TIGAR protein, to try and obtain a ligand bound X-ray structure.

At this point in time, no biophysical characterisation has been made of the compounds described within this report to assess their binding affinity for TIGAR. This type of data could potentially be obtained through a technique known as a Differential Scanning Fluorimetry assay, which assesses the thermal melt temperature of both the apo protein and the ligand bound structure to produce a temperature differential (ΔT). A high ΔT is indicative of a ligand with a strong binding affinity for the selected protein. The data obtained from this assay would effectively complement the already generated competitive assay data and provide further support for ligand interaction with TIGAR.

6.2. Metabolic enhancement

As described in Section 4.3.1.2. lead compounds **338** and **348** both exhibited a significant increase in metabolic instability, within the hepatocyte assay (**338** clearance 54.9 μL/min/10^6 cells, $t_{1/2}$ 25.2 min, **348** 88.8 μL/min/10^6 cells, $t_{1/2}$ 15.6 min) compared to the microsomal S9 assay (**338** clearance 0.89 μL/min/mg protein, $t_{1/2}$ 781 min **348** clearance 10.8 μL/min/mg protein, $t_{1/2}$ 64.5 min). A known reason for this difference is the enhanced phase II metabolism of compounds, as this type of metabolism is more prolific in hepatocyte studies than microsomal.[80] Increased phase II metabolism would most likely be occurring through glucuronidation (conjugation of a glucose unit) of the carboxylic acid head group. Potential future work could involve the exchange of the carboxylic acid head group for the tetrazole bioisostere (compound **357**, Figure 117). Tetrazole functionalities are known to mimic the electronic and structural properties of carboxylic acid groups, whilst also exhibiting enhanced metabolic stability.[100] Previous SAR studies on this project highlighted that the tetrazole moiety could be incorporated as a carboxylic acid replacement, that retained approximately equivalent potency. Future work on the project may be able to use this tactic for improving the metabolic profile of ligands **338** and **348**, through resistance towards phase II metabolism.

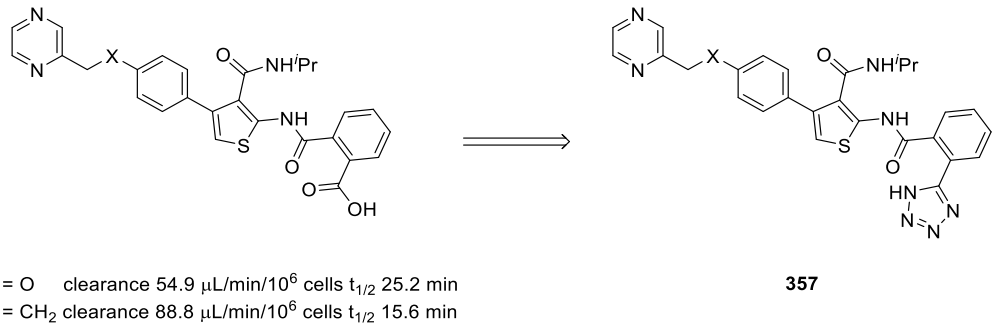

Figure 117: Proposed tetrazole scaffold upon modification of ligands 338 and 348.

6.3. Selectivity data

Selectivity data was determined for phenylethyl ligand **184** (Figure 118) and described in Section 4.3.2. Future work on the project will include submitting lead compound **330** to undergo the same selectivity profile as ligand **184**, against the panel of tyrosine phosphatases. This study will be crucial for confirming that the same levels of selectivity have been retained during development of the lead compounds. It will also be very interesting to observe if selectivity towards TIGAR has improved, during the optimisation phase of the SAR, progressing from ligand **184** to lead compound **338**.

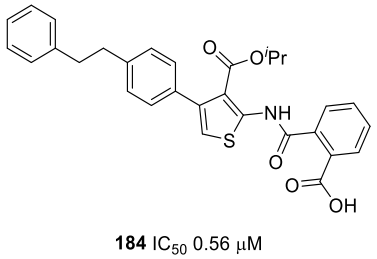

Figure 118: Ligand 184 used for selectivity studies.

If the option becomes feasible, it would also be extremely beneficial to be able to generate selectivity data for ligand **338** against a panel of histidine phosphatases. Being selective against the tyrosine phosphatase family would be considered excellent, however, obtaining selectivity against the histidine phosphatase family would significantly enhance the efficiency of the chemical probes within this series and aid future cell/*in vivo* studies.

6.4. Future cell and potential *in vivo* studies

Immediate future work will consist of running probe compound **338** (Figure 119) through the same cell studies that were performed using ligand **184**. This will include employing the same glucose-fed and glucose-starved (glycerol-fed) experimental set-ups described in Section 4.3.3. to determine the cellular activity levels of derivative **338**. These studies will establish whether these ligands can still permeate cell membranes, interact/bind with the target protein and induce a desirable downstream functional effect.

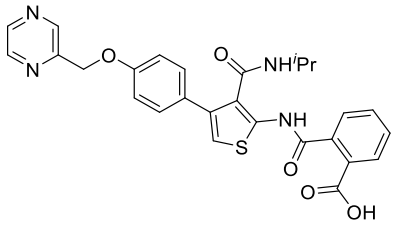

338

Figure 119: Lead compound 338.

If initial cell studies appear promising, then further investigations, that can assess the therapeutic activity of **338**, will be performed. This may include using Western Blot analysis to quantify the levels of apoptosis induced within malignant cell lines (FA6), through the inhibition of TIGAR, by probe **338**.

If the favoured DMPK profile for compound **338** can be combined with sufficient selectivity data and satisfactory cellular activity, then an efficient chemical probe will have been developed, that is capable of undergoing *in vivo* studies within a mouse model, in the Vousden research group. This would allow the final aim of the project, described in Section 2.0. to be achieved. *In vivo* studies using a robust chemical probe, will allow for further dissection and increased understanding, of the fundamental biology associated with TIGAR.

7. Experimental

General: All commercially available reagents and chemicals were used without any further purification unless otherwise indicated. Microwave reactions were carried out using a BIOTAGE initiator microwave.

Purification: Purification was performed by flash column chromatography, with chromatography grade silica 60 Å particle size 35-70 micron from Fisher Scientific, using the solvent systems stated and also by an Agilent technologies semi-preparative LC-MS (Liquid chromatography-mass spectrometry). Final products were dried through the utilisation of a high vacuum system installed in the fume hood. LC-MS spectra were obtained using an Agilent technologies semi-preparative LC-MS, with a gradient of 5-95% to 100-0% (Acetonitrile/water).

NMR spectroscopy: ^{1}H and ^{13}C NMR were carried out using a Bruker Avance 3 (^{1}H 400 MHz and ^{13}C 101 MHz) and a Bruker Avance 500 (^{1}H 500 MHz and ^{13}C 125 MHz) as stated. The spectra were recorded in the deuterated solvents $CDCl_3$ (chloroform), $(CD_3)_2SO$ (dimethyl sulfoxide) and CD_3OD (methanol). Multiplicities were indicated as follows: s (singlet); br s (broad singlet); d (doublet); t (triplet); dd (doublet of doublets); tt (triplet of triplets); m (multiplet); app t (apparent triplet) etc… Coupling constants (*J*) were given in Hertz. Chemical shifts were reported in parts per million (ppm) relative to tetramethylsilane (TMS) as an internal standard. Peaks with δ values of 7.26, 2.50, 3.31 ppm (^{1}H NMR) and 77, 40, 49 ppm (^{13}C NMR) correspond to the residual solvent peak for $CDCl_3$, $(CD_3)_2SO$ and CD_3OD respectively.

Melting point analysis: Melting points were measured on a Stuart automatic melting point apparatus, SMP40.

Infrared: IR spectra were recorded from solid samples using a SHIMADZU IRAFFINITY-1 spectrophotometer with a Perkin Elmer Universal ATR (attenuated total reflectance) sampling accessory. Absorption frequencies are reported in wavenumbers (cm^{-1}).

7.1. General Procedures

General Procedure A: Phosphonic acid preparation.[58]

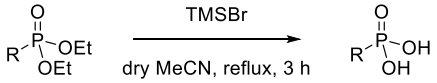

The appropriate phosphonate (1.0 eq.) was dissolved in dry acetonitrile (MeCN) (0.13 M). Bromotrimethylsilane (TMSBr) (19.5 eq.) was added dropwise to the stirred solution, under nitrogen, and the reaction mixture was heated to 65 °C for 3 hours. The volatiles were removed *in vacuo* before the resulting residue was co-evaporated multiple times with toluene (PhMe) / methanol (MeOH). Aqueous MeOH was then added and the solution was evaporated to dryness to afford the desired phosphonic acid.

General Procedure B: Amido lactone preparation.[61-62]

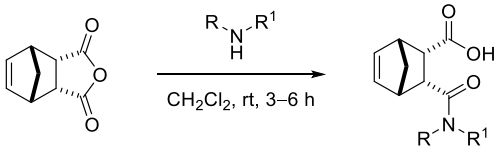

To a solution of endic anhydride (1.0 eq.) in anhydrous dichloromethane (CH_2Cl_2) (0.90 M) was added the appropriate amine (1.0 eq.). The reaction mixture was stirred at room temperature until completion, which was monitored by TLC. The resultant precipitate was filtered *via* Buchner funnel and subsequently washed with cold CH_2Cl_2, before being air-dried.

General Procedure C: Squaric acid derivative preparation.[67]

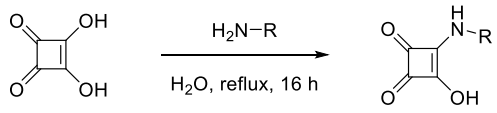

To a solution of squaric acid (1.0 eq.) in deionised H_2O (0.17 M) was added, with stirring, the appropriate amine (0.95 eq.). The reaction mixture was heated to reflux for 16 h before being allowed to cool to room temperature. The resultant precipitate was collected by vacuum filtration. The crude product was purified by flash column chromatography using a CH_2Cl_2/MeOH gradient to yield the desired product.

General Procedure D: Gewald synthesis.[68]

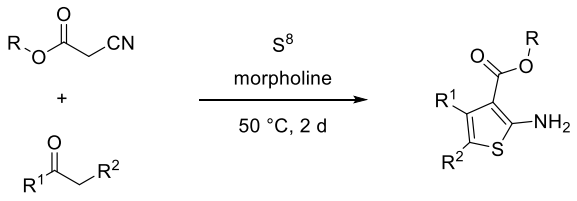

A microwave vial equipped with a stirrer bar, was charged with elemental sulfur (1.0 eq.) and morpholine (1.0 eq.), which were stirred until total dissolution of the sulfur occurred. The appropriate cyanoacetate (2.0 eq.) and the appropriate ketone (1.0 eq.) were subsequently added before the microwave vial was sealed. The neat reaction mixture was then heated to 50 °C for 2 days. Crude products were purified directly by flash column chromatography to afford the desired products.

General Procedure E: Anhydride ring-opening.[68]

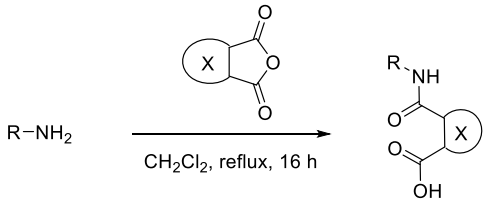

To a solution of the appropriate amine derivatives (1.0 eq.) in anhydrous CH_2Cl_2 (0.05 M) was added cyclic anhydride (1.0 eq.). The mixture was refluxed overnight under an inert atmosphere (N_2). The reaction mixture was concentrated under reduced pressure and purified directly by flash column chromatography to yield the desired product.

General Procedure F: Esterification.[96]

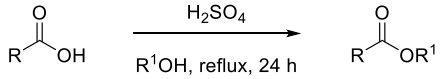

To a stirred solution of the selected carboxylic acid (1.0 eq.) in the appropriate alcohol (0.1 M), was added a few drops of sulfuric acid (H_2SO_4). The reaction mixture was stirred and heated to reflux for 24 h before the mixture was concentrated under reduced pressure, The resultant residue was dissolved in EtOAc (20 mL) which was washed with $NaHCO_3$ (15 mL), brine (15 mL), filtered and dried over

$MgSO_4$ before being concentrated under reduced pressure. Crude products were purified by flash column chromatography to yield the desired ester.

General Procedure G: Hydrolysis.[93]

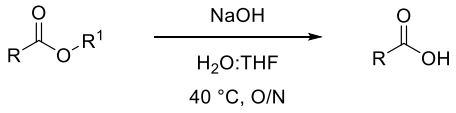

The appropriate ester derivative was dissolved in THF:H_2O (1:1) (0.4 M). A solution of 2 M NaOH (0.1 M) was added and the reaction mixture was heated to 40 °C overnight. The reaction mixture was allowed to cool to room temperature and was subsequently diluted with dH_2O (10 mL). The aqueous layer was extracted with ethyl acetate (10 mL) and then acidified with conc. HCl to pH 5. The aqueous layer was then extracted with ethyl acetate (3 × 10 mL) and the combined organic extracts were dried over $MgSO_4$, filtered and concentrated under reduced pressure to afford the appropriate carboxylic acid.

General Procedure H: Alkylation.[111]

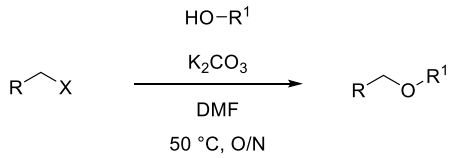

The appropriate halogen/pseudo halogen derivative (1.2 eq.) and phenol derivative (1.0 eq.) were dissolved in dimethylformamide (DMF) (0.2 M), before potassium carbonate (K_2CO_3) (3.0 eq.) was subsequently added. The resulting solution was stirred overnight at 50 °C. The reaction was then quenched with deionised H_2O (80 mL) before being extracted with CH_2Cl_2 (5 × 50 mL). The organic extracts were combined, dried over $MgSO_4$, filtered and concentrated under reduced pressure. Crude products were purified by flash column chromatography to yield the desired product.

General Procedure I: Amide bond formation.[107]

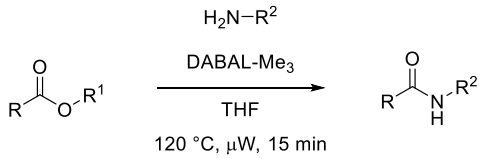

Neat samples of the appropriate amine (1.0 eq.) and methyl ester (1.0 eq.) derivatives and DABAL-Me_3 (0.8 eq.), were placed in a microwave vial, purged with N_2, before dry THF was added (0.6 M). The vial was irradiated in a Biotage microwave reactor at 130 °C for 15 minutes before being allowed to cool to room temperature. The reactions were quenched with aqueous solutions of Rochelle salt (saturated potassium sodium tartrate, 2 M) (Care: methane liberated). Extraction with CH_2Cl_2 (4 × 20 mL), drying over $MgSO_4$, filtration and subsequent concentration under reduced pressure provided crude products. Further purification by flash column chromatography, yielded the desired product.

General Procedure J: Mesylation.[113]

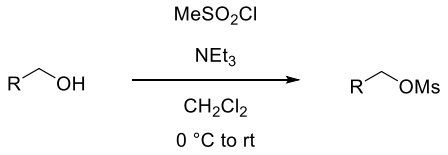

A solution of the appropriate alcohol (1.0 eq.) in anhydrous CH_2Cl_2 (0.78 M) was cooled to 0 °C under a nitrogen atmosphere. NEt_3 (1.1 eq.) was added and the mixture was stirred for 10-15 minutes, before methane sulfonyl chloride (1.1 eq.) was added dropwise, while keeping the temperature below 10 °C. The reaction mixture was then stirred at room temperature for 1 hour, quenched with water (40 mL) and extracted with CH_2Cl_2 (3 × 50 mL). The organic extracts were combined before being dried with $MgSO_4$, filtered and concentrated under reduced pressure to provide the desired mesylated derivative as a brown residue.

7.2. Phosphonate series

Diethyl (hydroxy(phenyl)methyl)phosphonate (23)[16]

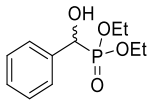

To a solution of tetrahydrofuran (THF) (63.0 mL, 0.30 M) at -20 °C was added sodium hydride (NaH) (498 mg, 20.7 mmol) followed by the dropwise addition of diethyl phosphite (2.67 mL, 20.7 mmol). The solution was stirred at this temperature for 20 minutes before a solution of benzaldehyde (1.92 mL, 18.8 mmol) in THF (50.0 mL, 0.38 M) was added. The solution was stirred for an additional 30 minutes before the reaction mixture was quenched with 5% saturated aqueous ammonium chloride (NH_4Cl) solution (63 mL). The mixture was then extracted with ethyl acetate (EtOAc) (3 × 80 mL). The combined organic extracts were washed with brine (150 mL), dried over magnesium sulfate ($MgSO_4$), filtered and concentrated under reduced pressure. Further purification *via* flash column chromatography (dry loading, CH_2Cl_2 4:1 EtOAc, isocratic) afforded the *title compound* as an off-white solid (2.93 g, 12.0 mmol, 64%). **mp** 84–86 °C; **IR** (ATR)/cm^{-1} 3412 (br), 3246, 2921, 1264, 1044; **^{1}H NMR** (500 MHz, $CDCl_3$) δ (ppm) 7.48 (d, 2H, *J* 7.5 Hz, 2 × Ar*H*), 7.35 (app t, *J* 8.0 Hz, 2H, 2 × Ar*H*), 7.32–7.27 (m, 1H, Ar*H*), 5.01 (dd, J_{PH} 11.0 Hz, *J* 5.5 Hz, 1H, OHC*H*PO) 4.13 (br s, 1H, CHO*H*), 4.07–3.94 (m, 4H, 2 × POCH_2CH$_3$), 1.26 (td, *J* 7.0 Hz, J_{PH} 1.5 Hz, 3H, POCH$_2$CH_3), 1.21 (td, *J* 7.0 Hz, J_{PH} 1.5 Hz, 3H, POCH$_2$CH_3); **^{13}C NMR** (125 MHz, $CDCl_3$) δ (ppm) 136.6, 128.3, 128.1, 127.1 (d, J_{PC} 6.3 Hz), 70.9 (d, J_{PC} 157.5 Hz) 63.3 (d, J_{PC} 7.5 Hz), 63.1 (d, J_{PC} 7.5 Hz), 16.4 (d, J_{PC} 5.0 Hz), 16.3 (d, J_{PC} 5.0 Hz) (2 carbons missing); **^{31}P NMR** (202 MHz, $CDCl_3$) δ (ppm) 21.5–21.2 (m, 1P, CH(OH)*P*O) **LRMS** (ES + APCI) *m/z*: calc. for $C_{11}H_{17}O_4P$ 244.1, found 245.1 $[M+H]^+$.

Diethyl benzoylphosphonate (24)[16]

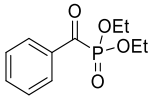

To a solution of oxalyl chloride (139 μL, 1.64 mmol) and CH_2Cl_2 (10.0 mL, 0.08 M) at -78 °C was added dropwise, *via* a syringe, dimethyl sulfoxide (DMSO) (128 μL, 1.80 mmol). The resulting solution was stirred at this temperature for 10 minutes

before a solution of compound **2** (200 mg, 0.82 mmol) in CH_2Cl_2 (6.0 mL, 0.14 M) was added dropwise. After stirring for a further 15 minutes, the reaction mixture was treated with trimethylamine (Et_3N) (660 μL, 4.76 mmol) and then allowed to warm to ambient temperature. The mixture was washed with H_2O (20 mL) and the aqueous portion was then extracted with CH_2Cl_2 (2 × 20 mL). The combined organic layers were washed with a 1% aqueous solution of hydrochloric acid (HCl) (4 × 50 mL). No further purification was required and so, the *title compound* was afforded as a yellow oil (187 mg, 0.77 mmol, 94%). **IR** (ATR)/cm^{-1} 3034, 2911, 1715, 1252, 1014; **^{1}H NMR** (500 MHz, $CDCl_3$) δ (ppm) 8.26 (d, 2H, *J* 8.0 Hz, 2 × Ar*H*), 7.63 (t, *J* 7.5 Hz, 1H, Ar*H*), 7.50 (app t, *J* 7.5 Hz, 2H, 2 × Ar*H*), 4.31–4.24 (m, 4H, 2 × POC*H*$_2$CH$_3$), 1.37 (t, 6H, 2 × POCH$_2$C*H*$_3$); **^{13}C NMR** (125 MHz, $CDCl_3$) δ (ppm) 199.2 (d, J_{PC} 173.8 Hz), 135.7 (d, J_{PC} 63.8 Hz), 134.9, 129.9, 128.9, 64.1 (d, J_{PC} 7.5 Hz), 16.5 (d, J_{PC} 5.0 Hz); **^{31}P NMR** (202 MHz, $CDCl_3$) δ (ppm) 1.29 (p, J_{PC} 7.9 Hz, 1P, CO*P*O(OCH$_2$CH$_3$)$_2$); **LRMS** (ES + APCI) *m/z*: calc. for $C_{11}H_{15}O_4P$ 242.1, found 242.9 $[M+H]^+$.

Diethyl (fluoro(phenyl)methyl)phosphonate (25)[16]

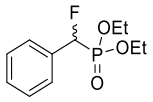

To a solution of diethyl aminosulfurtrifluoride (DAST) (240 μL, 1.78 mmol) in CH_2Cl_2 (0.74 mL, 1.66 M) at -78 °C was added rapidly, *via* syringe, a precooled (-78 °C) solution of **2** (300 mg, 1.23 mmol) in CH_2Cl_2 (7.70 mL, 0.16 M). The mixture was stirred at -78 °C for 3–4 minutes and then raised immediately to room temperature. After 1 hour of stirring at room temperature, the reaction was quenched with a saturated aqueous sodium hydrogen carbonate ($NaHCO_3$) solution (10 mL), followed by extraction with CH_2Cl_2 (3 × 15 mL). The combined organic extracts were dried over $MgSO_4$, filtered and then concentrated under reduced pressure. Further purification was carried out *via* flash column chromatography (dry loading, CH_2Cl_2 9:1 EtOAc, isocratic) to afford the *title compound* as a colourless oil (188 mg, 0.76 mmol, 62%). **IR** (ATR)/cm^{-1} 3032, 2930, 1259, 1022; **^{1}H NMR** (500 MHz, $CDCl_3$) δ (ppm) 7.47 (d, 2H, *J* 7.5 Hz, 2 × Ar*H*), 7.42–7.33 (m, 3H, 3 × Ar*H*), 5.67 (dd, J_{PH} 45.0 Hz, J_{FH} 8.0 Hz, 1H, FC*H*PO), 4.16–3.98 (m, 4H, 2 × POC*H*$_2$CH$_3$), 1.29–1.22 (m, 6H, 2 × POCH$_2$C*H*$_3$); **^{13}C NMR** (125 MHz,

$CDCl_3$) δ (ppm) 132.9 (d, J_{PC} 17.5 Hz), 129.1, 128.5 (d, J_{PC} 2.5 Hz), 126.8 (app t, $J_{PC + FC}$ 6.3 Hz), 89.4 (dd, J_{PC} 182.5 Hz, J_{FC} 168.8 Hz), 63.5 (d, J_{PC} 7.0 Hz), 63.3 (d, J_{PC} 7.0 Hz), 16.4 (d, 4.0 Hz), 16.3 (d, J_{PC} 4.0 Hz); **^{31}P NMR** (202 MHz, $CDCl_3$) δ (ppm) 6.39 (app t p, J_{FP} 116 Hz, J 8.0 Hz, 1P, CHF*P*O(OCH$_2$CH$_3$)$_2$); **^{19}F NMR** (471 MHz, $CDCl_3$) δ (ppm) -200.6 (dd, J_{PF} 84.5 Hz, J 44.5 Hz, 1F, CHF*P*O(OCH$_2$CH$_3$)$_2$)); **LRMS** (ES + APCI) *m/z*: calc. for $C_{11}H_{16}FO_3P$ 246.1, found 247.1 $[M+H]^+$.

Diethyl (difluoro(phenyl)methyl)phosphonate (26)[16]

To a solution of **3** (130 mg, 0.54 mmol), in CH_2Cl_2 (3.60 mL, 0.15 M) at 0 °C was added DAST (0.71 mL, 5.37 mmol). The reaction mixture was stirred at 0 °C for 1 hour before the ice bath was removed and the mixture was stirred for a further 2 hours at room temperature. The solution was then diluted with CH_2Cl_2 (20 mL) and then slowly added to an ice cold saturated aqueous solution of $NaHCO_3$ (50 mL). The aqueous portion was then extracted with CH_2Cl_2 (3 × 20 mL) and the combined organic extracts were washed with brine, dried over $MgSO_4$, filtered and then concentrated under reduced pressure. Purification was performed *via* flash column chromatography (dry loading, CH_2Cl_2 9:1 EtOAc, isocratic) to afford the *title compound* as a colourless oil (53 mg, 0.20 mmol, 37 %). **IR** (ATR)/cm^{-1} 3022, 2989, 1270, 1038; **^{1}H NMR** (500 MHz, $CDCl_3$) δ (ppm) 7.62 (d, 2H, J 8.0 Hz, 2 × Ar*H*), 7.50–7.42 (m, 1H, 3 × Ar*H*), 4.25–4.09 (m, 4H, 2 × POC*H*$_2$CH$_3$), 1.30 (td, J 7.5 Hz, J_{PH} 0.5 Hz, 6H, 2 × POCH$_2$C*H*$_3$); **^{13}C NMR** (125 MHz, $CDCl_3$) δ (ppm) 132.9 (td, J_{FC} 22.0 Hz, J_{PC} 14.0 Hz), 131.1, 128.7, 126.5 (J_{FC} 7.0 Hz, J_{PC} 2.5 Hz), 118.4 (td, J_{FC} 262.0 Hz, J_{PC} 217.0 Hz), 65.1 (d, J_{PC} 7.0 Hz), 16.6 (d, J_{PC} 5.5 Hz); **^{31}P NMR** (202 MHz, $CDCl_3$) δ (ppm) 6.39 (tp, J_{FP} 115.5 Hz, J 7.5 Hz, 1P, C(F$_2$)*P*O(OCH$_2$CH$_3$)$_2$); **^{19}F NMR** (471 MHz, $CDCl_3$) δ (ppm) -108.4 (d, J_{PF} 116.0 Hz, 2F, C(*F*$_2$)*P*O(OCH$_2$CH$_3$)$_2$); **LRMS** (ES + APCI) *m/z*: calc. for $C_{11}H_{15}F_2O_3P$ 264.1, found 265.0 $[M+H]^+$.

Tetraethyl (1,3-phenylene*bis*(hydroxymethylene))*bis*(phosphonate) (28)

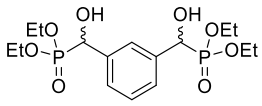

To a solution of THF (50.0 mL, 0.30 M) at -20 °C was added NaH (77 mg, 3.2 mmol) followed by the drop-wise addition of diethyl phosphite (4.61 mL, 35.8 mmol). The solution was stirred at this temperature for 20 minutes before a solution of isophthalaldehyde (1.68 mL, 14.9 mmol) in THF (40.0 mL, 0.37 M) was added. The solution was stirred for an additional 30 minutes before the reaction mixture was quenched with 5% saturated aqueous NH_4Cl solution (65 mL). The mixture was then extracted with EtOAc (3 × 50 mL). The combined organic extracts were washed with brine (100 mL), dried over $MgSO_4$, filtered and concentrated under reduced pressure. Further purification *via* flash column chromatography (dry loading, CH_2Cl_2 4:1 EtOAc, isocratic) afforded the *title compound* as an off-white solid (4.10 g, 1.0 mol, 67%). **mp** 86–89 °C; **IR** (ATR)/cm^{-1} 3248 (br), 3056, 2984, 1228, 1017; **^{1}H NMR** (500 MHz, $CDCl_3$) δ (ppm) 7.68–7.63 (m, 1H, Ar*H*), 7.43–7.39 (m, 2H, 2 × Ar*H*), 7.34 (t, *J* 7.5 Hz, 1H, Ar*H*), 4.99 (app dt, J_{PH} 11.5 Hz, *J* 5.0 Hz, 2H, 2 × OHC*H*PO) 4.27 (dd, J_{PH} 11.5 Hz, *J* 5.5 Hz, 1H, POCHO*H*), 4.24 (dd, J_{PH} 11.5 Hz, *J* 5.5 Hz, 1H, POCHO*H*), 4.11–3.90 (m, 8H, 4 × POC*H*$_2$CH$_3$), 1.26 (app q, *J* 6.5 Hz, 6H, 2 × POCH$_2$C*H*$_3$), 1.20 (app q, *J* 6.5 Hz, 6H, 2 × POCH$_2$C*H*$_3$); **^{13}C NMR** (125 MHz, $CDCl_3$) δ (ppm) 137.3, 128.5–128.4 (m), 127.3–127.2 (m), 126.4–126.2 (m), 70.1 (d, J_{PC} 158.5 Hz), 63.6 (d, J_{PC} 4.0 Hz), 63.5 (d, J_{PC} 4.0 Hz), 16.8 (d, J_{PC} 6.5 Hz), 16.7 (d, J_{PC} 6.5 Hz); **^{31}P NMR** (202 MHz, $CDCl_3$) δ (ppm) 21.4–21.1 (m, 2P, 2 × *P*OCHOH); **LRMS** (ES + APCI) *m/z*: calc. for $C_{16}H_{28}O_8P_2$ 410.1, found 411.0 $[M+H]^+$; **HMRS** calc. for $C_{16}H_{29}O_8P_2$ 411.1338 $[M+H]^+$, found 411.1335 $[M+H]^+$.

Tetraethyl isophthaloyl*bis*(phosphonate) (29)[136]

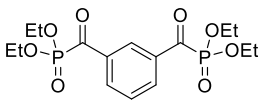

To a solution of oxalyl chloride (165 μL, 1.95 mmol) and CH_2Cl_2 (6.1 mL, 0.08 M) at -78 °C was added dropwise, *via* a syringe, DMSO (152 μL, 1.80 mmol). The resulting solution was stirred at this temperature for 10 minutes before a solution of

compound **7** (200 mg, 0.49 mmol) in CH_2Cl_2 (3.5 mL, 0.14 M) was added dropwise. After stirring for a further 15 minutes, the reaction mixture was treated with Et_3N (788 μL, 5.65 mmol) and then allowed to warm to room temperature. The mixture was washed with H_2O (20 mL) and the aqueous portion was then extracted with CH_2Cl_2 (2 × 20 mL). The combined organic layers were washed with a 1% aqueous solution of HCl (4 × 50 mL). No further purification was required and so, the *title compound* (187 mg, 0.77 mmol, 94%) was afforded as a yellow oil. **IR** (ATR)/cm^{-1} 3021, 2976, 1768, 1248, 1022; **^{1}H NMR** (500 MHz, $CDCl_3$) δ (ppm) 9.04 (s, 1H, Ar*H*), 8.54 (dd, *J* 8.0 Hz, 2.0 Hz, 2H, 2 × Ar*H*), 7.68 (t, *J* 8.0 Hz, 1H, Ar*H*), 4.37–4.24 (m, 8H, 4 × POC*H*$_2$CH$_3$), 1.41 (t, *J* 7.0 Hz, 12H, 4 × POCH$_2$C*H*$_3$); **^{13}C NMR** (125 MHz, $CDCl_3$) δ (ppm) 202.9 (d, J_{PC} 128.5 Hz) 138.2–138.0 (m), 129.7–129.6 (m), 128.1–128.0 (m), 124.5–124.4 (m), 63.8 (d, J_{PC} 5.5 Hz), 16.0 (d, J_{PC} 7.0 Hz); **^{31}P NMR** (202 MHz, $CDCl_3$) δ (ppm) 15.6–15.3 (m, 2P, 2 × *P*OCO); **LRMS** (ES + APCI) *m/z*: calc. for $C_{16}H_{24}O_8P_2$ 406.1, found 407.1 $[M+H]^+$.

Tetraethyl (1,3-phenylene*bis*(fluoromethylene))*bis*(phosphonate) (30)

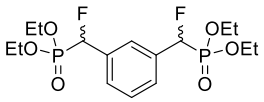

To a solution of DAST (412 μL, 3.12 mmol) in CH_2Cl_2 (0.58 mL, 1.66 M) at -78 °C was added rapidly, *via* syringe, a precooled (-78 °C) solution of **7** (400 mg, 0.97 mmol) in CH_2Cl_2 (6.10 mL, 0.16 M). The mixture was stirred at -78 °C for 3–4 minutes and then raised immediately to room temperature. After 1 hour of stirring at room temperature, the reaction was quenched with a saturated aqueous $NaHCO_3$ solution (10 mL), followed by extraction with CH_2Cl_2 (3 × 15 mL). The combined organic extracts were dried over $MgSO_4$, filtered and then concentrated under reduced pressure. Further purification was carried out *via* flash column chromatography (dry loading, CH_2Cl_2 9:1 EtOAc, isocratic) to afford the *title compound* as a colourless oil (312 mg, 0.76 mmol, 78%). **IR** (ATR)/cm^{-1} 3033, 2932, 1257, 1014, 965; **^{1}H NMR** (500 MHz, $CDCl_3$) δ (ppm) 7.56 (s, 1H, Ar*H*), 7.51 (d, *J* 7.5 Hz, 2H, 2 × Ar*H*), 7.45 (t, *J* 7.5 Hz, 1H, Ar*H*), 5.75 (dd, J_{PH} 8.0 Hz, *J* 3.0 Hz, 1H, POC*H*F), 5.66 (dd, J_{PH} 8.0 Hz, *J* 3.0 Hz, 1H, POC*H*F), 4.19–3.99 (m, 8H, 4 × POC*H*$_2$CH$_3$), 1.33–1.24 (m, 12H, 4 × POCH$_2$C*H*$_3$); **^{13}C NMR** (125 MHz, $CDCl_3$) δ (ppm) 133.8 (d, J_{PC} 19.5 Hz), 129.0, 127.9–127.6 (m), 125.2 (app dt,

J_{PC} 29.5 Hz, J_{FC} 6.5 Hz), 89.5 (dd, J_{PC} 183.0 Hz, J_{FC} 168.5 Hz), 89.4 (dd, J_{PC} 183.0 Hz, J_{FC} 168.5 Hz), 64.2 (d, J_{PC} 7.0 Hz), 64.1 (d, J_{PC} 7.0 Hz), 63.8 (d, J_{PC} 7.0 Hz), 16.8–16.6 (m); **^{31}P NMR** (202 MHz, $CDCl_3$) δ (ppm) 14.5 (d sextets, J_{FP} 84.5 Hz, J 7.5 Hz, 2P, 2 × FCH*P*O(OCH_2CH_3)$_2$); **^{19}F NMR** (471 MHz, $CDCl_3$) δ (ppm) -201.4 (dd, J_{PF} 50.5 Hz, J 45.0 Hz, 1F, *F*CHPO), -201.6 (dd, J_{PF} 50.5 Hz, J 45.0 Hz, 1F, *F*CHPO), **LRMS** (ES + APCI) *m/z*: calc. for $C_{16}H_{26}F_2O_6P_2$ 414.1, found 415.0 $[M+H]^+$; **HMRS** calc. for $C_{16}H_{27}F_2O_6P_2$ 415.1251 $[M+H]^+$, found 415.1253 $[M+H]^+$.

Diethyl benzylphosphonate (32)[56]

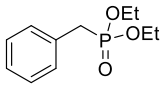

To a solution of degassed THF (12 mL, 0.19 M), containing H_2O (1.5 μL, 0.08 mmol) was added Palladium acetate ($Pd(OAc)_2$) (34 mg, 0.15 mmol), Xantphos (174 mg, 0.30 mmol) and di-isopropylethylamine (DIPEA) (340 μL, 1.50 mmol). The mixture was refluxed for 15 minutes before diethyl phosphite (193 μL, 1.5 mmol) and benzyl bromide (268 μL, 2.25 mmol) in a solution of degassed THF (4.0 mL, 0.56 M) were added. The reaction mixture was then refluxed for a further 3 hours. The volatiles were removed *in vacuo* and the resultant residue was partitioned between CH_2Cl_2 and a saturated aqueous $NaHCO_3$ solution. The aqueous phase was extracted with CH_2Cl_2 (3 × 10 mL) and the combined organic extracts were then dried over $MgSO_4$, filtered and concentrated under reduced pressure. Purification was performed *via* flash column chromatography (dry loading, CH_2Cl_2 4:1 EtOAc, isocratic) to afford the *title compound* (119 mg, 0.52 mmol, 35%) as a colourless oil. **IR** (ATR)/cm^{-1} 3021, 2982, 1247; **^{1}H NMR** (500 MHz, $CDCl_3$) δ (ppm) 7.33–7.27 (m, 4H, 4 × Ar*H*), 7.25–7.21 (m, 1H, Ar*H*), 4.05–3.94 (m, 4H, 2 × POC*H*$_2$CH$_3$), 3.14 (d, J_{PH} 21.5 Hz, 2H, C*H*$_2$PO), 1.23 (t, J 7.0 Hz, 6H, 2 × POCH$_2$C*H*$_3$); **^{13}C NMR** (125 MHz, $CDCl_3$) δ (ppm) 131.8 (d, J_{PC} 10.0 Hz), 129.9 (d, J_{PC} 6.5 Hz), 128.7, 128.6, 127.0, 63.3 (d, J_{PC} 6.5 Hz), 33.9 (d, J_{PC} 137.5 Hz), 16.5 (d, J_{PC} 6.5 Hz); **^{31}P NMR** (202 MHz, $CDCl_3$) δ (ppm) 26.4 (septet, J 7.5 Hz, 1P, $CH_2PO(OCH_2CH_3)_2$), **LRMS** (ES + APCI) *m/z*: calc. for $C_{11}H_{17}O_3P$ 228.1, found 229.1 $[M+H]^+$.

Diethyl phenethylphosphonate (34)[57]

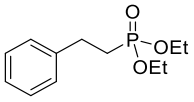

To a solution of diethyl phosphite (600 mg, 4.34 mmol) in dry dimethylformamide (DMF) (22.0 mL, 0.20 M) was added caesium carbonate (Cs_2CO_3) (4.25 g, 13.0 mmol) and tetrabutylammonium iodide (4.81 g, 13.0 mmol) with vigorous stirring for 1 hour at room temperature under an N_2 atmosphere. At this point, (2-bromoethyl)benzene (1.78 mL, 13.0 mmol) was added and the reaction mixture was stirred for an additional 1 hour. The resulting milky-white suspension was then poured into H_2O (30 mL) and extracted with EtOAc (3 × 30 mL). The combined organic extracts were washed with H_2O (2 × 30 mL), brine (30 mL) and then dried over $MgSO_4$, filtered and concentrated under reduced pressure. Purification was carried out *via* flash column chromatography (dry loading, CH_2Cl_2 7:3 EtOAc, isocratic) to afford the *title compound* (592 mg, 2.44 mmol, 56%) as a colourless oil. **IR** (ATR)/cm^{-1} 3018, 2986, 1242, 1024; **^{1}H NMR** (500 MHz, $CDCl_3$) δ (ppm) 7.31–7.26 (m, 2H, 2 × Ar*H*), 7.22–7.17 (m, 3H, 3 × Ar*H*), 4.14–4.01 (m, 4H, 2 × POC*H*$_2$CH$_3$), 2.94–2.88 (m, 2H, CH$_2$C*H*$_2$PO), 2.09–1.97 (m, 2H, C*H*$_2$CH$_2$PO), 1.31 (t, *J* 7.0 Hz, 6H, 2 × POCH$_2$C*H*$_3$); **^{13}C NMR** (125 MHz, $CDCl_3$) δ (ppm) 141.0 (d, J_{PC} 17.5 Hz), 128.6, 128.1, 126.3, 61.6 (d, *J* 6.5 Hz), 28.6 (d, J_{PC} 4.5 Hz), 27.6 (d, J_{PC} 138.5 Hz), 16.5 (d, J_{PC} 6.0 Hz); **^{31}P NMR** (202 MHz, $CDCl_3$) δ (ppm) 30.8 (app nonet, *J* 8.5 Hz, 1P, CH$_2$CH$_2$*P*O(OCH$_2$CH$_3$)$_2$); **LRMS** (ES + APCI) *m/z*: calc. for $C_{12}H_{19}O_3P$ 242.1, found 243.1 $[M+H]^+$.

Tetraethyl (1,3-phenylene*bis*(methylene))*bis*(phosphonate) (36)

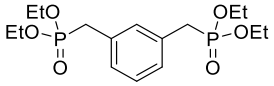

To a solution of degassed THF (15.0 mL, 0.10 M), containing H_2O (1.5 μL, 0.08 mmol) was added $Pd(OAc)_2$ (45 mg, 0.20 mmol), Xantphos (234 mg, 0.40 mmol) and DIPEA (457 μL, 2.63 mmol). The mixture was refluxed for 15 minutes before diethyl phosphite (260 μL, 2.02 mmol) and 1,3-*bis*(bromomethyl)benzene (400 mg, 1.51 mmol) in a solution of degassed THF (5.0 mL, 0.30 M) were added. The reaction mixture was then refluxed for a further

3 hours. The volatiles were removed *in vacuo* and the resultant residue was partitioned between CH_2Cl_2 and a saturated aqueous $NaHCO_3$ solution. The aqueous phase was extracted with CH_2Cl_2 (3 × 10 mL) and the combined organic extracts were then dried over $MgSO_4$, filtered and concentrated under reduced pressure. Purification was performed *via* flash column chromatography (dry loading, CH_2Cl_2 4:1 EtOAc, isocratic) to afford the *title compound* (209 mg, 0.55 mmol, 37%) as an orange oil. **IR** (ATR)/cm^{-1} 3011, 2984, 1244, 1017; **^{1}H NMR** (500 MHz, $CDCl_3$) δ (ppm) 7.25–7.23 (m, 1H, Ar*H*), 7.22–7.17 (m, 3H, 3 × Ar*H*), 4.06–3.96 (m, 8H, 4 × POC*H*$_2$CH$_3$), 3.12 (d, J_{PH} 21.5 Hz, 4H, 2 × C*H*$_2$PO), 1.24 (t, *J* 7.0 Hz, 12H, 4 × POCH$_2$C*H*$_3$); **^{13}C NMR** (125 MHz, $CDCl_3$) δ (ppm) 132.3–132.2 (m), 131.5 (t, 7.0 Hz), 128.9 (t, J_{PC} 3.0 Hz), 128.7 (t, J_{PC} 5.0 Hz), 62.5–62.3 (m), 33.9 (d, J_{PC} 137.5 Hz), 16.8–16.6 (m); **^{31}P NMR** (202 MHz, $CDCl_3$) δ (ppm) 26.2 (app septet, *J* 8.0 Hz, 2P, 2 × CH$_2$*P*O(OCH$_2$CH$_3$)$_2$); **LRMS** (ES + APCI) *m/z*: calc. for $C_{16}H_{28}O_6P_2$ 378.1, found 379.0 $[M+H]^+$; **HMRS** calc. for $C_{16}H_{29}O_6P_2$ 379.1440 $[M+H]^+$, found 379.1437 $[M+H]^+$.

7.3. Phosphonic acid series

(Hydroxy(phenyl)methyl)phosphonic acid (37)[58]

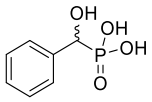

Following General Procedure A, compound **23** (200 mg, 0.82 mmol) afforded the *title compound* (139 mg, 0.95 mmol, 90%) as a brown residue. **IR** (ATR)/cm^{-1} 3373 br, 3058, 1396, 1033; **^{1}H NMR** (500 MHz, DMSO-d_6) δ (ppm) 7.41–7.12 (m, 5H, 5 × Ar*H*), 4.71 (d, J_{PH} 14.0 Hz, 1H, POC*H*(OH)); **^{13}C NMR** (125 MHz, DMSO-d_6) δ (ppm) 140.1, 128.0, 127.8 (d, J_{PC} 5.0 Hz), 127.4, 70.5 (d, J_{PC} 158.5 Hz); **^{31}P NMR** (202 MHz, DMSO-d_6) δ (ppm) 18.9 (app d, *J* 13.0 Hz, 1P, $(OH)_2$*P*OCHOH); **LRMS** (ES + APCI) *m/z*: calc. for $C_7H_9O_4P$ 188.0, found 187.0 $[M–H]^+$.

Phenethylphosphonic acid (38)[99]

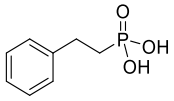

Following General Procedure A, compound **34** (200 mg, 0.83 mmol) afforded the *title compound* (122 mg, 0.66 mmol, 79%) as an off-white powder. **mp** 112–114 °C; **IR** (ATR)/cm^{-1} 3008, 2932, 2913 br, 1238, 1011; **^{1}H NMR** (500 MHz, DMSO-d_6) δ (ppm) 7.28 (app t, *J* 7.5 Hz, 2H, 2 × Ar*H*), 7.22 (d, *J* 7.5 Hz, 2H, 2 × Ar*H*), 7.18 (t, *J* 7.5 Hz, 1H, Ar*H*), 2.81–2.71 (m, 2H, CH_2CH$_2$PO), 1.86–1.75 (m, 2H, CH$_2$CH_2PO); **^{13}C NMR** (125 MHz, DMSO-d_6) δ (ppm) 141.9 (d, J_{PC} 17.5 Hz), 128.4, 127.9, 125.9, 29.5 (d, J_{PC} 153.5 Hz), 28.9 (d, J_{PC} 22.5 Hz); **^{31}P NMR** (202 MHz, DMSO-d_6) δ (ppm) 24.8 (app septet, *J* 8.0 Hz, 1P, CH$_2$CH$_2$*P*O$(OH)_2$); **LRMS** (ES + APCI) *m/z*: calc. for $C_8H_{11}O_3P$ 186.0, found 185.0 $[M–H]^+$.

(1,3-Phenylene*bis*(methylene))diphosphonic acid (39)

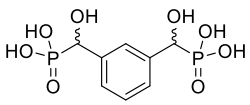

Following General Procedure A, compound **28** (250 mg, 0.61 mmol) afforded the *title compound* (120 mg, 0.40 mmol, 83%) as an orange gum. **IR** (ATR)/cm^{-1}

3208 br, 2970, 1238, 1017; **^{1}H NMR** (500 MHz, DMSO-d_6) δ (ppm) 7.50–7.15 (m, 4H, 4 × Ar*H*), 6.30–4.90 (m, 6H, 6 × O*H*), 4.67 (app s, 2H, 2 × PO*CH*OH); **^{13}C NMR** (125 MHz, DMSO-d_6) δ (ppm) 138.9 (d, J_{PC} 7.5 Hz), 126.7 (d, J_{PC} 15.0 Hz), 126.4, 125.9 (d, 21.5 Hz), 70.2 (d, J_{PC} 156.5 Hz); **^{31}P NMR** (202 MHz, DMSO-d_6) δ (ppm) 18.7 (app q, *J* 7.0 Hz, 2P, 2 × $(OH)_2$*P*OCHOH); **LRMS** (ES + APCI) *m/z*: calc. for $C_8H_{12}O_8P_2$ 298.0, found 297.0 $[M–H]^-$; **HMRS** calc. for $C_8H_{11}O_8P_2$ 296.9935 $[M–H]^-$, found 296.9930 $[M–H]^-$.

(1,3-Phenylene*bis*(fluoromethylene))diphosphonic acid (40)[137]

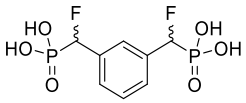

Following General Procedure A, compound **30** (250 mg, 0.60 mmol) afforded the *title compound* (118 mg, 0.39 mmol, 81%) as a brown gum. **IR** (ATR)/cm^{-1} 3140 br, 2945, 1222, 1033, 1015; **^{1}H NMR** (500 MHz, DMSO-d_6) δ (ppm) 9.01–8.29 (m, 4H, 4 × OH), 7.55–7.33 (m, 4H, 4 × Ar*H*), 5.67 (app d, *J* 42.0 Hz, 2H, 2 × POC*H*F); **^{13}C NMR** (125 MHz, DMSO-d_6) δ (ppm) 134.7 (dd, J_{FC} 20.0 Hz, J_{PC} 6.5 Hz), 127.7 (app d, *J* 7.5 Hz), 127.1 (app d, *J* 12.5 Hz), 125.7, 90.0 (dd, J_{FC} 176.5 Hz, J_{PC} 158.5 Hz); **^{31}P NMR** (202 MHz, DMSO-d_6) δ (ppm) 10.9 (app d, J_{FP} 80.5 Hz, 2P, $(OH)_2$*P*OCHF); **^{19}F NMR** (471 MHz, DMSO-d_6) δ (ppm) -196.4 (dd, J_{PF} 80.0 Hz, *J* 42.5 Hz, 1F, POCH*F*), 196.6 (dd, J_{PF} 80.0 Hz, *J* 42.5 Hz, 1F, POCH*F*); **LRMS** (ES + APCI) *m/z*: calc. for $C_8H_{10}F_2O_6P_2$ 302.0, found 301.1 $[M–H]^+$.

7.4. Amido acid series

Endic anhydride (44)[64]

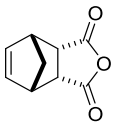

To a 100 mL conical flask was added maleic anhydride (6.00 g, 60.0 mmol) which was subsequently dissolved in EtOAc (4.0 M) *via* heating to reflux. Hexane (4.0 M) was then added and the mixture was cooled to 0 °C in an ice/water bath. To the ice-cold solution was added cyclopentadiene (freshly cracked from di-cyclopentadiene) (10.0 M) and the solution swirled until the exothermic reaction had finished and the adduct separated as a white solid. The mixture was heated (reflux) to dissolve the solid and then left to stand undisturbed to allow crystallisation to occur. Subsequent filtration afforded the *title compound* as a white crystalline solid (9.16 g, 55.8 mmol, 93%). **mp** 182–184 °C; **IR** (ATR)/cm^{-1} 2967, 1678; **^{1}H NMR** (500 MHz, $CDCl_3$) δ (ppm) 6.29 (s, 2H, C*H*=C*H*), 3.57 (app br s, 2H, 2 × CHC*H*COOCO), 3.49 (app br s, 2H, 2 × C*H*CHCOOCO), 1.76 (d, *J* 9.0 Hz, 1H, CH*H*), 1.56 (d, *J* 9.0 Hz, 1H, C*H*H); **^{13}C NMR** (125 MHz, $CDCl_3$) δ (ppm) 171.4, 135.6, 52.8, 47.2, 46.2; **LRMS** (ES + APCI) *m/z*: calc. for $C_9H_8O_3$ 164.0, found 165.1 $[M+H]^+$.

(±)-(1*R*,2*S*,3*R*,4*S*)-3-(Benzylcarbamoyl)bicyclo[2.2.1]hept-5-ene-2-carboxylic acid (45)[61]

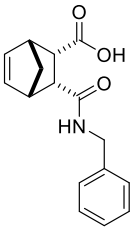

Following General Procedure B, compound **44** (250 mg, 1.53 mmol) and benzylamine (163 mg, 1.53 mmol) afforded the *title compound* (364 mg, 1.34 mmol, 93%) as an off-white solid. **mp** 142–144 °C; **IR**(ATR)/cm^{-1} 3369, 3066, 2978 br, 1731, 1662, 1539; **^{1}H NMR** (500 MHz, DMSO-d_6) δ (ppm) 11.59 (br s, 1H, COO*H*), 8.23 (t, *J* 6.0 Hz, 1H, CON*H*), 7.30 (t, *J* 7.5 Hz, 2H, 2 × Ar*H*), 7.25 (d, *J* 7.0 Hz, 2H, 2 × Ar*H*), 7.22 (t, *J* 7.5 Hz, 1H, Ar*H*), 6.20 (dd, *J* 5.5 Hz, 3.0 Hz, 1H, CH=C*H*CH), 5.93 (dd, *J* 5.5 Hz, 3.0 Hz, 1H, CH=C*H*CH), 4.25–4.17 (m,

2H, CONHCH_2), 3.25 (app dd, *J* 10.0 Hz, 3.0 Hz, 1H, CHC*H*COOH), 3.11 (app dd, *J* 10.0 Hz, 3.0 Hz, 1H, CHC*H*CONH), 2.99 (app s, 1H, CH=CHC*H*CH), 2.95 (app s, 1H, CH=CHC*H*CH), 1.29 (d, *J* 8.0 Hz, 1H, CH*H*), 1.24 (d, *J* 8.0 Hz, 1H, C*H*H); **^{13}C NMR** (125 MHz, DMSO-d_6) δ (ppm) 173.6, 171.1, 139.8, 135.1, 133.5, 128.1, 127.1, 126.5, 48.4, 48.2, 48.2, 46.9, 42.0, 39.5; **LRMS** (ES + APCI) *m/z*: calc. for $C_{16}H_{18}NO_3$ 271.12, found 272.0 $[M+H]^+$.

(±)-(1*R*,2*S*,3*R*,4*S*)-3-(Phenylcarbamoyl)bicyclo[2.2.1]hept-5-ene-2-carboxylic acid (46)[61]

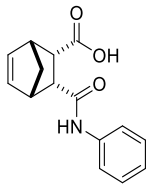

Following General Procedure B, compound **44** (150 mg, 0.91 mmol) and aniline (85 mg, 0.91 mmol) afforded the *title compound* (188 mg, 0.81 mmol, 80%) as an off-white solid. **mp** 133–135 °C; **IR**(ATR)/cm^{-1} 3284, 3125, 2978 br, 1684, 1588, 1539; **^{1}H NMR** (500 MHz, DMSO-d_6) δ (ppm) 11.61 (br s, 1H, COO*H*), 9.81 (s, 1H, CON*H*), 7.51 (d, *J* 8.0 Hz, 2H, 2 × Ar*H*), 7.24 (app t, *J* 7.5 Hz, 2H, 2 × Ar*H*), 6.98 (t, *J* 7.5 Hz, 1H, Ar*H*), 6.20 (dd, *J* 5.0 Hz, 3.0 Hz, 1H, CH=C*H*CH), 6.03 (dd, *J* 5.0 Hz, 3.0 Hz, 1H, CH=C*H*CH), 3.36 (app dd, *J* 10.0 Hz, 3.0 Hz, 1H, CHC*H*COOH), 3.21 (app dd, *J* 10.0 Hz, 3.0 Hz, 1H, CHC*H*CONH), 3.07 (app s, 1H, CH=CHC*H*CH), 3.00 (app s, 1H, CH=CHC*H*CH), 1.32 (d, *J* 8.0 Hz, 1H, CH*H*), 1.27 (d, *J* 8.0 Hz, 1H, C*H*H); **^{13}C NMR** (125 MHz, DMSO-d_6) δ (ppm) 173.0, 169.7, 139.2, 134.6, 133.5, 128.1, 122.3, 118.6, 48.8, 48.4, 47.8, 46.4, 45.1; **LRMS** (ES + APCI) *m/z*: calc. for $C_{15}H_{15}NO_3$ 257.11, found 258.0 $[M+H]^+$.

(±)-(1*R*,2*S*,3*R*,4*S*)-3-(Pyrrolidine-1-carbonyl)bicyclo[2.2.1]hept-5-ene-2-carboxylic acid (47)[62]

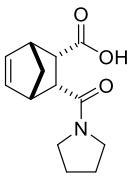

Following General Procedure B, compound **44** (150 mg, 0.91 mmol) and pyrrolidine (65 mg, 0.91 mmol) afforded the *title compound* (180 mg, 0.77 mmol, 84%) as an

off-white solid. **mp** 176–177 °C; **IR**(ATR)/cm^{-1} 2963, 2870 br, 1718, 1590; **^{1}H NMR** (500 MHz, DMSO-d_6) δ (ppm) 11.71 (br s, 1H, COO*H*), 6.15 (dd, *J* 5.0 Hz, 3.0 Hz, 1H, CH=C*H*CH), 6.01 (dd, *J* 5.0 Hz, 3.0 Hz, 1H, CH=C*H*CH), 3.48–3.37 (m, 2H, CH_2NCO), 3.31 (app dd, *J* 10.0 Hz, 3.0 Hz, 1H, CHC*H*COOH), 3.25 (app dd, *J* 10.0 Hz, 3.0 Hz, 1H, CHC*H*CON), 3.22–3.12 (m, 2H, CH_2NCO), 3.01 (app s, 1H, CH=CHC*H*CH), 2.95 (app s, 1H, CH=CHC*H*CH), 1.89–1.65 (m, 4H, $CH_2CH_2CH_2$NCO), 1.31 (d, *J* 8.0 Hz, 1H, CH*H*), 1.21 (d, *J* 8.0 Hz, 1H, C*H*H); **^{13}C NMR** (125 MHz, DMSO-d_6) δ (ppm) 173.3, 169.9, 136.0, 133.1, 48.2, 47.8, 47.4, 45.9, 45.8, 45.6, 45.4, 25.6, 23.8; **LRMS** (ES + APCI) *m/z*: calc. for $C_{13}H_{17}NO_3$ 235.12, found 236.1 $[M+H]^+$.

(±)-(1*R*,2*S*,3*R*,4*S*)-3-(Morpholine-4-carbonyl)bicyclo[2.2.1]hept-5-ene-2-carboxylic acid (48)[62]

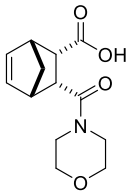

Following General Procedure B, compound **44** (150 mg, 0.91 mmol) and morpholine (79 mg, 0.91 mmol) afforded the *title compound* (150 mg, 0.60 mmol, 65%) as an off-white solid. **mp** 171–173 °C; **IR**(ATR)/cm^{-1} 2975, 2863 br, 1711, 1606; **^{1}H NMR** (500 MHz, DMSO-d_6) δ (ppm) 11.76 (br s, 1H, COO*H*), 6.28 (dd, *J* 5.0 Hz, 3.0 Hz, 1H, CH=C*H*CH), 5.92 (dd, *J* 5.0 Hz, 3.0 Hz, 1H, CH=C*H*CH), 3.61–3.41 (m, 6H, CH_2NCO), 3.35 (app dd, *J* 10.0 Hz, 3.0 Hz, 1H, CHC*H*COOH), 3.31 (app dd, *J* 10.0 Hz, 3.0 Hz, 1H, CHC*H*CON), 3.23–3.16 (m, 1H, OCH_2CH_2NCO), 3.12–3.08 (m, 1H, OCH_2CH_2NCO), 3.05 (app s, 1H, CH=CHC*H*CH), 2.91 (app s, 1H, CH=CHC*H*CH), 1.32 (d, *J* 8.0 Hz, 1H, CH*H*), 1.22 (d, *J* 8.0 Hz, 1H, C*H*H); **^{13}C NMR** (125 MHz, DMSO-d_6) δ (ppm) 173.2, 170.7, 137.2, 132.2, 65.9, 65.7, 48.2, 47.6, 46.5, 46.2, 46.0, 45.1, 41.7; **LRMS** (ES + APCI) *m/z*: calc. for $C_{13}H_{17}NO_4$ 251.12, found 252.1 $[M+H]^+$.

(±)-(1*R*,2*S*,3*R*,4*S*)-3-(Pyridin-2-ylcarbamoyl)bicyclo[2.2.1]hept-5-ene-2-carboxylic acid (49)[138]

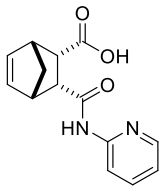

Following General Procedure B, compound **44** (150 mg, 0.91 mmol) and pyridine-2-amine (85 mg, 0.91 mmol) afforded the *title compound* (220 mg, 0.85 mmol, 93%) as an off-white solid. **mp** 159–161 °C; **IR**(ATR)/cm^{-1} 3098, 2980, 2871 br, 1711, 1582, 1552; **^{1}H NMR** (500 MHz, DMSO-d_6) δ (ppm) 11.64 (br s, 1H, COO*H*), 10.32 (s, 1H, CON*H*), 8.26 (d, *J* 4.0 Hz, 1H, Ar*H*), 7.96 (d, *J* 8.5 Hz, 1H, Ar*H*), 7.69 (app t, *J* 8.0 Hz, 1H, Ar*H*), 7.02 (app t, *J* 6.5 Hz, 1H, Ar*H*), 6.17 (dd, *J* 5.0 Hz, 3.0 Hz, 1H, CH=C*H*CH), 6.06 (dd, *J* 5.0 Hz, 3.0 Hz, 1H, CH=C*H*CH), 3.48 (app dd, *J* 10.0 Hz, 3.0 Hz, 1H, CHC*H*COOH), 3.24 (app dd, *J* 10.0 Hz, 3.0 Hz, 1H, CHC*H*CONH), 3.07 (app s, 1H, CH=CHC*H*CH), 3.01 (app s, 1H, CH=CHC*H*CH), 1.30 (d, *J* 8.0 Hz, 1H, CH*H*), 1.27 (d, *J* 8.0 Hz, 1H, C*H*H); **^{13}C NMR** (125 MHz, DMSO-d_6) δ (ppm) 173.3, 170.1, 152.4, 147.7, 137.8, 134.7, 134.2, 118.8, 113.3, 48.9, 48.8, 48.2, 46.6, 45.6; **LRMS** (ES + APCI) *m/z*: calc. for $C_{14}H_{14}N_2O_3$ 258.10, found 259.0 $[M+H]^+$.

(±)-(1*R*,2*S*,3*R*,4*S*)-3-(Pyridin-3-ylcarbamoyl)bicyclo[2.2.1]hept-5-ene-2-carboxylic acid (50)

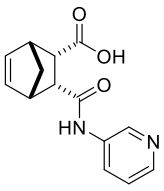

Following General Procedure B, compound **44** (150 mg, 0.91 mmol) and pyridine-3-amine (85 mg, 0.91 mmol) afforded the *title compound* (224 mg, 0.87 mmol, 95%) as an off-white solid. **mp** 234–236 °C; **IR**(ATR)/cm^{-1} 3274, 2969, 2868 br, 1694, 1590, 1543; **^{1}H NMR** (500 MHz, DMSO-d_6) δ (ppm) 11.70 (br s, 1H, COO*H*), 10.03 (s, 1H, CON*H*), 8.67 (d, *J* 2.5 Hz, 1H, Ar*H*), 8.20 (dd, *J* 5.0 Hz, 1.5 Hz, 1H, Ar*H*), 7.94 (ddd, *J* 8.5 Hz, 2.5 Hz, 1.5 Hz, 1H, Ar*H*), 7.29 (dd, *J* 8.5 Hz, 5.0 Hz, 1H, Ar*H*), 6.18 (dd, *J* 5.0 Hz, 3.0 Hz, 1H, CH=C*H*CH), 6.07

(dd, *J* 5.0 Hz, 3.0 Hz, 1H, CH=C*H*CH), 3.38 (app dd, *J* 10.0 Hz, 3.0 Hz, 1H, CHC*H*COOH), 3.26 (app dd, *J* 10.0 Hz, 3.0 Hz, 1H, CHC*H*CONH), 3.09 (app s, 1H, CH=CHC*H*CH), 3.03 (app s, 1H, CH=CHC*H*CH), 1.35 (d, *J* 8.0 Hz, 1H, CH*H*), 1.28 (d, *J* 8.0 Hz, 1H, C*H*H); **^{13}C NMR** (125 MHz, DMSO-d_6) δ (ppm) 173.3, 170.1, 143.6, 140.7, 136.1, 134.8, 134.1, 125.8, 123.4, 49.1, 48.8, 48.1, 46.6, 45.5; **LRMS** (ES + APCI) *m/z*: calc. for $C_{14}H_{14}N_2O_3$ 258.10, found 259.0 $[M+H]^+$; **HMRS** calc. for $C_{14}H_{13}N_2O_3$ 257.0932 $[M–H]^-$, found 257.0931 $[M–H]^-$.

(±)-(1*R*,2*S*,3*R*,4*S*)-Bicyclo[2.2.1]hept-5-ene-2,3-dicarboxylic acid (51)

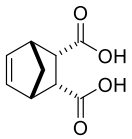

Compound **44** (1.00 g, 6.09 mmol) was placed in a 100 mL eschmeyer flask, followed by the addition of deionised H_2O (0.40 M). The contents were heated until the solid had fully dissolved before the resultant solution was left to stand undisturbed to cool to room temperature. Crystallisation was induced *via* a glass rod to produce small needles which were subsequently collected by filtration to afford the *title compound* (998 mg, 5.48 mmol, 90%) as off-white crystalline needles. **mp** 120–122 °C; **IR**(ATR)/cm^{-1} 2949, 2755 br, 1696; **^{1}H NMR** (500 MHz, DMSO-d_6) δ (ppm) 11.77 (br s, 2H, 2 × COO*H*), 6.10 (s, 2H, 2 × CHCH=C*H*CH), 3.19 (s, 2H, 2 × CHC*H*COOH), 3.00 (s, 1H, 2 × CH=CHC*H*CH), 1.32 (d, *J* 8.0 Hz, 1H, C*H*H), 1.25 (d, *J* 8.0 Hz, 1H, C*H*H); **^{13}C NMR** (125 MHz, DMSO-d_6) δ (ppm) 173.3, 134.6, 48.1, 47.7 45.8; **LRMS** (ES + APCI) *m/z*: calc. for $C_9H_{10}O_4$ 182.06, found 183.1 $[M+H]^+$; **HMRS** calc. for $C_9H_9O_4$ 181.0506 $[M–H]^-$, found 181.0508 $[M–H]^-$.

7.5. Squaric acid series

3-Hydroxy-4-(naphthalen-1-ylamino)cyclobut-3-ene-1,2-dione (54)[67]

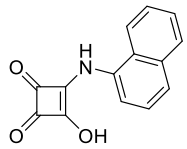

Following General Procedure C, squaric acid **53** (100 mg, 0.88 mmol) and naphthalene-1-amine (120 mg, 0.84 mmol), after purification *via* flash column chromatography (dry loading, CH_2Cl_2 20:1 MeOH, CH_2Cl_2 4:1 MeOH), afforded the *title compound* (174 mg, 0.73 mmol, 95%) as a pale yellow solid. **mp** 248–250 °C; **IR**(ATR)/cm^{-1} 3207, 2876 br, 1798, 1630, 1523; **^{1}H NMR** (500 MHz, MeOH-d_4) δ (ppm) 9.65 (br s, 1H, COC(=C)N*H*), 8.14 (d, *J* 8.5 Hz, 1H, Ar*H*), 7.87 (d, *J* 7.5, Hz, 1H, Ar*H*), 7.67–7.61 (m, 2H, 2 × Ar*H*), 7.56–7.49 (m, 2H, 2 × Ar*H*), 7.44 (app t, *J* 8.0 Hz, 1H, Ar*H*); **^{13}C NMR** (125 MHz, MeOH-d_4) δ (ppm) 200.0, 189.4, 179.2, 135.7, 135.0, 129.5, 127.2, 127.1, 126.8, 125.2, 122.4, 118.8 (2 carbons missing); **LRMS** (ES + APCI) *m/z*: calc. for $C_{14}H_9NO_3$ 239.1, found 240.1 $[M+H]^+$.

3-((4-Fluorophenyl)amino)-4-hydroxycyclobut-3-ene-1,2-dione (55)[67]

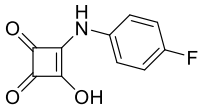

Following General Procedure C, squaric acid **53** (150 mg, 1.32 mmol) and 4-fluoroaniline (140 mg, 1.25 mmol), after purification *via* flash column chromatography (dry loading, CH_2Cl_2 20:1 MeOH, CH_2Cl_2 4:1 MeOH), afforded the *title compound* (210 mg, 1.01 mmol, 77%) as a grey solid. **mp** >250 °C; **IR**(ATR)/cm^{-1} 3194, 3135, 2965 br, 1804, 1668, 1506; **^{1}H NMR** (500 MHz, DMSO-d_6) δ (ppm) 9.28 (s, 1H, COC(=C)N*H*), 7.69–7.63 (m, 2H, 2 × Ar*H*), 7.01 (app t, *J* 8.5 Hz, 2H, 2 × Ar*H*); **^{13}C NMR** (125 MHz, DMSO-d_6) δ (ppm) 201.9, 187.7, 177.7, 156.7 (d, 235.0 Hz), 137.9, 118.6, 118.5, 115.3, 115.1; **^{19}F NMR** (125 MHz, DMSO-d_6) δ (ppm) 124.5 (app octet, *J* 4.0 Hz, 1F, *F*ArC$(CH)_2(CH)_2$); **LRMS** (ES + APCI) *m/z*: calc. for $C_{10}H_6FNO_3$ 207.0, found 208.0 $[M+H]^+$.

3-Hydroxy-4-((4-methoxyphenyl)amino)cyclobut-3-ene-1,2-dione (56)[67]

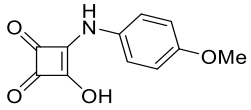

Following General Procedure C, squaric acid **53** (150 mg, 1.32 mmol) and 4-methoxyaniline (154 mg, 1.25 mmol), after purification *via* flash column chromatography (dry loading CH_2Cl_2 20:1 MeOH, CH_2Cl_2 4:1 MeOH), afforded the *title compound* (191 mg, 0.87 mmol, 70%) as a yellow solid. **mp** >250 °C; **IR**(ATR)/cm^{-1} 3191, 3071, 2963 br, 1820, 1675, 1593; **^{1}H NMR** (500 MHz, DMSO-d_6) δ (ppm) 10.33 (s, 1H, COC(=C)N*H*), 7.32 (d, *J* 8.5 Hz, 2H, 2 × Ar*H*), 6.91 (d, *J* 8.5, Hz, 2H, 2 × Ar*H*); **^{13}C NMR** (125 MHz, DMSO-d_6) δ (ppm) 186.5, 170.5, 131.7, 120.6, 114.2, 55.3 (3 carbons missing); **LRMS** (ES + APCI) *m/z*: calc. for $C_{10}H_9NO_4$ 219.1, found 220.0 $[M+H]^+$.

3-((4-Bromophenyl)amino)-4-hydroxycyclobut-3-ene-1,2-dione (57)

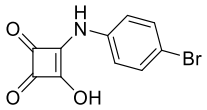

Following General Procedure C, squaric acid **53** (150 mg, 1.32 mmol) and 4-bromoaniline (226 mg, 1.25 mmol), after purification *via* flash column chromatography (dry loading, CH_2Cl_2 20:1 MeOH, CH_2Cl_2 4:1 MeOH), afforded the *title compound* (253 mg, 0.95 mmol, 76%) as a yellow solid. **mp** >250 °C; **IR**(ATR)/cm^{-1} 3179, 3049, 2965 br, 1817, 1683, 1539; **^{1}H NMR** (500 MHz, DMSO-d_6) δ (ppm) 10.42 (s, 1H, COC(=C)N*H*), 7.49 (d, *J* 8.5 Hz, 2H, 2 × Ar*H*), 7.41 (d, *J* 8.5, Hz, 2H, 2 × Ar*H*); **^{13}C NMR** (125 MHz, DMSO-d_6) δ (ppm) 188.8, 184.9, 171.1, 138.4, 131.8, 120.7, 114.9 (1 carbon missing); **LRMS** (ES + APCI) *m/z*: calc. for $C_{10}H_6{}^{79}BrNO_3$ 267.0, found 267.9 $[M+H]^+$; **HMRS** calc. for $C_{10}H_7{}^{79}BrNO_3$ 267.9604 $[M+H]^+$, found 267.9608 $[M+H]^+$.

7.6. Thiophene amido acid series

Methyl 2-amino-4-(4-bromophenyl)thiophene-3-carboxylate (68)[68]

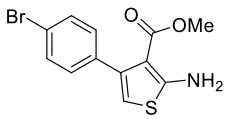

Following General Procedure D, methyl 2-cyanoacetate (991 mg, 10.0 mmol) and 4-bromoacetophenone (995 mg, 5.0 mmol), after purification *via* flash column chromatography (dry loading, Hexane 10:1 EtOAc, Hexane 5:1 EtOAc), afforded the *title compound* (689 mg, 1.99 mmol, 44%) as a pale yellow solid. **mp** 151–153 °C; **IR**(ATR)/cm^{-1} 3447, 3317, 3179, 2952, 1670, 1599; **^{1}H NMR** (500 MHz, $CDCl_3$) δ (ppm) 7.44 (d, *J* 8.5 Hz, 2H, 2 × Ar*H*), 7.16 (d, *J* 8.5 Hz, 2H, 2 × Ar*H*), 6.10 (br s, 2H, NH_2), 6.05 (s, 1H, C=C*H*S), 3.58 (s, 3H, COOCH_3); **^{13}C NMR** (125 MHz, $CDCl_3$) δ (ppm) 166.0, 164.3, 140.4, 137.3, 130.6, 121.1, 106.1, 105.6, 50.8 (1 carbon missing); **LRMS** (ES + APCI) *m/z*: calc. for $C_{12}H_{10}{}^{81}BrNO_2S$ 313.0, found 314.0 $[M+H]^+$; **HMRS** calc. for $C_{12}H_{11}{}^{81}BrNO_2S$ 313.9667 $[M+H]^+$, found 313.9668 $[M+H]^+$.

Ethyl 2-amino-4-(4-bromophenyl)thiophene-3-carboxylate (69)[68]

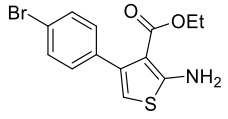

Following General Procedure D, ethyl 2-cyanoacetate (1.13 g, 10.0 mmol) and 4-bromoacetophenone (995 mg, 5.0 mmol), after purification *via* flash column chromatography (dry loading, Hexane 10:1 EtOAc, Hexane 5:1 EtOAc), afforded the *title compound* (650 mg, 1.99 mmol, 40%) as an off-white solid. **mp** 122–124 °C; **IR**(ATR)/cm^{-1} 3451, 3332, 3110, 2982, 1660, 1565; **^{1}H NMR** (500 MHz, $CDCl_3$) δ (ppm) 7.44 (d, *J* 8.5 Hz, 2H, 2 × Ar*H*), 7.17 (d, *J* 8.5 Hz, 2H, 2 × Ar*H*), 6.09 (br s, 2H, NH_2), 6.05 (s, 1H, C=C*H*S), 4.06 (q, *J* 7.0 Hz, 2H, COOCH_2CH$_3$), 0.99 (t, *J* 7.0 Hz, 3H, COOCH$_2$CH_3); **^{13}C NMR** (125 MHz, $CDCl_3$) δ (ppm) 165.6, 164.1, 140.5, 137.6, 130.8, 130.5, 121.0, 105.6, 105.9, 59.7, 13.9; **LRMS** (ES + APCI) *m/z*: calc. for $C_{13}H_{12}{}^{81}BrNO_2S$ 326.98, found 327.9 $[M+H]^+$; **HMRS** calc. for $C_{13}H_{13}{}^{81}BrNO_2S$ 327.9824 $[M+H]^+$, found 327.9825 $[M+H]^+$.

Ethyl 4-([1,1'-biphenyl]-4-yl)-2-aminothiophene-3-carboxylate (70)

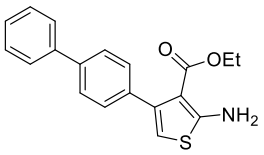

Following General Procedure D, ethyl 2-cyanoacetate (1.13 g, 10.0 mmol) and 1-([1,1'-biphenyl]-4-yl)ethan-1-one (981 mg, 5.0 mmol), after purification *via* flash column chromatography (dry loading, Hexane 7:1 EtOAc, Hexane 5:1 EtOAc), afforded the *title compound* (598 mg, 1.85 mmol, 37%) as a yellow solid. **mp** 124–126 °C; **IR**(ATR)/cm^{-1} 3456, 3338, 3075, 2958, 1642, 1568, 1544; **^{1}H NMR** (500 MHz, $CDCl_3$) δ (ppm) 7.64 (d, *J* 7.5 Hz, 2H, 2 × Ar*H*), 7.56 (d, *J* 8.0 Hz, 2H, 2 × Ar*H*), 7.46 (app t, *J* 7.5 Hz, 2H, 2 × Ar*H*), 7.38 (d, *J* 8.0 Hz, 2H, 2 × Ar*H*), 7.36 (d, *J* 7.0 Hz, 1H, Ar*H*), 6.12 (s, 1H, C=C*H*S), 6.09 (br s, 2H, NH_2), 4.08 (q, *J* 7.0 Hz, 2H, COOCH_2CH$_3$), 0.98 (d, *J* 7.0 Hz, 3H, COOCH$_2$CH_3); **^{13}C NMR** (125 MHz, $CDCl_3$) δ (ppm) 165.9, 164.0, 141.4, 141.2, 139.8, 137.7, 129.5, 128.9, 127.3, 127.2, 126.1, 106.3, 105.7, 59.7, 13.9; **LRMS** (ES + APCI) *m/z*: calc. for $C_{19}H_{17}NO_2S$ 323.1, found 324.0 $[M+H]^+$; **HMRS** calc. for $C_{19}H_{18}NO_2S$ 324.1053 $[M+H]^+$, found 324.1053 $[M+H]^+$.

Isopropyl 2-amino-4-(4-bromophenyl)thiophene-3-carboxylate (71)[68]

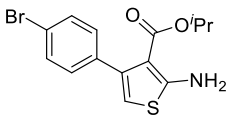

Following General Procedure D, isopropyl 2-cyanoacetate (1.27 g, 10.0 mmol) and 4-bromoacetophenone (995 mg, 5.0 mmol), after purification *via* flash column chromatography (dry loading, Hexane 10:1 EtOAc, Hexane 5:1 EtOAc), afforded the *title compound* (638 mg, 1.88 mmol, 38%) as a pale yellow solid. **mp** 124–126 °C; **IR**(ATR)/cm^{-1} 3444, 3332, 3105, 2978, 1645, 1577, 1532; **^{1}H NMR** (500 MHz, $CDCl_3$) δ (ppm) 7.43 (d, *J* 7.5 Hz, 2H, 2 × Ar*H*), 7.15 (d, *J* 7.5 Hz, 2H, 2 × Ar*H*), 6.09 (br s, 2H, NH_2), 6.04 (s, 1H, C=C*H*S), 4.98 (septet, *J* 6.0 Hz, 1H, COOC*H*(CH$_3$)$_2$), 1.00 (d, *J* 6.0 Hz, 6H, COOCH(CH_3)$_2$); **^{13}C NMR** (125 MHz, $CDCl_3$) δ (ppm) 165.2, 163.9, 140.5, 137.8, 130.9, 130.4, 120.9, 106.5, 105.8, 67.3, 21.8; **LRMS** (ES + APCI) *m/z*: calc. for $C_{14}H_{14}{}^{81}BrNO_2S$ 341.0, found 342.0

$[M+H]^+$; **HMRS** calc. for $C_{14}H_{15}{}^{81}BrNO_2S$ 341.9980 $[M+H]^+$, found 341.9980 $[M+H]^+$.

Isopropyl 4-([1,1'-biphenyl]-4-yl)-2-aminothiophene-3-carboxylate (72)

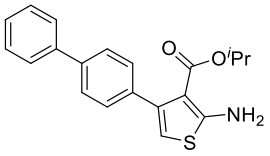

Following General Procedure D, isopropyl 2-cyanoacetate (1.27 g, 10.0 mmol) and 1-([1,1'-biphenyl]-4-yl)ethan-1-one (981 mg, 5.0 mmol), after purification *via* flash column chromatography (dry loading, Hexane 10:1 EtOAc), afforded the *title compound* (678 mg, 2.01 mmol, 40%) as an off-white solid. **mp** 144–146 °C; **IR**(ATR)/cm^{-1} 3447, 3341, 3107, 2976, 1746, 1586, 1478; **^{1}H NMR** (400 MHz, $CDCl_3$) δ (ppm) 7.63 (d, *J* 8.4 Hz, 2H, 2 × Ar*H*), 7.55 (d, *J* 8.0 Hz, 2H, 2 × Ar*H*), 7.46 (t, *J* 7.6 Hz, 2H, 2 × Ar*H*), 7.39–7.33 (m, 3H, 3 × Ar*H*), 6.11 (s, 1H, C=C*H*S), 6.09 (br s, 2H, NH_2), 4.99 (septet, *J* 6.4 Hz, 1H, COOC*H*$(CH_3)_2$), 0.99 (d, *J* 6.4 Hz, 6H, COOCH(CH_3)$_2$); **^{13}C NMR** (101 MHz, $CDCl_3$) δ (ppm) 165.4, 163.8, 141.6, 141.3, 139.8, 137.9, 129.6, 128.9, 127.3, 127.2, 126.1, 106.8, 105.6, 67.2, 21.8; **LRMS** (ES + APCI) *m/z*: calc. for $C_{20}H_{19}NO_2S$ 337.1, found 338.0 $[M+H]^+$; **HMRS** calc. for $C_{20}H_{20}NO_2S$ 338.1209 $[M+H]^+$, found 338.1211 $[M+H]^+$.

***tert*-Butyl 2-amino-4-(4-bromophenyl)thiophene-3-carboxylate (73)**

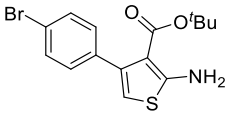

Following General Procedure D, *tert*-butyl 2-cyanoacetate (1.41 g, 10.0 mmol) and 4-bromoacetophenone (995 mg, 5.0 mmol), after purification *via* flash column chromatography (dry loading, Hexane 20:1 EtOAc), afforded the *title compound* (712 mg, 2.01 mmol, 40%) as a yellow solid. **mp** 84–86 °C; **IR**(ATR)/cm^{-1} 3418, 3317, 3116, 2975, 1644, 1577, 1487; **^{1}H NMR** (400 MHz, $CDCl_3$) δ (ppm) 7.44 (d, *J* 8.4 Hz, 2H, 2 × Ar*H*), 7.14 (d, *J* 8.4 Hz, 2H, 2 × Ar*H*), 6.08 (br s, 2H, NH_2), 6.00 (s, 1H, C=C*H*S), 1.23 (s, 9H, COOC(CH_3)$_3$); **^{13}C NMR** (101 MHz, $CDCl_3$) δ (ppm) 165.2, 163.5, 140.5, 138.1, 131.9, 130.7, 130.5, 120.6, 105.5, 80.5, 28.1;

LRMS (ES + APCI) *m/z*: calc. for $C_{15}H_{16}{}^{79}BrNO_2S$ 353.0, found 354.0 $[M+H]^+$; **HMRS** calc. for $C_{15}H_{17}{}^{79}BrNO_2S$ 354.0158 $[M+H]^+$, found 354.0161 $[M+H]^+$.

***tert*-Butyl 4-([1,1'-biphenyl]-4-yl)-2-aminothiophene-3-carboxylate (74)**

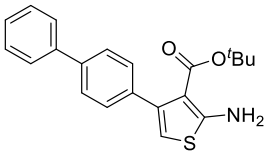

Following General Procedure D, *tert*-butyl 2-cyanoacetate (1.41 g, 10.0 mmol) and 1-([1,1'-biphenyl]-4-yl)ethan-1-one (981 mg, 5.0 mmol), after purification *via* flash column chromatography (dry loading, DCM 1:1 PhMe), afforded the *title compound* (715 mg, 2.04 mmol, 41%) as an off-white solid. **mp** 123–125 °C; **IR**(ATR)/cm^{-1} 3477, 3341, 3068, 2980, 1681, 1578, 1476; **^{1}H NMR** (400 MHz, $CDCl_3$) δ (ppm) 7.65–7.61 (m, 2H, 2 × Ar*H*), 7.56 (d, *J* 8.4 Hz, 2H, 2 × Ar*H*), 7.45 (app t, *J* 7.2 Hz, 2H, 2 × Ar*H*), 7.39–7.31 (m, 3H, 3 × Ar*H*), 6.09 (s, 1H, C=C*H*S), 6.03 (br s, 2H, NH_2), 1.23 (s, 9H, COOC(CH_3)$_3$); **^{13}C NMR** (101 MHz, $CDCl_3$) δ (ppm) 165.5, 163.3, 141.5, 141.3, 139.7, 138.3, 129.5, 128.9, 127.3, 127.2, 126.3, 107.9, 105.4, 80.4, 28.1; **LRMS** (ES + APCI) *m/z*: calc. for $C_{21}H_{21}NO_2S$ 351.1, found 352.0 $[M+H]^+$; **HMRS** calc. for $C_{21}H_{22}NO_2S$ 352.1366 $[M+H]^+$, found 352.1367 $[M+H]^+$.

Butyl 4-([1,1'-biphenyl]-4-yl)-2-aminothiophene-3-carboxylate (75)

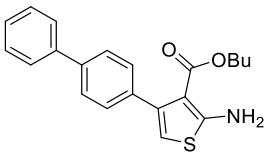

Following General Procedure D, butyl 2-cyanoacetate (1.41 g, 10.0 mmol) and 1-([1,1'-biphenyl]-4-yl)ethan-1-one (980 mg, 5.0 mmol), after purification *via* flash column chromatography (dry loading, Hexane 10:1 EtOAc), afforded the *title compound* (522 mg, 1.40 mmol, 30%) as a yellow solid. **mp** 309–311 °C; **IR**(ATR)/cm^{-1} 3435, 3327, 3026, 2929, 2864, 1649, 1590, 1530, 1495, 1261, 1142; **^{1}H NMR** (500 MHz, $CDCl_3$) δ (ppm) 7.62 (d, *J* 8.0 Hz, 2H, 2 × Ar*H*), 7.55 (d, *J* 8.0 Hz, 2H, 2 × Ar*H*), 7.45 (app t, *J* 8.0 Hz, 2H, 2 × Ar*H*), 7.39–7.32 (m, 3H, 3 × Ar*H*), 6.13 (br s, 2H, NH_2), 6.09 (s, 1H, C=C*H*S), 4.02 (t, *J* 7.0 Hz, 2H, OCH_2), 1.34–1.26 (m, 2H, OCH_2CH_2CH$_2$), 1.01–0.95 (m, 2H, CH$_2$CH_2CH$_3$), 0.69 (t, *J* 7.0 Hz, 3H, CH$_2$CH$_2$CH_3); **^{13}C NMR** (125 MHz, $CDCl_3$) δ (ppm) 166.1, 164.1,

141.4, 141.2, 139.9, 137.8, 129.5, 128.9, 127.3, 127.2, 126.2, 106.3, 105.7, 63.7, 30.6, 19.2, 13.8; **LRMS** (ES + APCI) *m/z*: calc. for $C_{21}H_{21}NO_2S$ 351.1 found 352.0 $[M+H]^+$; **HMRS** calc. for $C_{21}H_{22}NO_2S$ 352.1366 $[M+H]^+$, found 352.1367 $[M+H]^+$.

Isobutyl 4-([1,1'-biphenyl]-4-yl)-2-aminothiophene-3-carboxylate (76)

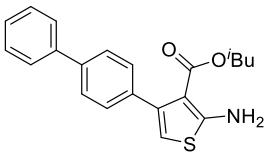

Following General Procedure D, isobutyl 2-cyanoacetate (1.41 g, 10.0 mmol) and 1-([1,1'-biphenyl]-4-yl)ethan-1-one (980 mg, 5.0 mmol), after purification *via* flash column chromatography (dry loading, Hexane 10:1 EtOAc), afforded the *title compound* (689 mg, 1.96 mmol, 39%) as a pale yellow solid. **mp** 68–70 °C; **IR**(ATR)/cm^{-1} 3411, 3303, 3027, 2931, 1642, 1588, 1525, 1486, 1391, 1257, 1209; **^{1}H NMR** (500 MHz, $CDCl_3$) δ (ppm) 7.64–7.59 (m, 2H, 2 × Ar*H*), 7.54 (d, *J* 8.0 Hz, 2H, 2 × Ar*H*), 7.46 (app t, *J* 8.0 Hz, 2H, 2 × Ar*H*), 7.40–7.34 (m, 3H, 3 × Ar*H*), 6.15 (br s, 2H, NH_2), 6.09 (s, 1H, C=C*H*S), 3.81 (d, *J* 7.0 Hz, 2H, OCH_2), 1.64–1.53 (m, 1H, OCH_2C*H*), 0.59 (d, *J* 7.0 Hz, 6H, CH(CH_3)$_2$); **^{13}C NMR** (125 MHz, $CDCl_3$) δ (ppm) 166.2, 164.2, 141.4, 141.3, 139.9, 137.9, 129.5, 128.9, 127.3, 127.2, 126.4, 106.3, 105.7, 70.3, 27.3, 19.0; **LRMS** (ES + APCI) *m/z*: calc. for $C_{21}H_{21}NO_2S$ 351.1 found 352.0 $[M+H]^+$; **HMRS** calc. for $C_{21}H_{22}NO_2S$ 352.1366 $[M+H]^+$, found 352.1367 $[M+H]^+$.

Allyl 4-([1,1'-biphenyl]-4-yl)-2-aminothiophene-3-carboxylate (77)

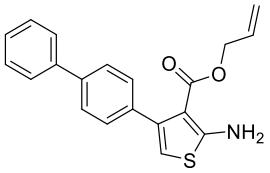

Following General Procedure D, allyl 2-cyanoacetate (301 mg, 1.20 mmol) and 1-([1,1'-biphenyl]-4-yl)ethan-1-one (236 mg, 2.40 mmol), after purification *via* flash column chromatography (dry loading, Hexane 10:1 EtOAc), afforded the *title compound* as a partially purified yellow solid.

Selected data; **^{1}H NMR** (500 MHz, $CDCl_3$) δ (ppm) 7.62 (d, *J* 8.0 Hz, 2H, 2 × Ar*H*), 7.55 (d, *J* 8.0 Hz, 2H, 2 × Ar*H*), 7.45 (app t, *J* 8.0 Hz, 2H, 2 × Ar*H*), 7.40–7.32 (m,

3H, 3 × Ar*H*), 6.12 (s, 1H, C=C*H*S), 6.11 (br s, 2H, NH_2), 5.69–5.59 (m, 1H, OCH_2CHCH_2), 4.98 (dd, *J* 10.5 Hz, 1.0 Hz, 1H, $OCH_2CHCH_{cis}(H)$), 4.88 (dd, *J* 17.0 Hz, 1.0 Hz, 1H, $OCH_2CHCH(H_{trans})$), 4.54 (d, *J* 5.5 Hz, 2H, OCH_2CHCH_2).

Benzyl 2-amino-4-(4-bromophenyl)thiophene-3-carboxylate (78)

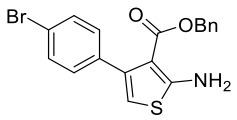

Following General Procedure D, benzyl 2-cyanoacetate (1.75 g, 10.0 mmol) and 4-bromoacetophenone (995 mg, 5.0 mmol), after purification *via* flash column chromatography (dry loading, Hexane 5:1 EtOAc), afforded the *title compound* (789 mg, 2.03 mmol, 41%) as a pale yellow solid. **mp** 116–118 °C; **IR**(ATR)/cm^{-1} 3449, 3323, 3099, 2960, 1668, 1569, 1480; **^{1}H NMR** (400 MHz, $CDCl_3$) δ (ppm) 7.33 (d, *J* 8.4 Hz, 2H, 2 × Ar*H*), 7.31–7.27 (m, 3H, 3 × Ar*H*), 7.13 (d, *J* 8.4 Hz, 2H, 2 × Ar*H*), 6.94 (dd, *J* 5.2 Hz, 2.0 Hz, 2H, 2 × Ar*H*), 6.17 (br s, 2H, NH_2), 6.05 (s, 1H, C=C*H*S), 5.08 (s, 2H, $COOCH_2$); **^{13}C NMR** (101 MHz, $CDCl_3$) δ (ppm) 167.3, 165.4, 164.6, 140.4, 137.5, 137.4, 135.6, 130.7, 130.6, 128.4, 128.0, 127.9, 121.1, 105.9, 105.7, 65.7; **LRMS** (ES + APCI) *m/z*: calc. for $C_{18}H_{14}{}^{79}BrNO_2S$ 387.0, found 387.9 $[M+H]^+$; **HMRS** calc. for $C_{18}H_{15}{}^{79}BrNO_2S$ 388.0001 $[M+H]^+$, found 388.0004 $[M+H]^+$.

Benzyl 4-([1,1'-biphenyl]-4-yl)-2-aminothiophene-3-carboxylate (79)

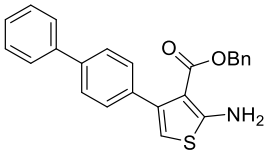

Following General Procedure D, benzyl 2-cyanoacetate (1.75 g, 10.0 mmol) and 1-([1,1'-biphenyl]-4-yl)ethan-1-one (981 mg, 5.0 mmol), after purification *via* flash column chromatography (dry loading, Hexane 5:1 EtOAc), afforded the *title compound* (737 mg, 1.91 mmol, 38%) as an off-white solid. **mp** 119–121 °C; **IR**(ATR)/cm^{-1} 3434, 3325, 3109, 2947, 1657, 1537, 1403; **^{1}H NMR** (400 MHz, $CDCl_3$) δ (ppm) 7.59 (dd, *J* 8.0 Hz, 1.2 Hz, 2H, 2 × Ar*H*), 7.50–7.43 (m, 4H, 4 × Ar*H*), 7.36 (app t, *J* 8.4 Hz, 4H, 4 × Ar*H*), 7.16–7.10 (m, 2H, 2 × Ar*H*), 6.93–6.89 (m, 2H, 2 × Ar*H*), 6.15 (br s, 2H, NH_2), 6.10 (s, 1H, C=C*H*S), 5.09 (s, 2H,

COOCH_2); **^{13}C NMR** (101 MHz, $CDCl_3$) δ (ppm) 165.6, 164.5, 141.3, 141.1, 139.8, 137.5, 135.8, 129.5, 129.1, 128.8, 128.7, 128.3, 127.7, 127.3, 127.2, 126.3, 105.8, 65.5; **LRMS** (ES + APCI) *m/z*: calc. for $C_{24}H_{19}NO_2S$ 385.1, found 386.0 $[M+H]^+$; **HMRS** calc. for $C_{24}H_{20}NO_2S$ 386.1209 $[M+H]^+$, found 386.1211 $[M+H]^+$.

2-((4-(4-Bromophenyl)-3-(methoxycarbonyl)thiophen-2-yl)carbamoyl)benzoic acid (80)

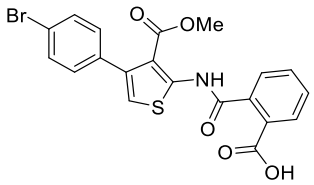

Following General Procedure E, compound **68** (300 mg, 0.96 mmol) and phthalic anhydride (143 mg, 0.96 mmol), after purification *via* flash column chromatography (dry loading, Hexane 5:1 EtOAc, CH_2Cl_2 95:5 MeOH), afforded the *title compound* (345 mg, 0.75 mmol, 78%) as an pale green solid. **mp** 120–122 °C; **IR**(ATR)/cm^{-1} 3248, 3159, 3026 br, 2952, 1725, 1664, 1599, 1534, 1513; **^{1}H NMR** (500 MHz, DMSO-d_6) δ (ppm) 13.30 (br s, 1H, COO*H*) 11.93 (br s, 1H, CON*H*), 7.89 (d, *J* 7.0 Hz, 1H, Ar*H*), 7.72–7.63 (m, 3H, 3 × Ar*H*), 7.55 (d, *J* 8.5 Hz, 2H, 2 × Ar*H*), 7.28 (d, *J* 8.5 Hz, 2H, 2 × Ar*H*), 7.05 (s, 1H, C=C*H*S), 3.60 (s, 3H, COOCH_3); **^{13}C NMR** (125 MHz, DMSO-d_6) δ (ppm) 168.0, 165.9, 164.9, 147.9, 144.3, 137.6, 135.9, 135.2, 131.3, 130.7, 130.6, 130.5, 129.8, 127.9, 120.4, 116.5, 112.6, 51.6; **LRMS** (ES + APCI) *m/z*: calc. for $C_{20}H_{14}{}^{81}BrNO_5S$ 461.0, found 461.8 $[M+H]^+$; **HMRS** calc. for $C_{20}H_{13}{}^{79}BrNO_5S$ 457.9703 $[M–H]^-$, found 457.9694 $[M–H]^-$.

2-((4-(4-Bromophenyl)-3-(ethoxycarbonyl)thiophen-2-yl)carbamoyl)benzoic acid (58)[68]

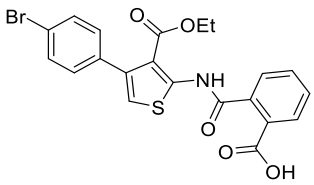

Following General Procedure E, compound **69** (250 mg, 0.77 mmol) and phthalic anhydride (120 mg, 0.77 mmol), after purification *via* flash column chromatography (dry loading, Hexane 5:1 EtOAc, CH_2Cl_2 95:5 MeOH), afforded the

title compound (252 mg, 0.53 mmol, 69%) as an off-white solid. **mp** 160–162 °C; **IR**(ATR)/cm^{-1} 3593, 3310, 3110, 2986, 1675, 1653, 1563, 1537; **^{1}H NMR** (500 MHz, DMSO-d_6) δ (ppm) 13.30 (br s, 1H, COO*H*) 12.03 (br s, 1H, CON*H*), 7.89 (app d, *J* 7.0 Hz, 1H, Ar*H*), 7.71–7.61 (m, 3H, 3 × Ar*H*), 7.56 (d, *J* 8.0 Hz, 2H, 2 × Ar*H*), 7.27 (d, *J* 8.0 Hz, 2H, 2 × Ar*H*), 7.04 (s, 1H, C=C*H*S), 4.07 (q, *J* 7.0 Hz, 2H, COOCH_2CH$_3$), 0.96 (t, *J* 7.0 Hz, 3H, COOCH$_2$CH_3); **^{13}C NMR** (125 MHz, DMSO-d_6) δ (ppm) 168.9, 166.3, 164.5, 148.2, 137.6, 136.2, 134.8, 130.9, 130.5, 130.4, 129.9, 127.9, 120.3, 116.0, 112.5, 60.4, 13.4 (2 carbons missing); **LRMS** (ES + APCI) *m/z*: calc. for $C_{21}H_{16}{}^{81}BrNO_5S$ 474.99, found 475.9 $[M+H]^+$.

2-((4-([1,1'-Biphenyl]-4-yl)-3-(ethoxycarbonyl)thiophen-2-yl)carbamoyl)benzoic acid (81)[68]

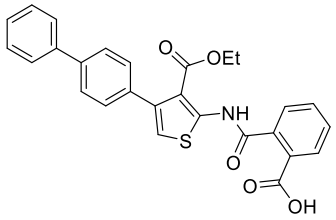

Following General Procedure E, compound **70** (250 mg, 0.77 mmol) and phthalic anhydride (115 mg, 0.77 mmol), after purification *via* flash column chromatography (dry loading, Hexane 5:1 EtOAc, CH_2Cl_2 95:5 MeOH), afforded the *title compound* (220 mg, 0.46 mmol, 60%) as a yellow solid. **mp** 135–137 °C; **IR**(ATR)/cm^{-1} 3030, 2963, 1724, 1662, 1576, 1528; **^{1}H NMR** (500 MHz, DMSO-d_6) δ (ppm) 13.42 (br s, 1H, COO*H*) 12.33 (br s, 1H, CON*H*), 7.90 (app d, *J* 7.0 Hz, 1H, Ar*H*), 7.70 (app d, *J* 7.5, 3H, 3 × Ar*H*), 7.66 (d, *J* 8.0 Hz, 2H, 2 × Ar*H*), 7.65–7.58 (m, 2H, 2 × Ar*H*), 7.48 (app t, 7.5 Hz, 2H, 2 × Ar*H*), 7.40 (d, *J* 8.0 Hz, 2H, 2 × Ar*H*), 7.38 (t, *J* 7.5 Hz, 1H, Ar*H*), 7.05 (s, 1H, C=C*H*S), 4.09 (q, *J* 7.0 Hz, 2H, COOCH_2CH$_3$), 0.97 (t, *J* 7.0 Hz, 3H, COOCH$_2$CH_3); **^{13}C NMR** (125 MHz, DMSO-d_6) δ (ppm) 168.5, 166.1, 164.7, 147.8, 139.8, 138.8, 138.5, 136.0, 134.9, 134.8, 130.8, 130.5, 129.9, 129.3, 128.9, 127.9, 127.4, 126.5, 125.9, 115.7, 112.9, 60.4, 13.4; **LRMS** (ES + APCI) *m/z*: calc. for $C_{27}H_{21}NO_5S$ 471.11, found 471.9 $[M+H]^+$.

2-((4-(4-Bromophenyl)-3-(isopropoxycarbonyl)thiophen-2-yl)carbamoyl)benzoic acid (82)[68]

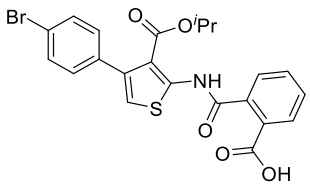

Following General Procedure E, compound **71** (300 mg, 0.88 mmol) and phthalic anhydride (132 mg, 0.88 mmol), after purification *via* flash column chromatography (dry loading, Hexane 5:1 EtOAc, CH_2Cl_2 95:5 MeOH), afforded the *title compound* (340 mg, 0.70 mmol, 79%) as an off-white solid. **mp** 158–160 °C; **IR**(ATR)/cm^{-1} 3555, 3335 br, 3274, 3088, 2973, 1701, 1653, 1569, 1539; **^{1}H NMR** (500 MHz, DMSO-d_6) δ (ppm) 13.35 (br s, 1H, COO*H*) 11.89 (br s, 1H, CON*H*), 7.90 (d, *J* 7.0 Hz, 1H, Ar*H*), 7.71–7.60 (m, 3H, 3 × Ar*H*), 7.56 (d, *J* 8.0 Hz, 2H, 2 × Ar*H*), 7.25 (d, *J* 8.0 Hz, 2H, 2 × Ar*H*), 7.01 (s, 1H, C=C*H*S), 4.90 (septet, *J* 6.0 Hz, 1H, COOC*H*$(CH_3)_2$), 0.96 (d, *J* 6.0 Hz, 6H, COOCH(C*H*$_3)_2$); **^{13}C NMR** (125 MHz, DMSO-d_6) δ (ppm) 168.1, 166.1, 164.1, 148.3, 141.8, 137.7, 136.4, 135.3, 131.2, 131.0, 130.6, 130.4, 129.9, 127.7, 120.3, 115.9, 112.6, 68.2, 21.1; **LRMS** (ES + APCI) *m/z*: calc. for $C_{22}H_{18}{}^{81}BrNO_5S$ 489.0, found 489.9 $[M+H]^+$.

2-((4-([1,1'-Biphenyl]-4-yl)-3-(isopropoxycarbonyl)thiophene-2-yl)carbamoyl)benzoic acid (83)

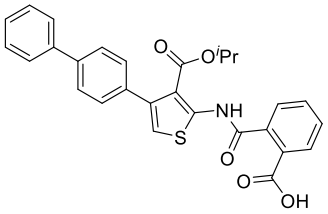

Following General Procedure E, compound **72** (200 mg, 0.59 mmol) and phthalic anhydride (88 mg, 0.59 mmol), after purification *via* flash column chromatography (dry loading, Hexane 5:1 EtOAc, CH_2Cl_2 95:5 MeOH), afforded the *title compound* (232 mg, 0.48 mmol, 81%) as an off-white solid. **mp** 166–168 °C; **IR**(ATR)/cm^{-1} 3563 br, 3278, 3099, 2967, 1696, 1675, 1645, 1532; **^{1}H NMR** (400 MHz, DMSO-d_6) δ (ppm) 13.36 (br s, 1H, COO*H*), 11.88 (br s, 1H, CON*H*), 7.91 (dd, *J* 6.8 Hz, 1.6 Hz, 1H, Ar*H*), 7.72–7.62 (m, 7H, 7 × Ar*H*), 7.48 (t, *J* 7.2 Hz,

2H, 2 × Ar*H*), 7.41–7.35 (m, 3H, 3 × Ar*H*), 7.04 (s, 1H, C=C*H*S), 4.92 (septet, *J* 6.0 Hz, 1H, COOC*H*(CH_3)$_2$), 0.97 (d, *J* 6.4 Hz, 6H, COOCH(C*H*$_3$)$_2$); **^{13}C NMR** (101 MHz, DMSO-d_6) δ (ppm) 167.9 165.9, 164.3, 147.9, 139.8, 138.8, 138.7, 136.3, 135.4, 131.9, 131.3, 130.6, 129.9, 129.4, 128.9, 127.7, 127.4, 126.5, 125.8, 115.6, 113.0, 68.2, 21.3; **LRMS** (ES + APCI) *m/z*: calc. for $C_{28}H_{23}NO_5S$ 485.13, found 486.0 $[M+H]^+$; **HMRS** calc. for $C_{28}H_{22}NO_5S$ 484.1224 $[M–H]^-$, found 484.1219 $[M–H]^-$.

2-((4-(4-Bromophenyl)-3-(*tert*-butoxycarbonyl)thiophen-2-yl)carbamoyl)benzoic acid (84)

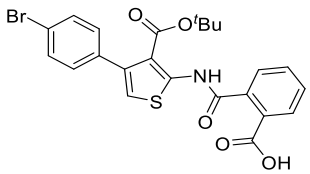

Following General Procedure E, compound **73** (200 mg, 0.56 mmol) and phthalic anhydride (84 mg, 0.56 mmol), after purification *via* flash column chromatography (dry loading, Hexane 5:1 EtOAc, CH_2Cl_2 95:5 MeOH), afforded the *title compound* (212 mg, 0.42 mmol, 76%) as an off-white solid. **mp** 183–185 °C; **IR**(ATR)/cm^{-1} 3313 br, 3269, 3116, 2984, 1722, 1657, 1640, 1537; **^{1}H NMR** (400 MHz, DMSO-d_6) δ (ppm) 12.03 (br s, 1H, COO*H*), 7.90 (dd, *J* 8.4 Hz, 3.6 Hz, 1H, Ar*H*), 7.64–7.53 (m, 5H, 5 × Ar*H*), 7.23 (d, *J* 8.4 Hz, 2H, 2 × Ar*H*), 6.94 (s, 1H, C=C*H*S), 1.18 (s, 1H, COOC(C*H*$_3$)$_3$; **^{13}C NMR** (101 MHz, DMSO-d_6) δ (ppm) 176.3, 166.8, 163.9, 148.4, 137.9, 136.9, 135.2, 130.9, 130.5, 130.2, 129.9, 127.6, 120.1, 115.6, 113.2, 81.5, 27.4 (2 carbons missing); **LRMS** (ES + APCI) *m/z*: calc. for $C_{23}H_{20}{}^{81}BrNO_5S$ 503.1, found 503.9 $[M+H]^+$; **HMRS** calc. for $C_{23}H_{19}{}^{81}BrNO_5S$ 502.0152 $[M–H]^-$, found 502.0143 $[M–H]^-$.

2-((4-([1,1'-Biphenyl]-4-yl)-3-(tert-butoxycarbonyl)thiophen-2-yl)carbamoyl)benzoic acid (85)

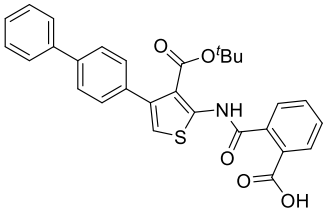

Following General Procedure E, compound **74** (200 mg, 0.57 mmol) and phthalic anhydride (85 mg, 0.57 mmol), after purification *via* flash column chromatography (dry loading, Hexane 5:1 EtOAc, CH_2Cl_2 95:5 MeOH), afforded the *title compound* (197 mg, 0.39 mmol, 69%) as a pale yellow solid. **mp** 163–165 °C; **IR**(ATR)/cm^{-1} 3088, 2980, 1720, 1658, 1586, 1526; **^{1}H NMR** (400 MHz, DMSO-d_6) δ (ppm) 12.26 (br s, 1H, COO*H*), 7.90 (dd, *J* 6.4 Hz, 2.4 Hz, 1H, Ar*H*), 7.71–7.65 (m, 4H, 4 × Ar*H*), 7.60 (dd, *J* 6.8 Hz, 2.4 Hz, 1H, Ar*H*), 7.56–7.51 (m, 2H, 2 × Ar*H*), 7.47 (t, *J* 7.2 Hz, 2H, 2 × Ar*H*), 7.39–7.35 (m, 3H, 3 × Ar*H*), 6.95 (s, 1H, C=C*H*S), 1.19 (s, 9H, COOC(CH_3)$_3$); **^{13}C NMR** (101 MHz, DMSO-d_6) δ (ppm) 169.7, 167.1, 164.1, 148.2, 139.9, 138.8, 138.7, 136.9, 136.7, 135.1, 130.1, 129.9, 129.6, 129.3, 128.9, 127.6, 127.4, 126.5, 125.8, 115.1, 113.6, 81.3, 27.4; **LRMS** (ES + APCI) *m/z*: calc. for $C_{29}H_{25}NO_5S$ 499.2, found 500.0 $[M+H]^+$; **HMRS** calc. for $C_{29}H_{24}NO_5S$ 498.1381 $[M–H]^-$, found 498.1382 $[M–H]^-$.

2-((4-([1,1'-Biphenyl]-4-yl)-3-(butoxycarbonyl)thiophen-2-yl)carbamoyl)benzoic acidcarboxylate (86)

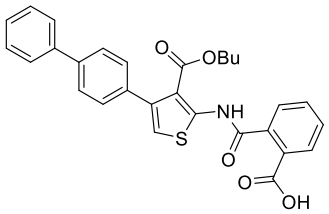

Following General Procedure E, compound **75** (100 mg, 0.28 mmol) and phthalic anhydride (43 mg, 0.28 mmol), after purification *via* flash column chromatography (dry loading, Petroleum ether 3:1 EtOAc, CH_2Cl_2 9:1 MeOH), afforded the *title compound* (118 mg, 0.24 mmol, 83%) as an off-white solid. **mp** 189–191 °C; **IR**(ATR)/cm^{-1} 3027, 2955, 1720, 1655, 1525, 1497, 1396, 1255, 1210; **^{1}H NMR** (500 MHz, DMSO-d_6) δ (ppm) 13.48 (br s, 1H, COO*H*), 12.73 (br s, 1H, CON*H*), 7.88 (dd, *J* 5.5 Hz, 3.5 Hz, 1H, Ar*H*), 7.71–7.67 (m, 3H, 3 × Ar*H*), 7.66 (d, *J* 8.0 Hz, 2H, 2 × Ar*H*), 7.61–7.55 (m, 2H, 2 × Ar*H*), 7.48 (app t, *J* 7.5 Hz, 2H, 2 × Ar*H*), 7.41–7.35 (m, 3H, 3 × Ar*H*), 7.01 (s, 1H, C=C*H*S), 4.04 (t, *J* 6.0 Hz, 2H, OCH_2), 1.35–1.27 (m, 2H, OCH$_2$CH_2CH$_2$), 0.98–0.88 (m, 2H, CH$_2$CH_2CH$_3$), 0.62 (t, *J* 7.0 Hz, 3H, CH$_2$CH$_2$CH_3); **^{13}C NMR** (125 MHz, DMSO-d_6) δ (ppm) 169.1, 166.4, 164.8, 148.0, 139.9, 138.8, 138.5, 136.2, 134.7, 130.3, 130.1, 129.9, 129.2, 128.9, 127.9, 127.4, 126.5, 125.9, 115.7, 115.6, 112.8, 64.2, 29.7, 18.5, 13.4; **LRMS**

(ES + APCI) *m/z*: calc. for $C_{29}H_{25}NO_5S$ 499.1, found 500.0 $[M+H]^+$; **HMRS** calc. for $C_{29}H_{26}NO_5S$ 500.1526 $[M+H]^+$, found 500.1520 $[M+H]^+$.

2-((4-([1,1'-Biphenyl]-4-yl)-3-(isobutoxycarbonyl)thiophen-2-yl)carbamoyl)benzoic acid (87)

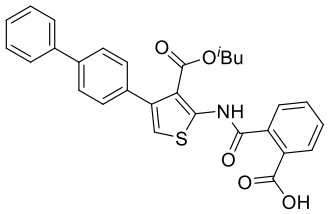

Following General Procedure E, compound **76** (100 mg, 0.28 mmol) and phthalic anhydride (43 mg, 0.28 mmol), after purification *via* flash column chromatography (dry loading, Petroleum ether 3:1 EtOAc, CH_2Cl_2 9:1 MeOH), afforded the *title compound* (110 mg, 0.22 mmol, 77%) as an off-white solid. **mp** 139–141 °C; **IR**(ATR)/cm^{-1} 3007, 2946, 1720, 1655, 1525, 1499, 1396, 1255, 1209; **^{1}H NMR** (500 MHz, DMSO-d_6) δ (ppm) 13.51 (br s, 1H, COO*H*), 12.98 (br s, 1H, CON*H*), 7.88 (dd, *J* 5.0 Hz, 2.0 Hz, 1H, Ar*H*), 7.71–7.63 (m, 5H, 5 × Ar*H*), 7.59–7.53 (m, 2H, 2 × Ar*H*), 7.48 (app t, *J* 7.5 Hz, 2H, 2 × Ar*H*), 7.41–7.35 (m, 3H, 3 × Ar*H*), 7.01 (s, 1H, C=C*H*S), 3.84 (d, *J* 6.5 Hz, 2H, OCH_2), 1.63 (septet, *J* 6.5 Hz, 1H, $OCH_2CH(CH_3)_2$), 0.57 (d, *J* 6.5 Hz, 3H, $CH_2CH_2CH_3$); **^{13}C NMR** (125 MHz, DMSO-d_6) δ (ppm) 167.2, 166.5, 164.9, 148.0, 139.9, 138.9, 138.4, 136.3, 134.5, 130.2, 130.1, 130.0, 129.8, 129.1, 128.9, 128.0, 127.4, 126.5, 126.1, 115.5, 112.9, 70.5, 26.8, 18.6; **LRMS** (ES + APCI) *m/z*: calc. for $C_{29}H_{25}NO_5S$ 499.1, found 500.0 $[M+H]^+$; **HMRS** calc. for $C_{29}H_{26}NO_5S$ 500.1526 $[M+H]^+$, found 500.1520 $[M+H]^+$.

2-((4-([1,1'-Biphenyl]-4-yl)-3-((allyloxy)carbonyl)thiophen-2-yl)carbamoyl)benzoic acid (88)

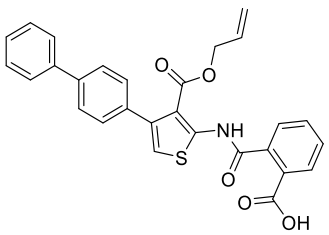

Following General Procedure E, partially purified compound **77** (200 mg, 0.60 mmol) and phthalic anhydride (88 mg, 0.60 mmol), after purification *via* flash column chromatography (dry loading, Petroleum ether 3:1 EtOAc, CH_2Cl_2 9:1 MeOH), afforded the *title compound* (198 mg, 0.41 mmol, 34%) as an off-white solid. **mp** 124–126 °C; **IR**(ATR)/cm^{-1} 3072, 2933, 1724, 1657, 1649, 1525, 1499, 1398, 1253, 1207; **^{1}H NMR** (500 MHz, DMSO-d_6) δ (ppm) 13.28 (br s, 1H, COO*H*), 7.91–7.87 (m, 1H, Ar*H*), 7.75–7.71 (m, 1H, Ar*H*), 7.69 (d, *J* 8.0 Hz, 2H, 2 × Ar*H*), 7.65 (d, *J* 8.0 Hz, 2H, 2 × Ar*H*), 7.64–7.58 (m, 2H, 2 × Ar*H*), 7.49 (app t, *J* 8.0 Hz, 2H, 2 × Ar*H*), 7.41 (d, *J* 8.0 Hz, 2H, 2 × Ar*H*), 7.38 (t, *J* 8.0 Hz, 1H, Ar*H*), 7.06 (s, 1H, C=C*H*S), 5.79–5.69 (m, 1H, OCH_2CHCH_2), 5.01 (d, J_{cis} 10.5 Hz, J_{gem} 1.0 Hz, 1H, OCH_2CHCHH), (d, J_{trans} 17.5 Hz, 1H, OCH_2CHCHH), 4.60 (d, *J* 5.5 Hz, 2H, OCH_2CHCH_2); **^{13}C NMR** (125 MHz, DMSO-d_6) δ (ppm) 168.6, 166.1, 164.3, 147.9, 139.9, 138.9, 138.5, 135.9, 134.8, 132.8, 131.9, 130.7, 130.5, 129.9, 129.2, 128.9, 128.0, 127.4, 126.5, 126.0, 117.6, 115.9, 112.8, 65.0; **LRMS** (ES + APCI) *m/z*: calc. for $C_{28}H_{21}NO_5S$ 483.1, found 484.0 $[M+H]^+$; **HMRS** calc. for $C_{28}H_{22}NO_5S$ 484.1213 $[M+H]^+$, found 484.1208 $[M+H]^+$.

2-((3-((benzyloxy)carbonyl)-4-(4-bromophenyl)thiophen-2-yl)carbamoyl) benzoic acid (89)

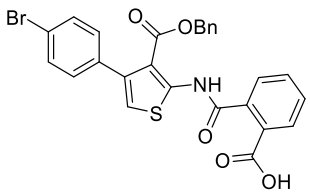

Following General Procedure E, compound **78** (200 mg, 0.52 mmol) and phthalic anhydride (77 mg, 0.52 mmol), after purification *via* flash column chromatography (dry loading, Hexane 5:1 EtOAc, CH_2Cl_2 95:5 MeOH), afforded the *title compound* (240 mg, 0.45 mmol, 86%) as an off-white solid. **mp** 158–160 °C; **IR**(ATR)/cm^{-1} 3353 br, 3251, 3064, 2975, 1724, 1662, 1653, 1534; **^{1}H NMR** (400 MHz, DMSO-d_6) δ (ppm) 13.21 (br s, 1H, COO*H*), 7.90 (dd, *J* 7.2 Hz, 2.0 Hz, 1H, Ar*H*), 7.67 (dd, *J* 7.2 Hz, 1.6 Hz, 1H, Ar*H*), 7.58–7.50 (m, 2H, 2 × Ar*H*), 7.45 (d, *J* 8.4 Hz, 2H, 2 × Ar*H*), 7.29–7.18 (m, 5H, 5 × Ar*H*), 7.05 (d, *J* 6.8 Hz, 2H, 2 × Ar*H*), 6.99 (s, 1H, C=C*H*S), 5.13 (s, 2H, $COOCH_2$); **^{13}C NMR** (101 MHz, DMSO-d_6) δ (ppm) 169.9, 166.6, 164.2, 148.2, 137.5, 136.9, 136.2,

136.1, 135.3, 134.4, 134.2, 130.6, 130.2, 130.1, 129.5, 128.1, 127.9, 127.8, 120.4, 115.9, 112.5, 108.2, 66.2; **LRMS** (ES + APCI) *m/z*: calc. for $C_{26}H_{18}{}^{79}BrNO_5S$ 535.1, found 535.8 $[M+H]^+$; **HMRS** calc. for $C_{26}H_{17}{}^{79}BrNO_5S$ 534.0016 $[M–H]^-$, found 534.0010 $[M–H]^-$.

2-((4-([1,1'-Biphenyl]-4-yl)-3-((benzyloxy)carbonyl)thiophen-2-yl)carbamoyl)benzoic acid (90)

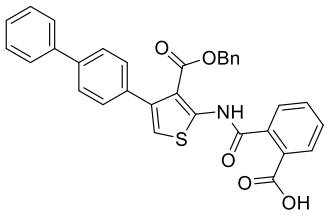

Following General Procedure E, compound **79** (200 mg, 0.52 mmol) and phthalic anhydride (77 mg, 0.52 mmol), after purification *via* flash column chromatography (dry loading, Hexane 5:1 EtOAc, CH_2Cl_2 95:5 MeOH), afforded the *title compound* (177 mg, 0.33 mmol, 64%) as an off-white solid. **mp** 173–175 °C; **IR**(ATR)/cm^{-1} 3256, 3057, 2989, 1722, 1658, 1651, 1532; **^{1}H NMR** (400 MHz, DMSO-d_6) δ (ppm) 13.09 (br s, 1H, COO*H*), 7.88 (d, *J* 7.2 Hz, 1H, Ar*H*), 7.72 (d, *J* 7.2 Hz, 1H, Ar*H*), 7.67 (d, *J* 8.4 Hz, 2H, 2 × Ar*H*), 7.58 (d, *J* 8.4 Hz, 2H, 2 × Ar*H*), 7.56–7.46 (m, 4H, 4 × Ar*H*), 7.39 (app dt, *J* 7.6 Hz, 1H, Ar*H*), 7.35 (d, *J* 8.4 Hz, 2H, 2 × Ar*H*), 7.23–7.09 (m, 5H, 5 × Ar*H*), 7.01 (s, 1H, C=C*H*S), 5.19 (s, 2H, COOCH_2); **^{13}C NMR** (101 MHz, DMSO-d_6) δ (ppm) 170.6, 166.6, 164.4, 147.5, 147.4, 139.8, 138.8, 138.2, 135.9, 135.5, 133.6, 133.5, 130.2, 130.1, 128.9, 128.5, 128.1, 128.0, 127.8, 126.5, 126.1, 115.5, 113.2, 66.2 (3 carbons missing); **LRMS** (ES + APCI) *m/z*: calc. for $C_{32}H_{23}NO_5S$ 533.1, found 534.0 $[M+H]^+$; **HMRS** calc. for $C_{32}H_{22}NO_5S$ 532.1224 $[M–H]^-$, found 532.1216 $[M–H]^-$.

4-(4-Bromophenyl)-2-(2-carboxybenzamido)thiophene-3-carboxylic acid (91)

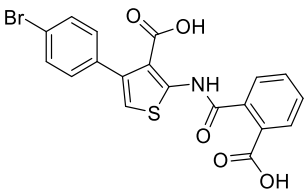

Following General Procedure G, compound **58** (150 mg, 0.32 mmol) and NaOH (132 mg, 0.88 mmol), afforded the *title compound* (101 mg, 0.23 mmol, 71%) as an

off-white solid. **mp** 198–200 °C; **IR**(ATR)/cm^{-1} 3360 br, 3291, 3054, 2922, 1673, 1682, 1513; **^{1}H NMR** (500 MHz, DMSO-d_6) δ (ppm) 12.98 (br s, 2H, 2 × COO*H*), 7.88 (d, *J* 7.0 Hz, 1H, Ar*H*), 7.72–7.64 (m, 3H, 3 × Ar*H*), 7.52 (d, *J* 8.0 Hz, 2H, 2 × Ar*H*), 7.29 (d, *J* 8.0 Hz, 2H, 2 × Ar*H*), 6.95 (s, 1H, C=C*H*S); **^{13}C NMR** (125 MHz, DMSO-d_6) δ (ppm) 165.5, 138.4, 136.7, 131.9, 131.8, 131.2, 130.9, 130.8, 130.3, 129.7, 127.6, 127.3, 120.2, 115.8, 106.9 (1 carbon missing); **LRMS** (ES + APCI) *m/z*: calc. for $C_{19}H_{12}{}^{79}BrNO_5S$ 444.9, found 445.8 $[M+H]^+$; **HMRS** calc. for $C_{19}H_{10}{}^{79}BrNO_5S$ 221.4737 $[M–2H]^{2-}$, found 221.4739 $[M–2H]^{2-}$.

4-([1,1'-Biphenyl]-4-yl)-2-(2-carboxybenzamido)thiophene-3-carboxylic acid (92)

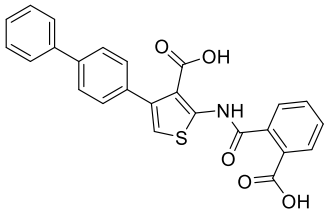

Following General Procedure G, compound **81** (150 mg, 0.32 mmol) and NaOH (132 mg, 0.88 mmol), afforded the *title compound* (108 mg, 0.24 mmol, 76%) as an off-white solid. **mp** 201–203 °C; **IR**(ATR)/cm^{-1} 3366 br, 3291, 3029, 2924, 1668, 1582, 1523; **^{1}H NMR** (500 MHz, DMSO-d_6) δ (ppm) 13.18 (br s, 2H, 2 × COO*H*), 11.67 (br s, 1H, CON*H*), 7.92 (d, *J* 7.5 Hz, 1H, Ar*H*), 7.77–7.68 (m, 5H, 5 × Ar*H*), 7.65 (d, *J* 8.0 Hz, 2H, 2 × Ar*H*), 7.48 (app t, *J* 8.0 Hz, 2H, 2 × Ar*H*), 7.43 (d, *J* 8.0 Hz, 2H, 2 × Ar*H*), 7.37 (t, *J* 7.5 Hz, 1H, Ar*H*), 7.01 (s, 1H, C=C*H*S); **^{13}C NMR** (125 MHz, DMSO-d_6) δ (ppm) 167.3, 166.7, 165.6, 148.7, 139.8, 139.1, 138.7, 136.4, 135.8, 132.1, 130.8, 130.7, 129.9, 129.5, 128.9, 127.6, 127.4, 126.6, 125.8, 115.8, 112.7; **LRMS** (ES + APCI) *m/z*: calc. for $C_{25}H_{17}NO_5S$ 443.1, found 443.9 $[M+H]^+$; **HMRS** calc. for $C_{25}H_{16}NO_5S$ 442.0755 $[M–H]^-$, found 442.0759 $[M–H]^-$.

2-((4-([1,1'-Biphenyl]-4-yl)-3-(isopropoxycarbonyl)thiophen-2-yl)carbamoyl)benzenesulfonic acid (95)

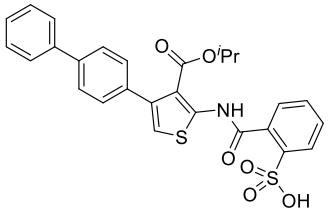

Following General Procedure E, compound **72** (100 mg, 0.30 mmol) and 4,5,6,7-tetrahydroisobenzofuran-1,3-dione (55 mg, 0.30 mmol), after purification *via* flash column chromatography (dry loading, CH_2Cl_2 48:2 MeOH, CH_2Cl_2 9:1 MeOH), afforded the *title compound* (96 mg, 0.18 mmol, 62%) as an off-white solid. **mp** 176–178 °C; **IR**(ATR)/cm^{-1} 3270 br, 3025, 2976, 2926, 1656, 1528, 1498, 1409, 1292, 1251, 1217, 1100, 1024; **^{1}H NMR** (400 MHz, DMSO-d_6) δ (ppm) 11.88 (s, 1H, CON*H*), 7.85 (dd, *J* 7.2 Hz, 1.6 Hz, 1H, Ar*H*), 7.70 (d, *J* 8.4 Hz, 2H, 2 × Ar*H*), 7.66 (d, *J* 8.4 Hz, 2H, 2 × Ar*H*), 7.59 (dd, *J* 7.2 Hz, 1.6 Hz, 1H, Ar*H*), 7.57–7.45 (m, 5H, 5 × Ar*H*), 7.40–7.34 (m, 3H, 3 × Ar*H*), 7.02 (s, 1H, C=C*H*S), 4.86 (septet, *J* 6.0 Hz, 1H, COOC*H*$(CH_3)_2$), 0.97 (d, *J* 6.0 Hz, 6H, COOCH$(CH_3)_2$); **^{13}C NMR** (101 MHz, DMSO-d_6) δ (ppm) 166.1, 163.1, 146.5, 144.7, 139.9, 138.7, 138.6, 136.4, 132.6, 130.1, 129.6, 129.2, 129.1, 129.0, 128.9, 127.4, 126.5, 125.9, 115.4, 114.0, 67.8, 21.1; **LRMS** (ES + APCI) *m/z*: calc. for $C_{27}H_{23}NO_6S_2$ 521.1, found 522.0 $[M+H]^+$; **HMRS** calc. for $C_{27}H_{22}NO_6S_2$ 520.0894 $[M–H]^-$, found 520.0903 $[M–H]^-$.

Ethyl 2-(1*H*-tetrazol-5-yl)benzoate (97)

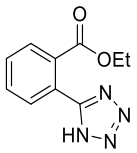

A solution of ethyl 2-cyanobenzoate **96** (2.00 g, 11.40 mmol), sodium azide (2.22 g, 34.20 mmol) and triethylamine hydrochloride (4.71 g, 34.22 mmol) in toluene (40 mL, 0.29 M) was heated to 100 °C for 4.5 hours. The mixture was cooled to room temperature and H_2O (150 mL) was added. The suspension was stirred for a further 10 minutes before the aqueous phase was separated and transferred to a round-bottomed flask, cooled to 0 °C and acidified with conc. HCl. The resultant precipitate was collected by filtration, washed with H_2O (100 mL) and vacuum dried to afford the *title compound* (1.45 g, 7.11 mmol, 62%) as an off-white solid. **mp** 146–148 °C; **IR**(ATR)/cm^{-1} 3061, 2986, 2937, 1718, 1587, 1389, 1260, 1087; **^{1}H NMR** (500 MHz, $CDCl_3$) δ (ppm) 14.66 (br s, 1H, NN*H*), 8.60 (d, *J* 7.0 Hz, 1H, Ar*H*), 8.16 (d, *J* 8.0 Hz, 1H, Ar*H*), 7.76 (app td, *J* 8.0, 1.0 Hz, 1H, Ar*H*), 7.64 (d, *J* 8.0, 1.0 Hz, 1H, Ar*H*), 4.46 (q, *J* 7.0 Hz, 2H, COOC$H_2$$CH_3$), 1.43 (t, *J* 7.0 Hz, 3H, COOCH$_2$CH_3); **^{13}C NMR** (125 MHz, $CDCl_3$) δ (ppm) 168.7, 153.9, 133.5,

132.1, 131.9, 131.3, 128.9, 124.1, 63.0, 14.1; **LRMS** (ES + APCI) *m/z*: calc. for $C_{10}H_{10}N_4O_2$ 218.1, found 219.0 $[M+H]^+$; **HMRS** calc. for $C_{10}H_{11}N_4O_2$ 219.0877 $[M+H]^+$, found 219.0871 $[M+H]^+$.

2-(1*H*-Tetrazol-5-yl)benzoic acid (98)

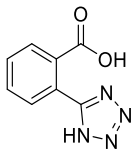

Following General Procedure G, compound **97** (200 mg, 0.92 mmol) afforded the *title compound* (170 mg, 0.89 mmol, 98%) as an off-white solid. **Mp** 200–202 °C; **IR**(ATR)/cm^{-1} 3043, 2982, 2852 br, 1697, 1586, 1493, 1418, 1305, 1273; **^{1}H NMR** (500 MHz, DMSO-d_6) δ (ppm) 14.68 (br s, 1H, NN*H*), 13.29 (br s, 1H, COO*H*), 8.01 (dd, *J* 7.5 Hz, 1.5 Hz, 1H, Ar*H*), 7.77–7.69 (m, 2H, 2 × Ar*H*), 7.65 (dd, *J* 7.5 Hz, 1.5 Hz, 1H, Ar*H*); **^{13}C NMR** (125 MHz, DMSO-d_6) δ (ppm) 167.2, 154.8, 131.9, 131.9, 130.9, 130.8, 130.3, 125.1; **LRMS** (ES + APCI) *m/z*: calc. for $C_8H_6N_4O_2$ 190.0, found 189.1 $[M–H]^-$; **HMRS** calc. for $C_8H_5N_4O_2$ 189.0418 $[M–H]^-$, found 189.0413 $[M–H]^-$.

Isopropyl 2-(2-(1*H*-tetrazol-5-yl)benzamido)-4-(4-bromophenyl)thiophene-3-carboxylate (99)

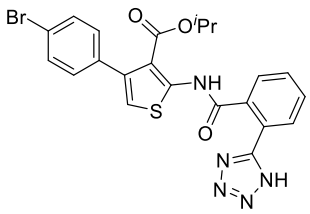

To a suspension of compound **71** (142 mg, 0.42 mmol) and compound **98** (80 mg, 0.42 mmol) in anhydrous THF (1.4 mL, 0.3 M), were added successively diisopropylethyl amine (DIPEA) (220 µL, 1.26 mmol) T3P (≥50 wt. % ethyl acetate) (188 µL, 0.63 mmol). The reaction mixture was stirred overnight at room temperature and then diluted with water (10 mL) and CH_2Cl_2 (10 mL). The layers were separated and the aqueous layer was extracted with CH_2Cl_2 (2 × 10 mL). The combined organic extracts were dried over $MgSO_4$, filtered and concentrated under reduced pressure. Further purification *via* flash column chromatography (dry loading,

Hexane 5:1 EtOAc, CH_2Cl_2 95:5 MeOH) afforded the *title compound* (70 mg, 0.14 mmol, 33%) as an off-white solid. **mp** 168–170 °C; **IR**(ATR)/cm^{-1} 3365 br, 3254, 3076, 2943, 1703, 1646, 1573, 1521, 1373, 1291; **^{1}H NMR** (500 MHz, DMSO-d_6) δ (ppm) 11.41 (br s, 1H, CON*H*), 7.97 (dd, *J* 7.5 Hz, 1.0 Hz, 1H, Ar*H*), 7.68 (dd, *J* 7.5 Hz, 1.0 Hz, 1H, Ar*H*), 7.63 (app td, *J* 7.5 Hz, 1.0 Hz, 1H, Ar*H*), 7.56–7.50 (m, 3H, 3 × Ar*H*), 7.25 (d, *J* 8.5 Hz, 2H, 2 × Ar*H*), 6.98 (s, 1H, C=C*H*S), 4.82 (septet, *J* 6.0 Hz, 1H, COOC*H*$(CH_3)_2$), 0.90 (d, *J* 6.0 Hz, 6H, COOCH$(CH_3)_2$); **^{13}C NMR** (125 MHz, DMSO-d_6) δ (ppm) 170.5, 166.3, 163.8, 158.1, 148.8, 137.8, 136.6, 133.4, 131.1, 130.8, 130.3, 129.2, 128.4, 128.1, 120.2, 115.8, 111.9, 68.1, 21.1; **LRMS** (ES + APCI) *m/z*: calc. for $C_{22}H_{18}{}^{81}BrN_5O_3S$ 511.0, found 511.8 $[M+H]^+$; **HMRS** calc. for $C_{22}H_{19}{}^{81}BrN_5O_3S$ 512.0386 $[M+H]^+$, found 512.0381 $[M+H]^+$.

Isopropyl 2-(2-(1*H*-tetrazol-5-yl)benzamido)-4-([1,1'-biphenyl]-4-yl)thiophene-3-carboxylate (100)

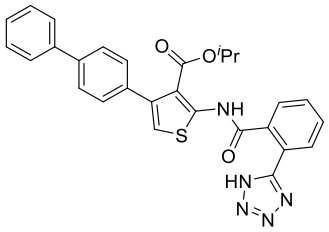

To a suspension of compound **72** (150 mg, 0.45 mmol) and compound **98** (85 mg, 0.45 mmol) in anhydrous THF (1.5 mL, 0.3 M), were added successively DIPEA (233 μL, 1.34 mmol) and T3P (≥50 wt. % ethyl acetate) (199 μL, 0.67 mmol). The reaction mixture was stirred overnight at room temperature and then diluted with water (10 mL) and CH_2Cl_2 (10 mL). The layers were separated and the aqueous layer was extracted with CH_2Cl_2 (2 × 10 mL). The combined organic extracts were dried over $MgSO_4$, filtered and concentrated under reduced pressure. Further purification *via* flash column chromatography (dry loading, Hexane 5:1 EtOAc, CH_2Cl_2 95:5 MeOH) afforded the *title compound* (82 mg, 0.16 mmol, 36%) as an off-white solid. **mp** 181–183 °C; **IR**(ATR)/cm^{-1} 3258, 3053, 2979, 1716, 1651, 1527, 1409, 1255, 1222, 1101; **^{1}H NMR** (400 MHz, DMSO-d_6) δ (ppm) 11.48 (br s, 1H, CON*H*), 7.93 (dd, *J* 7.6 Hz, 0.8 Hz, 1H, Ar*H*), 7.83 (dd, *J* 7.6 Hz, 0.8 Hz, 1H, Ar*H*), 7.77–7.63 (m, 6H, 6 × Ar*H*), 7.48 (app t, *J* 7.6 Hz, 2H, 2 × Ar*H*), 7.41–7.34 (m, 3H, 3 × Ar*H*), 7.03 (s, 1H, C=C*H*S), 4.87 (septet, *J* 6.4 Hz, 1H, COOC*H*$(CH_3)_2$), 0.93 (d, *J* 6.4 Hz,

6H, COOCH(CH_3)$_2$); **^{13}C NMR** (125 MHz, DMSO-d_6) δ (ppm) 165.2, 164.2, 156.4, 148.3, 138.8, 136.3, 131.3, 129.9, 129.8, 129.5, 129.0, 128.9, 128.5, 127.4, 126.5, 125.9, 125.7, 115.7, 112.7, 68.2, 21.1; **LRMS** (ES + APCI) *m/z*: calc. for $C_{28}H_{23}N_5O_3S$ 509.2, found 510.0 $[M+H]^+$; **HMRS** calc. for $C_{28}H_{24}N_5O_3S$ 510.1594 $[M+H]^+$, found 510.1589 $[M+H]^+$.

Ethyl 4-(4-bromophenyl)-2-(2-(ethoxycarbonyl)benzamido)thiophene-3-carboxylate (101)

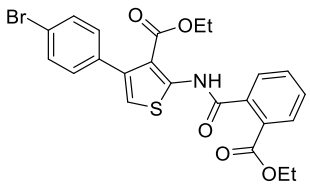

Following General Procedure F, compound **58** (150 mg, 0.32 mmol) was refluxed in ethanol (EtOH) (5.0 mL) containing a few drops of H_2SO_4 to afford, after purification *via* flash column chromatography (dry loading, petroleum ether 6:1 EtOAc, isocratic), the *title compound* (100 mg, 0.20 mmol, 63%) as an off-white solid. **mp** 178–180 °C; **IR**(ATR)/cm^{-1} 3257, 3057, 2988, 1724, 1673, 1651, 1545; **^{1}H NMR** (500 MHz, $CDCl_3$) δ (ppm) 11.58 (s, 1H, CON*H*), 7.98 (d, *J* 7.5 Hz, 1H, Ar*H*), 7.63–7.55 (m, 3H, 3 × Ar*H*), 7.47 (d, *J* 8.0 Hz, 2H, 2 × Ar*H*), 7.18 (d, *J* 8.0 Hz, 2H, 2 × Ar*H*), 6.66 (s, 1H, C=C*H*S), 4.33 (q, *J* 7.5 Hz, 2H, COOCH_2CH$_3$), 4.06 (q, *J* 7.0 Hz, 2H, COOCH_2CH$_3$), 1.28 (t, *J* 7.0 Hz, 3H, COOCH$_2$CH_3), 0.96 (t, *J* 7.0 Hz, 3H, COOCH$_2$CH_3); **^{13}C NMR** (125 MHz, $CDCl_3$) δ (ppm) 166.4, 166.2, 166.0, 150.5, 138.8, 136.9, 136.3, 132.3, 131.1, 130.8, 130.7, 130.6, 130.3, 127.6, 121.3, 115.8, 111.9, 61.9, 60.8, 14.1, 13.7; **LRMS** (ES + APCI) *m/z*: calc. for $C_{23}H_{20}{}^{79}BrNO_5S$ 501.0, found 501.9 $[M+H]^+$; **HMRS** calc. for $C_{23}H_{21}{}^{79}BrNO_5S$ 502.0318 $[M+H]^+$, found 502.0310 $[M+H]^+$.

Isopropyl 4-([1,1'-biphenyl]-4-yl)-2-(2-(methoxycarbonyl)benzamido)thiophene-3-carboxylate (102)

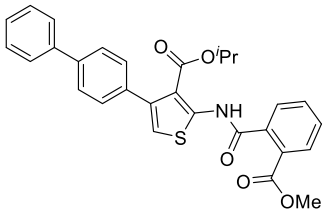

Following General Procedure F, compound **83** (100 mg, 0.21 mmol) was refluxed in MeOH (2.0 mL) containing a few drops of H_2SO_4 to afford, after purification *via* flash column chromatography (dry loading, petroleum ether 6:1 EtOAc, isocratic), the *title compound* (91 mg, 0.18 mmol, 88%) as an off-white solid. **mp** 169–171 °C; **IR**(ATR)/cm^{-1} 3240, 3086, 3025, 2978, 2926, 1727, 1677, 1656, 1543, 1277, 1230, 1139, 1104; **^{1}H NMR** (500 MHz, $CDCl_3$) δ (ppm) 11.68 (s, 1H, CON*H*), 7.96 (d, *J* 8.0 Hz, 1H, Ar*H*), 7.68–7.61 (m, 4H, 4 × Ar*H*), 7.61–7.56 (m, 3H, 3 × Ar*H*), 7.47 (app t, *J* 8.0 Hz, 2H, 2 × Ar*H*), 7.40–7.35 (m, 3H, 3 × Ar*H*), 6.72 (s, 1H, C=C*H*S), 4.97 (septet, *J* 6.0 Hz, 1H, COOC*H*$(CH_3)_2$), 3.90 (s, 3H, COOCH_3), 0.97 (d, *J* 6.0 Hz, 6H, COOCH(CH_3)$_2$); **^{13}C NMR** (125 MHz, $CDCl_3$) δ (ppm) 167.0, 166.0, 165.7, 150.0, 141.2, 140.1, 139.8, 137.3, 136.4, 132.3, 130.8, 130.5, 130.2, 129.9, 129.0, 127.7, 127.4, 127.2, 126.2, 115.5, 112.8, 68.6, 52.9, 21.5; **LRMS** (ES + APCI) *m/z*: calc. for $C_{29}H_{25}NO_5S$ 499.2, found 500.2 $[M+H]^+$; **HMRS** calc. for $C_{29}H_{24}NO_5S$ 498.1381 $[M–H]^-$, found 498.1393 $[M–H]^-$.

2-((4-(4-Bromophenyl)-3-(isopropoxycarbonyl)thiophen-2-yl)carbamoyl)-3-hydroxybenzoic acid and 2-((4-(4-bromophenyl)-3-(isopropoxycarbonyl)thiophen-2-yl)carbamoyl)-6-hydroxybenzoic acid (1:1) (104)

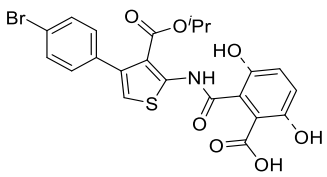

Following General Procedure E, compound **71** (50 mg, 0.15 mmol) and 4-hydroxyisobenzofuran-1,3-dione (25 mg, 0.15 mmol), after purification *via* flash column chromatography (dry loading, Hexane 4:1 EtOAc, CH_2Cl_2 9.5:0.5 MeOH), afforded the *title compound* (36 mg, 0.07 mmol, 49%) as an off-white solid. **mp** 151–152 °C; **IR**(ATR)/cm^{-1} 3248, 3064, 2976, 2928, 1721, 1658, 1600, 1580, 1537, 1513, 1385, 1290, 1262, 1221, 1100; **^{1}H NMR** (400 MHz, DMSO-d_6) δ (ppm) 10.96 (s, 1H, ArO*H*), 7.54 (d, *J* 8.0 Hz, 2H, 2 × Ar*H*), 7.29–7.22 (m, 3H, 3 × Ar*H*), 6.91 (s, 1H, C=C*H*S), 6.83 (dd, *J* 8.0 Hz, 0.8 Hz, 1H, Ar*H*), 6.66 (dd, *J* 8.0 Hz, 0.8 Hz, 1H, Ar*H*), 4.85 (septet, *J* 6.4 Hz, 1H, COOC*H*$(CH_3)_2$), 0.91 (d, *J* 6.4 Hz, 6H, COOCH(CH_3)$_2$), 1:1 mixture of regioisomers; **^{13}C NMR** (101 MHz, DMSO-d_6) δ (ppm) 169.8, 168.4, 164.2, 163.1, 150.2, 137.9, 137.7, 136.9, 132.2, 131.2, 130.2,

120.1, 118.1, 117.0, 115.5, 115.2, 110.4, 67.9, 21.1; **LRMS** (ES + APCI) *m/z*: calc. for $C_{22}H_{18}{}^{79}BrNO_6S$ 503.0, found 503.9 $[M+H]^+$; **HMRS** calc. for $C_{22}H_{19}{}^{79}BrNO_6S$ 504.0111 $[M+H]^+$, found 504.0108 $[M+H]^+$.

2-((4-([1,1'-Biphenyl]-4-yl)-3-(isopropoxycarbonyl)thiophen-2-yl)carbamoyl)-3-hydroxybenzoic acid and 2-((4-([1,1'-biphenyl]-4-yl)-3-(isopropoxycarbonyl)thiophen-2-yl)carbamoyl)-6-hydroxybenzoic acid (1:0.33) (105)

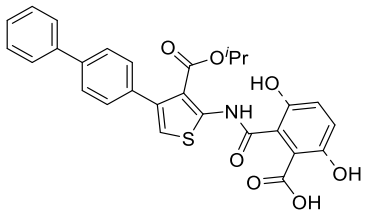

Following General Procedure E, compound **72** (50 mg, 0.15 mmol) and 4-hydroxyisobenzofuran-1,3-dione (25 mg, 0.15 mmol), after purification *via* flash column chromatography (dry loading, Hexane 4:1 EtOAc, CH_2Cl_2 9:1 MeOH), afforded the *title compound* (61 mg, 0.12 mmol, 82%) as an off-white solid. **mp** 144–146 °C; **IR**(ATR)/cm^{-1} 3522, 3033, 2979, 2928, 1657, 1625, 1595, 1530, 1486, 1448, 1396, 1292, 1259, 1225, 1101; **^{1}H NMR** (400 MHz, DMSO-d_6) δ (ppm) 13.36 (br s, 1H, COO*H*), 10.99 (s, 1H, ArO*H*), 7.69 (d, *J* 8.4 Hz, 2H, 2 × Ar*H*), 7.65 (d, *J* 8.4 Hz, 2H, 2 × Ar*H*), 7.48 (app t, *J* 7.2 Hz, 2H, 2 × Ar*H*), 7.36 (d, *J* 8.4 Hz, 2H, 2 × Ar*H*), 7.36–7.31 (m, 1H, Ar*H*), 7.26 (t, *J* 7.2 Hz, 1H, Ar*H*), 7.18 (t, *J* 7.2 Hz, 0.33H, Ar*H*), 6.93 (s, 1H, C=C*H*S), 6.83 (d, *J* 8.4 Hz, 1H, Ar*H*), 6.75 (d, *J* 8.4 Hz, 0.33H, Ar*H*), 6.68 (d, *J* 8.4 Hz, 1H, Ar*H*), 6.55 (d, *J* 8.4 Hz, 0.33H, Ar*H*), 4.86 (septet, *J* 6.4 Hz, 1H, COOC*H*$(CH_3)_2$), 0.91 (d, *J* 6.4 Hz, 6H, COOCH$(CH_3)_2$), 1:0.33 mixture of regioisomers; **^{13}C NMR** (101 MHz, DMSO-d_6) δ (ppm) 170.0, 169.8, 168.4, 168.2, 164.6, 164.4, 163.1, 162.9, 150.1, 149.9, 140.0, 138.7, 138.6, 137.8, 136.9, 136.7, 131.4, 131.2, 131.0, 130.9, 129.7, 129.6, 129.0, 129.0, 127.5, 127.4, 126.6, 126.5, 125.7, 125.6, 120.1, 119.9, 118.3, 118.2, 117.5, 117.1, 115.9, 115.6, 115.1, 114.8, 110.9, 110.8, 67.9, 21.1 (2 carbons missing); **LRMS** (ES + APCI) *m/z*: calc. for $C_{28}H_{23}NO_6S$ 501.1, found 502.0 $[M+H]^+$; **HMRS** calc. for $C_{28}H_{24}NO_6S$ 502.1319 $[M+H]^+$, found 502.1315 $[M+H]^+$.

4-((4-(4-Bromophenyl)-3-(isopropoxycarbonyl)thiophen-2-yl)carbamoyl)isophthalic acid and 2-((4-(4-bromophenyl)-3-(isopropoxycarbonyl)thiophen-2-yl)carbamoyl)terephthalic acid (1.38:1.18) (106)

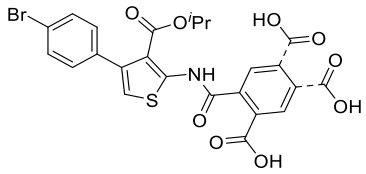

Following General Procedure E, compound **71** (50 mg, 0.15 mmol) and 1,3-dioxo-1,3-dihydroisobenzofuran-5-carboxylic acid (30 mg, 0.30 mmol), after purification *via* flash column chromatography (dry loading, Hexane 4:1 EtOAc, CH_2Cl_2 9:1 MeOH 0.1% acetic acid), afforded the *title compound* (57 mg, 0.11 mmol, 73%) as an off-white solid. **mp** 183–185 °C; **IR**(ATR)/cm^{-1} 3323, 3073, 2954, 2928, 1723, 1678, 1636, 1593, 1537, 1511, 1385, 1291, 1258, 1221, 1103; **^{1}H NMR** (500 MHz, DMSO-d_6) δ (ppm) 14.43 (br s, 2H, COO*H*), 8.55–8.44 (m, 1.38H, Ar*H*), 8.35–8.25 (m, 1.18H, Ar*H*), 8.05–7.88 (m, 2H, Ar*H*), 7.83–7.75 (m, 1.38H, Ar*H*), 7.70–7.63 (m, 1.18H, Ar*H*), 7.55 (d, *J* 8.5 Hz, 4H, 2 × Ar*H*), 7.23 (d, *J* 8.5 Hz, 4H, 2 × Ar*H*), 7.00–6.93 (m, 2H, C=C*H*S), 4.97–4.87 (m, 2H, COOC*H*(CH_3)$_2$), 1.02 (d, *J* 6.0 Hz, 12H, COOCH(C*H*$_3$)$_2$), 1.38:1.18 mixture of regioisomers; **^{13}C NMR** (101 MHz, DMSO-d_6) δ (ppm) 171.0, 170.3, 170.1, 167.1, 167.0, 163.9, 163.9, 147.6, 137.4, 137.4, 136.5, 135.0, 132.7, 132.5, 131.6, 131.4, 131.1, 130.9, 130.7, 130.7, 130.5, 129.7, 129.6, 127.8, 120.1, 115.5, 68.1, 21.2 (12 carbons missing); **LRMS** (ES + APCI) *m/z*: calc. for $C_{23}H_{18}{}^{79}BrNO_7S$ 531.0, found 530.0 $[M–H]^-$; **HMRS** calc. for $C_{23}H_{17}{}^{79}BrNO_7S$ 529.9915 $[M–H]^-$, found 529.9923 $[M–H]^-$.

4-((4-([1,1'-Biphenyl]-4-yl)-3-(isopropoxycarbonyl)thiophen-2-yl)carbamoyl)isophthalic acid and 2-((4-([1,1'-biphenyl]-4-yl)-3-(isopropoxycarbonyl)thiophen-2-yl)carbamoyl)terephthalic acid (1.26:1.10) (107)

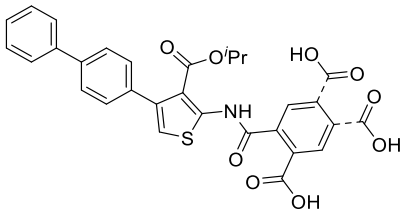

Following General Procedure E, compound **72** (50 mg, 0.15 mmol) and 1,3-dioxo-1,3-dihydroisobenzofuran-5-carboxylic acid (29 mg, 0.30 mmol), after purification *via* flash column chromatography (dry loading, Hexane 4:1 EtOAc, CH_2Cl_2 9:1 MeOH 0.1% acetic acid), afforded the *title compound* (63 mg, 0.12 mmol, 80%) as an off-white solid. **mp** 216–219 °C; **IR**(ATR)/cm^{-1} 3464, 3316, 3104, 2976, 1698, 1649, 1582, 1538, 1493, 1374, 1257, 1225, 1103; **^{1}H NMR** (500 MHz, DMSO-d_6) δ (ppm) 14.73 (br s, 4H, 2 × COO*H*), 8.46–8.40 (m, 1.26H, Ar*H*), 8.35–8.30 (m, 1.10H, Ar*H*), 8.03–7.90 (m, 2H, Ar*H*), 7.82–7.78 (m, 2H, Ar*H*), 7.72–7.65 (m, 8H, 4 × Ar*H*), 7.48 (app t, *J* 8.0 Hz, 4H, 2 × Ar*H*), 7.41–7.35 (m, 6H, 3 × Ar*H*), 7.00 (s, 2H, C=C*H*S), 5.00–4.92 (m, 2H, COOC*H*$(CH_3)_2$), 1.09–1.03 (m, 12H, COOCH(C*H*$_3)_2$), 1.26:1.10 mixture of regioisomers; **^{13}C NMR** (101 MHz, DMSO-d_6) δ (ppm) 169.8, 169.7, 169.6, 166.5, 166.4, 164.1, 164.1, 146.8, 141.5, 140.6, 139.9, 139.4, 138.8, 138.7, 138.4, 138.3, 136.8, 136.7, 136.5, 136.2, 136.2, 129.8, 129.1, 129.1, 129.0, 128.9, 128.6, 127.4, 126.6, 126.5, 125.9, 125.9, 115.3, 68.1, 21.2 (13 carbons missing); **LRMS** (ES + APCI) *m/z*: calc. for $C_{29}H_{23}NO_7S$ 529.1, found 528.1 $[M–H]^-$; **HMRS** calc. for $C_{29}H_{22}NO_7S$ 528.1122 $[M–H]^-$, found 528.1127 $[M–H]^-$.

3-Acetamido-2-((4-(4-bromophenyl)-3-(isopropoxycarbonyl)thiophen-2-yl)carbamoyl)benzoic acid and 2-acetamido-6-((4-(4-bromophenyl)-3-(isopropoxycarbonyl)thiophen-2-yl)carbamoyl)benzoic acid (1.35:0.65) (108)

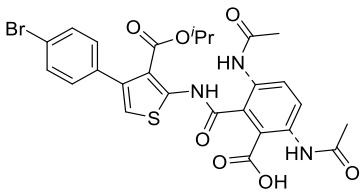

Following General Procedure E, compound **71** (100 mg, 0.30 mmol) and *N*-(1,3-dioxo-1,3-dihydroisobenzofuran-4-yl)acetamide (61 mg, 0.30 mmol), after purification *via* flash column chromatography (dry loading, Hexane 3:1 EtOAc,

CH_2Cl_2 9:1 MeOH), afforded the *title compound* (100 mg, 0.16 mmol, 54%) as an off-white solid. **mp** 197–199 °C; **IR**(ATR)/cm^{-1} 3237, 3036, 2925, 2862, 1703, 1664, 1601, 1573, 1537, 1513, 1387, 1291, 1221, 1103; **^{1}H NMR** (400 MHz, DMSO-d_6) δ (ppm) 13.36 (br s, 2H, COO*H*), 11.18–11.02 (m, 2H, CH_3CONH), 8.53 (d, *J* 8.0 Hz, 1.35H, Ar*H*), 7.83–7.75 (m, 0.65H, Ar*H*), 7.61–7.53 (m, 4H, 2 × Ar*H*), 7.52–7.46 (m, 0.65H, Ar*H*), 7.41–7.31 (m, 2H, Ar*H*), 7.29–7.20 (m, 4H, 2 × Ar*H*), 7.02 (d, *J* 8.0 Hz, 1.35H, Ar*H*), 6.97–6.89 (m, 2H, C=C*H*S), 4.86 (septet, *J* 6.0 Hz, 2H, COOC*H*$(CH_3)_2$), 2.10–1.90 (m, 6H, NHCOCH_3), 0.92 (d, *J* 6.0 Hz, 12H, COOCH$(CH_3)_2$), 1.35:0.65 mixture of regioisomers; **^{13}C NMR** (101 MHz, DMSO-d_6) δ (ppm) 169.0, 168.3, 168.2, 168.0, 165.2, 165.1, 164.2, 164.0, 150.2, 139.8, 137.7, 137.6, 136.9, 136.7, 131.2, 131.1, 130.3, 130.2, 129.6, 129.1, 126.9, 124.6, 120.7, 120.2, 120.1, 120.1, 115.5, 115.2, 111.3, 110.6, 67.9, 25.1, 21.1 (7 carbons missing); **LRMS** (ES + APCI) *m/z*: calc. for $C_{24}H_{21}{}^{79}BrN_2O_6S$ 544.0, found 543.0 $[M–H]^-$; **HMRS** calc. for $C_{24}H_{20}{}^{79}BrN_2O_6S$ 543.0231 $[M–H]^-$, found 543.0244 $[M–H]^-$.

2-((4-([1,1'-Biphenyl]-4-yl)-3-(isopropoxycarbonyl)thiophen-2-yl)carbamoyl)-6-acetamidobenzoic acid and 2-((4-([1,1'-biphenyl]-4-yl)-3-(isopropoxycarbonyl)thiophen-2-yl)carbamoyl)-3-acetamidobenzoic acid (1.39:0.61) (109)

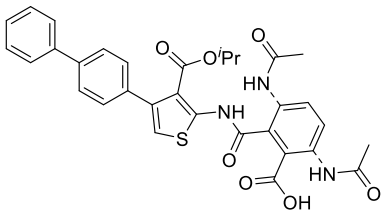

Following General Procedure E, compound **72** (100 mg, 0.30 mmol) and *N*-(1,3-dioxo-1,3-dihydroisobenzofuran-4-yl)acetamide (61 mg, 0.30 mmol), after purification *via* flash column chromatography (dry loading, Hexane 2:1 EtOAc, CH_2Cl_2 9:1 MeOH), afforded the *title compound* (98 mg, 0.18 mmol, 61%) as an off-white solid. **mp** 172–174 °C; **IR**(ATR)/cm^{-1} 3249, 3036, 2979, 2928, 1678, 1617, 1593, 1536, 1493, 1461, 1397, 1295, 1246, 1221, 1103; **^{1}H NMR** (400 MHz, DMSO-d_6) δ (ppm) 13.37 (br s, 2H, COO*H*), 11.22–11.08 (m, 2H, CH_3CONH), 8.53 (d, *J* 8.0 Hz, 1.39H, Ar*H*), 7.82–7.76 (m, 0.61H, Ar*H*), 7.72–7.63 (m, 8H, 4 × Ar*H*), 7.61–7.56 (m, 0.61H, Ar*H*), 7.48 (app t, *J* 8.0 Hz, 4H, 2 × Ar*H*), 7.41–7.36 (m, 6H,

3 × Ar*H*), 7.36–7.32 (m, 2H, Ar*H*), 7.04 (d, *J* 8.0 Hz, 1.39H, Ar*H*), 6.99–6.92 (m, 2H, C=C*H*S), 4.87 (septet, *J* 6.0 Hz, 2H, COOC*H*$(CH_3)_2$), 2.09–1.93 (m, 6H, $NHCOCH_3$), 0.92 (d, *J* 6.0 Hz, 12H, $COOCH(CH_3)_2$), 1.39:0.61 mixture of regioisomers; **^{13}C NMR** (101 MHz, DMSO-d_6) δ (ppm) 169.1, 168.3, 168.1, 168.0, 165.0, 164.4, 164.2, 150.0, 140.0, 139.9, 139.7, 138.8, 138.7, 138.6, 137.8, 136.7, 136.5, 129.6, 129.5, 129.1, 129.0, 127.4, 127.4, 126.6, 126.5, 125.7, 125.6, 124.7, 120.7, 120.1, 114.8, 110.9, 67.9, 25.1, 21.1 (13 carbons missing); **LRMS** (ES + APCI) *m/z*: calc. for $C_{30}H_{26}N_2O_6S$ 542.2, found 541.2 $[M–H]^-$; **HMRS** calc. for $C_{30}H_{25}N_2O_6S$ 541.1439 $[M–H]^-$, found 541.1448 $[M–H]^-$.

2-((4-(4-Bromophenyl)-3-(isopropoxycarbonyl)thiophen-2-yl)carbamoyl)-6-chlorobenzoic acid and 2-((4-(4-bromophenyl)-3-(isopropoxycarbonyl)thiophen-2-yl)carbamoyl)-3-chlorobenzoic acid (1.27:1.08) (110)

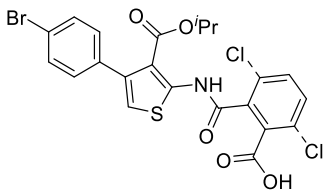

Following General Procedure E, compound **71** (50 mg, 0.15 mmol) and 4-hydroxyisobenzofuran-1,3-dione (25 mg, 0.15 mmol), after purification *via* flash column chromatography (dry loading, Hexane 4:1 EtOAc, CH_2Cl_2 9:1 MeOH), afforded the *title compound* (60 mg, 0.11 mmol, 74%) as an off-white solid. **mp** 220–222 °C; **IR**(ATR)/cm^{-1} 3558, 3057, 2976, 2932, 1721, 1658, 1603, 1582, 1539, 1515, 1465, 1387, 1290, 1264, 1223, 1100; **^{1}H NMR** (500 MHz, DMSO-d_6) δ (ppm) 12.35 (br s, 1H, COO*H*), 11.05 (s, 1H, ArO*H*), 7.95 (d, *J* 6.4 Hz, 1.27H, Ar*H*), 7.74–7.64 (m, 1.08H, Ar*H*), 7.60–7.53 (m, 4H, 2 × Ar*H*), 7.52–7.45 (m, 2H, 2 × Ar*H*), 7.39–7.31 (m, 1H, Ar*H*), 7.30–7.21 (m, 4H, 2 × Ar*H*), 7.19–7.11 (m, 1H, Ar*H*), 7.05–6.91 (m, 2H, C=C*H*S), 4.98–4.80 (m, 2H, COOC*H*$(CH_3)_2$), 1.07–0.87 (m, 12H, $COOCH(CH_3)_2$, 1.27:1.08 mixture of regioisomers; **^{13}C NMR** (125 MHz, DMSO-d_6) δ (ppm) 167.8, 167.6, 165.2, 165.2, 164.3, 149.8, 146.4, 142.8, 140.2, 137.7, 137.6, 136.7, 136.4, 135.1, 134.9, 131.8, 131.2, 130.8, 130.5, 130.3, 130.0, 129.9, 129.0, 128.9, 128.2, 128.1, 127.2, 126.5, 120.2, 116.1, 115.4, 110.8, 68.1, 68.0, 21.2, 21.1 (2 carbons missing); **LRMS** (ES + APCI) *m/z*: calc. for $C_{22}H_{17}{}^{81}Br^{35}ClNO_5S$ 522.8,

found 523.8 $[M+H]^+$; **HMRS** calc. for $C_{22}H_{18}{}^{79}Br^{35}ClNO_5S$ 521.9767 $[M+H]^+$, found 521.9772 $[M+H]^+$.

2-((4-([1,1'-Biphenyl]-4-yl)-3-(isopropoxycarbonyl)thiophen-2-yl)carbamoyl)-6-chlorobenzoic acid and 2-((4-([1,1'-biphenyl]-4-yl)-3-(isopropoxycarbonyl)thiophen-2-yl)carbamoyl)-3-chlorobenzoic acid (1.13:0.87) (111)

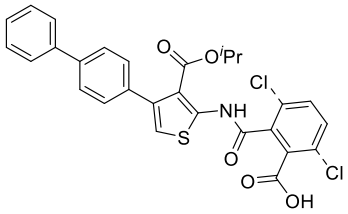

Following General Procedure E, compound **72** (50 mg, 0.15 mmol) and 4-chloroisobenzofuran-1,3-dione (25 mg, 0.15 mmol), after purification *via* flash column chromatography (dry loading, Hexane 4:1 EtOAc, CH_2Cl_2 9:1 MeOH), afforded the *title compound* (55 mg, 0.11 mmol, 71%) as an off-white solid. **mp** 214–216 °C; **IR**(ATR)/cm^{-1} 3230, 3025, 2974, 2924, 1721, 1651, 1580, 1528, 1403, 1294, 1258, 1100; **^{1}H NMR** (400 MHz, DMSO-d_6) δ (ppm) 14.41 (br s, 1H, COO*H*), 14.09 (br s, 1H, CON*H*), 7.90 (d, *J* 8.0 Hz, 1.13H, Ar*H*), 7.83 (d, *J* 2.4 Hz, 0.87H, Ar*H*), 7.78–7.73 (m, 2H, Ar*H*), 7.72–7.63 (m, 8H, 4 × Ar*H*), 7.53–7.50 (m, 2H, Ar*H*), 7.48 (t, *J* 8.0 Hz, 4H, 2 × Ar*H*), 7.41–7.33 (m, 6H, 3 × Ar*H*), 7.04–7.00 (m, 2H, C=C*H*S), 5.01–4.89 (m, 2H, COOC*H*$(CH_3)_2$), 1.08–1.02 (m, 12H, COOCH$(CH_3)_2$), 1.13:0.87 mixture of regioisomers; **^{13}C NMR** (101 MHz, DMSO-d_6) δ (ppm) 168.9, 168.1, 165.6, 165.1, 164.1, 164.1, 146.5, 140.0, 139.8, 138.8, 138.7, 138.2, 138.2, 136.1, 136.0, 134.9, 134.8, 133.2, 132.6, 131.1, 130.8, 129.9, 129.8, 129.0, 128.3, 128.2, 127.4, 126.6, 126.5, 126.1, 126.0, 115.4, 115.3, 68.2, 21.2 (11 carbons missing); **LRMS** (ES + APCI) *m/z*: calc. for $C_{28}H_{22}{}^{35}ClNO_5S$ 519.1, found 519.9 $[M+H]^+$; **HMRS** calc. for $C_{28}H_{23}{}^{35}ClNO_5S$ 520.098 $[M+H]^+$, found 520.0973 $[M+H]^+$.

2-((4-(4-Bromophenyl)-3-(isopropoxycarbonyl)thiophen-2-yl)carbamoyl)-4-fluorobenzoic acid and 2-((4-(4-bromophenyl)-3-(isopropoxycarbonyl)thiophen-2-yl)carbamoyl)-5-fluorobenzoic acid (1:0.6) (112)

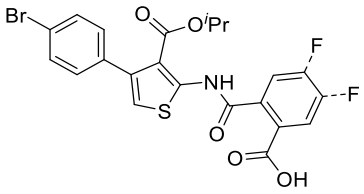

Following General Procedure E, compound **71** (50 mg, 0.15 mmol) and 5-fluoroisobenzofuran-1,3-dione (25 mg, 0.15 mmol), after purification *via* flash column chromatography (dry loading, Hexane 5:1 EtOAc, CH_2Cl_2 9:1 MeOH), afforded the *title compound* (72 mg, 0.14 mmol, 97%) as an off-white solid. **mp** 130–132 °C; **IR**(ATR)/cm^{-1} 3262, 3096, 2976, 2930, 1721, 1658, 1584, 1537, 1515, 1407, 1385, 1290, 1257, 1230, 1100; **^{1}H NMR** (500 MHz, DMSO-d_6) δ (ppm) 13.46 (br s, 2H, COO*H*), 12.90 (br s, 2H, CON*H*), 8.00 (dd, *J* 9.0 Hz, 6.0 Hz, 1H, Ar*H*), 7.77 (dd, *J* 9.0 Hz, 6.0 Hz, 0.6H, Ar*H*), 7.62–7.63 (m, 6H, 3 × Ar*H*), 7.46–7.33 (m, 2H, Ar*H*), 7.28–7.22 (m, 4H, 2 × Ar*H*), 7.04–6.98 (m, 2H, C=C*H*S), 4.96–4.86 (m, 2H, COOC*H*$(CH_3)_2$), 1.04–0.96 (m, 12H, COOCH$(CH_3)_2$, 1:0.6 mixture of regioisomers; **^{13}C NMR** (125 MHz, DMSO-d_6) δ (ppm) 167.7, 165.5, 165.0, 164.0, 163.9, 163.7, 161.8, 147.6, 147.5, 137.6, 137.5, 136.3, 136.3, 133.2, 133.1, 130.8, 130.7, 130.5, 120.2, 120.2, 117.1, 117.0, 116.5, 116.4, 116.0, 115.8, 115.1, 115.0, 113.4, 68.2, 21.1 (7 carbons missing); **^{19}F NMR** (471 MHz, DMSO-d_6) δ (ppm) -110.0–(-110.4) (m, 1F, Ar*F*); **LRMS** (ES + APCI) *m/z*: calc. for $C_{22}H_{17}{}^{81}BrFNO_5S$ 506.4, found 507.7 $[M+H]^+$; **HMRS** calc. for $C_{22}H_{18}{}^{79}BrFNO_5S$ 506.0068 $[M+H]^+$, found 506.0061 $[M+H]^+$.

2-((4-([1,1'-Biphenyl]-4-yl)-3-(isopropoxycarbonyl)thiophen-2-yl)carbamoyl)-4-fluorobenzoic acid and 2-((4-([1,1'-biphenyl]-4-yl)-3-(isopropoxycarbonyl)thiophen-2-yl)carbamoyl)-5-fluorobenzoic acid (1.27:1.78) (113)

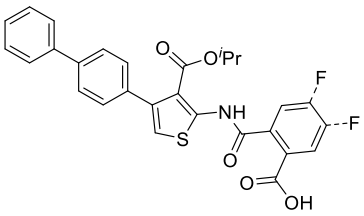

Following General Procedure E, compound **72** (50 mg, 0.15 mmol) and 5-fluoroisobenzofuran-1,3-dione (22 mg, 0.15 mmol), after purification *via* flash

column chromatography (dry loading, Hexane 4:1 EtOAc, CH_2Cl_2 9:1 MeOH), afforded the *title compound* (66 mg, 0.13 mmol, 88%) as an off-white solid. **mp** 161–163 °C; **IR**(ATR)/cm^{-1} 3248, 3026, 2974, 2924, 1725, 1658, 1573, 1528, 1495, 1409, 1385, 1288, 1257, 1229, 1102; **^{1}H NMR** (500 MHz, DMSO-d_6) δ (ppm) 13.49 (br s, 2H, COO*H*), 8.00 (dd, *J* 8.5 Hz, 6.0 Hz, 1.27H, Ar*H*), 7.91–7.79 (m, 1.78H, Ar*H*), 7.72–7.65 (m, 8H, 4 × Ar*H*), 7.61–7.56 (m, 2H, Ar*H*), 7.48 (app t, *J* 8.0 Hz, 4H, 2 × Ar*H*), 7.45–7.40 (m, 2H, Ar*H*), 7.40–7.35 (m, 6H, 3 × Ar*H*), 7.06–7.01 (m, 2H, C=C*H*S), 4.99–4.89 (m, 2H, COOC*H*$(CH_3)_2$), 1.05–0.99 (m, 12H, COOCH(C*H*$_3)_2$, 1.27:1.78 mixture of regioisomers; **^{13}C NMR** (125 MHz, DMSO-d_6) δ (ppm) 167.7, 165.4, 164.9, 164.2, 164.1, 161.8, 147.3, 147.1, 140.0, 138.8, 138.8, 138.5, 138.4, 136.2, 136.1, 133.2, 133.2, 132.1, 132.0, 129.3, 129.2, 129.0, 127.4, 126.5, 125.9, 125.9, 117.2, 117.1, 117.0, 117.0, 116.6, 116.4, 116.4, 116.1, 115.8, 115.6, 115.4, 115.2, 115.0, 114.7, 114.6, 113.8, 68.2, 68.2, 21.2, 21.2; **^{19}F NMR** (471 MHz, DMSO-d_6) δ (ppm) -109.9–(-110.3) (m, 1F, Ar*F*); **LRMS** (ES + APCI) *m/z*: calc. for $C_{28}H_{22}FNO_5S$ 503.1, found 503.9 $[M+H]^+$; **HMRS** calc. for $C_{28}H_{23}FNO_5S$ 504.1275 $[M+H]^+$, found 504.1268 $[M+H]^+$.

2-((4-(4-Bromophenyl)-3-(isopropoxycarbonyl)thiophen-2-yl)carbamoyl)-5-chlorobenzoic acid and 2-((4-(4-bromophenyl)-3-(isopropoxycarbonyl)thiophen-2-yl)carbamoyl)-4-chlorobenzoic acid (1.33:0.79) (114)

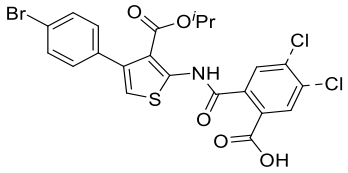

Following General Procedure E, compound **71** (50 mg, 0.15 mmol) and 5-chloroisobenzofuran-1,3-dione (27 mg, 0.15 mmol), after purification *via* flash column chromatography (dry loading, Hexane 4:1 EtOAc, CH_2Cl_2 9:1 MeOH), afforded the *title compound* (68 mg, 0.13 mmol, 89%) as an off-white solid. **mp** 209–211 °C; **IR**(ATR)/cm^{-1} 3230, 3088, 2976, 2928, 1719, 1654, 1572, 1535, 1509, 1374, 1292, 1258, 1219, 1100; **^{1}H NMR** (500 MHz, DMSO-d_6) δ (ppm) 14.37 (br s, 1H, COO*H*), 14.02 (br s, 1H, CON*H*), 7.89 (d, *J* 8.0 Hz, 1.33H, Ar*H*), 7.81 (br s, 0.79H, Ar*H*), 7.76–7.71 (m, 2H, Ar*H*), 7.56 (d, *J* 8.0 Hz, 4H, 2 × Ar*H*), 7.54–7.47 (m, 2H, Ar*H*), 7.23 (d, *J* 8.0 Hz, 4H, 2 × Ar*H*), 7.01–6.97 (m, 2H, C=C*H*S), 4.98–4.88 (m, 2H, COOC*H*$(CH_3)_2$), 1.06–1.00 (m, 12H, COOCH(C*H*$_3)_2$, 1.33:0.79

mixture of regioisomers; **^{13}C NMR** (125 MHz, DMSO-d_6) δ (ppm) 168.7, 168.0, 165.8, 165.2, 163.8, 163.8, 149.9, 137.4, 137.3, 136.3, 136.3, 135.4, 134.8, 133.1, 132.6, 132.1, 130.8, 130.7, 130.6, 130.6, 129.8, 128.2, 128.1, 120.2, 115.7, 115.7, 114.2, 113.9, 68.2, 21.2 (8 carbons missing); **LRMS** (ES + APCI) *m/z*: calc. for $C_{22}H_{17}{}^{81}Br^{35}ClNO_5S$ 522.8, found 523.8 $[M+H]^+$; **HMRS** calc. for $C_{22}H_{18}{}^{79}Br^{35}ClNO_5S$ 521.9772 $[M+H]^+$, found 521.9767 $[M+H]^+$.

2-((4-([1,1'-Biphenyl]-4-yl)-3-(isopropoxycarbonyl)thiophen-2-yl)carbamoyl)-5-chlorobenzoic acid and 2-((4-([1,1'-biphenyl]-4-yl)-3-(isopropoxycarbonyl)thiophen-2-yl)carbamoyl)-4-chlorobenzoic acid (1.33:0.42) (115)

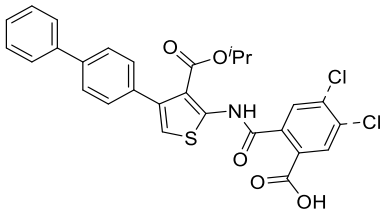

Following General Procedure E, compound **72** (50 mg, 0.15 mmol) and 5-chloroisobenzofuran-1,3-dione (28 mg, 0.15 mmol), after purification *via* flash column chromatography (dry loading, Hexane 4:1 EtOAc, CH_2Cl_2 9:1 MeOH), afforded the *title compound* (62 mg, 0.12 mmol, 81%) as an off-white solid. **mp** 193–195 °C; **IR**(ATR)/cm^{-1} 3273, 3026, 2960, 2924, 2852, 1721, 1658, 1602, 1582, 1530, 1500, 1394, 1292, 1262, 1223, 1102; **^{1}H NMR** (400 MHz, DMSO-d_6) δ (ppm) 12.30 (br s, 1H, COO*H*), 11.09 (br s, 1H, CON*H*), 7.98 (d, *J* 7.6 Hz, 1.33H, Ar*H*), 7.91 (d, *J* 7.6 Hz, 0.42H, Ar*H*), 7.74–7.63 (m, 8H, 4 × Ar*H*), 7.62–7.57 (m, 2H, Ar*H*), 7.56–7.51 (m, 2H, Ar*H*), 7.50–7.44 (m, 4H, 2 × Ar*H*), 7.41–7.34 (m, 4H, 2 × Ar*H*), 7.33–7.12 (m, 2H, Ar*H*), 7.06–6.95 (m, 2H, C=C*H*S), 5.02–4.80 (m, 2H, COOC*H*$(CH_3)_2$), 1.05–0.87 (m, 12H, COOCH$(CH_3)_2$, 1.33:0.42 mixture of regioisomers; **^{13}C NMR** (101 MHz, DMSO-d_6) δ (ppm) 168.0, 167.9, 165.1, 165.0, 164.5, 163.4, 149.4, 146.3, 140.0, 139.9, 139.4, 138.8, 138.8, 138.7, 138.5, 136.6, 136.2, 135.1, 132.7, 131.9, 131.3, 130.4, 129.7, 129.6, 129.2, 129.1, 129.0, 128.6, 127.6, 127.4, 127.1, 126.8, 126.6, 125.9, 125.7, 115.8, 115.1, 114.6, 111.3, 68.2, 68.1, 21.2, 21.1 (3 carbons missing); **LRMS** (ES + APCI) *m/z*: calc. for $C_{28}H_{22}{}^{35}ClNO_5S$ 519.1, found 519.9 $[M+H]^+$; **HMRS** calc. for $C_{28}H_{23}{}^{35}ClNO_5S$ 520.0980 $[M+H]^+$, found 520.0973 $[M+H]^+$.

2-((4-(4-Bromophenyl)-3-(isopropoxycarbonyl)thiophen-2-yl)carbamoyl)-5-(*tert*-butyl)benzoic acid and 2-((4-(4-bromophenyl)-3-(isopropoxycarbonyl)thiophen-2-yl)carbamoyl)-4-(*tert*-butyl)benzoic acid (0.79:1.23) (116)

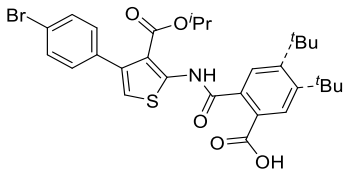

Following General Procedure E, compound **71** (50 mg, 0.15 mmol) and 5-(*tert*-butyl)isobenzofuran-1,3-dione (31 mg, 0.15 mmol), after purification *via* flash column chromatography (dry loading, Hexane 4:1 EtOAc, CH_2Cl_2 9:1 MeOH), afforded the *title compound* (60 mg, 0.10 mmol, 68%) as an off-white solid. **mp** 139–141 °C; **IR**(ATR)/cm^{-1} 3242, 3026, 2974, 2954, 2922, 1721, 1658, 1599, 1580, 1537, 1526, 1455, 1387, 1290, 1264, 1221, 1100; **^{1}H NMR** (400 MHz, DMSO-d_6) δ (ppm) 13.26 (br s, 2H, COO*H*), 12.76 (br s, 2H, CON*H*), 7.88 (br s, 0.79H, Ar*H*), 7.85 (d, *J* 8.0 Hz, 1.23H, Ar*H*), 7.69–7.63 (m, 2H, Ar*H*), 7.63–7.58 (m, 2H, Ar*H*), 7.58–7.52 (m, 4H, 2 × Ar*H*), 7.24 (d, *J* 8.4 Hz, 4H, 2 × Ar*H*), 7.01–6.96 (m, 2H, C=C*H*S), 4.98–4.84 (m, 2H, COOC*H*(CH_3)$_2$), 1.36–1.30 (m, 18H, C(CH_3)$_3$), 1.02–0.96 (m, 12H, COOCH(CH_3)$_2$, 0.79:1.23 mixture of regioisomers; **^{13}C NMR** (101 MHz, DMSO-d_6) δ (ppm) 168.8, 168.7, 166.8, 166.4, 164.1, 164.0, 153.0, 148.0, 137.6, 137.5, 136.4, 130.8, 130.5, 130.2, 130.0, 128.0, 127.2, 127.1, 126.6, 124.8, 122.0, 120.2, 115.7, 115.6, 112.9, 68.2, 34.7, 34.6, 30.8, 21.2 (12 carbons missing); **LRMS** (ES + APCI) *m/z*: calc. for $C_{26}H_{26}{}^{79}BrNO_5S$ 543.1, found 543.9 $[M+H]^+$; **HMRS** calc. for $C_{26}H_{27}{}^{79}BrNO_5S$ 544.0788 $[M+H]^+$, found 544.0785 $[M+H]^+$.

2-((4-([1,1'-Biphenyl]-4-yl)-3-(isopropoxycarbonyl)thiophen-2-yl)carbamoyl)-5-(*tert*-butyl)benzoic acid and 2-((4-([1,1'-biphenyl]-4-yl)-3-(isopropoxycarbonyl)thiophen-2-yl)carbamoyl)-4-(*tert*-butyl)benzoic acid (0.84:1.26) (117)

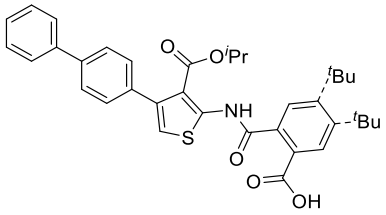

Following General Procedure E, compound **72** (50 mg, 0.15 mmol) and 5-fluoroisobenzofuran-1,3-dione (31 mg, 0.15 mmol), after purification *via* flash column chromatography (dry loading, Hexane 4:1 EtOAc, CH_2Cl_2 9:1 MeOH), afforded the *title compound* (71 mg, 0.13 mmol, 88%) as an off-white solid. **mp** 138–140 °C; **IR**(ATR)/cm^{-1} 3255, 3061, 2976, 2926, 1721, 1658, 1606, 1574, 1537, 1511, 1403, 1292, 1258, 1221, 1100; **^{1}H NMR** (500 MHz, DMSO-d_6) δ (ppm) 13.38 (br s, 1H, COO*H*), 12.61 (br s, 2H, CON*H*), 7.89 (br s, 0.84H, Ar*H*), 7.87 (d, *J* 8.5 Hz, 1.26H, Ar*H*), 7.72–7.63 (m, 10H, 5 × Ar*H*), 7.63–7.58 (m, 2H, Ar*H*), 7.48 (app t, *J* 8.0 Hz, 4H, 2 × Ar*H*), 7.42–7.34 (m, 6H, 3 × Ar*H*), 7.03–6.98 (m, 2H, C=C*H*S), 4.97–4.87 (m, 2H, COOC*H*$(CH_3)_2$), 1.35–1.31 (m, 18H, C(CH_3)$_3$), 1.01–0.96 (m, 12H, COOCH(CH_3)$_2$, 0.84:1.26 mixture of regioisomers; **^{13}C NMR** (125 MHz, DMSO-d_6) δ (ppm) 169.3, 168.8, 166.7, 166.3, 164.3, 164.2, 153.0, 147.8, 139.9, 138.8, 138.5, 136.3, 135.1, 132.0, 130.2, 129.3, 129.0, 127.9, 127.4, 127.1, 126.6, 126.5, 125.8, 124.7, 124.1, 115.4, 115.3, 113.1, 68.1, 68.1, 34.7, 34.6, 30.8, 30.8, 21.2 (15 carbons missing); **LRMS** (ES + APCI) *m/z*: calc. for $C_{32}H_{31}NO_5S$ 541.2, found 542.0 $[M+H]^+$; **HMRS** calc. for $C_{32}H_{30}NO_5S$ 540.1850 $[M–H]^-$, found 540.1853 $[M–H]^-$.

3-((4-(4-Bromophenyl)-3-(isopropoxycarbonyl)thiophen-2-yl)carbamoyl)-2-naphthoic acid (118)

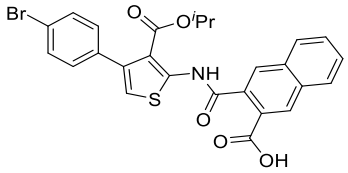

Following General Procedure E, compound **71** (100 mg, 0.29 mmol) and naphtho[2,3-c]furan-1,3-dione (58 mg, 0.29 mmol), after purification *via* flash column chromatography (dry loading, Hexane 4:1 EtOAc, CH_2Cl_2 95:5 MeOH), afforded the *title compound* (163 mg, 0.27 mmol, 92%) as an off-white solid. **mp** 166–168 °C; **IR**(ATR)/cm^{-1} 3240, 3084, 2963, 1714, 1588, 1537, 1396, 1258, 1233; **^{1}H NMR** (400 MHz, DMSO-d_6) δ (ppm) 12.83 (br s, 1H, COO*H*), 8.48 (s, 1H, Ar*H*), 8.24 (s, 1H, Ar*H*), 8.06–8.01 (m, 2H, 2 × Ar*H*), 7.65–7.60 (m, 2H, 2 × Ar*H*), 7.56 (d, *J* 8.4 Hz, 2H, 2 × Ar*H*), 7.25 (d, *J* 8.4 Hz, 2H, 2 × Ar*H*), 6.98 (s, 1H, C=C*H*S), 4.90 (septet, *J* 6.4 Hz, 1H, COOC*H*$(CH_3)_2$), 0.97 (d, *J* 6.4 Hz, 6H, COOCH(CH_3)$_2$); **^{13}C NMR** (101 MHz, DMSO-d_6) δ (ppm) 169.9, 166.9, 164.1,

148.5, 137.6, 136.5, 134.6, 133.0, 132.9, 132.4, 130.9, 130.5, 130.1, 128.4, 128.2, 127.9, 127.7, 127.5, 120.2, 115.6, 112.5, 68.1, 21.2; **LRMS** (ES + APCI) *m/z*: calc. for $C_{26}H_{20}{}^{79}BrNO_5S$ 537.0, found 537.9 $[M+H]^+$; **HMRS** calc. for $C_{26}H_{19}{}^{79}BrNO_5S$ 536.0173 $[M–H]^-$, found 536.0181 $[M–H]^-$.

3-((4-([1,1'-Biphenyl]-4-yl)-3-(isopropoxycarbonyl)thiophen-2-yl)carbamoyl)-2-naphthoic acid (119)

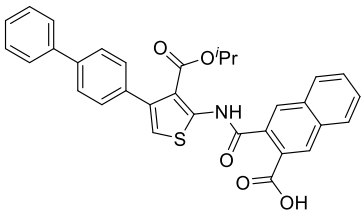

Following General Procedure E, compound **72** (100 mg, 0.29 mmol) and naphtho[2,3-c]furan-1,3-dione (58 mg, 0.29 mmol), after purification *via* flash column chromatography (dry loading, Hexane 4:1 EtOAc, CH_2Cl_2 95:5 MeOH), afforded the *title compound* (101 mg, 0.19 mmol, 65%) as an off-white solid. **mp** 180–182 °C; **IR**(ATR)/cm^{-1} 3284, 3052, 2962, 1690, 1660, 1525, 1393, 1259, 1229, 1103, 1010; **^{1}H NMR** (500 MHz, DMSO-d_6) δ (ppm) 13.41 (br s, 1H, COO*H*), 12.29 (br s, 1H, CON*H*), 8.53 (s, 1H, Ar*H*), 8.31 (s, 1H, Ar*H*), 8.15–8.07 (m, 2H, 2 × Ar*H*), 7.73–7.65 (m, 6H, 6 × Ar*H*), 7.49 (t, *J* 7.5 Hz, 2H, 2 × Ar*H*), 7.43–7.35 (m, 3H, 3 × Ar*H*), 7.05 (s, 1H, C=C*H*S), 4.93 (septet, *J* 6.5 Hz, 1H, COOC*H*$(CH_3)_2$), 0.98 (d, *J* 6.5 Hz, 6H, COOCH(C*H*$_3)_2$); **^{13}C NMR** (125 MHz, DMSO-d_6) δ (ppm) 168.4, 166.2, 164.3, 153.5, 148.1, 139.9, 138.8, 138.6, 136.3, 132.8, 132.7, 132.6, 130.6, 129.4, 128.9, 128.7, 128.3, 128.2, 128.1, 128.0, 127.4, 126.5, 125.8, 115.5, 113.0, 68.2, 21.2; **LRMS** (ES + APCI) *m/z*: calc. for $C_{32}H_{25}NO_5S$ 535.1, found 536.0 $[M+H]^+$; **HMRS** calc. for $C_{32}H_{26}NO_5S$ 536.1526 $[M+H]^+$, found 536.1524 $[M+H]^+$.

2-((4-(4-Bromophenyl)-3-(isopropoxycarbonyl)thiophen-2-yl)carbamoyl)-4,5-dichlorobenzoic acid (120)

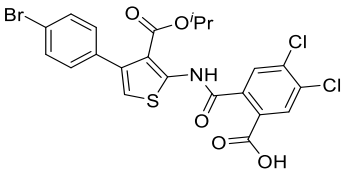

Following General Procedure E, compound **71** (50 mg, 0.15 mmol) and 5,6-dichloroisobenzofuran-1,3-dione (32 mg, 0.15 mmol), after purification *via* flash column chromatography (dry loading, Hexane 4:1 EtOAc, CH_2Cl_2 95:5 MeOH), afforded the *title compound* (77 mg, 0.14 mmol, 93%) as an off-white solid. **mp** 161–163 °C; **IR**(ATR)/cm^{-1} 3227, 3088, 2978, 1719, 1654, 1535, 1402, 1258; **^{1}H NMR** (500 MHz, DMSO-d_6) δ (ppm) 13.67 (br s, 1H, COO*H*), 8.05 (s, 1H, Ar*H*), 7.96 (s, 1H, Ar*H*), 7.56 (d, *J* 8.5 Hz, 2H, 2 × Ar*H*), 7.24 (d, *J* 8.5 Hz, 2H, 2 × Ar*H*), 7.02 (s, 1H, C=C*H*S), 4.92 (septet, *J* 6.5 Hz, 1H, COOC*H*$(CH_3)_2$), 1.02 (d, *J* 6.5 Hz, 6H, COOCH(C*H*$_3)_2$); **^{13}C NMR** (125 MHz, DMSO-d_6) δ (ppm) 166.7, 164.3, 163.8, 146.8, 137.4, 136.2, 134.3, 132.7, 132.2, 131.8, 131.7, 130.7, 130.6, 130.5, 120.2, 115.9, 114.1, 68.2, 21.2; **LRMS** (ES + APCI) *m/z*: calc. for $C_{22}H_{16}$ $^{79}Br^{35}Cl_2NO_5S$ 554.9, found 555.8 $[M+H]^+$; **HMRS** calc. for $C_{22}H_{17}$ $^{79}Br^{35}Cl_2NO_5S$ 555.9377 $[M+H]^+$, found 555.9382 $[M+H]^+$.

2-((4-([1,1'-Biphenyl]-4-yl)-3-(isopropoxycarbonyl)thiophen-2-yl)carbamoyl)-4,5-dichlorobenzoic acid (121)

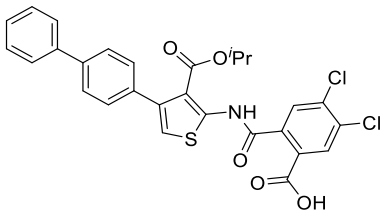

Following General Procedure E, compound **72** (50 mg, 0.15 mmol) and 5,6-dichloroisobenzofuran-1,3-dione (32 mg, 0.15 mmol), after purification *via* flash column chromatography (dry loading, Hexane 4:1 EtOAc, CH_2Cl_2 95:5 MeOH), afforded the *title compound* (73 mg, 0.13 mmol, 88%) as an off-white solid. **mp** 209–211 °C; **IR**(ATR)/cm^{-1} 3236, 3026, 2976, 1719, 1658, 1528, 1403, 1292; **^{1}H NMR** (500 MHz, DMSO-d_6) δ (ppm) 14.47 (br s, 1H, COO*H*), 8.04 (s, 1H, Ar*H*), 7.99 (s, 1H, Ar*H*), 7.72–7.68 (m, 2H, 2 × Ar*H*), 7.67 (d, *J* 8.0 Hz, 2H, 2 × Ar*H*), 7.51–7.45 (m, 2H, 2 × Ar*H*), 7.40–7.35 (m, 3H, 3 × Ar*H*), 7.05 (s, 1H, C=C*H*S), 4.96 (septet, *J* 6.5 Hz, 1H, COOC*H*$(CH_3)_2$), 1.06 (d, *J* 6.5 Hz, 6H, COOCH(C*H*$_3)_2$); **^{13}C NMR** (125 MHz, DMSO-d_6) δ (ppm) 166.9, 164.2, 164.0, 146.4, 139.8, 138.8, 138.3, 136.0, 134.2, 134.1, 132.7, 132.3, 131.5, 130.6, 129.0, 128.9, 127.4, 126.5, 125.9, 115.5, 114.6, 68.2, 21.2; **LRMS** (ES + APCI) *m/z*: calc. for $C_{28}H_{21}$ $^{35}Cl_2NO_5S$

553.1, found 553.8 $[M+H]^+$; **HMRS** calc. for $C_{28}H_{20}{}^{35}Cl_2NO_5S$ 552.0445 $[M–H]^-$, found 552.0453 $[M–H]^-$.

(*E*)-4-((3-(Isopropoxycarbonyl)-4-(4-phenethylphenyl)thiophen-2-yl)amino)-4-oxobut-2-enoic acid (122)

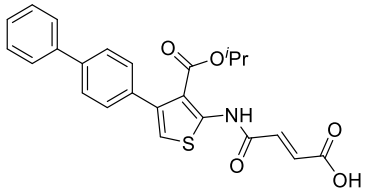

Following General Procedure E, compound **72** (100 mg, 0.30 mmol) and furan-2,5-dione (30 mg, 0.30 mmol), after purification *via* flash column chromatography (dry loading, Petroleum ether 5:1 EtOAc, CH_2Cl_2 9:1 MeOH), afforded the *title compound* (93 mg, 0.21 mmol, 72%) as an off-white solid. **mp** 140–142 °C; **IR**(ATR)/cm^{-1} 3237 br, 3023, 2976, 2930, 1716, 1662, 1586, 1526, 1483, 1446, 1292, 1229, 1100; **^{1}H NMR** (500 MHz, DMSO-d_6) δ (ppm) 15.75 (br s, 1H, COO*H*), 7.69 (d, *J* 8.0 Hz, 2H, 2 × Ar*H*), 7.66 (d, *J* 8.0 Hz, 2H, 2 × Ar*H*), 7.48 (app t, *J* 8.0 Hz, 2H, 2 × Ar*H*), 7.40–7.35 (m, 3H, 3 × Ar*H*), 6.99 (s, 1H, C=C*H*S), 6.25 (d, *J* 13.0 Hz, 1H, *H*C=CH), 6.08 (d, *J* 13.0 Hz, 1H, HC=C*H*), 4.99 (septet, *J* 6.0 Hz, 1H, COOC*H*$(CH_3)_2$), 1.13 (d, *J* 6.0 Hz, 6H, COOCH$(CH_3)_2$); **^{13}C NMR** (125 MHz, DMSO-d_6) δ (ppm) 167.8, 164.1, 163.1, 144.6, 139.8, 138.7, 138.1, 137.8, 135.8, 129.2, 128.9, 128.6, 127.4, 126.5, 126.2, 115.9, 115.3, 68.2, 21.3; **LRMS** (ES + APCI) *m/z*: calc. for $C_{24}H_{21}NO_5S$ 435.1, found 435.9 $[M+H]^+$; **HMRS** calc. for $C_{24}H_{20}NO_5S$ 434.1068 $[M–H]^-$, found 434.1073 $[M–H]^-$.

4-((4-([1,1'-Biphenyl]-4-yl)-3-(isopropoxycarbonyl)thiophen-2-yl)amino)-4-oxobutanoic acid (123)

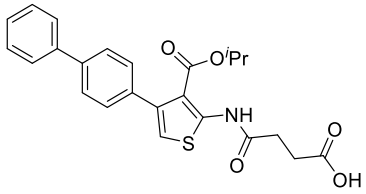

Following General Procedure E, compound **72** (100 mg, 0.29 mmol) and dihydrofuran-2,5-dione (30 mg, 0.29 mmol), after purification *via* flash column chromatography (dry loading, Petroleum ether 5:1 EtOAc, CH_2Cl_2 9:1 MeOH),

afforded the *title compound* (62 mg, 0.14 mmol, 48%) as an off-white solid. **mp** 135–137 °C; **IR**(ATR)/cm^{-1} 3259 br, 3086, 2971, 2921, 1742, 1693, 1664, 1521, 1398, 1296, 1217, 1104; **^{1}H NMR** (500 MHz, DMSO-d_6) δ (ppm) 12.29 (br s, 1H, COO*H*), 11.05 (s, 1H, CON*H*), 7.69 (d, *J* 8.0 Hz, 2H, 2 × Ar*H*), 7.65 (d, *J* 8.0 Hz, 2H, 2 × Ar*H*), 7.48 (app t, *J* 8.0 Hz, 2H, 2 × Ar*H*), 7.40–7.34 (m, 3H, 3 × Ar*H*), 6.95 (s, 1H, C=C*H*S), 4.96 (septet, *J* 6.0 Hz, 1H, COOC*H*(CH$_3$)$_2$), 2.77 (t, *J* 6.0 Hz, 2H, C*H*$_2$CH$_2$), 2.59 (t, *J* 6.0 Hz, 2H, CH$_2$C*H*$_2$), 0.99 (d, *J* 6.0 Hz, 6H, COOCH(C*H*$_3$)$_2$); **^{13}C NMR** (125 MHz, DMSO-d_6) δ (ppm) 173.5, 169.7, 164.1, 148.0, 139.9, 138.7, 138.6, 136.4, 129.4, 128.9, 127.4, 126.5, 125.7, 115.3, 112.1, 68.1, 30.8, 28.8, 21.1; **LRMS** (ES + APCI) *m/z*: calc. for $C_{24}H_{23}NO_5S$ 437.1, found 437.9 $[M+H]^+$; **HMRS** calc. for $C_{24}H_{22}NO_5S$ 436.1224 $[M–H]^-$, found 436.1229 $[M–H]^-$.

6-((4-([1,1'-Biphenyl]-4-yl)-3-(isopropoxycarbonyl)thiophen-2-yl)carbamoyl)cyclohex-3-ene-1-carboxylic acid (124)

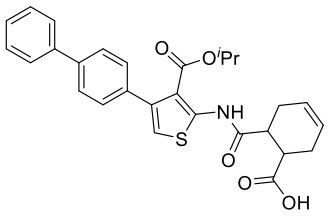

Following General Procedure E, compound **72** (100 mg, 0.30 mmol) and 3a,4,7,7a-tetrahydroisobenzofuran-1,3-dione (45 mg, 0.30 mmol), after purification *via* flash column chromatography (dry loading, Petroleum ether 4:1 EtOAc, CH_2Cl_2 9:1 MeOH), afforded the *title compound* (30 mg, 0.06 mmol, 21%) as an off-white solid. **mp** 206–208 °C; **IR**(ATR)/cm^{-1} 3244 br, 3025, 2978, 2924, 2850, 1703, 1688, 1647, 1545, 1528, 1402, 1294, 1245, 1098; **^{1}H NMR** (500 MHz, DMSO-d_6) δ (ppm) 12.34 (br s, 1H, COO*H*), 11.30 (s, 1H, CON*H*), 7.69 (d, *J* 8.0 Hz, 2H, 2 × Ar*H*), 7.65 (d, *J* 8.0 Hz, 2H, 2 × Ar*H*), 7.48 (app t, *J* 8.0 Hz, 2H, 2 × Ar*H*), 7.40–7.35 (m, 3H, 3 × Ar*H*), 6.94 (s, 1H, C=C*H*S), 5.73–5.70 (m, 2H, C*H*=C*H*), 4.98 (septet, *J* 6.0 Hz, 1H, COOC*H*(CH$_3$)$_2$), 3.21–3.16 (m, 1H, NHCOCHC*H*COOH), 3.14–3.08 (m 1H, NHCOC*H*CHCOOH), 2.42–2.34 (m, 2H, CH$_2$CH=CHC*H*$_2$), 0.98 (d, *J* 6.0 Hz, 6H, COOCH(C*H*$_3$)$_2$), (2 protons missing); **^{13}C NMR** (125 MHz, DMSO-d_6) δ (ppm) 174.3, 171.0, 164.5, 148.9, 139.9, 138.8, 138.7, 136.6, 129.6, 128.9, 127.4, 126.5, 125.8, 125.7, 124.4, 115.3, 111.6, 68.1, 40.2, 39.8, 26.1, 25.3, 21.2; **LRMS**

(ES + APCI) *m/z*: calc. for $C_{28}H_{27}NO_5S$ 489.2, found 490.0 $[M+H]^+$; **HMRS** calc. for $C_{28}H_{26}NO_5S$ 488.1537 $[M–H]^-$, found 488.1543 $[M–H]^-$.

3-((4-([1,1'-Biphenyl]-4-yl)-3-(isopropoxycarbonyl)thiophen-2-yl)carbamoyl)pyrazine-2-carboxylic acid (125)

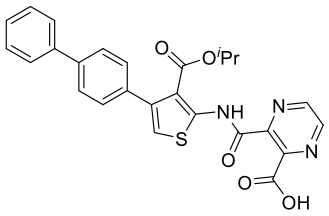

Following General Procedure E, compound **72** (50 mg, 0.15 mmol) and furo[3,4-*b*]pyrazine-5,7-dione (55 mg, 0.30 mmol), after purification *via* flash column chromatography (dry loading, petroleum ether 3:1 EtOAc, CH_2Cl_2 9:1 MeOH), afforded the *title compound* (70 mg, 0.14 mmol, 97%) as an off-white solid. **mp** 189–191 °C; **IR**(ATR)/cm^{-1} 3532 br, 3029, 2976, 2928, 1716, 1660, 1634, 1526, 1496, 1364, 1292, 1234, 1202, 1102, 1082; **^{1}H NMR** (500 MHz, DMSO-d_6) δ (ppm) 12.57 (br s, 1H, COO*H*), 8.78 (d, *J* 2.5 Hz, 1H, Ar*H*), 8.67 (app br s, 1H, Ar*H*), 7.70 (d, *J* 8.0 Hz, 2H, 2 × Ar*H*), 7.66 (d, *J* 8.0 Hz, 2H, 2 × Ar*H*), 7.48 (app t, *J* 8.0 Hz, 2H, 2 × Ar*H*), 7.43–7.35 (m, 3H, 3 × Ar*H*), 7.06 (s, 1H, C=C*H*S), 5.01 (septet, *J* 6.0 Hz, 1H, COOC*H*$(CH_3)_2$), 1.03 (d, *J* 6.0 Hz, 6H, COOCH(C*H*$_3)_2$); **^{13}C NMR** (125 MHz, DMSO-d_6) δ (ppm) 168.0, 163.9, 161.1, 155.3, 148.2, 146.9, 141.5, 141.4, 139.9, 139.1, 138.8, 136.4, 129.6, 128.9, 127.4, 126.5, 125.7, 115.9, 112.6, 68.2, 21.2; **LRMS** (ES + APCI) *m/z*: calc. for $C_{26}H_{21}N_3O_5S$ 487.1, found 488.0 $[M+H]^+$; **HMRS** calc. for $C_{26}H_{20}N_3O_5S$ 486.1129 $[M–H]^-$, found 486.1134 $[M–H]^-$.

Isopropyl 2-amino-4-(pyridin-3-yl)thiophene-3-carboxylate (147)

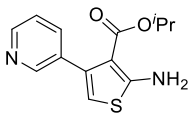

Following General Procedure D, isopropyl 2-cyanoacetate (1.27 g, 10.0 mmol) and 1-(pyridin-3-yl)ethan-1-one (606 mg, 5.0 mmol), after purification *via* flash column chromatography (dry loading, Hexane 2:1 EtOAc), afforded the *title compound* (678 mg, 2.01 mmol, 52%) as an off-white solid. **mp** 154–156 °C; **IR**(ATR)/cm^{-1} 3513, 3397, 3094, 2975, 1651, 1539, 1496; **^{1}H NMR** (400 MHz, $CDCl_3$) δ (ppm)

8.53 (dd, *J* 2.0 Hz, 0.8 Hz, 1H, Ar*H*), 8.52 (dd, *J* 4.8 Hz, 1.6 Hz, 1H, Ar*H*), 7.59 (app dt, *J* 7.6 Hz, 2.0 Hz, 1H, Ar*H*), 7.23 (m, *J* 7.6 Hz, 4.8 Hz, 0.8 Hz, 1H, Ar*H*), 6.27 (br s, 2H, NH_2), 6.08 (s, 1H, C=C*H*S), 4.97 (septet, *J* 6.4 Hz, 1H, COOC*H*(CH_3)$_2$), 0.96 (d, *J* 6.4 Hz, 6H, COOCH(CH_3)$_2$); **^{13}C NMR** (101 MHz, $CDCl_3$) δ (ppm) 165.1, 164.4, 149.8, 147.9, 137.9, 136.5, 134.7, 122.3, 106.5, 106.2, 67.3, 21.8; **LRMS** (ES + APCI) *m/z*: calc. for $C_{13}H_{14}N_2O_2S$ 262.1 found 263.0 $[M+H]^+$; **HMRS** calc. for $C_{13}H_{15}N_2O_2S$ 263.0849 $[M+H]^+$, found 263.0849 $[M+H]^+$.

Isopropyl 2-amino-4-(pyridin-4-yl)thiophene-3-carboxylate (148)

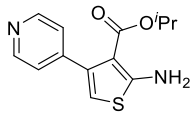

Following General Procedure D, isopropyl 2-cyanoacetate (1.27 g, 10.0 mmol) and 1-(pyridin-4-yl)ethan-1-one (606 mg, 5.0 mmol), after purification *via* flash column chromatography (dry loading, Hexane 2:1 EtOAc), afforded the *title compound* (654 mg, 2.50 mmol, 50%) as an off-white solid. **mp** 156–158 °C; **IR**(ATR)/cm^{-1} 3386, 3354, 3094, 2982, 1660, 1534, 1496; **^{1}H NMR** (400 MHz, $CDCl_3$) δ (ppm) 8.54 (dd, *J* 4.8 Hz, 2.0 Hz, 2H, 2 × Ar*H*), 7.21 (dd, *J* 4.8 Hz, 2.0 Hz, 2H, 2 × Ar*H*), 6.28 (br s, 2H, NH_2), 6.10 (s, 1H, C=C*H*S), 4.98 (septet, *J* 6.0 Hz, 1H, COOC*H*(CH_3)$_2$), 0.98 (d, *J* 6.4 Hz, 6H, COOCH(CH_3)$_2$); **^{13}C NMR** (101 MHz, $CDCl_3$) δ (ppm) 164.9, 164.4, 148.9, 146.7, 139.1, 124.2, 106.8, 105.7, 67.5, 21.7; **LRMS** (ES + APCI) *m/z*: calc. for $C_{13}H_{14}N_2O_2S$ 262.1 found 263.0 $[M+H]^+$; **HMRS** calc. for $C_{13}H_{15}N_2O_2S$ 263.0849 $[M+H]^+$, found 263.0850 $[M+H]^+$.

Isopropyl 2-amino-4-(2,4-dimethylthiazol-5-yl)thiophene-3-carboxylate (149)

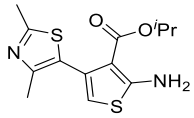

Following General Procedure D, isopropyl 2-cyanoacetate (1.27 g, 10.0 mmol) and 1-(2,4-dimethylthiazol-5-yl)ethan-1-one (776 mg, 5.0 mmol), after purification *via* flash column chromatography (dry loading, Hexane 1:1 EtOAc), afforded the *title compound* (667 mg, 2.25 mmol, 45%) as an off-white solid. **mp** 158–160 °C **IR**(ATR)/cm^{-1} 3380, 3200, 3094, 2962, 1722, 1651, 1580; **^{1}H NMR** (400 MHz, $CDCl_3$) δ (ppm) 6.16 (s, 1H, C=C*H*S), 6.15 (br s, 2H, NH_2), 4.97 (septet, *J* 6.4 Hz,

1H, COOC*H*(CH_3)$_2$), 2.65 (s, 3H, NC(C*H*$_3$)S), 2.19 (s, 3H, NC(C*H*$_3$)C), 1.03 (d, *J* 6.0 Hz, 6H, COOCH(C*H*$_3$)$_2$); **^{13}C NMR** (101 MHz, $CDCl_3$) δ (ppm) 164.9, 163.6, 163.0, 149.1, 129.9, 126.5, 108.8, 107.0, 67.1, 21.8, 19.1, 15.5; **LRMS** (ES + APCI) *m/z*: calc. for $C_{13}H_{16}N_2O_2S_2$ 296.1 found 297.0 $[M+H]^+$; **HMRS** calc. for $C_{13}H_{17}N_2O_2S_2$ 297.0726 $[M+H]^+$, found 297.0721 $[M+H]^+$.

Isopropyl 2-amino-4-(naphthalen-1-yl)thiophene-3-carboxylate (150)

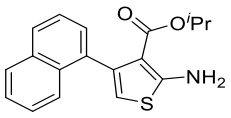

Following General Procedure D, isopropyl 2-cyanoacetate (1.27 g, 10.0 mmol) and 1-(naphthalen-1-yl)ethan-1-one (850 mg, 5.0 mmol), after purification *via* flash column chromatography (dry loading, Hexane 10:1 EtOAc), afforded the *title compound* (641 mg, 2.06 mmol, 41%) as a pale yellow solid. **mp** 73–75 °C; **IR**(ATR)/cm^{-1} 3408, 3264, 3093, 2974, 1649, 1582, 1270; **^{1}H NMR** (500 MHz, $CDCl_3$) δ (ppm) 7.83 (d, *J* 8.0 Hz, 1H, Ar*H*), 7.81 (d, *J* 8.0 Hz, 1H, Ar*H*), 7.67 (d, *J* 8.0 Hz, 1H, Ar*H*), 7.46–7.40 (m, 2H, 2 × Ar*H*), 7.39–7.31 (m, 2H, 2 × Ar*H*), 6.19 (s, 1H, C=C*H*S), 6.16 (br s, 2H, N*H*$_2$), 4.62 (septet, *J* 6.0 Hz, 1H, COOC*H*(CH_3)$_2$), 0.53 (d, *J* 6.5 Hz, 3H, COOCH(C*H*$_3$)$_2$), 0.17 (d, *J* 6.5 Hz, 3H, COOCH(C*H*$_3$)$_2$); **^{13}C NMR** (101 MHz, $CDCl_3$) δ (ppm) 165.3, 163.4, 139.7, 137.4, 133.6, 133.2, 127.9, 127.3, 126.5, 126.2, 125.8, 125.5, 125.1, 108.2, 106.1, 66.3, 21.3, 20.5; **LRMS** (ES + APCI) *m/z*: calc. for $C_{18}H_{17}NO_2S$ 311.1 found 312.0 $[M+H]^+$; **HMRS** calc. for $C_{18}H_{16}NO_2S$ 310.0907 $[M–H]^-$, found 310.0916 $[M–H]^-$.

Isopropyl 2-amino-4-(naphthalen-2-yl)thiophene-3-carboxylate (151)

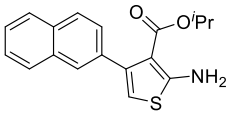

Following General Procedure D, isopropyl 2-cyanoacetate (1.27 g, 10.0 mmol) and 1-(naphthalen-2-yl)ethan-1-one (850 mg, 5.0 mmol), after purification *via* flash column chromatography (dry loading, Hexane 10:1 EtOAc), afforded the *title compound* (670 mg, 2.15 mmol, 43%) as a pale yellow solid. **mp** 72–74 °C **IR**(ATR)/cm^{-1} 3452, 3341, 3103, 2971, 1643, 1573, 1481, 1270, 1102; **^{1}H NMR** (500 MHz, $CDCl_3$) δ (ppm) 7.86–7.80 (m, 2H, 2 × Ar*H*), 7.76 (d, *J* 7.5 Hz, 2H,

2 × Ar*H*), 7.50–7.45 (m, 2H, 2 × Ar*H*), 7.45–7.41 (m, 1H, Ar*H*), 6.15 (s, 1H, C=C*H*S), 6.12 (br s, 2H NH_2), 4.96 (septet, *J* 6.0 Hz, 1H, COOC*H*(CH_3)$_2$), 0.87 (d, *J* 6.0 Hz, 6H, COOCH(CH_3)$_2$); **^{13}C NMR** (125 MHz, $CDCl_3$) δ (ppm) 165.4, 163.9, 141.8, 136.4, 133.1, 132.6, 128.4, 127.9, 127.7, 127.2, 126.4, 125.9, 125.7, 106.8, 105.9, 67.2, 21.7; **LRMS** (ES + APCI) *m/z*: calc. for $C_{18}H_{17}NO_2S$ 311.1 found 312.0 $[M+H]^+$; **HMRS** calc. for $C_{18}H_{18}NO_2S$ 312.1053 $[M+H]^+$, found 312.1054 $[M+H]^+$.

Isopropyl 2-amino-4-(quinolin-3-yl)thiophene-3-carboxylate (152)

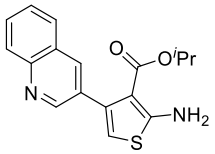

Following General Procedure D, isopropyl 2-cyanoacetate (1.27 g, 10.0 mmol) and 1-(quinolin-3-yl)ethan-1-one (856 mg, 5.0 mmol), after purification *via* flash column chromatography (dry loading, Hexane 3:1 EtOAc), afforded the *title compound* (880 mg, 2.82 mmol, 56%) as an orange solid. **mp** 164–166 °C; **IR**(ATR)/cm^{-1} 3384, 3236, 3074, 2979, 1672, 1586, 1493, 1372, 1272, 1222, 1095; **^{1}H NMR** (500 MHz, $CDCl_3$) δ (ppm) 8.86 (d, *J* 2.0 Hz, 1H, Ar*H*), 8.11 (d, *J* 8.5 Hz, 1H, Ar*H*), 8.03 (d, *J* 2.0 Hz, 1H, Ar*H*), 7.79 (d, *J* 8.5 Hz, 1H, Ar*H*), 7.69 (ddd, *J* 8.5 Hz, 7.0 Hz, 2.0 Hz, 1H, Ar*H*), 7.57–7.52 (m, 1H, Ar*H*), 6.32 (br s, 2H, NH_2), 6.18 (s, 1H, C=C*H*S), 4.96 (septet, *J* 6.0 Hz, 1H, COOC*H*(CH_3)$_2$), 0.88 (d, *J* 6.0 Hz, 6H, COOCH(CH_3)$_2$); **^{13}C NMR** (101 MHz, $CDCl_3$) δ (ppm) 165.1, 164.5, 151.9, 146.9, 138.0, 134.4, 132.0, 129.2, 129.1, 127.8, 127.6, 126.7, 106.9, 106.2, 67.4, 21.7; **LRMS** (ES + APCI) *m/z*: calc. for $C_{17}H_{16}N_2O_2S$ 312.1 found 313.0 $[M+H]^+$; **HMRS** calc. for $C_{17}H_{17}N_2O_2S$ 313.1009 $[M+H]^+$, found 313.1005 $[M+H]^+$.

Isopropyl 2-amino-4-(isoquinolin-4-yl)thiophene-3-carboxylate (153)

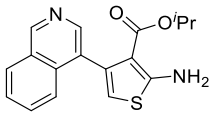

Following General Procedure D, isopropyl 2-cyanoacetate (1.27 g, 10.0 mmol) and 1-(quinolin-3-yl)ethan-1-one (856 mg, 5.0 mmol), after purification *via* flash column chromatography (dry loading, Hexane 3:1 EtOAc), afforded the *title compound*

(684 mg, 2.19 mmol, 44%) as an off-white solid. **mp** 148–150 °C; **IR**(ATR)/cm^{-1} 3366, 3213, 3048, 2973, 1657, 1601, 1488, 1409, 1274, 1097; **^{1}H NMR** (400 MHz, $CDCl_3$) δ (ppm) 9.22 (s, 1H, Ar*H*), 8.39 (s, 1H, Ar*H*), 7.97 (dd, *J* 7.0 Hz, 2.0 Hz, 1H, Ar*H*), 7.70–7.65 (m, 1H, Ar*H*), 7.62–7.53 (m, 2H, 2 × Ar*H*), 6.32 (br s, 2H, NH_2), 6.22 (s, 1H, C=C*H*S), 4.63 (septet, *J* 6.0 Hz, 1H, COOC*H*$(CH_3)_2$), 0.56 (d, *J* 6.0 Hz, 3H, COOCH(C*H*$_3$)$_2$), 0.19 (d, *J* 6.0 Hz, 3H, COOCH(C*H*$_3$)$_2$); **^{13}C NMR** (101 MHz, $CDCl_3$) δ (ppm) 165.0, 164.0, 151.8, 142.1, 136.2, 135.7, 130.9, 130.2, 127.9, 127.4, 126.9, 125.5, 107.7, 107.1, 66.6, 21.4, 20.6; **LRMS** (ES + APCI) *m/z*: calc. for $C_{17}H_{16}N_2O_2S$ 312.1 found 313.0 $[M+H]^+$; **HMRS** calc. for $C_{17}H_{17}N_2O_2S$ 313.1005 $[M+H]^+$, found 313.1008 $[M+H]^+$.

Isopropyl 2-amino-4-(quinoxalin-2-yl)thiophene-3-carboxylate (154)

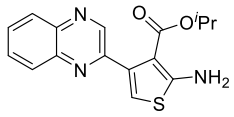

Following General Procedure D, isopropyl 2-cyanoacetate (1.27 g, 10.0 mmol) and 1-(quinoxalin-2-yl)ethan-1-one (861 mg, 5.0 mmol), after purification *via* flash column chromatography (dry loading, Hexane 4:1 EtOAc), afforded the *title compound* (951 mg, 3.04 mmol, 61%) as an off-white solid. **mp** 136–138 °C **IR**(ATR)/cm^{-1} 3412, 3277, 3142, 2978, 1671, 1584, 1495, 1266, 1087; **^{1}H NMR** (500 MHz, $CDCl_3$) δ (ppm) 8.86 (s, 1H, Ar*H*), 8.13–8.08 (m, 2H, 2 × Ar*H*), 7.79–7.72 (m, 2H, 2 × Ar*H*), 6.53 (s, 1H, C=C*H*S), 6.27 (br s, 2H NH_2), 4.96 (septet, *J* 6.5 Hz, 1H, COOC*H*$(CH_3)_2$), 0.86 (d, *J* 6.0 Hz, 6H, COOCH(C*H*$_3$)$_2$); **^{13}C NMR** (125 MHz, $CDCl_3$) δ (ppm) 164.7, 164.5, 152.0, 146.9, 141.7, 141.1, 137.8, 130.0, 129.5, 129.4, 129.1, 109.8, 105.9, 67.7, 21.7; **LRMS** (ES + APCI) *m/z*: calc. for $C_{16}H_{15}N_3O_2S$ 313.1 found 314.0 $[M+H]^+$; **HMRS** calc. for $C_{16}H_{16}N_3O_2S$ 314.0958 $[M+H]^+$, found 314.0961 $[M+H]^+$.

Isopropyl 2-amino-4-(7-methoxybenzofuran-2-yl)thiophene-3-carboxylate (155)

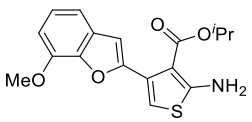

Following General Procedure D, isopropyl 2-cyanoacetate (1.27 g, 10.0 mmol) and 1-(7-methoxybenzofuran-2-yl)ethan-1-one (950 mg, 5.0 mmol), after purification *via*

flash column chromatography (dry loading, Hexane 5:1 EtOAc), afforded the *title compound* (710 mg, 2.14 mmol, 43%) as an off-white solid. **mp** 106–108 °C; **IR**(ATR)/cm^{-1} 3427, 3321, 3103, 2976, 1645, 1586; **^{1}H NMR** (400 MHz, $CDCl_3$) δ (ppm) 7.18–7.10 (m, 2H, 2 × Ar*H*), 6.81–6.77 (m, 2H, 2 × Ar*H*), 6.55 (s, 1H, C=C*H*S), 6.11 (br s, 2H, NH_2), 5.07 (septet, *J* 6.0 Hz, 1H, COOC*H*$(CH_3)_2$), 3.99 (s, 3H, OCH_3), 1.04 (d, *J* 6.4 Hz, 6H, COOCH(C$H_3)_2$); **^{13}C NMR** (101 MHz, $CDCl_3$) δ (ppm) 164.9, 163.6, 152.9, 145.3, 143.8, 130.6, 130.0, 123.3, 113.4, 109.4, 106.4, 106.1, 105.1, 67.4, 56.1, 21.7; **LRMS** (ES + APCI) *m/z*: calc. for $C_{17}H_{17}NO_4S$ 331.1 found 332.0 $[M+H]^+$; **HMRS** calc. for $C_{17}H_{18}NO_4S$ 332.0951 $[M+H]^+$, found 332.0953 $[M+H]^+$.

Isopropyl 2-amino-4-(2-oxo-2,3-dihydrobenzo[d]oxazol-6-yl)thiophene-3-carboxylate (156)

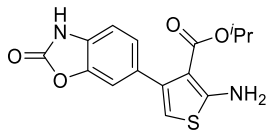

Following General Procedure D, isopropyl 2-cyanoacetate (1.27 g, 10.0 mmol) and 6-acetylbenzo[*d*]oxazol-2(3*H*)-one (885 mg, 5.0 mmol), after purification *via* flash column chromatography (dry loading, Hexane 3:1 EtOAc), afforded the *title compound* (200 mg, 0.63 mmol, 13%) as a yellow residue. **IR**(ATR)/cm^{-1} 3541 br, 3166, 3033, 2947, 2839, 1640, 1446, 1377; **^{1}H NMR** (400 MHz, DMSO-d_6) δ (ppm) 11.58 (br s, 1H, OCON*H*), 7.37 (br s, 2H, NH_2), 7.13 (app t, *J* 1.2 Hz, 1H, Ar*H*), 7.01 (app d, *J* 0.8 Hz, 2H, 2 × Ar*H*), 6.16 (s, 1H, C=C*H*S), 4.85 (septet, *J* 6.0 Hz, 1H, COOC*H*$(CH_3)_2$), 0.92 (d, *J* 6.0 Hz, 6H, COOCH(C$H_3)_2$); **^{13}C NMR** (101 MHz, DMSO-d_6) δ (ppm) 165.0, 164.2, 154.6, 142.5, 139.8, 132.5, 128.9, 124.2, 110.3, 108.3, 105.0, 103.2, 65.9, 21.4; **LRMS** (ES + APCI) *m/z*: calc. for $C_{15}H_{14}N_2O_4S$ 318.1 found 319.0 $[M+H]^+$; **HMRS** calc. for $C_{15}H_{15}N_2O_4S$ 319.0748 $[M+H]^+$, found 319.0747 $[M+H]^+$.

Isopropyl 2-amino-4-(4-morpholinophenyl)thiophene-3-carboxylate (157)

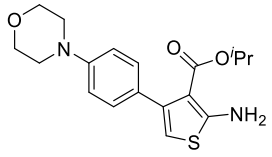

Following General Procedure D, isopropyl 2-cyanoacetate (358 mg, 2.82 mmol) and 1-(4-morpholinophenyl)ethan-1-one (289 mg, 1.41 mmol), after purification *via* flash column chromatography (dry loading, Hexane 4:1 EtOAc), afforded the *title compound* as a partially purified pale yellow solid.

Selected data; **^{1}H NMR** (500 MHz, $CDCl_3$) δ (ppm) 7.20 (d, *J* 8.5 Hz, 2H, 2 × Ar*H*), 6.86 (d, *J* 8.5 Hz, 2H, 2 × Ar*H*), 6.03 (br s, 2H, NH_2), 6.01 (s, 1H, C=C*H*S), 4.99 (septet, *J* 6.5 Hz, 1H, COOC*H*$(CH_3)_2$), 3.91–3.87 (m, 4H, O(CH_2CH_2)CH_2CH_2N), 3.18–3.14 (m, 4H, N(CH_2CH_2)CH_2CH_2O), 1.01 (d, *J* 6.5 Hz, 6H, COOCH(CH_3)$_2$).

Isopropyl 4-(4-(1*H*-imidazol-1-yl)phenyl)-2-aminothiophene-3-carboxylate (158)

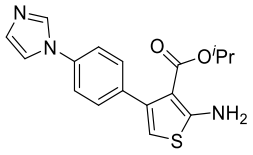

Following General Procedure D, isopropyl 2-cyanoacetate (1.27 g, 10.0 mmol) and 1-([1,1'-biphenyl]-4-yl)ethan-1-one (931 mg, 5.0 mmol), after purification *via* flash column chromatography (dry loading, EtOAc 5:1 Hexane), afforded the *title compound* (745 mg, 2.28 mmol, 46%) as an off-white solid. **mp** 104–106 °C; **IR**(ATR)/cm^{-1} 3383, 3277, 3141, 2983, 1668, 1595, 1504, 1396, 1255, 1097; **^{1}H NMR** (500 MHz, $CDCl_3$) δ (ppm) 7.88 (s, 1H, Ar*H*), 7.42–7.38 (m, 2H, 2 × Ar*H*), 7.36–7.32 (m, 2H, 2 × Ar*H*), 7.30 (app t, *J* 1.5 Hz, 1H, Ar*H*), 7.22 (app t, *J* 1.5 Hz, 1H, Ar*H*), 6.14 (br s, 2H, NH_2), 6.09 (s, 1H, C=C*H*S), 4.99 (septet, *J* 6.5 Hz, 1H, COOC*H*$(CH_3)_2$), 1.00 (d, *J* 6.5 Hz, 6H, COOCH(CH_3)$_2$); **^{13}C NMR** (125 MHz, $CDCl_3$) δ (ppm) 165.1, 164.0, 140.4, 138.3, 136.2, 135.8, 130.7, 130.6, 120.4, 118.4, 106.4, 106.0, 62.3, 21.9; **LRMS** (ES + APCI) *m/z*: calc. for $C_{17}H_{17}N_3O_2S$ 327.1 found 328.0 $[M+H]^+$; **HMRS** calc. for $C_{17}H_{18}N_3O_2S$ 328.1114 $[M+H]^+$, found 328.1116 $[M+H]^+$.

Isopropyl 2-amino-4-(4-cyanophenyl)thiophene-3-carboxylate (159)

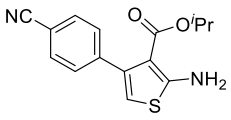

Following General Procedure D, isopropyl 2-cyanoacetate (1.27 g, 10.0 mmol) and 4-acetylbenzonitrile (726 mg, 5.0 mmol), after purification *via* flash column

chromatography (dry loading, Hexane 7:1 EtOAc), afforded the *title compound* (470 mg, 1.64 mmol, 33%) as an off-white solid. **mp** 104–106 °C; **IR**(ATR)/cm^{-1} 3414, 3312, 3103, 2986, 2226, 1668, 1591, 1500; **^{1}H NMR** (400 MHz, $CDCl_3$) δ (ppm) 7.59 (d, *J* 8.4 Hz, 2H, 2 × Ar*H*), 7.38 (d, *J* 8.4 Hz, 2H, 2 × Ar*H*), 6.20 (br s, 2H, NH_2), 6.07 (s, 1H, C=C*H*S), 4.97 (septet, *J* 6.0 Hz, 1H, COOC*H*(CH_3)$_2$), 0.96 (d, *J* 6.4 Hz, 6H, COOCH(CH_3)$_2$); **^{13}C NMR** (101 MHz, $CDCl_3$) δ (ppm) 164.8, 164.3, 143.6, 139.8, 131.1, 129.9, 119.2, 110.4, 106.6, 105.8, 67.4, 21.7; **LRMS** (ES + APCI) *m/z*: calc. for $C_{15}H_{14}N_2O_2S$ 286.1 found 287.0 $[M+H]^+$; **HMRS** calc. for $C_{15}H_{15}N_2O_2S$ 287.0849 $[M+H]^+$, found 287.0852 $[M+H]^+$.

Isopropyl 2-amino-4-(4-ethynylphenyl)thiophene-3-carboxylate (160)

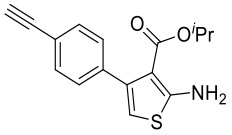

Following General Procedure D, isopropyl 2-cyanoacetate (1.27 g, 10.0 mmol) and 1-(4-ethynylphenyl)ethan-1-one (720 mg, 5.0 mmol), after purification *via* flash column chromatography (dry loading, Hexane 8:1 EtOAc), afforded the *title compound* (445 mg, 1.56 mmol, 31%) as an off-white solid. **mp** 78–80 °C; **IR**(ATR)/cm^{-1} 3459, 3338, 3102, 2985, 2946, 2132, 1668, 1580, 1493, 1387, 1261, 1095; **^{1}H NMR** (500 MHz, $CDCl_3$) δ (ppm) 7.42 (d, *J* 8.0 Hz, 2H, 2 × Ar*H*), 7.24 (d, *J* 8.0 Hz, 2H, 2 × Ar*H*), 6.09 (br s, 2H, NH_2), 6.05 (s, 1H, C=C*H*S), 4.98 (septet, *J* 6.5 Hz, 1H, COOC*H*(CH_3)$_2$), 3.09 (s, 1H, CC*H*), 0.98 (d, *J* 6.0 Hz, 6H, COOCH(CH_3)$_2$); **^{13}C NMR** (125 MHz, $CDCl_3$) δ (ppm) 165.2, 163.9, 140.9, 139.5, 131.2, 129.2, 120.5, 106.5, 105.9, 84.0, 77.2, 67.3, 21.8; **LRMS** (ES + APCI) *m/z*: calc. for $C_{16}H_{15}NO_2S$ 285.1 found 286.0 $[M+H]^+$; **HMRS** calc. for $C_{16}H_{14}NO_2S$ 284.0751 $[M–H]^-$, found 284.0757 $[M–H]^-$.

Isopropyl 2-amino-4-(4-phenoxyphenyl)thiophene-3-carboxylate (161)

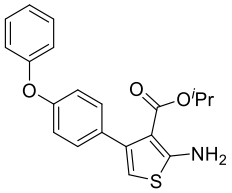

Following General Procedure D, isopropyl 2-cyanoacetate (1.27 g, 10.0 mmol) and 1-(4-phenoxyphenyl)ethan-1-one (532 mg, 2.5 mmol), after purification *via* flash column chromatography (dry loading, Hexane 10:1 EtOAc), afforded the *title compound* (266 mg, 0.75 mmol, 30%) as an off-white solid. **mp** 101–103 °C; **IR**(ATR)/cm^{-1} 3438, 3323, 3102, 2975, 1659, 1573, 1488, 1227, 1101; **^{1}H NMR** (500 MHz, $CDCl_3$) δ (ppm) 7.34 (app t, *J* 7.5 Hz, 2H, 2 × Ar*H*), 7.25 (d, *J* 9.0 Hz, 2H, 2 × Ar*H*), 7.09 (t, *J* 7.5 Hz, 1H, Ar*H*), 7.03 (d, *J* 7.5 Hz, 2H, 2 × Ar*H*), 6.96 (d, *J* 9.0 Hz, 2H, 2 × Ar*H*), 6.09 (br s, 2H, NH_2), 6.05 (s, 1H, C=C*H*S), 5.00 (septet, *J* 6.5 Hz, 1H, COOC*H*$(CH_3)_2$), 1.04 (d, *J* 6.5 Hz, 3H, COOCH(CH_3)$_2$); **^{13}C NMR** (125 MHz, $CDCl_3$) δ (ppm) 165.4, 163.8, 157.7, 156.3, 141.1, 134.0, 130.6, 129.8, 123.2, 118.8, 117.9, 106.7, 105.5, 67.2, 21.9; **LRMS** (ES + APCI) *m/z*: calc. for $C_{20}H_{19}NO_3S$ 353.1 found 354.0 $[M+H]^+$; **HMRS** calc. for $C_{20}H_{20}NO_3S$ 354.1158 $[M+H]^+$, found 354.1160 $[M+H]^+$.

Isopropyl 2-amino-4-(4-benzylphenyl)thiophene-3-carboxylate (162)

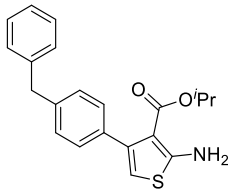

Following General Procedure D, isopropyl 2-cyanoacetate (1.27 g, 10.0 mmol) and 1-(4-benzylphenyl)ethan-1-one (525 mg, 2.5 mmol), after purification *via* flash column chromatography (dry loading, Hexane 10:1 EtOAc), afforded the *title compound* (380 mg, 1.08 mmol, 43%) as an off-white solid. **mp** 83–85 °C; **IR**(ATR)/cm^{-1} 3412, 3303, 3100, 2975, 1634, 1582, 1495, 1272, 1103; **^{1}H NMR** (500 MHz, $CDCl_3$) δ (ppm) 7.29 (app t, *J* 7.5 Hz, 2H, 2 × Ar*H*), 7.25–7.18 (m, 5H, 5 × Ar*H*), 7.15 (d, *J* 7.5 Hz, 2H, 2 × Ar*H*), 6.07 (br s, 2H, NH_2), 6.04 (s, 1H, C=C*H*S), 4.97 (septet, *J* 6.0 Hz, 1H, COOC*H*$(CH_3)_2$), 4.02 (s, 2H, CH_2), 0.95 (d, *J* 6.0 Hz, 3H, COOCH(CH_3)$_2$); **^{13}C NMR** (125 MHz, $CDCl_3$) δ (ppm) 165.4, 163.7, 141.7, 141.5, 139.8, 136.6, 129.3, 129.0, 128.5, 127.9, 126.1, 106.8, 105.3, 67.1, 41.8, 21.7; **LRMS** (ES + APCI) *m/z*: calc. for $C_{21}H_{21}NO_2S$ 351.1 found 352.0 $[M+H]^+$; **HMRS** calc. for $C_{21}H_{22}NO_2S$ 352.1366 $[M+H]^+$, found 352.1368 $[M+H]^+$.

Isopropyl 2-amino-4-(4-(benzyloxy)phenyl)thiophene-3-carboxylate (163)

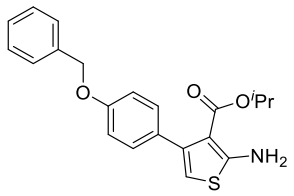

Following General Procedure D, isopropyl 2-cyanoacetate (387 g, 3.04 mmol) and 1-(4-(benzyloxy)phenyl)ethan-1-one (344 mg, 1.52 mmol), after purification *via* flash column chromatography (dry loading, Hexane 9:1 EtOAc), afforded the *title compound* as a partially purified yellow solid.

Selected data; **^{1}H NMR** (500 MHz, $CDCl_3$) δ (ppm) 7.43–7.36 (m, 5H, 5 × Ar*H*), 7.20 (d, *J* 8.5 Hz, 2H, 2 × Ar*H*), 6.92 (d, *J* 8.5 Hz, 2H, 2 × Ar*H*), 6.04 (br s, 2H, NH_2), 6.01 (s, 1H, C=C*H*S), 5.10 (s, 2H, OCH_2), 4.97 (septet, *J* 6.0 Hz, 1H, COOC*H*$(CH_3)_2$), 0.98 (d, *J* 6.0 Hz, 6H, COOCH(CH_3)$_2$).

Isopropyl 2-amino-4-(4-phenethylphenyl)thiophene-3-carboxylate (164)

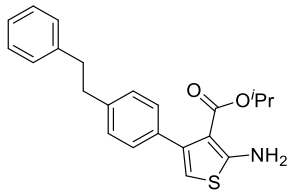

Following General Procedure D, isopropyl 2-cyanoacetate (1.27 g, 10.0 mmol) and 1-(4-phenethylphenyl)ethan-1-one (1.12 g, 5.0 mmol), after purification *via* flash column chromatography (dry loading, Hexane 10:1 EtOAc), afforded the *title compound* (496 mg, 1.36 mmol, 26%) as an off-white solid. **mp** 75–77 °C; **IR**(ATR)/cm^{-1} 3427, 3319, 3020, 2979, 2856, 1636, 1575, 1499, 1268, 1103; **^{1}H NMR** (500 MHz, $CDCl_3$) δ (ppm) 7.32–7.27 (m, 2H, 2 × Ar*H*), 7.25–7.18 (m, 5H, 5 × Ar*H*), 7.14 (d, *J* 8.0 Hz, 2H, 2 × Ar*H*), 6.05 (br s, 2H, NH_2), 6.04 (s, 1H, C=C*H*S), 4.97 (septet, *J* 6.0 Hz, 1H, COOC*H*$(CH_3)_2$), 2.95 (s, 4H, CH_2CH_2), 0.97 (d, *J* 6.0 Hz, 3H, COOCH(CH_3)$_2$); **^{13}C NMR** (125 MHz, $CDCl_3$) δ (ppm) 165.4, 163.6, 141.9, 141.8, 140.5, 136.5, 129.2, 128.6, 128.5, 127.4, 126.1, 106.9, 105.4, 67.1, 38.2, 37.7, 21.8; **LRMS** (ES + APCI) *m/z*: calc. for $C_{22}H_{23}NO_2S$ 365.1 found 366.0 $[M+H]^+$; **HMRS** calc. for $C_{22}H_{24}NO_2S$ 366.1522 $[M+H]^+$, found 366.1525 $[M+H]^+$.

Isopropyl 2-amino-4-(3-(benzyloxy)phenyl)thiophene-3-carboxylate (165)

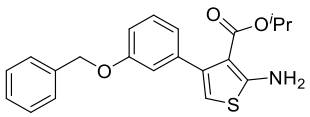

Following General Procedure D, isopropyl 2-cyanoacetate (1.01 g, 7.95 mmol) and 1-(3-(benzyloxy)phenyl)ethan-1-one (900 mg, 3.98 mmol), after purification *via* flash column chromatography (dry loading, Hexane 10:1 EtOAc, isocratic), afforded the *title compound* (700 mg, 1.91 mmol, 48%) as an off-white solid. **mp** 87–89 °C; **IR**(ATR)/cm^{-1} 3431, 3329, 3100, 2977, 2929, 1659, 1575, 1486, 1398, 1272, 1238, 1103; **^{1}H NMR** (500 MHz, $CDCl_3$) δ (ppm) 7.44 (d, *J* 7.5 Hz, 2H, 2 × Ar*H*), 7.38 (app t, *J* 7.5 Hz, 2H, 2 × Ar*H*), 7.32 (app d, *J* 7.0 Hz, 1H, Ar*H*), 7.21 (app t, *J* 7.5 Hz, 1H, Ar*H*), 6.95–6.86 (m, 3H, 3 × Ar*H*), 6.08–6.03 (m, 3H, C=C*H*S, NH_2), 5.07 (s, 2H, OCH_2), 4.96 (septet, *J* 6.5 Hz, 1H, COOC*H*$(CH_3)_2$), 0.85 (d, *J* 6.5 Hz, 6H, COOCH(CH_3)$_2$); **^{13}C NMR** (125 MHz, $CDCl_3$) δ (ppm) 165.4, 163.6, 158.1, 141.6, 140.2, 137.3, 128.7, 128.3, 128.0, 127.6, 122.2, 115.9, 113.4, 106.9, 105.5, 70.1, 67.1, 21.7; **LRMS** (ES + APCI) *m/z*: calc. for $C_{21}H_{21}NO_3S$ 367.1, found 368.0 $[M+H]^+$; **HMRS** calc. for $C_{21}H_{22}NO_3S$ 368.1315 $[M+H]^+$, found 368.1317 $[M+H]^+$.

Isopropyl 2-amino-4-(2-(benzyloxy)phenyl)thiophene-3-carboxylate (166)

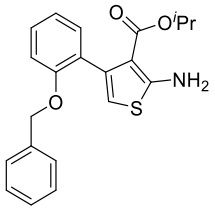

Following General Procedure D, isopropyl 2-cyanoacetate (1.01 g, 7.95 mmol) and 1-(2-(benzyloxy)phenyl)ethan-1-one (900 mg, 3.98 mmol), after purification *via* flash column chromatography (dry loading, Hexane 10:1 EtOAc, isocratic), afforded the *title compound* (505 mg, 1.38 mmol, 35%) as an off-white solid. **mp** 92–94 °C; **IR**(ATR)/cm^{-1} 3416, 3308, 3044, 2975, 2934, 1642, 1594, 1495, 1385, 1268, 1238, 1104; **^{1}H NMR** (500 MHz, $CDCl_3$) δ (ppm) 7.30–7.25 (m, 2H, 2 × Ar*H*), 7.25–7.19 (m, 4H, 4 × Ar*H*), 7.19 (d, *J* 7.5 Hz, 1H, Ar*H*), 6.92 (t, *J* 7.5 Hz, 1H, Ar*H*), 6.86 (d, *J* 7.5 Hz, 1H, Ar*H*), 6.05 (s, 1H, C=C*H*S), 5.95(br s, 2H, NH_2), 4.98 (s, 2H, OCH_2), 4.86 (septet, *J* 6.0 Hz, 1H, COOC*H*$(CH_3)_2$), 0.85 (d, *J* 6.0 Hz, 6H, COOCH(CH_3)$_2$);

^{13}C NMR (125 MHz, $CDCl_3$) δ (ppm) 165.4, 162.6, 156.5, 137.8, 137.5, 130.3, 129.3, 128.4, 128.3, 127.5, 126.7, 120.4, 112.1, 107.8, 105.6, 70.0, 66.6, 21.6; **LRMS** (ES + APCI) *m/z*: calc. for $C_{21}H_{21}NO_3S$ 367.1, found 368.0 $[M+H]^+$; **HMRS** calc. for $C_{21}H_{22}NO_3S$ 368.1315 $[M+H]^+$, found 368.1317 $[M+H]^+$.

2-((4-([1,1'-Biphenyl]-4-yl)-3-((benzyloxy)carbonyl)thiophen-2-yl)carbamoyl)benzoic acid (167)

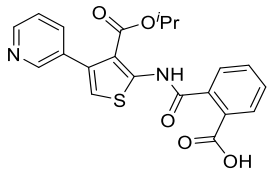

Following General Procedure E, compound **147** (200 mg, 0.76 mmol) and phthalic anhydride (113 mg, 0.76 mmol), after purification *via* flash column chromatography (dry loading, Hexane 3:1 EtOAc, CH_2Cl_2 95:5 MeOH), afforded the *title compound* (198 mg, 0.48 mmol, 64%) as an off-white solid. **mp** 188–190 °C; **IR**(ATR)/cm^{-1} 3084, 2963, 1714, 1658, 1616, 1537; **^{1}H NMR** (400 MHz, DMSO-d_6) δ (ppm) 12.58 (br s, 1H, COO*H*), 8.52 (dd, *J* 4.8 Hz, 1.6 Hz, 1H, Ar*H*), 8.49 (app d, *J* 1.6 Hz, 1H, Ar*H*), 7.90 (d, *J* 7.4 Hz, 1H, Ar*H*), 7.70 (dt, *J* 7.6 Hz, 2.0 Hz, 1H, Ar*H*), 7.60 (dd, *J* 6.4 Hz, 2.4 Hz, 1H, Ar*H*), 7.55–7.45 (m, 2H, 2 × Ar*H*), 7.39 (dd, *J* 7.6 Hz, 4.4 Hz, 1H, Ar*H*), 7.05 (s, 1H, C=C*H*S), 4.88 (septet, *J* 6.0 Hz, 1H, COOC*H*(CH_3)$_2$), 0.94 (d, *J* 6.0 Hz, 6H, COOCH(C*H*$_3$)$_2$); **^{13}C NMR** (101 MHz, DMSO-d_6) δ (ppm) 169.8, 167.2, 163.9, 149.0, 148.9, 147.9, 136.2, 135.3, 134.7, 133.2, 130.1, 130.0, 129.4, 129.0, 127.7, 122.7, 116.4, 112.4, 68.2, 21.2; **LRMS** (ES + APCI) *m/z*: calc. for $C_{21}H_{18}N_2O_5S$ 410.1, found 411.0 $[M+H]^+$; **HMRS** calc. for $C_{21}H_{17}N_2O_5S$ 409.0864 $[M–H]^-$, found 409.0863 $[M–H]^-$.

2-((3-(Isopropoxycarbonyl)-4-(pyridin-4-yl)thiophen-2-yl)carbamoyl)benzoic acid (168)

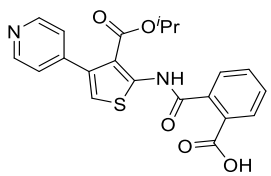

Following General Procedure E, compound **148** (200 mg, 0.76 mmol) and phthalic anhydride (113 mg, 0.76 mmol), after purification *via* flash column

chromatography (dry loading, Hexane 1:1 EtOAc, CH_2Cl_2 95:5 MeOH), afforded the *title compound* (220 mg, 0.54 mmol, 71%) as an off-white solid. **mp** 203–205 °C; **IR**(ATR)/cm^{-1} 3086, 2980, 1714, 1658, 1604, 1521; **^{1}H NMR** (400 MHz, DMSO-d_6) δ (ppm) 12.92 (br s, 1H, COO*H*), 8.55 (d, *J* 6.0 Hz, 2H, 2 × Ar*H*), 7.91 (dd, *J* 8.4 Hz, 2.0 Hz, 1H, Ar*H*), 7.63 (dd, *J* 6.4 Hz, 1.2 Hz, 1H, Ar*H*), 7.55–7.46 (m, 2H, 2 × Ar*H*), 7.31 (d, *J* 6.0 Hz, 2H, 2 × Ar*H*), 7.11 (s, 1H, C=C*H*S), 4.92 (septet, *J* 6.4 Hz, 1H, COOC*H*(CH_3)$_2$), 0.98 (d, *J* 6.0 Hz, 6H, COOCH(C*H*$_3$)$_2$); **^{13}C NMR** (101 MHz, DMSO-d_6) δ (ppm) 170.1, 167.1, 163.8, 148.9, 148.6, 148.5, 144.8, 137.3, 136.2, 134.5, 130.1, 130.0, 129.3, 127.8, 123.8, 116.8, 112.3, 68.3, 21.1; **LRMS** (ES + APCI) *m/z*: calc. for $C_{21}H_{18}N_2O_5S$ 410.1, found 411.0 $[M+H]^+$; **HMRS** calc. for $C_{21}H_{17}N_2O_5S$ 409.0864 $[M–H]^-$, found 409.0862 $[M–H]^-$.

2-((4-(2,4-dimethylthiazol-5-yl)-3-(isopropoxycarbonyl)thiophen-2-yl)carbamoyl)benzoic acid (169)

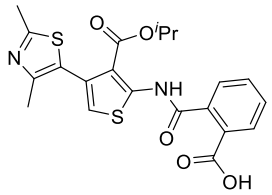

Following General Procedure E, compound **149** (200 mg, 0.67 mmol) and phthalic anhydride (100 mg, 0.67 mmol), after purification *via* flash column chromatography (dry loading, Hexane 2:1 EtOAc, CH_2Cl_2 95:5 MeOH), afforded the *title compound* (142 mg, 0.32 mmol, 48%) as an off-white solid. **mp** 155–157 °C; **IR**(ATR)/cm^{-1} 3057, 2978, 1716, 1658, 1611, 1532; **^{1}H NMR** (400 MHz, DMSO-d_6) δ (ppm) 12.64 (br s, 1H, COO*H*), 8.89 (dd, *J* 6.8 Hz, 2.0 Hz, 1H, Ar*H*), 7.61 (dd, *J* 6.4 Hz, 2.4 Hz, 1H, Ar*H*), 7.55–7.47 (m, 2H, 2 × Ar*H*), 7.08 (s, 1H, C=C*H*S), 4.88 (septet, *J* 6.4 Hz, 1H, COOC*H*(CH_3)$_2$), 2.62 (s, 3H, NC(C*H*$_3$)S), 2.09 (s, 3H, NC(C*H*$_3$)C), 0.99 (d, *J* 6.0 Hz, 6H, COOCH(C*H*$_3$)$_2$); **^{13}C NMR** (101 MHz, DMSO-d_6) δ (ppm) 169.9, 167.2, 163.6, 162.4, 148.5, 148.3, 137.1, 134.7, 130.1, 130.0, 129.4, 127.7, 127.3, 124.9, 118.5, 113.2, 67.9, 21.2, 18.6, 15.2; **LRMS** (ES + APCI) *m/z*: calc. for $C_{21}H_{20}N_2O_5S_2$ 444.1, found 445.0 $[M+H]^+$; **HMRS** calc. for $C_{21}H_{19}N_2O_5S_2$ 443.0741 $[M–H]^-$, found 443.0743 $[M–H]^-$.

2-((3-(Isopropoxycarbonyl)-4-(naphthalen-1-yl)thiophen-2-yl)carbamoyl)benzoic acid (170)

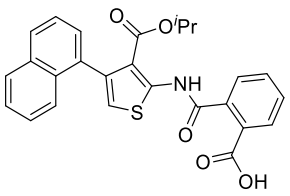

Following General Procedure E, compound **150** (250 mg, 0.80 mmol) and phthalic anhydride (119 mg, 0.80 mmol), after purification *via* flash column chromatography (dry loading, Hexane 2:1 EtOAc, CH_2Cl_2 95:5 MeOH), afforded the *title compound* (140 mg, 0.31 mmol, 38%) as an off-white solid. **mp** 190–192 °C; **IR**(ATR)/cm^{-1} 3248, 3054, 2976, 1699, 1673, 1651, 1548, 1292; **^{1}H NMR** (500 MHz, DMSO-d_6) δ (ppm) 13.32 (br s, 1H, COO*H*), 11.46 (s, 1H, CON*H*), 7.99–7.90 (m, 3H, 3 × Ar*H*), 7.78–7.62 (m, 3H, 3 × Ar*H*), 7.55–7.41 (m, 4H, 4 × Ar*H*), 7.36 (d, *J* 7.0 Hz, 1H, Ar*H*), 7.11 (s, 1H, C=C*H*S), 4.54 (septet, *J* 6.0 Hz, 1H, COOC*H*$(CH_3)_2$), 0.47 (d, *J* 6.0 Hz, 3H, COOCH(C*H*$_3$), 0.12 (d, *J* 6.0 Hz, 3H, COOCH(C*H*$_3$); **^{13}C NMR** (101 MHz, DMSO-d_6) δ (ppm) 167.4, 165.6, 164.2, 148.6, 137.0, 135.8, 135.6, 132.7, 132.1, 130.9, 130.8, 129.8, 128.1, 127.9, 127.6, 127.4, 126.3, 125.9, 125.6, 125.4, 125.1, 116.3, 113.6, 67.2, 20.7, 19.9; **LRMS** (ES + APCI) *m/z*: calc. for $C_{26}H_{21}NO_5S$ 459.1, found 460.0 $[M+H]^+$; **HMRS** calc. for $C_{26}H_{21}NO_5SNa$ 482.1033 $[M+Na]^+$, found 482.1024 $[M+Na]^+$.

2-((3-(Isopropoxycarbonyl)-4-(naphthalen-2-yl)thiophen-2-yl)carbamoyl)benzoic acid (171)

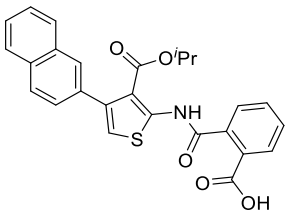

Following General Procedure E, compound **151** (250 mg, 0.80 mmol) and phthalic anhydride (119 mg, 0.80 mmol), after purification *via* flash column chromatography (dry loading, Hexane 5:1 EtOAc, CH_2Cl_2 95:5 MeOH), afforded the *title compound* (314 mg, 0.68 mmol, 86%) as an off-white solid. **mp** 120–122 °C; **IR**(ATR)/cm^{-1} 3051, 2976, 1723, 1658, 1651, 1537, 1221; **^{1}H NMR** (400 MHz,

DMSO-d_6) δ (ppm) 13.47 (br s, 1H, COO*H*), 12.05 (s, 1H, CON*H*), 7.96–7.86 (m, 4H, 4 × Ar*H*), 7.84 (s, 1H, Ar*H*), 7.72–7.60 (m, 3H, 3 × Ar*H*), 7.55–7.49 (m, 2H, 2 × Ar*H*), 7.46 (dd, *J* 8.4 Hz, 1.6 Hz, 1H, Ar*H*), 7.09 (s, 1H, C=C*H*S), 4.89 (septet, *J* 6.4 Hz, 1H, COOC*H*(CH_3)$_2$), 0.85 (d, *J* 6.4 Hz, 6H, COOCH(C*H*$_3$)$_2$); **^{13}C NMR** (101 MHz, DMSO-d_6) δ (ppm) 168.3, 166.2, 164.3, 148.2, 138.9, 135.3, 134.7, 133.4, 132.5, 131.9, 130.9, 130.5, 129.9, 127.8, 127.7, 127.4, 126.9, 126.6, 126.1, 125.9, 115.9, 112.9, 68.1, 21.1; **LRMS** (ES + APCI) *m/z*: calc. for $C_{26}H_{21}NO_5S$ 459.1, found 460.0 $[M+H]^+$; **HMRS** calc. for $C_{26}H_{21}NO_5SNa$ 482.1033 $[M+Na]^+$, found 482.1024 $[M+Na]^+$.

2-((3-(Isopropoxycarbonyl)-4-(quinolin-3-yl)thiophen-2-yl)carbamoyl)benzoic acid (172)

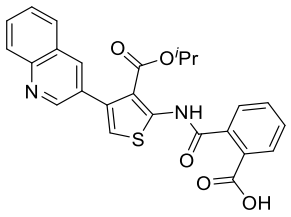

Following General Procedure E, compound **152** (200 mg, 0.64 mmol) and phthalic anhydride (95 mg, 0.64 mmol), after purification *via* flash column chromatography (dry loading, Hexane 2:1 EtOAc, CH_2Cl_2 95:5 MeOH), afforded the *title compound* (210 mg, 0.46 mmol, 71%) as an off-white solid. **mp** 201–203 °C; **IR**(ATR)/cm^{-1} 3256, 3044, 2914, 2849, 1724, 1679, 1655, 1534, 1499, 1402, 1251, 1220, 1097; **^{1}H NMR** (400 MHz, DMSO-d_6) δ (ppm) 12.89 (br s, 1H, COO*H*), 8.83 (d, *J* 2.0 Hz, 1H, Ar*H*), 8.27 (d, *J* 2.0 Hz, 1H, Ar*H*), 8.04 (d, *J* 8.0 Hz, 1H, Ar*H*), 8.00 (d, *J* 8.0 Hz, 1H, Ar*H*), 7.92–7.86 (m, 1H, Ar*H*), 7.81–7.73 (m, 1H, Ar*H*), 7.70–7.60 (m, 1H, Ar*H*), 7.59–7.46 (m, 3H, 3 × Ar*H*), 7.21 (s, 1H, C=C*H*S), 4.89 (septet, *J* 6.4 Hz, 1H, COOC*H*(CH_3)$_2$), 0.87 (d, *J* 6.4 Hz, 6H, COOCH(C*H*$_3$)$_2$); **^{13}C NMR** (101 MHz, DMSO-d_6) δ (ppm) 169.3, 166.9, 163.9, 151.2, 148.8, 146.3, 135.4, 134.3, 130.5, 130.2, 130.0, 129.3, 128.9, 128.6, 128.0, 127.4, 127.1, 126.8, 117.0, 112.7, 68.2, 21.1; **LRMS** (ES + APCI) *m/z*: calc. for $C_{25}H_{20}N_2O_5S$ 460.1, found 461.0 $[M+H]^+$; **HMRS** calc. for $C_{25}H_{19}N_2O_5S$ 459.1020 $[M–H]^-$, found 459.1025 $[M–H]^-$.

2-((3-(Isopropoxycarbonyl)-4-(isoquinolin-4-yl)thiophen-2-yl)carbamoyl)benzoic acid (173)

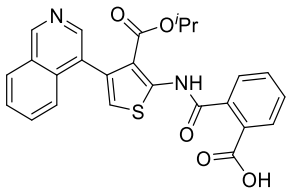

Following General Procedure E, compound **153** (200 mg, 0.64 mmol) and phthalic anhydride (95 mg, 0.64 mmol), after purification *via* flash column chromatography (dry loading, Hexane 1:1 EtOAc, CH_2Cl_2 95:5 MeOH), afforded the *title compound* (270 mg, 0.59 mmol, 92%) as an off-white solid. **mp** 210–212 °C; **IR**(ATR)/cm^{-1} 3197, 3048, 2912, 2849, 1731, 1681, 1655, 1536, 1381, 1246, 1220, 1097; **^{1}H NMR** (400 MHz, DMSO-d_6) δ (ppm) 13.58 (br s, 1H, COO*H*), 11.90 (s, 1H, CON*H*), 9.33 (s, 1H, Ar*H*), 8.35 (s, 1H, Ar*H*), 8.18 (d, *J* 8.0 Hz, 1H, Ar*H*), 7.94–7.89 (m, 1H, Ar*H*), 7.75–7.56 (m, 5H, 5 × Ar*H*), 7.51 (d, *J* 8.0 Hz, 1H, Ar*H*), 7.19 (s, 1H, C=C*H*S), 4.56 (septet, *J* 6.0 Hz, 1H, COOC*H*$(CH_3)_2$), 0.55–0.10 (m, 6H, COOCH$(CH_3)_2$); **^{13}C NMR** (101 MHz, DMSO-d_6) δ (ppm) 168.4, 166.6, 163.8, 151.8, 149.2, 141.8, 135.3, 135.1, 133.2, 130.8, 130.6, 130.5, 129.9, 129.4, 128.9, 127.8, 127.6, 127.5, 127.2, 124.4, 117.2, 113.5, 67.3, 20.3; **LRMS** (ES + APCI) *m/z*: calc. for $C_{25}H_{20}N_2O_5S$ 460.1, found 461.0 $[M+H]^+$; **HMRS** calc. for $C_{25}H_{19}N_2O_5S$ 459.1020 $[M–H]^-$, found 459.1028 $[M–H]^-$.

2-((3-(Isopropoxycarbonyl)-4-(quinoxalin-2-yl)thiophen-2-yl)carbamoyl)benzoic acid (174)

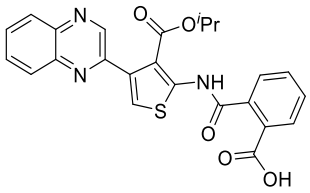

Following General Procedure E, compound **154** (200 mg, 0.64 mmol) and phthalic anhydride (95 mg, 0.64 mmol), after purification *via* flash column chromatography (dry loading, Hexane 2:1 EtOAc, CH_2Cl_2 95:5 MeOH), afforded the *title compound* (246 mg, 0.53 mmol, 84%) as an off-white solid. **mp** 152–154 °C; **IR**(ATR)/cm^{-1} 3248, 3086, 2976, 1712, 1660, 1537, 1511, 1402, 1255, 1217, 1100; **^{1}H NMR** (500 MHz, DMSO-d_6) δ (ppm) 13.63 (br s, 1H, COO*H*), 9.09 (s, 1H, Ar*H*),

8.12 (d, *J* 7.5 Hz, 1H, Ar*H*), 8.03 (d, *J* 7.5 Hz, 1H, Ar*H*), 7.93–7.82 (m, 3H, 3 × Ar*H*), 7.71 (d, *J* 7.5 Hz, 1H, Ar*H*), 7.56 (s, 1H, C=C*H*S), 7.54–7.45 (m, 2H, 2 × Ar*H*), 4.93 (septet, *J* 6.0 Hz, 1H, COOC*H*$(CH_3)_2$), 0.90 (d, *J* 6.0 Hz, 6H, COOCH(C*H*$_3)_2$); **^{13}C NMR** (125 MHz, DMSO-*d*$_6$) δ (ppm) 170.1, 167.1, 163.7, 150.4, 147.6, 145.9, 140.9, 140.5, 138.3, 135.1, 133.8, 132.5, 130.4, 130.2, 129.8, 128.9, 128.8, 128.4, 126.8, 119.5, 113.7, 68.3, 21.2; **LRMS** (ES + APCI) *m/z*: calc. for $C_{24}H_{19}N_3O_5S$ 461.1, found 462.0 $[M+H]^+$; **HMRS** calc. for $C_{24}H_{20}N_3O_5S$ 462.1118 $[M+H]^+$, found 462.1115 $[M+H]^+$.

2-((3-(Isopropoxycarbonyl)-4-(7-methoxybenzofuran-2-yl)thiophen-2-yl)carbamoyl)benzoic acid (175)

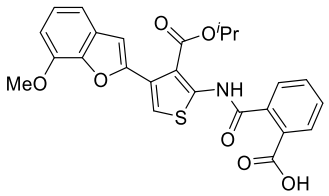

Following General Procedure E, compound **155** (200 mg, 0.61 mmol) and phthalic anhydride (90 mg, 0.61 mmol), after purification *via* flash column chromatography (dry loading, Hexane 3:1 EtOAc, CH_2Cl_2 95:5 MeOH), afforded the *title compound* (240 mg, 0.50 mmol, 83%) as an off-white solid. **mp** 139–141 °C; **IR**(ATR)/cm^{-1} 3246, 2976, 2837, 1721, 1660, 1651, 1537, 1258; **^{1}H NMR** (500 MHz, DMSO-*d*$_6$) δ (ppm) 12.64 (br s, 1H, COO*H*), 7.94–7.89 (m, 1H, Ar*H*), 7.74–7.68 (m, 1H, Ar*H*), 7.64–7.57 (m, 2H, 2 × Ar*H*), 7.45 (s, 1H, Ar*H*), 7.21 (d, *J* 7.5 Hz, 1H, Ar*H*), 7.16 (app t, *J* 7.5 Hz, 1H, Ar*H*), 6.98 (s, 1H, C=C*H*S), 6.93 (d, *J* 7.5 Hz, 1H, Ar*H*), 5.00 (septet, *J* 6.5 Hz, 1H, COOC*H*$(CH_3)_2$), 3.93 (s, 3H, OC*H*$_3$), 1.03 (d, *J* 6.5 Hz, 6H, COOCH(C*H*$_3)_2$); **^{13}C NMR** (125 MHz, DMSO-*d*$_6$) δ (ppm) 168.8, 166.4, 163.8, 151.4, 147.7, 144.8, 143.1, 134.8, 134.4, 130.5, 130.1, 129.9, 128.1, 127.1, 123.6, 118.6, 113.1, 112.8, 106.9, 104.6, 68.4, 55.8, 21.1 (1 carbon missing); **LRMS** (ES + APCI) *m/z*: calc. for $C_{25}H_{21}NO_7S$ 479.1, found 479.9 $[M+H]^+$; **HMRS** calc. for $C_{25}H_{20}NO_7S$ 478.0966 $[M–H]^-$, found 478.0970 $[M–H]^-$.

2-((3-(Isopropoxycarbonyl)-4-(2-oxo-2,3-dihydrobenzo[*d*]oxazol-6-yl)thiophen-2-yl)carbamoyl)benzoic acid (176)

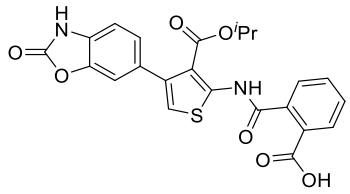

Following General Procedure E, compound **156** (140 mg, 0.44 mmol) and phthalic anhydride (66 mg, 0.44 mmol), after purification *via* flash column chromatography (dry loading, Hexane 2:1 EtOAc, CH_2Cl_2 95:5 MeOH), afforded the *title compound* (171 mg, 0.37 mmol, 83%) as an off-white solid. **mp** 142–144 °C; **IR**(ATR)/cm^{-1} 3337 br, 3043, 2978, 1738, 1714, 1658, 1651, 1521, 1258, 1223, 1095; **^{1}H NMR** (500 MHz, DMSO-d_6) δ (ppm) 13.28 (br s, 1H, COO*H*), 11.72 (s, 1H, CON*H*), 11.37 (s, 1H, CON*H*), 7.91 (d, *J* 7.5 Hz, 1H, Ar*H*), 7.76–7.71 (m, 1H, Ar*H*), 7.70–7.65 (m, 2H, 2 × Ar*H*), 7.24 (s, 1H, Ar*H*), 7.08 (br s, 2H, 2 × Ar*H*), 6.99 (s, 1H, C=C*H*S), 4.90 (septet, *J* 6.0 Hz, 1H, COOC*H*$(CH_3)_2$), 0.93 (d, *J* 6.0 Hz, 6H, COOCH(C*H*$_3)_2$); **^{13}C NMR** (125 MHz, DMSO-d_6) δ (ppm) 167.3, 165.7, 164.3, 154.4, 148.2, 142.7, 138.6, 135.8, 132.1, 131.0, 130.8, 130.6, 129.9, 129.4, 127.5, 124.5, 115.9, 112.7, 110.5, 108.7, 68.1, 21.1; **LRMS** (ES + APCI) *m/z*: calc. for $C_{23}H_{18}N_2O_7S$ 466.1, found 467.0 $[M+H]^+$; **HMRS** calc. for $C_{23}H_{17}N_2O_7S$ 465.0762 $[M–H]^-$, found 465.0767 $[M–H]^-$.

2-((3-(Isopropoxycarbonyl)-4-(4-morpholinophenyl)thiophen-2-yl)carbamoyl)benzoic acid (177)

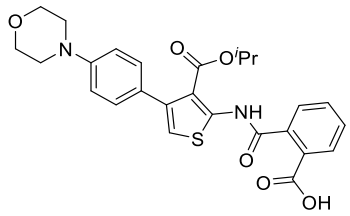

Following General Procedure E, compound **157** (200 mg, 0.58 mmol) and phthalic anhydride (86 mg, 0.58 mmol), after purification *via* flash column chromatography (dry loading, Hexane 2:1 EtOAc, CH_2Cl_2 95:5 MeOH), afforded the *title compound* (240 mg, 0.82 mmol, 34%**) as an off-white solid. **mp** 150–152 °C; **IR**(ATR)/cm^{-1} 3247, 3089, 2975, 1714, 1657, 1610, 1525, 1374, 1222, 1101; **^{1}H**

NMR (500 MHz, DMSO-d_6) δ (ppm) 13.32 (br s, 1H, COO*H*), 11.88 (br s, 1H, CON*H*), 7.90 (d, *J* 7.5 Hz, 1H, Ar*H*), 7.72–7.60 (m, 3H, 3 × Ar*H*), 7.16 (d, *J* 8.5 Hz, 2H, 2 × Ar*H*), 6.93 (d, *J* 8.5 Hz, 2H, 2 × Ar*H*), 6.88 (s, 1H, C=C*H*S), 4.91 (septet, *J* 6.0 Hz, 1H, COOC*H*$(CH_3)_2$), 3.75 (t, *J* 5.0 Hz, 4H, CH_2OCH_2), 3.11 (t, *J* 5.0 Hz, 4H, CH_2NCH_2), 0.99 (d, *J* 6.0 Hz, 6H, COOCH(CH_3)$_2$); **^{13}C NMR** (125 MHz, DMSO-d_6) δ (ppm) 165.8, 164.5, 163.6, 150.2, 147.5, 139.1, 135.4, 131.2, 130.5, 129.9, 129.4, 127.8, 127.7, 114.6, 114.2, 113.2, 79.2, 68.0, 66.0, 48.6, 21.2; **LRMS** (ES + APCI) *m/z*: calc. for $C_{26}H_{26}N_2O_6S$ 494.2, found 495.0 $[M+H]^+$; **HMRS** calc. for $C_{26}H_{27}N_2O_6S$ 495.1584 $[M+H]^+$, found 495.1580 $[M+H]^+$.

2-((4-(4-(1*H*-Imidazol-1-yl)phenyl)-3-(isopropoxycarbonyl)thiophen-2-yl)carbamoyl)benzoic acid (178)

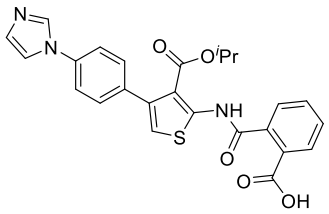

Following General Procedure E, compound **158** (200 mg, 0.61 mmol) and phthalic anhydride (91 mg, 0.61 mmol), after purification *via* flash column chromatography (dry loading, EtOAc, CH_2Cl_2 9:1 MeOH), afforded the *title compound* (217 mg, 0.46 mmol, 75%) as an off-white solid. **mp** 163–165 °C; **IR**(ATR)/cm^{-1} 3044, 2936, 1718, 1651, 1588, 1525, 1456, 1396, 1255, 1222; **^{1}H NMR** (500 MHz, DMSO-d_6) δ (ppm) 13.29 (br s, 1H, COO*H*), 8.29 (s, 1H, Ar*H*), 7.90–7.86 (m, 1H, Ar*H*), 7.78 (app br s, 1H, Ar*H*), 7.71–7.64 (m, 3H, 3 × Ar*H*), 7.57–7.50 (m, 2H, 2 × Ar*H*), 7.42 (d, *J* 8.5 Hz, 2H, 2 × Ar*H*), 7.12 (app br s, 1H, Ar*H*), 7.01 (s, 1H, C=C*H*S), 4.93 (septet, *J* 6.0 Hz, 1H, COOC*H*$(CH_3)_2$), 1.02 (d, *J* 6.0 Hz, 6H, COOCH(CH_3)$_2$); **^{13}C NMR** (125 MHz, DMSO-d_6) δ (ppm) 166.6, 166.5, 164.1, 147.7, 137.7, 135.7, 135.6, 135.4, 134.3, 130.2, 130.1, 130.0, 129.9, 128.9, 128.1, 128.0, 119.4, 117.9, 115.6, 113.3, 68.2, 21.2; **LRMS** (ES + APCI) *m/z*: calc. for $C_{25}H_{21}N_3O_5S$ 475.1, found 476.0 $[M+H]^+$; **HMRS** calc. for $C_{25}H_{22}N_3O_5S$ 476.1275 $[M+H]^+$, found 476.1269 $[M+H]^+$.

2-((4-(4-Cyanophenyl)-3-(isopropoxycarbonyl)thiophen-2-yl)carbamoyl)benzoic acid (179)

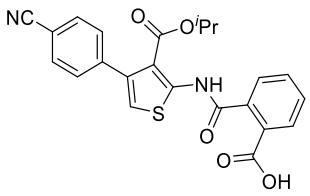

Following General Procedure E, compound **159** (200 mg, 0.69 mmol) and phthalic anhydride (104 mg, 0.69 mmol), after purification *via* flash column chromatography (dry loading, Hexane 5:1 EtOAc, CH_2Cl_2 95:5 MeOH), afforded the *title compound* (237 mg, 0.55 mmol, 79%) as an off-white solid. **mp** 171–173 °C; **IR**(ATR)/cm^{-1} 3103, 2986, 2226, 1715, 1668, 1593, 1537; **^{1}H NMR** (400 MHz, DMSO-d_6) δ (ppm) 12.49 (br s, 1H, COO*H*), 7.93 (dd, *J* 6.8 Hz, 4.4 Hz, 1H, Ar*H*), 7.83 (d, *J* 8.0 Hz, 2H, 2 × Ar*H*), 7.62 (dd, *J* 4.8 Hz, 2.4 Hz, 1H, Ar*H*), 7.58–7.52 (m, 2H, 2 × Ar*H*), 7.50 (d, *J* 8.0 Hz, 2H, 2 × Ar*H*), 7.08 (s, 1H, C=C*H*S), 4.89 (septet, *J* 6.0 Hz, 1H, COOC*H*$(CH_3)_2$), 0.95 (d, *J* 6.4 Hz, 6H, COOCH(C*H*$_3)_2$); **^{13}C NMR** (101 MHz, DMSO-d_6) δ (ppm) 169.5, 166.9, 163.8, 148.7, 142.2, 137.2, 136.3, 134.7, 131.6, 130.2, 130.1, 129.8, 129.7, 127.8, 118.9, 116.7, 112.4, 109.6, 68.3, 21.1; **LRMS** (ES + APCI) *m/z*: calc. for $C_{23}H_{18}N_2O_5S$ 434.1, found 435.0 $[M+H]^+$; **HMRS** calc. for $C_{23}H_{17}N_2O_5S$ 433.0864 $[M–H]^-$, found 433.0863 $[M–H]^-$.

2-((4-(4-Ethynylphenyl)-3-(isopropoxycarbonyl)thiophen-2-yl)carbamoyl)benzoic acid (180)

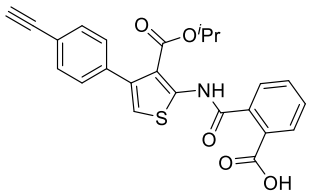

Following General Procedure E, compound **160** (280 mg, 0.98 mmol) and phthalic anhydride (146 mg, 0.98 mmol), after purification *via* flash column chromatography (dry loading, Petroleum ether 3:1 EtOAc, CH_2Cl_2 9:1 MeOH), afforded the *title compound* (370 mg, 0.85 mmol, 87%) as an off-white solid. **mp** 180–182 °C; **IR**(ATR)/cm^{-1} 3273, 3200, 3091, 2979, 1744, 1651, 1547, 1521, 1398, 1270, 1212, 1104, 1067; **^{1}H NMR** (500 MHz, DMSO-d_6) δ (ppm) 13.39 (br s, 1H,

COO*H*), 12.07 (br s, 1H, CON*H*), 7.90 (dd, *J* 7.0 Hz, 1.5 Hz, 1H, Ar*H*), 7.72–7.59 (m, 3H, 3 × Ar*H*), 7.47 (d, *J* 8.0 Hz, 2H, 2 × Ar*H*), 7.31 (d, *J* 8.0 Hz, 2H, 2 × Ar*H*), 7.02 (s, 1H, C=C*H*S), 4.91 (septet, *J* 6.0 Hz, 1H, COOC*H*$(CH_3)_2$), 4.20 (s, 1H, CC*H*), 0.96 (d, *J* 6.0 Hz, 6H, COOCH(C*H*$_3)_2$); **^{13}C NMR** (125 MHz, DMSO-d_6) δ (ppm) 168.1, 166.1, 164.1, 148.2, 138.1, 137.7, 135.2, 131.0, 130.9, 130.8, 130.6, 129.9, 129.1, 127.8, 120.3, 116.0, 112.8, 83.5, 80.9, 68.2, 21.1; **LRMS** (ES + APCI) *m/z*: calc. for $C_{24}H_{19}NO_5S$ 433.1, found 434.0 $[M+H]^+$; **HMRS** calc. for $C_{24}H_{18}NO_5S$ 432.0911 $[M–H]^-$, found 432.0912 $[M–H]^-$.

2-((3-(Isopropoxycarbonyl)-4-(4-phenoxyphenyl)thiophen-2-yl)carbamoyl)benzoic acid (181)

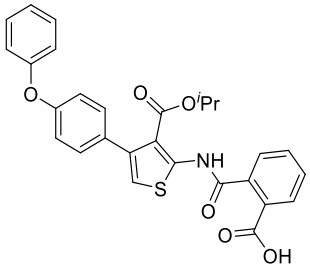

Following General Procedure E, compound **161** (266 mg, 0.75 mmol) and phthalic anhydride (112 mg, 0.75 mmol), after purification *via* flash column chromatography (dry loading, Hexane 3:1 EtOAc, CH_2Cl_2 95:5 MeOH), afforded the *title compound* (278 mg, 0.55 mmol, 74%) as an off-white solid. **mp** 126–128 °C; **IR**(ATR)/cm^{-1} 3260, 3031, 2977, 1718, 1681, 1657, 1519, 1488, 1223, 1101; **^{1}H NMR** (500 MHz, DMSO-d_6) δ (ppm) 13.34 (br s, 1H, COO*H*), 12.19 (br s, 1H, CON*H*), 7.89 (d, *J* 8.0 Hz, 1H, Ar*H*), 7.71–7.58 (m, 3H, 3 × Ar*H*), 7.40 (app t, *J* 7.5 Hz, 2H, 2 × Ar*H*), 7.31 (d, *J* 8.5 Hz, 2H, 2 × Ar*H*), 7.15 (t, *J* 7.5 Hz, 1H, Ar*H*), 7.02 (app t, *J* 9.0 Hz, 4H, 4 × Ar*H*), 6.97 (s, 1H, C=C*H*S), 4.93 (septet, *J* 6.0 Hz, 1H, COOC*H*$(CH_3)_2$), 1.01 (d, *J* 6.0 Hz, 6H, COOCH(C*H*$_3)_2$); **^{13}C NMR** (125 MHz, DMSO-d_6) δ (ppm) 168.4, 166.2, 164.3, 156.9, 155.7, 148.2, 138.3, 135.3, 132.5, 130.9, 130.5, 130.4, 130.1, 130.0, 129.9, 127.7, 123.4, 118.4, 117.9, 115.4, 112.8, 68.1, 21.2; **LRMS** (ES + APCI) *m/z*: calc. for $C_{28}H_{23}NO_6S$ 501.1, found 502.0 $[M+H]^+$; **HMRS** calc. for $C_{28}H_{24}NO_6S$ 502.1319 $[M+H]^+$, found 502.1313 $[M+H]^+$.

2-((4-(4-Benzylphenyl)-3-(isopropoxycarbonyl)thiophen-2-yl)carbamoyl)benzoic acid (182)

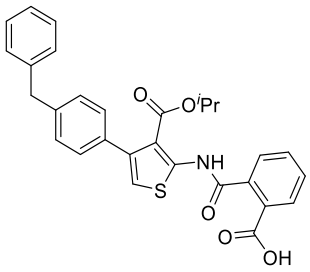

Following General Procedure E, compound **162** (340 mg, 0.97 mmol) and phthalic anhydride (144 mg, 0.97 mmol), after purification *via* flash column chromatography (dry loading, Hexane 3:1 EtOAc, CH_2Cl_2 95:5 MeOH), afforded the *title compound* (403 mg, 0.81 mmol, 83%) as an off-white solid. **mp** 161–163 °C; **IR**(ATR)/cm^{-1} 3238, 3057, 2977, 1722, 1651, 1599, 1525, 1411, 1222, 1101; **^{1}H NMR** (500 MHz, DMSO-d_6) δ (ppm) 13.41 (br s, 1H, COO*H*), 11.92 (br s, 1H, CON*H*), 7.90 (d, *J* 7.0 Hz, 1H, Ar*H*), 7.70–7.58 (m, 3H, 3 × Ar*H*), 7.31–7.15 (m, 9H, 9 × Ar*H*), 6.93 (s, 1H, C=C*H*S), 4.87 (septet, *J* 6.5 Hz, 1H, COOC*H*$(CH_3)_2$), 3.97 (s, 2H, CH_2), 0.90 (d, *J* 6.5 Hz, 6H, COOCH(CH_3)$_2$); **^{13}C NMR** (125 MHz, DMSO-d_6) δ (ppm) 168.2, 166.0, 164.3, 147.9, 141.4, 140.1, 138.9, 135.3, 134.8, 131.1, 130.5, 129.9, 128.9, 128.6, 128.3, 127.9, 127.7, 125.9, 115.2, 113.0, 79.2, 68.0, 40.8, 21.1; **LRMS** (ES + APCI) *m/z*: calc. for $C_{29}H_{25}NO_5S$ 499.1, found 500.0 $[M+H]^+$; **HMRS** calc. for $C_{29}H_{26}NO_5S$ 500.1526 $[M+H]^+$, found 500.1520 $[M+H]^+$.

2-((4-(4-(Benzyloxy)phenyl)-3-(isopropoxycarbonyl)thiophen-2-yl)carbamoyl)benzoic acid (183)

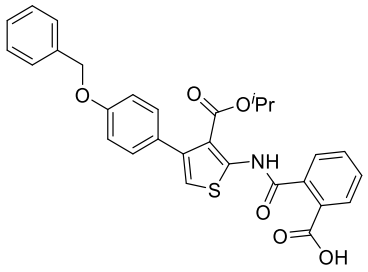

Following General Procedure E, compound **163** (280 mg, 0.76 mmol) and phthalic anhydride (114 mg, 0.76 mmol), after purification *via* flash column chromatography (dry loading, Hexane 4:1 EtOAc, CH_2Cl_2 95:5 MeOH), afforded the

title compound (201 mg, 0.39 mmol, 26%**) as an off-white solid. **mp** 163–165 °C; **IR**(ATR)/cm^{-1} 3234, 3033, 2981, 1700, 1673, 1646, 1547, 1525, 1374, 1218, 1099; **^{1}H NMR** (500 MHz, DMSO-d_6) δ (ppm) 13.31 (br s, 1H, COO*H*), 11.60 (br s, 1H, CON*H*), 7.90 (d, *J* 7.5 Hz, 1H, Ar*H*), 7.72–7.63 (m, 3H, 3 × Ar*H*), 7.45 (d, *J* 7.0 Hz, 2H, 2 × Ar*H*), 7.39 (app t, *J* 7.0 Hz, 2H, 2 × Ar*H*), 7.32 (t, *J* 7.0 Hz, 1H, Ar*H*), 7.20 (d, *J* 8.5 Hz, 2H, 2 × Ar*H*), 6.99 (d, *J* 8.5 Hz, 2H, 2 × Ar*H*), 6.91 (s, 1H, C=C*H*S), 5.16 (s, 2H, CH_2O), 4.89 (septet, *J* 6.0 Hz, 1H, COOC*H*(CH$_3$)$_2$), 0.93 (d, *J* 6.0 Hz, 6H, COOCH(CH_3)$_2$); **^{13}C NMR** (125 MHz, DMSO-d_6) δ (ppm) 167.6, 165.7, 164.4, 157.4, 147.9, 138.8, 137.2, 135.6, 131.7, 130.7, 129.9, 129.8, 129.6, 128.4, 127.7, 127.6, 127.5, 115.1, 113.9, 112.9, 79.2, 69.1, 68.1, 21.1; **LRMS** (ES + APCI) *m/z*: calc. for $C_{29}H_{25}NO_6S$ 515.1, found 516.0 $[M+H]^+$. **HMRS** calc. for $C_{29}H_{26}NO_6S$ 516.1475 $[M+H]^+$, found 516.1469 $[M+H]^+$.

2-((3-(Isopropoxycarbonyl)-4-(4-phenethylphenyl)thiophen-2-yl)carbamoyl)benzoic acid (184)

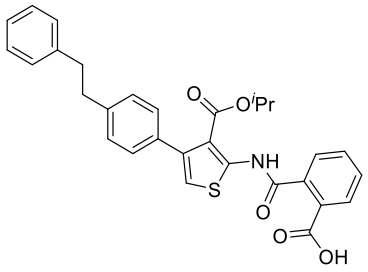

Following General Procedure E, compound **164** (400 mg, 1.09 mmol) and phthalic anhydride (163 mg, 1.09 mmol), after purification *via* flash column chromatography (dry loading, Hexane 3:1 EtOAc, CH_2Cl_2 95:5 MeOH), afforded the *title compound* (444 mg, 0.87 mmol, 79%) as an off-white solid. **mp** 94–96 °C; **IR**(ATR)/cm^{-1} 3243, 3024, 2977, 1722, 1651, 1627, 1525, 1411, 1259, 1103; **^{1}H NMR** (500 MHz, DMSO-d_6) δ (ppm) 13.33 (br s, 1H, COO*H*), 11.94 (br s, 1H, CON*H*), 7.90 (d, *J* 8.0 Hz, 1H, Ar*H*), 7.71–7.60 (m, 3H, 3 × Ar*H*), 7.30–7.24 (m, 4H, 4 × Ar*H*), 7.23–7.15 (m, 5H, 5 × Ar*H*), 6.93 (s, 1H, C=C*H*S), 4.89 (septet, *J* 6.5 Hz, 1H, COOC*H*(CH$_3$)$_2$), 2.91 (s, 4H, CH_2CH_2), 0.94 (d, *J* 6.5 Hz, 6H, COOCH(CH_3)$_2$); **^{13}C NMR** (125 MHz, DMSO-d_6) δ (ppm) 168.1, 165.9, 164.4, 147.7, 141.4, 140.3, 139.0, 135.3, 134.6, 131.2, 131.1, 130.6, 129.9, 128.7, 128.4, 128.2, 127.7, 127.5, 125.8, 115.3, 113.1, 68.0, 37.1, 36.6, 21.1; **LRMS** (ES + APCI)

m/z: calc. for $C_{30}H_{27}NO_5S$ 513.1, found 514.0 $[M+H]^+$; **HMRS** calc. for $C_{30}H_{28}NO_5S$ 514.1683 $[M+H]^+$, found 514.1678 $[M+H]^+$.

2-((4-(3-(Benzyloxy)phenyl)-3-(isopropoxycarbonyl)thiophen-2-yl)carbamoyl)benzoic acid (185)

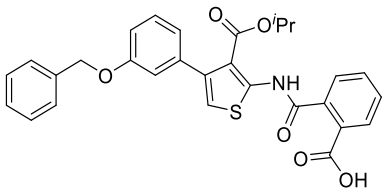

Following General Procedure E, compound **165** (300 mg, 0.82 mmol) and phthalic anhydride (121 mg, 0.82 mmol), after purification *via* flash column chromatography (dry loading, Petroleum ether 3:1 EtOAc, CH_2Cl_2 9:1 MeOH), afforded the *title compound* (322 mg, 0.63 mmol, 77%) as an off-white solid. **mp** 133–135 °C; **IR**(ATR)/cm^{-1} 3278 br, 3068, 2981, 1714, 1668, 1644, 1540, 1515, 1411, 1257, 1222, 1103; **^{1}H NMR** (500 MHz, DMSO-d_6) δ (ppm) 12.87 (br s, 1H, COO*H*), 7.89 (app t, *J* 5.0 Hz, 1H, Ar*H*), 7.67 (app t, *J* 5.0 Hz, 1H, Ar*H*), 7.59–7.52 (m, 2H, 2 × Ar*H*), 7.45 (d, *J* 7.5 Hz, 2H, 2 × Ar*H*), 7.39 (app t, *J* 7.5 Hz, 2H, 2 × Ar*H*), 7.33 (app t, *J* 7.5 Hz, 1H, Ar*H*), 7.27 (t, *J* 8.0 Hz, 1H, Ar*H*), 6.98 (d, *J* 8.0 Hz, 1H, Ar*H*), 6.95 (s, 1H, C=C*H*S), 6.93 (br s, 1H, Ar*H*), 6.86 (d, *J* 7.5 Hz, 1H, Ar*H*), 5.12 (s, 2H, OCH_2), 4.89 (septet, *J* 6.5 Hz, 1H, COOC*H*$(CH_3)_2$), 0.97 (d, *J* 6.5 Hz, 6H, COOCH(CH_3)$_2$); **^{13}C NMR** (125 MHz, DMSO-d_6) δ (ppm) 169.4, 166.5, 164.2, 157.7, 147.5, 138.7, 138.5, 137.1, 136.1, 134.7, 130.2, 130.0, 129.8, 128.6, 128.4, 127.9, 127.8, 127.6, 121.3, 115.4, 115.2, 113.3, 113.2, 69.2, 67.9, 21.1; **LRMS** (ES + APCI) *m/z*: calc. for $C_{29}H_{25}NO_6S$ 515.1, found 516.0 $[M+H]^+$; **HMRS** calc. for $C_{29}H_{24}NO_6S$ 514.1330 $[M–H]^-$, found 514.1337 $[M–H]^-$.

2-((4-(2-(Benzyloxy)phenyl)-3-(isopropoxycarbonyl)thiophen-2-yl)carbamoyl)benzoic acid (186)

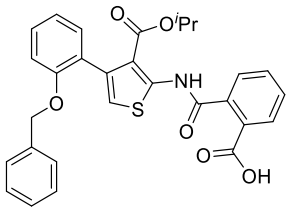

Following General Procedure E, compound **166** (210 mg, 0.57 mmol) and phthalic anhydride (84 mg, 0.57 mmol), after purification *via* flash column chromatography (dry loading, Petroleum ether 3:1 EtOAc, CH_2Cl_2 9:1 MeOH), afforded the *title compound* (242 mg, 0.47 mmol, 82%) as an off-white solid. **mp** 91–93 °C; **IR**(ATR)/cm^{-1} 3176 br, 3035, 2979, 1726, 1659, 1651, 1540, 1519, 1398, 1259, 1220, 1101; **^{1}H NMR** (500 MHz, DMSO-d_6) δ (ppm) 13.35 (br s, 1H, COO*H*), 11.99 (br s, 1H, CON*H*), 7.90–7.84 (m, 1H, Ar*H*), 7.68–7.55 (m, 3H, 3 × Ar*H*), 7.35–7.27 (m, 3H, 3 × Ar*H*), 7.27–7.21 (m, 3H, 3 × Ar*H*), 7.17 (d, *J* 8.0 Hz, 1H, Ar*H*), 7.04 (d, *J* 8.0 Hz, 1H, Ar*H*), 6.96 (app t, *J* 8.0 Hz, 1H, Ar*H*), 6.89 (s, 1H, C=C*H*S), 5.05 (s, 2H, OCH_2), 4.78 (septet, *J* 6.0 Hz, 1H, COOC*H*$(CH_3)_2$), 0.83 (d, *J* 6.0 Hz, 6H, COOCH(C$H_3)_2$); **^{13}C NMR** (125 MHz, DMSO-d_6) δ (ppm) 172.3, 171.8, 166.3, 164.3, 155.7, 147.3, 137.2, 135.6, 135.5, 130.4, 130.3, 130.0, 129.8, 128.5, 128.3, 127.6, 127.4, 127.3, 126.7, 120.2, 115.3, 113.9, 111.9, 68.9, 67.5, 20.9; **LRMS** (ES + APCI) *m/z*: calc. for $C_{29}H_{25}NO_6S$ 515.1, found 514.1 [M–H]$^-$; **HMRS** calc. for $C_{29}H_{24}NO_6S$ 514.1330 [M–H]$^-$, found 514.1333 [M–H]$^-$.

1-(4-(Pyridin-2-yl)phenyl)ethan-1-one (190)

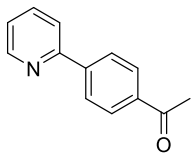

A solution of 2-iodo pyridine (300 mg, 1.46 mmol), (4-acetylphenyl)boronic acid (360 mg, 2.20 mmol), and K_2CO_3 (405 mg, 2.93 mmol) in dioxane:H_2O (3:1) (14.5 mL, 0.10 M), was purged with nitrogen for 10 minutes before [1,1′-Bis(diphenylphosphino)ferrocene]dichloropalladium(II) (Pd(dppf)Cl_2) (54 mg, 0.08 mmol) was added. The reaction mixture was subjected to microwave irradiation at 120 °C for 90 minutes. The reaction was then cooled to room temperature, diluted with CH_2Cl_2 (50 mL) and filtered through Celite®. The filtrate was subsequently concentrated under reduced pressure. The residue was purified *via* flash column chromatography (dry loading, petroleum ether 1:2 EtOAc isocratic) to afford the *title compound* (226 mg, 1.15 mmol, 78%) as an off-white solid. **mp** 109–111 °C; **IR**(ATR)/cm^{-1} 3048, 2920, 1675, 1605, 1584, 1355, 1266; **^{1}H NMR** (500 MHz, $CDCl_3$) δ (ppm) 8.73 (d, *J* 5.0 Hz, 1H, Ar*H*), 8.10 (d, *J* 8.5 Hz, 2H, 2 × Ar*H*), 8.06 (d, *J* 8.5 Hz, 2H, 2 × Ar*H*), 7.79 (app dd, *J* 5.0 Hz, 1.0 Hz, 2H, 2 × Ar*H*), 7.29

(app q, *J* 5.0 Hz, 1H, Ar*H*), 2.65 (s, 3H, CH_3), **^{13}C NMR** (125 MHz, $CDCl_3$) δ (ppm) 197.9, 156.2, 150.1, 143.8, 137.3, 137.1, 128.9, 127.2, 123.1, 121.2, 26.9; **LRMS** (ES + APCI) *m/z*: calc. for $C_{13}H_{11}NO$ 197.1, found 198.1 $[M+H]^+$; **HMRS** calc. for $C_{13}H_{12}NO$ 198.0911 $[M+H]^+$, found 198.0913 $[M+H]^+$.

1-(4-(Pyridin-3-yl)phenyl)ethan-1-one (191)

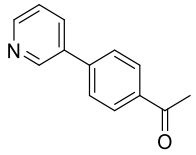

A solution of 3-bromo pyridine (400 mg, 2.53 mmol), (4-acetylphenyl)boronic acid (623 mg, 3.80 mmol), and K_2CO_3 (699 mg, 5.06 mmol) in dioxane:H_2O (3:1) (14.5 mL, 0.17 M), was purged with nitrogen for 10 minutes before Pd(dppf)Cl_2 (93 mg, 0.13 mmol) was added. The reaction mixture was subjected to microwave irradiation at 120 °C for 90 minutes. The reaction was then cooled to room temperature, diluted with CH_2Cl_2 (50 mL) and filtered through Celite®. The filtrate was subsequently concentrated under reduced pressure. The residue was purified *via* flash column chromatography (dry loading, petroleum ether 1:2 EtOAc isocratic) to afford the *title compound* (230 mg, 1.17 mmol, 46%) as an off-white solid. **mp** 105–107 °C; **IR**(ATR)/cm^{-1} 3025, 2963, 1671, 1608, 1573, 1401, 1257; **^{1}H NMR** (500 MHz, $CDCl_3$) δ (ppm) 8.89 (s, 1H, Ar*H*), 8.65 (d, *J* 5.0 Hz, 1H, Ar*H*), 8.07 (d, *J* 8.0 Hz, 2H, 2 × Ar*H*), 7.91 (d, *J* 8.0 Hz, 1H, Ar*H*), 7.68 (d, *J* 8.0 Hz, 2H, 2 × Ar*H*), 7.40 (dd, *J* 8.0 Hz, 5.0 Hz, 1H, Ar*H*), 2.65 (s, 3H, CH_3), **^{13}C NMR** (125 MHz, $CDCl_3$) δ (ppm) 197.7, 149.5, 148.5, 142.5, 136.7, 135.6, 134.6, 129.3, 127.4, 123.8, 26.8; **LRMS** (ES + APCI) *m/z*: calc. for $C_{13}H_{11}NO$ 197.1, found 198.1 $[M+H]^+$; **HMRS** calc. for $C_{13}H_{12}NO$ 198.0911 $[M+H]^+$, found 198.0914 $[M+H]^+$.

1-(4-(Pyridin-4-yl)phenyl)ethan-1-one (192)

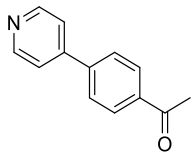

A solution of 4-iodo pyridine (500 mg, 2.44 mmol), (4-acetylphenyl)boronic acid (600 mg, 3.66 mmol), and K_2CO_3 (675 mg, 4.88 mmol) in dioxane:H_2O (3:1)

(14.5 mL, 0.17 M), was purged with nitrogen for 10 minutes before $Pd(dppf)Cl_2$ (89 mg, 0.12 mmol) was added. The reaction mixture was subjected to microwave irradiation at 120 °C for 90 minutes. The reaction was then cooled to room temperature, diluted with CH_2Cl_2 (50 mL) and filtered through Celite®. The filtrate was subsequently concentrated under reduced pressure. The residue was purified *via* flash column chromatography (dry loading, petroleum ether 1:3 EtOAc isocratic) to afford the *title compound* (226 mg, 1.15 mmol, 78%) as an off-white solid. **mp** 101–103 °C; **IR**(ATR)/cm^{-1} 3061, 2921, 1681, 1603, 1590, 1402, 1357, 1264, 805; **^{1}H NMR** (500 MHz, $CDCl_3$) δ (ppm) 8.71 (d, *J* 6.0 Hz, 2H, 2 × Ar*H*), 8.07 (d, *J* 8.5 Hz, 2H, 2 × Ar*H*), 7.73 (d, *J* 8.5 Hz, 2H, 2 × Ar*H*), 7.53 (d, *J* 6.0 Hz, 2H, 2 × Ar*H*), 2.65 (s, 3H, CH_3), **^{13}C NMR** (125 MHz, $CDCl_3$) δ (ppm) 197.6, 150.7, 147.2, 142.8, 137.5, 129.3, 127.4, 121.8, 26.9; **LRMS** (ES + APCI) *m/z*: calc. for $C_{13}H_{11}NO$ 197.1, found 198.1 $[M+H]^+$; **HMRS** calc. for $C_{13}H_{12}NO$ 198.0913 $[M+H]^+$, found 198.0911 $[M+H]^+$.

1-(4-(Phenylethynyl)phenyl)ethan-1-one (193)

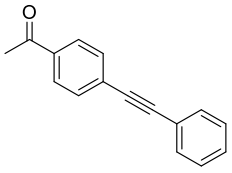

A solution of 4-bromo acetophenone (600 mg, 3.01 mmol), copper(I) iodide (517 mg, 2.71 mmol), tetrabutylammonium iodide (TBAI) (3.67 g, 9.90 mmol) and NEt_3 (4.0 mL, 29.0 mmol) in DMF (20 mL, 0.15 M) was purged with nitrogen for 10 minutes before *bis*-(triphenylphosphine)-palladium dichloride ($Pd(PPh_3)_2Cl_2$) (846 mg, 1.21 mmol) was added. After the mixture was stirred at room temperature for 10 minutes, phenyl acetylene (1.65 mL, 15.0 mmol) was added, and the reaction mixture was heated at 70 °C for 4 hours. The reaction was then cooled to room temperature, diluted with CH_2Cl_2 (50 mL) and filtered through Celite®. The filtrate was subsequently washed with 1 N HCl (30 mL), water (2 × 30 mL), and brine (30 mL), before being filtered, dried over $MgSO_4$ and concentrated under reduced pressure. The residue was purified *via* flash column chromatography (dry loading, Hexane 20:1 EtOAc isocratic) to afford the *title compound* (550 mg, 2.50 mmol, 83%) as an off-white solid. **mp** 88–90 °C; **IR**(ATR)/cm^{-1} 3057, 2960, 2218, 1677, 1603, 1486, 1262, 961; **^{1}H NMR** (500 MHz, $CDCl_3$) δ (ppm) 7.94

(d, *J* 8.5 Hz, 2H, 2 × Ar*H*), 7.61 (d, *J* 8.5 Hz, 2H, 2 × Ar*H*), 7.58–7.52 (m, 2H, 2 × Ar*H*), 7.40–7.35 (m, 3H, 3 × Ar*H*), 2.62 (s, 3H, CH_3), **^{13}C NMR** (125 MHz, $CDCl_3$) δ (ppm) 197.3, 136.2, 131.8, 131.7, 128.8, 128.5, 128.3, 128.2, 122.7, 92.7, 88.6, 26.6; **LRMS** (ES + APCI) *m/z*: calc. for $C_{16}H_{12}O$ 220.1, found 221.1 $[M+H]^+$; **HMRS** calc. for $C_{16}H_{13}O$ 221.0961 $[M+H]^+$, found 221.0962 $[M+H]^+$.

Isopropyl 2-amino-4-(4-(pyridin-2-yl)phenyl)thiophene-3-carboxylate (194)

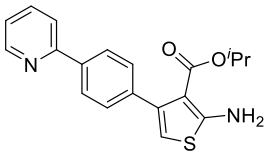

Following General Procedure D, isopropyl 2-cyanoacetate (259 mg, 2.04 mmol) and compound **190** (200 mg, 1.02 mmol), after purification *via* flash column chromatography (dry loading, petroleum ether 4:1 EtOAc), afforded the *title compound* (140 mg, 0.41 mmol, 41%) as an off-white solid. **mp** 146–148 °C; **IR**(ATR)/cm^{-1} 3401, 3206, 3102, 2981, 2931, 1662, 1588, 1469, 1393, 1261, 1093; **^{1}H NMR** (500 MHz, $CDCl_3$) δ (ppm) 8.71 (d, *J* 3.5 Hz, 1H, Ar*H*), 7.96 (d, *J* 8.0 Hz, 2H, 2 × Ar*H*), 7.78–7.74 (m, 2H, 2 × Ar*H*), 7.40 (d, *J* 8.0 Hz, 2H, 2 × Ar*H*), 7.25–7.21 (m, 1H, Ar*H*), 6.15–6.06 (m, 3H, (NH_2, C=C*H*S)), 4.98 (septet, *J* 6.0 Hz, 1H, COOC*H*$(CH_3)_2$), 0.98 (d, *J* 6.0 Hz, 6H, COOCH(CH_3)$_2$); **^{13}C NMR** (125 MHz, $CDCl_3$) δ (ppm) 165.4, 163.9, 157.5, 149.8, 141.4, 139.6, 137.9, 136.9, 129.6, 125.9, 122.1, 120.5, 106.7, 105.8, 67.3, 21.8; **LRMS** (ES + APCI) *m/z*: calc. for $C_{19}H_{18}N_2O_2S$ 338.1 found 339.0 $[M+H]^+$; **HMRS** calc. for $C_{19}H_{19}N_2O_2S$ 339.1162 $[M+H]^+$, found 339.1163 $[M+H]^+$.

Isopropyl 2-amino-4-(4-(pyridin-3-yl)phenyl)thiophene-3-carboxylate (195)

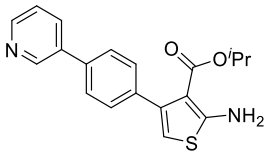

Following General Procedure D, isopropyl 2-cyanoacetate (297 mg, 2.34 mmol) and compound **191** (230 mg, 1.17 mmol), after purification *via* flash column chromatography (dry loading, petroleum ether 2:1 EtOAc), afforded the

title compound (188 mg, 0.56 mmol, 48%) as an off-white solid. **mp** 138–140 °C; **IR**(ATR)/cm^{-1} 3411, 3282, 3102, 2979, 2931, 1659, 1599, 1489, 1385, 1262, 1090; **^{1}H NMR** (500 MHz, $CDCl_3$) δ (ppm) 8.90 (s, 1H, Ar*H*), 8.61 (app s, 1H, Ar*H*), 7.90 (d, *J* 8.0 Hz, 1H, Ar*H*), 7.54 (d, *J* 8.0 Hz, 2H, 2 × Ar*H*), 7.40 (d, *J* 8.0 Hz, 2H, 2 × Ar*H*), 7.38 (dd, *J* 8.0 Hz, 5.0 Hz, 1H, Ar*H*), 6.13–6.09 (m, 3H, (NH_2, C=C*H*S)), 4.99 (septet, *J* 6.0 Hz, 1H, COOC*H*(CH_3)$_2$), 0.99 (d, *J* 6.0 Hz, 6H, COOCH(C*H*$_3$)$_2$); **^{13}C NMR** (125 MHz, $CDCl_3$) δ (ppm) 165.2, 163.9, 148.5, 148.4, 141.2, 138.8, 136.8, 136.4, 134.3, 129.9, 126.1, 123.8, 106.7, 105.8, 67.3, 21.8; **LRMS** (ES + APCI) *m/z*: calc. for $C_{19}H_{18}N_2O_2S$ 338.1 found 339.0 $[M+H]^+$; **HMRS** calc. for $C_{19}H_{19}N_2O_2S$ 339.1162 $[M+H]^+$, found 339.1164 $[M+H]^+$.

Isopropyl 2-amino-4-(4-(pyridin-4-yl)phenyl)thiophene-3-carboxylate (196)

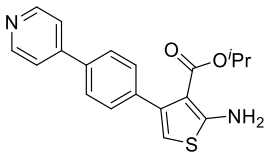

Following General Procedure D, isopropyl 2-cyanoacetate (259 mg, 2.04 mmol) and compound **192** (200 mg, 1.02 mmol), after purification *via* flash column chromatography (dry loading, petroleum ether 4:1 EtOAc), afforded the *title compound* (167 mg, 0.49 mmol, 49%) as an off-white solid. **mp** 138–140 °C; **IR**(ATR)/cm^{-1} 3412, 3254, 3057, 2921, 1666, 1595, 1495, 1393, 1257, 1099; **^{1}H NMR** (500 MHz, $CDCl_3$) δ (ppm) 9.10–8.70 (m, 2H, 2 × Ar*H*), 7.65–7.55 (m, 4H, 4 × Ar*H*), 7.41 (d, *J* 8.5 Hz, 2H, 2 × Ar*H*), 6.11 (s, 1H, C=C*H*S), 6.10 (br s, 2H, NH_2), 4.99 (septet, *J* 6.5 Hz, 1H, COOC*H*(CH_3)$_2$), 0.99 (d, *J* 6.5 Hz, 6H, COOCH(C*H*$_3$)$_2$); **^{13}C NMR** (125 MHz, $CDCl_3$) δ (ppm) 165.2, 163.9, 150.3, 148.5, 141.0, 139.9, 136.6, 130.0, 125.9, 121.7, 106.6, 105.9, 67.3, 21.8; **LRMS** (ES + APCI) *m/z*: calc. for $C_{19}H_{18}N_2O_2S$ 338.1 found 339.0 $[M+H]^+$; **HMRS** calc. for $C_{19}H_{19}N_2O_2S$ 339.1162 $[M+H]^+$, found 339.1163 $[M+H]^+$.

Isopropyl 2-amino-4-(4-(phenylethynyl)phenyl)thiophene-3-carboxylate (197)

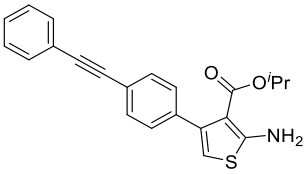

Following General Procedure D, isopropyl 2-cyanoacetate (229 mg, 1.80 mmol) and compound **193** (198 mg, 0.90 mmol), after purification *via* flash column chromatography (dry loading, Hexane 10:1 EtOAc), afforded the *title compound* as a partially purified yellow solid.

Selected data; **^{1}H NMR** (500 MHz, $CDCl_3$) δ (ppm) 7.55 (app dd, *J* 8.0 Hz, 2.0 Hz, 2H, 2 × Ar*H*), 7.48 (d, *J* 8.0 Hz, 2H, 2 × Ar*H*), 7.38–7.32 (m 3H, 3 × Ar*H*), 7.27 (d, *J* 8.0 Hz, 2H, 2 × Ar*H*), 6.10 (br s, 2H, NH_2), 6.07 (s, 1H, C=C*H*S), 4.99 (septet, *J* 6.5 Hz, 1H, COOC*H*$(CH_3)_2$), 1.01 (d, *J* 6.5 Hz, 6H, COOCH(CH_3)$_2$).

2-((3-(Isopropoxycarbonyl)-4-(4-(pyridin-2-yl)phenyl)thiophen-2-yl)carbamoyl)benzoic acid (198)

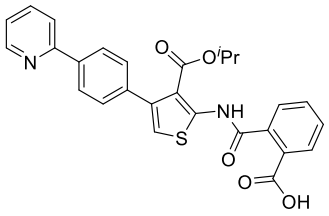

Following General Procedure E, compound **194** (130 mg, 0.38 mmol) and phthalic anhydride (57 mg, 0.38 mmol), after purification *via* flash column chromatography (dry loading, Petroleum ether 2:1 EtOAc, CH_2Cl_2 9:1 MeOH), afforded the *title compound* (72 mg, 0.15 mmol, 39%) as an off-white solid. **mp** 180–182 °C; **IR**(ATR)/cm^{-1} 3241, 3219, 3056, 2981, 1714, 1659, 1586, 1527, 1395, 1257, 1223, 1101; **^{1}H NMR** (500 MHz, DMSO-d_6) δ (ppm) 13.79 (br s, 1H, COO*H*), 8.68 (d, *J* 4.0 Hz, 1H, Ar*H*), 8.09 (d, *J* 8.0 Hz, 2H, 2 × Ar*H*), 7.99 (d, *J* 8.0 Hz, 1H, Ar*H*), 7.92–7.84 (m, 2H, 2 × Ar*H*), 7.70 (d, *J* 6.5 Hz, 1H, Ar*H*), 7.54–7.45 (m, 2H, 2 × Ar*H*), 7.41 (d, *J* 8.0 Hz, 2H, 2 × Ar*H*), 7.35 (dd, *J* 6.5 Hz, 5.0 Hz, 1H), 7.02 (s, 1H, C=C*H*S), 4.94 (septet, *J* 6.0 Hz, 1H, COOC*H*$(CH_3)_2$), 1.02 (d, *J* 6.0 Hz, 6H, COOCH(CH_3)$_2$); **^{13}C NMR** (125 MHz, DMSO-d_6) δ (ppm) 170.1, 166.7, 164.2, 155.7, 149.6, 138.4, 138.2, 137.7, 137.2, 131.9, 130.3, 130.2, 130.0, 129.6, 129.0, 128.9, 128.3, 126.8, 125.8, 122.5, 120.1, 115.4, 68.1, 21.2; **LRMS** (ES + APCI) *m/z*: calc. for $C_{27}H_{22}N_2O_5S$ 486.1, found 487.0 $[M+H]^+$; **HMRS** calc. for $C_{27}H_{21}N_2O_5S$ 485.1177 $[M–H]^-$, found 485.1178 $[M–H]^-$.

2-((3-(Isopropoxycarbonyl)-4-(4-(pyridin-3-yl)phenyl)thiophen-2-yl)carbamoyl)benzoic acid (199)

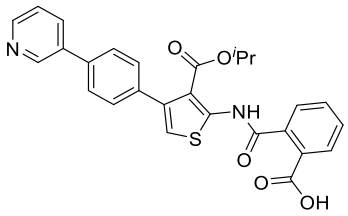

Following General Procedure E, compound **195** (180 mg, 0.53 mmol) and phthalic anhydride (79 mg, 0.53 mmol), after purification *via* flash column chromatography (dry loading, Petroleum ether 2:1 EtOAc, CH_2Cl_2 9:1 MeOH), afforded the *title compound* (225 mg, 0.46 mmol, 87%) as an off-white solid. **mp** 192–194 °C; **IR**(ATR)/cm^{-1} 3472 br, 3042, 2981, 1714, 1651, 1614, 1521, 1395, 1253, 1220, 1101; **^{1}H NMR** (500 MHz, DMSO-d_6) δ (ppm) 13.22 (br s, 1H, COO*H*), 8.93 (d, *J* 1.5 Hz, 1H, Ar*H*), 8.58 (dd, *J* 4.5 Hz, 1.5 Hz, 1H, Ar*H*), 8.11 (app dt, *J* 7.5 Hz, 1.5 Hz, 1H, Ar*H*), 7.90 (dd, *J* 7.5 Hz, 1.5 Hz, 1H, Ar*H*), 7.74 (d, *J* 8.0 Hz, 2H, 2 × Ar*H*), 7.65 (dd, *J* 7.0 Hz, 1.0 Hz, 1H, Ar*H*), 7.54–7.46 (m, 3H, 3 × Ar*H*), 7.41 (d, *J* 8.0 Hz, 1H, Ar*H*), 7.01 (s, 1H, C=C*H*S), 4.92 (septet, *J* 6.5 Hz, 1H, COOC*H*(CH_3)$_2$), 1.00 (d, *J* 6.5 Hz, 6H, COOCH(C*H*$_3$)$_2$); **^{13}C NMR** (125 MHz, DMSO-d_6) δ (ppm) 170.3, 166.9, 164.1, 148.6, 147.7, 147.5, 138.2, 137.9, 137.0, 135.6, 135.3, 134.3, 133.9, 130.1, 129.9, 129.4, 129.0, 128.0, 126.1, 123.9, 115.3, 113.2, 68.1, 21.2; **LRMS** (ES + APCI) *m/z*: calc. for $C_{27}H_{22}N_2O_5S$ 486.1, found 487.0 $[M+H]^+$; **HMRS** calc. for $C_{27}H_{21}N_2O_5S$ 485.1177 $[M–H]^-$, found 485.1178 $[M–H]^-$.

2-((3-(Isopropoxycarbonyl)-4-(4-(pyridin-4-yl)phenyl)thiophen-2-yl)carbamoyl)benzoic acid (200)

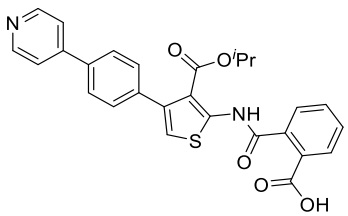

Following General Procedure E, compound **196** (80 mg, 0.24 mmol) and phthalic anhydride (35 mg, 0.24 mmol), after purification *via* flash column

chromatography (dry loading, Petroleum ether 2:1 EtOAc, CH_2Cl_2 9:1 MeOH), afforded the *title compound* (62 mg, 0.13 mmol, 54%) as an off-white solid. **mp** 174–176 °C; **IR**(ATR)/cm^{-1} 3451 br, 3063, 2978, 2925, 1727, 1640, 1510, 1471, 1357, 1153, 1037, 768; **^{1}H NMR** (500 MHz, DMSO-d_6) δ (ppm) 14.02 (br s, 1H, COO*H*), 8.64 (d, *J* 6.5 Hz, 1H, Ar*H*), 7.88–7.78 (m, 3H, 3 × Ar*H*), 7.77–7.68 (m, 2H, 2 × Ar*H*), 7.51–7.42 (m, 5H, 5 × Ar*H*), 7.38 (d, *J* 6.5 Hz, 1H, Ar*H*), 7.03 (s, 1H, C=C*H*S), 4.94 (septet, *J* 6.0 Hz, 1H, COOC*H*$(CH_3)_2$), 1.03 (d, *J* 6.0 Hz, 6H, COOCH(C*H*$_3)_2$); **^{13}C NMR** (125 MHz, DMSO-d_6) δ (ppm) 169.9, 166.7, 164.0, 150.3, 146.6, 138.1, 137.9, 135.6, 133.6, 130.2, 130.1, 129.6, 129.3, 129.2, 129.0, 128.4, 126.7, 126.1, 120.9, 115.5, 68.1, 21.2; **LRMS** (ES + APCI) *m/z*: calc. for $C_{27}H_{22}N_2O_5S$ 486.1, found 487.0 $[M+H]^+$; **HMRS** calc. for $C_{27}H_{21}N_2O_5S$ 485.1177 $[M–H]^-$, found 485.1178 $[M–H]^-$.

2-((3-(Isopropoxycarbonyl)-4-(4-(phenylethynyl)phenyl)thiophen-2-yl)carbamoyl)benzoic acid (201)

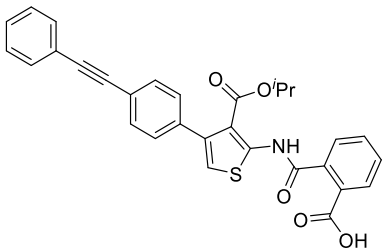

Following General Procedure E, compound **197** (185 mg, 0.51 mmol) and phthalic anhydride (76 mg, 0.51 mmol), after purification *via* flash column chromatography (dry loading, Petroleum ether 4:1 EtOAc, CH_2Cl_2 95:5 MeOH), afforded the *title compound* (139 mg, 0.27 mmol, 30%**) as an off-white solid. **mp** 159–161 °C; **IR**(ATR)/cm^{-1} 3557, 3278, 3117, 2964, 2218, 1703, 1670, 1640, 1536, 1409, 1264, 1216, 1101; **^{1}H NMR** (500 MHz, DMSO-d_6) δ (ppm) 13.51 (br s, 1H, COO*H*), 12.63 (br s, 1H, CON*H*), 7.91–7.87 (m, 1H, Ar*H*), 7.72–7.65 (m, 1H, Ar*H*), 7.62–7.52 (m, 6H, 6 × Ar*H*), 7.47–7.41 (m, 3H, 3 × Ar*H*), 7.35 (d, *J* 8.0 Hz, 2H, 2 × Ar*H*), 7.03 (s, 1H, C=C*H*S), 4.93 (septet, *J* 6.0 Hz, 1H, COOC*H*$(CH_3)_2$), 1.00 (d, *J* 6.0 Hz, 6H, COOCH(C*H*$_3)_2$); **^{13}C NMR** (125 MHz, DMSO-d_6) δ (ppm) 168.8, 166.4, 164.1, 147.9, 138.1, 137.5, 134.8, 131.4, 130.6, 130.4, 130.3, 130.2, 130.0, 129.1, 128.8, 128.7, 127.9, 122.3, 120.8, 115.9, 112.9, 89.6, 89.4, 68.2, 21.2;

LRMS (ES + APCI) *m/z*: calc. for $C_{30}H_{23}NO_5S$ 509.1, found 510.0 $[M+H]^+$; **HMRS** calc. for $C_{30}H_{22}NO_5S$ 508.1224 $[M–H]^-$, found 508.1227 $[M–H]^-$.

1-([1,1'-Biphenyl]-4-yl)butan-1-one (205)

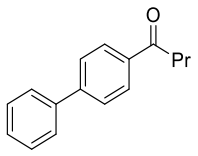

1-(4-Bromophenyl)butan-1-one (530 mg, 2.33 mmol), (4-phenyl)boronic acid (427 mg, 3.50 mmol) and K_2CO_3 (675 mg, 4.88 mmol) in dioxane:H_2O (3:1) (11.7 mL, 0.20 M), was purged with nitrogen for 10 minutes before Pd(dppf)Cl_2 (85 mg, 0.12 mmol) was added. The reaction mixture was subjected to microwave irradiation at 120 °C for 90 minutes. The reaction was then cooled to room temperature, diluted with CH_2Cl_2 (50 mL) and filtered through Celite®. The filtrate was subsequently concentrated under reduced pressure. The residue was purified *via* flash column chromatography (dry loading, Hexane 10:1 EtOAc isocratic) to afford the *title compound* (498 mg, 2.22 mmol, 95%) as an off-white solid. **mp** 94–96 °C; **IR**(ATR)/cm^{-1} 3056, 3036, 2958, 2934, 2870, 1677, 1602, 1402, 1372, 1219, 1004; **^{1}H NMR** (500 MHz, $CDCl_3$) δ (ppm) 8.04 (d, *J* 8.5 Hz, 2H, 2 × Ar*H*), 7.68 (d, *J* 8.5 Hz, 2H, 2 × Ar*H*), 7.65–7.61 (m, 2H, 2 × Ar*H*), 7.48 (app t, *J* 8.5 Hz, 2H, 2 × Ar*H*), 7.43–7.37 (m, 1H, Ar*H*), 2.98 (t, *J* 7.5 Hz, 2H, C$H_2$$CH_2CH_3$), 1.80 (app sextet, *J* 7.5 Hz, 2H, CH_2CH_2CH_3), 1.03 (t, *J* 7.5 Hz, 3H, CH_2CH_2CH_3); **^{13}C NMR** (125 MHz, $CDCl_3$) δ (ppm) 200.2, 145.7, 140.1, 136.0, 129.1, 128.8, 128.3, 127.4, 127.3, 40.7, 18.0, 14.1; **LRMS** (ES + APCI) *m/z*: calc. for $C_{16}H_{16}O$ 224.1, found 225.3 $[M+H]^+$; **HMRS** calc. for $C_{16}H_{15}O$ 223.1128 $[M–H]^-$, found 223.1133 $[M–H]^-$.

Isopropyl 4-([1,1'-biphenyl]-4-yl)-2-amino-5-methylthiophene-3-carboxylate (206)

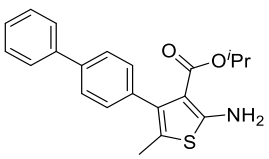

Following General Procedure D, isopropyl 2-cyanoacetate (1.27 g, 10.0 mmol) and 1-([1,1'-biphenyl]-4-yl)propan-1-one (1.05 g, 5.0 mmol), after purification *via* flash

column chromatography (dry loading, Hexane 10:1 EtOAc), afforded the *title compound* (589 mg, 1.68 mmol, 36%) as a yellow oil. **IR**(ATR)/cm^{-1} 3434, 3326, 3029, 2978, 1658, 1575, 1487, 1400, 1269, 1107; **^{1}H NMR** (400 MHz, $CDCl_3$) δ (ppm) 7.71–7.55 (m, 4H, 4 × Ar*H*), 7.53–7.44 (m, 3H, 3 × Ar*H*), 7.39 (tt, *J* 7.6 Hz, 1.2 Hz, 1H, Ar*H*), 7.30–7.25 (m, 1H, Ar*H*), 6.18 (br s, 1H, NH_2), 6.03 (br s, 1H, NH_2), 5.28 (septet, *J* 6.0 Hz, 0.5H, COOC*H*$(CH_3)_2$), 4.93 (septet, *J* 6.0 Hz, 0.5H, COOC*H*$(CH_3)_2$), 2.43 (s, 1.5 H, SCCH_3), 2.13 (s, 1.5 H, SCCH_3), 1.41 (d, *J* 6.0 Hz, 3H, COOCH(CH_3)$_2$), 0.92 (d, *J* 6.0 Hz, 3H, COOCH(CH_3)$_2$); **^{13}C NMR** (101 MHz, $CDCl_3$) δ (ppm) 165.9, 165.3, 162.9, 160.9, 141.4, 140.7, 139.7, 139.4, 137.5, 136.0, 133.4, 131.8, 130.3, 130.1, 129.3, 128.9, 128.8, 128.8, 127.5, 127.2, 127.2, 127.1, 127.1, 127.0, 126.2, 119.1, 117.1, 108.3, 107.5, 104.9, 67.2, 66.8, 22.3, 21.6, 16.5, 13.1 (4 carbons missing); **LRMS** (ES + APCI) *m/z*: calc. for $C_{21}H_{21}NO_2S$ 351.1 found 352.0 $[M+H]^+$; **HMRS** calc. for $C_{21}H_{22}NO_2S$ 352.1366 $[M+H]^+$, found 352.1368 $[M+H]^+$.

Isopropyl 4-([1,1'-biphenyl]-4-yl)-2-amino-5-ethylthiophene-3-carboxylate (207)

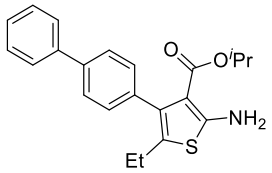

Following General Procedure D, isopropyl 2-cyanoacetate (567 mg, 4.46 mmol) and compound **205** (500 mg, 2.23 mmol), after purification *via* flash column chromatography (dry loading, Hexane 10:1 EtOAc), afforded the *title compound* (263 mg, 0.72 mmol, 29%) as a yellow oil. **IR**(ATR)/cm^{-1} 3430, 3318, 3025, 2971, 2928, 2868, 1658, 1573, 1485, 1396, 1262, 1186, 1104; **^{1}H NMR** (500 MHz, $CDCl_3$) δ (ppm) 7.65 (d, *J* 7.5 Hz, 2H, 2 × Ar*H*), 7.57 (d, *J* 7.5 Hz, 2H, 2 × Ar*H*), 7.47 (app t, *J* 7.5 Hz, 2H, 2 × Ar*H*), 7.36 (t, *J* 7.5 Hz, 1H, Ar*H*), 7.24 (d, *J* 7.5 Hz, 2H, 2 × Ar*H*), 6.00 (br s, 2H, NH_2), 4.88 (septet, *J* 6.0 Hz, 1H, COOC*H*$(CH_3)_2$), 2.48 (q, *J* 7.5 Hz, 2H, CH_2CH$_3$), 1.12 (t, *J* 7.5 Hz, 3H, CH$_2$CH_3), 0.87 (d, *J* 6.0 Hz, 6H, COOCH(CH_3)$_2$); **^{13}C NMR** (125 MHz, $CDCl_3$) δ (ppm) 165.4, 160.9, 141.4, 139.4, 137.6, 135.2, 130.2, 128.9, 127.2, 127.1, 126.2, 125.3, 107.4, 66.6, 21.6, 21.2, 16.6; **LRMS** (ES + APCI) *m/z*: calc. for $C_{22}H_{23}NO_2S$ 365.1 found 366.1 $[M+H]^+$; **HMRS** calc. for $C_{22}H_{24}NO_2S$ 366.1522 $[M+H]^+$, found 366.1523 $[M+H]^+$.

2-((4-([1,1'-Biphenyl]-4-yl)-3-(isopropoxycarbonyl)-5-methylthiophen-2-yl)carbamoyl)benzoic acid (208)

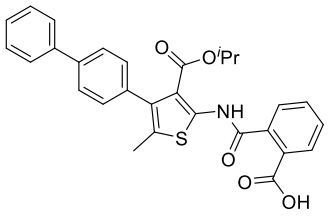

Following General Procedure E, compound **206** (270 mg, 0.77 mmol) and phthalic anhydride (114 mg, 0.77 mmol), after purification *via* flash column chromatography (dry loading, Hexane 3:1 EtOAc, CH_2Cl_2 95:5 MeOH), afforded the *title compound* (210 mg, 0.42 mmol, 55%) as an orange solid. **mp** 128–130 °C; **IR**(ATR)/cm^{-1} 3253, 3026, 2977, 2933, 1714, 1657, 1621, 1527, 1385, 1255, 1222, 1103; **^{1}H NMR** (500 MHz, DMSO-d_6) δ (ppm) (1:1 mixture of rotamers) 13.53 (br s, 1H, COO*H*), 12.25–11.80 (m, 1H, CON*H*), 7.92–7.88 (m, 1H, Ar*H*), 7.80–7.73 (m, 1H, Ar*H*), 7.73–7.67 (m, 3H, 3 × Ar*H*), 7.67–7.59 (m, 3H, 3 × Ar*H*), 7.59–7.52 (m, 1H, Ar*H*), 7.52–7.46 (m, 2H, 2 × Ar*H*), 7.45–7.32 (m, 1H, Ar*H*), 7.28–7.19 (m, 1H, Ar*H*), 5.12 (septet, *J* 6.0 Hz, 1H, COOC*H*(CH$_3$)$_2$), 4.78 (septet, *J* 6.0 Hz, 1H, COOC*H*(CH$_3$)$_2$), 2.39 (s, 1H, CC*H*$_3$), 2.19 (s, 2H, CC*H*$_3$), 1.30 (d, *J* 6.0 Hz, 2H, COOCH(C*H*$_3$)$_2$), 0.84 (d, *J* 6.0 Hz, 4H, COOCH(C*H*$_3$)$_2$); **^{13}C NMR** (125 MHz, DMSO-d_6) δ (ppm) (1:1 mixture of rotamers) 169.1, 168.9, 166.6, 165.2, 165.0, 164.6, 150.0, 147.6, 145.5, 140.5, 139.9, 139.7, 139.1, 138.2, 137.3, 136.4, 135.8, 135.6, 134.7, 133.0, 131.1, 130.8, 130.6, 130.4, 130.4, 130.0, 129.5, 129.5, 129.4, 129.3, 128.2, 128.1, 127.9, 127.6, 127.1, 127.0, 126.9, 126.4, 125.8, 115.6, 114.8, 114.1, 69.0, 68.1, 22.1, 21.5, 15.8, 13.2; **LRMS** (ES + APCI) *m/z*: calc. for $C_{29}H_{25}NO_5S$ 499.2, found 500.0 [M+H]$^+$; **HMRS** calc. for $C_{29}H_{24}NO_5S$ 498.1381 [M–H]$^+$, found 498.1388 [M–H]$^+$.

2-((4-([1,1'-Biphenyl]-4-yl)-5-ethyl-3-(isopropoxycarbonyl)thiophen-2-yl)carbamoyl)benzoic acid (209)

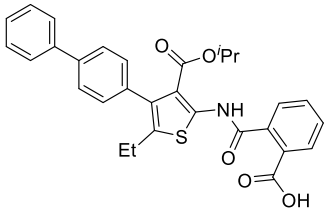

Following General Procedure E, compound **207** (90 mg, 0.25 mmol) and phthalic anhydride (36 mg, 0.25 mmol), after purification *via* flash column chromatography (dry loading, Hexane 4:1 EtOAc, CH_2Cl_2 95:5 MeOH), afforded the *title compound* (73 mg, 0.14 mmol, 58%) as an off-white solid. **mp** 132–134 °C; **IR**(ATR)/cm^{-1} 3255, 3071, 3025, 2963, 2926, 2852, 1725, 1682, 1653, 1528, 1385, 1299, 1255, 1223, 1098; **^{1}H NMR** (500 MHz, DMSO-d_6) δ (ppm) 13.41 (br s, 1H, COO*H*), 12.00 (br s, 1H, CON*H*), 7.89 (d, *J* 7.0 Hz, 1H, Ar*H*), 7.73–7.66 (m, 4H, 4 × Ar*H*), 7.66–7.57 (m, 3H, 3 × Ar*H*), 7.49 (app t, *J* 8.0 Hz, 2H, 2 × Ar*H*), 7.38 (t, *J* 7.0 Hz, 1H, Ar*H*), 7.26 (d, *J* 8.0 Hz, 2H, 2 × Ar*H*), 4.77 (septet, *J* 6.0 Hz, 1H, COOC*H*$(CH_3)_2$), 2.57 (q, *J* 7.5 Hz, 2H, C$H_2$$CH_3$), 1.14 (t, *J* 7.5 Hz, 3H, CH_2CH_3), 0.82 (d, *J* 6.0 Hz, 6H, COOCH(CH_3)$_2$); **^{13}C NMR** (125 MHz, DMSO-d_6) δ (ppm) 168.5, 166.1, 164.2, 145.1, 140.0, 138.7, 136.2, 136.0, 135.3, 133.6, 132.9, 130.6, 130.3, 130.0, 129.9, 129.0, 127.6, 127.4, 126.6, 125.9, 113.6, 67.5, 21.0, 20.6, 16.4; **LRMS** (ES + APCI) *m/z*: calc. for $C_{30}H_{27}NO_5S$ 513.2, found 514.2 $[M+H]^+$; **HMRS** calc. for $C_{30}H_{26}NO_5S$ 512.1537 $[M–H]^-$, found 512.1543 $[M–H]^-$.

2-((4-([1,1'-Biphenyl]-4-yl)-3-((benzyloxy)carbonyl)thiophen-2-yl)carbamoyl)-4,5-dichlorobenzoic acid (211)

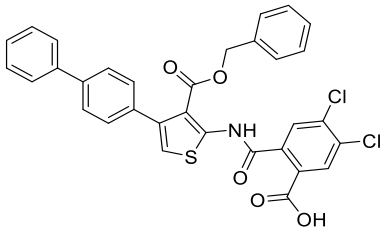

Following General Procedure E, compound **90** (50 mg, 0.13 mmol) and 5,6-dichloroisobenzofuran-1,3-dione (30 mg, 0.13 mmol), after purification *via* flash column chromatography (dry loading, Hexane 3:1 EtOAc, CH_2Cl_2 95:5 MeOH), afforded the *title compound* (38 mg, 0.06 mmol, 49%) as an off-white solid. **mp** 155–157 °C; **IR**(ATR)/cm^{-1} 3271, 3057, 2959, 1727, 1660, 1575, 1527, 1395, 1259, 1214; **^{1}H NMR** (500 MHz, DMSO-d_6) δ (ppm) 14.52 (br s, 1H, COO*H*), 8.06 (s, 1H, Ar*H*), 8.04 (s, 1H, Ar*H*), 7.67 (d, *J* 8.0 Hz, 2H, 2 × Ar*H*), 7.59 (d, *J* 8.0 Hz, 2H, 2 × Ar*H*), 7.49 (app t, *J* 8.0 Hz, 2H, 2 × Ar*H*), 7.41–7.33 (m, 3H, 3 × Ar*H*), 7.24–7.14 (m, 5H, 5 × Ar*H*), 7.08 (s, 1H, C=C*H*S), 5.21 (s, 2H, CH_2); **^{13}C NMR** (125 MHz, DMSO-d_6) δ (ppm) 166.8, 164.2, 163.7, 146.1, 139.8, 138.8, 138.2, 135.6, 135.5, 133.7, 132.9, 132.4, 131.9, 130.9, 128.9, 128.8, 128.1, 128.1, 128.0,

127.8, 127.4, 126.5, 126.2, 116.0, 114.5, 66.3; **LRMS** (ES + APCI) *m/z*: calc. for $C_{32}H_{21}{}^{35,37}Cl_2NO_5S$ 603.0, found 603.8 $[M+H]^+$; **HMRS** calc. for $C_{32}H_{20}{}^{35,35}Cl_2NO_5S$ 600.0445 $[M–H]^-$, found 600.0463 $[M–H]^-$.

2-((4-([1,1'-Biphenyl]-4-yl)-3-(isopropoxycarbonyl)-5-methylthiophen-2-yl)carbamoyl)-4,5-dichlorobenzoic acid (212)

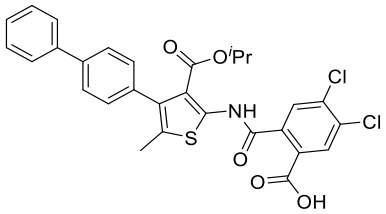

Following General Procedure E, compound **206** (50 mg, 0.14 mmol) and 5,6-dichloroisobenzofuran-1,3-dione (22 mg, 0.14 mmol), after purification *via* flash column chromatography (dry loading, Hexane 3:1 EtOAc, CH_2Cl_2 95:5 MeOH), afforded the *title compound* (42 mg, 0.07 mmol, 52%) as an off-white solid. **mp** 210–212 °C; **IR**(ATR)/cm^{-1} 3248, 3027, 2975, 1722, 1651, 1614, 1532, 1385, 1227, 1103; **^{1}H NMR** (500 MHz, DMSO-d_6) δ (ppm) 13.24 (br s, 1H, COO*H*), 8.04 (s, 1H, Ar*H*), 7.91 (s, 1H, Ar*H*), 7.73–7.66 (m, 4H, 4 × Ar*H*), 7.48 (app t, *J* 7.5 Hz, 2H, 2 × Ar*H*), 7.38 (t, *J* 7.0 Hz, 1H, Ar*H*), 7.25 (d, *J* 8.0 Hz, 2H, 2 × Ar*H*), 4.79 (septet, *J* 6.0 Hz, 1H, COOC*H*$(CH_3)_2$), 2.20 (s, 3H, CH_3), 0.89 (d, *J* 6.0 Hz, 6H, COOCH(CH_3)$_2$); **^{13}C NMR** (125 MHz, DMSO-d_6) δ (ppm) 166.8, 164.3, 163.8, 143.6, 139.9, 138.6, 135.8, 134.5, 134.1, 132.5, 132.1, 131.4, 130.3, 129.9, 128.9, 127.4, 126.5, 125.9, 125.4, 114.9, 79.2, 67.6, 21.0, 12.7; **LRMS** (ES + APCI) *m/z*: calc. for $C_{29}H_{23}{}^{35}Cl_2NO_5S$ 567.1, found 567.9 $[M+H]^+$; **HMRS** calc. for $C_{29}H_{24}{}^{35}Cl_2NO_5S$ 568.0747 $[M+H]^+$, found 568.0743 $[M+H]^+$.

4,5-Dichloro-2-((3-(isopropoxycarbonyl)-4-(4-phenethylphenyl)thiophen-2-yl)carbamoyl)benzoic acid (213)

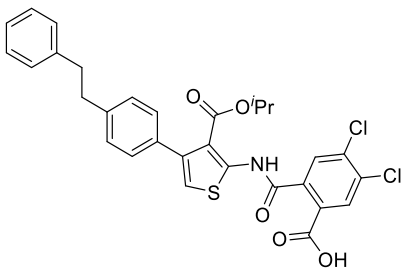

Following General Procedure E, compound **184** (50 mg, 0.14 mmol) and 5,6-dichloroisobenzofuran-1,3-dione (30 mg, 0.14 mmol), after purification *via* flash column chromatography (dry loading, Hexane 2:1 EtOAc, CH_2Cl_2 95:5 MeOH), afforded the *title compound* (75 mg, 0.13 mmol, 94%) as an off-white solid. **mp** 141–142 °C; **IR**(ATR)/cm^{-1} 3233, 3024, 2977, 1722, 1651, 1614, 1525, 1395, 1259, 1225, 1101; **^{1}H NMR** (500 MHz, DMSO-d_6) δ (ppm) 13.79 (br s, 1H, COO*H*), 8.05 (s, 1H, Ar*H*), 7.98 (s, 1H, Ar*H*), 7.30–7.14 (m, 9H, 9 × Ar*H*), 6.94 (s, 1H, C=C*H*S), 4.92 (septet, *J* 6.0 Hz, 1H, COOC*H*$(CH_3)_2$), 2.90 (s, 4H, CH_2CH_2), 1.00 (d, *J* 6.0 Hz, 6H, COOCH(CH_3)$_2$); **^{13}C NMR** (125 MHz, DMSO-d_6) δ (ppm) 169.4, 167.4, 166.7, 164.1, 163.9, 145.9, 141.4, 140.3, 138.7, 134.4, 132.7, 132.2, 131.9, 130.6, 128.4, 128.3, 128.2, 127.7, 125.8, 115.2, 114.7, 68.1, 37.0, 36.6, 21.2; **LRMS** (ES + APCI) *m/z*: calc. for $C_{30}H_{25}{}^{35}Cl_2NO_5S$ 581.1, found 581.9 $[M+H]^+$; **HMRS** calc. for $C_{30}H_{26}{}^{35}Cl_2NO_5S$ 582.0903 $[M+H]^+$, found 582.0900 $[M+H]^+$.

Benzyl 2-amino-4-(4-phenethylphenyl)thiophene-3-carboxylate (214)

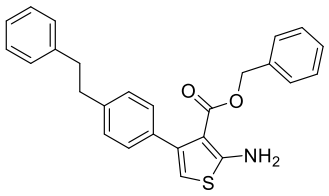

Following General Procedure D, benzyl 2-cyanoacetate (1.75 g, 10.0 mmol) and 1-(4-phenethylphenyl)ethan-1-one (1.12 g, 5.0 mmol), after purification *via* flash column chromatography (dry loading, Hexane 10:1 EtOAc), afforded the *title compound* (579 mg, 1.40 mmol, 28%) as an off-white solid. **mp** 104–106 °C; **IR**(ATR)/cm^{-1} 3433, 3327, 3107, 3026, 2918, 2854, 1644, 1584, 1484, 1259, 1117; **^{1}H NMR** (500 MHz, $CDCl_3$) δ (ppm) 7.32–7.27 (m, 2H, 2 × Ar*H*), 7.24–7.17 (m, 8H, 8 × Ar*H*), 7.05 (d, *J* 8.0 Hz, 2H, 2 × Ar*H*), 6.95–6.91 (m, 2H, 2 × Ar*H*), 6.09 (br s, 2H, NH_2), 6.04 (s, 1H, C=C*H*S), 5.07 (s, 2H, OCH_2), 2.91 (s, 4H, CH_2CH_2); **^{13}C NMR** (125 MHz, $CDCl_3$) δ (ppm) 165.6, 164.4, 142.1, 141.7, 140.6, 136.2, 136.0, 129.1, 128.6, 128.5, 128.3, 127.9, 127.8, 127.6, 126.1, 106.0, 105.6, 65.5, 38.0, 37.9; **LRMS** (ES + APCI) *m/z*: calc. for $C_{26}H_{23}NO_2S$ 413.1 found 414.0 $[M+H]^+$; **HMRS** calc. for $C_{26}H_{24}NO_2S$ 414.1522 $[M+H]^+$, found 414.1521 $[M+H]^+$.

2-((3-((Benzyloxy)carbonyl)-4-(4-phenethylphenyl)thiophen-2-yl)carbamoyl)benzoic acid (215)

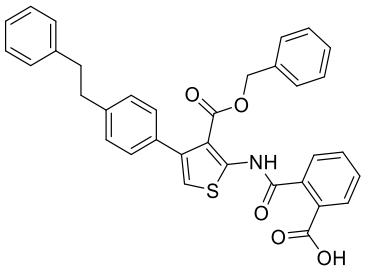

Following General Procedure E, compound **214** (50 mg, 0.12 mmol) and phthalic anhydride (18 mg, 0.12 mmol), after purification *via* flash column chromatography (dry loading, Hexane 3:1 EtOAc, CH_2Cl_2 9:1 MeOH), afforded the *title compound* (60 mg, 0.11 mmol, 68%) as an off-white solid. **mp** 113–115 °C; **IR**(ATR)/cm^{-1} 3059, 3026, 2921, 2853, 1724, 1651, 1621, 1521, 1395, 1281, 1212; **^{1}H NMR** (500 MHz, DMSO-d_6) δ (ppm) 13.83 (br s, 1H, COO*H*), 13.32 (br s, 1H, CON*H*), 7.87 (d, *J* 7.0 Hz, 1H, Ar*H*), 7.71 (d, *J* 7.0 Hz, 1H, Ar*H*), 7.58–7.50 (m, 2H, 2 × Ar*H*), 7.31–7.24 (m, 4H, 4 × Ar*H*), 7.24–7.14 (m, 8H, 8 × Ar*H*), 7.09 (d, *J* 7.0 Hz, 2H, 2 × Ar*H*), 6.93 (s, 1H, C=C*H*S), 5.15 (s, 2H, CH_2), 2.88 (s, 4H, CH_2CH_2); **^{13}C NMR** (125 MHz, DMSO-d_6) δ (ppm) 167.9, 166.3, 164.5, 148.8, 147.2, 141.6, 140.3, 138.6, 138.0, 135.5, 135.2, 130.2, 130.1, 130.0 128.3, 128.2, 128.1, 128.0, 127.8, 125.8, 115.2, 113.2, 66.1, 36.9, 36.8; **LRMS** (ES + APCI) *m/z*: calc. for $C_{34}H_{27}NO_5S$ 561.2, found 562.0 $[M+H]^+$; **HMRS** calc. for $C_{34}H_{26}NO_5S$ 560.1537 $[M–H]^-$, found 560.1547 $[M–H]^-$.

3-((3-(Isopropoxycarbonyl)-4-(4-phenethylphenyl)thiophen-2-yl)carbamoyl)bicyclo[2.2.1]hept-5-ene-2-carboxylic acid (216)

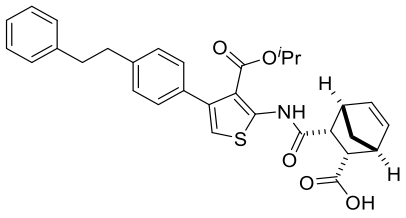

Following General Procedure E, compound **164** (150 mg, 0.41 mmol) and (3a*R*,4*S*,7*R*,7a*S*)-3a,4,7,7a-tetrahydro-4,7-methanoisobenzofuran-1,3-dione (68 mg, 0.41 mmol), after purification *via* flash column chromatography (dry loading, Petroleum ether 5:1 EtOAc, CH_2Cl_2 9:1 MeOH), afforded the *title compound* (81 mg, 0.15 mmol, 37%) as an off-white solid. **mp** 157–159 °C; **IR**(ATR)/cm^{-1} 3280 br, 3100, 2986, 2944, 1737, 1687, 1646, 1527, 1398, 1298, 1236, 1103; **^{1}H NMR** (500 MHz, DMSO-d_6) δ (ppm) 12.17 (br s, 1H, COO*H*), 11.09 (s, 1H,

CON*H*), 7.30–7.20 (m, 4H, 4 × Ar*H*), 7.22–7.17 (m, 3H, 3 × Ar*H*), 7.16 (d, *J* 8.0 Hz, 2H, 2 × Ar*H*), 6.83 (s, 1H, C=C*H*S), 6.29–6.26 (m, 2H, *H*C=C*H*), 4.93 (septet, *J* 6.0 Hz, 1H, COOC*H*(CH_3)$_2$), 3.02 (br s, 1H, COC*H*C*H*), 2.99 (br s, 1H, COC*H*C*H*), 2.97–2.92 (m, 4H, CH_2CH_2), 2.85 (d, *J* 10.0 Hz, 1H, C(C*H*H)C), 2.57 (d, *J* 10.0 Hz, 1H, C(CH*H*)C), 2.18 (d, *J* 8.0 Hz, 1H, CC*H*C), 1.37 (d, *J* 8.0 Hz, 1H, CC*H*C), 0.95 (d, *J* 6.0 Hz, 6H, COOCH(CH_3)$_2$); **^{13}C NMR** (125 MHz, $CDCl_3$) δ (ppm) 174.0, 170.8, 164.3, 148.1, 141.4, 140.2, 138.9, 138.3, 137.8, 134.8, 128.7, 128.3, 128.2, 127.4, 125.8, 115.0, 111.9, 67.9, 47.8, 47.6, 45.9, 45.0, 44.3, 37.1, 36.6, 21.1; **LRMS** (ES + APCI) *m/z*: calc. for $C_{31}H_{31}NO_5S$ 529.2, found 530.0 $[M+H]^+$; **HMRS** calc. for $C_{31}H_{30}NO_5S$ 528.1850 $[M–H]^-$, found 528.1856 $[M–H]^-$.

3-((3-(Isopropoxycarbonyl)-4-(4-phenethylphenyl)thiophen-2-yl)carbamoyl)bicyclo[2.2.1]hept-5-ene-2-carboxylic acid (217)

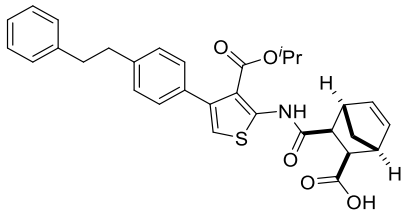

Following General Procedure E, compound **164** (100 mg, 0.27 mmol) and (3a*R*,4*R*,7*S*,7a*S*)-3a,4,7,7a-tetrahydro-4,7-methanoisobenzofuran-1,3-dione (45 mg, 0.27 mmol), after purification *via* flash column chromatography (dry loading, Petroleum ether 5:1 EtOAc, CH_2Cl_2 9:1 MeOH), afforded the *title compound* (30 mg, 0.06 mmol, 21%) as an off-white solid. **mp** 132–134 °C; **IR**(ATR)/cm^{-1} 3273 br, 3089, 2962, 2934, 1739, 1696, 1651, 1530, 1400, 1300, 1238, 1104; **^{1}H NMR** (500 MHz, DMSO-d_6) δ (ppm) 7.31–7.27 (m, 2H, 2 × Ar*H*), 7.24–7.18 (m, 5H, 5 × Ar*H*), 7.17 (d, *J* 8.0 Hz, 2H, 2 × Ar*H*), 7.09 (s, 1H, C=C*H*S), 6.29–6.24 (m, 2H, *H*C=C*H*), 4.93 (septet, *J* 6.0 Hz, 1H, COOC*H*(CH_3)$_2$), 3.53–3.47 (m, 4H, 2 × COC*H*C*H*), 2.94–2.88 (m, 4H, CH_2CH_2), 1.79 (d, *J* 9.0 Hz, 1H, C(C*H*H)C), 1.61 (d, *J* 9.0 Hz, 1H, C(CH*H*)C), 1.00 (d, *J* 6.0 Hz, 6H, COOCH(CH_3)$_2$); **^{13}C NMR** (125 MHz, $CDCl_3$) δ (ppm) 173.0, 169.7, 164.4, 148.7, 141.4, 140.1, 138.9, 135.7, 134.9, 134.1, 128.8, 128.3, 128.2, 127.4, 125.8, 114.7, 111.3, 67.8, 49.2, 49.1, 48.4, 46.2, 45.7, 37.1, 36.6, 21.1; **LRMS** (ES + APCI) *m/z*: calc. for $C_{31}H_{31}NO_5S$ 529.2, found 530.0 $[M+H]^+$; **HMRS** calc. for $C_{31}H_{30}NO_5S$ 528.1850 $[M–H]^-$, found 528.1856 $[M–H]^-$.

Methyl 2-amino-4-(4-phenethylphenyl)thiophene-3-carboxylate (219)

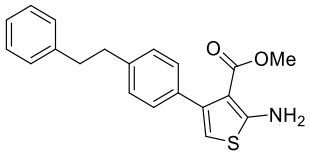

Following General Procedure D, methyl cyanoacetate (884 mg, 8.92 mmol) and 1-(4-phenethylphenyl)ethan-1-one (1.00 g, 4.46 mmol), after purification *via* flash column chromatography (dry loading, Hexane 10:1 EtOAc), afforded the *title compound* (559 mg, 1.66 mmol, 37%) as a pale yellow solid. **mp** 114–116 °C; **IR**(ATR)/cm^{-1} 3458, 3305, 3177, 3097, 3021, 2945, 2854, 1669, 1602, 1496, 1435, 1396, 1309, 1212, 1182, 1100; **^{1}H NMR** (500 MHz, $CDCl_3$) δ (ppm) 7.33–7.27 (m, 2H, 2 × Ar*H*), 7.25–7.19 (m, 5H, 5 × Ar*H*), 7.15 (d, *J* 8.0 Hz, 2H, 2 × Ar*H*), 6.07 (br s, 2H, NH_2), 6.06 (s, 1H, C=C*H*S), 3.59 (s, 3H, CH_3), 3.01–2.93 (m, 4H, CH_2CH_2); **^{13}C NMR** (125 MHz, $CDCl_3$) δ (ppm) 166.2, 164.1, 142.0, 141.6, 140.5, 136.0, 128.9, 128.6, 128.5, 127.6, 126.0, 105.9, 105.7, 50.7, 38.0, 37.8; **LRMS** (ES + APCI) *m/z*: calc. for $C_{20}H_{19}NO_2S$ 337.1 found 338.0 $[M+H]^+$; **HMRS** calc. for $C_{20}H_{18}NO_2S$ 336.1064 $[M–H]^-$, found 336.1072 $[M–H]^-$.

2-Amino-*N*-ethyl-4-(4-phenethylphenyl)thiophene-3-carboxamide (220)

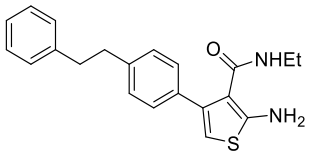

Following General Procedure I, compound **219** (150 mg, 0.45 mmol), ethanamine hydrochloride (36 mg, 0.45 mmol) and NEt_3 (124 μL, 0.90 mmol), after purification *via* flash column chromatography (dry loading, Petroleum ether 4:1 EtOAc, isocratic), afforded the *title compound* (60 mg, 0.17 mmol, 38%) as an off-white solid. **mp** 113–115 °C; **IR**(ATR)/cm^{-1} 3378, 3263, 3058, 2960, 1606, 1578, 1509, 1481, 1390, 1249, 1073; **^{1}H NMR** (500 MHz, $CDCl_3$) δ (ppm) 7.31–7.26 (m, 4H, 4 × Ar*H*), 7.24–7.17 (m, 5H, 5 × Ar*H*), 6.19 (br s, 2H, NH_2), 6.05 (s, 1H, C=C*H*S), 5.04 (app br s, 1H, CON*H*), 3.14 (app sextet, *J* 7.0 Hz, 2H, CONHCH_2CH_3), 3.02–2.92 (br s, 4H, C_6H_5CH_2CH_2), 0.82 (t, *J* 7.0 Hz, 3H, CONHCH_2CH_3); **^{13}C NMR** (125 MHz, $CDCl_3$) δ (ppm) 165.9, 161.6, 142.1, 141.5, 139.1, 134.8, 129.4, 128.9, 128.6, 128.5, 126.2, 108.7, 105.7, 37.9, 37.6, 33.8, 14.6; **LRMS** (ES + APCI) *m/z*:

calc. for $C_{21}H_{22}N_2OS$ 350.1, found 351.0 $[M+H]^+$; **HMRS** calc. for $C_{21}H_{23}N_2OS$ 351.1526 $[M+H]^+$, found 351.1527 $[M+H]^+$.

2-Amino-*N*-isopropyl-4-(4-phenethylphenyl)thiophene-3-carboxamide (221)

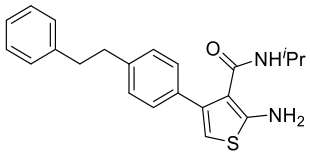

Following General Procedure I, compound **219** (200 mg, 0.59 mmol) and isopropylamine (51 µL, 0.59 mmol), after purification *via* flash column chromatography (dry loading, Petroleum ether 5:1 EtOAc, isocratic), afforded the *title compound* (160 mg, 0.55 mmol, 74%) as an off-white solid. **mp** 98–100 °C; **IR**(ATR)/cm^{-1} 3393, 3274, 3153, 3021, 2958, 1623, 1591, 1511, 1495, 1452, 1385, 1251, 1178, 818; **^{1}H NMR** (400 MHz, $CDCl_3$) δ (ppm) 7.33–7.26 (m, 4H, 4 × Ar*H*), 7.25–7.18 (m, 5 H, 5 × Ar*H*), 6.19 (br s, 2H, NH_2), 6.05 (s, 1H, C=C*H*S), 4.92 (d, *J* 6.8 Hz, 1H, CON*H*), 4.06–3.92 (m, 1H, CONHC*H*$(CH_3)_2$), 3.03–2.91 (m, 4H, CH_2CH_2), 0.84 (d, *J* 6.4 Hz, 6H, CONHCH(CH_3)$_2$); **^{13}C NMR** (101 MHz, $CDCl_3$) δ (ppm) 165.1, 161.5, 142.1, 141.5, 139.1, 134.9, 129.5, 128.9, 128.8, 128.6, 126.2, 108.9, 105.6, 40.8, 38.0, 37.6, 22.6; **LRMS** (ES + APCI) *m/z*: calc. for $C_{22}H_{24}N_2OS$ 364.2, found 365.0 $[M+H]^+$; **HMRS** calc. for $C_{22}H_{25}N_2OS$ 365.1682 $[M+H]^+$, found 365.1683 $[M+H]^+$.

2-Amino-*N*-cyclopropyl-4-(4-phenethylphenyl)thiophene-3-carboxamide (222)

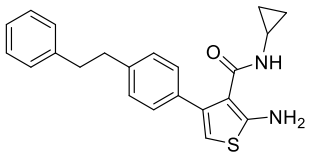

Following General Procedure I, compound **219** (150 mg, 0.45 mmol) and cyclopropanamine (31 µL, 0.45 mmol), after purification *via* flash column chromatography (dry loading, Petroleum ether 2:1 EtOAc, isocratic), afforded the *title compound* (112 mg, 0.31 mmol, 69%) as a pale yellow solid. **mp** 96–98 °C; **IR**(ATR)/cm^{-1} 3398, 3268, 3025, 2941, 2854, 1604, 1580, 1511, 1495, 1454, 1387, 1314, 1264, 1028; **^{1}H NMR** (500 MHz, $CDCl_3$) δ (ppm) 7.30 (app t, *J* 7.5 Hz, 2H, 2 × Ar*H*), 7.25–7.19 (m, 7H, 7 × Ar*H*), 6.25 (br s, 2H, NH_2), 6.03 (s, 1H, C=C*H*S),

5.14 (app br s, 1H, CON*H*), 3.01–2.92 (m, 4H, $C_6H_5CH_2CH_2$), 2.61 (app octet, *J* 3.5 Hz, 1H, CONHC*H*), 0.61 (app q, *J* 6.0 Hz, 2H, CONHCH(CH_2)CH_2) 0.09–0.04 (m, 2H, CONHCH(CH_2)CH_2); **^{13}C NMR** (125 MHz, $CDCl_3$) δ (ppm) 167.4, 161.9, 142.2, 141.5, 139.0, 134.7, 129.4, 128.9, 128.6, 126.2, 108.3, 105.6, 37.9, 37.6, 22.1, 6.6 (1 carbon missing); **LRMS** (ES + APCI) *m/z*: calc. for $C_{22}H_{22}N_2OS$ 362.1, found 363.0 $[M+H]^+$; **HMRS** calc. for $C_{22}H_{22}N_2OSNa$ 385.1335 $[M+Na]^+$, found 385.1336 $[M+Na]^+$.

2-Amino-*N*-cyclobutyl-4-(4-phenethylphenyl)thiophene-3-carboxamide (223)

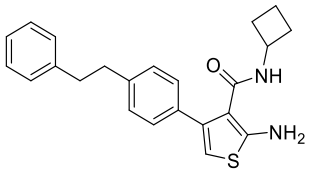

Following General Procedure I, compound **219** (150 mg, 0.45 mmol) and cyclobutanamine (38 μL, 0.45 mmol), after purification *via* flash column chromatography (dry loading, Petroleum ether 4:1 EtOAc, isocratic), afforded the *title compound* (128 mg, 0.34 mmol, 77%) as a pale yellow solid. **mp** 107–109 °C; **IR**(ATR)/cm^{-1} 3389, 3264, 3099, 2973, 2928, 2854, 1619, 1582, 1504, 1452, 1389, 1316, 1257, 1076; **^{1}H NMR** (500 MHz, $CDCl_3$) δ (ppm) 7.33–7.27 (m, 4H, 4 × Ar*H*), 7.27–7.24 (m, 4H, 4 × Ar*H*), 7.23–7.19 (m, 3H, 3 × Ar*H*), 6.22 (br s, 2H, NH_2), 6.05 (s, 1H, C=C*H*S), 5.14 (d, *J* 5.5 Hz, 1H, CON*H*), 4.30 (app sextet, *J* 8.0 Hz, 1H, CONHC*H*), 3.03–2.93 (m, 4H, $C_6H_5CH_2CH_2$), 2.19–2.11 (m, 2H, CONHCH(CH_2)CH_2), 1.64–1.48 (m, 2H, CONHCH(CH_2)CH_2) 1.38–1.24 (m, 2H, CONHCH(CH_2)CH_2CH_2); **^{13}C NMR** (125 MHz, $CDCl_3$) δ (ppm) 164.9, 161.8, 142.3, 141.5, 139.1, 134.9, 129.6, 128.9, 128.6, 126.2, 108.5, 105.6, 44.2, 38.1, 37.6, 31.1, 15.3 (1 carbon missing); **LRMS** (ES + APCI) *m/z*: calc. for $C_{23}H_{24}N_2OS$ 376.2, found 377.0 $[M+H]^+$; **HMRS** calc. for $C_{23}H_{25}N_2OS$ 377.1667 $[M+H]^+$, found 377.1666 $[M+H]^+$.

2-Amino-*N*-cyclopentyl-4-(4-phenethylphenyl)thiophene-3-carboxamide (224)

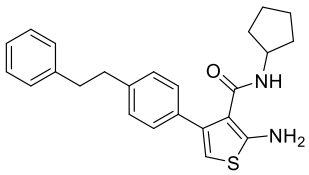

Following General Procedure I, compound **219** (150 mg, 0.45 mmol) and cyclopentanamine (44 μL, 0.45 mmol), after purification *via* flash column chromatography (dry loading, Petroleum ether 5:1 EtOAc, isocratic), afforded the *title compound* (143 mg, 0.37 mmol, 82%) as a pale yellow solid. **mp** 119–121 °C; **IR**(ATR)/cm^{-1} 3395, 3266, 3095, 2960, 2861, 1600, 1580, 1504, 1452, 1323, 1240, 1076; **^{1}H NMR** (500 MHz, $CDCl_3$) δ (ppm) 7.34–7.26 (m, 6H, 6 × Ar*H*), 7.26–7.19 (m, 3H, 3 × Ar*H*), 6.23 (br s, 2H, NH_2), 6.05 (s, 1H, C=C*H*S), 5.09 (d, *J* 6.0 Hz, 1H, CON*H*), 4.14 (app sextet, *J* 7.0 Hz, 1H, CONHC*H*), 3.01–2.91 (m, 4H, $C_6H_5CH_2CH_2$), 1.72 (app sextet, *J* 6.0 Hz, 2H, CONHCH(CH_2CH_2)CH_2CH_2) 1.48–1.38 (m, 2H, CONHCH(CH_2CH_2)CH_2CH_2), 1.31–1.21 (m, 2H, CONHCH(CH_2CH_2)CH_2CH_2), 1.06–0.97 (m, 2H, CONHCH(CH_2CH_2)CH_2CH_2); **^{13}C NMR** (125 MHz, $CDCl_3$) δ (ppm) 165.4, 161.5, 142.2, 141.6, 139.1, 135.0, 129.5, 128.9, 128.6, 128.5, 126.2, 108.9, 105.6, 50.7, 38.1, 37.7, 35.1, 23.5; **LRMS** (ES + APCI) *m/z*: calc. for $C_{24}H_{26}N_2OS$ 390.2, found 391.0 $[M+H]^+$; **HMRS** calc. for $C_{24}H_{27}N_2OS$ 391.1839 $[M+H]^+$, found 391.1840 $[M+H]^+$.

2-Amino-*N*-cyclohexyl-4-(4-phenethylphenyl)thiophene-3-carboxamide (225)

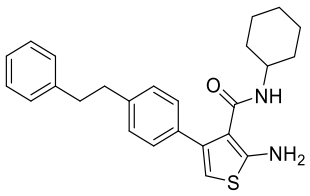

Following General Procedure I, compound **219** (150 mg, 0.45 mmol) and cyclohexanamine (51 μL, 0.45 mmol), after purification *via* flash column chromatography (dry loading, Petroleum ether 5:1 EtOAc, isocratic), afforded the *title compound* (130 mg, 0.32 mmol, 72%) as an pale yellow solid. **mp** 102–104 °C; **IR**(ATR)/cm^{-1} 3396, 3270, 3021, 2926, 2852, 1619, 1582, 1504, 1452, 1325, 1257; **^{1}H NMR** (500 MHz, $CDCl_3$) δ (ppm) 7.33–7.27 (m, 4H, 4 × Ar*H*), 7.25–7.19 (m, 5H, 5 × Ar*H*), 6.22 (br s, 2H, NH_2), 6.05 (s, 1H, C=C*H*S), 5.09 (d, *J* 6.0 Hz, 1H, CON*H*), 3.80–3.72 (m, 1H, CONHC*H*), 3.02–2.91 (m, 4H, $C_6H_5CH_2CH_2$), 1.64 (dd, *J* 12.0 Hz, 3.5 Hz, 2H, CONHCH(CH_2CH_2)CH_2CH_2) 1.49–1.33 (m, 3H, CONHCH(CH_2CH_2)$CH_2C(H)H$), 1.30–1.20 (m, 2H, CONHCH(CH_2CH_2)CH_2CH_2), 1.05 (app q, *J* 12.0 Hz, 1H, CONHCH(CH_2CH_2)$CH_2C(H)H$), 0.84–0.74 (m, 2H, CONHCH(CH_2CH_2)$CH_2CH_2CH_2$); **^{13}C NMR** (125 MHz, $CDCl_3$) δ (ppm) 165.1,

161.6, 142.2, 141.5, 139.1, 134.9, 129.6, 128.9, 128.6, 128.5, 126.2, 108.9, 105.6, 47.2, 38.1, 37.7, 32.6, 25.6, 24.3; **LRMS** (ES + APCI) *m/z*: calc. for $C_{25}H_{28}N_2OS$ 404.2, found 405.1 $[M+H]^+$; **HMRS** calc. for $C_{25}H_{29}N_2OS$ 405.1995 $[M+H]^+$, found 405.1994 $[M+H]^+$.

2-Amino-*N*-cycloheptyl-4-(4-phenethylphenyl)thiophene-3-carboxamide (226)

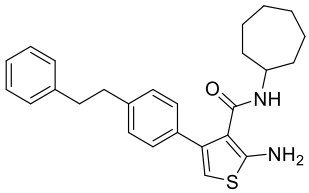

Following General Procedure I, compound **219** (150 mg, 0.45 mmol) and cycloheptanamine (57 μL, 0.45 mmol), after purification *via* flash column chromatography (dry loading, Petroleum ether 5:1 EtOAc, isocratic), afforded the *title compound* (110 mg, 0.26 mmol, 59%) as a pale yellow solid. **mp** 38–40 °C; **IR**(ATR)/cm^{-1} 3382, 3270, 3021, 2909, 2807, 1619, 1561, 1509, 1452, 1385, 1297, 1268, 1113; **^{1}H NMR** (400 MHz, $CDCl_3$) δ (ppm) 7.34–7.28 (m, 4H, 4 × Ar*H*), 7.28–7.26 (m, 1H, Ar*H*), 7.26–7.19 (m, 3H, 3 × Ar*H*), 6.23 (br s, 2H, NH_2), 6.04 (s, 1H, C=C*H*S), 5.14 (d, *J* 7.6 Hz, 1H, CON*H*), 3.94 (app nonet, *J* 5.0 Hz, 1H, CONHC*H*), 3.02–2.91 (m, 4H, $C_6H_5CH_2CH_2$), 1.73–1.74 (m, 2H, CONHCH($CH_2CH_2CH_2$)$CH_2CH_2CH_2$), 1.53–1.43 (m, 2H, CONHCH($CH_2CH_2CH_2$)$CH_2CH_2CH_2$), 1.40–1.23 (m, 6H, CONHCH($CH_2CH_2CH_2$)$CH_2CH_2CH_2$), 1.12–1.02 (m, 2H, CONHCH($CH_2CH_2CH_2$)$CH_2CH_2CH_2$); **^{13}C NMR** (101 MHz, $CDCl_3$) δ (ppm) 164.8, 161.6, 142.1, 141.6, 139.1, 135.0, 129.6, 128.9, 128.6, 128.5, 126.2, 108.8, 105.5, 49.4, 38.1, 37.7, 34.7, 28.3, 23.8; **LRMS** (ES + APCI) *m/z*: calc. for $C_{26}H_{30}N_2OS$ 418.2, found 419.0 $[M+H]^+$; **HMRS** calc. for $C_{26}H_{31}N_2OS$ 419.2152 $[M+H]^+$, found 419.2151 $[M+H]^+$.

2-Amino-*N*-((1*S*,4*R*)-bicyclo[2.2.1]heptan-2-yl)-4-(4-phenethylphenyl)thiophene-3-carboxamide (227)

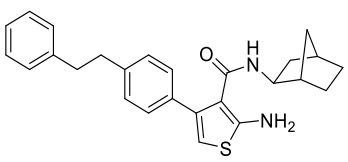

Following General Procedure I, compound **219** (150 mg, 0.45 mmol) and (1*R*,4*S*)-bicyclo[2.2.1]heptan-2-amine (53 μL, 0.45 mmol), after purification *via* flash column chromatography (dry loading, Petroleum ether 5:1 EtOAc, isocratic), afforded the *title compound* (127 mg, 0.31 mmol, 69%) as a pale yellow solid. **mp** 83–85 °C; **IR**(ATR)/cm^{-1} 3421, 3383, 3264, 3021, 2947, 2909, 2867, 1619, 1582, 1511, 1474, 1452, 1390, 1318, 1253, 1076; **^{1}H NMR** (500 MHz, $CDCl_3$) δ (ppm) 7.34–7.26 (m, 6H, 6 × Ar*H*), 7.25–7.20 (m, 3H, 3 × Ar*H*), 6.24 (br s, 2H, NH_2), 6.04 (s, 1H, C=C*H*S), 5.02 (d, *J* 6.5 Hz, 1H, CON*H*), 3.68–3.61 (m, 1H, CONHC*H*), 3.00–2.89 (m, 4H, $C_6H_5CH_2CH_2$), 2.06–1.91 (m, 2H, 2 × bicycle C*H*), 1.62–1.55 (m, 1H, bicycle C*H*), 1.45–1.30 (m, 2H, 2 × bicycle C*H*), 1.20–1.12 (m, 1H, bicycle C*H*), 1.06–0.99 (m, 1H, bicycle C*H*), 0.91 (d, *J* 10.0 Hz, 1H, bicycle C*H*), 0.64–0.57 (m, 2H, 2 × bicycle C*H*); **^{13}C NMR** (125 MHz, $CDCl_3$) δ (ppm) 165.1, 161.6, 142.3, 141.6, 139.0, 135.1, 129.6, 128.9, 128.6, 128.5, 126.3, 108.8, 105.5, 52.2, 42.4, 40.2, 38.2, 37.8, 35.5, 35.4, 28.3, 26.5; **LRMS** (ES + APCI) *m/z*: calc. for $C_{26}H_{28}N_2OS$ 416.2, found 417.0 $[M+H]^+$; **HMRS** calc. for $C_{26}H_{29}N_2OS$ 417.1995 $[M+H]^+$, found 417.1996 $[M+H]^+$.

2-Amino-*N*-(cyclohexylmethyl)-4-(4-phenethylphenyl)thiophene-3-carboxamide (228)

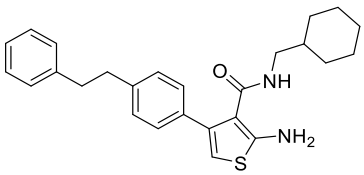

Following General Procedure I, compound **219** (150 mg, 0.45 mmol) and cyclohexylmethanamine (58 μL, 0.45 mmol), after purification *via* flash column chromatography (dry loading, Petroleum ether 5:1 EtOAc, isocratic), afforded the *title compound* (134 mg, 0.32 mmol, 72%) as a pale yellow solid. **mp** 44–46 °C; **IR**(ATR)/cm^{-1} 3389, 3276, 3023, 2922, 2850, 1612, 1593, 1515, 1448, 1385, 1318, 1270; **^{1}H NMR** (500 MHz, $CDCl_3$) δ (ppm) 7.33–7.28 (m, 4H, 4 × Ar*H*), 7.26–7.19 (m, 5H, 5 × Ar*H*), 6.28 (br s, 2H, NH_2), 6.04 (s, 1H, C=C*H*S), 5.20 (app br s, 1H, CON*H*), 3.00–2.92 (m, 6H, $C_6H_5CH_2CH_2$, CONHCH_2), 1.65–1.55 (m, 3H, $CONHCH_2CH(CH_2CH_2CH_2)CH_2CH_2$), 1.34 (d, *J* 13.0 Hz, 2H, $CONHCH_2CH(CH_2CH_2CH_2)CH_2CH_2$), 1.15–1.00 (m, 4H, $CONHCH_2CH(CH_2CH_2CH_2)CH_2CH_2$), 0.70–0.60 (m, 2H,

$CONHCH_2CH(CH_2CH_2C\mathit{H}_2)CH_2CH_2$); **^{13}C NMR** (125 MHz, $CDCl_3$) δ (ppm) 166.0, 161.5, 142.2, 141.6, 139.1, 135.1, 129.5, 128.9, 128.6, 128.5, 126.3, 108.9, 105.8, 45.4, 38.0, 37.8, 30.8, 26.4, 25.9 (1 carbon missing); **LRMS** (ES + APCI) *m/z*: calc. for $C_{26}H_{30}N_2OS$ 418.2, found 419.1 $[M+H]^+$; **HMRS** calc. for $C_{26}H_{30}N_2OSNa$ 441.1963 $[M+Na]^+$, found 441.1962 $[M+Na]^+$.

2-Amino-4-(4-phenethylphenyl)-*N*-(prop-2-yn-1-yl)thiophene-3-carboxamide (229)

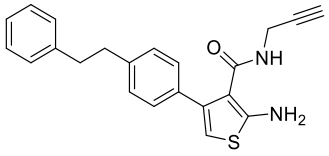

Following General Procedure I, compound **219** (150 mg, 0.45 mmol) and prop-2-yn-1-amine (30 μL, 0.45 mmol), after purification *via* flash column chromatography (dry loading, Petroleum ether 5:1 EtOAc, isocratic), afforded the *title compound* (64 mg, 0.18 mmol, 40%) as an off-white solid. **mp** 76–78 °C; **IR**(ATR)/cm^{-1} 3411, 3309, 3266, 3023, 2919, 2852, 1606, 1573, 1521, 1495, 1468, 1307, 1257; **^{1}H NMR** (400 MHz, $CDCl_3$) δ (ppm) 7.33–7.27 (m, 4H, 4 × Ar*H*), 7.25-–7.17 (m, 5H, 5 × Ar*H*), 6.29 (br s, 2H, NH_2), 6.05 (s, 1H, C=C*H*S), 5.29 (br s, 1H, CON*H*), 3.90 (dd, *J* 5.6 Hz, 2.8 Hz, 2H, $CONHCH_2$), 3.02–2.92 (m, 4H, CH_2CH_2), 2.06 (t, *J* 2.4 Hz, 1H, $CONHCH_2CCH$); **^{13}C NMR** (101 MHz, $CDCl_3$) δ (ppm) 165.7, 162.6, 157.7, 142.2, 141.6, 139.0, 134.5, 129.4, 129.1, 128.6, 128.5, 126.2, 105.7, 79.8, 70.9, 37.9, 37.7, 28.7; **LRMS** (ES + APCI) *m/z*: calc. for $C_{22}H_{20}N_2OS$ 360.1, found 361.0 $[M+H]^+$; **HMRS** calc. for $C_{22}H_{21}N_2OS$ 361.1369 $[M+H]^+$, found 361.1368 $[M+H]^+$.

2-Amino-4-(4-phenethylphenyl)-*N*-(2,2,2-trifluoroethyl)thiophene-3-carboxamide (230)

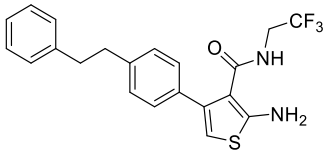

Following General Procedure I, compound **219** (150 mg, 0.45 mmol) and 2,2,2-trifluoroethan-1-amine (35 μL, 0.45 mmol), after purification *via* flash column

chromatography (dry loading, Petroleum ether 8:1 EtOAc, isocratic), afforded the *title compound* (143 mg, 0.35 mmol, 80%) as an off-white solid. **mp** 101–103 °C; **IR**(ATR)/cm^{-1} 3406, 3304, 3264, 3028, 2922, 2859, 1619, 1580, 1519, 1495, 1470, 1392, 1255, 1141; **^{1}H NMR** (400 MHz, $CDCl_3$) δ (ppm) 7.33–7.27 (m, 4H, 4 × Ar*H*), 7.26–7.17 (m, 5H, 5 × Ar*H*), 6.31 (br s, 2H, NH_2), 6.06 (s, 1H, C=C*H*S), 5.36 (app br s, 1H, CON*H*), 3.77 (dq, *J* 9.2 Hz, 8.8 Hz, 2H, CONHC$H_2$$CF_3$), 3.02–2.92 (m, 4H, C$H_2CH_2$); **^{13}C NMR** (101 MHz, $CDCl_3$) δ (ppm) 165.8, 163.3, 142.4, 141.5, 138.9, 134.2, 129.3, 129.2, 128.6, 128.5, 126.2, 124.2 ($J_{C\text{-}F}$ 280.0 Hz, NHC$H_2$$CF_3$), 107.2, 105.8, 40.0 ($J_{C\text{-}F}$ 34.5 Hz NHC$H_2$$CF_3$), 37.8, 37.6; **^{19}F NMR** (376 MHz, $CDCl_3$) δ (ppm) -72.27 (t, *J* 9.2 Hz, 3F, NHC$H_2$$CF_3$); **LRMS** (ES + APCI) *m/z*: calc. for $C_{21}H_{19}F_3N_2OS$ 404.1, found 405.0 $[M+H]^+$; **HMRS** calc. for $C_{21}H_{20}F_3N_2OS$ 405.1243 $[M+H]^+$, found 405.1242 $[M+H]^+$.

2-Amino-4-(4-phenethylphenyl)-*N*-phenylthiophene-3-carboxamide (231)

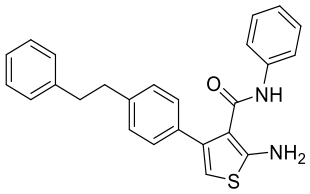

Following General Procedure I, compound **219** (150 mg, 0.45 mmol) and aniline (41 μL, 0.45 mmol), after purification *via* flash column chromatography (dry loading, Petroleum ether 4:1 EtOAc, isocratic), afforded the *title compound* (85 mg, 0.21 mmol, 48%) as a pale yellow solid. **mp** 145–147 °C; **IR**(ATR)/cm^{-1} 3421, 3385, 3259, 3053, 2913, 2852, 1630, 1580, 1515, 1495, 1379, 1318, 1251, 1076; **^{1}H NMR** (500 MHz, $CDCl_3$) δ (ppm) 7.38 (d, *J* 8.0 Hz, 2H, 2 × Ar*H*), 7.30 (d, *J* 8.0 Hz, 2H, 2 × Ar*H*), 7.28 (d, *J* 7.0 Hz, 2H, 2 × Ar*H*), 7.25–7.16 (m, 5H, 5 × Ar*H*), 7.04 (d, *J* 8.0 Hz, 2H, 2 × Ar*H*), 6.99 (t, *J* 8.0 Hz, 1H, Ar*H*), 6.96 (br s, 1H, CON*H*), 6.39 (br s, 2H, NH_2), 6.11 (s, 1H, C=C*H*S), 3.06–2.94 (m, 4H, C_6H_5CH_2CH_2); **^{13}C NMR** (125 MHz, $CDCl_3$) δ (ppm) 164.2, 163.1, 142.6, 141.5, 138.7, 138.1, 134.6, 129.7, 129.3, 128.9, 128.6, 128.5, 126.3, 123.7, 119.6, 108.4, 105.7, 38.1, 37.8; **LRMS** (ES + APCI) *m/z*: calc. for $C_{25}H_{22}N_2OS$ 398.1, found 399.0 $[M+H]^+$; **HMRS** calc. for $C_{25}H_{23}N_2OS$ 399.1526 $[M+H]^+$, found 399.1525 $[M+H]^+$.

2-Amino-*N*-(2-methoxyethyl)-4-(4-phenethylphenyl)thiophene-3-carboxamide (232)

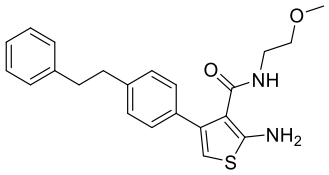

Following General Procedure I, compound **219** (150 mg, 0.45 mmol) and 2-methoxyethan-1-amine (38 μL, 0.45 mmol), after purification *via* flash column chromatography (dry loading, Petroleum ether 2:1 EtOAc, isocratic), afforded the *title compound* (125 mg, 0.33 mmol, 74%) as an off-white solid. **mp** 106–108 °C; **IR**(ATR)/cm^{-1} 3389, 3266, 3025, 2917, 2870, 1597, 1580, 1511, 1496, 1454, 1383, 1273, 1123; **^{1}H NMR** (500 MHz, $CDCl_3$) δ (ppm) 7.33–7.27 (m, 4H, 4 × Ar*H*), 7.25–7.18 (m, 5H, 5 × Ar*H*), 6.23 (br s, 2H, NH_2), 6.04 (s, 1H, C=C*H*S), 5.49 (app br s, 1H, CON*H*), 3.33 (app q, *J* 5.0 Hz, 2H, CONHC$H_2$$CH_2$$OCH_3$), 3.22 (t, *J* 5.0 Hz, 2H, CONHCH$_2$C$H_2$$OCH_3$), 3.11 (s, 3H, CONHCH$_2$$CH_2$$OCH_3$), 3.00–2.92 (m, 4H, $C_6H_5CH_2CH_2$); **^{13}C NMR** (125 MHz, $CDCl_3$) δ (ppm) 166.1, 161.8, 141.9, 141.6, 139.3, 134.7, 129.3, 128.8, 128.6, 126.2, 108.5, 105.8, 71.0, 58.7, 38.8, 37.9, 37.8, (1 carbon missing); **LRMS** (ES + APCI) *m/z*: calc. for $C_{22}H_{24}N_2O_2S$ 380.2, found 381.0 $[M+H]^+$; **HMRS** calc. for $C_{22}H_{25}N_2O_2S$ 381.1631 $[M+H]^+$, found 381.1630 $[M+H]^+$.

2-Amino-*N*-(3-methoxypropyl)-4-(4-phenethylphenyl)thiophene-3-carboxamide (233)

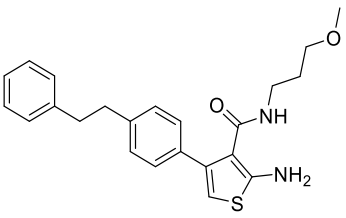

Following General Procedure I, compound **219** (150 mg, 0.45 mmol) and 3-methoxypropan-1-amine (45 μL, 0.45 mmol), after purification *via* flash column chromatography (dry loading, Petroleum ether 2:1 EtOAc, isocratic), afforded the *title compound* (139 mg, 0.35 mmol, 79%) as an off-white solid. **mp** 105–107 °C; **IR**(ATR)/cm^{-1} 3421, 3367, 3264, 3021, 2919, 2870, 2857, 1628, 1606, 1587, 1521,

1454, 1387, 1279, 1112; **^{1}H NMR** (500 MHz, $CDCl_3$) δ (ppm) 7.33–7.27 (m, 4H, 4 × Ar*H*), 7.25–7.18 (m, 5H, 5 × Ar*H*), 6.20 (br s, 2H, NH_2), 6.05 (s, 1H, C=C*H*S), 5.30 (app br s, 1H, CON*H*), 3.22 (app q, *J* 6.0 Hz, 2H, CONHCH_2CH$_2$CH$_2$OCH$_3$), 3.19 (s, 3H, CONHCH$_2$CH$_2$CH$_2$OCH_3), 3.18–3.14 (m, 2H, CONHCH$_2$CH$_2$CH_2OCH$_3$), 3.00–2.92 (m, 4H, C$_6$H$_5$CH_2CH_2), 1.51 (app pentet, *J* 6.0 Hz, 2H, CONHCH$_2$CH_2CH$_2$OCH$_3$); **^{13}C NMR** (125 MHz, $CDCl_3$) δ (ppm) 166.0, 161.6, 142.0, 141.6, 139.1, 134.8, 129.3, 128.9, 128.6, 126.2, 108.8, 105.8, 70.6, 58.8, 37.9, 37.7, 36.6, 29.5 (1 carbon missing); **LRMS** (ES + APCI) *m/z*: calc. for $C_{23}H_{26}N_2O_2S$ 394.2, found 395.0 $[M+H]^+$; **HMRS** calc. for $C_{23}H_{27}N_2O_2S$ 395.1788 $[M+H]^+$, found 395.1786 $[M+H]^+$.

2-Amino-4-(4-phenethylphenyl)-*N*-(piperidin-1-yl)thiophene-3-carboxamide (234)

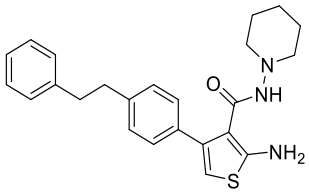

Following General Procedure I, compound **219** (150 mg, 0.45 mmol) and piperidin-1-amine (48 μL, 0.45 mmol), after purification *via* flash column chromatography (dry loading, Petroleum ether 1:1 EtOAc, isocratic), afforded the *title compound* as a partially purified yellow solid.

Selected data; **^{1}H NMR** (500 MHz, $CDCl_3$) δ (ppm) 7.33–7.29 (m, 2H, 2 × Ar*H*), 7.21–7.17 (m, 5H, 5 × Ar*H*), 7.09 (d, *J* 7.5 Hz, 2H, 2 × Ar*H*), 6.29 (br s, 2H, NH_2), 6.01 (s, 1H, C=C*H*S), 2.90–2.86 (m, 4H, C$_6$H$_5$CH_2CH_2), 2.69–2.63 (m, 4H, N(CH_2CH$_2$CH$_2$)CH_2CH$_2$), 1.58–1.47 (m, 6H, N(CH$_2$CH_2CH_2)CH$_2$CH_2).

2-Amino-4-(4-phenethylphenyl)-*N*-(tetrahydro-2*H*-pyran-4-yl)thiophene-3-carboxamide (235)

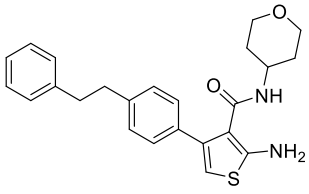

Following General Procedure I, compound **219** (150 mg, 0.45 mmol) and tetrahydro-2*H*-pyran-4-amine (46 μL, 0.45 mmol), after purification *via* flash column chromatography (dry loading, Petroleum ether 2:1 EtOAc, isocratic), afforded the *title compound* (100 mg, 0.25 mmol, 55%) as an off-white solid. **mp** 103–105 °C; **IR**(ATR)/cm^{-1} 3396, 3263, 3023, 2924, 2850, 1625, 1561, 1509, 1385, 1260, 1115; **^{1}H NMR** (500 MHz, $CDCl_3$) δ (ppm) 7.34–7.27 (m, 4H, 4 × Ar*H*), 7.26–7.18 (m, 5H, 5 × Ar*H*), 6.24 (br s, 2H, NH_2), 6.05 (s, 1H, C=C*H*S), 5.10 (d, *J* 6.5 Hz, 1H, CON*H*), 4.01–3.90 (m, 1H, CONHC*H*CH_2), 3.69–3.62 (m, 2H, CONHCH(CH_2CH_2)CH_2CH_2O), 3.39 (t, *J* 10.0 Hz, 2H, CONHCH(CH_2CH_2)CH_2CH_2O), 3.03–2.92 (m, 4H, $C_6H_5CH_2CH_2$), 1.68 (app d, *J* 12.0 Hz, 2H, CONHCH(CH_2CH_2)CH_2CH_2O), 1.07–0.97 (m, 2H, CONHCH(CH_2CH_2)CH_2CH_2O); **^{13}C NMR** (125 MHz, $CDCl_3$) δ (ppm) 165.3, 162.0, 142.4, 141.5, 139.0, 134.9, 129.5, 128.9, 128.6, 128.5, 126.2, 108.4, 105.8, 66.4, 44.7, 37.9, 37.6, 32.7; **LRMS** (ES + APCI) *m/z*: calc. for $C_{24}H_{26}N_2O_2S$ 406.2, found 407.0 $[M+H]^+$; **HMRS** calc. for $C_{24}H_{27}N_2O_2S$ 407.1788 $[M+H]^+$, found 407.1789 $[M+H]^+$.

2-Amino-4-(4-phenethylphenyl)-*N*-(tetrahydrofuran-3-yl)thiophene-3-carboxamide (236)

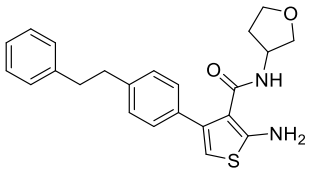

Following General Procedure I, compound **219** (82 mg, 0.45 mmol) and tetrahydrofuran-2-amine (21 μL, 0.45 mmol), after purification *via* flash column chromatography (dry loading, Petroleum ether 1:1 EtOAc, isocratic), afforded the *title compound* as a partially purified yellow solid.

Selected data; **^{1}H NMR** (500 MHz, $CDCl_3$) δ (ppm) 7.32–7.25 (m, 2H, 2 × Ar*H*), 7.25–7.16 (m, 5H, 5 × Ar*H*), 7.13 (d, *J* 7.5 Hz, 2H, 2 × Ar*H*), 6.10 (s, 1H, C=C*H*S), 4.37–4.26 (m, 1H, CONHC*H*(CH_2CH_2)CH_2O), 4.22 (app t, *J* 7.5 Hz, 1H, CONHCH(CH_2CH_2)C(*H*)HO), 3.92–3.79 (m, 2H, CONHCH(CH_2CH_2)CH_2O), 3.71 (app t, *J* 7.5 Hz, 1H, CONHCH(CH_2CH_2)C(H)*H*O), 2.98–2.90 (m, 1H, $C_6H_5CH_2CH_2$), 1.91–1.72 (m, 2H, CONHCH(CH_2CH_2)CH_2O).

2-Amino-4-(4-phenethylphenyl)-*N*-((tetrahydrofuran-3-yl)methyl)thiophene-3-carboxamide (237)

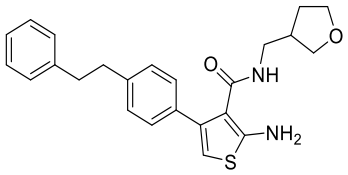

Following General Procedure I, compound **219** (150 mg, 0.45 mmol) and (tetrahydrofuran-3-yl)methanamine (46 μL, 0.45 mmol), after purification *via* flash column chromatography (dry loading, Petroleum ether 2:1 EtOAc, isocratic), afforded the *title compound* (133 mg, 0.33 mmol, 74%) as an off-white solid. **mp** 110–112 °C; **IR**(ATR)/cm^{-1} 3417, 3281, 3108, 3021, 2928, 2865, 1632, 1573, 1515, 1495, 1454, 1389, 1305, 1249, 1074, 907; **^{1}H NMR** (500 MHz, $CDCl_3$) δ (ppm) 7.34–7.26 (m, 5H, 5 × Ar*H*), 7.26–7.18 (m, 4H, 4 × Ar*H*), 6.26 (br s, 2H, NH_2), 6.04 (s, 1H, C=C*H*S), 5.22 (app br s, 1H, CON*H*), 3.75–3.69 (app td, *J* 8.0 Hz, 5.5 Hz, 1H, CONHCH_2CH(C(*H*)H)CH_2CH_2O), 3.63 (app q, *J* 8.0 Hz, 1H, CONHCH_2CH(CH_2)CH_2C(*H*)HO), 3.58 (app t, *J* 8.0 Hz, 1H, CONHCH_2CH(CH_2)CH_2C(H)*H*O), 3.21–3.13 (m, 2H, CONHC*H*$_2$CH(CH_2)CH_2CH_2O), 3.13–3.06 (m, 1H, CONHCH_2CH(C(H)*H*)CH_2CH_2O), 3.00–2.92 (m, 4H, C_6H_5C*H*$_2$C*H*$_2$), 2.13 (app septet, *J* 8.0 Hz, 1H, CONHCH_2C*H*), 1.81–1.73 (m, 1H, CONHCH_2CH(CH_2)C(*H*)HCH_2O), 1.35–1.26 (m, 1H, CONHCH_2CH(CH_2)C(H)*H*CH_2O); **^{13}C NMR** (125 MHz, $CDCl_3$) δ (ppm) 166.1, 162.0, 142.3, 141.5, 138.9, 135.0, 129.4, 129.0, 128.6, 128.5, 126.3, 108.3, 105.9, 71.9, 67.8, 41.8, 39.2, 37.9, 37.6, 30.1; **LRMS** (ES + APCI) *m/z*: calc. for $C_{24}H_{26}N_2O_2S$ 406.2, found 407.0 $[M+H]^+$; **HMRS** calc. for $C_{24}H_{27}N_2O_2S$ 407.1788 $[M+H]^+$, found 407.1787 $[M+H]^+$.

2-Amino-4-(4-phenethylphenyl)-*N*-((tetrahydrofuran-2-yl)methyl)thiophene-3-carboxamide (238)

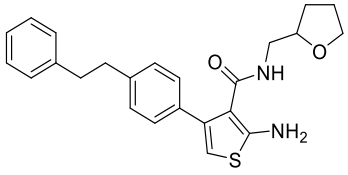

Following General Procedure I, compound **219** (150 mg, 0.45 mmol) and (tetrahydrofuran-2-yl)methanamine (46 μL, 0.45 mmol), after purification *via* flash column chromatography (dry loading, Petroleum ether 2:1 EtOAc, isocratic), afforded the *title compound* (108 mg, 0.27 mmol, 60%) as an off-white solid. **mp** 102–104 °C; **IR**(ATR)/cm^{-1} 3391, 3253, 3023, 2915, 2861, 1617, 1573, 1519, 1493, 1450, 1392, 1257, 1087; **^{1}H NMR** (500 MHz, $CDCl_3$) δ (ppm) 7.33–7.27 (m, 4H, 4 × Ar*H*), 7.25–7.19 (m, 5H, 5 × Ar*H*), 6.23 (br s, 2H, NH_2), 6.04 (s, 1H, C=C*H*S), 5.45 (app br s, 1H, CON*H*), 3.71 (app pentet, *J* 5.5 Hz, 1H, CONHCH$_2$C*H*O), 3.54 (t, *J* 6.5 Hz, 2H, CONHCH$_2$CHOCH_2), 3.35 (app dt, *J* 13.5 Hz, 4.5 Hz, 1H, CONHC(*H*)HCHO), 3.35 (app dt, *J* 13.5 Hz, 5.5 Hz, 1H, CONHC(H)*H*CHO), 3.00–2.92 (m, 4H, $C_6H_5CH_2CH_2$), 1.83–1.67 (m, 3H, CONHCH$_2$CHOCH$_2$CH_2CH_2), 1.39–1.31 (m, 1H, CONHCH$_2$CHOCH$_2$CH$_2$CH_2); **^{13}C NMR** (125 MHz, $CDCl_3$) δ (ppm) 166.2, 161.8, 141.9, 141.7, 139.3, 134.8, 129.3, 128.9, 128.6, 126.2, 108.6, 105.8, 67.9, 42.5, 38.0, 37.9, 28.5, 25.8 (2 carbons missing); **LRMS** (ES + APCI) *m/z*: calc. for $C_{24}H_{26}N_2O_2S$ 406.2, found 407.0 $[M+H]^+$. **HMRS** calc. for $C_{24}H_{27}N_2O_2S$ 407.1788 $[M+H]^+$, found 407.1786 $[M+H]^+$.

_N_-((1,3-Dioxolan-2-yl)methyl)-2-amino-4-(4-phenethylphenyl)thiophene-3-carboxamide (239)

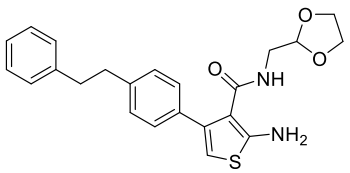

Following General Procedure I, compound **219** (150 mg, 0.45 mmol) and (1,3-dioxolan-2-yl)methanamine (42 μL, 0.45 mmol), after purification *via* flash column chromatography (dry loading, Petroleum ether 2:1 EtOAc, isocratic), afforded the *title compound* (116 mg, 0.28 mmol, 64%) as an off-white solid. **mp** 117–119 °C; **IR**(ATR)/cm^{-1} 3396, 3279, 3099, 2950, 2913, 2868, 1615, 1602, 1578, 1511, 1470, 1454, 1403, 1257, 1056, 1019; **^{1}H NMR** (500 MHz, $CDCl_3$) δ (ppm) 7.33–7.27 (m, 4H, 4 × Ar*H*), 7.25–7.19 (m, 5H, 5 × Ar*H*), 6.28 (br s, 2H, NH_2), 6.03 (s, 1H, C=C*H*S), 5.42 (app br s, 1H, CON*H*), 4.77 (t, *J* 3.5 Hz, 1H, CONHCH$_2$C*H*(O)O), 3.75–3.67 (m, 4H, CONHCH$_2$CH(OCH_2)OCH_2), 3.39 (dd, *J* 5.5 Hz, 3.5 Hz, 2H, CONHCH_2CH(O)O), 3.02–2.92 (m, 4H, $C_6H_5CH_2CH_2$);

^{13}C NMR (125 MHz, $CDCl_3$) δ (ppm) 166.2, 162.2, 141.9, 141.6, 139.2, 134.8, 129.4, 128.9, 128.6, 126.2, 108.3, 105.8, 101.8, 65.1, 41.2, 38.0, 37.8 (1 carbon missing); **LRMS** (ES + APCI) *m/z*: calc. for $C_{23}H_{24}N_2O_3S$ 408.2, found 409.0 $[M+H]^+$; **HMRS** calc. for $C_{23}H_{25}N_2O_3S$ 409.1580 $[M+H]^+$, found 409.1581 $[M+H]^+$.

2-Amino-*N*-((1-methylpyrrolidin-2-yl)methyl)-4-(4-phenethylphenyl)thiophene-3-carboxamide (240)

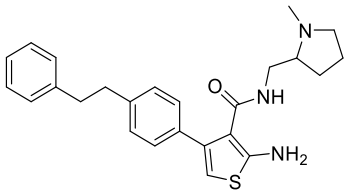

Following General Procedure I, compound **219** (150 mg, 0.45 mmol) and (1-methylpyrrolidin-2-yl)methanamine (55 μL, 0.45 mmol), after purification *via* flash column chromatography (dry loading, Petroleum ether 1:2 EtOAc, isocratic), afforded the *title compound* (160 mg, 0.38 mmol, 86%) as an off-white solid. **mp** 98–100 °C; **IR**(ATR)/cm^{-1} 3389, 3272, 3021, 2928, 2854, 2779, 1602, 1573, 1509, 1495, 1454, 1385, 1260, 1104, 1074, 1022; **^{1}H NMR** (500 MHz, $CDCl_3$) δ (ppm) 7.34–7.26 (m, 4H, 4 × Ar*H*), 7.26–7.18 (m, 5H, 5 × Ar*H*), 6.24 (br s, 2H, NH_2), 6.02 (s, 1H, C=C*H*S), 5.63 (app br s, 1H, CON*H*), 3.51 (app ddd, *J* 13.5 Hz, 7.0 Hz, 2.5 Hz, 1H, $CONHCH_2CH(NCH_3)CH_2$), 3.00–2.89 (m, 5H, $C_6H_5CH_2CH_2$, $CONHCH(H)CH(NCH_3)CH_2CH_2$), 2.77–2.67 (m, 1H, $CONHCH(H)CH(N(CH_3)CH_2)CH_2CH_2$), 2.15–1.93 (m, 5H, $CONHCH_2CH(N(CH_3)CH_2)CH_2CH_2$), 1.63–1.53 (m, 1H, $CONHCH_2CH(N(CH_3)CH_2)CH(H)CH_2$), 1.53–1.44 (m, 1H, $CONHCH_2CH(N(CH_3)CH_2)CH(H)CH_2$), 1.44–1.32 (m, 1H, $CONHCH_2CH(N(CH_3)CH_2)CH_2CH(H)$), 1.23–1.12 (m, 1H, $CONHCH_2CH(N(CH_3)CH_2)CH_2CH(H)$); **^{13}C NMR** (125 MHz, $CDCl_3$) δ (ppm) 166.5, 161.6, 141.7, 141.7, 139.4, 135.0, 129.3, 128.8, 128.6, 128.5, 126.2, 108.8, 105.8, 63.6, 60.0, 40.2, 40.0, 38.0, 37.9, 28.5, 22.2; **LRMS** (ES + APCI) *m/z*: calc. for $C_{25}H_{29}N_3OS$ 419.2, found 420.0 $[M+H]^+$; **HMRS** calc. for $C_{25}H_{30}N_3OS$ 420.2104 $[M+H]^+$, found 420.2105 $[M+H]^+$.

2-Amino-*N*-(2-morpholinoethyl)-4-(4-phenethylphenyl)thiophene-3-carboxamide (241)

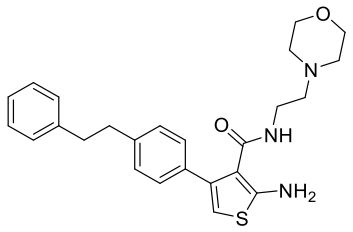

Following General Procedure I, compound **219** (150 mg, 0.45 mmol) and 2-morpholinoethan-1-amine (58 μL, 0.45 mmol), after purification *via* flash column chromatography (dry loading, Petroleum ether 1:2 EtOAc, isocratic), afforded the *title compound* (130 mg, 0.30 mmol, 67%) as an off-white solid. **mp** 84–86 °C; **IR**(ATR)/cm^{-1} 3391, 3285, 3023, 2922, 2854, 2809, 1615, 1574, 1511, 1454, 1387, 1270, 1115, 1022; **^{1}H NMR** (500 MHz, $CDCl_3$) δ (ppm) 7.35–7.27 (m, 4H, 4 × Ar*H*), 7.22 (app t, *J* 7.5 Hz, 5H, 5 × Ar*H*), 6.17 (br s, 2H, NH_2), 6.05 (s, 1H, C=C*H*S), 5.66 (app br s, 1H, CON*H*), 3.47 (app br s, 4H, $CONHCH_2CH_2N(CH_2CH_2)CH_2CH_2O$), 3.28 (app q, *J* 5.5 Hz, 2H, $CONHCH_2CH_2N$), 3.98–2.90 (m, 4H, $C_6H_5CH_2CH_2$), 2.21 (t, *J* 5.5 Hz, 2H, $CONHCH_2CH_2N$), 2.16 (app br s, 4H, $CONHCH_2CH_2N(CH_2CH_2)CH_2CH_2O$); **^{13}C NMR** (125 MHz, $CDCl_3$) δ (ppm) 165.9, 161.6, 141.6, 141.5, 139.3, 134.9, 129.3, 128.7, 128.6, 128.5, 126.3, 108.6, 106.0, 66.8, 56.8, 53.1, 37.8, 37.7, 35.5; **LRMS** (ES + APCI) *m/z*: calc. for $C_{25}H_{29}N_3O_2S$ 435.2, found 436.0 $[M+H]^+$; **HMRS** calc. for $C_{25}H_{30}N_3O_2S$ 436.2053 $[M+H]^+$, found 436.2054 $[M+H]^+$.

2-((3-(Ethylcarbamoyl)-4-(4-phenethylphenyl)thiophen-2-yl)carbamoyl)benzoic acid (242)

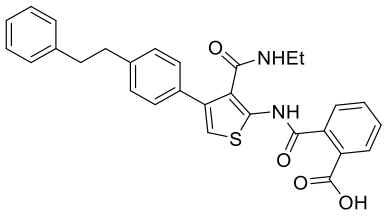

Following General Procedure E, compound **220** (50 mg, 0.14 mmol) and phthalic anhydride (20 mg, 0.14 mmol), after purification *via* flash column chromatography (dry loading, Petroleum ether 1:1 EtOAc, CH_2Cl_2 9:1 MeOH),

afforded the *title compound* (35 mg, 0.07 mmol, 49%) as an off-white solid. **mp** 130–132 °C; **IR**(ATR)/cm^{-1} 3411, 3021, 2960, 2922, 1719, 1656, 1610, 1561, 1519, 1396, 1292, 1258, 1229, 1074, 1020; **^{1}H NMR** (500 MHz, DMSO-d_6) δ (ppm) 13.69 (br s, 1H, COO*H*), 13.16 (br s, 1H, CON*H*CS), 7.86–7.79 (m, 1H, Ar*H*), 7.78–7.71 (m, 1H, Ar*H*), 7.61–7.47 (m, 3H, 2 × Ar*H*, CON*H*CH$_2$), 7.32 (d, *J* 8.0 Hz, 2H, 2 × Ar*H*), 7.31–7.22 (m, 6H, 6 × Ar*H*), 7.18 (app t, *J* 7.0 Hz, 1H, Ar*H*), 6.98 (s, 1H, C=C*H*S), 3.14 (app pentet, *J* 7.0 Hz, 2H, CONHC*H*$_2$CH$_3$), 2.90 (br s, 4H, C$_6$H$_5$C*H*$_2$C*H*$_2$), 0.92 (t, *J* 7.0 Hz, 3H, CONHCH$_2$C*H*$_3$); **^{13}C NMR** (125 MHz, DMSO-d_6) δ (ppm) 170.2, 165.6, 164.4, 141.7, 141.5, 140.6, 137.3, 133.8, 133.6, 130.1, 129.9, 129.4, 128.7, 128.4, 128.3, 128.3, 128.2, 127.9, 125.8, 119.7, 114.6, 36.9, 36.7, 33.8, 14.0; **LRMS** (ES + APCI) *m/z*: calc. for $C_{29}H_{26}N_2O_4S$ 498.2, found 499.0 $[M+H]^+$; **HMRS** calc. for $C_{29}H_{25}N_2O_4S$ 497.1541 $[M–H]^-$, found 497.1550 $[M–H]^-$.

2-((3-(Isopropylcarbamoyl)-4-(4-phenethylphenyl)thiophen-2-yl)carbamoyl)benzoic acid (243)

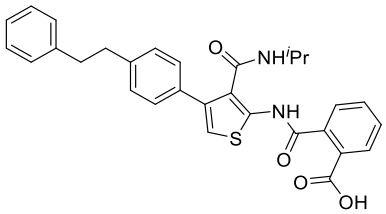

Following General Procedure E, compound **221** (85 mg, 0.23 mmol) and phthalic anhydride (35 mg, 0.23 mmol), after purification *via* flash column chromatography (dry loading, Petroleum ether 2:1 EtOAc, CH_2Cl_2 9:1 MeOH), afforded the *title compound* (81 mg, 0.16 mmol, 68%) as an off-white solid. **mp** 132–134 °C; **IR**(ATR)/cm^{-1} 3406 br, 3058, 3023, 2965, 2921, 1719, 1667, 1613, 1591, 1519, 1392, 1258, 1229, 1006; **^{1}H NMR** (400 MHz, DMSO-d_6) δ (ppm) 13.62 (br s, 1H, COO*H*), 13.21 (br s, 1H, CON*H*), 7.83 (dd, *J* 5.2 Hz, 3.2 Hz, 1H, Ar*H*), 7.73 (dd, *J* 5.2 Hz, 3.2 Hz, 1H, Ar*H*), 7.53 (dd, *J* 5.2 Hz, 3.2 Hz, 2H, 2 × Ar*H*), 7.35–7.29 (m, 2H, 2 × Ar*H*), 7.29–7.23 (m, 6H, 6 × Ar*H*), 7.21–7.14 (m, 1H, Ar*H*), 6.97 (s, 1H, C=C*H*S), 3.93 (app octet, *J* 6.4 Hz, 1H, CONHC*H*(CH$_3$)$_2$), 2.91 (br s, 4H, C*H*$_2$C*H*$_2$), 0.94 (d, *J* 6.4 Hz, 6H, CONHCH(C*H*$_3$)$_2$); **^{13}C NMR** (101 MHz, DMSO-d_6) δ (ppm) 171.2, 166.6, 165.6, 163.6, 142.0, 141.4, 140.8, 137.3, 133.6, 130.2, 129.9, 129.7, 128.6, 128.4, 128.3, 128.3, 128.2, 128.1, 125.8,

119.5, 114.6, 40.7, 36.9, 36.6, 21.9; **LRMS** (ES + APCI) *m/z*: calc. for $C_{30}H_{28}N_2O_4S$ 512.2, found 513.0 $[M+H]^+$; **HMRS** calc. for $C_{30}H_{27}N_2O_4S$ 511.1697 $[M–H]^-$, found 511.1703 $[M–H]^-$.

2-((3-(Cyclopropylcarbamoyl)-4-(4-phenethylphenyl)thiophen-2-yl)carbamoyl)benzoic acid (244)

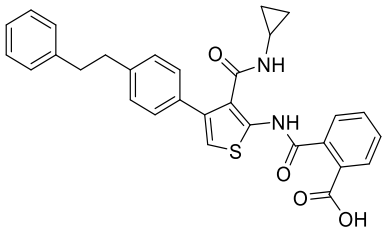

Following General Procedure E, compound **222** (80 mg, 0.22 mmol) and phthalic anhydride (32 mg, 0.22 mmol), after purification *via* flash column chromatography (dry loading, Petroleum ether 1:1 EtOAc, CH_2Cl_2 9:1 MeOH), afforded the *title compound* (72 mg, 0.16 mmol, 64%) as an off-white solid. **mp** 115–117 °C; **IR**(ATR)/cm^{-1} 3395 br, 3261, 3086, 3017, 2921, 1721, 1606, 1580, 1511, 1454, 1390, 1250, 1204, 1007; **^{1}H NMR** (500 MHz, DMSO-d_6) δ (ppm) 13.73 (br s, 1H, COO*H*), 13.12 (br s, 1H, CON*H*CS), 7.86–7.81 (m, 1H, Ar*H*), 7.79–7.75 (m, 1H, Ar*H*), 7.71 (br s, 1H, CON*H*CH), 7.56–7.48 (m, 2H, 2 × Ar*H*), 7.32–7.25 (m, 6H, 6 × Ar*H*), 7.24 (d, *J* 8.0 Hz, 2H, 2 × Ar*H*), 7.18 (app tt, *J* 7.0 Hz, 2.0 Hz, 1H, Ar*H*), 6.97 (s, 1H, C=C*H*S), 2.90 (br s, 4H, $C_6H_5CH_2CH_2$), 2.68 (app octet, *J* 7.0 Hz, 1H, CONHC*H*), 0.53 (td, *J* 7.0 Hz, 5.0 Hz, 2H, CONHCH(CH_2)CH_2), 0.37–0.31 (m, 2H, CONHCH(CH_2)CH_2); **^{13}C NMR** (125 MHz, DMSO-d_6) δ (ppm) 170.2, 165.9, 165.7, 141.5, 141.4, 140.6, 137.3, 133.8, 133.5, 130.1, 129.9, 129.3, 128.8, 128.4, 128.3, 128.3, 128.2, 127.8, 125.8, 119.7, 114.5, 36.9, 36.6, 22.5, 5.6; **LRMS** (ES + APCI) *m/z*: calc. for $C_{30}H_{26}N_2O_4S$ 510.2, found 511.0 $[M+H]^+$; **HMRS** calc. for $C_{30}H_{25}N_2O_4S$ 509.1541 $[M–H]^+$, found 509.1537 $[M–H]^+$.

2-((3-(Cyclobutylcarbamoyl)-4-(4-phenethylphenyl)thiophen-2-yl)carbamoyl)benzoic acid (245)

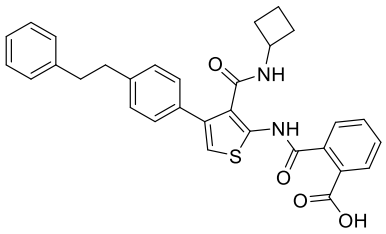

Following General Procedure E, compound **223** (85 mg, 0.22 mmol) and phthalic anhydride (33 mg, 0.22 mmol), after purification *via* flash column chromatography (dry loading, Petroleum ether 2:1 EtOAc, CH_2Cl_2 9:1 MeOH), afforded the *title compound* (77 mg, 0.15 mmol, 65%) as an off-white solid. **mp** 118–120 °C; **IR**(ATR)/cm^{-1} 3389 br, 3062, 2969, 2941, 1721, 1656, 1608, 1587, 1519, 1444, 1398, 1294, 1260, 987; **^{1}H NMR** (500 MHz, DMSO-d_6) δ (ppm) 13.64 (br s, 1H, COO*H*), 13.23 (br s, 1H, CON*H*CS), 7.86–7.81 (m, 1H, Ar*H*), 7.73 (app t, *J* 4.5 Hz, 1H, Ar*H*), 7.64 (br s, 1H, CON*H*CH), 7.56–7.48 (m, 2H, 2 × Ar*H*), 7.32 (d, *J* 8.0 Hz, 2H, 2 × Ar*H*), 7.30–7.23 (m, 6H, 6 × Ar*H*), 7.20–7.15 (m, 1H, Ar*H*), 6.98 (s, 1H, C=C*H*S), 4.25 (app sextet, *J* 8.0 Hz, 1H, CONHC*H*), 2.90 (br s, 4H, $C_6H_5CH_2CH_2$), 2.11–2.02 (m, 2H, CONHCH(CH_2)CH_2), 1.68 (app quintet, *J* 9.0 Hz, 2H, CONHCH(CH_2)CH_2), 1.60–1.69 (m, 2H, CONHCH(CH_2)CH_2CH_2); **^{13}C NMR** (125 MHz, DMSO-d_6) δ (ppm) 170.5, 166.3, 164.1, 142.7, 141.9, 141.2, 137.8, 134.5, 134.1, 130.6, 130.5, 129.9, 129.1, 128.8, 128.8, 128.7, 128.5, 126.3, 124.2, 119.7, 115.1, 44.8, 37.5, 37.1, 30.2, 15.4; **LRMS** (ES + APCI) *m/z*: calc. for $C_{31}H_{28}N_2O_4S$ 524.2, found 525.0 $[M+H]^+$; **HMRS** calc. for $C_{31}H_{27}N_2O_4S$ 523.1697 $[M–H]^+$, found 523.1695 $[M–H]^+$.

2-((3-(Cyclopentylcarbamoyl)-4-(4-phenethylphenyl)thiophen-2-yl)carbamoyl)benzoic acid (246)

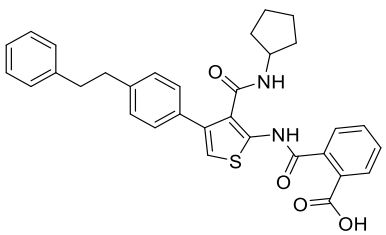

Following General Procedure E, compound **224** (90 mg, 0.23 mmol) and phthalic anhydride (34 mg, 0.23 mmol), after purification *via* flash column chromatography (dry loading, Petroleum ether 2:1 EtOAc, CH_2Cl_2 9:1 MeOH), afforded the *title compound* (80 mg, 0.15 mmol, 64%) as an off-white solid. **mp** 122–124 °C; **IR**(ATR)/cm^{-1} 3406 br, 3060, 3021, 2935, 2857, 1721, 1666, 1610, 1587, 1515, 1454, 1396, 1290, 1255, 1227, 1074; **^{1}H NMR** (500 MHz, DMSO-d_6) δ (ppm) 13.73 (br s, 2H, CON*H*CS, COO*H*), 7.86–7.81 (m, 1H, Ar*H*), 7.75–7.70 (m, 1H, Ar*H*), 7.55–7.49 (m, 2H, 2 × Ar*H*), 7.32 (d, *J* 8.5 Hz, 2H, 2 × Ar*H*), 7.30–7.24 (m, 6H, 6 × Ar*H*), 7.23–7.16 (m, 2H, CON*H*CH, Ar*H*), 6.95 (s, 1H, C=C*H*S), 4.09 (app sextet, *J* 7.0 Hz, 1H, CONHC*H*), 2.90 (br s, 4H, $C_6H_5CH_2CH_2$), 1.74–1.64 (m, 2H, CONHCH(CH_2CH_2)CH_2CH_2), 1.43–1.35 (m, 4H, CONHCH(CH_2CH_2)CH_2CH_2), 1.28–1.20 (m, 2H, CONHCH(CH_2CH_2)CH_2CH_2); **^{13}C NMR** (125 MHz, DMSO-d_6) δ (ppm) 170.1, 165.8, 164.1, 142.5, 141.4, 140.9, 137.3, 134.1, 133.7, 130.1, 129.9, 129.4, 128.5, 128.3, 128.2, 128.1, 127.6, 125.8, 123.7, 118.9, 114.5, 50.7, 37.0, 36.6, 31.8, 23.1; **LRMS** (ES + APCI) *m/z*: calc. for $C_{32}H_{30}N_2O_4S$ 538.2, found 539.0 $[M+H]^+$; **HMRS** calc. for $C_{32}H_{29}N_2O_4S$ 537.1854 $[M–H]^-$, found 537.1858 $[M–H]^-$.

2-((3-(Cyclohexylcarbamoyl)-4-(4-phenethylphenyl)thiophen-2-yl)carbamoyl)benzoic acid (247)

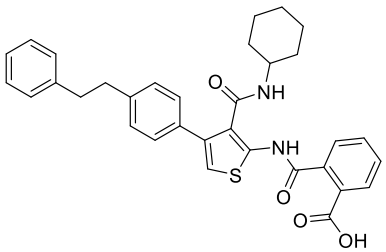

Following General Procedure E, compound **225** (88 mg, 0.22 mmol) and phthalic anhydride (32 mg, 0.22 mmol), after purification *via* flash column chromatography (dry loading, Petroleum ether 3:1 EtOAc, CH_2Cl_2 9:1 MeOH), afforded the *title compound* (82 mg, 0.50 mmol, 68%) as an off-white solid. **mp** 133–135 °C; **IR**(ATR)/cm^{-1} 3406 br, 3266, 3025, 2924, 2852, 1723, 1671, 1619, 1580, 1509, 1452, 1392, 1257, 1223, 1074; **^{1}H NMR** (400 MHz, DMSO-d_6) δ (ppm) 13.80–12.70 (m, 2H, CON*H*CS, COO*H*), 7.83 (dd, *J* 5.2 Hz, 3.6 Hz, 1H, Ar*H*), 7.73–7.68 (m, 1H, Ar*H*), 7.59–7.51 (m, 2H, 2 × Ar*H*), 7.33 (d, *J* 8.0 Hz, 2H, 2 × Ar*H*),

7.31–7.24 (m, 6H, 6 × Ar*H*), 7.21–7.16 (m, 1H, Ar*H*), 7.07 (br s, 1H, CON*H*CH), 6.96 (s, 1H, C=C*H*S), 3.70–3.59 (m, 1H, CONHC*H*), 2.91 (br s, 4H, $C_6H_5CH_2CH_2$), 1.68 (app d, *J* 10.0 Hz, 2H, CONHCH(CH_2CH_2)CH_2CH_2), 1.51–1.40 (m, 3H, CONHCH(CH_2CH_2)$CH_2C(H)H$), 1.22–1.12 (m, 2H, CONHCH(CH_2CH_2)CH_2CH_2), 1.08–0.91 (m, 3H, CONHCH(CH_2CH_2)$CH_2C(H)HCH_2$); **^{13}C NMR** (125 MHz, DMSO-d_6) δ (ppm) 169.5, 165.7, 163.6, 142.7, 141.4, 141.0, 137.2, 134.6, 133.6, 130.2, 129.9, 129.8, 128.4, 128.4, 128.3, 128.3, 128.2, 128.2, 125.8, 118.6, 114.8, 47.5, 37.0, 36.6, 31.5, 25.1, 24.1; **LRMS** (ES + APCI) *m/z*: calc. for $C_{33}H_{32}N_2O_4S$ 552.2, found 553.0 $[M+H]^+$; **HMRS** calc. for $C_{33}H_{31}N_2O_4S$ 551.2015 $[M–H]^+$, found 551.2013 $[M–H]^+$.

2-((3-(Cycloheptylcarbamoyl)-4-(4-phenethylphenyl)thiophen-2-yl)carbamoyl)benzoic acid (248)

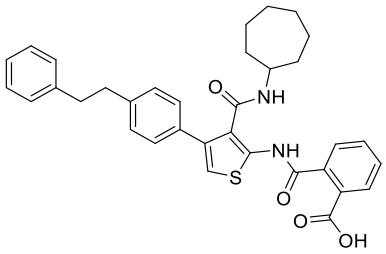

Following General Procedure E, compound **226** (85 mg, 0.20 mmol) and phthalic anhydride (30 mg, 0.20 mmol), after purification *via* flash column chromatography (dry loading, Petroleum ether 2:1 EtOAc, CH_2Cl_2 9:1 MeOH), afforded the *title compound* (70 mg, 0.15 mmol, 61%) as an off-white solid. **mp** 127–129 °C; **IR**(ATR)/cm^{-1} 3408, 3060, 2924, 2850, 1725, 1666, 1610, 1589, 1519, 1455, 1398, 1281, 1255, 1074; **^{1}H NMR** (500 MHz, DMSO-d_6) δ (ppm) 13.74 (br s, 1H, COO*H*), 13.25 (br s, 1H, CON*H*CS), 7.86–7.81 (m, 1H, Ar*H*), 7.74–7.69 (m, 1H, Ar*H*), 7.55–7.48 (m, 2H, 2 × Ar*H*), 7.32 (d, *J* 8.0 Hz, 2H, 2 × Ar*H*), 7.31–7.24 (m, 6H, 6 × Ar*H*), 7.19 (app tt, *J* 6.5 Hz, 2.0 Hz, 1H, Ar*H*), 7.12 (br s, 1H, CON*H*CH), 6.94 (s, 1H, C=C*H*S), 3.84 (app nonet, *J* 4.0 Hz, 1H, CONHC*H*), 2.90 (br s, 4H, $C_6H_5CH_2CH_2$), 1.76–1.67 (m, 2H, CONHCH($CH_2CH_2CH_2$)$CH_2CH_2CH_2$), 1.51–1.43 (m, 2H, CONHCH($CH_2CH_2CH_2$)$CH_2CH_2CH_2$), 1.42–1.33 (m, 4H, CONHCH($CH_2CH_2CH_2$)$CH_2CH_2CH_2$), 1.33–1.26 (m, 2H, CONHCH($CH_2CH_2CH_2$)$CH_2CH_2CH_2$), 1.26–1.17 (m, 2H, CONHCH($CH_2CH_2CH_2$)$CH_2CH_2CH_2$); **^{13}C NMR** (125 MHz, DMSO-d_6) δ (ppm)

170.1, 165.8, 163.4, 142.7, 141.4, 140.9, 137.3, 134.1, 133.7, 130.1, 129.9, 129.4, 128.5, 128.4, 128.3, 128.3, 128.2, 128.2, 125.8, 118.8, 114.6, 49.7, 37.1, 36.7, 33.5, 27.8, 23.4; **LRMS** (ES + APCI) *m/z*: calc. for $C_{34}H_{34}N_2O_4S$ 566.2, found 567.0 $[M+H]^+$; **HMRS** calc. for $C_{34}H_{33}N_2O_4S$ 565.2167 $[M–H]^-$, found 565.2177 $[M–H]^-$.

2-((3-(((1*S*,4*R*)-bicyclo[2.2.1]heptan-2-yl)carbamoyl)-4-(4-phenethylphenyl)thiophen-2-yl)carbamoyl)benzoic acid (249)

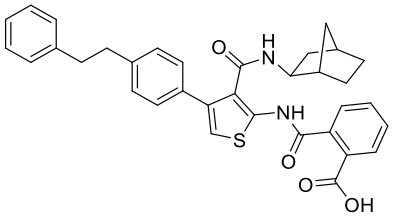

Following General Procedure E, compound **227** (80 mg, 0.19 mmol) and phthalic anhydride (28 mg, 0.19 mmol), after purification *via* flash column chromatography (dry loading, Petroleum ether 1:1 EtOAc, CH_2Cl_2 9:1 MeOH), afforded the *title compound* (77 mg, 0.14 mmol, 71%) as an off-white solid. **mp** 150–152 °C; **IR**(ATR)/cm^{-1} 3408, 3025, 2945, 2865, 1725, 1660, 1619, 1580, 1515, 1454, 1392, 1279, 1257, 1020; **^{1}H NMR** (500 MHz, DMSO-d_6) δ (ppm) 13.35 (br s, 2H, COO*H*, CON*H*CS), 7.84 (dd, *J* 5.5 Hz, 3.5 Hz, 1H, Ar*H*), 7.73–7.67 (m, 1H, Ar*H*), 7.58–7.52 (m, 2H, 2 × Ar*H*), 7.35–7.24 (m, 8H, 8 × Ar*H*), 7.22–7.16 (m, 1H, Ar*H*), 6.95 (app br s, 2H, C=C*H*S, CON*H*CH), 3.61–3.54 (m, 1H, CONHC*H*), 2.95–2.86 (m, 4H, $C_6H_5CH_2CH_2$), 2.07–2.01 (m, 2H, 2 × bicycle C*H*), 1.47 (dd, *J* 12.5 Hz, 8.5 Hz, 1H, bicycle C*H*), 1.41–1.29 (m, 2H, 2 × bicycle C*H*), 1.10–0.95 (m, 3H, 3 × bicycle C*H*), 0.94–0.86 (m, 2H, 2 × bicycle C*H*); **^{13}C NMR** (125 MHz, DMSO-d_6) δ (ppm) 169.4, 165.7, 163.7, 142.8, 141.4, 141.0, 137.4, 134.6, 134.4, 133.7, 130.1, 129.9, 129.8, 128.4, 128.4, 128.3, 128.3, 128.2, 125.9, 118.6, 114.6, 52.3, 41.3, 38.3, 37.1, 36.7, 34.9, 34.8, 27.9, 25.9; **LRMS** (ES + APCI) *m/z*: calc. for $C_{34}H_{32}N_2O_4S$ 564.2, found 565.0 $[M+H]^+$; **HMRS** calc. for $C_{34}H_{31}N_2O_4S$ 563.2010 $[M–H]^-$, found 563.2021 $[M–H]^-$.

2-((3-((Cyclohexylmethyl)carbamoyl)-4-(4-phenethylphenyl)thiophen-2-yl)carbamoyl)benzoic acid (250)

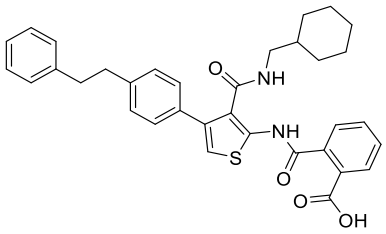

Following General Procedure E, compound **228** (88 mg, 0.21 mmol) and phthalic anhydride (31 mg, 0.21 mmol), after purification *via* flash column chromatography (dry loading, Petroleum ether 2:1 EtOAc, CH_2Cl_2 9:1 MeOH), afforded the *title compound* (83 mg, 0.16 mmol, 70%) as an off-white solid. **mp** 151–153 °C; **IR**(ATR)/cm^{-1} 3408, 3086, 2919, 2850, 1721, 1660, 1610, 1589, 1519, 1448, 1394, 1281, 1258; **^{1}H NMR** (500 MHz, DMSO-d_6) δ (ppm) 13.68 (br s, 1H, COO*H*), 13.29 (br s, 1H, CON*H*CS), 7.85–7.81 (m, 1H, Ar*H*), 7.74–7.69 (m, 1H, Ar*H*), 7.55–7.49 (m, 2H, 2 × Ar*H*), 7.37 (br s, 1H, CON*H*CH), 7.33 (d, *J* 8.0 Hz, 2H, 2 × Ar*H*), 7.31–7.23 (m, 6H, 6 × Ar*H*), 7.19 (app t, *J* 7.0 Hz, 1H, Ar*H*), 6.95 (s, 1H, C=C*H*S), 2.94 (app t, *J* 6.0 Hz, 2H, CONHCH_2), 2.90 (br s, 4H, $C_6H_5CH_2CH_2$), 1.61–1.51 (m, 3H, $CONHCH_2CH(CH_2CH_2)CH_2CH_2CH_2$), 1.42 (d, *J* 13.0 Hz, 2H, $CONHCH_2CH(CH_2CH_2)CH_2CH_2CH_2$), 1.31–1.21 (m, 1H, $CONHCH_2CH(CH_2C(H)H)CH_2CH_2CH_2$), 1.13–1.00 (m, 3H, $CONHCH_2CH(CH_2C(H)H)CH_2CH_2CH_2$), 0.74–0.64 (m, 2H, $CONHCH_2CH(CH_2CH_2)CH_2CH_2CH_2$); **^{13}C NMR** (125 MHz, DMSO-d_6) δ (ppm) 170.1, 165.7, 164.7, 142.2, 141.5, 140.8, 137.3, 134.1, 133.7, 130.1, 129.9, 129.5, 129.5, 129.4, 128.5, 128.3, 128.2, 128.1, 125.9, 119.3, 114.6, 45.3, 37.0, 36.9, 36.7, 30.3, 25.9, 25.4; **LRMS** (ES + APCI) *m/z*: calc. for $C_{34}H_{34}N_2O_4S$ 566.2, found 567.0 $[M+H]^+$; **HMRS** calc. for $C_{34}H_{34}N_2O_4SNa$ 589.2111 $[M+Na]^+$, found 589.2111 $[M+Na]^+$.

2-((4-(4-Phenethylphenyl)-3-(prop-2-yn-1-ylcarbamoyl)thiophen-2-yl)carbamoyl)benzoic acid (251)

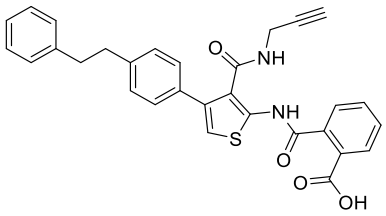

Following General Procedure E, compound **229** (60 mg, 0.17 mmol) and phthalic anhydride (25 mg, 0.17 mmol), after purification *via* flash column chromatography (dry loading, Petroleum ether 1:1 EtOAc, CH_2Cl_2 9:1 MeOH), afforded the *title compound* (72 mg, 0.14 mmol, 85%) as an off-white solid. **mp** 87–89 °C; **IR**(ATR)/cm^{-1} 3409 br, 3268, 3054, 3023, 2894, 1719, 1613, 1573, 1519, 1454, 1394, 1258, 1223, 1019; **^{1}H NMR** (500 MHz, DMSO-d_6) δ (ppm) 14.15 (br s, 1H, COO*H*), 13.15 (br s, 1H, CON*H*CS), 8.31 (br s, 1H, CON*H*CH_2), 7.86–7.76 (m, 2H, 2 × Ar*H*), 7.56–7.48 (m, 2H, 2 × Ar*H*), 7.35 (d, *J* 8.0 Hz, 2H, 2 × Ar*H*), 7.32–7.25 (m, 4H, 4 × Ar*H*), 7.23 (d, *J* 8.0 Hz, 2H, 2 × Ar*H*), 7.21–7.17 (m, 1H, Ar*H*), 7.01 (s, 1H, C=C*H*S), 3.97 (dd, *J* 5.5 Hz, 2.5 Hz, 2H, CONHCH_2), 3.07 (s, 1H, CH_2CC*H*), 2.89 (br s, 4H, CH_2CH_2); **^{13}C NMR** (125 MHz, DMSO-d_6) δ (ppm) 168.2, 165.5, 164.4, 141.7, 141.6, 140.4, 137.5, 137.2, 133.4, 130.1, 129.4, 128.9, 128.4, 128.3, 128.2, 128.2, 128.1, 127.7, 125.8, 119.5, 114.6, 80.7, 72.9, 36.9, 36.7, 28.6; **LRMS** (ES + APCI) *m/z*: calc. for $C_{30}H_{24}N_2O_4S$ 508.1, found 509.0 $[M+H]^+$; **HMRS** calc. for $C_{30}H_{23}N_2O_4S$ 507.1384 $[M–H]^+$, found 507.1380 $[M–H]^+$.

2-((4-(4-Phenethylphenyl)-3-((2,2,2-trifluoroethyl)carbamoyl)thiophen-2-yl)carbamoyl)benzoic acid (252)

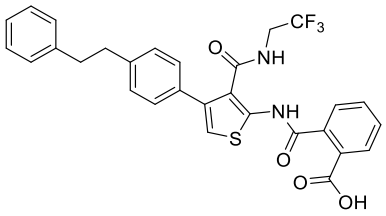

Following General Procedure E, compound **230** (95 mg, 0.24 mmol) and phthalic anhydride (35 mg, 0.24 mmol), after purification *via* flash column chromatography (dry loading, Petroleum ether 2:1 EtOAc, CH_2Cl_2 9:1 MeOH), afforded the *title compound* (73 mg, 0.13 mmol, 53%) as an off-white solid. **mp** 82–

84 °C; **IR**(ATR)/cm^{-1} 3396, 3250, 3026, 2935, 2855, 1719, 1671, 1630, 1578, 1519, 1454, 1392, 1255, 1223, 1156, 935; **^{1}H NMR** (500 MHz, DMSO-d_6) δ (ppm) 13.75 (br s, 1H, COO*H*), 13.22 (br s, 1H, CON*H*CS), 8.62 (br s, 1H, CON*H*CH$_2$), 7.84 (dd, *J* 5.5 Hz, 3.5 Hz, 1H, Ar*H*), 7.82–7.76 (m, 1H, Ar*H*), 7.53 (dd, *J* 5.5 Hz, 3.5 Hz, 2H, 2 × Ar*H*), 7.31 (d, *J* 8.0 Hz, 2H, 2 × Ar*H*), 7.30–7.24 (m, 4H, 4 × Ar*H*), 7.21 (d, *J* 8.0 Hz, 2H, 2 × Ar*H*), 7.20–7.16 (m, 1H, Ar*H*), 7.03 (s, 1H, C=C*H*S), 3.99 (app sextet, *J* 7.0 Hz, 2H, CONHC*H*$_2$CF$_3$), 2.89 (br s, 4H, C*H*$_2$C*H*$_2$); **^{13}C NMR** (125 MHz, DMSO-d_6) δ (ppm) 169.7, 165.6, 165.4, 141.9, 141.5, 140.5, 137.3, 134.9, 134.0, 133.9, 133.3, 130.2, 130.1, 129.6, 128.9, 128.3, 128.2, 127.6, 125.8, 124.8 ($J_{C\text{-}F}$ 278.0 Hz, NHCH$_2$*C*F$_3$), 119.2, 114.8, 40.4 ($J_{C\text{-}F}$ 33.0 Hz, NH*C*H$_2$CF$_3$), 36.9, 36.7; **^{19}F NMR** (376 MHz, DMSO-d_6) δ (ppm) -69.87 (t, *J* 7.9 Hz, 3F, NHCH$_2$C*F*$_3$); **LRMS** (ES + APCI) *m/z*: calc. for $C_{29}H_{23}F_3N_2O_4S$ 552.1, found 553.0 $[M+H]^+$; **HMRS** calc. for $C_{29}H_{22}F_3N_2O_4S$ 551.1253 $[M–H]^+$, found 551.1253 $[M–H]^+$.

2-((4-(4-Phenethylphenyl)-3-(phenylcarbamoyl)thiophen-2-yl)carbamoyl)benzoic acid (253)

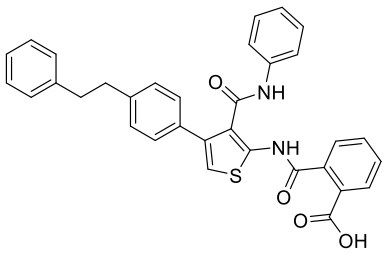

Following General Procedure E, compound **231** (72 mg, 0.18 mmol) and phthalic anhydride (27 mg, 0.18 mmol), after purification *via* flash column chromatography (dry loading, Petroleum ether 2:1 EtOAc, CH_2Cl_2 9:1 MeOH), afforded the *title compound* (48 mg, 0.09 mmol, 49%) as an off-white solid. **mp** 131–133 °C; **IR**(ATR)/cm^{-1} 3382, 3257, 3056, 3023, 2926, 2852, 1719, 1686, 1630, 1578, 1515, 1495, 1390, 1314, 1245, 1199, 1076; **^{1}H NMR** (500 MHz, DMSO-d_6) δ (ppm) 13.83 (br s, 1H, COO*H*), 13.14 (br s, 1H, CON*H*CS), 9.97 (br s, 1H, CON*H*C$_6$H$_5$), 7.86–7.79 (m, 1H, Ar*H*), 7.77–7.69 (m, 1H, Ar*H*), 7.58–7.46 (m, 4H, 4 × Ar*H*), 7.35 (d, *J* 6.5 Hz, 2H, 2 × Ar*H*), 7.30–7.13 (m, 9H, 9 × Ar*H*), 7.07–6.99 (m, 2H, Ar*H*, C=C*H*S), 2.92–2.83 (br s, 4H, C$_6$H$_5$C*H*$_2$C*H*$_2$); **^{13}C NMR** (125 MHz, DMSO-d_6) δ (ppm) 169.6, 166.1, 163.1, 141.6, 141.5, 140.4, 139.0,

137.7, 134.6, 133.8, 130.0, 129.9, 129.7, 128.7, 128.3, 128.3, 128.2, 127.7, 125.8, 123.8, 123.4, 120.9, 120.2, 119.9, 114.8, 36.9, 36.7; **LRMS** (ES + APCI) *m/z*: calc. for $C_{33}H_{26}N_2O_4S$ 546.2, found 547.0 $[M+H]^+$; **HMRS** calc. for $C_{33}H_{25}N_2O_4S$ 545.1541 $[M–H]^-$, found 545.1547 $[M–H]^-$.

2-((3-((2-Methoxyethyl)carbamoyl)-4-(4-phenethylphenyl)thiophen-2-yl)carbamoyl)benzoic acid (254)

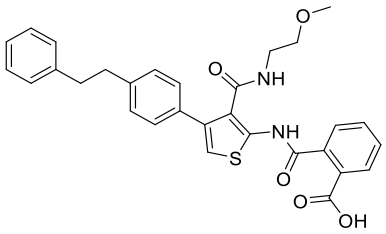

Following General Procedure E, compound **232** (86 mg, 0.23 mmol) and phthalic anhydride (34 mg, 0.23 mmol), after purification *via* flash column chromatography (dry loading, Petroleum ether 1:2 EtOAc, CH_2Cl_2 9:1 MeOH), afforded the *title compound* (70 mg, 0.13 mmol, 59%) as an off-white solid. **mp** 112–114 °C; **IR**(ATR)/cm^{-1} 3389, 3264, 3028, 2915, 2878, 1721, 1638, 1580, 1561, 1509, 1452, 1398, 1275, 1240, 1123, 1087; **^{1}H NMR** (500 MHz, DMSO-d_6) δ (ppm) 14.03 (br s, 1H, COO*H*), 7.83 (d, *J* 7.0 Hz, 1H, Ar*H*), 7.75 (d, *J* 7.0 Hz, 1H, Ar*H*), 7.68 (app br s, 1H, CON*H*CH_2), 7.48 (app pentet, *J* 7.0 Hz, 2H, 2 × Ar*H*), 7.33 (d, *J* 8.0 Hz, 2H, 2 × Ar*H*), 7.31–7.22 (m, 6H, 6 × Ar*H*), 7.19 (app t, *J* 7.0 Hz, 1H, Ar*H*), 6.96 (s, 1H, C=C*H*S), 3.33–3.27 (m, 4H, CONHCH_2CH_2OCH_3), 3.11 (s, 3H, CONHCH_2CH_2OCH_3), 2.93–2.88 (m, 4H, C_6H_5CH_2CH_2); **^{13}C NMR** (125 MHz, DMSO-d_6) δ (ppm) 171.0, 165.8, 164.8, 142.2, 141.5, 140.6, 138.3, 137.2, 133.6, 130.1, 130.0, 128.8, 128.7, 128.3, 128.3, 128.2, 127.8, 125.8, 123.7, 119.2, 114.5, 70.0, 57.7, 38.7, 37.0, 36.7; **LRMS** (ES + APCI) *m/z*: calc. for $C_{30}H_{28}N_2O_5S$ 528.2, found 528.9 $[M+H]^+$; **HMRS** calc. for $C_{30}H_{27}N_2O_5S$ 527.1646 $[M–H]^-$, found 527.1652 $[M–H]^-$.

2-((3-((3-Methoxypropyl)carbamoyl)-4-(4-phenethylphenyl)thiophen-2-yl)carbamoyl)benzoic acid (255)

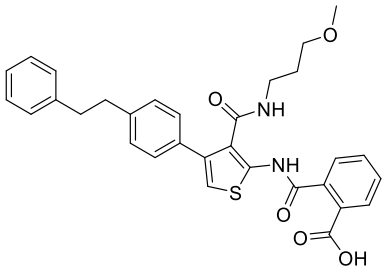

Following General Procedure E, compound **233** (88 mg, 0.22 mmol) and phthalic anhydride (33 mg, 0.22 mmol), after purification *via* flash column chromatography (dry loading, Petroleum ether 1:2 EtOAc, CH_2Cl_2 9:1 MeOH), afforded the *title compound* (79 mg, 0.15 mmol, 65%) as an off-white solid. **mp** 113–115 °C; **IR**(ATR)/cm^{-1} 3408, 3251, 3025, 2919, 2861, 1721, 1608, 1587, 1519, 1485, 1454, 1390, 1290, 1258, 1113; **^{1}H NMR** (500 MHz, DMSO-d_6) δ (ppm) 14.10 (br s, 1H, COO*H*), 7.81 (d, *J* 7.0 Hz, 1H, Ar*H*), 7.77 (d, *J* 7.0 Hz, 1H, Ar*H*), 7.68 (br s, 1H, CON*H*CH_2), 7.48 (app pentet, *J* 7.0 Hz, 2H, 2 × Ar*H*), 7.32 (d, *J* 8.0 Hz, 2H, 2 × Ar*H*), 7.31–7.22 (m, 6H, 6 × Ar*H*), 7.18 (app t, *J* 7.0 Hz, 1H, Ar*H*), 6.96 (s, 1H, C=C*H*S), 3.21–3.15 (m, 4H, CONHC$H_2$$CH_2CH_2$$OCH_3$), 3.12 (s, 3H, CONHC$H_2$ $CH_2CH_2OCH_3$), 2.90 (br s, 4H, $C_6H_5CH_2CH_2$), 1.57 (app pentet, 2H, CONHCH_2C$H_2$$CH_2OCH_3$); **^{13}C NMR** (125 MHz, DMSO-d_6) δ (ppm) 171.0, 165.7, 164.7, 141.7, 141.5, 140.5, 138.4, 137.3, 133.7, 133.3, 130.0, 129.9, 128.9, 128.8, 128.3, 128.3, 128.2, 127.8, 125.8, 119.7, 114.5, 69.8, 57.8, 37.0, 36.7, 36.5, 28.6; **LRMS** (ES + APCI) *m/z*: calc. for $C_{31}H_{30}N_2O_5S$ 542.2, found 543.0 $[M+H]^+$; **HMRS** calc. for $C_{31}H_{29}N_2O_5S$ 541.1803 $[M–H]^-$, found 541.1811 $[M–H]^-$.

2-((4-(4-Phenethylphenyl)-3-(piperidin-1-ylcarbamoyl)thiophen-2-yl)carbamoyl)benzoic acid (256)

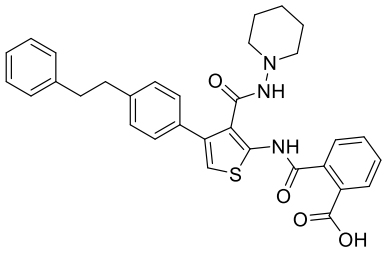

Following General Procedure E, compound **234** (51 mg, 0.13 mmol) and phthalic anhydride (19 mg, 0.13 mmol), after purification *via* flash column chromatography (dry loading, Petroleum ether 1:2 EtOAc, CH_2Cl_2 9:1 MeOH), afforded the *title compound* (23 mg, 0.04 mmol, 9%**) as an off-white solid. **mp** 117–119 °C; **IR**(ATR)/cm^{-1} 3404 br, 3272, 3021, 2928, 2852, 1719, 1638, 1582, 1504, 1452, 1390, 1258, 1076, 1011; **^{1}H NMR** (500 MHz, DMSO-d_6) δ (ppm) 14.48 (br s, 1H, COO*H*), 8.96–8.80 (m, 1H, CON*H*N), 7.84 (d, *J* 7.0 Hz, 1H, Ar*H*), 7.75 (d, *J* 7.0 Hz, 1H, Ar*H*), 7.52–7.43 (m, 2H, 2 × Ar*H*), 7.33 (d, *J* 8.0 Hz, 2H, 2 × Ar*H*), 7.30–7.20 (m, 6H, 6 × Ar*H*), 7.19–7.13 (m, 1H, Ar*H*), 6.99 (s, 1H, C=C*H*S), 2.89 (br s, 4H, $C_6H_5CH_2CH_2$), 2.66–2.56 (m, 4H, CONHN(CH_2)CH_2), 1.54–1.46 (m, 4H, CONHN(CH_2CH_2)CH_2CH_2), 1.30–1.24 (m, 2H, CONHN(CH_2CH_2)$CH_2CH_2CH_2$); **^{13}C NMR** (125 MHz, DMSO-d_6) δ (ppm) 171.5, 165.2, 162.4, 141.4, 141.0, 140.5, 137.4, 133.6, 132.2, 130.3, 129.9, 129.4, 128.4, 128.2, 128.2, 128.1, 127.7, 127.2, 125.8, 119.4, 114.3, 54.9, 36.9, 36.6, 24.9, 23.0; **LRMS** (ES + APCI) *m/z*: calc. for $C_{32}H_{31}N_3O_4S$ 553.2, found 554.0 $[M+H]^+$; **HMRS** calc. for $C_{32}H_{30}N_3O_4S$ 552.1963 $[M–H]^-$, found 552.1974 $[M–H]^-$.

2-((4-(4-Phenethylphenyl)-3-((tetrahydro-2*H*-pyran-4-yl)carbamoyl)thiophen-2-yl)carbamoyl)benzoic acid (257)

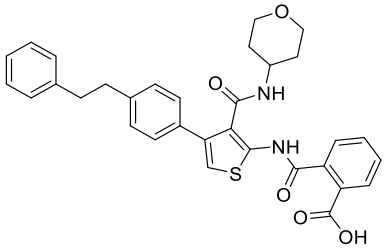

Following General Procedure E, compound **235** (78 mg, 0.19 mmol) and phthalic anhydride (28 mg, 0.19 mmol), after purification *via* flash column chromatography (dry loading, Petroleum ether 1:2 EtOAc, CH_2Cl_2 9:1 MeOH), afforded the *title compound* (64 mg, 0.12 mmol, 60%) as an off-white solid. **mp** 138–140 °C; **IR**(ATR)/cm^{-1} 3256, 3076, 2937, 2856, 1721, 1668, 1609, 1576, 1523, 1489, 1393, 1268, 1116, 1101; **^{1}H NMR** (500 MHz, DMSO-d_6) δ (ppm) 14.47 (br s, 1H, COO*H*), 7.80 (d, *J* 7.0 Hz, 2H, 2 × Ar*H*), 7.70 (app br s, 1H, CON*H*CH_2), 7.48 (app pentet, *J* 7.0 Hz, 2H, 2 × Ar*H*), 7.33 (d, *J* 8.0 Hz, 2H, 2 × Ar*H*), 7.31–7.22 (m, 6H, 6 × Ar*H*), 7.18 (app t, *J* 7.0 Hz, 1H, Ar*H*), 6.97 (s, 1H, C=C*H*S), 3.96–3.87

(m, 1H, CONHC*H*), 3.71 (app d, *J* 11.0 Hz, 2H, CONHCH(CH_2CH_2)CH_2C*H_2*O), 3.29 (t, *J* 11.0 Hz, 2H, CONHCH(CH_2C*H_2*)CH_2CH_2O), 2.90 (br s, 4H, C_6H_5C*H_2C*H_2*), 1.73 (app d, *J* 11.0 Hz, 2H, CONHCH(CH_2CH_2)C*H_2*CH_2O), 1.29–1.20 (m, 2H, CONHCH(C*H_2*CH_2)CH_2CH_2O); **^{13}C NMR** (125 MHz, DMSO-*d_6*) δ (ppm) 170.9, 165.5, 163.9, 141.5, 141.4, 140.6, 137.3, 133.7, 133.0, 130.1, 130.0, 129.0, 128.7, 128.3, 128.2, 128.2, 127.8, 127.6, 125.8, 119.9, 114.3, 65.8, 45.2, 37.0, 36.6, 31.7; **LRMS** (ES + APCI) *m/z*: calc. for $C_{32}H_{30}N_2O_5S$ 554.2, found 555.0 $[M+H]^+$; **HMRS** calc. for $C_{32}H_{29}N_2O_5S$ 553.1803 $[M–H]^-$, found 553.1811 $[M–H]^-$.

2-((4-(4-Phenethylphenyl)-3-((tetrahydrofuran-3-yl)carbamoyl)thiophen-2-yl)carbamoyl)benzoic acid (258)

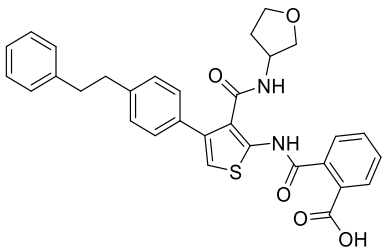

Following General Procedure E, compound **236** (68 mg, 0.17 mmol) and phthalic anhydride (24 mg, 0.17 mmol), after purification *via* flash column chromatography (dry loading, Petroleum ether 1:3 EtOAc, CH_2Cl_2 9:1 MeOH), afforded the *title compound* (52 mg, 0.10 mmol, 39%**) as an off-white solid. **mp** 121–123 °C; **IR**(ATR)/cm^{-1} 3396, 3025, 2967, 2857, 1719, 1606, 1582, 1517, 1454, 1403, 1296, 1258, 1076; **^{1}H NMR** (500 MHz, DMSO-*d_6*) δ (ppm) 14.49 (br s, 1H, COO*H*), 7.97 (app br s, 1H, CON*H*CH), 7.85 (d, *J* 7.0 Hz, 2H, 2 × Ar*H*), 7.48 (app pentet, *J* 7.0 Hz, 2H, 2 × Ar*H*), 7.32 (d, *J* 8.0 Hz, 2H, 2 × Ar*H*), 7.30–7.22 (m, 6H, 6 × Ar*H*), 7.18 (app t, *J* 7.0 Hz, 1H, Ar*H*), 6.97 (s, 1H, C=C*H*S), 4.43–4.34 (m, 1H, CONHC*H*CH_2O), 3.73 (dd, *J* 9.0 Hz, 6.5 Hz, 1H, CONHCH(CH_2)CH(*H*)OCH_2), 3.63–3.52 (m, 2H, CONHCH(CH_2)CH_2OC*H_2*), 3.43 (dd, *J* 9.0 Hz, 4.0 Hz, 1H, CONHCH(CH_2)C*H*(H)OCH_2), 2.90 (br s, 4H, C_6H_5C*H_2C*H_2*), 2.03–1.94 (m, 1H, CONHCH(C(H)*H*)CH_2OCH_2), 1.71–1.61 (m, 1H, CONHCH(C(*H*)H)CH_2OCH_2); **^{13}C NMR** (125 MHz, DMSO-*d_6*) δ (ppm) 171.1, 165.5, 164.7, 141.6, 141.5, 140.6, 137.3, 133.7, 133.0, 130.1, 129.1, 128.8, 128.7, 128.4, 128.3, 128.2, 127.8, 125.8, 125.5, 119.8, 114.3, 71.9, 66.2, 50.0, 37.0, 36.7, 31.7; **LRMS** (ES + APCI) *m/z*: calc.

for $C_{31}H_{28}N_2O_5S$ 540.2, found 541.0 $[M+H]^+$; **HMRS** calc. for $C_{31}H_{27}N_2O_5S$ 539.1646 $[M–H]^-$, found 539.1655 $[M–H]^-$.

2-((4-(4-Phenethylphenyl)-3-(((tetrahydrofuran-3-yl)methyl)carbamoyl)thiophen-2-yl)carbamoyl)benzoic acid (259)

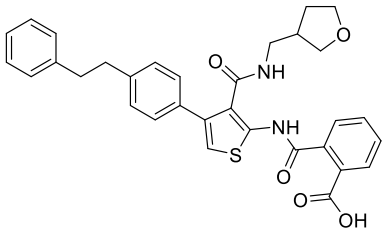

Following General Procedure E, compound **237** (86 mg, 0.21 mmol) and phthalic anhydride (31 mg, 0.21 mmol), after purification *via* flash column chromatography (dry loading, Petroleum ether 1:2 EtOAc, CH_2Cl_2 9:1 MeOH), afforded the *title compound* (70 mg, 0.13 mmol, 60%) as an off-white solid. **mp** 128–130 °C; **IR**(ATR)/cm^{-1} 3409, 3054, 2958, 2926, 2854, 1721, 1667, 1608, 1587, 1519, 1483, 1396, 1292, 1258, 1072, 1020; **^{1}H NMR** (500 MHz, DMSO-d_6) δ (ppm) 14.25 (br s, 1H, COO*H*), 7.87 (app br s, 1H, CON*H*CH_2), 7.81 (d, *J* 7.0 Hz, 1H, Ar*H*), 7.78 (d, *J* 7.0 Hz, 1H, Ar*H*), 7.48 (app pentet, *J* 7.0 Hz, 2H, 2 × Ar*H*), 7.32 (d, *J* 8.0 Hz, 2H, 2 × Ar*H*), 7.30–7.22 (m, 6H, 6 × Ar*H*), 7.18 (app t, *J* 7.0 Hz, 1H, Ar*H*), 6.96 (s, 1H, C=C*H*S), 3.63 (app q, *J* 8.0 Hz, 1H, $CONHCH_2CH(CH(H))CH_2CH_2O$), 3.56–3.48 (m, 2H, $CONHCH_2CH(CH_2)CH_2CH_2O$), 3.24 (dd, *J* 8.0 Hz, 5.5 Hz, 1H, $CONHCH_2CH(CH(H))CH_2CH_2O$), 3.19–3.06 (m, 2H, $CONHCH_2CH(CH_2)CH_2CH_2O$), 2.89 (br s, 4H, $C_6H_5CH_2CH_2$), 2.28 (app septet, *J* 7.0 Hz, 1H, $CONHCH_2CH(CH_2)CH_2CH_2O$), 1.77 (app sextet, *J* 7.0 Hz, 1H, $CONHCH_2CH(CH_2)C(H)HCH_2O$), 1.39 (app sextet, *J* 7.0 Hz, 1H, $CONHCH_2CH(CH_2)C(H)HCH_2O$); **^{13}C NMR** (125 MHz, DMSO-d_6) δ (ppm) 171.1, 165.6, 164.9, 141.5, 140.6, 138.5, 137.3, 133.7, 133.1, 130.1, 130.0, 129.0, 128.7, 128.3, 128.3, 128.2, 127.8, 127.6, 125.8, 119.9, 114.4, 70.6, 66.7, 42.1, 38.3, 37.0, 36.7, 29.6; **LRMS** (ES + APCI) *m/z*: calc. for $C_{32}H_{30}N_2O_5S$ 554.2, found 555.0 $[M+H]^+$; **HMRS** calc. for $C_{32}H_{29}N_2O_5S$ 553.1803 $[M–H]^-$, found 553.1810 $[M–H]^-$.

2-((4-(4-Phenethylphenyl)-3-(((tetrahydrofuran-2-yl)methyl)carbamoyl)thiophen-2-yl)carbamoyl)benzoic acid (260)

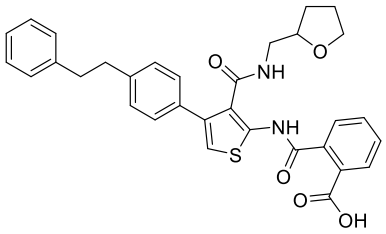

Following General Procedure E, compound **238** (90 mg, 0.24 mmol) and phthalic anhydride (33 mg, 0.22 mmol), after purification *via* flash column chromatography (dry loading, Petroleum ether 1:2 EtOAc, CH_2Cl_2 9:1 MeOH), afforded the *title compound* (82 mg, 0.15 mmol, 67%) as an off-white solid. **mp** 119–121 °C; **IR**(ATR)/cm^{-1} 3404, 3060, 2922, 1721, 1667, 1610, 1587, 1517, 1454, 1394, 1258, 1227, 1074, 1022; **^{1}H NMR** (500 MHz, DMSO-d_6) δ (ppm) 13.99 (br s, 1H, COO*H*), 7.83 (d, *J* 7.0 Hz, 1H, Ar*H*), 7.74 (d, *J* 7.0 Hz, 1H, Ar*H*), 7.68 (br s, 1H, CON*H*CH_2), 7.48 (app pentet, *J* 7.0 Hz, 2H, 2 × Ar*H*), 7.33 (d, *J* 8.0 Hz, 2H, 2 × Ar*H*), 7.31–7.22 (m, 6H, 6 × Ar*H*), 7.19 (app t, *J* 7.0 Hz, 1H, Ar*H*), 6.95 (s, 1H, C=C*H*S), 3.80 (app pentet, *J* 6.5 Hz, 1H, CONHCH$_2$C*H*O), 3.57 (app q, *J* 6.5 Hz, 1H, CONHCH$_2$CH(CH$_2$CH$_2$)OC(*H*)H), 3.43 (app q, *J* 6.5 Hz, 1H, CONHCH$_2$CH(CH$_2$CH$_2$)OC(H)*H*), 3.31–3.34 (m, 1H, CONHC(*H*)HCHO), 3.14 (app dt, *J* 13.5 Hz, 5.5 Hz, 1H, CONHC(H)*H*CHO), 2.90 (br s, 4H, $C_6H_5CH_2CH_2$), 1.76–1.64 (m, 3H, CONHCH$_2$CH(CH_2C(*H*)H)OCH$_2$), 1.43–1.34 (m, 1H, CONHCH$_2$CH(CH$_2$C(H)*H*)OCH$_2$); **^{13}C NMR** (125 MHz, DMSO-d_6) δ (ppm) 171.0, 166.0, 164.9, 142.3, 141.5, 140.6, 138.0, 137.3, 133.8, 133.6, 130.0, 129.9, 128.9, 128.6, 128.3, 128.3, 128.2, 127.9, 125.8, 119.1, 114.5, 76.4, 66.9, 43.0, 36.9, 36.7, 28.4, 25.0; **LRMS** (ES + APCI) *m/z*: calc. for $C_{32}H_{30}N_2O_5S$ 554.2, found 555.0 $[M+H]^+$; **HMRS** calc. for $C_{32}H_{29}N_2O_5S$ 553.1803 $[M–H]^-$, found 553.1810 $[M–H]^-$.

2-((3-(((1,3-Dioxolan-2-yl)methyl)carbamoyl)-4-(4-phenethylphenyl)thiophen-2-yl)carbamoyl)benzoic acid (261)

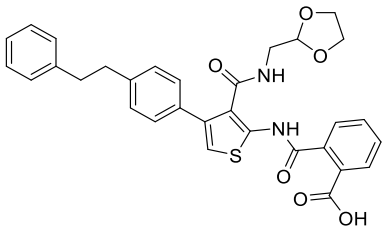

Following General Procedure E, compound **239** (68 mg, 0.17 mmol) and phthalic anhydride (24 mg, 0.17 mmol), after purification *via* flash column chromatography (dry loading, Petroleum ether 1:2 EtOAc, CH_2Cl_2 9:1 MeOH), afforded the *title compound* (53 mg, 0.10 mmol, 57%) as an off-white solid. **mp** 128–130 °C; **IR**(ATR)/cm^{-1} 3398, 3019, 2937, 2887, 1723, 1654, 1604, 1580, 1515, 1454, 1402, 1258, 1139, 1020; **^{1}H NMR** (500 MHz, DMSO-d_6) δ (ppm) 14.00 (br s, 1H, COO*H*), 7.85 (d, *J* 7.0 Hz, 1H, Ar*H*), 7.75 (d, *J* 7.0 Hz, 1H, Ar*H*), 7.70 (br s, 1H, CON*H*CH_2), 7.48 (app pentet, *J* 7.0 Hz, 2H, 2 × Ar*H*), 7.34 (d, *J* 8.0 Hz, 2H, 2 × Ar*H*), 7.32–7.23 (m, 6H, 6 × Ar*H*), 7.19 (app t, *J* 7.0 Hz, 1H, Ar*H*), 6.95 (s, 1H, C=C*H*S), 4.88 (t, *J* 4.0 Hz, 1H, $CONHCH_2CHO(O)$), 3.79–3.66 (m, 4H, $CONHCH_2CH(OCH_2)OCH_2$), 3.34 (app t, *J* 4.0 Hz, 2H, $CONHCH_2CH(OCH_2)OCH_2$), 2.90 (br s, 4H, $C_6H_5CH_2CH_2$); **^{13}C NMR** (125 MHz, DMSO-d_6) δ (ppm) 171.0, 166.0, 164.9, 142.7, 141.5, 140.6, 138.2, 137.2, 133.7, 133.6, 130.1, 129.9, 128.9, 128.7, 128.4, 128.2, 127.9, 127.6, 125.8, 118.6, 114.5, 101.1, 64.3, 41.6, 37.0, 36.7; **LRMS** (ES + APCI) *m/z*: calc. for $C_{31}H_{28}N_2O_6S$ 556.2, found 557.0 $[M+H]^+$; **HMRS** calc. for $C_{31}H_{27}N_2O_6S$ 555.1595 $[M–H]^-$, found 555.1608 $[M–H]^-$.

2-((3-(((1-Methylpyrrolidin-2-yl)methyl)carbamoyl)-4-(4-phenethylphenyl)thiophen-2-yl)carbamoyl)benzoic acid (262)

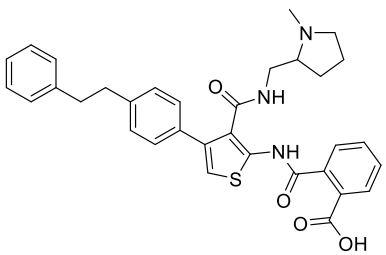

Following General Procedure E, compound **240** (108 mg, 0.26 mmol) and phthalic anhydride (37 mg, 0.26 mmol), after purification *via* flash column chromatography (dry loading, Petroleum ether 1:2 EtOAc, CH_2Cl_2 9:1 MeOH), afforded the *title compound* (86 mg, 0.15 mmol, 59%) as an off-white solid. **mp** 139–141 °C; **IR**(ATR)/cm^{-1} 3443, 3049, 2943, 2885, 1719, 1653, 1634, 1558, 1532, 1489, 1376, 1275, 1238, 1061; **^{1}H NMR** (500 MHz, DMSO-d_6) δ (ppm) 15.36 (br s, 1H, COO*H*), 11.66 (br s, 1H, CON*H*CS), 8.56 (app br s, 1H, CON*H*CH_2), 8.12–8.04 (m, 1H, Ar*H*), 7.82 (d, *J* 7.0 Hz, 1H, Ar*H*), 7.52 (app pentet, *J* 7.0 Hz, 2H, 2 × Ar*H*), 7.32 (d, *J* 8.0 Hz, 2H, 2 × Ar*H*), 7.30–7.22 (m, 6H, 6 × Ar*H*), 7.19 (app t, *J* 7.0 Hz, 1H, Ar*H*), 7.05 (s, 1H, C=C*H*S), 4.05–3.70 (m, 2H, CONHC*H*$_2$CH(N(CH_3)CH_2)CH_2CH_2), 3.20–3.09 (m, 1H, CONHCH$_2$C*H*(N(CH_3)CH_2)CH_2CH_2), 3.00–2.80 (m, 9H, CONHCH$_2$CH(N(C*H*$_3$)C*H*$_2$)CH_2CH_2, $C_6H_5CH_2CH_2$), 2.06–1.75 (m, 4H, CONHCH$_2$CH(N(CH_3)CH_2)C*H*$_2$C*H*$_2$); **^{13}C NMR** (125 MHz, DMSO-d_6) δ (ppm) 172.2, 167.4, 164.1, 142.0, 140.9, 139.8, 139.2, 137.5, 133.9, 131.4, 131.1, 129.8, 129.6, 129.3, 128.9, 128.7, 127.7, 126.3, 121.5, 114.8, 114.6, 66.8, 56.1, 55.3, 37.4, 37.2, 26.3, 20.7, 19.9; **LRMS** (ES + APCI) *m/z*: calc. for $C_{33}H_{33}N_3O_4S$ 567.2, found 568.0 $[M+H]^+$; **HMRS** calc. for $C_{33}H_{32}N_3O_4S$ 566.2119 $[M–H]^-$, found 566.2131 $[M–H]^-$.

2-((3-((2-Morpholinoethyl)carbamoyl)-4-(4-phenethylphenyl)thiophen-2-yl)carbamoyl)benzoic acid (263)

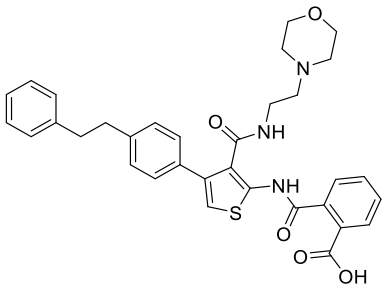

Following General Procedure E, compound **241** (88 mg, 0.20 mmol) and phthalic anhydride (30 mg, 0.20 mmol), after purification *via* flash column chromatography (dry loading, Petroleum ether 1:4 EtOAc, CH_2Cl_2 9:1 MeOH), afforded the *title compound* (51 mg, 0.09 mmol, 43%) as an off-white solid. **mp** 113–115 °C; **IR**(ATR)/cm^{-1} 3391, 3281, 3023, 2924, 2855, 1716, 1660, 1615, 1583,

1515, 1455, 1394, 1262, 1117, 1072; **^{1}H NMR** (500 MHz, DMSO-d_6) δ (ppm) 13.60 (br s, 2H, COO*H*, CON*H*CS), 7.82 (d, *J* 7.0 Hz, 1H, Ar*H*), 7.80–7.72 (m, 2H, Ar*H*, CON*H*CH_2), 7.54 (app pentet, *J* 7.0 Hz, 2H, 2 × Ar*H*), 7.32 (d, *J* 8.0 Hz, 2H, 2 × Ar*H*), 7.31–7.24 (m, 6H, 6 × Ar*H*), 7.19 (app t, *J* 7.0 Hz, 1H, Ar*H*), 7.00 (s, 1H, C=C*H*S), 3.56 (app br s, 4H, $CONHCH_2CH_2N(CH_2CH_2)CH_2CH_2O$), 3.33 (app q, *J* 5.5 Hz, 2H, $CONHCH_2CH_2N$), 2.90 (br s, 4H, $C_6H_5CH_2CH_2$), 2.66–2.55 (m, 6H, $CONHCH_2CH_2N(CH_2CH_2)CH_2CH_2O$); **^{13}C NMR** (125 MHz, DMSO-d_6) δ (ppm) 170.6, 165.2, 165.0, 141.5, 141.2, 140.7, 137.2, 136.9, 133.5, 132.8, 130.6, 129.7, 129.4, 128.9, 128.4, 128.3, 128.2, 127.8, 125.8, 119.4, 114.9, 64.9, 56.1, 52.1, 36.9, 36.7, 35.2; **LRMS** (ES + APCI) *m/z*: calc. for $C_{33}H_{33}N_3O_5S$ 583.2, found 584.0 $[M+H]^+$; **HMRS** calc. for $C_{33}H_{32}N_3O_5S$ 582.2068 $[M–H]^+$, found 582.2068 $[M–H]^+$.

Methyl 2-((4-acetylphenoxy)methyl)benzoate (269)

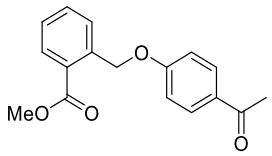

Following General procedure H, methyl 2-(bromomethyl)benzoate (2.00 g, 8.81 mmol) and 1-(4-hydroxyphenyl)ethan-1-one (1.00 g, 7.34 mmol), after purification *via* flash column chromatography (dry loading, Petroleum ether 3:1 EtOAc, isocratic), afforded the *title compound* (1.83 g, 6.44 mmol, 88%) as an off-white solid. **mp** 81–83 °C; **IR**(ATR)/cm^{-1} 3083, 2949, 1714, 1659, 1601, 1575, 1510, 1434, 1270, 1246, 1181, 1090; **^{1}H NMR** (500 MHz, $CDCl_3$) δ (ppm) 8.04 (d, *J* 8.0 Hz, 1H, Ar*H*), 7.93 (d, *J* 8.0 Hz, 2H, 2 × Ar*H*), 7.71 (d, *J* 8.0 Hz, 1H, Ar*H*), 7.59 (app t, *J* 8.0 Hz, 1H, Ar*H*), 7.39 (app t, *J* 8.0 Hz, 1H, Ar*H*), 7.02 (d, *J* 8.0 Hz, 2H, 2 × Ar*H*), 5.57 (s, 2H, OCH_2), 3.90 (s, 3H, OCH_3), 2.55 (s, 3H, CH_3); **^{13}C NMR** (125 MHz, $CDCl_3$) δ (ppm) 196.9, 167.4, 162.7, 138.9, 132.8, 131.0, 130.8, 130.7, 127.8, 127.7, 127.5, 114.7, 68.4, 52.3, 26.5; **LRMS** (ES + APCI) *m/z*: calc. for $C_{17}H_{16}O_4$ 284.1, found 285.0 $[M+H]^+$; **HMRS** calc. for $C_{17}H_{17}O_4$ 285.1121 $[M+H]^+$, found 285.1122 $[M+H]^+$.

Methyl 3-((4-acetylphenoxy)methyl)benzoate (270)

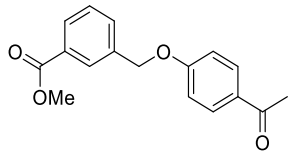

Following General procedure H, methyl 3-(bromomethyl)benzoate (2.00 g, 8.81 mmol) and 1-(4-hydroxyphenyl)ethan-1-one (1.00 g, 7.34 mmol), after purification *via* flash column chromatography (dry loading, Petroleum ether 3:1 EtOAc, isocratic), afforded the *title compound* (1.93 g, 6.80 mmol, 93%) as an off-white solid. **mp** 95–97 °C; **IR**(ATR)/cm^{-1} 3076, 2959, 1713, 1679, 1599, 1586, 1512, 1450, 1380, 1249, 1205, 1171, 1108; **^{1}H NMR** (500 MHz, $CDCl_3$) δ (ppm) 8.12 (s, 1H, Ar*H*), 8.02 (d, *J* 8.0 Hz, 1H, Ar*H*), 7.94 (d, *J* 8.0 Hz, 2H, 2 × Ar*H*), 7.63 (d, *J* 8.0 Hz, 1H, Ar*H*), 7.48 (app t, *J* 8.0 Hz, 1H, Ar*H*), 7.01 (d, *J* 8.0 Hz, 2H, 2 × Ar*H*), 5.17 (s, 2H, OCH_2), 3.93 (app d, *J* 1.5 Hz, 3H, OCH_3), 2.55 (app d, *J* 1.5 Hz, 3H, CH_3); **^{13}C NMR** (125 MHz, $CDCl_3$) δ (ppm) 196.8, 166.9, 162.5, 136.8, 131.9, 130.9, 130.8, 130.7, 129.6, 128.9, 128.7, 114.7, 69.7, 52.4, 26.5; **LRMS** (ES + APCI) *m/z*: calc. for $C_{17}H_{16}O_4$ 284.1, found 285.0 $[M+H]^+$; **HMRS** calc. for $C_{17}H_{17}O_4$ 285.1121 $[M+H]^+$, found 285.1122 $[M+H]^+$.

Methyl 4-((4-acetylphenoxy)methyl)benzoate (271)

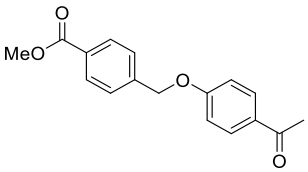

Following General procedure H, methyl 4-(bromomethyl)benzoate (1.56 g, 6.81 mmol) and 1-(4-hydroxyphenyl)ethan-1-one (773 mg, 5.67 mmol), after purification *via* flash column chromatography (dry loading, Petroleum ether 3:1 EtOAc, isocratic), afforded the *title compound* (1.53 g, 5.39 mmol, 95%) as an off-white solid. **mp** 120–122 °C; **IR**(ATR)/cm^{-1} 3065, 2921, 2873, 1718, 1670, 1601, 1579, 1512, 1365, 1285, 1253, 1108, 1019; **^{1}H NMR** (500 MHz, $CDCl_3$) δ (ppm) 8.06 (d, *J* 8.0 Hz, 2H, 2 × Ar*H*), 7.94 (d, *J* 8.5 Hz, 2H, 2 × Ar*H*), 7.50 (d, *J* 8.0 Hz, 2H, 2 × Ar*H*), 7.00 (d, *J* 8.5 Hz, 2H, 2 × Ar*H*), 5.20 (s, 2H, OCH_2), 3.93 (s, 3H, OCH_3), 2.55 (s, 3H, CH_3); **^{13}C NMR**

(125 MHz, $CDCl_3$) δ (ppm) 196.8, 166.9, 162.4, 141.5, 130.9, 130.8, 130.1, 127.2, 127.1, 114.7, 69.6, 52.3, 26.5; **LRMS** (ES + APCI) *m/z*: calc. for $C_{17}H_{16}O_4$ 284.1, found 285.0 $[M+H]^+$; **HMRS** calc. for $C_{17}H_{17}O_4$ 285.1121 $[M+H]^+$, found 285.1123 $[M+H]^+$.

Methyl 2-((4-acetylphenoxy)methyl)benzoate (272)

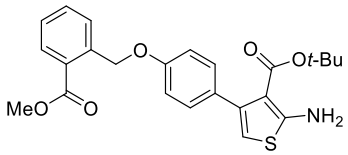

Following General Procedure D, *tert*-butyl 2-cyanoacetate (895 mg, 6.34 mmol) and compound **269** (900 mg, 3.17 mmol), after purification *via* flash column chromatography (dry loading, petroleum ether 10:1 EtOAc, isocratic), afforded the *title compound* (373 mg, 0.85 mmol, 27%) as an off-white solid. **mp** 44–46 °C; **IR**(ATR)/cm^{-1} 3412, 3318, 3026, 2925, 1714, 1660, 1603, 1575, 1501, 1240, 1136, 1030; **^{1}H NMR** (500 MHz, $CDCl_3$) δ (ppm) 8.03 (d, *J* 7.5 Hz, 1H, Ar*H*), 7.76 (d, *J* 7.5 Hz, 1H, Ar*H*), 7.54 (app t, *J* 7.5 Hz, 1H, Ar*H*), 7.37 (app t, *J* 7.5 Hz, 1H, Ar*H*), 7.19 (d, *J* 8.0 Hz, 2H, 2 × Ar*H*), 6.93 (d, *J* 8.0 Hz, 2H, 2 × Ar*H*), 6.06–5.93 (m, 3H, C=C*H*S, NH_2), 5.53 (s, 2H, OCH_2), 3.92 (s, 3H, OCH_3), 1.22 (s, 9H, COOC(CH_3)$_3$); **^{13}C NMR** (125 MHz, $CDCl_3$) δ (ppm) 167.5, 165.5, 163.2, 157.7, 141.5, 140.0, 132.7, 132.0, 130.9, 130.1, 127.8, 127.5, 127.3, 113.9, 108.0, 105.0, 80.3, 68.3, 52.2, 28.2; **LRMS** (ES + APCI) *m/z*: calc. for $C_{24}H_{25}NO_5S$ 439.1, found 440.0 $[M+H]^+$; **HMRS** calc. for $C_{24}H_{26}NO_5S$ 440.1526 $[M+H]^+$, found 440.1527 $[M+H]^+$.

***tert*-Butyl 2-amino-4-(4-((3-(methoxycarbonyl)benzyl)oxy)phenyl)thiophene-3-carboxylate (273)**

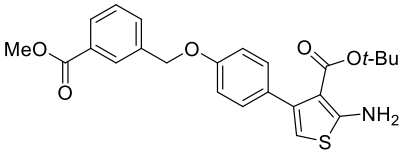

Following General Procedure D, *tert*-butyl 2-cyanoacetate (995 mg, 7.04 mmol) and compound **270** (1.00 g, 3.52 mmol), after purification *via* flash column chromatography (dry loading, petroleum ether 10:1 EtOAc, isocratic), afforded the

title compound (402 mg, 0.92 mmol, 26%) as an off-white solid. **mp** 110–112 °C; **IR**(ATR)/cm^{-1} 3427, 3321, 3102, 2921, 2866, 1713, 1659, 1586, 1501, 1395, 1279, 1210, 1175; **^{1}H NMR** (500 MHz, $CDCl_3$) δ (ppm) 8.13 (s, 1H, Ar*H*), 8.00 (d, *J* 8.0 Hz, 1H, Ar*H*), 7.65 (d, *J* 8.0 Hz, 1H, Ar*H*), 7.46 (app t, *J* 8.0 Hz, 1H, Ar*H*), 7.19 (d, *J* 8.5 Hz, 2H, 2 × Ar*H*), 6.92 (d, *J* 8.5 Hz, 2H, 2 × Ar*H*), 6.03–5.96 (m, 3H, C=C*H*S, NH_2), 5.13 (s, 2H, OCH_2), 3.93 (s, 3H, OCH_3), 1.21 (s, 9H, COOC(CH_3)$_3$); **^{13}C NMR** (125 MHz, $CDCl_3$) δ (ppm) 167.0, 165.5, 163.2, 157.6, 141.4, 137.8, 132.2, 131.9, 130.7, 130.1, 129.3, 128.8, 128.6, 114.0, 107.9, 105.1, 80.3, 69.6, 52.3, 28.2; **LRMS** (ES + APCI) *m/z*: calc. for $C_{24}H_{25}NO_5S$ 439.1, found 440.0 $[M+H]^+$; **HMRS** calc. for $C_{24}H_{26}NO_5S$ 440.1526 $[M+H]^+$, found 440.1525 $[M+H]^+$.

tert-Butyl 2-amino-4-(4-((4-(methoxycarbonyl)benzyl)oxy)phenyl)thiophene-3-carboxylate (274)

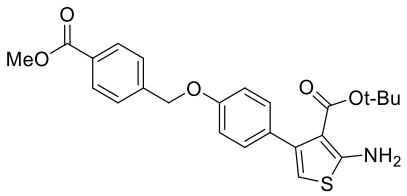

Following General Procedure D, *tert*-butyl 2-cyanoacetate (895 mg, 6.34 mmol) and compound **271** (900 mg, 3.17 mmol), after purification *via* flash column chromatography (dry loading, petroleum ether 10:1 EtOAc, isocratic), afforded the *title compound* (445 mg, 1.05 mmol, 33%) as an off-white solid. **mp** 123–125 °C; **IR**(ATR)/cm^{-1} 3414, 3316, 3102, 2973, 2854, 1722, 1644, 1582, 1501, 1393, 1277, 1238, 1101; **^{1}H NMR** (500 MHz, $CDCl_3$) δ (ppm) 8.05 (d, *J* 8.5 Hz, 2H, 2 × Ar*H*), 7.51 (d, *J* 8.5 Hz, 2H, 2 × Ar*H*), 7.19 (d, *J* 8.5 Hz, 2H, 2 × Ar*H*), 6.91 (d, *J* 8.5 Hz, 2H, 2 × Ar*H*), 6.01–5.97 (m, 3H, C=C*H*S, NH_2), 5.16 (s, 2H, OCH_2), 3.93 (s, 3H, OCH_3), 1.21 (s, 9H, COOC(CH_3)$_3$); **^{13}C NMR** (125 MHz, $CDCl_3$) δ (ppm) 166.9, 165.5, 163.2, 157.5, 142.6, 141.3, 132.3, 130.1, 130.0, 129.8, 127.0, 113.9, 107.9, 105.1, 80.3, 69.5, 52.3, 28.2; **LRMS** (ES + APCI) *m/z*: calc. for $C_{24}H_{25}NO_5S$ 439.1, found 440.0 $[M+H]^+$; **HMRS** calc. for $C_{24}H_{26}NO_5S$ 440.1526 $[M+H]^+$, found 440.1525 $[M+H]^+$.

2-((3-(*tert*-Butoxycarbonyl)-4-(4-((2-(methoxycarbonyl)benzyl)oxy)phenyl)thiophen-2-yl)carbamoyl)benzoic acid (275)

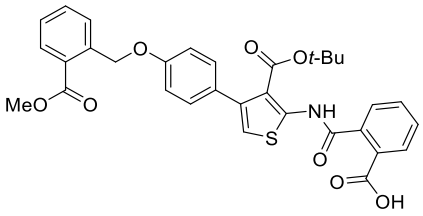

Following General Procedure E, compound **272** (330 mg, 0.75 mmol) and phthalic anhydride (111 mg, 0.75 mmol), after purification *via* flash column chromatography (dry loading, Petroleum ether 2:1 EtOAc, CH_2Cl_2 9.5:0.5 MeOH), afforded the *title compound* (192 mg, 0.33 mmol, 44%) as an off-white solid. **mp** 151–153 °C; **IR**(ATR)/cm^{-1} 3219 br, 3096, 2979, 1724, 1713, 1651, 1543, 1525, 1395, 1264, 1233, 1162, 1036; **^{1}H NMR** (500 MHz, DMSO-d_6) δ (ppm) 13.30 (br s, 1H, COO*H*), 11.45 (br s, 1H, CON*H*), 7.91 (app t, *J* 7.5 Hz, 2H, 2 × Ar*H*), 7.73–7.59 (m, 5H, 5 × Ar*H*), 7.47 (app t, *J* 7.5 Hz, 1H, Ar*H*), 7.20 (d, *J* 8.0 Hz, 2H, 2 × Ar*H*), 6.97 (d, *J* 8.0 Hz, 2H, 2 × Ar*H*), 6.88 (s, 1H, C=C*H*S), 5.46 (s, 2H, OCH_2), 3.83 (s, 3H, CH_3), 1.17 (s, 9H, COOC(CH_3)$_3$); **^{13}C NMR** (125 MHz, DMSO-d_6) δ (ppm) 173.8, 167.1, 166.9, 164.4, 157.3, 138.9, 138.6, 138.3, 132.6, 132.4, 130.7, 130.6, 130.5, 130.3, 130.2, 129.9, 129.8, 128.7, 128.6, 127.9, 127.8, 127.7, 114.9, 113.9, 81.4, 67.5, 52.1, 27.4; **LRMS** (ES + APCI) *m/z*: calc. for $C_{32}H_{29}NO_8S$ 587.2, found 586.1 $[M–H]^-$; **HMRS** calc. for $C_{32}H_{28}NO_8S$ 586.1541 $[M–H]^-$, found 586.1540 $[M–H]^-$.

2-((3-(*tert*-Butoxycarbonyl)-4-(4-((3-(methoxycarbonyl)benzyl)oxy)phenyl)thiophen-2-yl)carbamoyl)benzoic acid (276)

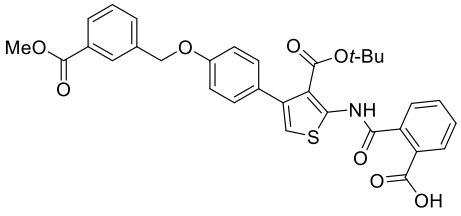

Following General Procedure E, compound **273** (300 mg, 0.67 mmol) and phthalic anhydride (101 mg, 0.67 mmol), after purification *via* flash column

chromatography (dry loading, Petroleum ether 2:1 EtOAc, CH_2Cl_2 9:1 MeOH), afforded the *title compound* (207 mg, 0.51 mmol, 52%) as an off-white solid. **mp** 187–189 °C; **IR**(ATR)/cm^{-1} 3267 br, 3120, 3042, 2947, 1722, 1659, 1651, 1521, 1393, 1287, 1231, 1160, 1108; **^{1}H NMR** (500 MHz, DMSO-d_6) δ (ppm) 13.35 (br s, 1H, COO*H*), 11.81 (br s, 1H, CON*H*), 8.05 (s, 1H, Ar*H*), 7.95–7.85 (m, 2H, 2 × Ar*H*), 7.73 (d, *J* 8.0 Hz, 1H, Ar*H*), 7.70–7.59 (m, 3H, 3 × Ar*H*), 7.55 (app t, *J* 8.0 Hz, 1H, Ar*H*), 7.18 (d, *J* 8.5 Hz, 2H, 2 × Ar*H*), 7.02 (d, *J* 8.5 Hz, 2H, 2 × Ar*H*), 6.86 (s, 1H, C=C*H*S), 5.25 (s, 2H, OCH_2), 3.86 (s, 3H, CH_3), 1.14 (s, 9H, COOC(CH_3)$_3$); **^{13}C NMR** (125 MHz, DMSO-d_6) δ (ppm) 172.1, 166.1, 164.3, 157.1, 147.8, 138.9, 138.1, 135.4, 132.2, 130.5, 130.3, 129.9, 129.9, 129.8, 128.9, 128.5, 127.9, 127.6, 127.5, 114.9, 114.1, 113.7, 81.3, 68.4, 52.2, 27.4 (2 carbons missing); **LRMS** (ES + APCI) *m/z*: calc. for $C_{32}H_{29}NO_8S$ 587.2, found 586.1 [M–H]$^-$; **HMRS** calc. for $C_{32}H_{28}NO_8S$ 586.1541 [M–H]$^-$, found 586.1551 [M–H]$^-$.

2-((3-(*tert*-Butoxycarbonyl)-4-(4-((4-(methoxycarbonyl)benzyl)oxy)phenyl)thiophen-2-yl)carbamoyl)benzoic acid (277)

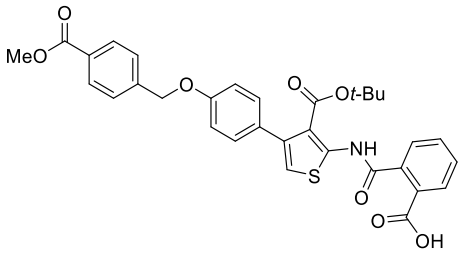

Following General Procedure E, compound **274** (220 mg, 0.50 mmol) and phthalic anhydride (74 mg, 0.50 mmol), after purification *via* flash column chromatography (dry loading, Petroleum ether 3:1 EtOAc, CH_2Cl_2 9:1 MeOH), afforded the *title compound* (213 mg, 0.36 mmol, 74%) as an off-white solid. **mp** 169–171 °C; **IR**(ATR)/cm^{-1} 3325 br, 3280, 3124, 2979, 1722, 1675, 1642, 1540, 1521, 1409, 1274, 1248, 1164, 1103; **^{1}H NMR** (500 MHz, DMSO-d_6) δ (ppm) 13.34 (br s, 1H, COO*H*), 11.41 (br s, 1H, CON*H*), 7.97 (d, *J* 8.0 Hz, 2H, 2 × Ar*H*), 7.86 (app t, *J* 4.0 Hz, 1H, Ar*H*), 7.64 (app t, *J* 4.0 Hz, 1H, Ar*H*), 7.62–7.53 (m, 4H, 4 × Ar*H*), 7.18 (d, *J* 8.5 Hz, 2H, 2 × Ar*H*), 7.01 (d, *J* 8.5 Hz, 2H, 2 × Ar*H*), 6.84 (s, 1H, C=C*H*S), 5.26 (s, 2H, OCH_2), 3.86 (s, 3H, CH_3), 1.17 (s, 9H, COOC(CH_3)$_3$); **^{13}C NMR** (125 MHz, DMSO-d_6) δ (ppm) 170.5, 168.7, 166.0, 164.1, 157.1, 147.6,

142.8, 142.5, 138.8, 134.7, 131.0, 130.4, 130.2, 129.9, 129.8, 129.3, 128.9, 128.1, 127.8, 127.3, 114.7, 114.1, 81.1, 68.5, 52.1, 27.4; **LRMS** (ES + APCI) *m/z*: calc. for $C_{32}H_{29}NO_8S$ 587.2, found 586.1 $[M–H]^-$. **HMRS** calc. for $C_{32}H_{28}NO_8S$ 586.1530 $[M–H]^-$, found 586.1540 $[M–H]^-$.

2-((3-(*tert*-Butoxycarbonyl)-4-(4-((2-carboxybenzyl)oxy)phenyl)thiophen-2-yl)carbamoyl)benzoic acid (278)

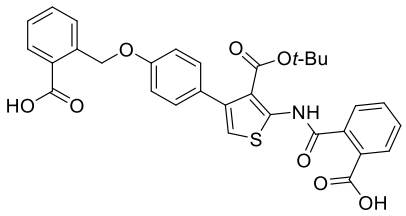

Following General Procedure G, compound **275** (100 mg, 0.17 mmol) and NaOH (1.70 mL, 0.1 M), afforded the *title compound* (70 mg, 0.12 mmol, 72%) as an off-white solid. **mp** 132–134 °C; **IR**(ATR)/cm^{-1} 3167 br, 3035, 2957, 1694, 1660, 1651, 1579, 1521, 1393, 1302, 1229, 1160, 1138, 1030; **^{1}H NMR** (500 MHz, DMSO-d_6) δ (ppm) 13.16 (br s, 2H, 2 × COO*H*), 11.30 (br s, 1H, CON*H*), 7.94 (d, *J* 8.0 Hz, 1H, Ar*H*), 7.92 (d, *J* 8.0 Hz, 1H, Ar*H*), 7.77–7.65 (m, 3H, 3 × Ar*H*), 7.63 (d, *J* 8.0 Hz, 1H, Ar*H*), 7.58 (app t, *J* 8.0 Hz, 1H, Ar*H*), 7.44 (app t, *J* 8.0 Hz, 1H, Ar*H*), 7.20 (d, *J* 8.5 Hz, 2H, 2 × Ar*H*), 6.97 (d, *J* 8.5 Hz, 2H, 2 × Ar*H*), 6.89 (s, 1H, C=C*H*S), 5.50 (s, 2H, OCH_2), 1.16 (s, 9H, COOC(CH_3)$_3$); **^{13}C NMR** (125 MHz, DMSO-d_6) δ (ppm) 168.1, 167.3, 165.6, 164.5, 157.4, 148.1, 139.1, 138.5, 135.9, 132.1, 132.0, 130.8, 130.6, 130.5, 130.2, 130.1, 130.0, 129.9, 129.8, 129.2, 127.5, 115.1, 113.9, 113.5, 81.5, 67.6, 27.4; **LRMS** (ES + APCI) *m/z*: calc. for $C_{31}H_{27}NO_8S$ 573.1, found 572.2 $[M–H]^-$; **HMRS** calc. for $C_{31}H_{26}NO_8S$ 572.1385 $[M–H]^-$, found 572.1386 $[M–H]^-$.

2-((3-(*tert*-Butoxycarbonyl)-4-(4-((3-carboxybenzyl)oxy)phenyl)thiophen-2-yl)carbamoyl)benzoic acid (279)

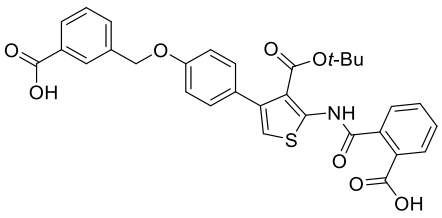

Following General Procedure G, compound **276** (100 mg, 0.17 mmol) and NaOH (1.70 mL, 0.1 M), afforded the *title compound* (66 mg, 0.12 mmol, 68%) as an off-white solid. **mp** 184–186 °C; **IR**(ATR)/cm^{-1} 3245 br, 3171, 2985, 2921, 1722, 1694, 1660, 1521, 1411, 1393, 1302, 1231, 1160, 1138; **^{1}H NMR** (500 MHz, DMSO-d_6) δ (ppm) 13.26 (br s, 1H, COO*H*), 13.03 (br s, 1H, COO*H*), 11.29 (br s, 1H, CON*H*), 8.03 (s, 1H, Ar*H*), 7.91 (d, *J* 7.5 Hz, 1H, Ar*H*), 7.89 (d, *J* 7.5 Hz, 1H, Ar*H*), 7.76–7.66 (m, 4H, 4 × Ar*H*), 7.52 (app t, *J* 7.5 Hz, 1H, Ar*H*), 7.19 (d, *J* 8.5 Hz, 2H, 2 × Ar*H*), 7.02 (d, *J* 8.5 Hz, 2H, 2 × Ar*H*), 6.89 (s, 1H, C=C*H*S), 5.24 (s, 2H, OCH_2), 1.13 (s, 9H, COOC(CH_3)$_3$); **^{13}C NMR** (125 MHz, DMSO-d_6) δ (ppm) 167.3, 167.1, 165.6, 164.5, 157.2, 148.1, 139.1, 137.8, 135.9, 132.1, 131.7, 130.9, 130.8, 130.2, 129.9, 129.8, 129.6, 128.7, 128.6, 128.1, 127.5, 115.1, 114.1, 113.5, 81.5, 68.5, 27.4; **LRMS** (ES + APCI) *m/z*: calc. for $C_{31}H_{27}NO_8S$ 573.1, found 572.1 [M–H]$^-$; **HMRS** calc. for $C_{31}H_{26}NO_8S$ 572.1385 [M–H]$^-$, found 572.1383 [M–H]$^-$.

2-((3-(*tert*-Butoxycarbonyl)-4-(4-((4-carboxybenzyl)oxy)phenyl)thiophen-2-yl)carbamoyl)benzoic acid (280)

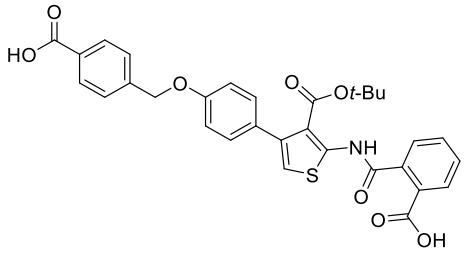

Following General Procedure G, compound **277** (100 mg, 0.17 mmol) and NaOH (1.70 mL, 0.1 M), afforded the *title compound* (64 mg, 0.11 mmol, 66%) as an off-white solid. **mp** 230–232 °C; **IR**(ATR)/cm^{-1} 3224 br, 3066, 2976, 2868, 1688, 1679, 1651, 1580, 1521, 1415, 1297, 1234, 1162, 1020; **^{1}H NMR** (500 MHz, DMSO-d_6) δ (ppm) 13.20 (br s, 1H, COO*H*), 12.96 (br s, 1H, COO*H*), 12.28 (br s, 1H, CON*H*), 8.00–7.88 (m, 3H, 3 × Ar*H*), 7.77–7.65 (m, 3H, 3 × Ar*H*), 7.56 (d, *J* 8.0 Hz, 2H, 2 × Ar*H*), 7.19 (d, *J* 8.0 Hz, 2H, 2 × Ar*H*), 7.01 (d, *J* 8.0 Hz, 2H, 2 × Ar*H*), 6.87 (s, 1H, C=C*H*S), 5.25 (s, 2H, OCH_2), 1.14 (s, 9H, COOC(CH_3)$_3$); **^{13}C NMR** (125 MHz, DMSO-d_6) δ (ppm) 167.3, 167.1, 165.6, 164.5, 157.2, 148.1, 139.1, 135.9, 132.2, 130.8, 130.5, 130.3, 130.2, 130.1, 130.0, 129.9, 129.5, 129.4, 127.5, 127.4, 127.2, 115.2, 114.1, 113.5, 81.5, 68.5, 27.4; **LRMS** (ES + APCI) *m/z*:

calc. for $C_{31}H_{27}NO_8S$ 573.1, found 572.1 $[M–H]^-$; **HMRS** calc. for $C_{31}H_{26}NO_8S$ 572.1385 $[M–H]^-$, found 572.1384 $[M–H]^-$.

1-(4-(Prop-2-yn-1-yloxy)phenyl)ethan-1-one (282)

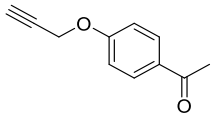

Following General procedure H, 3-bromoprop-1-yne (1.31 g, 8.81 mmol) and 1-(4-hydroxyphenyl)ethan-1-one (1.00 g, 7.34 mmol), after purification *via* flash column chromatography (dry loading, Petroleum ether 10:1 EtOAc, isocratic), afforded the *title compound* (1.23 g, 7.05 mmol, 96%) as an off-white solid. **mp** 66–68 °C; **IR**(ATR)/cm^{-1} 3221, 3085, 2925, 2122, 1659, 1601, 1577, 1508, 1422, 1357, 1242, 1186, 1019; **^{1}H NMR** (500 MHz, $CDCl_3$) δ (ppm) 7.95 (d, *J* 8.0 Hz, 2H, 2 × Ar*H*), 7.01 (d, *J* 8.0 Hz, 2H, 2 × Ar*H*), 4.76 (s, 2H, OCH_2), 2.56 (s, 3H, CH_3), 2.55–2.53 (m, 1H, CC*H*); **^{13}C NMR** (125 MHz, $CDCl_3$) δ (ppm) 196.8, 161.4, 131.2, 130.7, 114.7, 77.9, 76.3, 55.9, 26.5; **LRMS** (ES + APCI) *m/z*: calc. for $C_{11}H_{10}O_2$ 174.1, found 175.1 $[M+H]^+$; **HMRS** calc. for $C_{11}H_{11}O_2$ 175.0750 $[M+H]^+$, found 175.0754 $[M+H]^+$.

2-(4-Acetylphenoxy)acetonitrile (284)

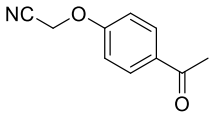

Following General procedure H, 2-bromoacetonitrile (1.15 g, 9.55 mmol) and 1-(4-hydroxyphenyl)ethan-1-one (1.00 g, 7.34 mmol), after purification *via* flash column chromatography (dry loading, Petroleum ether 3:1 EtOAc, isocratic), afforded the *title compound* (1.28 g, 7.31 mmol, 99%) as an off-white solid. **mp** 86–88 °C; **IR**(ATR)/cm^{-1} 3074, 2925, 2239, 1675, 1601, 1579, 1508, 1355, 1246, 1186, 1041; **^{1}H NMR** (500 MHz, $CDCl_3$) δ (ppm) 7.98 (d, *J* 9.0 Hz, 2H, 2 × Ar*H*), 7.02 (d, *J* 9.0 Hz, 2H, 2 × Ar*H*), 4.84 (s, 2H, OCH_2), 2.57 (s, 3H, CH_3); **^{13}C NMR** (125 MHz, $CDCl_3$) δ (ppm) 196.6, 160.0, 132.5, 130.9, 130.8, 114.6, 53.4, 26.6; **LRMS** (ES + APCI) *m/z*: calc. for $C_{10}H_9NO_2$ 175.1, found 176.1 $[M+H]^+$; **HMRS** calc. for $C_{10}H_{10}NO_2$ 176.0706 $[M+H]^+$, found 176.0705 $[M+H]^+$.

1-(4-((1*H*-1,2,3-Triazol-5-yl)methoxy)phenyl)ethan-1-one (285)

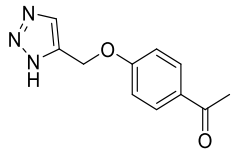

A solution of compound **282** (1.00 g, 5.75 mmol), azidotrimethylsilane (1.20 mL, 8.62 mmol) and copper iodide (CuI) (55 mg, 0.29 mmol) in 9:1 DMF/MeOH (11 mL, 0.52 M) was heated to 95 °C in a sealed vessel for 12 hours. The mixture was concentrated under reduced pressure, the resulting oil was diluted with CH_2Cl_2 (20 mL) and the undissolved solids were filtered off. The filtrate was concentrated under reduced pressure to afford the *title compound* (1.18 g, 5.44 mmol, 95%) as an off-white solid. **mp** 88–90 °C; **IR**(ATR)/cm^{-1} 3271, 3163 br, 3023, 2927, 1644, 1599, 1573, 1506, 1422, 1361, 1246, 1177, 1001; **^{1}H NMR** (500 MHz, $CDCl_3$) δ (ppm) 7.94 (d, *J* 8.5 Hz, 2H, 2 × Ar*H*), 7.80 (s, 1H, Ar*H*), 7.03 (d, *J* 8.0 Hz, 2H, 2 × Ar*H*), 5.30 (s, 2H, OCH_2), 2.96 (s, 1H, NN*H*), 2.56 (s, 3H, CH_3); **^{13}C NMR** (125 MHz, $CDCl_3$) δ (ppm) 197.2, 162.2, 130.9, 130.8, 114.7, 77.4, 61.8, 36.7, 26.5; **LRMS** (ES + APCI) *m/z*: calc. for $C_{11}H_{11}N_3O_2$ 217.1, found 218.1 $[M+H]^+$; **HMRS** calc. for $C_{11}H_{12}N_3O_2$ 218.0924 $[M+H]^+$, found 218.0925 $[M+H]^+$.

1-(4-((1*H*-Tetrazol-5-yl)methoxy)phenyl)ethan-1-one (286)

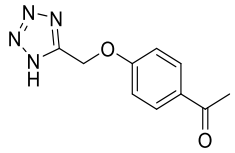

A solution of compound **284** (1.00 g, 5.71 mmol), sodium azide (1.12 g, 17.10 mmol) and triethylamine hydrochloride (2.40 g, 17.10 mmol) in toluene (20 mL, 0.29 M) was heated to 100 °C for 4.5 hours. The mixture was cooled to room temperature and H_2O (80 mL) was added. The suspension was stirred for a further 10 minutes before the aqueous phase was separated and transferred to a round-bottomed flask, cooled to 0 °C and acidified with conc. HCl. The resultant precipitate was collected by filtration, washed with H_2O (50 mL) and vacuum dried to afford the *title compound* (1.08 g, 4.97 mmol, 87%) as an off-white solid. **mp** 164–166 °C; **IR**(ATR)/cm^{-1} 3135, 3037, 2929, 2879 br, 1644, 1592, 1514, 1443, 1363, 1257, 1171, 1041; **^{1}H NMR** (500 MHz, DMSO-d_6) δ (ppm) 12.15 (br s, 1H, NN*H*), 7.96

(d, *J* 8.5 Hz, 2H, 2 × Ar*H*), 7.17 (d, *J* 8.5 Hz, 2H, 2 × Ar*H*), 5.60 (s, 2H, OCH_2), 2.53 (s, 3H, CH_3); **^{13}C NMR** (125 MHz, DMSO-d_6) δ (ppm) 196.3, 161.1, 130.8, 130.5, 114.6, 59.5, 26.5, (1 carbon missing); **LRMS** (ES + APCI) *m/z*: calc. for $C_{10}H_{10}N_4O_2$ 218.1, found 219.0 $[M+H]^+$; **HMRS** calc. for $C_{10}H_{11}N_4O_2$ 219.0877 $[M+H]^+$, found 219.0877 $[M+H]^+$.

Isopropyl 4-(4-((1*H*-1,2,3-triazol-5-yl)methoxy)phenyl)-2-aminothiophene-3-carboxylate (287)

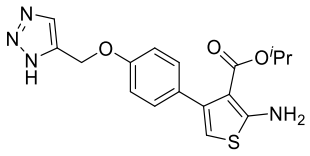

Following General Procedure D, isopropyl 2-cyanoacetate (820 mg, 6.45 mmol) and compound **285** (700 mg, 3.22 mmol), after purification *via* flash column chromatography (dry loading, Petroleum ether 2:1 EtOAc, isocratic), afforded the *title compound* (554 mg, 1.55 mmol, 48%) as a pale yellow solid. **mp** 60–62 °C; **IR**(ATR)/cm^{-1} 3446, 3310, 3152, 2981, 2929, 1659, 1575, 1497, 1398, 1270, 1218, 1101, 1017; **^{1}H NMR** (500 MHz, $CDCl_3$) δ (ppm) 7.81 (s, 1H, Ar*H*), 7.21 (d, *J* 8.5 Hz, 2H, 2 × Ar*H*), 6.93 (d, *J* 8.5 Hz, 2H, 2 × Ar*H*), 6.15–5.95 (m, 3H, C=C*H*S, NH_2), 5.26 (s, 2H, OCH_2), 4.98 (septet, *J* 6.0 Hz, 1H, COOC*H*(CH_3)$_2$), 0.98 (d, *J* 6.0 Hz, 6H, COOCH(CH_3)$_2$); **^{13}C NMR** (125 MHz, $CDCl_3$) δ (ppm) 165.4, 163.8, 157.3, 144.0, 141.3, 132.1, 131.9, 130.4, 113.7, 106.7, 105.3, 67.2, 61.8, 21.8; **LRMS** (ES + APCI) *m/z*: calc. for $C_{17}H_{18}N_4O_3S$ 358.1, found 359.0 $[M+H]^+$; **HMRS** calc. for $C_{17}H_{19}N_4O_3S$ 359.1172 $[M+H]^+$, found 359.1176 $[M+H]^+$.

Isopropyl 4-(4-((1*H*-tetrazol-5-yl)methoxy)phenyl)-2-aminothiophene-3-carboxylate (288)

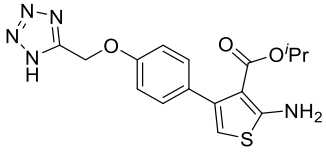

Following General Procedure D, isopropyl 2-cyanoacetate (583 mg, 4.58 mmol) and compound **286** (500 mg, 2.29 mmol), after purification *via* flash column chromatography (dry loading, EtOAc, CH_2Cl_2 9:1 MeOH, CH_2Cl_2 8:2 MeOH),

afforded the *title compound* (236 mg, 0.66 mmol, 29%) as a pale yellow solid. **mp** 146–148 °C; **IR**(ATR)/cm^{-1} 3476, 3345, 3107 br, 3044, 2981, 2931, 1724, 1660, 1567, 1499, 1398, 1262, 1233, 1104; **^{1}H NMR** (500 MHz, DMSO-*d*$_6$) δ (ppm) 12.42 (br s, 1H, NN*H*), 7.33 (br s, 2H, NH_2), 7.15 (d, *J* 8.5 Hz, 2H, 2 × Ar*H*), 6.98 (d, *J* 8.5 Hz, 2H, 2 × Ar*H*), 6.09 (s, 1H, C=C*H*S), 5.34 (s, 2H, OCH_2), 4.84 (septet, *J* 6.5 Hz, 1H, COOC*H*(CH$_3$)$_2$), 0.92 (d, *J* 6.5 Hz, 6H, COOCH(CH_3)$_2$); **^{13}C NMR** (125 MHz, DMSO-*d*$_6$) δ (ppm) 164.9, 164.4, 156.7, 154.9, 140.0, 131.5, 129.8, 113.5, 104.4, 103.4, 65.9, 60.2, 21.4; **LRMS** (ES + APCI) *m/z*: calc. for $C_{16}H_{17}N_5O_3S$ 359.1, found 358.0 [M–H]$^-$; **HMRS** calc. for $C_{16}H_{16}N_5O_3S$ 358.0979 [M–H]$^-$, found 358.0977 [M–H]$^-$.

2-((4-(4-((1*H*-1,2,3-Triazol-5-yl)methoxy)phenyl)-3-(isopropoxycarbonyl)thiophen-2-yl)carbamoyl)benzoic acid (289)

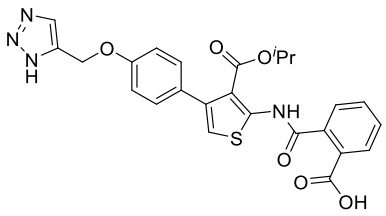

Following General Procedure E, compound **287** (150 mg, 0.42 mmol) and phthalic anhydride (62 mg, 0.42 mmol), after purification *via* flash column chromatography (dry loading, Petroleum ether 1:2 EtOAc, CH_2Cl_2 9:1 MeOH), afforded the *title compound* (70 mg, 0.14 mmol, 33%) as an off-white solid. **mp** 177–179 °C; **IR**(ATR)/cm^{-1} 3226 br, 3104, 2986, 2892, 1714, 1659, 1651, 1540, 1521, 1387, 1283, 1259, 1222, 1101; **^{1}H NMR** (500 MHz, DMSO-*d*$_6$) δ (ppm) 15.11 (br s, 1H, NN*H*), 14.01–13.30 (a br s, 2H, COO*H*, CON*H*), 7.95 (a br s, 1H, Ar*H*), 7.85 (d, *J* 7.5 Hz, 1H, Ar*H*), 7.67 (d, *J* 7.5 Hz, 1H, Ar*H*), 7.54–7.43 (m, 2H, 2 × Ar*H*), 7.20 (d, *J* 8.5 Hz, 2H, 2 × Ar*H*), 7.02 (d, *J* 8.5 Hz, 2H, 2 × Ar*H*), 6.86 (s, 1H, C=C*H*S), 5.21 (s, 2H, OCH_2), 4.91 (septet, *J* 6.5 Hz, 1H, COOC*H*(CH$_3$)$_2$), 0.99 (d, *J* 6.5 Hz, 6H, COOCH(CH_3)$_2$); **^{13}C NMR** (125 MHz, DMSO-*d*$_6$) δ (ppm) 170.2, 166.9, 164.3, 157.1, 153.4, 147.6, 138.5, 137.9, 134.5, 134.4, 130.0, 129.9, 129.8, 129.7, 129.1, 127.9, 114.6, 113.9, 113.2, 67.9, 60.8, 21.2; **LRMS** (ES + APCI) *m/z*: calc. for $C_{25}H_{22}N_4O_6S$ 506.1, found 507.0 [M+H]$^+$; **HMRS** calc. for $C_{25}H_{23}N_4O_6S$ 507.1333 [M+H]$^+$, found 507.1327 [M+H]$^+$.

2-((4-(4-((1*H*-Tetrazol-5-yl)methoxy)phenyl)-3-(isopropoxycarbonyl)thiophen-2-yl)carbamoyl)benzoic acid (290)

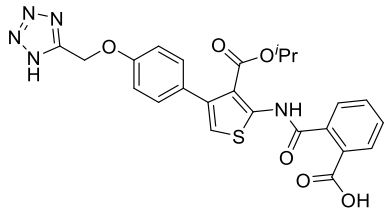

Following General Procedure E, compound **288** (100 mg, 0.28 mmol) and phthalic anhydride (41 mg, 0.28 mmol), after purification *via* flash column chromatography (dry loading, CH_2Cl_2 9:1 MeOH, CH_2Cl_2 8:2 MeOH), afforded the *title compound* (72 mg, 0.04 mmol, 10%) as an off-white solid. **mp** 221–223 °C; **IR**(ATR)/cm^{-1} 3425, 3245, 3100 br, 3023, 2983, 1713, 1649, 1607, 1519, 1398, 1259, 1220, 1101; **^{1}H NMR** (500 MHz, DMSO-d_6) δ (ppm) 13.90–12.90 (a br s, 2H, COO*H*, NN*H*), 7.86 (d, *J* 7.0 Hz, 1H, Ar*H*), 7.65 (d, *J* 7.0 Hz, 1H, Ar*H*), 7.53–7.44 (m, 2H, 2 × Ar*H*), 7.17 (d, *J* 8.5 Hz, 2H, 2 × Ar*H*), 7.03 (d, *J* 8.5 Hz, 2H, 2 × Ar*H*), 6.85 (s, 1H, C=C*H*S), 5.12 (s, 2H, OCH_2), 4.92 (septet, *J* 6.5 Hz, 1H, COOC*H*$(CH_3)_2$), 1.01 (d, *J* 6.5 Hz, 6H, COOCH$(CH_3)_2$); **^{13}C NMR** (125 MHz, DMSO-d_6) δ (ppm) 170.4, 166.8, 164.4, 157.9, 157.3, 149.9, 149.2, 138.6, 130.0, 129.9, 129.5, 129.1, 128.9, 128.7, 128.1, 114.3, 113.8, 106.7, 67.9, 61.9, 21.3; **LRMS** (ES + APCI) *m/z*: calc. for $C_{24}H_{21}N_5O_6S$ 507.1, found 506.0 [M–H]$^-$; **HMRS** calc. for $C_{24}H_{20}N_5O_6S$ 506.1140 [M–H]$^-$, found 506.1145 [M–H]$^-$.

Thiazol-5-ylmethyl methanesulfonate (299)

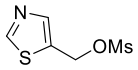

Following General Procedure J, thiazol-5-ylmethanol (1.10 g, 9.57 mmol) and methane sulfonyl chloride (0.89 mL, 11.48 mmol) afforded the *title compound* as a partially clean and chemically unstable brown residue.

Selected data; **^{1}H NMR** (500 MHz, $CDCl_3$) δ (ppm) 8.81 (s, 1H, Ar*H*), 7.85 (s, 1H, Ar*H*), 4.84 (s, 2H, CH_2), 3.67 (s, 3H, SO_2CH_3).

Oxazol-5-ylmethyl methanesulfonate (300)

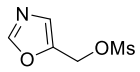

Following General Procedure J, oxazol-5-ylmethanol (1.00 g, 10.09 mmol) and methane sulfonyl chloride (0.95 mL, 12.11 mmol) afforded the *title compound* as a partially clean and chemically unstable brown residue.

Selected data; **^{1}H NMR** (500 MHz, $CDCl_3$) δ (ppm) 8.06 (s, 1H, Ar*H*), 7.95 (s, 1H, Ar*H*), 4.62 (s, 2H, CH_2), 3.67 (s, 3H, SO_2CH_3).

Pyridin-2-ylmethyl methanesulfonate (301)

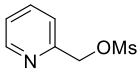

Following General Procedure J, pyridin-2-ylmethanol (2.00 g, 18.32 mmol) and methane sulfonyl chloride (1.71 mL, 22.01 mmol) afforded the *title compound* as a partially clean and chemically unstable brown residue.

Selected data; **^{1}H NMR** (500 MHz, $CDCl_3$) δ (ppm) 8.64 (d, *J* 4.5 Hz, 1H, Ar*H*), 7.81 (app td, *J* 7.5 Hz, 1.5 Hz, 1H, Ar*H*), 7.52 (d, *J* 7.5 Hz, 1H, Ar*H*), 7.34 (dd, *J* 7.5 Hz, 4.5 Hz, 1H, Ar*H*), 5.36 (s, 2H, CH_2), 3.10 (s, 3H, SO_2CH_3).

Pyridin-3-ylmethyl methanesulfonate (302)

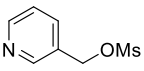

Following General Procedure J, pyridin-3-ylmethanol (1.10 g, 10.10 mmol) and methane sulfonyl chloride (1.00 mL, 12.10 mmol) afforded the *title compound* as a partially clean and chemically unstable brown residue.

Selected data; **^{1}H NMR** (500 MHz, $CDCl_3$) δ (ppm) 8.69 (d, *J* 1.5 Hz, 1H, Ar*H*), 8.62 (dd, *J* 5.0 Hz, 1.5 Hz, 1H, Ar*H*), 7.89–7.84 (m, 1H, Ar*H*), 7.42 (dd, *J* 7.5 Hz, 5.0 Hz, 1H, Ar*H*), 4.62 (s, 2H, CH_2), 3.67 (s, 3H, SO_2CH_3).

Pyridin-4-ylmethyl methanesulfonate (303)

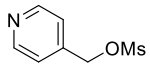

Following General Procedure J, pyridin-3-ylmethanol (1.10 g, 10.10 mmol) and methane sulfonyl chloride (1.00 mL, 12.10 mmol) afforded the *title compound* as a partially clean and chemically unstable brown residue.

Selected data; **^{1}H NMR** (500 MHz, $CDCl_3$) δ (ppm) 8.70 (d, *J* 6.5 Hz, 2H, 2 × Ar*H*), 7.50 (d, *J* 6.5 Hz, 2H, 2 × Ar*H*), 4.62 (s, 2H, CH_2), 3.00 (s, 3H, SO_2CH_3).

Pyrazin-2-ylmethyl methanesulfonate (304)

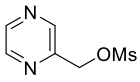

Following General Procedure J, pyrazin-2-ylmethanol (1.00 g, 9.08 mmol) and methane sulfonyl chloride (0.85 mL, 10.90 mmol) afforded the *title compound* as a partially clean and chemically unstable brown residue.

Selected data; **^{1}H NMR** (500 MHz, $CDCl_3$) δ (ppm) 8.75 (s, 1H, Ar*H*), 8.62–8.58 (m, 2H, 2 × Ar*H*), 5.37 (s, 2H, CH_2), 3.12 (s, 3H, SO_2CH_3).

Quinolin-5-ylmethyl methanesulfonate (305)

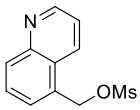

Following General Procedure J, quinolin-5-ylmethanol (1.00 g, 6.28 mmol) and methane sulfonyl chloride (0.60 mL, 7.53 mmol) afforded the *title compound* as a partially clean and chemically unstable brown residue.

Selected data; **^{1}H NMR** (500 MHz, $CDCl_3$) δ (ppm) 8.99 (d, *J* 4.0 Hz, 1H, Ar*H*), 8.54 (d, *J* 8.5 Hz, 1H, Ar*H*), 8.15 (d, *J* 8.5 Hz, 1H, Ar*H*), 7.69 (app t, *J* 8.5 Hz, 1H, Ar*H*), 7.63–7.59 (m, 1H, Ar*H*), 7.54 (dd, *J* 8.5 Hz, 4.0 Hz, 1H, Ar*H*), 5.03 (s, 2H, CH_2), 3.67 (s, 3H, SO_2CH_3).

Quinolin-6-ylmethyl methanesulfonate (306)

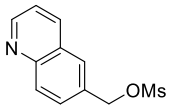

Following General Procedure J, quinolin-6-ylmethanol (1.00 g, 6.28 mmol) and methane sulfonyl chloride (0.60 mL, 7.53 mmol) afforded the *title compound* as a partially clean and chemically unstable brown residue.

Selected data; **^{1}H NMR** (500 MHz, $CDCl_3$) δ (ppm) 8.97 (dd, *J* 4.5 Hz, 1.5 Hz, 1H, Ar*H*), 8.23 (d, *J* 8.0 Hz, 1H, Ar*H*), 8.18 (d, *J* 8.5 Hz, 1H, Ar*H*), 7.86 (d, *J* 1.5 Hz, 1H, Ar*H*), 7.78 dd, *J* 8.5 Hz, 1.5 Hz, 1H, Ar*H*), 7.49 (dd, *J* 8.5 Hz, 4.5 Hz, 1H, Ar*H*), 4.78 (s, 2H, CH_2), 3.67 (s, 3H, SO_2CH_3).

1-(4-(Thiazol-5-ylmethoxy)phenyl)ethan-1-one (307)

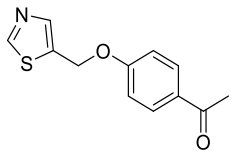

Following General procedure H, compound **299** (1.70 g, 8.81 mmol) and 1-(4-hydroxyphenyl)ethan-1-one (1.00 g, 7.34 mmol), after purification *via* flash column chromatography (dry loading, Petroleum ether 1:1 EtOAc, isocratic), afforded the *title compound* (1.65 g, 7.08 mmol, 96%) as an off-white solid. **mp** 54–56 °C; **IR**(ATR)/cm^{-1} 3111, 3066, 2990, 1668, 1599, 1515, 1411, 1365, 1259, 1181, 1027; **^{1}H NMR** (500 MHz, $CDCl_3$) δ (ppm) 8.84 (s, 1H, Ar*H*), 7.94 (d, *J* 8.5 Hz, 2H, 2 × Ar*H*), 7.93 (s, 1H, Ar*H*), 7.00 (d, *J* 8.5 Hz, 2H, 2 × Ar*H*), 5.35 (s, 2H, OCH_2), 2.56 (s, 3H, CH_3); **^{13}C NMR** (125 MHz, $CDCl_3$) δ (ppm) 196.8, 161.8, 154.5, 142.9, 133.4, 131.3, 130.8, 114.7, 62.6, 26.5; **LRMS** (ES + APCI) *m/z*: calc. for $C_{12}H_{11}NO_2S$ 233.1, found 234.0 $[M+H]^+$; **HMRS** calc. for $C_{12}H_{12}NO_2S$ 234.0583 $[M+H]^+$, found 234.0585 $[M+H]^+$.

1-(4-(Oxazol-5-ylmethoxy)phenyl)ethan-1-one (308)

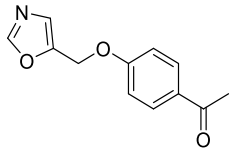

Following General procedure H, compound **300** (950 mg, 4.38 mmol) and 1-(4-hydroxyphenyl)ethan-1-one (500 mg, 3.65 mmol), after purification via flash column chromatography (dry loading, Petroleum ether 1:1 EtOAc, isocratic), afforded the title compound (708 mg, 3.26 mmol, 89%) as an off-white solid. **mp** 146–148 °C; **IR**(ATR)/cm^{-1} 3238, 3092, 2933, 2873, 1668, 1597, 1499, 1428, 1361, 1244, 1175, 1101, 1011, 941; **^{1}H NMR** (500 MHz, $CDCl_3$) δ (ppm) 7.95 (d, *J* 8.5 Hz, 2H, 2 × ArH), 7.92 (s, 1H, ArH), 7.19 (s, 1H, ArH), 7.01 (d, *J* 8.5 Hz, 2H, 2 × Ar*H*), 5.15 (s, 2H, OCH_2), 2.56 (s, 3H, CH_3); **^{13}C NMR** (125 MHz, $CDCl_3$) δ (ppm) 196.8, 161.8, 151.9, 147.1, 131.3, 130.8, 126.7, 114.6, 60.1, 26.5; **LRMS** (ES + APCI) *m/z*: calc. for $C_{12}H_{11}NO_3$ 217.1, found 218.0 $[M+H]^+$; **HMRS** calc. for $C_{12}H_{10}NO_3$ 216.0666 $[M–H]^-$, found 216.0670 $[M–H]^-$.

1-(4-(Pyridin-2-ylmethoxy)phenyl)ethan-1-one (309)

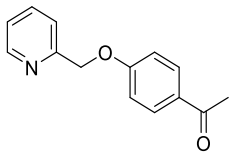

Following General procedure H, compound **301** (988 mg, 5.29 mmol) and 1-(4-hydroxyphenyl)ethan-1-one (600 mg, 4.41 mmol), after purification *via* flash column chromatography (dry loading, Petroleum ether 2:1 EtOAc, isocratic), afforded the *title compound* (462 mg, 2.04 mmol, 46%) as an off-white solid. **mp** 91–93 °C; **IR**(ATR)/cm^{-1} 3307, 3072, 2921, 2860, 1668, 1594, 1575, 1514, 1419, 1363, 1264, 1183, 1045; **^{1}H NMR** (500 MHz, $CDCl_3$) δ (ppm) 8.61 (d, *J* 5.0 Hz, 1H, Ar*H*), 7.93 (d, *J* 9.0 Hz, 2H, 2 × Ar*H*), 7.72 (td, *J* 8.0 Hz, 1.5 Hz, 1H, Ar*H*), 7.49 (d, *J* 8.0 Hz, 1H, Ar*H*), 7.24 (dd, *J* 8.0 Hz, 5.0 Hz, 1H, Ar*H*), 7.02 (d, *J* 9.0 Hz, 2H, 2 × Ar*H*), 5.27 (s, 2H, OCH_2), 2.55 (s, 3H, CH_3); **^{13}C NMR** (125 MHz, $CDCl_3$) δ (ppm) 196.8, 162.3, 156.6, 149.5, 137.1, 130.9, 130.8, 123.0, 121.5, 114.7, 70.9, 26.5; **LRMS** (ES + APCI) *m/z*: calc. for $C_{14}H_{13}NO_2$ 227.1, found 228.1 $[M+H]^+$; **HMRS** calc. for $C_{14}H_{14}NO_2$ 228.1019 $[M+H]^+$, found 228.1021 $[M+H]^+$.

1-(4-(Pyridin-3-ylmethoxy)phenyl)ethan-1-one (310)

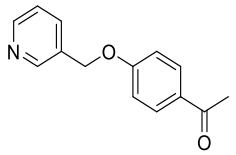

Following General procedure H, compound **302** (988 mg, 5.29 mmol) and 1-(4-hydroxyphenyl)ethan-1-one (600 mg, 4.41 mmol), after purification *via* flash column chromatography (dry loading, Petroleum ether 1:1 EtOAc, isocratic), afforded the *title compound* (620 mg, 2.73 mmol, 62%) as an off-white solid. **mp** 65–67 °C; **IR**(ATR)/cm^{-1} 3306, 3031, 2936, 1668, 1599, 1580, 1512, 1417, 1357, 1248, 1169, 993; **^{1}H NMR** (500 MHz, $CDCl_3$) δ (ppm) 8.71 (s, 1H, Ar*H*), 8.62 (d, *J* 4.0 Hz, 1H, Ar*H*), 7.94 (d, *J* 9.0 Hz, 2H, 2 × Ar*H*), 7.77 (d, *J* 8.0 Hz, 1H, Ar*H*), 7.34 (dd, *J* 8.0 Hz, 4.0 Hz, 1H, Ar*H*), 7.01 (d, *J* 9.0 Hz, 2H, 2 × Ar*H*), 5.15 (s, 2H, OCH_2), 2.56 (s, 3H, CH_3); **^{13}C NMR** (125 MHz, $CDCl_3$) δ (ppm) 196.8, 162.3, 149.9, 149.1, 135.4, 131.9, 131.1, 130.8, 123.7, 114.6, 67.8, 26.5; **LRMS** (ES + APCI) *m/z*: calc. for $C_{14}H_{13}NO_2$ 227.1, found 228.1 $[M+H]^+$; **HMRS** calc. for $C_{14}H_{14}NO_2$ 228.1019 $[M+H]^+$, found 228.1020 $[M+H]^+$.

1-(4-(Pyridin-4-ylmethoxy)phenyl)ethan-1-one (311)

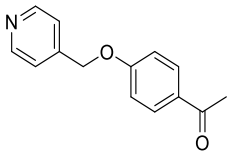

Following General procedure H, compound **303** (988 mg, 5.29 mmol) and 1-(4-hydroxyphenyl)ethan-1-one (600 mg, 4.41 mmol), after purification *via* flash column chromatography (dry loading, Petroleum ether 1:1 EtOAc, isocratic), afforded the *title compound* (547 mg, 2.41 mmol, 55%) as an off-white solid. **mp** 80–82 °C; **IR**(ATR)/cm^{-1} 3318, 3076, 2912, 1662, 1597, 1562, 1512, 1419, 1359, 1251, 1173, 1045; **^{1}H NMR** (500 MHz, $CDCl_3$) δ (ppm) 8.56 (d, *J* 5.5 Hz, 2H, 2 × Ar*H*), 7.87 (d, *J* 9.0 Hz, 2H, 2 × Ar*H*), 7.28 (d, *J* 5.5 Hz, 2H, 2 × Ar*H*), 6.92 (d, *J* 9.0 Hz, 2H, 2 × Ar*H*), 5.09 (s, 2H, OCH_2), 2.48 (s, 3H, CH_3); **^{13}C NMR** (125 MHz, $CDCl_3$) δ (ppm) 196.7, 162.0, 150.3, 145.4, 131.2, 130.8, 121.5, 114.6, 68.3, 26.5; **LRMS** (ES + APCI) *m/z*: calc. for $C_{14}H_{13}NO_2$ 227.1, found 228.1 $[M+H]^+$; **HMRS** calc. for $C_{14}H_{14}NO_2$ 228.1019 $[M+H]^+$, found 228.1021 $[M+H]^+$.

1-(4-(Pyrazin-2-ylmethoxy)phenyl)ethan-1-one (312)

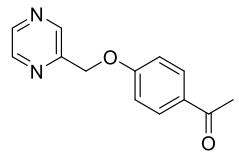

Following General procedure H, compound **304** (1.80 g, 9.57 mmol) and 1-(4-hydroxyphenyl)ethan-1-one (1.09 g, 7.98 mmol), after purification *via* flash column chromatography (dry loading, Petroleum ether 1:1 EtOAc, isocratic), afforded the *title compound* (1.29 g, 5.64 mmol, 70%) as an off-white solid. **mp** 144–146 °C; **IR**(ATR)/cm^{-1} 3316, 3087, 2912, 1664, 1603, 1580, 1515, 1411, 1359, 1257, 1190, 1060, 1021; **^{1}H NMR** (500 MHz, $CDCl_3$) δ (ppm) 8.82 (s, 1H, Ar*H*), 8.60–8.56 (m, 2H, 2 × Ar*H*), 7.95 (d, *J* 9.0 Hz, 2H, 2 × Ar*H*), 7.05 (d, *J* 9.0 Hz, 2H, 2 × Ar*H*), 5.30 (s, 2H, OCH_2), 2.56 (s, 3H, CH_3); **^{13}C NMR** (125 MHz, $CDCl_3$) δ (ppm) 196.8, 161.9, 151.9, 144.4, 144.1, 143.8, 131.3, 130.8, 114.7, 69.2, 26.5; **LRMS** (ES + APCI) *m/z*: calc. for $C_{13}H_{12}N_2O_2$ 228.1, found 229.0 $[M+H]^+$; **HMRS** calc. for $C_{13}H_{13}N_2O_2$ 229.0972 $[M+H]^+$, found 229.0974 $[M+H]^+$.

1-(4-(Quinolin-5-ylmethoxy)phenyl)ethan-1-one (313)

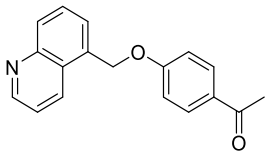

Following General procedure H, compound **305** (1.62 g, 6.84 mmol) and 1-(4-hydroxyphenyl)ethan-1-one (776 mg, 5.70 mmol), after purification via flash column chromatography (dry loading, Petroleum ether 1:1 EtOAc, isocratic), afforded the *title compound* (1.12 g, 4.06 mmol, 71%) as an off-white solid. **mp** 107–109 °C; **IR**(ATR)/cm^{-1} 3327, 3055, 2951, 2931, 1664, 1597, 1573, 1502, 1417, 1357, 1242, 1175, 998; **^{1}H NMR** (500 MHz, $CDCl_3$) δ (ppm) 8.96 (dd, *J* 4.0 Hz, 1.0 Hz, 1H, ArH), 8.38 (d, *J* 9.0 Hz, 1H, ArH), 8.14 (d, *J* 9.0 Hz, 1H, Ar*H*), 7.96 (d, *J* 8.5 Hz, 2H, 2 × ArH), 7.71 (app t, *J* 7.0 Hz, 1H, Ar*H*), 7.64 (d, *J* 7.0 Hz, 1H, Ar*H*), 7.45 (dd, *J* 9.0 Hz, 4.0 Hz, 1H, Ar*H*), 7.06 (d, *J* 8.5 Hz, 2H, 2 × ArH), 5.53 (s, 2H, OCH_2), 2.56 (s, 3H, CH_3); **^{13}C NMR** (125 MHz, $CDCl_3$) δ (ppm) 196.8, 162.4, 150.6, 148.8, 132.2, 132.1, 132.0, 131.0, 130.8, 128.9, 127.6, 126.9, 121.6,

114.7, 68.4, 26.5; **LRMS** (ES + APCI) *m/z*: calc. for $C_{18}H_{15}NO_2$ 277.1, found 278.0 $[M+H]^+$; **HMRS** calc. for $C_{18}H_{16}NO_2$ 278.1176 $[M+H]^+$, found 278.1177 $[M+H]^+$.

1-(4-(Quinolin-6-ylmethoxy)phenyl)ethan-1-one (314)

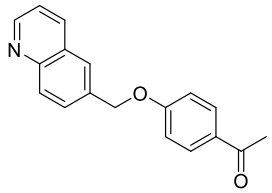

Following General procedure H, compound **306** (1.30 g, 5.49 mmol) and 1-(4-hydroxyphenyl)ethan-1-one (622 mg, 4.57 mmol), after purification via flash column chromatography (dry loading, Petroleum ether 1:1 EtOAc, isocratic), afforded the *title compound* (940 mg, 3.39 mmol, 74%) as an off-white solid. **mp** 125–127 °C; **IR**(ATR)/cm^{-1} 3344, 3020, 2946, 2851, 1677, 1599, 1510, 1463, 1355, 1253, 1175, 1008, 883; **^{1}H NMR** (500 MHz, $CDCl_3$) δ (ppm) 8.93 (d, *J* 4.0 Hz, 1H, ArH), 8.16 (app t, *J* 8.5 Hz, 2H, 2 × ArH), 7.95 (d, *J* 9.0 Hz, 2H, 2 × ArH), 7.88 (br s, 1H, Ar*H*), 7.76 (d, *J* 9.0 Hz, 1H, Ar*H*), 7.43 (dd, *J* 8.5 Hz, 4.0 Hz, 1H, Ar*H*), 7.05 (d, *J* 9.0 Hz, 2H, 2 × ArH), 5.32 (s, 2H, OCH_2), 2.55 (s, 3H, CH_3); **^{13}C NMR** (125 MHz, $CDCl_3$) δ (ppm) 196.8, 162.5, 150.9, 148.2, 136.2, 134.7, 130.9, 130.8, 130.3, 128.7, 128.3, 126.2, 121.7, 114.7, 69.9, 26.5; **LRMS** (ES + APCI) *m/z*: calc. for $C_{18}H_{15}NO_2$ 277.1, found 278.0 $[M+H]^+$; **HMRS** calc. for $C_{18}H_{16}NO_2$ 278.1176 $[M+H]^+$, found 278.1178 $[M+H]^+$.

Isopropyl 2-amino-4-(4-(thiazol-5-ylmethoxy)phenyl)thiophene-3-carboxylate (315)

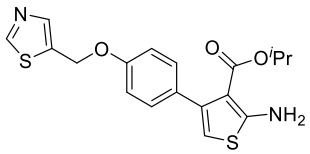

Following General Procedure D, Isopropyl 2-cyanoacetate (436 mg, 3.43 mmol) and compound **307** (400 mg, 1.72 mmol), after purification *via* flash column chromatography (dry loading, petroleum ether 3:1 EtOAc, isocratic), afforded the *title compound* (301 mg, 0.80 mmol, 47%) as an off-white solid. **mp** 168–170 °C; **IR**(ATR)/cm^{-1} 3394, 3269, 3139, 3096, 2973, 2858, 1659, 1592, 1501, 1370, 1262,

1233, 1099, 1019; **^{1}H NMR** (500 MHz, $CDCl_3$) δ (ppm) 8.82 (s, 1H, Ar*H*), 7.91 (s, 1H, Ar*H*), 7.22 (d, *J* 8.5 Hz, 2H, 2 × Ar*H*), 6.91 (d, *J* 8.5 Hz, 2H, 2 × Ar*H*), 6.07 (br s, 2H, NH_2), 6.01 (s, 1H, C=C*H*S), 5.32 (s, 2H, OCH_2), 4.98 (septet, *J* 6.0 Hz, 1H, COOC*H*$(CH_3)_2$), 0.98 (d, *J* 6.5 Hz, 6H, COOCH(CH_3)$_2$); **^{13}C NMR** (125 MHz, $CDCl_3$) δ (ppm) 165.4, 163.7, 157.1, 154.1, 142.5, 141.2, 134.4, 132.4, 130.4, 113.9, 106.7, 105.3, 67.1, 62.8, 21.8; **LRMS** (ES + APCI) *m/z*: calc. for $C_{18}H_{18}N_2O_3S_2$ 374.1, found 375.0 $[M+H]^+$; **HMRS** calc. for $C_{18}H_{19}N_2O_3S_2$ 375.0832 $[M+H]^+$, found 375.0833 $[M+H]^+$.

Isopropyl 2-amino-4-(4-(oxazol-5-ylmethoxy)phenyl)thiophene-3-carboxylate (316)

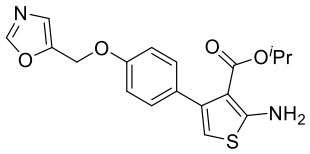

Following General Procedure D, isopropyl 2-cyanoacetate (821 mg, 6.45 mmol) and compound **308** (900 mg, 3.23 mmol), after purification *via* flash column chromatography (dry loading, Petroleum ether 3:1 EtOAc, isocratic), afforded the *title compound* (495 mg, 1.38 mmol, 43%) as an off-white solid. **mp** 54–56 °C; **IR**(ATR)/cm^{-1} 3411, 3303, 3130, 2981, 2921, 2853, 1651, 1588, 1528, 1497, 1398, 1264, 1225, 1103, 1086, 1021; **^{1}H NMR** (500 MHz, $CDCl_3$) δ (ppm) 7.91 (s, 1H, Ar*H*), 7.22 (d, *J* 8.5 Hz, 2H, 2 × Ar*H*), 7.17 (s, 1H, Ar*H*), 6.91 (d, *J* 8.5 Hz, 2H, 2 × Ar*H*), 6.06 (br s, 2H, NH_2), 6.01 (s, 1H, C=C*H*S), 5.10 (s, 2H, OCH_2), 4.99 (septet, *J* 6.5 Hz, 1H, COOC*H*$(CH_3)_2$), 0.99 (d, *J* 6.5 Hz, 6H, COOCH(CH_3)$_2$); **^{13}C NMR** (125 MHz, $CDCl_3$) δ (ppm) 165.4, 163.7, 157.1, 151.7, 147.9, 141.2, 132.5, 130.4, 126.3, 113.9, 106.7, 105.3, 67.1, 60.4, 21.8; **LRMS** (ES + APCI) *m/z*: calc. for $C_{18}H_{18}N_2O_4S$ 358.1, found 359.0 $[M+H]^+$; **HMRS** calc. for $C_{18}H_{19}N_2O_4S$ 359.1060 $[M+H]^+$, found 359.1061 $[M+H]^+$.

Isopropyl 2-amino-4-(4-(pyridin-2-ylmethoxy)phenyl)thiophene-3-carboxylate (317)

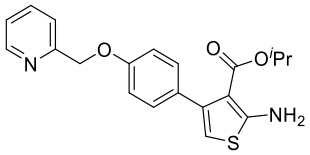

Following General Procedure D, isopropyl 2-cyanoacetate (527 mg, 4.14 mmol) and compound **309** (470 mg, 2.07 mmol), after purification *via* flash column chromatography (dry loading, petroleum ether 3:1 EtOAc, isocratic), afforded the *title compound* (355 mg, 0.96 mmol, 46%) as an off-white solid. **mp** 121–123 °C; **IR**(ATR)/cm^{-1} 3399, 3262, 3109, 2975, 2929, 1651, 1586, 1573, 1527, 1499, 1393, 1257, 1097, 1058; **^{1}H NMR** (500 MHz, $CDCl_3$) δ (ppm) 8.60 (d, *J* 4.5 Hz, 1H, Ar*H*), 7.70 (td, *J* 8.0 Hz, 2.0 Hz, 1H, Ar*H*), 7.54 (d, *J* 8.0 Hz, 1H, Ar*H*), 7.22 (dd, *J* 8.0 Hz, 4.5 Hz, 1H, Ar*H*), 7.20 (d, *J* 9.0 Hz, 2H, 2 × Ar*H*), 6.93 (d, *J* 9.0 Hz, 2H, 2 × Ar*H*), 6.07 (br s, 2H, NH_2), 6.00 (s, 1H, C=C*H*S), 5.24 (s, 2H, OCH_2), 4.96 (septet, *J* 6.5 Hz, 1H, COOC*H*$(CH_3)_2$), 0.96 (d, *J* 6.5 Hz, 6H, COOCH(C$H_3)_2$); **^{13}C NMR** (125 MHz, $CDCl_3$) δ (ppm) 165.4, 163.7, 157.6, 157.5, 149.4, 141.3, 136.9, 131.9, 130.4, 122.7, 121.5, 113.8, 106.8, 105.2, 70.8, 67.0, 21.8; **LRMS** (ES + APCI) *m/z*: calc. for $C_{20}H_{20}N_2O_3S$ 368.1, found 369.0 $[M+H]^+$; **HMRS** calc. for $C_{20}H_{20}N_2O_3SNa$ 391.1087 $[M+Na]^+$, found 391.1082 $[M+Na]^+$.

Isopropyl 2-amino-4-(4-(pyridin-3-ylmethoxy)phenyl)thiophene-3-carboxylate (318)

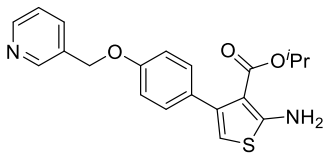

Following General Procedure D, isopropyl 2-cyanoacetate (627 mg, 4.93 mmol) and compound **310** (560 mg, 2.47 mmol), after purification *via* flash column chromatography (dry loading, petroleum ether 1:1 EtOAc, isocratic), afforded the *title compound* (425 mg, 1.15 mmol, 47%) as an off-white solid. **mp** 151–153 °C; **IR**(ATR)/cm^{-1} 3416, 3206, 3100, 2975, 2927, 1725, 1651, 1582, 1497, 1303, 1264, 1240, 1093; **^{1}H NMR** (500 MHz, $CDCl_3$) δ (ppm) 8.70 (d, *J* 1.5 Hz, 1H, Ar*H*), 8.59 (dd, *J* 5.0 Hz, 1.0 Hz, 1H, Ar*H*), 7.79 (d, *J* 8.0 Hz, 1H, Ar*H*), 7.32 (dd, *J* 8.0 Hz, 5.0 Hz, 1H, Ar*H*), 7.22 (d, *J* 9.0 Hz, 2H, 2 × Ar*H*), 6.93 (d, *J* 9.0 Hz, 2H, 2 × Ar*H*), 6.09 (br s, 2H, NH_2), 6.01 (s, 1H, C=C*H*S), 5.12 (s, 2H, OCH_2), 4.96 (septet, *J* 6.0 Hz, 1H, COOC*H*$(CH_3)_2$), 0.96 (d, *J* 6.0 Hz, 6H, COOCH(C$H_3)_2$); **^{13}C NMR** (125 MHz, $CDCl_3$) δ (ppm) 165.4, 163.7, 157.5, 157.5, 149.6, 149.2, 141.3, 135.4, 132.8, 132.1, 130.4, 123.6, 113.8, 106.8, 105.3, 67.8, 67.1, 21.8; **LRMS** (ES +

APCI) *m/z*: calc. for $C_{20}H_{20}N_2O_3S$ 368.1, found 369.0 $[M+H]^+$; **HMRS** calc. for $C_{20}H_{21}N_2O_3S$ 369.1267 $[M+H]^+$, found 369.1269 $[M+H]^+$.

Isopropyl 2-amino-4-(4-(pyridin-4-ylmethoxy)phenyl)thiophene-3-carboxylate (319)

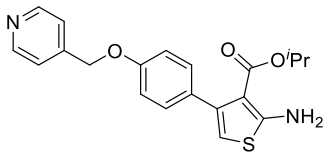

Following General Procedure D, isopropyl 2-cyanoacetate (392 mg, 3.08 mmol) and compound **311** (350 mg, 1.54 mmol), after purification *via* flash column chromatography (dry loading, petroleum ether 1:1 EtOAc, isocratic), afforded the *title compound* (230 mg, 0.63 mmol, 41%) as an off-white solid. **mp** 138–140 °C; **IR**(ATR)/cm^{-1} 3414, 3260, 3102, 2975, 2927, 1731, 1653, 1575, 1501, 1303, 1262, 1246, 1101; **^{1}H NMR** (500 MHz, $CDCl_3$) δ (ppm) 8.62 (d, *J* 5.5 Hz, 2H, 2 × Ar*H*), 7.37 (d, *J* 5.5 Hz, 2H, 2 × Ar*H*), 7.21 (d, *J* 8.5 Hz, 2H, 2 × Ar*H*), 6.89 (d, *J* 8.5 Hz, 2H, 2 × Ar*H*), 6.06 (br s, 2H, NH_2), 6.01 (s, 1H, C=C*H*S), 5.13 (s, 2H, OCH_2), 4.97 (septet, *J* 6.0 Hz, 1H, COOC*H*$(CH_3)_2$), 0.97 (d, *J* 6.0 Hz, 6H, COOCH(C$H_3)_2$); **^{13}C NMR** (125 MHz, $CDCl_3$) δ (ppm) 165.3, 163.7, 157.3, 150.2, 146.5, 141.2, 132.2, 130.4, 121.6, 113.7, 106.7, 105.3, 68.3, 67.1, 21.8; **LRMS** (ES + APCI) *m/z*: calc. for $C_{20}H_{20}N_2O_3S$ 368.1, found 369.0 $[M+H]^+$; **HMRS** calc. for $C_{20}H_{20}N_2O_3SNa$ 391.1087 $[M+Na]^+$, found 391.1084 $[M+Na]^+$.

Isopropyl 2-amino-4-(4-(pyrazin-2-ylmethoxy)phenyl)thiophene-3-carboxylate (320)

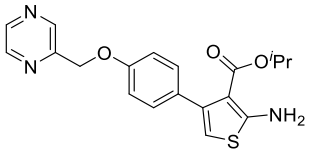

Following General Procedure D, isopropyl 2-cyanoacetate (669 mg, 5.26 mmol) and compound **312** (600 mg, 2.63 mmol), after purification *via* flash column chromatography (dry loading, petroleum ether 2:1 EtOAc, isocratic), afforded the *title compound* (350 mg, 0.95 mmol, 36%) as an off-white solid. **mp** 147–149 °C; **IR**(ATR)/cm^{-1} 3376, 3254, 3033, 2978, 2854, 1721, 1658, 1573, 1493, 1327, 1258, 1225, 1103; **^{1}H NMR** (500 MHz, $CDCl_3$) δ (ppm) 8.85 (s, 1H, Ar*H*), 8.59–8.53 (m,

2H, 2 × Ar*H*), 7.22 (d, *J* 8.5 Hz, 2H, 2 × Ar*H*), 6.94 (d, *J* 8.5 Hz, 2H, 2 × Ar*H*), 6.06 (br s, 2H, NH_2), 6.01 (s, 1H, C=C*H*S), 5.27 (s, 2H, OCH_2), 4.97 (septet, *J* 6.5 Hz, 1H, COOC*H*$(CH_3)_2$), 0.97 (d, *J* 6.5 Hz, 6H, COOCH(CH_3)$_2$); **^{13}C NMR** (125 MHz, $CDCl_3$) δ (ppm) 165.4, 163.7, 157.2, 152.9, 144.0, 143.9, 143.8, 141.2, 132.3, 130.5, 113.7, 106.8, 105.3, 69.2, 67.1, 21.8; **LRMS** (ES + APCI) *m/z*: calc. for $C_{19}H_{19}N_3O_3S$ 369.1, found 370.0 $[M+H]^+$; **HMRS** calc. for $C_{19}H_{20}N_3O_3S$ 370.1220 $[M+H]^+$, found 370.1221 $[M+H]^+$.

Isopropyl 2-amino-4-(4-(quinolin-5-ylmethoxy)phenyl)thiophene-3-carboxylate (321)

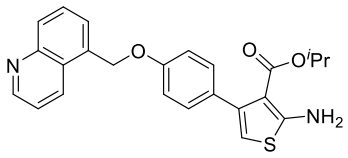

Following General Procedure D, isopropyl 2-cyanoacetate (642 mg, 5.05 mmol) and compound **313** (700 mg, 2.53 mmol), after purification *via* flash column chromatography (dry loading, Petroleum ether 2:1 EtOAc, isocratic), afforded the *title compound* (436 mg, 1.04 mmol, 41%) as an off-white solid. **mp** 138–140 °C; **IR**(ATR)/cm^{-1} 3397, 3234, 3106, 2970, 1727, 1668, 1599, 1575, 1501, 1303, 1236, 1177, 1103, 1010; **^{1}H NMR** (500 MHz, $CDCl_3$) δ (ppm) 8.96 (dd, *J* 4.0 Hz, 1.5 Hz, 1H, Ar*H*), 8.46 (d, *J* 8.5 Hz, 1H, Ar*H*), 8.12 (d, *J* 8.5 Hz, 1H, Ar*H*), 7.75–7.64 (m, 2H, 2 × Ar*H*), 7.46 (dd, *J* 8.5 Hz, 4.0 Hz, 1H, Ar*H*), 7.23 (d, *J* 8.5 Hz, 2H, 2 × Ar*H*), 6.98 (d, *J* 8.5 Hz, 2H, 2 × Ar*H*), 6.05 (br s, 2H, NH_2), 6.03 (s, 1H, C=C*H*S), 5.51 (s, 2H, OCH_2), 4.98 (septet, *J* 6.0 Hz, 1H, COOC*H*$(CH_3)_2$), 0.97 (d, *J* 6.0 Hz, 6H, COOCH(CH_3)$_2$); **^{13}C NMR** (125 MHz, $CDCl_3$) δ (ppm) 165.3, 163.7, 157.3, 150.5, 148.8, 141.3, 133.1, 132.6, 132.1, 130.7, 130.4, 129.0, 127.4, 127.1, 121.4, 113.9, 106.8, 105.3, 68.4, 67.1, 21.8; **LRMS** (ES + APCI) *m/z*: calc. for $C_{24}H_{22}N_2O_3S$ 418.1, found 419.0 $[M+H]^+$; **HMRS** calc. for $C_{24}H_{23}N_2O_3S$ 419.1424 $[M+H]^+$, found 419.1418 $[M+H]^+$.

Isopropyl 2-amino-4-(4-(quinolin-6-ylmethoxy)phenyl)thiophene-3-carboxylate (322)

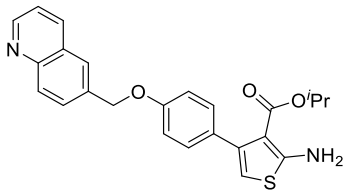

Following General Procedure D, isopropyl 2-cyanoacetate (826 mg, 6.50 mmol) and compound **314** (900 mg, 3.25 mmol), after purification *via* flash column chromatography (dry loading, Petroleum ether 2:1 EtOAc, isocratic), afforded the *title compound* (671 mg, 1.61 mmol, 49%) as an off-white solid. **mp** 160–162 °C; **IR**(ATR)/cm^{-1} 3383, 3225, 3098, 2981, 2929, 1724, 1651, 1594, 1575, 1497, 1461, 1398, 1268, 1233, 1177, 1101, 944; **^{1}H NMR** (500 MHz, $CDCl_3$) δ (ppm) 8.92 (dd, *J* 4.0 Hz, 1.0 Hz, 1H, Ar*H*), 8.16 (d, *J* 9.0 Hz, 1H, Ar*H*), 8.13 (d, *J* 9.0 Hz, 1H, Ar*H*), 7.90 (br s, 1H, Ar*H*), 7.79 (d, *J* 9.0 Hz, 1H, Ar*H*), 7.42 (d, *J* 9.0 Hz, 4.0 Hz, 1H, Ar*H*), 7.21 (d, *J* 9.0 Hz, 2H, 2 × Ar*H*), 6.96 (d, *J* 9.0 Hz, 2H, 2 × Ar*H*), 6.06 (br s, 2H, NH_2), 6.01 (s, 1H, C=C*H*S), 5.30 (s, 2H, OCH_2), 4.95 (septet, *J* 6.0 Hz, 1H, COOC*H*$(CH_3)_2$), 0.94 (d, *J* 6.0 Hz, 6H, COOCH(CH_3)$_2$); **^{13}C NMR** (125 MHz, $CDCl_3$) δ (ppm) 165.4, 163.7, 157.7, 150.7, 148.2, 141.4, 136.2, 135.8, 131.9, 130.4, 130.1, 128.9, 128.3, 126.0, 121.6, 113.9, 106.8, 105.2, 69.8, 67.0, 21.8; **LRMS** (ES + APCI) *m/z*: calc. for $C_{24}H_{22}N_2O_3S$ 418.1, found 419.0 $[M+H]^+$; **HMRS** calc. for $C_{24}H_{23}N_2O_3S$ 419.1424 $[M+H]^+$, found 419.1420 $[M+H]^+$.

2-((3-(Isopropoxycarbonyl)-4-(4-(thiazol-5-ylmethoxy)phenyl)thiophen-2-yl)carbamoyl)benzoic acid (323)

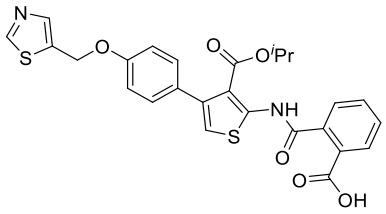

Following General Procedure E, compound **315** (150 mg, 0.40 mmol) and phthalic anhydride (60 mg, 0.40 mmol), after purification *via* flash column chromatography (dry loading, Petroleum ether 1:3 EtOAc, CH_2Cl_2 9:1 MeOH), afforded the *title compound* (133 mg, 0.25 mmol, 64%) as an off-white solid. **mp**

150–152 °C; **IR**(ATR)/cm^{-1} 3249 br, 3078, 2981, 2933, 1714, 1659, 1608, 1580, 1519, 1393, 1255, 1218, 1101; **^{1}H NMR** (500 MHz, DMSO-d_6) δ (ppm) 13.70–12.90 (app br s, 2H, COO*H*, NN*H*), 9.11 (s, 1H, Ar*H*), 8.02 (s, 1H, Ar*H*), 7.87 (d, *J* 7.0 Hz, 1H, Ar*H*), 7.65 (d, *J* 7.0 Hz, 1H, Ar*H*), 7.56–7.47 (m, 2H, 2 × Ar*H*), 7.21 (d, *J* 8.5 Hz, 2H, 2 × Ar*H*), 7.02 (d, *J* 8.5 Hz, 2H, 2 × Ar*H*), 6.87 (s, 1H, C=C*H*S), 5.43 (s, 2H, OCH_2), 4.90 (septet, *J* 6.0 Hz, 1H, COOC*H*$(CH_3)_2$), 0.97 (d, *J* 6.0 Hz, 6H, COOCH(C$H_3)_2$); **^{13}C NMR** (125 MHz, DMSO-d_6) δ (ppm) 169.9, 166.7, 164.3, 156.6, 155.2, 147.6, 142.8, 138.4, 137.2, 134.5, 134.2, 130.2, 130.1, 130.0, 129.8, 129.3, 127.9, 114.7, 114.2, 113.2, 67.9, 61.7, 21.2; **LRMS** (ES + APCI) *m/z*: calc. for $C_{26}H_{22}N_2O_6S_2$ 522.1, found 523.0 $[M+H]^+$; **HMRS** calc. for $C_{26}H_{23}N_2O_6S_2$ 523.0992 $[M+H]^+$, found 523.0985 $[M+H]^+$.

2-((3-(Isopropoxycarbonyl)-4-(4-(oxazol-5-ylmethoxy)phenyl)thiophen-2-yl)carbamoyl)benzoic acid (324)

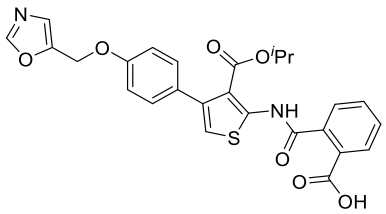

Following General Procedure E, compound **316** (100 mg, 0.28 mmol) and phthalic anhydride (42 mg, 0.28 mmol), after purification *via* flash column chromatography (dry loading, Petroleum ether 1:4 EtOAc, CH_2Cl_2 9:1 MeOH), afforded the *title compound* (75 mg, 0.15 mmol, 53%) as an off-white solid. **mp** 155–157 °C; **IR**(ATR)/cm^{-1} 3411 br, 3295, 3130, 2921, 2853, 1731, 1651, 1588, 1528, 1497, 1398, 1264, 1225, 1103; **^{1}H NMR** (500 MHz, DMSO-d_6) δ (ppm) 13.08 (br s, 1H, COO*H*), 8.41 (s, 1H, Ar*H*), 7.87 (d, *J* 7.0 Hz, 1H, Ar*H*), 7.63 (d, *J* 7.0 Hz, 1H, Ar*H*), 7.55–7.45 (m, 2H, 2 × Ar*H*), 7.34 (s, 1H, Ar*H*), 7.21 (d, *J* 8.5 Hz, 2H, 2 × Ar*H*), 7.02 (d, *J* 8.5 Hz, 2H, 2 × Ar*H*), 6.87 (s, 1H, C=C*H*S), 5.21 (s, 2H, OCH_2), 4.90 (septet, *J* 6.0 Hz, 1H, COOC*H*$(CH_3)_2$), 0.97 (d, *J* 6.0 Hz, 6H, COOCH(C$H_3)_2$); **^{13}C NMR** (125 MHz, DMSO-d_6) δ (ppm) 170.1, 166.8, 164.3, 156.7, 152.7, 147.5, 147.4, 138.4, 134.4, 130.2, 130.0, 129.9, 129.8, 129.1, 128.1, 128.0, 126.3, 114.6, 114.0, 113.3, 67.9, 59.2, 21.2; **LRMS** (ES + APCI) *m/z*: calc. for $C_{26}H_{22}N_2O_7S$ 506.1, found 507.0 $[M+H]^+$; **HMRS** calc. for $C_{26}H_{23}N_2O_7S$ 507.1220 $[M+H]^+$, found 507.1225 $[M+H]^+$.

2-((3-(Isopropoxycarbonyl)-4-(4-(pyridin-2-ylmethoxy)phenyl)thiophen-2-yl)carbamoyl)benzoic acid (325)

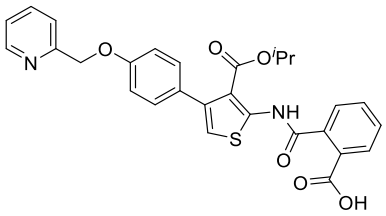

Following General Procedure E, compound **317** (300 mg, 0.82 mmol) and phthalic anhydride (121 mg, 0.82 mmol), after purification *via* flash column chromatography (dry loading, Petroleum ether 1:1 EtOAc, CH_2Cl_2 9:1 MeOH), afforded the *title compound* (189 mg, 0.37 mmol, 45%) as an off-white solid. **mp** 142–144 °C; **IR**(ATR)/cm^{-1} 3303 br, 3291, 2977, 1714, 1659, 1575, 1521, 1395, 1253, 1222, 1101; **^{1}H NMR** (500 MHz, DMSO-d_6) δ (ppm) 13.27 (br s, 1H, COO*H*), 8.58 (d, *J* 5.0 Hz, 1H, Ar*H*), 7.87 (dd, *J* 7.0 Hz, 1.5 Hz, 1H, Ar*H*), 7.82 (td, *J* 7.0 Hz, 1.5 Hz, 1H, Ar*H*), 7.64 (dd, *J* 6.5 Hz, 1.5 Hz, 1H, Ar*H*), 7.55–7.45 (m, 3H, 3 × Ar*H*), 7.34 (dd, *J* 7.0 Hz, 5.0 Hz, 1H, Ar*H*), 7.20 (d, *J* 9.0 Hz, 2H, 2 × Ar*H*), 7.00 (d, *J* 9.0 Hz, 2H, 2 × Ar*H*), 6.86 (s, 1H, C=C*H*S), 5.22 (s, 2H, OCH_2), 4.89 (septet, *J* 6.5 Hz, 1H, COOC*H*$(CH_3)_2$), 0.96 (d, *J* 6.5 Hz, 6H, COOCH$(CH_3)_2$); **^{13}C NMR** (125 MHz, DMSO-d_6) δ (ppm) 170.1, 166.7, 164.3, 157.2, 156.8, 149.1, 147.3, 138.4, 136.9, 134.3, 130.1, 130.0, 129.9, 129.8, 129.7, 129.0, 123.1, 122.9, 121.6, 114.5, 113.9, 113.4, 70.3, 67.9, 21.2; **LRMS** (ES + APCI) *m/z*: calc. for $C_{28}H_{24}N_2O_6S$ 516.1, found 517.0 $[M+H]^+$; **HMRS** calc. for $C_{28}H_{23}N_2O_6S$ 515.1282 $[M–H]^-$, found 515.1285 $[M–H]^-$.

2-((3-(Isopropoxycarbonyl)-4-(4-(pyridin-3-ylmethoxy)phenyl)thiophen-2-yl)carbamoyl)benzoic acid (326)

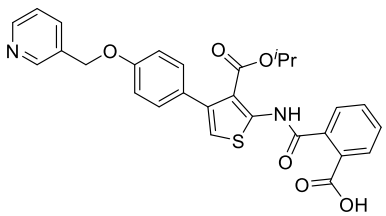

Following General Procedure E, compound **318** (400 mg, 1.09 mmol) and phthalic anhydride (161 mg, 1.09 mmol), after purification *via* flash column

chromatography (dry loading, Petroleum ether 1:1 EtOAc, CH_2Cl_2 9:1 MeOH), afforded the *title compound* (275 mg, 0.53 mmol, 49%) as an off-white solid. **mp** 175–177 °C; **IR**(ATR)/cm^{-1} 3401 br, 3269, 3070, 2884, 1722, 1651, 1608, 1521, 1395, 1285, 1222, 1103; **^{1}H NMR** (500 MHz, DMSO-d_6) δ (ppm) 13.46 (br s, 1H, COO*H*), 8.68 (s, 1H, Ar*H*), 8.54 (d, *J* 4.5 Hz, 1H, Ar*H*), 7.87 (app t, *J* 7.0 Hz, 2H, 2 × Ar*H*), 7.64 (d, *J* 7.0 Hz, 1H, Ar*H*), 7.53–7.40 (m, 3H, 3 × Ar*H*), 7.20 (d, *J* 8.5 Hz, 2H, 2 × Ar*H*), 7.02 (d, *J* 8.5 Hz, 2H, 2 × Ar*H*), 6.85 (s, 1H, C=C*H*S), 5.20 (s, 2H, OCH_2), 4.89 (septet, *J* 6.5 Hz, 1H, COOC*H*$(CH_3)_2$), 0.97 (d, *J* 6.5 Hz, 6H, COOCH(C$H_3)_2$); **^{13}C NMR** (125 MHz, DMSO-d_6) δ (ppm) 170.3, 168.8, 164.3, 157.1, 149.1, 149.0, 148.9, 147.3, 138.3, 135.5, 134.1, 132.7, 130.1, 129.9, 129.7, 128.8, 128.1, 123.6, 123.5, 114.5, 114.1, 113.4, 67.9, 66.9, 21.2; **LRMS** (ES + APCI) *m/z*: calc. for $C_{28}H_{24}N_2O_6S$ 516.1, found 517.0 $[M+H]^+$; **HMRS** calc. for $C_{28}H_{23}N_2O_6S$ 515.1282 $[M–H]^-$, found 515.1285 $[M–H]^-$.

2-((3-(Isopropoxycarbonyl)-4-(4-(pyridin-4-ylmethoxy)phenyl)thiophen-2-yl)carbamoyl)benzoic acid (327)

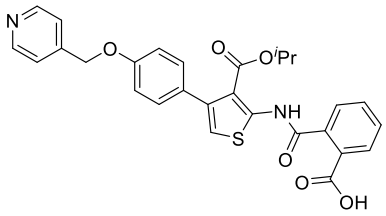

Following General Procedure E, compound **319** (200 mg, 0.54 mmol) and phthalic anhydride (81 mg, 0.54 mmol), after purification *via* flash column chromatography (dry loading, Petroleum ether 1:1 EtOAc, CH_2Cl_2 9:1 MeOH), afforded the *title compound* (177 mg, 0.34 mmol, 63%) as an off-white solid. **mp** 161–163 °C; **IR**(ATR)/cm^{-1} 3474 br, 3267, 3044, 2983, 1714, 1651, 1601, 1564, 1519, 1395, 1287, 1244, 1104, 1034; **^{1}H NMR** (500 MHz, DMSO-d_6) δ (ppm) 13.04 (br s, 1H, COO*H*), 8.57 (d, *J* 5.5 Hz, 2H, 2 × Ar*H*), 7.86 (d, *J* 7.0 Hz, 1H, Ar*H*), 7.64 (d, *J* 7.0 Hz, 1H, Ar*H*), 7.55–7.47 (m, 2H, 2 × Ar*H*), 7.44 (d, *J* 5.5 Hz, 2H, 2 × Ar*H*), 7.20 (d, *J* 8.5 Hz, 2H, 2 × Ar*H*), 7.02 (d, *J* 8.5 Hz, 2H, 2 × Ar*H*), 6.86 (s, 1H, C=C*H*S), 5.24 (s, 2H, OCH_2), 4.89 (septet, *J* 6.5 Hz, 1H, COOC*H*$(CH_3)_2$), 0.95 (d, *J* 6.5 Hz, 6H, COOCH(C$H_3)_2$); **^{13}C NMR** (125 MHz, DMSO-d_6) δ (ppm) 169.8, 166.7, 164.3, 156.9, 149.7, 147.5, 146.3, 138.4, 134.4, 131.8, 130.1, 130.0, 129.8, 129.3, 128.0, 121.8, 114.6, 114.5, 114.0, 113.3, 67.9, 67.4, 21.2; **LRMS** (ES +

APCI) *m/z*: calc. for $C_{28}H_{24}N_2O_6S$ 516.1, found 517.0 $[M+H]^+$; **HMRS** calc. for $C_{28}H_{24}N_2O_6SNa$ 539.1247 $[M+Na]^+$, found 539.1240 $[M+Na]^+$.

2-((3-(Isopropoxycarbonyl)-4-(4-(pyrazin-2-ylmethoxy)phenyl)thiophen-2-yl)carbamoyl)benzoic acid (328)

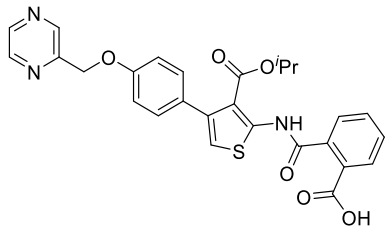

Following General Procedure E, compound **320** (140 mg, 0.38 mmol) and phthalic anhydride (56 mg, 0.38 mmol), after purification *via* flash column chromatography (dry loading, Petroleum ether 1:2 EtOAc, CH_2Cl_2 9:1 MeOH), afforded the *title compound* (20 mg, 0.04 mmol, 10%) as an off-white solid. **mp** 167–169 °C; **IR**(ATR)/cm^{-1} 3455 br, 3262, 3059, 2936, 1714, 1651, 1617, 1521, 1404, 1255, 1222, 1103; **^{1}H NMR** (500 MHz, DMSO-d_6) δ (ppm) 13.27 (br s, 1H, COO*H*), 12.25 (br s, 1H, CON*H*), 8.81 (s, 1H, Ar*H*), 8.67 (a br s, 1H, Ar*H*), 8.63 (d, *J* 2.0 Hz, 1H, Ar*H*), 7.88 (d, *J* 7.0 Hz, 1H, Ar*H*), 7.69 (d, *J* 7.0 Hz, 1H, Ar*H*), 7.66–7.57 (m, 2H, 2 × Ar*H*), 7.22 (d, *J* 8.5 Hz, 2H, 2 × Ar*H*), 7.04 (d, *J* 8.5 Hz, 2H, 2 × Ar*H*), 6.91 (s, 1H, C=C*H*S), 5.31 (s, 2H, OCH_2), 4.89 (septet, *J* 6.5 Hz, 1H, COOC*H*$(CH_3)_2$), 0.94 (d, *J* 6.5 Hz, 6H, COOCH$(CH_3)_2$); **^{13}C NMR** (125 MHz, DMSO-d_6) δ (ppm) 168.0, 165.9, 164.3, 157.0, 152.2, 147.6, 144.2, 144.1, 143.7, 138.6, 135.1, 131.0, 130.9, 130.5, 130.1, 130.0, 129.9, 127.9, 115.0, 113.9, 113.3, 68.4, 68.0, 21.2; **LRMS** (ES + APCI) *m/z*: calc. for $C_{27}H_{23}N_3O_6S$ 517.1, found 518.0 $[M+H]^+$; **HMRS** calc. for $C_{27}H_{23}N_3O_6SNa$ 540.1200 $[M+Na]^+$, found 540.1187 $[M+Na]^+$.

2-((3-(Isopropoxycarbonyl)-4-(4-(quinolin-5-ylmethoxy)phenyl)thiophen-2-yl)carbamoyl)benzoic acid (329)

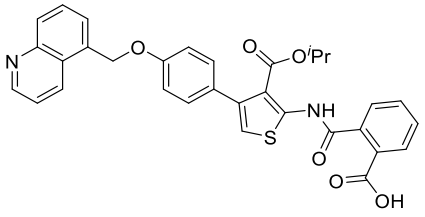

Following General Procedure E, compound **321** (150 mg, 0.36 mmol) and phthalic anhydride (53 mg, 0.36 mmol), after purification *via* flash column chromatography (dry loading, Petroleum ether 1:2 EtOAc, CH_2Cl_2 9:1 MeOH), afforded the *title compound* (104 mg, 0.18 mmol, 51%) as an off-white solid. **mp** 175–177 °C; **IR**(ATR)/cm^{-1} 3358 br, 3042, 2962, 2931, 1714, 1659, 1610, 1521, 1504, 1395, 1285, 1220, 1101; **^{1}H NMR** (500 MHz, DMSO-d_6) δ (ppm) 13.64 (br s, 1H, COO*H*), 13.38 (br s, 1H, CON*H*), 8.95 (dd, *J* 4.0 Hz, 1.5 Hz, 1H, Ar*H*), 8.56 (d, *J* 8.5 Hz, 1H, Ar*H*), 8.02 (d, *J* 7.5 Hz, 1H, Ar*H*), 7.85 (d, *J* 7.5 Hz, 1H, Ar*H*), 7.80–7.73 (m, 2H, 2 × Ar*H*), 7.67 (d, *J* 7.5 Hz, 1H, Ar*H*), 7.60 (dd, *J* 8.5 Hz, 4.0 Hz, 1H, Ar*H*), 7.55–7.45 (m 2H, 2 × Ar*H*), 7.22 (d, *J* 8.5 Hz, 2H, 2 × Ar*H*), 7.09 (d, *J* 8.5 Hz, 2H, 2 × Ar*H*), 6.87 (s, 1H, C=C*H*S), 5.63 (s, 2H, OCH_2), 4.90 (septet, *J* 6.0 Hz, 1H, COOC*H*$(CH_3)_2$), 0.97 (d, *J* 6.0 Hz, 6H, COOCH(C$H_3)_2$); **^{13}C NMR** (125 MHz, DMSO-d_6) δ (ppm) 169.9, 166.7, 164.3, 157.3, 150.4, 147.9, 147.4, 138.4, 134.4, 133.5, 132.4, 130.1, 130.0, 129.9, 129.7, 129.6, 129.2, 129.1, 128.9, 128.0, 126.9, 126.2, 121.5, 114.6, 114.2, 113.4, 67.9, 67.2, 21.2; **LRMS** (ES + APCI) *m/z*: calc. for $C_{32}H_{26}N_2O_6S$ 566.1, found 567.0 $[M+H]^+$; **HMRS** calc. for $C_{32}H_{27}N_2O_6S$ 567.1584 $[M+H]^+$, found 567.1574 $[M+H]^+$.

2-((3-(Isopropoxycarbonyl)-4-(4-(quinolin-6-ylmethoxy)phenyl)thiophen-2-yl)carbamoyl)benzoic acid (330)

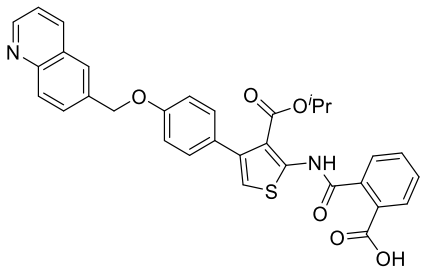

Following General Procedure E, compound **322** (150 mg, 0.36 mmol) and phthalic anhydride (53 mg, 0.36 mmol), after purification *via* flash column chromatography (dry loading, Petroleum ether 1:2 EtOAc, CH_2Cl_2 9:1 MeOH), afforded the *title compound* (112 mg, 0.20 mmol, 55%) as an off-white solid. **mp** 117–119 °C; **IR**(ATR)/cm^{-1} 3277 br, 3059, 2983, 1714, 1659, 1651, 1610, 1521, 1504, 1395, 1285, 1222, 1101, 1019; **^{1}H NMR** (500 MHz, DMSO-d_6) δ (ppm) 13.26 (app br s, 2H, COO*H*, CON*H*), 8.90 (dd, *J* 4.0 Hz, 1.0 Hz, 1H, Ar*H*), 8.37 (d, *J* 8.0 Hz, 1H, Ar*H*), 8.08–8.02 (m, 2H, 2 × Ar*H*), 7.89–7.81 (m, 2H, 2 × Ar*H*), 7.63 (d,

J 8.0 Hz, 1H, Ar*H*), 7.54 (dd, *J* 8.0 Hz, 4.0 Hz, 1H, Ar*H*), 7.53–7.44 (m 2H, 2 × Ar*H*), 7.20 (d, *J* 8.5 Hz, 2H, 2 × Ar*H*), 7.05 (d, *J* 8.5 Hz, 2H, 2 × Ar*H*), 6.85 (s, 1H, C=C*H*S), 5.37 (s, 2H, OCH_2), 4.86 (septet, *J* 6.5 Hz, 1H, COOC*H*$(CH_3)_2$), 0.89 (d, *J* 6.5 Hz, 6H, COOCH(CH_3)$_2$); **^{13}C NMR** (125 MHz, DMSO-d_6) δ (ppm) 170.3, 166.9, 164.3, 157.3, 150.6, 147.6, 147.3, 138.5, 136.0, 135.5, 134.5, 130.0, 129.9, 129.8, 129.7, 129.2, 129.1, 129.0, 129.0, 127.9, 127.7, 126.2, 121.7, 114.5, 114.2, 113.1, 68.9, 67.8, 21.1; **LRMS** (ES + APCI) *m/z*: calc. for $C_{32}H_{26}N_2O_6S$ 566.2, found 567.0 $[M+H]^+$; **HMRS** calc. for $C_{32}H_{27}N_2O_6S$ 567.1584 $[M+H]^+$, found 567.1578 $[M+H]^+$.

1-(3-Fluoro-4-(pyrazin-2-ylmethoxy)phenyl)ethan-1-one (333)

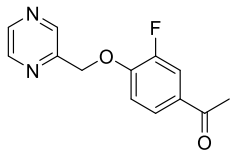

Pyrazin-2-yl methanol (1.50 g, 13.60 mmol), 1-(3,4-difluorophenyl)ethan-1-one (2.13 g, 13.60 mmol), K_2CO_3 (13.00 g, 95.40 mmol), 18-crown-6 (360 mg, 1.36 mmol), in PhMe (80 mL, 0.17 M), were stirred under reflux overnight. After cooling to room temperature, the reaction mixture was filtered through Celite® and washed through with ether (3 × 30 mL). The filtrate was concentrated under reduced pressure before purification by flash column chromatography (Petroleum ether 1:1 EtOAc, isocratic) afforded the *title compound* (2.84 g, 11.54 mmol, 85%) as an off-white solid. **mp** 123–125 °C; **IR**(ATR)/cm^{-1} 3012, 2943, 1664, 1578, 1513, 1433, 1385, 1273, 1197, 1147, 1061; **^{1}H NMR** (500 MHz, $CDCl_3$) δ (ppm) 8.87 (s, 1H, Ar*H*), 8.58 (app s, 2H, 2 × Ar*H*), 7.77–7.69 (m, 2H, 2 × Ar*H*), 7.09 (app t, *J* 8.0 Hz, 1H, Ar*H*), 5.37 (s, 2H, CH_2O), 2.55 (s, 3H, COCH_3); **^{13}C NMR** (125 MHz, $CDCl_3$) δ (ppm) 195.8, 152.4 ($J_{C\text{-}F}$ 247.4 Hz, 1F, ArF), 151.5, 150.4 ($J_{C\text{-}F}$ 10.9 Hz, 1F, ArF), 144.6, 144.1, 143.9, 131.7 ($J_{C\text{-}F}$ 5.0 Hz, 1F, ArF), 125.7 ($J_{C\text{-}F}$ 3.4 Hz, 1F, ArF), 116.5 ($J_{C\text{-}F}$ 18.9 Hz, 1F, ArF), 114.3, 70.2, 26.5; **^{19}F NMR** (376 MHz, $CDCl_3$) δ (ppm) -132.59–(-132.67) (m, 1F, Ar*F*); **LRMS** (ES + APCI) *m/z*: calc. for $C_{13}H_{11}FN_2O_2$ 246.1, found 247.0 $[M+H]^+$; **HMRS** calc. for $C_{13}H_{12}FN_2O_2$ 247.0877 $[M+H]^+$, found 247.0876 $[M+H]^+$.

Ethyl 2-amino-4-(4-(pyrazin-2-ylmethoxy)phenyl)thiophene-3-carboxylate (334)

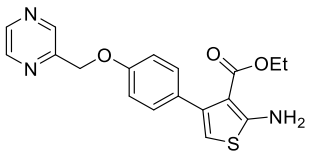

Following General Procedure D, ethyl 2-cyanoacetate (694 mg, 6.14 mmol) and compound **312** (700 mg, 3.06 mmol), after purification *via* flash column chromatography (dry loading, Petroleum ether 2:1 EtOAc, isocratic), afforded the *title compound* (484 mg, 1.37 mmol, 45%) as an off-white solid. **mp** 95–97 °C; **IR**(ATR)/cm^{-1} 3432, 3320, 3101, 2978, 2917, 2850, 1736, 1656, 1589, 1522, 1496, 1381, 1307, 1257, 1227, 1106, 1065, 1017; **^{1}H NMR** (500 MHz, $CDCl_3$) δ (ppm) 8.85 (s, 1H, Ar*H*), 8.58 (app t, *J* 2.5 Hz, 1H, Ar*H*), 8.55 (d, *J* 2.5 Hz, 1H, Ar*H*), 7.24 (d, *J* 8.5 Hz, 2H, 2 × Ar*H*), 6.95 (d, *J* 8.5 Hz, 2H, 2 × Ar*H*), 6.02 (app br s, 3H, C=C*H*S, NH_2), 5.27 (s, 2H, OCH_2), 4.05 (q, *J* 7.0 Hz, 2H, COOC$H_2$$CH_3$), 0.96 (t, *J* 7.0 Hz, 3H, $COOCH_2CH_3$); **^{13}C NMR** (125 MHz, $CDCl_3$) δ (ppm) 165.8, 164.0, 157.3, 152.9, 144.0, 143.9, 143.8, 141.1, 132.1, 130.4, 113.7, 106.3, 105.4, 69.2, 59.6, 14.0; **LRMS** (ES + APCI) *m/z*: calc. for $C_{18}H_{17}N_3O_3S$ 355.1, found 356.0 $[M+H]^+$. **HMRS** calc. for $C_{18}H_{18}N_3O_3S$ 356.1063 $[M+H]^+$, found 356.1064 $[M+H]^+$.

Ethyl 2-amino-4-(3-fluoro-4-(pyrazin-2-ylmethoxy)phenyl)thiophene-3-carboxylate (335)

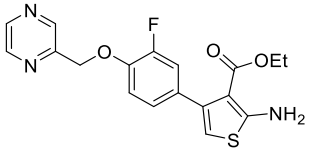

Following General Procedure D, ethyl 2-cyanoacetate (644 mg, 5.69 mmol) and compound **333** (700 mg, 2.84 mmol), after purification *via* flash column chromatography (dry loading, Petroleum ether 4:1 EtOAc, isocratic), afforded the *title compound* (464 mg, 1.24 mmol, 44%) as an off-white solid. **mp** 115–116 °C; **IR**(ATR)/cm^{-1} 3404, 3317, 3255, 3125, 2969, 2917, 2867, 1660, 1589, 1502, 1450, 1405, 1383, 1318, 1255, 1236, 1112, 1104, 1017, 831; **^{1}H NMR** (400 MHz, $CDCl_3$) δ (ppm) 8.90 (s, 1H, Ar*H*), 8.60–8.54 (m, 2H, 2 × Ar*H*), 7.12–7.06 (m, 1H, Ar*H*), 7.02–6.94 (m, 2H, 2 × Ar*H*), 6.11 (br s, 2H, NH_2), 6.04 (s, 1H, C=C*H*S), 5.33

(s, 2H, OCH_2), 4.06 (q, *J* 7.2 Hz, 2H, COOCH_2CH$_3$), 0.99 (t, *J* 7.2 Hz, 3H, COOCH$_2$CH_3); **^{13}C NMR** (101 MHz, $CDCl_3$) δ (ppm) 165.6, 164.2, 152.4, 151.9 ($J_{C\text{-}F}$ 246.4 Hz, 1F, ArF), 145.2 ($J_{C\text{-}F}$ 10.8 Hz, 1F, ArF), 144.2, 144.0, 143.9, 143.9, 140.0, 133.1 ($J_{C\text{-}F}$ 7.4 Hz, 1F, ArF), 124.9 ($J_{C\text{-}F}$ 3.7 Hz, 1F, ArF), 117.7 ($J_{C\text{-}F}$ 19.3 Hz, 1F, ArF), 114.6, 105.9, 70.6, 60.0, 14.0; **^{19}F NMR** (376 MHz, $CDCl_3$) δ (ppm) -135.4 (dd, *J* 12.4 Hz, 7.5 Hz, 1F, Ar*F*); **LRMS** (ES + APCI) *m/z*: calc. for $C_{18}H_{16}FN_3O_3S$ 373.1, found 374.0 $[M+H]^+$; **HMRS** calc. for $C_{18}H_{17}FN_3O_3S$ 374.0969 $[M+H]^+$, found 374.0970 $[M+H]^+$.

2-Amino-*N*-isopropyl-4-(4-(pyrazin-2-ylmethoxy)phenyl)thiophene-3-carboxamide (336)

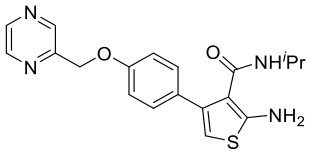

Following General Procedure I, compound **334** (150 mg, 0.42 mmol) and propan-2-amine (38 μL, 0.42 mmol), after purification *via* flash column chromatography (dry loading, Petroleum ether 1:1 EtOAc, isocratic), afforded the *title compound* (118 mg, 0.32 mmol, 76%) as an off-white solid. **mp** 113–115 °C; **IR**(ATR)/cm^{-1} 3406, 3354, 3257, 3147, 2967, 2922, 2867, 1621, 1591, 1515, 1502, 1452, 1383, 1255, 1236, 1186, 1059, 1017, 831; **^{1}H NMR** (400 MHz, $CDCl_3$) δ (ppm) 8.83 (s, 1H, Ar*H*), 8.61–8.54 (m, 2H, 2 × Ar*H*), 7.31 (d, *J* 8.8 Hz, 2H, 2 × Ar*H*), 7.04 (d, *J* 8.8 Hz, 2H, 2 × Ar*H*), 6.18 (br s, 2H, NH_2), 6.03 (s, 1H, C=C*H*S), 5.29 (s, 2H, OCH_2), 4.91 (d, *J* 6.4 Hz, 1H, CON*H*CH), 3.98 (app octet, *J* 6.8 Hz, 1H, CONHC*H*(CH$_3$)$_2$), 0.84 (d, *J* 6.8 Hz, 6H, CONHCH(CH_3)$_2$); **^{13}C NMR** (101 MHz, $CDCl_3$) δ (ppm) 165.1, 161.5, 158.1, 152.4, 144.2, 144.1, 143.8, 138.5, 130.9, 130.4, 115.0, 108.8, 105.6, 69.2, 40.8, 22.7; **LRMS** (ES + APCI) *m/z*: calc. for $C_{19}H_{20}N_4O_2S$ 368.1, found 369.0 $[M+H]^+$; **HMRS** calc. for $C_{19}H_{21}N_4O_2S$ 369.1380 $[M+H]^+$, found 369.1379 $[M+H]^+$.

2-Amino-4-(3-fluoro-4-(pyrazin-2-ylmethoxy)phenyl)-*N*-isopropylthiophene-3-carboxamide (337)

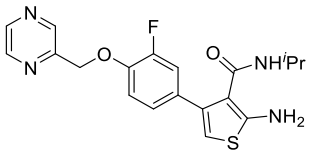

Following General Procedure I, compound **335** (200 mg, 0.54 mmol) and propan-2-amine (46 μL, 0.54 mmol), after purification *via* flash column chromatography (dry loading, Petroleum ether 1:1 EtOAc, isocratic), afforded the *title compound* (152 mg, 0.39 mmol, 73%) as an off-white solid. **mp** 118–120 °C; **IR**(ATR)/cm^{-1} 3419, 3348, 3255, 3099, 2967, 2926, 2868, 1612, 1573, 1515, 1455, 1383, 1271, 1247, 1113, 1020, 808; **^{1}H NMR** (500 MHz, $CDCl_3$) δ (ppm) 7.89 (s, 1H, Ar*H*), 8.58 (app br s, 2H, 2 × Ar*H*), 7.20–7.14 (m, 1H, Ar*H*), 7.11–7.05 (m, 2H, 2 × Ar*H*), 6.15 (br s, 2H, NH_2), 6.06 (s, 1H, C=C*H*S), 5.35 (s, 2H, OCH_2), 4.84 (d, *J* 6.5 Hz, 1H, CON*H*CH), 4.02 (app octet, *J* 7.0 Hz, 1H, CONHC*H*$(CH_3)_2$), 0.89 (d, *J* 7.0 Hz, 6H, CONHCH(CH_3)$_2$); **^{13}C NMR** (101 MHz, $CDCl_3$) δ (ppm) 164.9, 161.6, 152.5 ($J_{C\text{-}F}$ 250.0 Hz, 1F, ArF), 152.0, 146.2 ($J_{C\text{-}F}$ 10.7 Hz, 1F, ArF), 144.4, 144.1, 143.9, 137.4, 131.3 ($J_{C\text{-}F}$ 7.0 Hz, 1F, ArF), 125.4 ($J_{C\text{-}F}$ 3.2 Hz, 1F, ArF), 117.8 ($J_{C\text{-}F}$ 18.7 Hz, 1F, ArF), 115.7, 108.6, 106.2, 70.6, 40.9, 22.7; **^{19}F NMR** (376 MHz, $CDCl_3$) δ (ppm) -132.56–(-132.46) (m, 1F, Ar*F*); **LRMS** (ES + APCI) *m/z*: calc. for $C_{19}H_{19}FN_4O_2S$ 386.1, found 387.0 $[M+H]^+$; **HMRS** calc. for $C_{19}H_{20}FN_4O_2S$ 387.1286 $[M+H]^+$, found 387.1283 $[M+H]^+$.

2-((3-(Isopropylcarbamoyl)-4-(4-(pyrazin-2-ylmethoxy)phenyl)thiophen-2-yl)carbamoyl)benzoic acid (338)

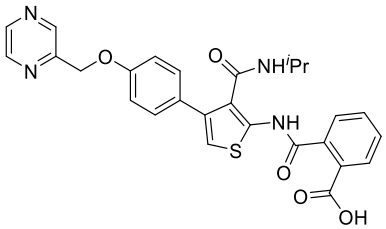

Following General Procedure E, compound **336** (80 mg, 0.22 mmol) and phthalic anhydride (32 mg, 0.22 mmol), after purification *via* flash column chromatography (dry loading, Petroleum ether 1:3 EtOAc, CH_2Cl_2 9:1 MeOH),

afforded the *title compound* (43 mg, 0.08 mmol, 38%) as an off-white solid. **mp** 149–151 °C; **IR**(ATR)/cm^{-1} 3396, 3240, 3058, 2973, 1719, 1654, 1606, 1573, 1519, 1402, 1284, 1255, 1219, 1154, 1020; **^{1}H NMR** (400 MHz, DMSO-d_6) δ (ppm) 13.98 (br s, 1H, COO*H*), 8.81 (s, 1H, Ar*H*), 8.70–8.60 (m, 2H, 2 × Ar*H*), 7.77 (d, *J* 7.2 Hz, 2H, 2 × Ar*H*), 7.50 (app pentet, *J* 7.2 Hz, 3H, 2 × Ar*H*, CON*H*CH), 7.35 (d, *J* 8.8 Hz, 2H, 2 × Ar*H*), 7.07 (d, *J* 8.8 Hz, 2H, 2 × Ar*H*), 6.94 (s, 1H, C=C*H*S), 5.30 (s, 2H, OCH_2), 3.96 (app octet, *J* 6.4 Hz, 1H, CONHC*H*$(CH_3)_2$), 0.92 (d, *J* 6.4 Hz, 6H, CONHCH(CH_3)$_2$); **^{13}C NMR** (101 MHz, DMSO-d_6) δ (ppm) 171.4, 165.6, 163.9, 157.3, 152.2, 144.2, 143.8, 141.5, 138.9, 136.8, 132.8, 130.2, 129.8, 129.3, 129.1, 129.0, 128.6, 119.8, 114.7, 114.0, 68.4, 40.7, 21.9, (1 carbon missing); **LRMS** (ES + APCI) *m/z*: calc. for $C_{27}H_{24}N_4O_5S$ 516.1, found 517.0 $[M+H]^+$; **HMRS** calc. for $C_{27}H_{23}N_4O_5S$ 515.1401 $[M–H]^-$, found 515.1402 $[M–H]^-$.

2-((4-(3-Fluoro-4-(pyrazin-2-ylmethoxy)phenyl)-3-(isopropylcarbamoyl)thiophen-2-yl)carbamoyl)benzoic acid (339)

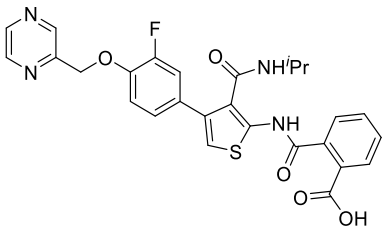

Following General Procedure E, compound **337** (90 mg, 0.23 mmol) and phthalic anhydride (34 mg, 0.23 mmol), after purification *via* flash column chromatography (dry loading, Petroleum ether 1:3 EtOAc, CH_2Cl_2 9:1 MeOH), afforded the *title compound* (58 mg, 0.11 mmol, 47%) as an off-white solid. **mp** 154–156 °C; **IR**(ATR)/cm^{-1} 3409, 3067, 2963, 2921, 1719, 1612, 1580, 1573, 1515, 1385, 1262, 1221, 1156, 1112, 1019; **^{1}H NMR** (400 MHz, DMSO-d_6) δ (ppm) 15.20 (br s, 1H, COO*H*), 8.82 (d, *J* 0.8 Hz, 1H, Ar*H*), 8.69 (app t, *J* 2.4 Hz, 1H, Ar*H*), 8.65 (d, *J* 2.4 Hz, 1H, Ar*H*), 7.95 (d, *J* 7.2 Hz, 1H, CON*H*CH), 7.85 (d, *J* 7.2 Hz, 1H, Ar*H*), 7.77 (d, *J* 7.2 Hz, 1H, Ar*H*), 7.52–7.40 (m, 2H, 2 × Ar*H*), 7.33–7.24 (m, 2H, 2 × Ar*H*), 7.18 (d, *J* 8.4 Hz, 1H, Ar*H*), 7.03 (s, 1H, C=C*H*S), 5.37 (s, 2H, OCH_2), 4.00 (app octet, *J* 6.8 Hz, 1H, CONHC*H*$(CH_3)_2$), 1.00 (d, *J* 6.8 Hz, 6H, CONHCH(CH_3)$_2$); **^{13}C NMR** (125 MHz, DMSO-d_6) δ (ppm) 171.4, 165.5, 163.7, 151.6, 151.3 ($J_{C\text{-}F}$ 242.0 Hz, 1F, ArF), 144.8 ($J_{C\text{-}F}$ 10.5 Hz, 1F, ArF), 144.4, 144.3, 143.8, 141.1, 139.1, 135.7, 132.5, 130.2, 129.9 ($J_{C\text{-}F}$ 4.0 Hz, 1F, ArF), 129.3, 128.5,

124.1 ($J_{C\text{-}F}$ 2.6 Hz, 1F, ArF), 120.4, 115.6 ($J_{C\text{-}F}$ 18.8 Hz, 1F, ArF), 115.3, 114.6, 69.4, 40.8, 21.8 (1 carbon missing); **^{19}F NMR** (376 MHz, $CDCl_3$) δ (ppm) -135.11 (app t, *J* 9.8 Hz, 1F, Ar*F*); **LRMS** (ES + APCI) *m/z*: calc. for $C_{27}H_{23}FN_4O_5S$ 534.1, found 535.0 $[M+H]^+$; **HMRS** calc. for $C_{27}H_{22}FN_4O_5S$ 533.1300 $[M–H]^-$, found 533.1307 $[M–H]^-$.

(*E*)-1-(4-(2-(Pyrazin-2-yl)vinyl)phenyl)ethan-1-one (341)

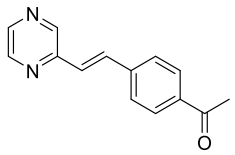

To a flame dried microwave vial was added 2-vinyl pyrazine (1.00 g, 9.42 mmol), 4-bromo acetophenone (2.25 g, 11.31 mmol), triphenyl phosphine (247 mg, 0.94 mmol), NEt_3 (1.91 g, 18.80 mmol) and 1-methyl-2-pyrrolidinone (2.70 mL, 0.47 M). The mixture was then degassed by bubbling nitrogen through it for 15 minutes. Palladium (II) acetate (106 mg, 0.47 mmol) was subsequently added and the mixture was again degassed by bubbling nitrogen through it for 10 minutes. The reaction mixture was heated at 120 °C overnight. The solution was allowed to cool to room temperature, before being filtered through Celite® and the filtrate was then concentrated under reduced pressure. Purification by flash column chromatography (Petroleum ether 2:1 EtOAc, isocratic) afforded the *title compound* (1.72 g, 7.68 mmol, 81%) as an off-white solid. **mp** 136–138 °C; **IR**(ATR)/cm^{-1} 3053, 3004, 2922, 2850, 1675, 1602, 1567, 1524, 1476, 1411, 1361, 1264, 1180, 1141, 1056, 1017, 844; **^{1}H NMR** (500 MHz, $CDCl_3$) δ (ppm) 8.67 (d, *J* 1.0 Hz, 1H, Ar*H*), 8.57 (app t, *J* 2.5 Hz, 1H, Ar*H*), 8.45 (d, *J* 2.5 Hz, 1H, Ar*H*), 7.99 (d, *J* 8.0 Hz, 2H, 2 × Ar*H*), 7.80 (d, *J* 16.0 Hz, 1H, C*H*=CH), 7.68 (d, *J* 8.0 Hz, 2H, 2 × Ar*H*), 7.27 (d, *J* 16.0 Hz, 1H, CH=C*H*), 2.63 (s, 3H, CH_3); **^{13}C NMR** (125 MHz, $CDCl_3$) δ (ppm) 197.5, 150.8, 144.6, 144.2, 143.5, 140.7, 137.2, 134.0, 129.1, 127.5, 126.7, 26.8; **LRMS** (ES + APCI) *m/z*: calc. for $C_{14}H_{12}N_2O$ 224.1, found 449.2 $[2M+H]^+$; **HMRS** calc. for $C_{14}H_{13}N_2O$ 225.1033 $[M+H]^+$, found 225.1023 $[M+H]^+$.

1-(4-(2-(Pyrazin-2-yl)ethyl)phenyl)ethan-1-one (342)

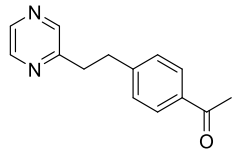

A round-bottomed flask was flame dried and purged with Nitrogen (× 3). To the flask was added Pd/C (71 mg, 0.67 mmol) and a solution of compound **341** (1.50 g, 6.69 mmol) in EtOAc/EtOH (1:1) (70 mL, 0.10 M). The mixture was then exposed to a Hydrogen (H_2) atmosphere by the application of vacuum, followed by a H_2 balloon. This sequence was repeated 5 times. H_2 was then bubbled through the mixture for 5–10 minutes. The reaction was allowed to stir at room temperature for 5 hours under a hydrogen atmosphere. Upon completion, the resulting solution was filtered through Celite® and the filtrate was concentrated under reduced pressure. Purification by flash column chromatography (Petroleum ether 1:1 EtOAc, isocratic) afforded the *title compound* (1.06 g, 4.71 mmol, 70%) as an off-white solid. **mp** 93–95 °C; **IR**(ATR)/cm^{-1} 3080, 3008, 2947, 2861, 1677, 1604, 1571, 1526, 1429, 1407, 1361, 1264, 1186, 1156, 1063, 1022, 849, 814; **^{1}H NMR** (500 MHz, $CDCl_3$) δ (ppm) 8.52 (s, 1H, Ar*H*), 8.41 (d, *J* 2.0 Hz, 1H, Ar*H*), 8.36 (app s, 1H, Ar*H*), 7.87 (d, *J* 8.0 Hz, 2H, 2 × Ar*H*), 7.26 (d, *J* 8.0 Hz, 2H, 2 × Ar*H*), 3.15 (app br s, 4H, CH_2CH_2), 2.58 (s, 3H, CH_3); **^{13}C NMR** (125 MHz, $CDCl_3$) δ (ppm) 197.8, 156.3, 146.6, 144.8, 144.3, 142.7, 135.6, 128.8, 36.8, 35.3, 26.7 (1 carbon missing); **LRMS** (ES + APCI) *m/z*: calc. for $C_{14}H_{14}N_2O$ 226.1, found 227.2 $[M+H]^+$; **HMRS** calc. for $C_{14}H_{15}N_2O$ 227.1179 $[M+H]^+$, found 227.1180 $[M+H]^+$.

Ethyl (*E*)-2-amino-4-(4-(2-(pyrazin-2-yl)vinyl)phenyl)thiophene-3-carboxylate (343)

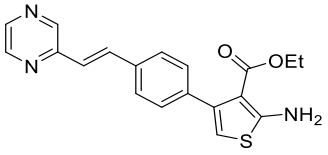

Following General Procedure D, ethyl 2-cyanoacetate (215 mg, 1.90 mmol) and compound **341** (213 mg, 0.95 mmol), after purification *via* flash column chromatography (dry loading, Petroleum ether 3:1 EtOAc, isocratic), afforded the *title compound* as a partially purified yellow solid.

Selected data; **^{1}H NMR** (500 MHz, $CDCl_3$) δ (ppm) 8.65 (d, *J* 1.5 Hz, 1H, Ar*H*), 8.55 (app t, *J* 1.5 Hz, 1H, Ar*H*), 8.40 (d, *J* 2.5 Hz, 1H, Ar*H*), 7.78 (d, *J* 16.0 Hz, 1H, C*H*=CH), 7.55 (d, *J* 8.5 Hz, 2H, 2 × Ar*H*), 7.33 (d, *J* 8.5 Hz, 2H, 2 × Ar*H*), 7.18 (d, *J* 16.0 Hz, 1H, CH=C*H*), 6.15–6.05 (m, 3H, NH_2, C=C*H*S), 4.07 (q, *J* 7.5 Hz, 2H, OCH_2CH$_3$), 0.97 (t, *J* 7.5 Hz, 3H, OCH$_2$CH_3).

Ethyl 2-amino-4-(4-(2-(pyrazin-2-yl)ethyl)phenyl)thiophene-3-carboxylate (344)

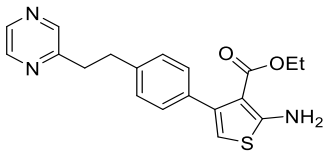

Following General Procedure D, ethyl 2-cyanoacetate (700 mg, 6.19 mmol) and compound **342** (700 mg, 3.10 mmol), after purification *via* flash column chromatography (dry loading, Petroleum ether 3:1 EtOAc, isocratic), afforded the *title compound* (559 mg, 1.58 mmol, 51%) as an off-white solid. **mp** 70–72 °C; **IR**(ATR)/cm^{-1} 3404, 3298, 3103, 2976, 2954, 2896, 1634, 1584, 1528, 1500, 1476, 1405, 1318, 1270, 1130, 1110, 1019, 942, 816; **^{1}H NMR** (400 MHz, $CDCl_3$) δ (ppm) 8.52 (app t, *J* 2.0 Hz, 1H, Ar*H*), 8.42–8.38 (m, 2H, 2 × Ar*H*), 7.20 (d, *J* 8.0 Hz, 2H, 2 × Ar*H*), 7.12 (d, *J* 8.0 Hz, 2H, 2 × Ar*H*), 6.13 (br s, 2H, NH_2), 6.02 (s, 1H, C=C*H*S), 4.03 (q, *J* 7.2 Hz, 2H, COOCH_2CH$_3$), 3.19–3.05 (m, 4H, CH_2CH_2), 0.92 (t, *J* 7.2 Hz, 3H, COOCH$_2$CH_3); **^{13}C NMR** (101 MHz, $CDCl_3$) δ (ppm) 165.8, 164.0, 156.9, 144.8, 144.2, 142.4, 141.5, 139.4, 136.6, 129.2, 127.4, 106.1, 105.5, 59.5, 37.3, 35.1, 13.9; **LRMS** (ES + APCI) *m/z*: calc. for $C_{19}H_{19}N_3O_2S$ 353.1, found 354.2 [M+H]$^+$; **HMRS** calc. for $C_{19}H_{20}N_3O_2S$ 354.1271 [M+H]$^+$, found 354.1269 [M+H]$^+$.

(*E*)-2-Amino-*N*-isopropyl-4-(4-(2-(pyrazin-2-yl)vinyl)phenyl)thiophene-3-carboxamide (345)

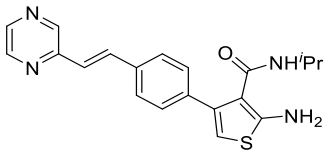

Following General Procedure I, compound **343** (130 mg, 0.46 mmol) and propan-2-amine (39 μL, 0.46 mmol), after purification *via* flash column chromatography (dry loading, Petroleum ether 2:1 EtOAc, isocratic), afforded the

title compound (91 mg, 0.25 mmol, 26%**) as an off-white solid. **mp** 99–101 °C; **IR**(ATR)/cm^{-1} 3415, 3285, 3045, 2963, 2924, 2867, 1621, 1573, 1513, 1468, 1385, 1260, 1173, 1138, 1017; **^{1}H NMR** (400 MHz, $CDCl_3$) δ (ppm) 8.66 (d, *J* 1.2 Hz, 1H, Ar*H*), 8.56 (app t, *J* 2.4 Hz, 1H, Ar*H*), 8.43 (d, *J* 2.4 Hz, 1H, Ar*H*), 7.79 (d, *J* 16.4 Hz, 1H, C*H*=CH), 7.64 (d, *J* 8.0 Hz, 2H, 2 × Ar*H*), 7.41 (d, *J* 8.0 Hz, 2H, 2 × Ar*H*), 7.22 (d, *J* 16.4 Hz, 1H, CH=C*H*), 6.16 (br s, 2H, NH_2), 6.12 (s, 1H, C=C*H*S), 4.88 (d, *J* 6.8 Hz, 1H, CON*H*CH), 4.01 (app octet, *J* 6.8 Hz, 1H, CONHC*H*$(CH_3)_2$), 0.87 (d, *J* 6.4 Hz, 6H, CONHCH(CH_3)$_2$); **^{13}C NMR** (125 MHz, $CDCl_3$) δ (ppm) 165.0, 161.7, 151.1, 144.5, 144.0, 143.1, 138.6, 137.7, 136.0, 134.4, 129.9, 127.5, 124.7, 108.7, 106.1, 41.0, 22.6; **LRMS** (ES + APCI) *m/z*: calc. for $C_{20}H_{20}N_4OS$ 364.1, found 365.2 $[M+H]^+$; **HMRS** calc. for $C_{20}H_{21}N_4OS$ 365.1431 $[M+H]^+$, found 365.1432 $[M+H]^+$.

2-Amino-*N*-isopropyl-4-(4-(2-(pyrazin-2-yl)ethyl)phenyl)thiophene-3-carboxamide (346)

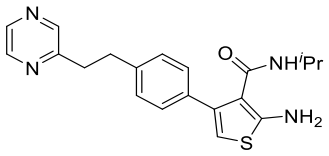

Following General Procedure I, compound **344** (200 mg, 0.57 mmol) and propan-2-amine (48 μL, 0.57 mmol), after purification *via* flash column chromatography (dry loading, Petroleum ether 1:1 EtOAc, isocratic), afforded the *title compound* (182 mg, 0.50 mmol, 88%) as an off-white solid. **mp** 80–82 °C; **IR**(ATR)/cm^{-1} 3411, 3279, 3063, 2963, 2924, 2863, 1621, 1574, 1515, 1455, 1383, 1258, 1173, 1059, 1020; **^{1}H NMR** (500 MHz, $CDCl_3$) δ (ppm) 8.53–8.50 (m, 1H, Ar*H*), 8.43–8.38 (m, 2H, 2 × Ar*H*), 7.26 (d, *J* 8.0 Hz, 2H, 2 × Ar*H*), 7.22 (d, *J* 8.0 Hz, 2H, 2 × Ar*H*), 6.23 (br s, 2H, NH_2), 6.02 (s, 1H, C=C*H*S), 4.85 (d, *J* 7.0 Hz, 1H, CON*H*CH), 3.95 (app octet, *J* 6.5 Hz, 1H, CONHC*H*$(CH_3)_2$), 3.17–3.09 (m, 4H, CH_2CH_2), 0.80 (d, *J* 6.5 Hz, 6H, CONHCH(CH_3)$_2$); **^{13}C NMR** (125 MHz, $CDCl_3$) δ (ppm) 165.0, 161.5, 156.5, 144.7, 144.3, 142.6, 141.1, 138.9, 135.2, 129.6, 128.7, 108.7, 105.6, 40.7, 37.1, 34.9, 22.5; **LRMS** (ES + APCI) *m/z*: calc. for $C_{20}H_{22}N_4OS$ 366.2, found 367.1 $[M+H]^+$; **HMRS** calc. for $C_{20}H_{23}N_4OS$ 367.1587 $[M+H]^+$, found 367.1588 $[M+H]^+$.

(*E*)-2-((3-(Isopropylcarbamoyl)-4-(4-(2-(pyrazin-2-yl)vinyl)phenyl)thiophen-2-yl)carbamoyl)benzoic acid (347)

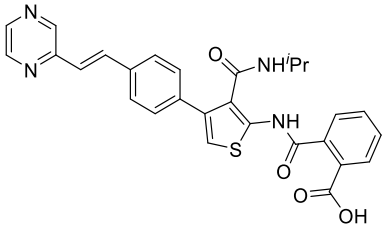

Following General Procedure E, compound **345** (36 mg, 0.10 mmol) and phthalic anhydride (14 mg, 0.10 mmol), after purification *via* flash column chromatography (dry loading, Petroleum ether 1:3 EtOAc, CH_2Cl_2 9:1 MeOH), afforded the *title compound* (34 mg, 0.07 mmol, 67%) as an off-white solid. **mp** 158–160 °C; **IR**(ATR)/cm^{-1} 3409, 3292, 3058, 2978, 2924, 1713, 1632, 1608, 1586, 1519, 1476, 1403, 1320, 1262, 1230, 1138, 1017, 847; **^{1}H NMR** (500 MHz, DMSO-d_6) δ (ppm) 14.71 (br s, 1H, COO*H*), 8.81 (s, 1H, Ar*H*), 8.63 (app br s, 1H, Ar*H*), 8.49 (d, *J* 2.5 Hz, 1H, Ar*H*), 7.88 (d, *J* 6.0 Hz, 1H, CON*H*CH), 7.85 (d, *J* 8.0 Hz, 1H, Ar*H*), 7.81 (d, *J* 16.0 Hz, 1H, C*H*=CH), 7.78 (d, *J* 8.0 Hz, 1H, Ar*H*), 7.70 (d, *J* 8.0 Hz, 2H, 2 × Ar*H*), 7.53–7.39 (m, 5H, 4 × Ar*H*, CH=C*H*), 7.11 (s, 1H, C=C*H*S), 4.03 (app octet, *J* 6.5 Hz, 1H, CONHC*H*(CH_3)$_2$), 1.02 (d, *J* 6.5 Hz, 6H, CONHCH(C*H*$_3$)$_2$); **^{13}C NMR** (125 MHz, DMSO-d_6) δ (ppm) 171.5, 165.5, 163.8, 150.7, 144.5, 143.8, 143.1, 141.1, 139.5, 136.9, 136.6, 134.7, 133.8, 132.4, 130.2, 130.0, 129.4, 128.4, 128.2, 127.2, 124.3, 120.6, 115.0, 40.9, 21.9; **LRMS** (ES + APCI) *m/z*: calc. for $C_{28}H_{24}N_4O_4S$ 512.2, found 513.2 $[M+H]^+$; **HMRS** calc. for $C_{28}H_{23}N_4O_4S$ 511.1445 $[M–H]^-$, found 511.1450 $[M–H]^-$.

2-((3-(Isopropylcarbamoyl)-4-(4-(2-(pyrazin-2-yl)ethyl)phenyl)thiophen-2-yl)carbamoyl)benzoic acid (348)

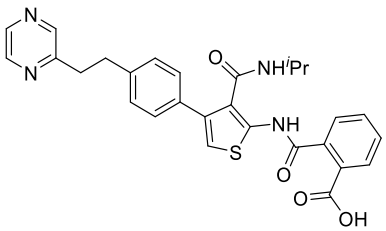

Following General Procedure E, compound **346** (100 mg, 0.27 mmol) and phthalic anhydride (40 mg, 0.27 mmol), after purification *via* flash column

chromatography (dry loading, Petroleum ether 1:4 EtOAc, CH_2Cl_2 9:1 MeOH), afforded the *title compound* (49 mg, 0.10 mmol, 35%) as an off-white solid. **mp** 129–131 °C; **IR**(ATR)/cm^{-1} 3406, 3296, 3103, 2974, 2922, 1719, 1632, 1586, 1524, 1478, 1403, 1318, 1264, 1230, 1130, 1020; **^{1}H NMR** (500 MHz, DMSO-d_6) δ (ppm) 14.29 (br s, 2H, COO*H*, CON*H*CS), 8.59–8.56 (m, 1H, Ar*H*), 8.55 (d, *J* 1.0 Hz, 1H, Ar*H*), 8.46 (d, *J* 2.5 Hz, 1H, Ar*H*), 7.83–7.75 (m, 2H, 2 × Ar*H*), 7.48 (app pentet, *J* 7.0 Hz, 2H, 2 × Ar*H*) 7.43 (app br s, 1H, CON*H*CH), 7.32 (d, *J* 8.0 Hz, 2H, 2 × Ar*H*), 7.23 (d, *J* 8.0 Hz, 2H, 2 × Ar*H*), 6.96 (s, 1H, C=C*H*S), 3.95 (app octet, *J* 6.5 Hz, 1H, CONHC*H*$(CH_3)_2$), 3.17–3.01 (m, 4H, CH_2CH_2), 0.93 (d, *J* 6.5 Hz, 6H, CONHCH(CH_3)$_2$); **^{13}C NMR** (101 MHz, DMSO-d_6) δ (ppm) 171.1, 165.7, 163.7, 156.3, 144.5, 144.0, 142.4, 141.7, 140.0, 138.8, 137.2, 133.8, 133.1, 130.1, 130.0, 129.0, 128.6, 128.2, 128.0, 119.8, 114.4, 40.8, 36.0, 33.9, 21.8; **LRMS** (ES + APCI) *m/z*: calc. for $C_{28}H_{26}N_4O_4S$ 514.2, found 515.2 $[M+H]^+$; **HMRS** calc. for $C_{28}H_{25}N_4O_4S$ 513.1602 $[M–H]^-$, found 513.1611 $[M–H]^-$.

2-((3-(Methoxycarbonyl)thiophen-2-yl)carbamoyl)benzoic acid (349)

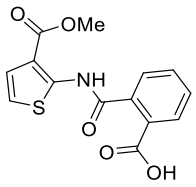

Following General Procedure E, methyl 2-aminothiophene-3-carboxylate (250 mg, 1.59 mmol), and phthalic anhydride (236 mg, 1.59 mmol), after purification *via* flash column chromatography (dry loading, hexane 10:1 EtOAc, CH_2Cl_2 95:5 MeOH), afforded the *title compound* (314 mg, 1.03 mmol, 65%) as a grey solid. **mp** 182–184 °C; **IR**(ATR)/cm^{-1} 3259, 3081, 2954, 1668, 1547, 1498; **^{1}H NMR** (500 MHz, DMSO-d_6) δ (ppm) 13.35 (br s, 1H, COO*H*), 11.34 (br s, 1H, CON*H*), 7.90 (d, *J* 7.0 Hz, 1H, Ar*H*), 7.70–7.62 (m, 3H, 3 × Ar*H*), 7.23 (d, *J* 5.5 Hz, 1H, Ar*H*), 7.10 (d, *J* 5.5 Hz, 1H, Ar*H*), 3.81 (s, 3H, COOCH_3), **^{13}C NMR** (125 MHz, DMSO-d_6) δ (ppm) 167.7, 165.6, 164.8, 147.9, 135.3, 131.6, 130.8, 129.8, 127.7, 123.6, 117.3, 112.9, 51.8 (1 carbon missing); **LRMS** (ES + APCI) *m/z*: calc. for $C_{14}H_{11}NO_5S$ 305.0, found 305.9 $[M+H]^+$; **HMRS** (ESI, -ve) *m/z*: calc. for $C_{14}H_{10}NO_5S$ 304.0285 $[M–H]^-$, found 304.0276 $[M–H]^-$.

Methyl 2-(2-(methoxycarbonyl)benzamido)thiophene-3-carboxylate (350)

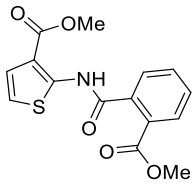

Following General Procedure F, compound **349** (100 mg, 0.33 mmol) was refluxed in MeOH (5.0 mL) containing a few drops of H_2SO_4 to afford, after purification *via* flash column chromatography (dry loading, petroleum ether 6:1 EtOAc, isocratic), the *title compound* (66 mg, 0.21 mmol, 63%) as an off-white solid. **mp** 107–109 °C; **IR**(ATR)/cm^{-1} 3271, 3127, 2952, 1727, 1671, 1550, 1498; **^{1}H NMR** (500 MHz, $CDCl_3$) δ (ppm) 11.27 (s, 1H, CON*H*), 7.93 (d, *J* 7.5 Hz, 1H, Ar*H*), 7.64–7.52 (m, 3H, 3 × Ar*H*), 7.22 (d, *J* 5.5 Hz, 1H, Ar*H*), 6.78 (d, *J* 5.5 Hz, 1H, Ar*H*), 3.83 (s, 3H, 2 × COOCH_3); **^{13}C NMR** (125 MHz, $CDCl_3$) δ (ppm) 166.9, 166.1, 165.6, 148.9, 135.9, 132.2, 130.8, 130.3, 130.1, 127.6, 123.9, 116.5, 113.1, 52.7, 51.8; **LRMS** (ES + APCI) *m/z*: calc. for $C_{15}H_{13}NO_5S$ 319.0, found 320.0 $[M+H]^+$; **HMRS** calc. for $C_{15}H_{14}NO_5S$ 320.0587 $[M+H]^+$, found 320.0589 $[M+H]^+$.

Isopropyl 2-(2-(methoxycarbonyl)benzamido)-4-(4-phenethylphenyl)thiophene-3-carboxylate (351)

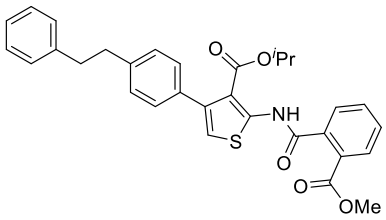

Following General Procedure F, compound **184** (156 mg, 0.30 mmol) and MeOH (3.0 mL, 0.1 M) with a few drops of H_2SO_4, after purification *via* flash column chromatography (dry loading, Petroleum ether 6:1 EtOAc isocratic), afforded the *title compound* (148 mg, 0.28 mmol, 93%) as an off-white solid. **mp** 117–119 °C; **IR**(ATR)/cm^{-1} 3221, 30296, 2981, 2931, 1731, 1672, 1642, 1553, 1430, 1279, 1259, 1106; **^{1}H NMR** (500 MHz, $CDCl_3$) δ (ppm) 11.66 (s, 1H, CON*H*), 7.95 (dd, *J* 7.0 Hz, 1.0 Hz, 1H, Ar*H*), 7.67–7.55 (m, 3H, 3 × Ar*H*), 7.60 (app t, *J* 7.5 Hz, 2H, 2 × Ar*H*), 7.25–7.14 (m, 7H, 7 × Ar*H*), 6.65 (s, 1H, C=C*H*S), 4.95 (septet, *J* 6.0 Hz, 1H, COOC*H*$(CH_3)_2$), 3.88 (s, 3H, OCH_3), 2.97 (s, 4H, CH_2CH_2), 0.94 (d, *J* 6.0 Hz, 6H, COOCH(C$H_3)_2$); **^{13}C NMR** (125 MHz, $CDCl_3$) δ (ppm) 167.0, 165.9, 165.8, 149.9, 141.9, 140.8, 140.2, 136.4, 135.8, 132.3, 130.8, 130.4, 130.2,

129.5, 128.6, 128.5, 127.7, 127.5, 126.1, 115.3, 112.8, 68.5, 52.9, 38.2, 37.7, 21.5; **LRMS** (ES + APCI) *m/z*: calc. for $C_{31}H_{29}NO_5S$ 527.2, found 528.0 $[M+H]^+$; **HMRS** calc. for $C_{31}H_{30}NO_5S$ 528.1839 $[M+H]^+$, found 528.1833 $[M+H]^+$.

8. References

1. Hunter, T., Protein kinases and phosphatases: The Yin and Yang of protein phosphorylation and signaling. *Cell* **1995,** *80*, 225-236.
2. Chen, M. J.; Dixon, J. E.; Manning, G., Genomics and evolution of protein phosphatases. *Sci Signal* **2017,** *10*. (accessed May 15th, 2019)
3. Bollu, L. R.; Mazumdar, A.; Savage, M. I.; Brown, P. H., Molecular Pathways: Targeting Protein Tyrosine Phosphatases in Cancer. *Clin Cancer Res* **2017,** *23*, 2136-2142.
4. Seifried, A.; Schultz, J.; Gohla, A., Human HAD phosphatases: structure, mechanism, and roles in health and disease. *FEBS Journal* **2013,** *280*, 549-571.
5. Millán, J. L., Alkaline Phosphatases. *Purinergic Signalling* **2006,** *2*, 335-341.
6. Hsu, P. L.; Yang, F.; Smith-Kinnaman, W.; Yang, W.; Song, J.-E.; Mosley, A. L.; Varani, G., Rtr1 Is a Dual Specificity Phosphatase That Dephosphorylates Tyr1 and Ser5 on the RNA Polymerase II CTD. *Journal of Molecular Biology* **2014,** *426*, 2970-2981.
7. Sacco, F.; Perfetto, L.; Castagnoli, L.; Cesareni, G., The human phosphatase interactome: An intricate family portrait. *Febs Letters* **2012,** *586*, 2732-2739.
8. Barford, D.; Das, A. K.; Egloff, M.-P., THE STRUCTURE AND MECHANISM OF PROTEIN PHOSPHATASES: Insights into Catalysis and Regulation. *Annual Review of Biophysics and Biomolecular Structure* **1998,** *27*, 133-164.
9. Hoff, R. H.; Wu, L.; Zhou, B.; Zhang, Z.-Y.; Hengge, A. C., Does Positive Charge at the Active Sites of Phosphatases Cause a Change in Mechanism? The Effect of the Conserved Arginine on the Transition State for Phosphoryl Transfer in the Protein-Tyrosine Phosphatase from Yersinia. *Journal of the American Chemical Society* **1999,** *121*, 9514-9521.
10. Johnson, L. N.; Lowe, E. D.; Noble, M. E. M.; Owen, D. J., The structural basis for substrate recognition and control by protein kinases. *FEBS Letters* **1998,** *430*, 1-11.
11. Huse, M.; Kuriyan, J., The Conformational Plasticity of Protein Kinases. *Cell* **2002,** *109*, 275-282.
12. Life tech. www.lifetechnologies.com. (accessed March 4th, 2017)
13. Bononi, A.; Agnoletto, C.; De Marchi, E.; et al., Protein Kinases and Phosphatases in the Control of Cell Fate. *Enzyme Research* **2011,** *2011*, 329098.
14. Beltrao, P.; Trinidad, J. C.; Fiedler, D.; Roguev, A.; Lim, W. A.; Shokat, K. M.; Burlingame, A. L.; Krogan, N. J., Evolution of Phosphoregulation: Comparison of Phosphorylation Patterns across Yeast Species. *PLoS Biology* **2009,** *7*, e1000134.
15. Ventura, J.-J.; Nebreda, Á. R., Protein kinases and phosphatases as therapeutic targets in cancer. *Clinical and Translational Oncology* **2006,** *8*, 153-160.
16. Shen, K.; Keng, Y.-F.; Wu, L.; Guo, X.-L.; Lawrence, D. S.; Zhang, Z.-Y., Acquisition of a Specific and Potent PTP1B Inhibitor from a Novel Combinatorial Library and Screening Procedure. *Journal of Biological Chemistry* **2001,** *276*, 47311-47319.
17. Andersen, H. S.; Olsen, O. H.; Iversen, L. F.; Sorensen, A. L.; Mortensen, S. B.; Christensen, M. S.; Branner, S.; Hansen, T. K.; Lau, J. F.; Jeppesen, L.; Moran, E. J.; Su, J.; Bakir, F.; Judge, L.; Shahbaz, M.; Collins, T.; Vo, T.; Newman, M. J.; Ripka, W. C.; Moller, N. P., Discovery and SAR of a novel selective and orally bioavailable nonpeptide classical competitive inhibitor class of protein-tyrosine phosphatase 1B. *J Med Chem* **2002,** *45*, 4443-59.
18. Shakespeare, W.; Yang, M.; Bohacek, R.; Cerasoli, F.; Stebbins, K.; Sundaramoorthi, R.; Azimioara, M.; Vu, C.; Pradeepan, S.; Metcalf, C., 3rd; Haraldson, C.; Merry, T.; Dalgarno, D.; Narula, S.; Hatada, M.; Lu, X.; van Schravendijk, M. R.; Adams, S.; Violette, S.; Smith, J.; Guan, W.; Bartlett, C.; Herson, J.; Iuliucci, J.; Weigele, M.; Sawyer, T., Structure-based design of an osteoclast-selective, nonpeptide src homology 2 inhibitor with in vivo antiresorptive activity. *Proc Natl Acad Sci U S A* **2000,** *97*, 9373-8.

19. Tonks, N. K., Protein tyrosine phosphatases: from genes, to function, to disease. *Nat Rev Mol Cell Biol* **2006,** *7*, 833-846.
20. De Munter, S.; Kohn, M.; Bollen, M., Challenges and opportunities in the development of protein phosphatase-directed therapeutics. *ACS Chem Biol* **2013,** *8*, 36-45.
21. Sakoff, J. A.; McCluskey, A., Protein phosphatase inhibition: structure based design. Towards new therapeutic agents. *Curr Pharm Des* **2004,** *10*, 1139-59.
22. Yadav, L.; Tamene, F.; Goos, H.; van Drogen, A.; Katainen, R.; Aebersold, R.; Gstaiger, M.; Varjosalo, M., Systematic Analysis of Human Protein Phosphatase Interactions and Dynamics. *Cell Syst* **2017,** *4*, 430-444 e5.
23. Fahs, S.; Lujan, P.; Kohn, M., Approaches to Study Phosphatases. *ACS Chem Biol* **2016,** *11*, 2944-2961.
24. Lazo, J. S.; McQueeney, K. E.; Sharlow, E. R., New Approaches to Difficult Drug Targets: The Phosphatase Story. *SLAS Discov* **2017**, 2472555217721142.
25. Stanford, S. M.; Bottini, N., Targeting Tyrosine Phosphatases: Time to End the Stigma. *Trends Pharmacol Sci* **2017,** *38*, 524-540.
26. Vintonyak, V. V.; Antonchick, A. P.; Rauh, D.; Waldmann, H., The therapeutic potential of phosphatase inhibitors. *Current Opinion in Chemical Biology* **2009,** *13*, 272-283.
27. Erbe, D. V.; Wang, S.; Zhang, Y. L.; Harding, K.; Kung, L.; Tam, M.; Stolz, L.; Xing, Y.; Furey, S.; Qadri, A.; Klaman, L. D.; Tobin, J. F., Ertiprotafib improves glycemic control and lowers lipids via multiple mechanisms. *Mol Pharmacol* **2005,** *67*, 69-77.
28. Hellmuth, K.; Grosskopf, S.; Lum, C. T.; Wurtele, M.; Roder, N.; von Kries, J. P.; Rosario, M.; Rademann, J.; Birchmeier, W., Specific inhibitors of the protein tyrosine phosphatase Shp2 identified by high-throughput docking. *Proc Natl Acad Sci U S A* **2008,** *105*, 7275-80.
29. Soellner, M. B.; Rawls, K. A.; Grundner, C.; Alber, T.; Ellman, J. A., Fragment-based substrate activity screening method for the identification of potent inhibitors of the Mycobacterium tuberculosis phosphatase PtpB. *J Am Chem Soc* **2007,** *129*, 9613-5.
30. Urbanek, R. A.; Suchard, S. J.; Steelman, G. B.; Knappenberger, K. S.; Sygowski, L. A.; Veale, C. A.; Chapdelaine, M. J., Potent reversible inhibitors of the protein tyrosine phosphatase CD45. *J Med Chem* **2001,** *44*, 1777-93.
31. Bensaad, K.; Tsuruta, A.; Selak, M. A.; Vidal, M. N. C.; Nakano, K.; Bartrons, R.; Gottlieb, E.; Vousden, K. H., TIGAR, a p53-Inducible Regulator of Glycolysis and Apoptosis. *Cell* **2006,** *126*, 107-120. (accessed June 11th, 2018)
32. Vousden, K. H.; Lu, X., Live or let die: the cell's response to p53. *Nat Rev Cancer* **2002,** *2*, 594-604.
33. Bourdon, J.-C.; Fernandes, K.; Murray-Zmijewski, F.; Liu, G.; Diot, A.; Xirodimas, D. P.; Saville, M. K.; Lane, D. P., p53 isoforms can regulate p53 transcriptional activity. *Genes & Development* **2005,** *19*, 2122-2137.
34. Rigden, Daniel J., The histidine phosphatase superfamily: structure and function. *Biochemical Journal* **2008,** *409*, 333-348. (accessed Novmber 10th, 2016)
35. Li, H.; Jogl, G., Structural and Biochemical Studies of TIGAR (TP53-induced Glycolysis and Apoptosis Regulator). *The Journal of Biological Chemistry* **2009,** *284*, 1748-1754. (accessed November 10th, 2016)
36. Lee, P.; Vousden, K. H.; Cheung, E. C., TIGAR, TIGAR, burning bright. *Cancer & Metabolism* **2014,** *2*, 1-1.
37. Yu, H.-P.; Xie, J.-M.; Li, B.; Sun, Y.-H.; Gao, Q.-G.; Ding, Z.-H.; Wu, H.-R.; Qin, Z.-H., TIGAR regulates DNA damage and repair through pentosephosphate pathway and Cdk5-ATM pathway. *Scientific Reports* **2015,** *5*, 9853.
38. Wanka, C.; Steinbach, J. P.; Rieger, J., Tp53-induced Glycolysis and Apoptosis Regulator (TIGAR) Protects Glioma Cells from Starvation-induced Cell Death by Up-regulating Respiration and Improving Cellular Redox Homeostasis. *The Journal of Biological Chemistry* **2012,** *287*, 33436-33446.

39. Cheung, Eric C.; Athineos, D.; Vousden, Karen H.; et al., TIGAR Is Required for Efficient Intestinal Regeneration and Tumorigenesis. *Developmental Cell* **2013,** *25*, 463-477. (accessed April 22nd, 2017)
40. Won, K. Y.; Lim, S.-J.; Kim, G. Y.; Kim, Y. W.; Han, S.-A.; Song, J. Y.; Lee, D.-K., Regulatory role of p53 in cancer metabolism via SCO2 and TIGAR in human breast cancer. *Human Pathology* **2012,** *43*, 221-228.
41. Lee, P.; Hock, A. K.; Vousden, K. H.; Cheung, E. C., p53- and p73-independent activation of TIGAR expression in vivo. *Cell Death Dis* **2015,** *6*, e1842.
42. Gerin, I.; Noel, G.; Bolsee, J.; Haumont, O.; Van Schaftingen, E.; Bommer, G. T., Identification of TP53-induced glycolysis and apoptosis regulator (TIGAR) as the phosphoglycolate-independent 2,3-bisphosphoglycerate phosphatase. *Biochem J* **2014,** *458*, 439-48.
43. Workman, P.; Collins, I., Probing the Probes: Fitness Factors For Small Molecule Tools. *Chemistry & Biology* **2010,** *17*, 561-577.
44. Chen, R.; Wierda, W. G.; Chubb, S.; Hawtin, R. E.; Fox, J. A.; Keating, M. J.; Gandhi, V.; Plunkett, W., Mechanism of action of SNS-032, a novel cyclin-dependent kinase inhibitor, in chronic lymphocytic leukemia. *Blood* **2009,** *113*, 4637-4645.
45. Lee, K. S.; Lee, H. K.; Hayflick, J. S.; Lee, Y. C.; Puri, K. D., Inhibition of phosphoinositide 3-kinase δ attenuates allergic airway inflammation and hyperresponsiveness in murine asthma model. *The FASEB Journal* **2006,** *20*, 455-465.
46. Arrowsmith, C. H.; Audia, J. E.; Austin, C.; *et al.*, The promise and peril of chemical probes. *Nat Chem Biol* **2015,** *11*, 536-541.
47. Frye, S. V., The art of the chemical probe. *Nat Chem Biol* **2010,** *6*, 159-161.
48. Kodadek, T., Rethinking screening. *Nat Chem Biol* **2010,** *6*, 162-165.
49. Fleisig, H.; El-Din El-Husseini, A.; Vincent, S. R., Regulation of ErbB4 phosphorylation and cleavage by a novel histidine acid phosphatase. *Neuroscience* **2004,** *127*, 91-100.
50. Zhou, W.; Yin, Y.; Weinheimer, A. S.; Kaur, N.; Carpino, N.; French, J. B., Structural and Functional Characterization of the Histidine Phosphatase Domains of Human Sts-1 and Sts-2. *Biochemistry* **2017,** *56*, 4637-4645.
51. Johnson, Louise N., The regulation of protein phosphorylation. *Biochemical Society Transactions* **2009,** *37*, 627-641.
52. van Erp, N. P.; Gelderblom, H.; Guchelaar, H.-J., Clinical pharmacokinetics of tyrosine kinase inhibitors. *Cancer Treatment Reviews* **2009,** *35*, 692-706.
53. Nottbohm, A. C.; Hergenrother, P. J.; Begley, T. P., Phosphate Mimics: Cyclic Compounds. In *Wiley Encyclopedia of Chemical Biology*, John Wiley & Sons, Inc.: 2007.
54. Elliott, T. S.; Slowey, A.; Ye, Y.; Conway, S. J., The use of phosphate bioisosteres in medicinal chemistry and chemical biology. *MedChemComm* **2012,** *3*, 735-751.
55. Xin, Z.; Oost, T. K.; Abad-Zapatero, C.; et al., Potent, selective inhibitors of protein tyrosine phosphatase 1B. *Bioorganic & Medicinal Chemistry Letters* **2003,** *13*, 1887-1890.
56. Lavén, G.; Stawinski, J., Palladium(0)-Catalyzed Benzylation of H-Phosphonate Diesters: An Efficient Entry to Benzylphosphonates. *Synlett* **2009,** *2009*, 225-228.
57. Cohen, R. J.; Fox, D. L.; Eubank, J. F.; Salvatore, R. N., Mild and efficient Cs2CO3-promoted synthesis of phosphonates. *Tetrahedron Letters* **2003,** *44*, 8617-8621.
58. Matulic-Adamic, J.; Haeberli, P.; Usman, N., Synthesis of 5'-Deoxy-5'-Difluoromethyl Phosphonate Nucleotide Analogs. *The Journal of Organic Chemistry* **1995,** *60*, 2563-2569.
59. Tulshian, D.; Czarniecki, M.; Doll, R. J.; Ahn, H. S., Synthesis and phosphodiesterase activity of carboxylic acid mimetics of cyclic guanosine 3',5'-monophosphate. *J Med Chem* **1993,** *36*, 1210-20.
60. Andersen, H. S.; Iversen, L. F.; Jeppesen, C. B.; Branner, S.; Norris, K.; Rasmussen, H. B.; Moller, K. B.; Moller, N. P., 2-(oxalylamino)-benzoic acid is a general, competitive inhibitor of protein-tyrosine phosphatases. *J Biol Chem* **2000,** *275*, 7101-8.

61. Tarabara, I. N.; Kas'yan, A. O.; Krishchik, O. V.; Shishkina, S. V.; Shishkin, O. V.; Kas'yan, L. I., Synthesis, Structure, and Transformations of New Endic Anhydride Derivatives. *Russian Journal of Organic Chemistry* **2002,** *38*, 1299-1308.
62. Kas'yan, L. I.; Krishchik, O. V.; Tarabara, I. N.; Kas'yan, A. O.; Pal'chikov, V. A., Lactonization of epoxyendic anhydride in reactions with amines. *Russian Journal of Organic Chemistry* **2006,** *42*, 501-508.
63. Dickson, R. S.; Dobney, B. J.; Eastwood, F. W., Preparation of cyclopentadiene from its dimer. *Journal of Chemical Education* **1987,** *64*, 898.
64. Arrieta, A.; Cossío, F. P.; Lecea, B., Direct Evaluation of Secondary Orbital Interactions in the Diels−Alder Reaction between Cyclopentadiene and Maleic Anhydride. *The Journal of Organic Chemistry* **2001,** *66*, 6178-6180.
65. Groaz, E.; Banti, D.; North, M., Synthesis of Cyclic and Macrocyclic Ethers Using Metathesis Reactions of Alkenes and Alkynes. *European Journal of Organic Chemistry* **2007,** *2007*, 3727-3745.
66. Hu, X.; Stebbins, C. E., Molecular docking and 3D-QSAR studies of Yersinia protein tyrosine phosphatase YopH inhibitors. *Bioorg Med Chem* **2005,** *13*, 1101-9.
67. Xie, J.; Comeau, A. B.; Seto, C. T., Squaric Acids: A New Motif for Designing Inhibitors of Protein Tyrosine Phosphatases. *Organic Letters* **2004,** *6*, 83-86.
68. Ye, D.; Zhang, Y.; Wang, F.; Zheng, M.; Zhang, X.; Luo, X.; Shen, X.; Jiang, H.; Liu, H., Novel thiophene derivatives as PTP1B inhibitors with selectivity and cellular activity. *Bioorganic & Medicinal Chemistry* **2010,** *18*, 1773-1782.
69. Hilmarsdottir, B.; Briem, E.; Halldorsson, S.; Kricker, J.; Ingthorsson, S.; Gustafsdottir, S.; Maelandsmo, G. M.; Magnusson, M. K.; Gudjonsson, T., Inhibition of PTP1B disrupts cell-cell adhesion and induces anoikis in breast epithelial cells. *Cell Death Dis* **2017,** *8*, e2769.
70. Kyriakou, E.; Schmidt, S.; Dodd, G. T.; Pfuhlmann, K.; Simonds, S. E.; Lenhart, D.; Geerlof, A.; Schriever, S. C.; De Angelis, M.; Schramm, K. W.; Plettenburg, O.; Cowley, M. A.; Tiganis, T.; Tschop, M. H.; Pfluger, P. T.; Sattler, M.; Messias, A. C., Celastrol Promotes Weight Loss in Diet-Induced Obesity by Inhibiting the Protein Tyrosine Phosphatases PTP1B and TCPTP in the Hypothalamus. *J Med Chem* **2018,** *61*, 11144-11157.
71. Krishnan, N.; Konidaris, K. F.; Gasser, G.; Tonks, N. K., A potent, selective, and orally bioavailable inhibitor of the protein-tyrosine phosphatase PTP1B improves insulin and leptin signaling in animal models. *J Biol Chem* **2018,** *293*, 1517-1525.
72. Feldhammer, M.; Uetani, N.; Miranda-Saavedra, D.; Tremblay, M. L., PTP1B: a simple enzyme for a complex world. *Crit Rev Biochem Mol Biol* **2013,** *48*, 430-45.
73. Maheshwari, N.; Karthikeyan, C.; Trivedi, P.; Moorthy, N., Recent Advances in Protein Tyrosine Phosphatase 1B Targeted Drug Discovery for Type II Diabetes and Obesity. *Curr Drug Targets* **2018,** *19*, 551-575.
74. Chowdhury, S.; Owens, K. N.; Herr, R. J.; Jiang, Q.; Chen, X.; Johnson, G.; Groppi, V. E.; Raible, D. W.; Rubel, E. W.; Simon, J. A., Phenotypic Optimization of Urea-Thiophene Carboxamides To Yield Potent, Well Tolerated, and Orally Active Protective Agents against Aminoglycoside-Induced Hearing Loss. *J Med Chem* **2018,** *61*, 84-97.
75. Van der Plas, S. E.; Kelgtermans, H.; De Munck, T.; Martina, S. L. X.; Dropsit, S.; Quinton, E.; De Blieck, A.; Joannesse, C.; Tomaskovic, L.; Jans, M.; Christophe, T.; van der Aar, E.; Borgonovi, M.; Nelles, L.; Gees, M.; Stouten, P.; Van Der Schueren, J.; Mammoliti, O.; Conrath, K.; Andrews, M., Discovery of N-(3-Carbamoyl-5,5,7,7-tetramethyl-5,7-dihydro-4H-thieno[2,3-c]pyran-2-yl)-lH-pyr azole-5-carboxamide (GLPG1837), a Novel Potentiator Which Can Open Class III Mutant Cystic Fibrosis Transmembrane Conductance Regulator (CFTR) Channels to a High Extent. *J Med Chem* **2018,** *61*, 1425-1435.
76. Bozorov, K.; Nie, L. F.; Zhao, J.; Aisa, H. A., 2-Aminothiophene scaffolds: Diverse biological and pharmacological attributes in medicinal chemistry. *Eur J Med Chem* **2017,** *140*, 465-493.

77. Thomas, J.; Jecic, A.; Vanstreels, E.; van Berckelaer, L.; Romagnoli, R.; Dehaen, W.; Liekens, S.; Balzarini, J., Pronounced anti-proliferative activity and tumor cell selectivity of 5-alkyl-2-amino-3-methylcarboxylate thiophenes. *Eur J Med Chem* **2017,** *132*, 219-235.
78. Jornada, D. H.; dos Santos Fernandes, G. F.; Chiba, D. E.; de Melo, T. R.; dos Santos, J. L.; Chung, M. C., The Prodrug Approach: A Successful Tool for Improving Drug Solubility. *Molecules* **2015,** *21*, 42.
79. Hoshi, A.; Sakamoto, T.; Takayama, J.; Xuan, M.; Okazaki, M.; Hartman, T. L.; Buckheit, R. W., Jr.; Pannecouque, C.; Cushman, M., Systematic evaluation of methyl ester bioisosteres in the context of developing alkenyldiarylmethanes (ADAMs) as non-nucleoside reverse transcriptase inhibitors (NNRTIs) for anti-HIV-1 chemotherapy. *Bioorg Med Chem* **2016,** *24*, 3006-3022.
80. Diana, G. D.; Volkots, D. L.; Nitz, T. J.; Bailey, T. R.; Long, M. A.; Vescio, N.; Aldous, S.; Pevear, D. C.; Dutko, F. J., Oxadiazoles as ester bioisosteric replacements in compounds related to disoxaril. Antirhinovirus activity. *J Med Chem* **1994,** *37*, 2421-36.
81. Huang, Y.; Domling, A., The Gewald multicomponent reaction. *Mol Divers* **2011,** *15*, 3-33.
82. Huang, X.-G.; Liu, J.; Ren, J.; Wang, T.; Chen, W.; Zeng, B.-B., A facile and practical one-pot synthesis of multisubstituted 2-aminothiophenes via imidazole-catalyzed Gewald reaction. *Tetrahedron* **2011,** *67*, 6202-6205.
83. Zhang, W.; Ma, L.; Yuan, L.; Xu, C.; Li, G.; Tao, M., An Efficient Synthesis of 2-Aminothiophenes via the Gewald Reaction Catalyzed by an N-Methylpiperazine-Functionalized Polyacrylonitrile Fiber. *Synthesis* **2012,** *45*, 45-52.
84. Thomas, J.; Jana, S.; Sonawane, M.; Fiey, B.; Balzarini, J.; Liekens, S.; Dehaen, W., A new four-component reaction involving the Michael addition and the Gewald reaction, leading to diverse biologically active 2-aminothiophenes. *Organic & Biomolecular Chemistry* **2017,** *15*, 3892-3900.
85. Weber, L., The Application of Multi-Component Reactions in Drug Discovery. *Current Medicinal Chemistry* **2002,** *9*, 2085-2093.
86. Dömling, A.; Wang, W.; Wang, K., Chemistry and Biology Of Multicomponent Reactions. *Chemical Reviews* **2012,** *112*, 3083-3135.
87. Slobbe, P.; Ruijter, E.; Orru, R. V. A., Recent applications of multicomponent reactions in medicinal chemistry. *MedChemComm* **2012,** *3*.
88. Kalinski, C.; Umkehrer, M.; Weber, L.; Kolb, J.; Burdack, C.; Ross, G., On the industrial applications of MCRs: molecular diversity in drug discovery and generic drug synthesis. *Molecular Diversity* **2010,** *14*, 513-522.
89. Hulme, C.; Ayaz, M.; Martinez-Ariza, G.; Medda, F.; Shaw, A., Recent Advances in Multicomponent Reaction Chemistry. In *Small Molecule Medicinal Chemistry*, 2015; pp 145-187.
90. Boström, J.; Brown, D. G.; Young, R. J.; Keserü, G. M., Expanding the medicinal chemistry synthetic toolbox. *Nature Reviews Drug Discovery* **2018,** *17*, 709-727.
91. Zarganes-Tzitzikas, T.; Dömling, A., Modern multicomponent reactions for better drug syntheses. *Organic Chemistry Frontiers* **2014,** *1*, 834-837.
92. Huang, W.; Li, J.; Tang, J.; Liu, H.; Shen, J.; Jiang, H., Microwave-Assisted Synthesis of 2-Amino-thiophene-3-Carboxylic Derivatives Under Solvent-Free Conditions. *Synthetic Communications* **2005,** *35*, 1351-1357.
93. Ueda, T.; Konishi, H.; Manabe, K., Trichlorophenyl Formate: Highly Reactive and Easily Accessible Crystalline CO Surrogate for Palladium-Catalyzed Carbonylation of Aryl/Alkenyl Halides and Triflates. *Organic Letters* **2012,** *14*, 5370-5373.
94. Dişli, A.; Salman, M., Synthesis of some new 5-substituted 1H-tetrazoles. *Russian Journal of Organic Chemistry* **2009,** *45*, 151.

95. Dunetz, J. R.; Xiang, Y.; Baldwin, A.; Ringling, J., General and Scalable Amide Bond Formation with Epimerization-Prone Substrates Using T3P and Pyridine. *Organic Letters* **2011,** *13*, 5048-5051.
96. Kamal, A.; Srikanth, P. S.; Vishnuvardhan, M. V. P. S.; Kumar, G. B.; Suresh Babu, K.; Hussaini, S. M. A.; Kapure, J. S.; Alarifi, A., Combretastatin linked 1,3,4-oxadiazole conjugates as a Potent Tubulin Polymerization inhibitors. *Bioorganic Chemistry* **2016,** *65*, 126-136.
97. Scott, J. S.; deSchoolmeester, J.; Kilgour, E.; Mayers, R. M.; Packer, M. J.; Hargreaves, D.; Gerhardt, S.; Ogg, D. J.; Rees, A.; Selmi, N.; Stocker, A.; Swales, J. G.; Whittamore, P. R. O., Novel Acidic 11β-Hydroxysteroid Dehydrogenase Type 1 (11β-HSD1) Inhibitor with Reduced Acyl Glucuronide Liability: The Discovery of 4-[4-(2-Adamantylcarbamoyl)-5-tert-butyl-pyrazol-1-yl]benzoic Acid (AZD8329). *Journal of Medicinal Chemistry* **2012,** *55*, 10136-10147.
98. Monrad, R. N.; Errey, J. C.; Barry, C. S.; Iqbal, M.; Meng, X.; Iddon, L.; Perrie, J. A.; Harding, J. R.; Wilson, I. D.; Stachulski, A. V.; Davis, B. G., Dissecting the reaction of Phase II metabolites of ibuprofen and other NSAIDS with human plasma protein. *Chem. Sci.* **2014,** *5*, 3789-3794.
99. Lassalas, P.; Gay, B.; Lasfargeas, C.; James, M. J.; Tran, V.; Vijayendran, K. G.; Brunden, K. R.; Kozlowski, M. C.; Thomas, C. J.; Smith, A. B.; Huryn, D. M.; Ballatore, C., Structure Property Relationships of Carboxylic Acid Isosteres. *Journal of Medicinal Chemistry* **2016,** *59*, 3183-3203.
100. Ballatore, C.; Huryn, D. M.; Smith, A. B., Carboxylic Acid (Bio)Isosteres in Drug Design. *ChemMedChem* **2013,** *8*, 385-395.
101. Dugave, C.; Demange, L., Cis−Trans Isomerization of Organic Molecules and Biomolecules: Implications and Applications†. *Chemical Reviews* **2003,** *103*, 2475-2532.
102. Wu, T. Y. H.; Schultz, P. G.; Ding, S., One-Pot Two-Step Microwave-Assisted Reaction in Constructing 4,5-Disubstituted Pyrazolopyrimidines. *Organic Letters* **2003,** *5*, 3587-3590.
103. Shi, Y.; Ye, H.; Link, K. H.; Putnam, M. C.; Hubner, I.; Dowdell, S.; Koh, J. T., Mutant-Selective Thyromimetics for the Chemical Rescue of Thyroid Hormone Receptor Mutants Associated with Resistance to Thyroid Hormone†. *Biochemistry* **2005,** *44*, 4612-4626.
104. Leeson, P. D.; Springthorpe, B., The influence of drug-like concepts on decision-making in medicinal chemistry. *Nature Reviews Drug Discovery* **2007,** *6*, 881-890.
105. Gleeson, M. P., Generation of a Set of Simple, Interpretable ADMET Rules of Thumb. *Journal of Medicinal Chemistry* **2008,** *51*, 817-834.
106. Meyers, J.; Carter, M.; Mok, N. Y.; Brown, N., On the origins of three-dimensionality in drug-like molecules. *Future Medicinal Chemistry* **2016,** *8*, 1753-1767.
107. Lee, D. S.; Amara, Z.; Poliakoff, M.; Harman, T.; Reid, G.; Rhodes, B.; Brough, S.; McInally, T.; Woodward, S., Investigating Scale-Up and Further Applications of DABAL-Me3 Promoted Amide Synthesis. *Organic Process Research & Development* **2015,** *19*, 831-840.
108. Biswas, K.; Prieto, O.; Goldsmith, P. J.; Woodward, S., Remarkably Stable (Me3Al)2?DABCO and Stereoselective Nickel-Catalyzed AlR3 (R=Me, Et) Additions to Aldehydes. *Angewandte Chemie International Edition* **2005,** *44*, 2232-2234.
109. Lipinski, C. A.; Lombardo, F.; Dominy, B. W.; Feeney, P. J., Experimental and computational approaches to estimate solubility and permeability in drug discovery and development settings. *Advanced Drug Delivery Reviews* **1997,** *23*, 3-25.
110. Ritchie, T. J.; Macdonald, S. J., The impact of aromatic ring count on compound developability--are too many aromatic rings a liability in drug design? *Drug Discov Today* **2009,** *14*, 1011-20.
111. Johnson, S. M.; Murphy, R. C.; Geiger, J. A.; DeRocher, A. E.; Zhang, Z.; Ojo, K. K.; Larson, E. T.; Perera, B. G. K.; Dale, E. J.; He, P.; Reid, M. C.; Fox, A. M. W.; Mueller, N. R.; Merritt, E. A.; Fan, E.; Parsons, M.; Van Voorhis, W. C.; Maly, D. J., Development

ofToxoplasma gondiiCalcium-Dependent Protein Kinase 1 (TgCDPK1) Inhibitors with Potent Anti-ToxoplasmaActivity. *Journal of Medicinal Chemistry* **2012,** *55*, 2416-2426.
112. Ueda, S.; Su, M.; Buchwald, S. L., Highly N2-Selective Palladium-Catalyzed Arylation of 1,2,3-Triazoles. *Angewandte Chemie International Edition* **2011,** *50*, 8944-8947.
113. Murphy, R. C.; Ojo, K. K.; Larson, E. T.; Castellanos-Gonzalez, A.; Perera, B. G. K.; Keyloun, K. R.; Kim, J. E.; Bhandari, J. G.; Muller, N. R.; Verlinde, C. L. M. J.; White, A. C.; Merritt, E. A.; Van Voorhis, W. C.; Maly, D. J., Discovery of Potent and Selective Inhibitors of CDPK1 from C. parvum and T. gondii. *ACS Medicinal Chemistry Letters* **2010,** *1*, 331-335.
114. Gillis, E. P.; Eastman, K. J.; Hill, M. D.; Donnelly, D. J.; Meanwell, N. A., Applications of Fluorine in Medicinal Chemistry. *Journal of Medicinal Chemistry* **2015,** *58*, 8315-8359.
115. Yerien, D. E.; Bonesi, S.; Postigo, A., Fluorination methods in drug discovery. *Organic & Biomolecular Chemistry* **2016,** *14*, 8398-8427.
116. Shah, P.; Westwell, A. D., The role of fluorine in medicinal chemistry. *Journal of Enzyme Inhibition and Medicinal Chemistry* **2008,** *22*, 527-540.
117. Xu, L.; Giese, R. W., Synthesis of pentafluorobenzyloxy mono- to tetra-fluoroacetophenones. *Journal of Fluorine Chemistry* **1994,** *67*, 47-51.
118. Bezou, P.; Hilberer, A.; Hadziioannou, G., Efficient Synthesis of p-Vinyl-trans-Stilbene. *Synthesis* **1996,** *1996*, 449-451.
119. Gramage-Doria, R.; Achelle, S.; Bruneau, C.; Robin-le Guen, F.; Dorcet, V.; Roisnel, T., Ruthenium(II)-Catalyzed C–H (Hetero)Arylation of Alkenylic 1,n-Diazines (n = 2, 3, and 4): Scope, Mechanism, and Application in Tandem Hydrogenations. *The Journal of Organic Chemistry* **2018,** *83*, 1462-1477.
120. Huang, L.; Li, H.; Li, L.; Niu, L.; Seupel, R.; Wu, C.; Cheng, W.; Chen, C.; Ding, B.; Brennan, P. E.; Yang, S., Discovery of Pyrrolo[3,2-d]pyrimidin-4-one Derivatives as a New Class of Potent and Cell-Active Inhibitors of P300/CBP-Associated Factor Bromodomain. *Journal of Medicinal Chemistry* **2019,** *62*, 4526-4542.
121. Chung, T. D. Y.; Terry, D. B.; Smith, L. H., In Vitro and In Vivo Assessment of ADME and PK Properties During Lead Selection and Lead Optimization - Guidelines, Benchmarks and Rules of Thumb. In *Assay Guidance Manual*, Sittampalam, G. S.; Coussens, N. P.; Brimacombe, K.; Grossman, A.; Arkin, M.; Auld, D.; Austin, C.; Baell, J.; Bejcek, B.; Caaveiro, J. M. M.; Chung, T. D. Y.; Dahlin, J. L.; Devanaryan, V.; Foley, T. L.; Glicksman, M.; Hall, M. D.; Haas, J. V.; Inglese, J.; Iversen, P. W.; Kahl, S. D.; Kales, S. C.; Lal-Nag, M.; Li, Z.; McGee, J.; McManus, O.; Riss, T.; Trask, O. J., Jr.; Weidner, J. R.; Wildey, M. J.; Xia, M.; Xu, X., Eds. Bethesda (MD), 2004.
122. Rizk, M. L.; Zou, L.; Savic, R. M.; Dooley, K. E., Importance of Drug Pharmacokinetics at the Site of Action. *Clinical and Translational Science* **2017,** *10*, 133-142.
123. Vorrink, S. U.; Zhou, Y.; Ingelman-Sundberg, M.; Lauschke, V. M., Prediction of Drug-Induced Hepatotoxicity Using Long-Term Stable Primary Hepatic 3D Spheroid Cultures in Chemically Defined Conditions. *Toxicological Sciences* **2018,** *163*, 655-665.
124. Lu, C., Comparison of Intrinsic Clearance in Liver Microsomes and Hepatocytes from Rats and Humans: Evaluation of Free Fraction and Uptake in Hepatocytes. *Drug Metabolism and Disposition* **2006,** *34*, 1600-1605.
125. J. Richardson, S.; Bai, A.; A. Kulkarni, A.; F. Moghaddam, M., Efficiency in Drug Discovery: Liver S9 Fraction Assay As a Screen for Metabolic Stability. *Drug Metabolism Letters* **2016,** *10*, 83-90.
126. Savjani, K. T.; Gajjar, A. K.; Savjani, J. K., Drug Solubility: Importance and Enhancement Techniques. *ISRN Pharmaceutics* **2012,** *2012*, 1-10.
127. Kerns, E.; Di, L., Automation in Pharmaceutical Profiling. *Journal of the Association for Laboratory Automation* **2005,** *10*, 114-123.
128. LeCluyse, E. L.; Alexandre, E., Isolation and Culture of Primary Hepatocytes from Resected Human Liver Tissue. In *Hepatocytes*, 2010; pp 57-82.

129. Hughes, J. P.; Rees, S.; Kalindjian, S. B.; Philpott, K. L., Principles of early drug discovery. *British Journal of Pharmacology* **2011,** *162*, 1239-1249.
130. Sotoud, H.; Gribbon, P.; Ellinger, B.; Reinshagen, J.; Boknik, P.; Kattner, L.; El-Armouche, A.; Eschenhagen, T., Development of a Colorimetric and a Fluorescence Phosphatase-Inhibitor Assay Suitable for Drug Discovery Approaches. *Journal of Biomolecular Screening* **2013,** *18*, 899-909.
131. Schürmann, M.; Janning, P.; Ziegler, S.; Waldmann, H., Small-Molecule Target Engagement in Cells. *Cell Chemical Biology* **2016,** *23*, 435-441.
132. Bartrons, R.; Simon-Molas, H.; Rodríguez-García, A.; Castaño, E.; Navarro-Sabaté, À.; Manzano, A.; Martinez-Outschoorn, U. E., Fructose 2,6-Bisphosphate in Cancer Cell Metabolism. *Frontiers in Oncology* **2018,** *8*.
133. Rajeshkumar, N. V.; Dutta, P.; Yabuuchi, S.; de Wilde, R. F.; Martinez, G. V.; Le, A.; Kamphorst, J. J.; Rabinowitz, J. D.; Jain, S. K.; Hidalgo, M.; Dang, C. V.; Gillies, R. J.; Maitra, A., Therapeutic Targeting of the Warburg Effect in Pancreatic Cancer Relies on an Absence of p53 Function. *Cancer Research* **2015,** *75*, 3355-3364.
134. Follia, L.; Ferrero, G.; Mandili, G.; Beccuti, M.; Giordano, D.; Spadi, R.; Satolli, M. A.; Evangelista, A.; Katayama, H.; Hong, W.; Momin, A. A.; Capello, M.; Hanash, S. M.; Novelli, F.; Cordero, F., Integrative Analysis of Novel Metabolic Subtypes in Pancreatic Cancer Fosters New Prognostic Biomarkers. *Frontiers in Oncology* **2019,** *9*.
135. Avila, M. A.; Chan, T. S.; Cassim, S.; Raymond, V.-A.; Gottschalk, S.; Merlen, G.; Zwingmann, C.; Lapierre, P.; Darby, P.; Mazer, C. D.; Bilodeau, M., Upregulation of Krebs cycle and anaerobic glycolysis activity early after onset of liver ischemia. *Plos One* **2018,** *13*.
136. Firouzabadi, H.; Iranpoor, N.; Sobhani, S., Preparation of α-ketophosphonates by oxidation of α-hydroxyphosphonates with neutral alumina supported potassium permanganate (NASPP) under solvent-free conditions and potassium permanganate in dry benzene. *Tetrahedron Letters* **2002,** *43*, 477-480.
137. Kotsikorou, E.; Sahota, G.; Oldfield, E., Bisphosphonate Inhibition of Phosphoglycerate Kinase: Quantitative Structure−Activity Relationship and Pharmacophore Modeling Investigation. *Journal of Medicinal Chemistry* **2006,** *49*, 6692-6703.
138. Badri, R.; Heidarizadeh, F., Steric Effects on the Formation of Imide 1,4-Diphenyl-1,4-epoxy-1,2,3,4-tetrahydronaphthalene-2,3-dicarboxylic Anhydride. *ChemInform* **2004,** *35*.

9. Appendix

9.1. Table of amino acids

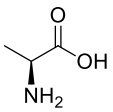

Alanine, Ala, A

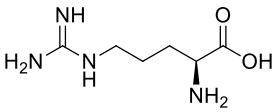

Arginine, Arg, R

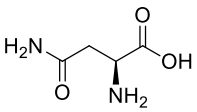

Asparagine, Asn, N

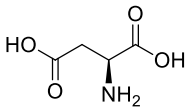

Aspartic acid, Asp, D

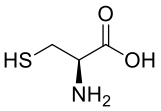

Cysteine, Cys, C

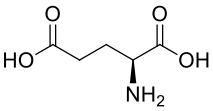

Glutamic acid, Glu, E

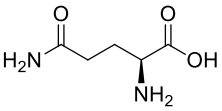

Glutamine, Gln, Q

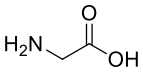

Glycine, Gly, G

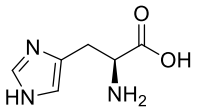

Histidine, His, H

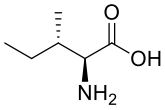

Isoleucine, Ile, I

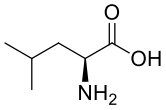

Leucine Leu, L

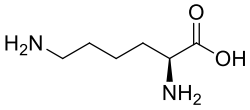

Lysine, Lys, K

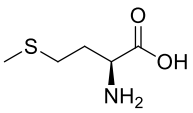

Methionine, Met, M

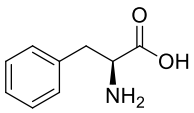

Phenylalanine, Phe, F

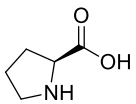

Proline, Pro, P

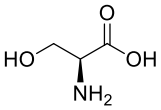

Serine, Ser, S

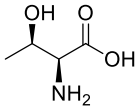

Threonine, Thr, T

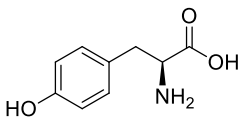

Tyrosine, Tyr, Y

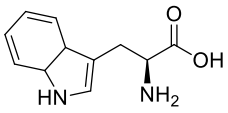

Tryptophan, Trp, W

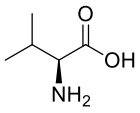

Valine, Val, V